THE MOMENT CARRYING CAPACITY OF SHORT PIER FOUNDATIONS IN CLAY

This thesis submitted in accordance with the requirements of the

University of Liverpool

for the degree of

Doctor in Philosophy

MUSTAFA LAMAN
(BSc., MSc.)

MARCH 1995

DECLARATION

I declare that no portion of the work referred to in this thesis has been submitted in support of an application for another degree or qualification of this or any other university or institute of learning.

....

MUSTAFA LAMAN

ABSTRACT

An investigation on the moment carrying capacity of short rigid pier foundations in saturated clay soil is described. The work includes extensive model studies (both conventional and centrifugal), numerical investigations, and the application of existing design formulae.

Pier foundations are widely used for transmission towers and gantries and for large road and railway hoardings and other elevated commercial signs, where moment carrying capacity is the dominant design requirement. In this study, the lateral pulling force is usually applied at a prototype height of 6 m above the level of the clay since this is the approximate height of railway power lines.

For both conventional and centrifugal experimental programs scale models of short pier foundations with different widths and lengths were used. The details of the experimental programs and the analysis of the test results are presented together with empirical relationships which have been derived between the moment carrying capacity and pier geometry. A very close fit is demonstrated between the moment-rotation values using these empirical equations and the observed data obtained from the model tests. The results show that the relationships between moment and rotation are non-linear but do not exhibit any peak values and that moment carrying capacity increases with increases in pier length and width. From comparisons of the results of centrifugal and conventional model tests, it is shown that for the same pier rotations, the moment carrying capacities observed in centrifugal model tests are significantly larger than those in conventional model tests.

Numerical analyses of these models were also carried out using the three-dimensional linear and non-linear finite element computer programs, developed in this study, and an existing axi-symmetric one, to assess the experimental work. The results from the non-linear computer analyses of the centrifuge models show good agreement with those at full-scale while those of the conventional models are significantly different.

The results of the finite element models are compared with those of experimental observations. The results from the three-dimensional finite element analysis, using a hyperbolic stress-strain model for the soil, are shown to provide satisfactory predictions of observed moment-rotation behaviour and working moment limits.

A numerical study of the effect of the pulling height on the moment/rotation behaviour of a rigid pier foundation was carried out. It is shown that the pulling height affects the moment/rotation performance of pier foundations for a pulling height/pier depth ratio < 2.5.

Some of the existing analytical approaches for predicting the ultimate behaviour of laterally loaded pile and pier foundations are examined. The methods of Brinch-Hansen (1961) and UIC/ORE (1957) are applied and the solutions obtained compared with the results from model tests and numerical analyses. It is shown that the latter considerably overestimates both the results of this study and those of Brinch-Hansen.

ACKNOWLEDGEMENTS

The author wishes to express his sincere gratitude and thanks to his supervisor, Dr. G.J.W. King, Senior Lecturer in Civil Engineering, for many stimulating discussions and continuous encouragement during the course of this investigation. His patient and careful evaluation of the manuscript were of invaluable assistance in the preparation of this thesis.

The author also expresses his gratitude to his nation who indirectly financed his expenses throughout the course of this research.

The help of Mr. A.J. Moorhouse, Senior Technician, Soil Mechanics Laboratory, Civil Engineering Department, in carrying out the experimental work is also gratefully acknowledged.

He also wishes to thank Prof. Erhan Kıral, Prof. Orhan Aksoğan, Prof. Salih Kırkgöz, Assoc. Prof. A. Kamil Tanrıkulu and Mr. Beytullah Temel of the Civil Engineering Department, University of Çukurova, for their heartfelt help and encouragement and my colleagues, M. Bouhicha, G. Najafian, M. Fienkeng, R. Nazir, O. Karim and others in the research room for the fun and co-operation during the course of this research.

Finally, the author would like also to thank his family for their constant support and encouragement throughout the course of this research.

TABLE OF CONTENTS

LIST OF TABLES

CHAPTER 2

CHAPTER 3

CHAPTER 4

CHAPTER 5

CHAPTER 6

CHAPTER 7

CHAPTER 8

APPENDIX B

LIST OF FIGURES

CHAPTER 2

CHAPTER 3

CHAPTER 4

CHAPTER 5

CHAPTER 6

CHAPTER 7

CHAPTER 8

APPENDIX A

APPENDIX B

APPENDIX E

LIST OF PLATES

CHAPTER 4

CHAPTER 5

LIST OF SYMBOLS

$\{B_{be}\}$	Vector of displacement boundary conditions
(E_p')	Correction coefficient to allow for height D′ of the soil replaced on the surface
$(M_R)_p$	Pure overturning moment
$\{d\}$	Nodal displacement vector of the whole system
$\{F\}$	Resultant nodal load vector of the whole system
$\{f\}$	An equivalent nodal force vector
$\{b\}$	Body force per unit volume
$\{d\}_e$	Nodal displacement vector of the element
$\{R\}$	Concentrated forces applied at the nodes
$\{t\}$	Surface forces per unit area
$[K]$	Overall stiffness matrix
$[B]$	Strain matrix
$[D]$	Elasticity matrix
$[J]$	Jacobian matrix
$[k]$	Element stiffness matrix
$[N]$	A set of shape functions
α_{t1}, α_{t2}, α_{t3}	Coefficient constants (centrifuge test)
α_{v1}, α_{v2}	Coefficient constants (conventional test)
β	A measure of the stiffness of the soil relative to that of the pile
β_{t1}	Intercept value of Moment/Cohesion against pier breadth curve (centrifuge test)
β_{t2}	Slope of Moment/Cohesion against pier geometry graph (centrifuge test)
β_{v1}	Intercept value of Moment/Cohesion against pier breadth curve (conventional test)
β_{v2}	Slope of Moment/Cohesion against pier geometry graph (conventional test)
γ	Density of soil (kg/m^3)
γ_b	Bulk unit weight
γ_m	Model specific weight
γ_p	Prototype specific weight
δ	Deflection
Δ	Horizontal deflection at ground level
ε	Axial strain
Θ	Rotation angle
ν	Poisson's ratio
ν_1	Poisson's ratio in the plane of isotropy
ν_2	Poisson's ratio representing the strain in the plane of isotropy

ν_s	Poisson's ratio of soil
$\xi\eta\zeta$	Serendipity co-ordinates system
π_e	Total potential energy of the individual element
$\sigma_1, \sigma_2, \sigma_3$	Principal stresses in 3D stress analysis
$\sigma_1 - \sigma_3$	Principal stress difference (deviator stress)
σ_1 and σ_3	Major and minor principal stresses
$\sigma_x, \sigma_y, \sigma_z$	Stresses in an element
ϕ	Apparent angle of internal friction of soil
Φ	Vector of surface tractions at the pile-soil interface
ω	Angular velocity
$\overline{\omega}$	Optimum angular velocity
a, b	Hyperbolic model parameters
A,B	Coefficients relating to a lateral load F and a moment loading M respectively
b	Width of pier perpendicular to B
B	Breadth of the pier parallel to the overturning force (m)
c	Shear strength of the soil
C_1	An empirical constant relating pier deflection to the laboratory strain
CPU	Central processing unit
c_u	Undrained shear strength of soil
d	Smaller of dimensions B and b (m)
D/B	Ratio of the depth to breadth of the pier
D	Depth of the pier (m)
DI	Pile diameter
D'	Depth of unconsolidated layer (m)
E	Young's modulus
E_1	Modulus of elasticity in the plane of isotropy
E_2	Modulus of elasticity in the direction perpendicular to the plane of isotropy
E_i	The initial modulus
E_p	Young's modulus of foundation
E_pI_p	Flexural stiffness of pile
E_s	Undrained modulus of the soil
E_t	Tangent modulus
E_{ur}	Unload/reload moduli
$[F_{be}]$	$(2p_{be} + q_{be})$ Square matrix of coefficients
F	Lateral load
F_m	Model force

F_p	Prototype force
G_2	Shear modulus in planes perpendicular to the plane of isotropy
H, P	Horizontal and axial loads
h_c	Depth of the cracks
I	Second moment of area
j	Number of nodes in each element
J	A constant which controls the depths at which P_u reaches 9cb for stiff soils
k	Modulus (in units of force/length^2)
K	Modulus of subgrade reaction (in units of force/length^3)
K_0	Coefficient of lateral earth pressure at rest
K_1, K_2, K	Coefficients in the UIC/ORE method
k_n	Unit normal stiffness
K_{qz}, K_{cz}	Passive earth pressure coefficients
k_s	Unit tangential stiffness
K_{ur}	Unloading-Reloading modulus number
L/D	Pulling height ratio
L	Pulling height
LL	Liquid Limit
LUGC	Liverpool University Geotechnical Centrifuge
m	Moisture content of clay (%)
M	Allowable moment at ground level (kNm)
M_B	Calculated moment limit
M_L	Corrected moment limit at ground level (kg m)
M_m	Model moment
M_{max}	Limit of overturning moment at large L for a prescribed displacement limit
M_p	Prototype moment
M_{pm}	Permissible moment at two thirds of the effective depth of the foundation (kN/m)
n, K	Hyperbolic Constants
n_h	Coefficient of subgrade reaction
N_i	Shape function for the i th node in the element
n_{ur}	Value of exponent
p	Soil pressure (kN/m^2)
$\overline{p}$	Soil reaction
p_{be}	Number of shaft segments
P	Soil resistance/unit length
P_θ	Force in the circumferential direction

P_a	Atmospheric pressure
PI	Plasticity Index
PL	Plastic Limit
P_m	Model pressure
p_{oz}	Effective overburden pressure at depth z
p_p	Passive pressure (kN/m^2)
P_p	Prototype pressure
P_r	Force in the radial direction
P_z	Force in the axial direction
q_{be}	Number of base elements
r	Radius
R_f	Failure ratio
RFOS	Reciprocal of the factor of safety of a soil element
rpm	Rotation per minute
s	Soil model height
S	Bending moment
S_G	Specific Gravity
u, v, w	Radial, axial, and circumferential displacements
u_i, v_i, w_i	Displacements of the i-th node
V	Slope
V_e	Volume of the hexahedron
w	Soil modulus at the level of the pile tip (in units of force/length^2)
W	Total vertical load including weight of foundation and pulling rod (kg)
w_i, w_j, w_k	Weight coefficients
x, y, z	Global co-ordinates
x	Distance between clay surface and top of the soil bin
x_0, y_0, z_0	Global co-ordinates of the centroid
y	Displacement
z	Length along pile

CHAPTER 1

INTRODUCTION

1.1 General

Foundations for transmission towers and gantries and for large road and railway hoardings and other elevated commercial signs have to be designed mainly to resist lateral loads applied high above ground level. A widely used type of foundation for these structures is the rigid pier which has to withstand large moments and relatively small vertical and horizontal forces. The techniques for the analyses of these foundations are not as advanced and as well understood as those for foundations subjected to vertical compressive loads, although the closely related problem of the laterally loaded pile has received considerable attention.

Pier foundations fulfil a similar function to piled foundations, the main differences being in the method of construction and the foundation sizes. Piers are characterised by geometries short (in length) and large, square or circular shaped, in cross-section. Piles are usually installed by driving or vibrating the structural member and displacing the ground while piers are installed by excavating or drilling a shaft, which may be cased or uncased depending on the soil conditions, and then filling the shaft with concrete. Piers and short bored-piles are synonymous.

In the past, the design of laterally loaded pile and pier foundations has been based upon empirical information mainly from full-scale tests or conventional model studies in the laboratory. In recent years techniques have been developed to predict the behaviour of laterally loaded pile and pier foundations which include centrifuge modelling, theoretical methods and, most recently, finite element and boundary element methods.

Although prototype tests would provide the most useful information, these are not often carried out because of the high cost of materials and labour, and because ground conditions are difficult to control and quantify. Use of the geotechnical centrifuge, however, offers an economical and practical alternative to large scale prototype testing to determine the behaviour of piles and piers subjected to lateral loading.

The theoretical methods for predicting the behaviour of laterally loaded pile and pier foundations have generally been based on either the modulus of subgrade reaction approach or elastic continuum methods.

The modulus of subgrade reaction approach, which was first introduced by Winkler in 1867, assumes that the foundation is supported upon a series of springs. The method has been widely used in foundation practice because it provides a relatively simple means of analysis and factors such as non-linearity, variation of soil stiffness with depth, and layering of the soil profile can sometimes be taken into account. However, there are some disadvantages of this soil model. It is difficult to assign values to the modulus of subgrade reaction which is dependent on the breadth of a foundation and is not an intrinsic soil property.

The elastic continuum approach, which assumes the soil to be an ideal elastic continuum, relies on separate numerical methods for analysing the foundation and the continuum and requires matching of deflection and pressure along the foundation/continuum interface using an iterative process. This method is more satisfactory than the modulus of subgrade reaction approach, as account is taken of the continuous nature of soil. However, there is also difficulty with this method in determining appropriate soil moduli.

The most recent methods for analyses of pier-soil behaviour are the finite element and boundary element methods. These methods require the use of a large computer for the solution of a given problem. Both analyses have received widespread attention in the last three decades.

Since stress-strain relationships for soil are generally non-linear, it is essential to allow for this in these analyses by incorporating a non-linear model for soil behaviour, particularly one which will not sustain tensile stresses. The hyperbolic model, proposed by Duncan and Chang (1970), for the mathematical modelling of soil behaviour gives reasonable predictions of stress dependent stress-strain curves for soils. It has been widely used in the finite element solution of boundary value problems. In the analysis, the loading is applied in a series of small increments and a modulus for each element is selected in accordance with the state of stress computed in the element at the beginning of each increment. Parameters required to define the model can be obtained from conventional triaxial compression tests.

1.2 Purpose and Scope of Present Investigation

This research is concerned with the study of the moment carrying capacity of rigid pier foundations in saturated clay soil. The work includes extensive laboratory model studies (both conventional and centrifugal), numerical investigations, and the application of existing design formulae. It is expected that the study will provide a better understanding of the behaviour of this type of foundation and hence facilitate improved design procedures.

Following the points highlighted in section 1.1, the following objectives were defined for the present investigation:

1) To perform conventional and centrifuge model tests for pier foundations embedded in saturated clay with the following specific intentions:

(i) To investigate the effect of the pier geometry on the moment carrying capacity and to obtain some empirical relationships from the tests.

(ii) To examine the suitability of these test methods and to point out where appropriate, their weaknesses.

2) To simulate the behaviour of piers using finite element models with the following specific intentions:

(i) To obtain some numerical results for laterally loaded pier foundations using an existing axi-symmetric two-dimensional finite element program, PIER2D, in order to make an approximate comparison with the results of the experimental investigations.

(ii) To develop a more versatile three-dimensional finite element program in order to examine the validity of the axi-symmetric program and to see whether considering the non-linear stress-strain behaviour of the clay shows improved correlation with experimental findings.

(iii) To carry on some parametric studies on the influence of artificial boundaries and on the effect of the pulling height and pier embedment on the moment/rotation behaviour of a rigid pier foundation using the computer programs.

3) To apply some existing design formulae for laterally loaded pile and pier foundations and to compare their results with those of this study.

4) To investigate the relative merits of the results of model tests, numerical analyses and some of the existing design formulae and to reach some conclusions on the validity of these different methods.

1.3 Structure of Thesis

A short description of the structure of the thesis is outlined below:

A review of the past experimental and analytical investigations carried out both on laterally loaded piles and on rigid piers in clay is given in Chapter 2. The resulting design formulae which are currently used for predicting the behaviour of single pile and rigid pier foundations under lateral loads and moments are also summarised.

The non-linear model proposed by Duncan and Chang (1970) for the mathematical modelling of soil behaviour is briefly reviewed in Chapter 3. In order to provide data for the numerical studies a series of conventional triaxial compression tests were carried out on the clay used to supplement the tests performed by previous research workers. The results of these tests and the derivation of appropriate soil parameters are also given in this chapter.

Chapter 4 is concerned with the conventional model studies of short pier foundations. It includes a description of the model piers and the clay used and a detailed description of the experimental apparatus and test procedure. The details of the experimental program and the analysis of the test results are presented together with an empirical relationship which has been derived between moment carrying capacity and pier geometry.

Chapter 5 is concerned with the centrifuge model studies of short pier foundations under a centrifugal acceleration of 40g. The basic principles and scaling laws of centrifuge modelling are reviewed. The Liverpool University Centrifuge and ancillary experimental apparatus are described together with the procedure for testing the model piers. The details of the experimental program and the results obtained from the tests are then presented and an alternative empirical equation, to the one obtained from the conventional model study, developed to fit the data.

Chapter 6 contains a detailed description of the finite element analyses performed on laterally loaded pier foundations. A brief description of the finite element method is presented. An existing axi-symmetric two-dimensional computer program, PIER2D, is described briefly and the three-dimensional computer programs, PIER3DLN and PIER3DNL, developed in this study are then presented in detail. The linear three-dimensional program is verified for a simple structural problem.

Chapter 7 is concerned with the results of the numerical analyses of short pier foundations using the three computer programs. The analyses of one of the piers tested is explained in considerable detail to demonstrate how the programs are used. The results of analyses of the other piers are then presented and discussed. An investigation carried out to determine the minimum distances required between the foundation and soil boundaries in order to reduce their effect is presented. In addition to analyses at full-scale geometry, the restricted prototype geometries modelled in the tests are also analysed. The effect of the pulling height on the moment/rotation behaviour of a rigid pier foundation using the 3-D linear program is considered. The results from the three finite element programs are compared for a range of pier geometries and the comparison of these results are discussed.

Chapter 8 is concerned with the comparisons of the results of moment-rotation behaviour observed in the conventional and centrifugal model tests with those predicted by the axi-symmetric and three-dimensional finite element models. Also, the validity of the empirical equations, which have been derived from the results of the model tests, between moment carrying capacity and pier geometry, are illustrated with respect to moment/rotation behaviour for typical experiments. Some of the existing design formulae, that are frequently used in the literature for predicting the behaviour of single pile and rigid pier foundations subjected to lateral loads and moments, are applied and the solutions obtained are compared with the results from model tests and numerical analyses.

Finally in Chapter 9, a summary of conclusions with regards to the present investigation are presented, together with recommendations for further research.

CHAPTER 2

LITERATURE REVIEW

2.1 Introduction

This chapter reports on the past experimental and analytical investigations carried out both on laterally loaded piles and on rigid piers in clay. Extensive literature is also available on rigid and flexural piles in sand and rigid and flexural pile groups in clay and sand based on model, field and centrifuge tests and analytical investigations. Since this study is on moment carrying capacity of short rigid pier foundations in clay, only the relevant literature is reviewed.

2.2 Analytical Approaches and Design Formulae

There are several methods for analysing single pile and rigid pier foundations subjected to lateral loads. These have been discussed by various workers, e.g. Banerjee and Driscoll (1976), Reese and Desai (1977), Poulos and Davis (1980) and Smith (1980). Banerjee and Driscoll (1976) have classified them into four main groups: The Winkler or the modulus of subgrade reaction method, the pile - soil interaction methods, the boundary element method and the finite element method. One of the earliest attempts to develop design formulae for short rigid pier foundations was derived by UIC/ORE (1957). Alternative design formulae have been developed by

Czerniak (1957), Broms (1964b), Brinch-Hansen (1961), McCorkle (1969), Reese and Welch (1975) and, Balfour Beatty Construction Ltd. (1986). An extensive review of these methods is presented in the following sections.

2.2.1 Limit state methods

2.2.1.1 The International Union of Railways / Office for Research and Experiments (UIC/ORE) method

A design method reported by Ramelot and Vandeperre (1950) was based on more than a thousand tests, on reduced scale models in dried pit sand. It gives the limiting moment at ground level of a short pile foundation and the following formula was proposed:

$$M_B = (M_R)_p \, E_p' \tag{2.1}$$

where

$(M_R)_p$ = pure overturning moment

(E_p') = correction coefficient to allow for height D′ of the soil replaced on the surface (unconsolidated ground)

Figure 2.1 shows the geometric configuration. The value of E_p' is given by

$$E_p' = 3.44\left[1 + \left[\frac{D'}{D}\right]^3\right] - 2.44\sqrt{\left[1 + \left[\frac{D'}{D}\right]^2\right]^3} \tag{2.2a}$$

where

D′ = depth of unconsolidated layer (m)

D = depth of the pier (m)

The pure overturning moment $(M_R)_p$ is given by the following formula which is apparently independent of soil strength,

$$(M_R)_p = K_1 B W + K_2 \gamma b D^3 \tag{2.2b}$$

where

B = breadth of the pier parallel to the overturning force (m)

W = total vertical load including weight of foundation and pulling rod (kg)

γ = density of soil (kg/m^3)

b = dimension perpendicular to the overturning force (m)

The values of K_1 and K_2 are obtained from the following empirical expressions;

$$K_1 = 0.5136 - \frac{0.175}{0.54 + \dfrac{b}{D}}$$

(2.2c)

$$K_2 = \left[2.8 - \frac{96.5}{68.5 + 3.375\left[\dfrac{W}{10\gamma bBd}\right]^3}\right]\left[1 + 0.45\frac{B}{b}\right]$$

where

d = smaller of dimensions B and b (m) (in the case of cylindrical piers b=B=d=0.8DI where DI is diameter of the pier)

UIC/ORE (1957) revised the relationship by introducing a surface profile factor K and for cohesive soils making a statistical correction to equation (2.1) based on the results of field tests carried out within the vicinity of railways tracks. Thus the following formula for moment limit at ground level in cohesive soils was proposed:

$$M_L = K \;\; 27.45 \; M_B^{2/3} \tag{2.3}$$

where

M_L = corrected moment limit at ground level (kg m)

K = surface profile factor (unity for flat ground)

M_B = calculated moment limit from equation (2.1)

A factor of safety must be applied to M_L to limit deflection.

2.2.1.2 Broms' method

Extensive theoretical studies on lateral load behaviour of piles in cohesive and cohesionless soils were carried out by Broms (1964a-b, 1965, 1981). Broms (1964b) developed a theory to calculate the ultimate lateral resistance of short rigid piles in cohesive saturated soils. He suggested a simplified lateral soil resistance distribution: zero from the ground surface to a depth of 1.5 times the pile diameter, and constant at an ultimate capacity of 9 times the undrained shear strength below this depth, as shown in figure 2.2. The method is simple and has been accepted by many foundation engineers for design of simple pole foundations.

The maximum moment occurs at the level where the total shear force in the pier is equal to zero which is at a depth (1.5DI + f) below ground surface. The values of the distance f, and the maximum moment, M_{max}, are given by:

$$f = \frac{F}{9\, c_u\, DI} \tag{2.4}$$

where

c_u = undrained shear strength of soil

and DI = pile diameter

and

$$M_{max} = F\,(\,L + 1.5DI + 0.5f\,) \tag{2.5}$$

where

F = lateral load

and L = pulling height

The part of the pier with the length g (located below the point of maximum bending moment) resists the bending moment M_{max}, and from the equilibrium requirements;

$$M_{max} = 2.25\; c_u\; DI\; g^2 \tag{2.6}$$

Broms' method yields conservative results for large pier foundations.

2.2.1.3 McCorkle's method

McCorkle (1969) suggested the following formula for determining the allowable moment at ground level which can be applied to side-bearing short pier foundations with plan cross-section constantly round or square throughout the depth:-

$$M = \frac{p_p B D^2 L}{3L + 2D} \tag{2.7}$$

where

M = allowable moment at ground level (kNm)

p_p = passive pressure (kN/m^2)

Values of p_p tabulated by McCorkle are given in table 2.1.

Clay Consistency	p_p (kN/m^2)
Very soft	$\langle$ 14.4
Soft	14.4 - 28.7
Medium	28.7 - 57.5
Stiff	57.5 - 115
Very stiff	115 - 230
Hard	$\rangle$ 230

Table 2.1 McCorkle passive pressure values (p_p).

This method does not recognise the fundamental difference between the stress dependent strength of cohesionless soils and the stress independent cohesive soils.

2.2.1.4 The Balfour Beatty method

Balfour Beatty (1986) developed a formula for designing pier foundations for overhead railway electrification gantries. The method was based on full scale observations from various sources. For cohesive soil, the method gives the permissible moment at two-thirds of the depth of the foundation as:-

$$M_{pm} = p\,D^2\,(\,B + 0.4\,) \qquad (2.8)$$

where

M_{pm} = permissible moment at two thirds of the effective depth of the foundation (kNm)

p = soil pressure constant (kN/m^2)

The value of the soil pressure constant, p, is dependent on clay consistency and ranges from 14 to 40 kN/m^2 as shown in table 2.2.

Clay Consistency	p (kN/m^2)
Firm clay	14 - 20
Stiff clay	20 - 30
Very stiff clay	30 - 40

Table 2.2 Balfour Beatty soil pressure constants (p).

Assuming the moment increases linearly from zero at the level of the applied horizontal force, the permissible moment at ground level can be defined as:-

$$M = M_{pm} \left[\frac{L}{L + \frac{2}{3} D} \right] \tag{2.9}$$

where

M = permissible moment at ground level

2.2.1.5 Brinch-Hansen's method

Brinch-Hansen (1961) developed a design formula based on ultimate strength theory and a pivot point. The method can be applied both to uniform and layered soils. The passive resistance diagram is divided into a convenient number of horizontal elements, n, of depth D/n shown in figure 2.3. The unit passive resistance of an element at a depth z below the ground surface is given by;

$$p_z = p_{oz} K_{qz} + c K_{cz} \tag{2.10}$$

where

p_{oz} = effective overburden pressure at depth z

c = shear strength of the soil (the undrained shearing strength c_u is used for short term loadings.)

K_{qz} and K_{cz} = passive earth pressure coefficients dependent on the soil properties, z and the foundation plan dimension.

Brinch-Hansen presented values of K_q and K_c in relation to the ratio of the depth z to the width of the pile B in the direction of rotation, as shown in figure 2.4.

The depth, a, of the point of rotation is found by a process of trial and error. Since the total passive resistance on each horizontal element is p_z D/n B, by taking moments about the point of application of lateral load,

$$\sum M = \sum_{z=0}^{a} p_z \frac{D}{n} (L+z)\, B - \sum_{z=a}^{D} p_z \frac{D}{n} (L+z)\, B \qquad (2.11a)$$

The point of rotation at depth a is correctly chosen when ΣM=0. Then the ultimate horizontal force F can be calculated by taking the moments about the point of rotation. Therefore

$$F(L + a) = \sum_{z=0}^{z=a} p_z \frac{D}{n} B(a - z) + \sum_{z=a}^{z=a+D} p_z \frac{D}{n} B(z - a) \qquad (2.11b)$$

Having obtained the horizontal force F, the ultimate bending moment at ground level is calculated as M=FL.

2.2.1.6 Murf and Hamilton's method

Murf and Hamilton (1993) proposed a three-dimensional collapse mechanism for the analysis of the ultimate strength of laterally loaded piles in clay under undrained conditions. The upper-bound method of plasticity was used to estimate the collapse load. The mechanism was capable of rationally accounting for many complexities such as strength, non-homogeneity, soil-pile adhesion, and suction on the back of the pile. Parametric studies showing the effect of these features were presented along with comparisons of model predictions with the centrifugal test results reported by Hamilton and Phillips (1991). Limiting values of ultimate soil resistance predicted from the collapse mechanism, which was as shallow as two diameters in depth, including adhesion and suction, were obtained, and agreed well with the results from experiments. An empirical equation was fitted to the analytical results to allow quick estimates of ultimate lateral loads for piles in commonly occurring soil profiles.

2.2.2 The modulus of subgrade reaction approach

The modulus of subgrade reaction approach was first introduced by Winkler in 1867. In this model, it is assumed that the reaction is proportional to the displacement. Thus;

$$p = K\,y \tag{2.12}$$

where,

p = soil pressure

K = modulus of subgrade reaction (in units of force/length^3)

y = displacement

Since 1867, many publications have dealt with this approach. The modulus of subgrade reaction can be assumed to be constant with depth or varying either linearly or nonlinearly with depth. Terzaghi (1955) and a number of investigators (e.g. Hetenyi (1946), McClelland and Focht (1956), Reese (1958), Georgiadis and Butterfield (1982), Pyke and Beikae (1984), Gabr and Borden (1990), Kramer (1992), Smith

(1987), Gabr et al. (1994)) have suggested procedures for obtaining the relationship between the soil pressure, p, and pile deflection, y, at various depths (p-y curves).

2.2.2.1 Constant Modulus of subgrade reaction

The differential equation for the problem of the laterally loaded pile modelled as a beam on elastic foundations is

$$E_p I_p \frac{d^4 y}{dz^4} + ky = 0 \qquad (2.13)$$

where

$E_p I_p$ = flexural stiffness of pile

z = length along pile

k = modulus (in units of force/length^2) = K x width or diameter of pile.

Solutions to equation (2.13) may be obtained either analytically or numerically (e.g Palmer and Thompson (1948)). For constant modulus, k, analytical solutions for flexible piles have been given by Matlock and Reese (1960) in terms of a characteristic length of pile defined by

$$T = \sqrt[4]{\frac{E_p I_p}{k}} \qquad (2.14)$$

They have presented a series of solutions containing similar groups of parameters in the form

$$y = \frac{F\,T^3}{E_p\,I_p} A_y + \frac{M\,T^2}{E_p\,I_p} B_y$$

$$S = \frac{F\,T^2}{E_p\,I_p} A_s + \frac{M\,T}{E_p\,I_p} B_s$$

$$M = F\,T\,A_m + M\,B_m \tag{2.15}$$

$$V = F\,A_v + \frac{M}{T} B_v$$

$$\bar{p} = \frac{F}{T} A_p + \frac{M}{T^2} B_p$$

where y, S, M, V and $\overline{p}$ are the displacement, slope, bending moment, shear force and soil reaction respectively. The A and B coefficients relate to a lateral load F and a moment loading M respectively. Analytical expressions for the coefficients A and B have been presented by Matlock and Reese (1960) in the form

$$A_y = \sqrt{2}\, e^{-\beta z} \cos \beta z \qquad B_y = e^{-\beta z} (\cos \beta z - \sin \beta z)$$

$$A_s = -\, e^{-\beta z} (\cos \beta z + \sin \beta z) \qquad B_s = -\, \sqrt{2}\, e^{-\beta z} (\cos \beta z)$$

$$A_m = \sqrt{2}\, e^{-\beta z} \sin \beta z \qquad B_m = e^{-\beta z} (\cos \beta z + \sin \beta z) \tag{2.16}$$

$$A_v = -\, e^{-\beta z} (\cos \beta z - \sin \beta z) \qquad B_v = -\, \sqrt{2}\, e^{-\beta z} (\sin \beta z)$$

$$A_p = A_y \qquad B_p = B_y$$

where β is a measure of the stiffness of the soil relative to that of the pile and is given by

$$\beta = \sqrt[4]{\frac{k}{4\, E_p\, I_p}} \propto \frac{1}{T} \tag{2.17}$$

Numerical values for the A and B coefficients at the ground level are shown in table 2.3.

Parameter	Lateral load	Moment
Deflection, y	$A_y = 1.41$	$B_y = 1.00$
Slope, s	$A_s = -1.00$	$B_s = -1.41$
Moment, m	$A_m = 0.00$	$B_m = 1.00$
Shear, v	$A_v = 1.00$	$B_v = 0.00$

Table 2.3 Ground-line values of deflection coefficients A and B for a single pile.

This assumption is usually accepted for overconsolidated clays. For horizontal load applied at ground level to a free-head pile Hetenyi (1946) obtained the solutions for horizontal displacements, slope, moment, and shear along the pile. Solutions for a pile in a two-layer system were presented by Davisson and Gill (1963). They concluded that the use of analytical results for a constant modulus, k, with depth might lead to underestimates of moment and deflection by a factor of 2.

The lateral deflection of piles is generally determined without taking into account the effect of vertical load. Davisson (1960) presented an analysis for a vertical pile subjected to moment, shear and axial load. It was based on the modulus of subgrade reaction approach. He assumed that the axial load was invariant with depth. The solutions for the governing differential equation was obtained using an analog computer and the results were presented in non-dimensional form. The results showed that for a given lateral load, the axial load magnified the pile head deflection and maximum moment in the pile. It was concluded that when the axial load was not within 10 % of the buckling load the increase in deflection and maximum moment was only marginal.

A simple theoretical approach to find a relationship between moment and rotation for a short rigid pier in clay, assuming a constant modulus, is presented by the Author in appendix A.

2.2.2.2 Modulus proportional to depth

The modulus of subgrade reaction approach has been improved by allowing the modulus, k, to vary along the length of the pile. This assumption is usually accepted as the best approximation for granular soils and normally consolidated clays. A comprehensive set of solutions for flexible piles have been also presented by Matlock and Reese (1961) and have been identical form to equation (2.15) but the characteristic length of the pile, T, was defined by:-

$$T = \sqrt[5]{\frac{E_p I_p}{n_h}} \qquad (2.18)$$

where n_h is the rate of increase of modulus k with depth. The charts for determining the coefficients A and B for the calculation of displacement, slope, bending moment, shear force and soil reaction were determined using finite difference methods by Matlock and Reese (1960). The charts for the calculation of displacement and bending moment are shown in figure 2.5 in which the A and B coefficients are related to a depth coefficient Z for various values of Z_{max}, where Z is equal to the depth z at any point divided by T (i.e. Z=x/T) and Z_{max} is equal to D/T.

Broms (1964b) developed a design formula for free-headed rigid piles, with a modulus of subgrade reaction constant with depth.

The lateral deflection at ground surface, y_0, is given by:

$$y_0 = \frac{4\,F\,[\,1 + 1.5\,(L/D)\,]}{k\,DI\,D} \tag{2.19}$$

where

F = lateral load

L = pulling height

k = modulus of subgrade reaction (force/length^2)

DI = diameter of pile

2.2.2.3 Czerniak's method

Czerniak (1957) derived a design formula for a rigid pile, in ground with a modulus of subgrade reaction proportional to depth, based on a pile pivot point. Figure 2.6 shows the geometry, the soil modulus and the pressure distributions along the rectangular pile. Dickin and Wei (1988) obtained a relationship between the moment, soil resistance and geometry for short circular pile in sand based on the Czerniak's method. The lateral load and the moment at ground level are given in terms of the soil modulus, horizontal deflection at ground level, pile depth and the distance of the point of rotation from the ground surface as;

$$F = \frac{w \, \Delta \, D}{6 \, a}(3a - 2D) \tag{2.20}$$

and

$$M = - \frac{w \, \Delta \, D^2}{12 \, a}(4a - 3D) \tag{2.21}$$

where

F = lateral load

w = the soil modulus at the level of the pile tip (in units of force/length^2)

Δ = horizontal deflection at ground level

a = the distance of the point of rotation from the ground surface

M = moment at ground level

Since M=FL, equations (2.20) and (2.21) give the following relation for depth of the pivot point

$$\frac{a}{D} = \frac{4\,L/D + 3}{6\,L/D + 4} \tag{2.22}$$

The relationship between a/D and L/D is plotted in figure 2.7. For any depth of pile D, it is clear that when pulling height is equal to zero, a/D is 3/4 and as the pulling height increases a/D approaches 2/3.

Combining equations (2.21) and (2.22) for a rectangular section pile the value of moment at ground level is obtained as;

$$M = \frac{w\,\Delta\,D^2}{24 + 18D/L} \tag{2.23}$$

From figure 2.6, the rotation θ of a free-head rigid pile at the ground surface may be expressed as $\theta=\Delta/a$. Hence combining equations (2.22) and (2.23), the value of moment at ground level, in terms of the rotation, may be obtained as;

$$M = \frac{w\,\theta\,D^3}{36 + 24\,D/L} \tag{2.24}$$

Hence the limit of overturning moment at large L for a prescribed displacement limit is given by;

$$M_{max} = \frac{w \Delta D^2}{24} \tag{2.25a}$$

or

$$M_{max} = \frac{w \theta D^3}{36} \tag{2.25b}$$

2.2.2.4 Stress-dependent modulus

Based on the equilibrium of a tetrahedron-shaped soil failure wedge under lateral load, Reese (1958) formulated an expression for the ultimate resistance of a laterally loaded pile in soft clay. The resulting ultimate resistance per unit length of pile consisted of three terms. The first indicated the resistance at ground surface, the second related to the increase in resistance with depth resulting from overburden pressure, and the third was a geometrically related restraint term. This method, which was then advanced by Matlock (1970) for soft clay and later extended by Reese and Welch (1975) for stiff clay, yielded non-linear predictions that approximate the actual behaviour of piles under lateral loading. Matlock (1970) found that the third term in Reese's expression did not agree with experimental observations and suggested an alternative approach based on p-y curves. The general procedure for obtaining a set of p-y curves at various depths along a pile in clay as proposed by Matlock (1970) and Reese and Welch (1975) was:

(i) From the results of triaxial compression tests on undisturbed samples, obtain the variation of undrained shear strength, the effective unit weight, γ, of the soil and the value of ε_{50}, the strain corresponding to one-half of maximum principal stress difference, $(\sigma_1 - \sigma_3)_{max}$ with depth.

(ii) Using the ε_{50} values, compute deflection y_{50} at one-half the ultimate soil reaction as

$$y_{50} = C_1\, b\, \epsilon_{50} \tag{2.26}$$

where

C_1 = an empirical constant relating pier deflection to the laboratory strain

and b = pile diameter

(iii) For a given depth, x, compute the ultimate soil resistance per unit length of pile, P_u, as

$$P_u = \left[3 + \frac{\gamma\, x}{c} + J\,\frac{x}{b} \right] c\, b \le 9\, c\, b \tag{2.27}$$

where

c = average undrained shear strength of soil from ground surface to depth x

and J = a constant which controls the depths at which P_u reaches 9cb for stiff soils

(iv) Compute points describing the P-y curve at depth x as

$$\frac{P}{P_u} = 0.5 \left[\frac{y}{y_{50}} \right]^n \tag{2.28}$$

where

P = soil resistance/unit length

y = deflection corresponding to P

n = an empirical constant

The values of parameters C_1, J and n for stiff clays proposed were 2.5, 0.5 and 1/4 respectively.

Vallabhan and Alikhanlou (1982) developed a discrete soil spring model for the analysis of short pier foundations in clay that were subjected to large lateral loads and overturning moments. In the model, the pier was assumed as a rigid structure and the displacements and rotations were considered to be small. The forces and resulting deformations of the pier-soil system are shown in figure 2.8. The proposed model to simulate these forces and displacements consisted of several discrete soil springs as shown in figure 2.9. Springs representing the bottom resisting moment, bottom friction, bottom vertical reaction, and side skin friction were added in addition to the lateral soil springs. The equations were developed on the assumption that the system was linear and elastic, and then they were extended to include non-linear behaviour of the soil springs. Results of analyses using the model were compared with field test data obtained by Bhushan et al. (1979) and Ismael and Klym (1978). The following conclusions were made from the study;

1. The load-displacement response of the pier obtained using only the lateral springs, neglecting the skin friction and the bottom resistances, showed poor agreement with the field test data.

2. After the addition of the resisting forces at the bottom and on the sides of the pier, the results of the analysis compared fairly well with the field test data.

3. The addition of a bell to the bottom of the pier increased the effect of the bottom resisting moment and the frictional force.

4. In a few cases, the predicted deflections of the piers were not as close to the actual measured deflections as was desired.

Yokoyama (1985) presented a simple and practical design method to analyze a laterally loaded pile by using a non-linear differential equation of the second order. The equation was derived as an approximate form of a non-linear differential equation of the fourth order. The method avoided the use of lengthy iterative procedures and was confirmed to be valid by comparing field test results with the numerical predictions.

2.2.3 Continuum Models

2.2.3.1 The Pile-Elastic Continuum Interaction Method

Analyses in which the pile or drilled pier is embedded in an elastic continuum having a constant modulus of elasticity, E, with depth or in some cases increasing linearly with depth were used by Douglas and Davis (1964) for buried footings. The method was then extended by Poulos (1971) to evaluate the interaction behaviour between a pile and a soil when the pile is subjected to horizontal load and moment. The soil surrounding the pile is modelled as an ideal, elastic homogeneous, isotropic mass, having constant elastic parameters E_s and ν_s. Soil displacements are evaluated from the Mindlin equation for horizontal displacement due to a horizontal load within a semi-infinite mass and the pile displacements are obtained from the equation of flexure of a thin strip. An iterative solution procedure is used until, the horizontal displacements of the soil and of the pile are equal along the length of the pile.

Pise (1984) carried out a theoretical study on a free-head pile subjected to a lateral load and moment at the ground surface. He assumed that the pile was embedded in a two layer soil system. Lateral pile head displacement, rotation and moment coefficients were presented in dimensionless terms thorough graphs. It was concluded that the results provided guidelines to predict the lateral response of free-head piles.

Sun an Pires (1993) proposed a simple approach for the analysis of pile-soil interaction under static and dynamic lateral loadings. The pile was treated as a shear beam and the soil was assumed to be a linear elastic material. The solutions for the static case were given as the limiting case when the circular frequency was equal to zero (ω=0). For this case, the pile head displacements were compared with the corresponding displacements obtained by Poulos's (1971a) method for a fixed-head pile and found to be in close agreement.

2.2.3.2 The Boundary Element Method

The boundary element method is a numerical technique that has been developed in recent years in the shadows of the finite difference and finite element methods. The method has been used for linear analyses (Banerjee and Driscoll, 1976) and also for non-linear analyses (Banerjee and Davies, 1978 and Wood, 1979) of laterally loaded piles. The analysis of a pile embedded in homogeneous soil by means of a boundary element formulation involves the integration of an appropriate elementary point force solution for the soil medium over the discretized surface elements of the pile-soil interface. The equations relating the displacements and surface tractions for the soil domain are then coupled with the compressibility and flexibility equations of the pile to generate the final system of equations (using the notation of Banerjee and Davies (1978)) as

$$[F_{be}]\ \{\Phi\} = \{B_{be}\} \tag{2.29}$$

where

$[F_{be}]$ = $(2p_{be} + q_{be})$ square matrix of coefficients

$\{\Phi\}$ = vector of surface tractions at the pile-soil interface

$\{B_{be}\}$ = vector of displacement boundary conditions

p_{be} = number of shaft segments

q_{be} = number of base elements

The final solution, relating the axial load P, the horizontal load H and the moment M at the pile head to the vertical displacement w, the horizontal displacement u and the rotation θ, is given by the global pile head flexibility equations

$$\begin{Bmatrix} w \\ u \\ \theta \end{Bmatrix} = \begin{bmatrix} f_{11} & f_{12} & f_{13} \\ f_{21} & f_{22} & f_{23} \\ f_{31} & f_{32} & f_{33} \end{bmatrix} \begin{Bmatrix} P \\ H \\ M \end{Bmatrix} \qquad (2.30)$$

where $f_{12} = f_{21}$, $f_{13} = f_{31}$ and $f_{23} = f_{32}$ and for vertical piles, $f_{12} = f_{13} = f_{21} = f_{31} = 0$. This method of analysis can be easily extended to deal with nonhomogeneous soils if a suitable point force solution for the problem is available. A number of computer programmes have been developed using this method such as PGROUP (Banerjee and Driscol (1975)) and DPILES (Budhu and Davies (1988)) for homogeneous soils and DEFPIG (Poulos (1979)) for nonhomogeneous soils.

In the PGROUP program, the soil was modelled as a homogeneous, linear elastic material. Banerjee and Davies (1980) upgraded this program to include a soil model with a linearly increasing modulus with depth and described a non-linear method of analysis in which volume cells were introduced into the soil domain to handle soil yielding.

The DEFPIG program was based on a simplified boundary element approach for single pile analyses and the calculation of the interaction factors for two equally loaded identical piles. Soil non-linearity was modelled by limiting the stresses at the pile-soil interface, while soil inhomogeneity was approximated with an averaging procedure using the point-load solutions of Mindlin (1936).

Davies and Budhu (1986) studied the non-linear load-deformation response of laterally loaded single piles embedded in heavily overconsolidated clays. The non-linear response of piles to lateral loading was obtained by coupling the equations describing the non-linear load-deformation behaviour of the soil with the equations describing the flexure of the pile. They found good agreement with the results of full-scale tests on laterally loaded piles and concluded that their method of analysis was useful in practice.

2.2.3.3 The Finite Element Method

In soil mechanics and foundation engineering one of the most rigorous numerical methods of solution is the finite element method (FEM). This now well established method, see for example Zienkiewicz (1977), King (1977), Desai and Abel (1972), Gallagher (1975), Martin and Carey (1973), Huebner (1975), Hinton and Owen (1979), Bathe (1982) and Burnett (1987), idealises the area to be analyzed as an assemblage of discrete elements interconnected at their nodal points. The FEM can permit realistic three-dimensional effects and computation of stress and deformations in and around the piles. It is also possible to study progressive development of stresses and deformations leading to demarcation of failure zones. The method requires the use of a large computer for the solution of a given problem. Although the use of three-dimensional finite element analysis is relatively expensive, with the introduction of the new generation of computers and development of efficient solving and data storage routines, its use has become fairly common. The application of the method to many different problems in soil mechanics including structure/soil interaction, slopes, seepage and pile foundations has been illustrated by King (1984).

(i) Beam - Spring Finite Element Method

Desai and Kuppusamy (1980) carried out a simple F.E. analysis in which they used beam bending elements for the structure and replaced the three-dimensional soil by non-linear springs in three coordinate directions as shown in figure 2.10. An incremental iterative procedure was used to simulate non-linear behaviour of the soil. Some construction sequences such as excavation and tie-bars were also considered. They compared numerical prediction with closed form solutions, laboratory and/or field observations and reported good agreement.

(ii) 2-D Continuum Finite Element Method

A commonly used simplification for axisymmetric structures under non-axisymmetric loads is to express the circumferential displacements as Fourier series so that the analysis becomes two-dimensional. This method was first developed by Wilson (1965) and was used for studying the problem of circular wells subjected to lateral loading by Desai and Chandrasekaran (1980). The well and soil were discretized using eight noded isoparametric finite elements and the interface between soil and well by six noded interface elements. They carried out a parametric study to obtain the influence factors for the displacement and rotation of a well in a homogeneous, isotropic and elastic soil. For horizontal and moment loading, the variations of the influence factors for displacement and rotation with the ratios of the depth of embedment to the diameter of the well and the total thickness of the soil stratum to the depth of embedment were presented.

This approach was also used by Chandrasekaran and King (1982) for analysing the behaviour of laterally loaded piles embedded in an elastic continuum. The computer program was written to allow consideration of arbitrary inhomogeneity in the soil deposit and also variable flexural rigidity along the length of piles. Free-head and fixed-head conditions were considered in the analysis. They evaluated non-dimensional influence coefficients for displacement and slope at the pile head and bending moment variations along the length for long piles for a homogeneous soil medium and for a medium in which the soil modulus was proportional to depth. They concluded that the influence of Poisson's ratio on the behaviour of laterally loaded piles was not significant. They also carried out two experiments on a model pile embedded in remoulded saturated clay in the centrifuge. Variations of bending moment and lateral deflection along the length of pile were presented together with the results obtained from the finite element analysis. The results were in close agreement.

A simplified approach to the finite element analysis of laterally loaded piles in a layered elastic medium was described by Verruijt and Kooijman (1989). It was assumed that horizontal displacements dominated the displacement field of the soil around the pile, so that a quasi-three-dimensional analysis was obtained. The pile was treated as a beam on elastic springs and two dimensional analyses of soil layers were carried out. The behaviour of pile and soil layers were coupled to satisfy equilibrium and compatibility conditions. The model was verified for two types of soil, namely a homogeneous elastic material and a medium having a modulus of elasticity proportional to depth, by comparison with results given by Poulos (1971a), Banerjee and Davies (1978) and Randolph (1981).

(iii) 3-D Continuum Finite Element Method

Selby and Arta (1991) developed a linear elastic finite element model for comparisons with a series of field tests on box-section piles under lateral loading. The shaft of each pile was modelled by 3-D prism elements occupying the full cross-section of the box section, but of reduced modulus so that the element was of equivalent stiffness to the webs of a box section. The surrounding soil was modelled by a mesh of 3-D prisms, of increasing modulus with depth in a sand layer or of uniform modulus in a clay layer. Horizontal loading was applied to the model by an imposed horizontal displacement of 20 mm. They compared the results for a single pile under horizontal load with published deflections and pile shaft moments given by Poulos (1971a). Results of the comparisons showed that fair agreement was obtained, the maximum difference being 33 %.

Trochanis et al. (1991a,b) used a three-dimensional finite element model to examine the effect of non-linear soil behaviour on the axial and lateral response of piles to monotonic and cyclic loading. The piles and the soil were modelled by quadratic 27-node elements (nine nodes per face) selected from the element library of ABAQUS, the commercial finite element package used for the work. The interface elements were quadratic 18-node elements comprising two nine-node surfaces compatible with the adjacent solid elements. The pile elements were assumed to remain elastic at all times, while the soil was idealized as either a linear elastic material or a Drucker-Prager elastoplastic material. The validity of the model was tested by comparing some of its results with those from previous studies. When subjected to lateral loads, the pile separated from the surrounding soil which caused a marked increase in lateral displacements. It was concluded that when subjected to combined axial and lateral loading, the axial capacity might actually increase, while the effect of a constant axial load on the response to cyclic lateral load was not significant.

Because of non-linearity of the stress-strain soil behaviour, pile response to lateral loading is also non-linear. Although finite element programs are generally formulated for linear behaviour there are many techniques available to simulate non-linear analyses, including the incremental method, the iterative method and the mixed method. In the iterative procedure the same change in external loading is repeatedly analyzed until stress and strain levels are compatible. In the incremental procedure the change in loading is analyzed in a series of steps, or increments while the stiffness changes according to stress level. By the mixed procedure the load is applied in small increments but iterations are performed after each load increment. The incremental method has great potential for use in geotechnical and structural engineering (Edwards 1979).

As seen in this section, the application of the finite element method to pile foundations has been described by several investigators. However, there is little published data which may be used to establish a rationale for the actual values of soil properties (such as shear modulus and its variation) which should be input into these analyses.

2.3 Additional Experimental Studies

A considerable number of model studies, as well as some full scale tests, have been carried out on laterally loaded piles and rigid piers over a large range of geometric and soil conditions. Prototype tests are not often carried out because of the high cost of materials and labour, and because ground conditions are difficult to control and quantify.

2.3.1 Field tests

Some of the first full scale field and small scale laboratory tests on the stability of non-uniform posts subjected to lateral loads in a granular soil and a silty clay were carried out by Shilts et al. (1948). They found that the location of the point of rotation was at that depth below which there was 0.324 of the vertical cross-sectional area of the embedded portion and that square sections had the same resistance to movement as round sections with a diameter equal to the diagonal of the square.

An extensive series of full scale tests involving gantry foundations carried out by Ramelot and Vandeperre (1950) was reported by the UIC/ORE (1957). Tests were performed along railway tracks or in the immediate proximity of the track. Loading was carried out until the failure of a foundation occurred. Two methods of applying the load were used, as shown in figure 2.11. With the first method, using a hand winch, the tests were completed in approximately fifteen minutes (fast tests) while with the second method, using dead weight, they were completed after several weeks or months (slow tests). Both prismatic and circular foundations were tested. The tests involved a large range of soils, e.g. clay, mixed gravel and sand. A design formula proposed by the UIC/ORE based on these tests is presented in section 2.2.1.1.

Matlock (1970) performed lateral load tests employing a steel pipe pile 325 mm in diameter and 12.8 m in length. It was driven into two clays near Lake Austin that had shear strengths of about 38 and 14 kPa. He analyzed the data and obtained experimental p-y curves. He recommended a design procedure using p-y curves for soft clay for short term static loading. The p-y curves and Matlock's procedure are explained in section 2.2.2.

Reese and Welch (1975) presented the results of a full scale instrumented lateral load test on a 0.76 m diameter and 13 m long pier loaded to a maximum load of 445 kN in stiff clay. The deflection of the top of the pier was found to be a non-linear function of load. Measured values of moment and deflection were compared with the computed values based on the p-y curve method and the overall agreement was good.

Bartolomey (1977) performed tests on single piles and a group of piles embedded in clay. He used prestressed concrete piles of 30 cm square section and 5 to 12 m long. It was found that piles subjected to both vertical and lateral load showed a 15 to 30 % higher resistance to lateral load than one which was subjected to only lateral load. It was also reported that cracks were observed at some depth below the ground level in piles subjected to lateral load only.

Ismael and Klym (1979) carried out full-scale tests on two instrumented piers in clay near Hamilton, Ontario. The first pier was 1.5 m in diameter and 12.6 m deep and the second was a 5.2 m deep belled pier with a 1.5 m diameter shaft and a 3 m diameter bell. The testing program consisted of uplift and lateral load tests. The soil profile at the site consisted of a firm to stiff brown fissured silty clay to a depth of about 2.4 m. This was underlain by a grey silty clay. The lateral loads were applied simultaneously to both piers and lateral displacements were recorded by dial gauges after each 45 kN load increment. At 169 kN, unloading/reloading cycles were carried out. The loads were then applied in 89 kN increments to a maximums of approximately 710 kN. The tests were analyzed using both the elastic subgrade theory and a non-linear method of analysis (Matlock (1970) and Reese and Welch (1975)), which essentially incorporated the subgrade theory and the non-linear response of soil behaviour. The elastic subgrade theory yielded conservative estimates of lateral deflections. The non-linear method of analysis yielded lateral deflections that were in good agreement with the actual behaviour of the footing under lateral load. Further, they concluded that the point of rotation lay at 71% of the depth for both piers with no apparent effect caused by the presence of the bell.

Bhushan et al. (1979) carried out field tests on full-sized instrumented drilled piers in hard overconsolidated clays to investigate their lateral response. Twelve piers with diameters between 0.61m and 1.22 m and lengths between 2.74 m to 6.71 m were tested. Eight of the piers were constructed in level ground and four were tested on slopes ranging from 20 to 50 degrees. Lateral loads up to 2670 kN were applied at a point 0.23 m above the ground surface. A computer program called COM622, based on the p-y curve method, was used to obtain theoretical results. It was suggested that drilled piers in hard clays can be designed to carry high lateral loads. The deflections computed from the program were generally larger than those observed especially at loads greater than one third of the ultimate load.

2.3.2 Conventional model tests

Bearing capacity, lateral soil pressure distribution on the pile shaft, and pile cap displacements for rigid piles jacked into clay and subjected to eccentric and inclined load have been reported by Meyerhof and Sastry (1985) and Sastry and Meyerhof (1986). Similar studies under central inclined loads were presented for vertical piles and pile groups in clay by Meyerhof (1981), Meyerhof and Yalcin (1984), Sastry et al. (1986) and in sand by Meyerhof et al. (1983).

Sastry and Meyerhof (1987) carried out model tests on an instrumented single rigid bored piles subjected to pure moment and horizontal load in saturated clay to investigate the lateral soil pressure distribution, pile capacity, and displacements. They also studied the influence of method of pile installation on the parameters mentioned by comparing the behaviour of bored piles with that of jacked piles. A hollow steel model pile, 1100 mm long, split longitudinally with an outside diameter of 74 mm and a wall thickness of 7 mm was employed as rigid pile foundation. It was instrumented with 18 pressure transducers to measure the lateral soil pressures and with a load cell to measure the base resistance. Two types of test were conducted. In the first, the pile was subjected to a pure moment caused by two equal and opposite vertical forces applied to a horizontal arm fixed to the top of the pile. In the second, a horizontal force was applied at ground level. It was concluded that, the net lateral soil pressure distribution at failure along the pile shaft and the pile capacity were unaffected by the method of installation. However the displacements of a bored pile were in general 1.5-3 times those of a jacked pile. It was found that the horizontal displacement and rotation of a bored pile could be closely estimated at any load level from elastic theory by using a soil modulus back-calculated for the appropriate load level from the results of unconfined compression tests.

Georgiadis et al. (1992) conducted a series of model tests to study pile response to cyclic lateral loads in a bed of soft, medium-plasticity, clay. Bending moments were monitored with strain gauges placed along the pile. Six lateral load tests were performed on 500 mm long aluminium, closed - ended, piles of 19 mm outside diameter and 1.5 mm wall thickness. The horizontal loads applied to the pile head at ground level were 38, 92, 146 and 202 N and were cycled ten times each. Average values (from the six tests) were used to interpret the results. Load - horizontal displacement and load - rotation relationships of the pile head were plotted. For all loading cycles similar relationships, demonstrating the non-linearity of the pile response even for low load levels, were obtained. They showed that cyclic lateral load had significant effect on the measured pile head lateral displacement and rotation. Correspondingly, the maximum bending moment measured at cycle 10 was about 20 percent higher than the one measured during the first cycle. Another important feature of the results was that the depth at which the bending moment reached its maximum value increased with increasing lateral load F, from 80 mm for F=38 N to 140 mm for F=202 N. Based on the measured pile response, a relationship was developed between the soil resistance and the lateral displacement. This relationship was incorporated into a numerical analysis to predict lateral pile response by treating the pile as an elastic beam on non-linear springs. They compared lateral load - pile head displacement and bending moment distribution along the depth at cycle 1 and 10 with the results determined using the p-y curve method of Matlock (1970) and Reese and Welch (1975). They concluded that measured pile head response was predicted fairly accurately for static loading but that for the tenth load cycle the prediction underestimated the response by more than 50%. Further, the difference between measured bending moments and those predicted was less than the difference in the corresponding pile head displacements, by an order of 10%. However the difference in bending moments was quite large at depths below the point where the maximum bending moment occurred.

2.3.3 <u>Centrifuge model testing</u>

The main purpose of using a centrifuge is to raise the overall level of stresses in the soil to that appropriate in field situations. Centrifuge model testing method has been widely accepted and has received widespread attention over the past sixty years by many researchers.

2.3.3.1 Background to the Centrifuge Modelling

Centrifugal testing was first suggested by Phillips in 1869 (Craig, 1989a) for testing models of a metal bridge for spanning the British Channel. However, practical use of the centrifuge was not seen until the 1930's when both Bucky (1931) in the USA and Pokrovsky (1933) and Davidenkov (1933) in the USSR began to use them. The first publication in mainstream geotechnical literature was by Pokrovsky and Fedorov (1936) at the First International Conference on Soil Mechanics and Foundation

Engineering (Craig, 1989b) in 1936. In the USA Bucky continued centrifuge modelling at the University of Columbia from 1931 to 1949 (Cheney, 1988). Following those initial studies, centrifugal modelling was accepted as the most reliable model testing method in soil mechanics and foundation engineering by many research workers in different countries and since then a lot of centrifuge centres have been constructed with a wide range of machine capacities and acceleration levels. Centrifuge research activities and/or literature from Japan, the USA, France, Denmark, the USSR, the United Kingdom to name a few were presented in the discussion session at the Eleventh International Conference on Soil Mechanics and Foundation Engineering in San Fransisco in August 1985. Some of those papers were published by Craig et al. (1988).

In the UK, the method was introduced by Schofield in the early 1960's and the first specialist geotechnical centrifuge was constructed at the University of Manchester Institute of Science and Technology (UMIST), in 1969 (Basset and Craig (1988)). Now there are six geotechnical centrifuges within the UK. There is a medium sized centrifuge in the University of Liverpool in use since 1978. A more complete description of the centrifuge used in this study is given in section 5.3 in Chapter 5.

The importance of centrifuge modelling of pile foundations has been discussed by many workers, e.g. Scott (1981), Craig (1985, 1989b). The application of centrifuge techniques for modelling pile foundations and results of some of the recent studies were reported by Craig (1988).

Centrifuge model testing of earth structures has not only received attention as a research tool, but also been recognised as a teaching aid in geotechnology. Craig (1988) reported that the use of a small centrifuge in a teaching laboratory provided a cheap and simple means of demonstrating the influence of gravity on earth structures in a dramatic manner. In the particular area of slope stability it provides a means of demonstrating the mechanics of failure, which would otherwise be unseen in the laboratory.

2.3.3.2 Centrifuge model tests

A series of nine model pile tests were carried out at the Cambridge University geotechnical centrifuge by Hamilton and Phillips (1991). The tests were conducted in fine china clay with a liquid limit of 69% and a plasticity index of 31%. Fixed-headed model piles with prototype geometries of 0.65 m to 2.45 m in diameter and 5.67 m to 23.23 m in length were tested under lateral load. In the tests the machine was operated between 49.3 g to 93.7 g. Soil resistance behaviour based on test results for static loading were compared with the results predicted by Matlock (1970), and the results of modelling-of-models tests were presented. The good agreement between pile head load-displacement behaviour and the derived p-y curves from tests indicated that modelling of models was successful. Results for monotonically loaded piles were shown to agree well with those predicted by established methods of analysis. It was concluded that the geotechnical centrifuge offered an economical and practical alternative to large scale field tests to determine the behaviour of piles subjected to cyclic, and large displacement, lateral loading.

2.4 Conclusion

As stated in this brief literature review, considerable research has been carried out on the ultimate load capacity of laterally loaded piles. Most of the studies, however, were on long piles subjected to large lateral loads and small moments. In this study, in order to understand the moment carrying capacity of short rigid piers more clearly, a comprehensive investigation including conventional and centrifugal modelling and numerical studies using the finite element method has been carried out.

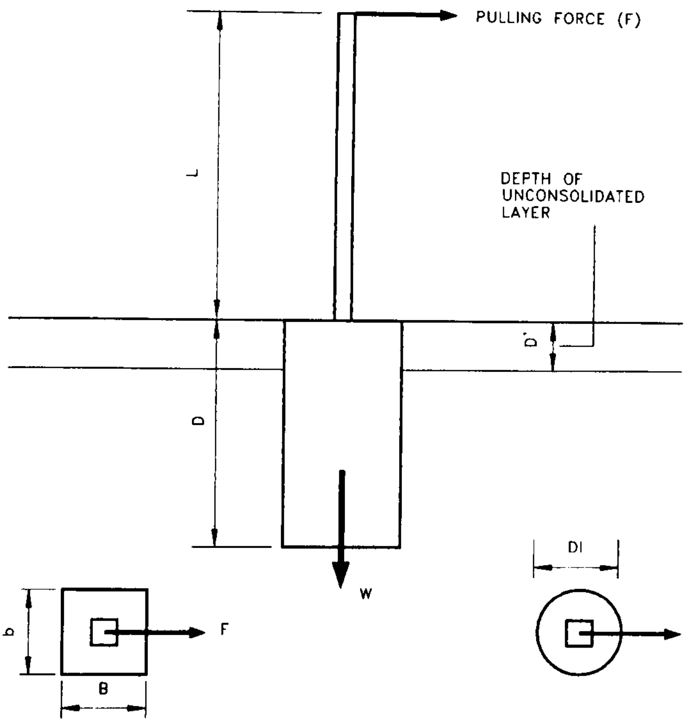

Figure 2.1 Geometric Configuration (UIC/ORE).

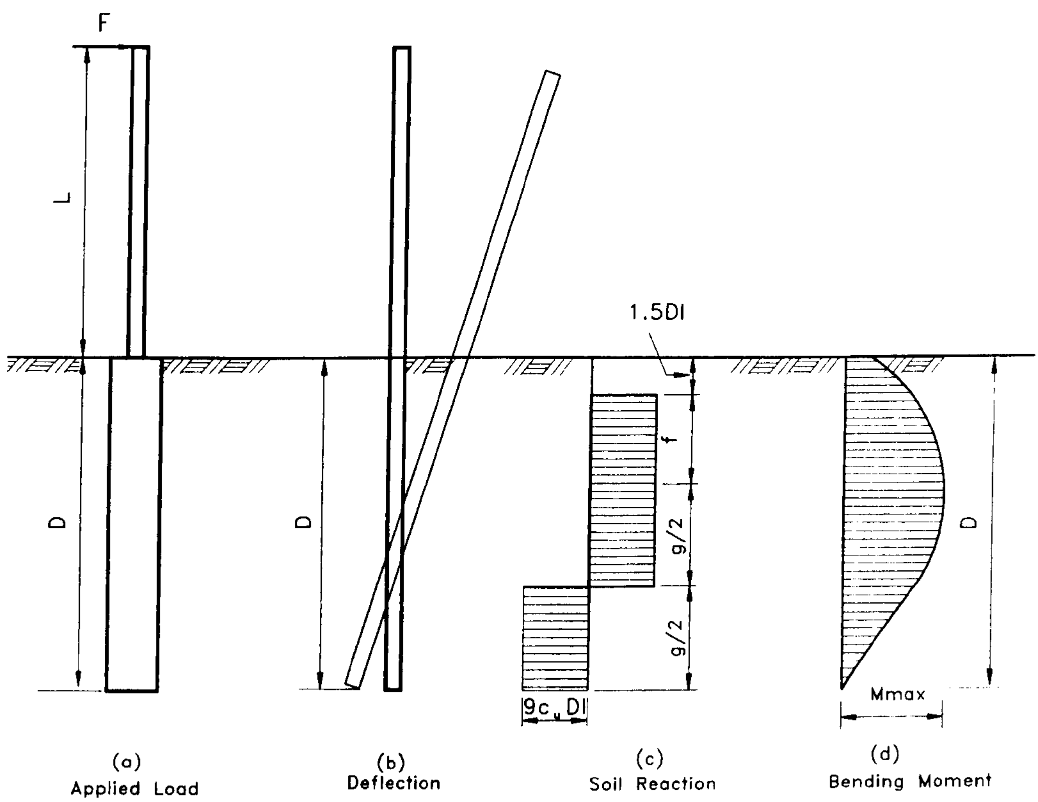

Figure 2.2 Failure Mode for Short Pile in Broms' Analysis.

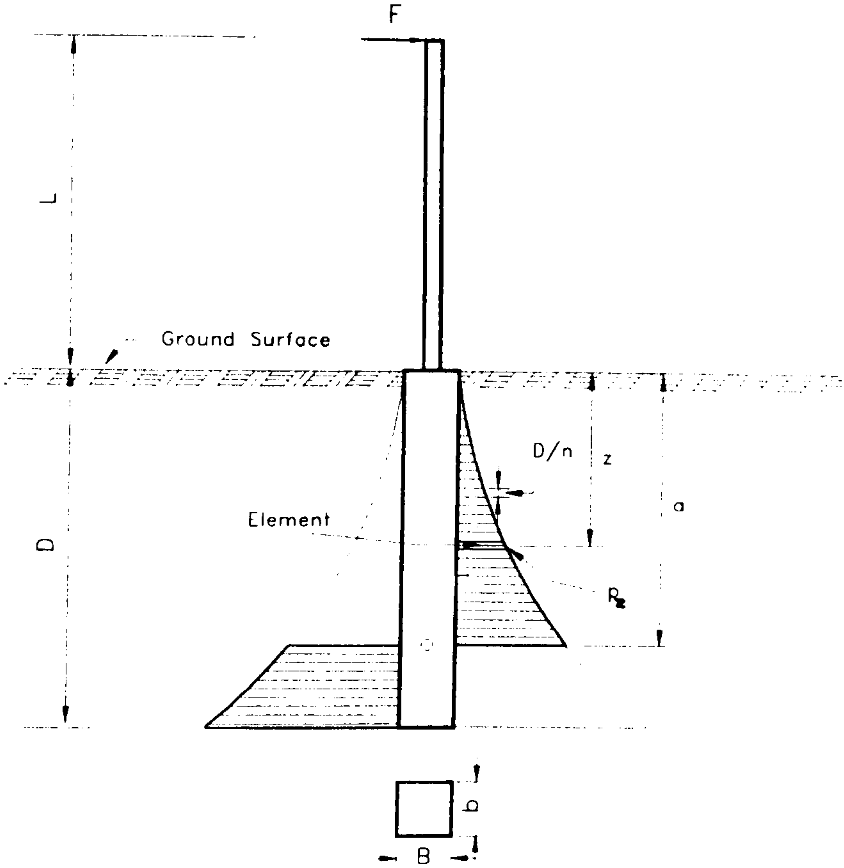

Figure 2.3 Soil Reactions in Brinch-Hansen's Formulae.

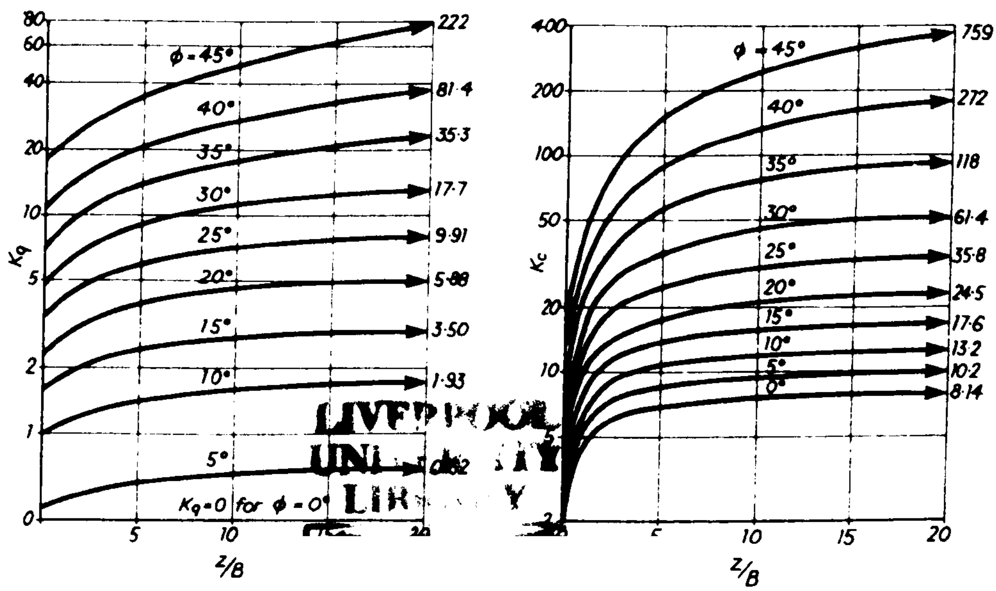

Figure 2.4 Brinch-Hansen's Coefficients K_q and K_c.

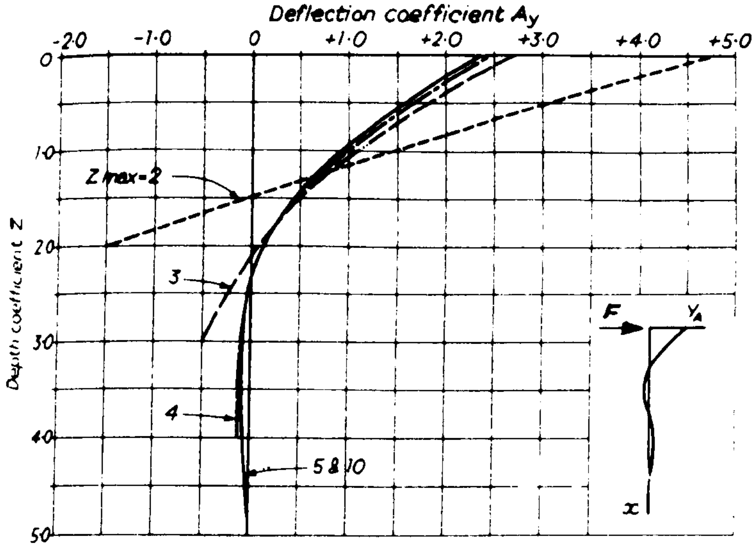

Coefficients for deflection

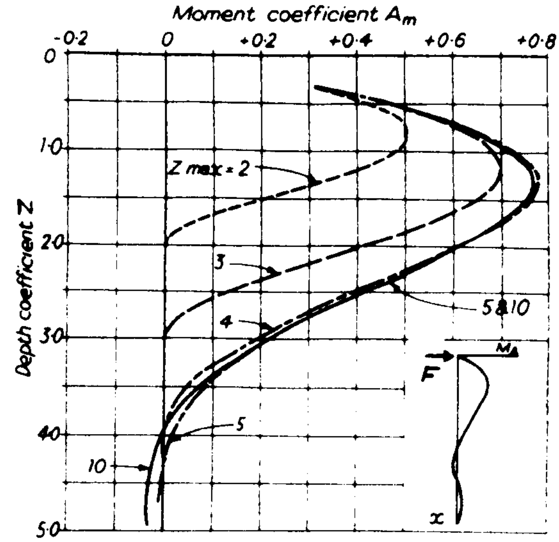

Coefficients for bending moment

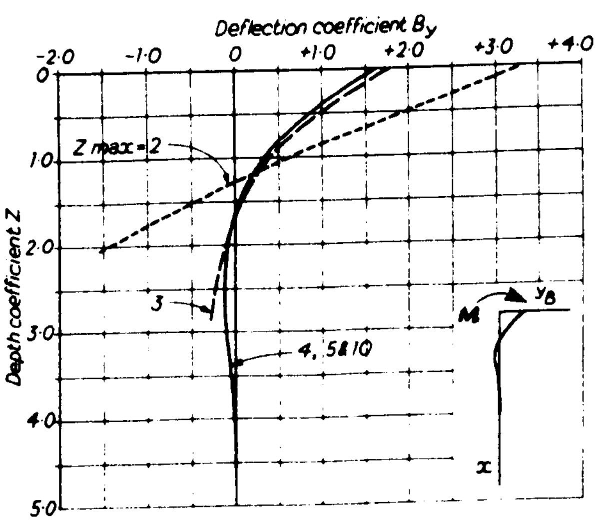

Coefficients for deflection

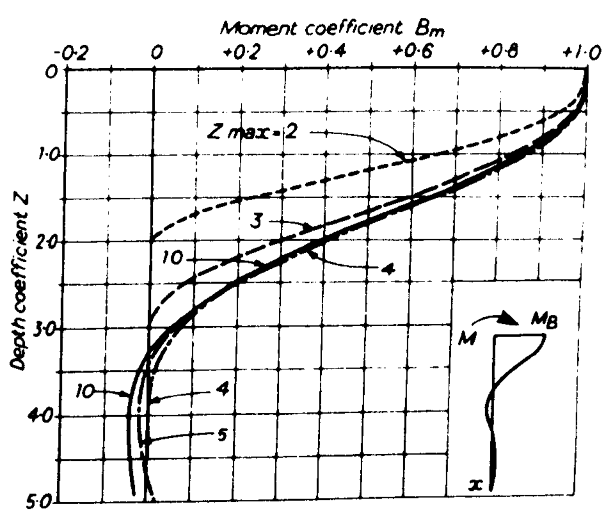

Coefficients for bending moment

Figure 2.5 Coefficients for Laterally Loaded Free-Headed Piles in Soil with Linearly Increasing Modulus (Matlock and Reese (1960)).

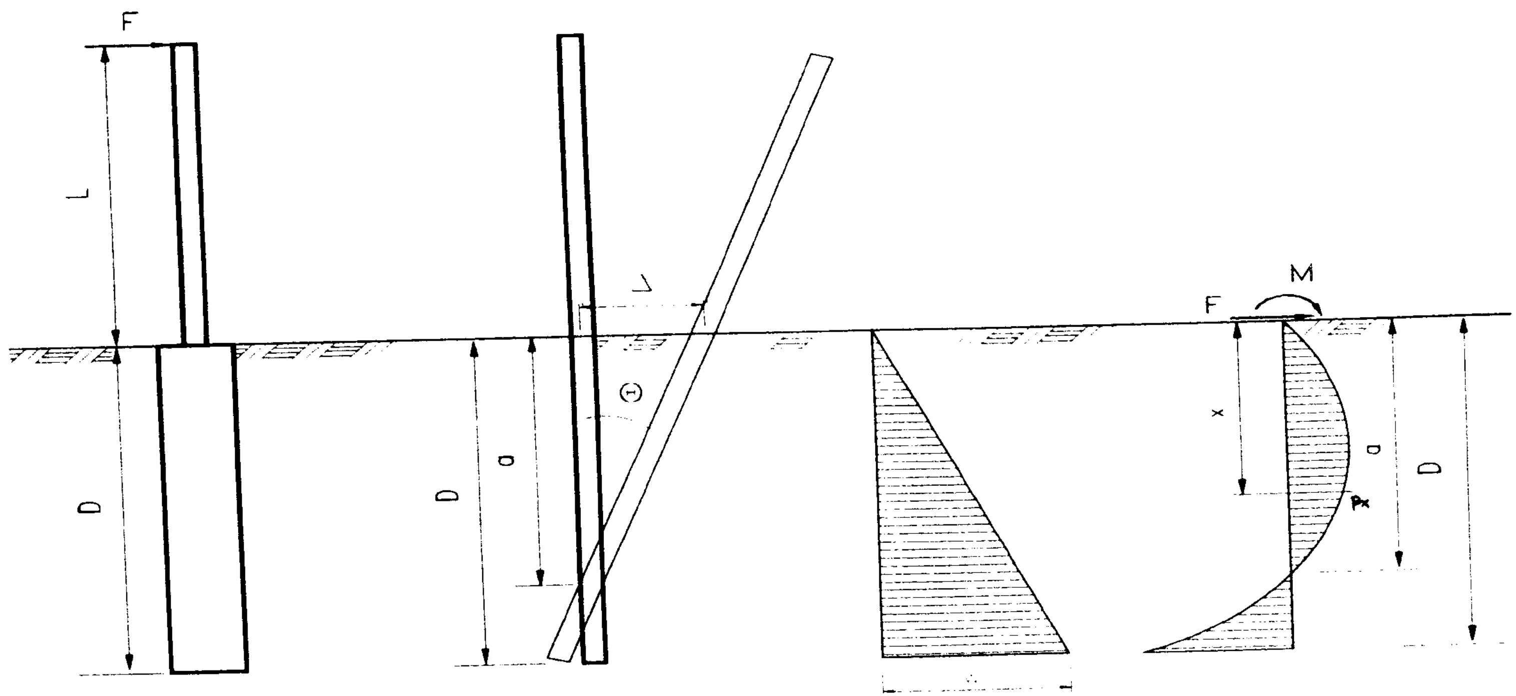

(a) Applied Load

(b) Pile Rotation

(c) Soil Modulus

(d) Pressure Diagram

Figure 2.6 Applied Load and Resistance of Pile in Czerniak's Method.

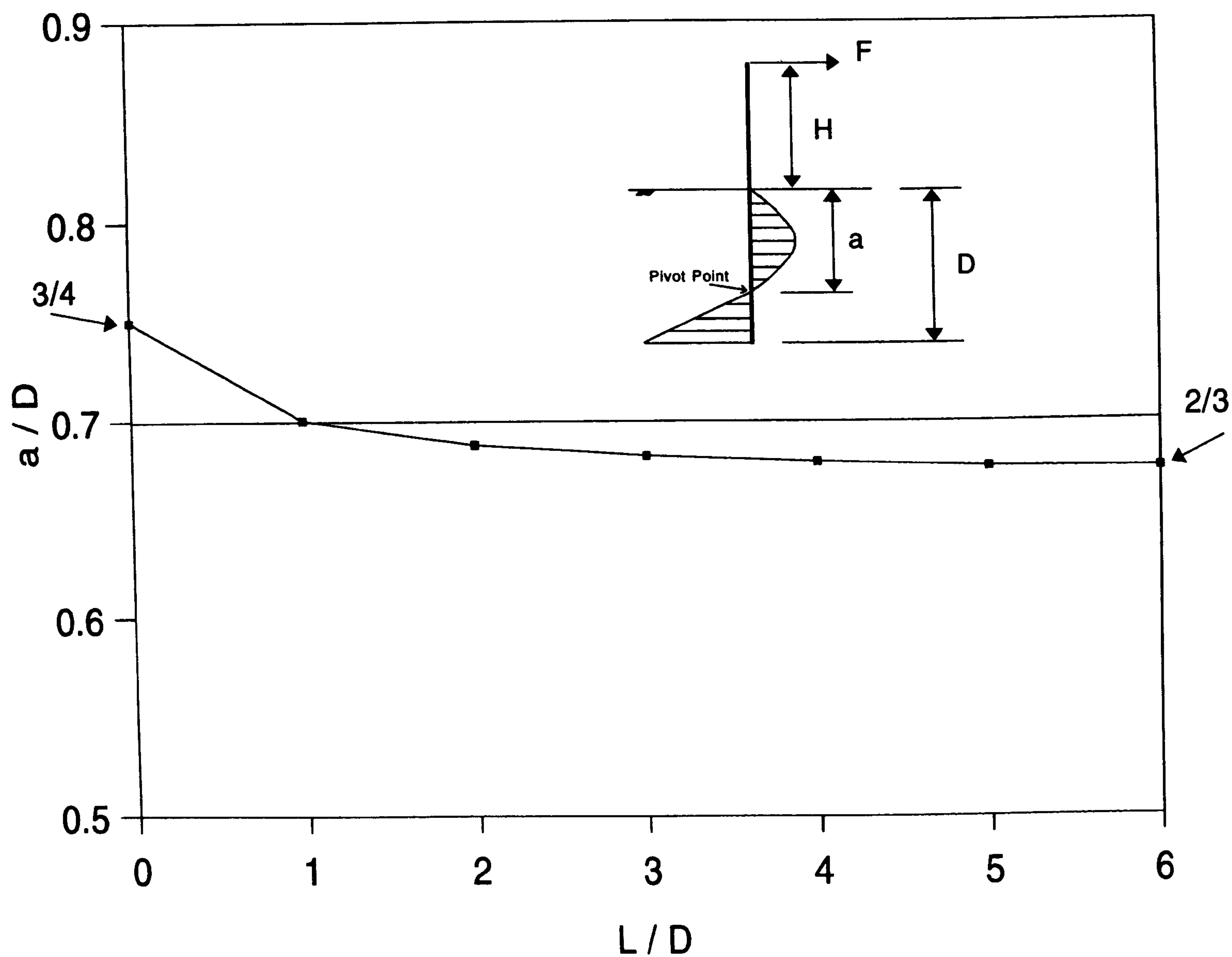

Figure 2.7 Effect of Pulling Height L on the Location of Pivot Point a.

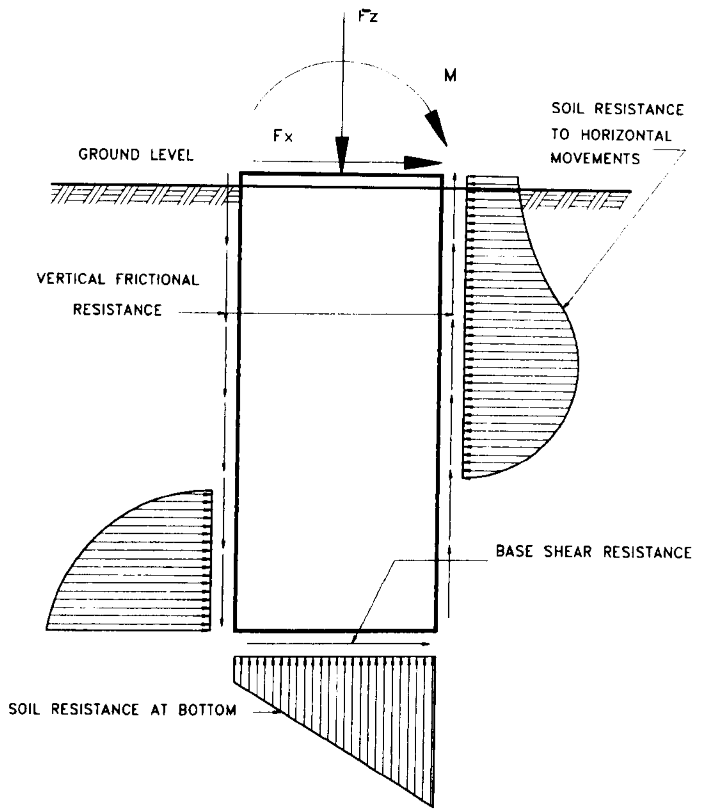

Figure 2.8 Forces Acting on the Pier (Vallabhan and Alikhanlou (1982)).

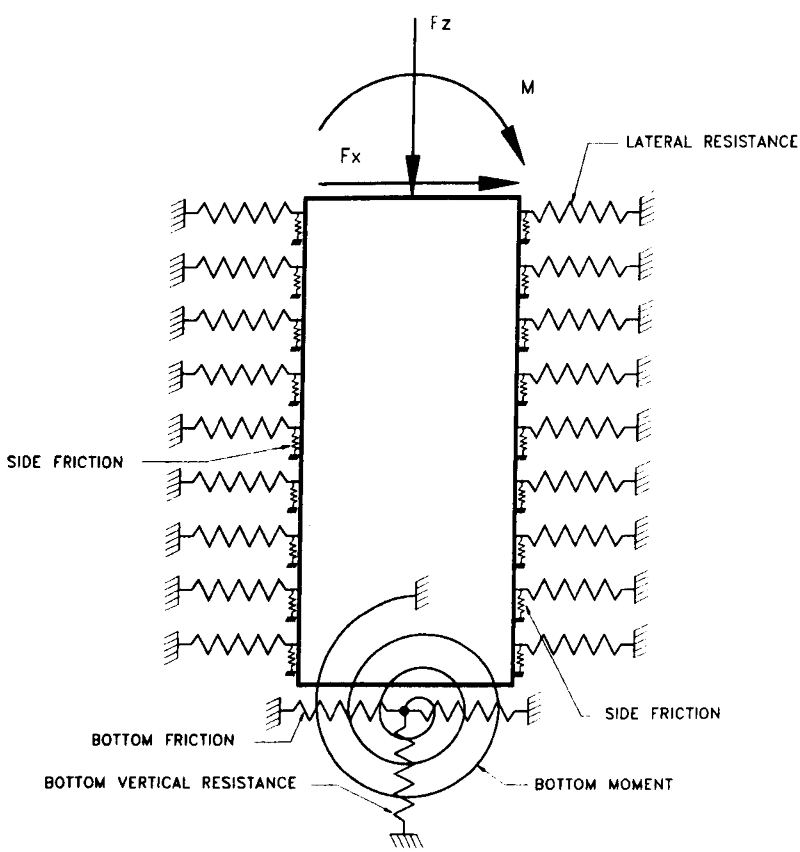

Figure 2.9 Vallabhan and Alikhanlou's (1982) Discrete Model.

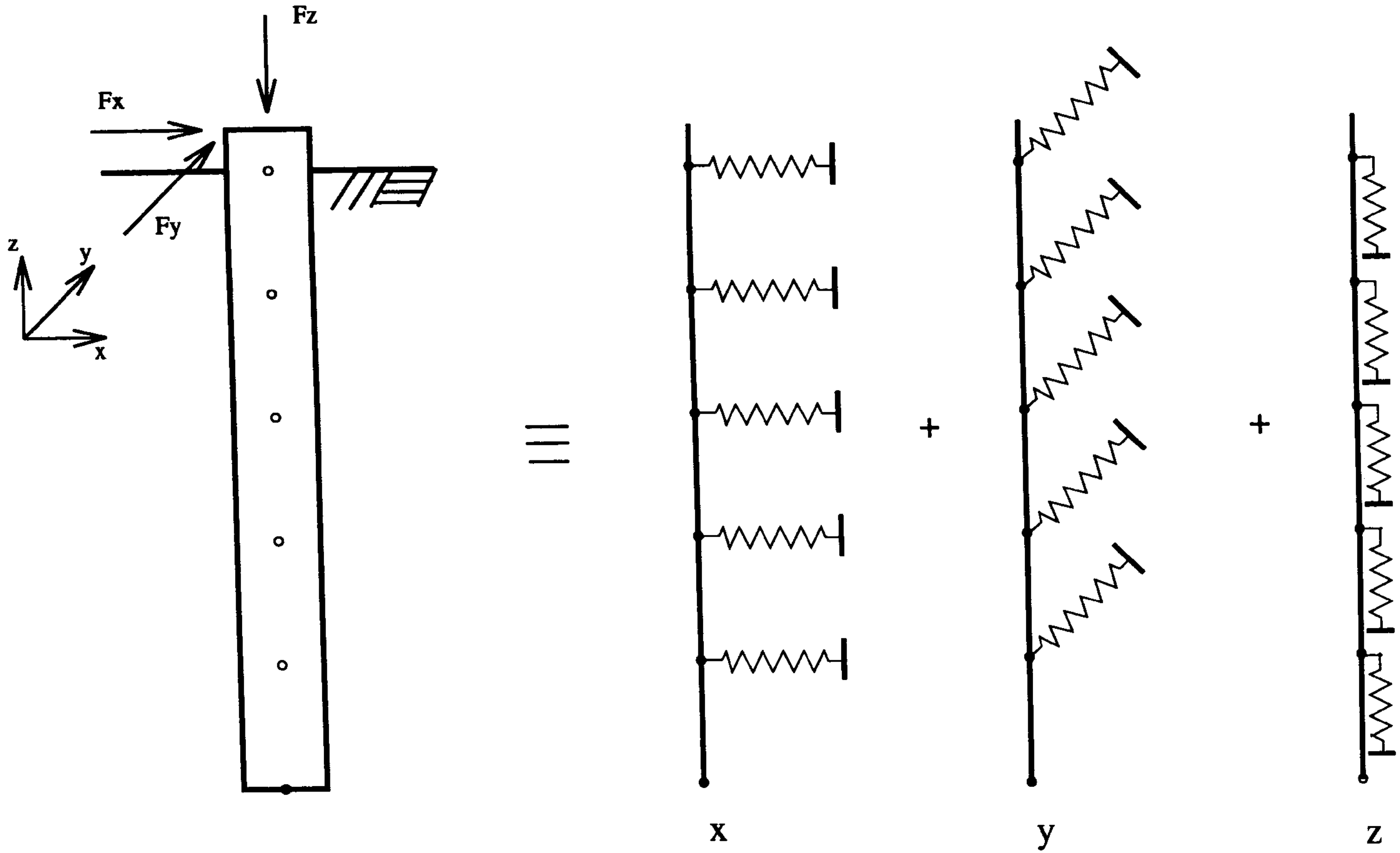

Figure 2.10 Soil Responses in x, y and z Directions (Desai and Kuppusamy (1980)).

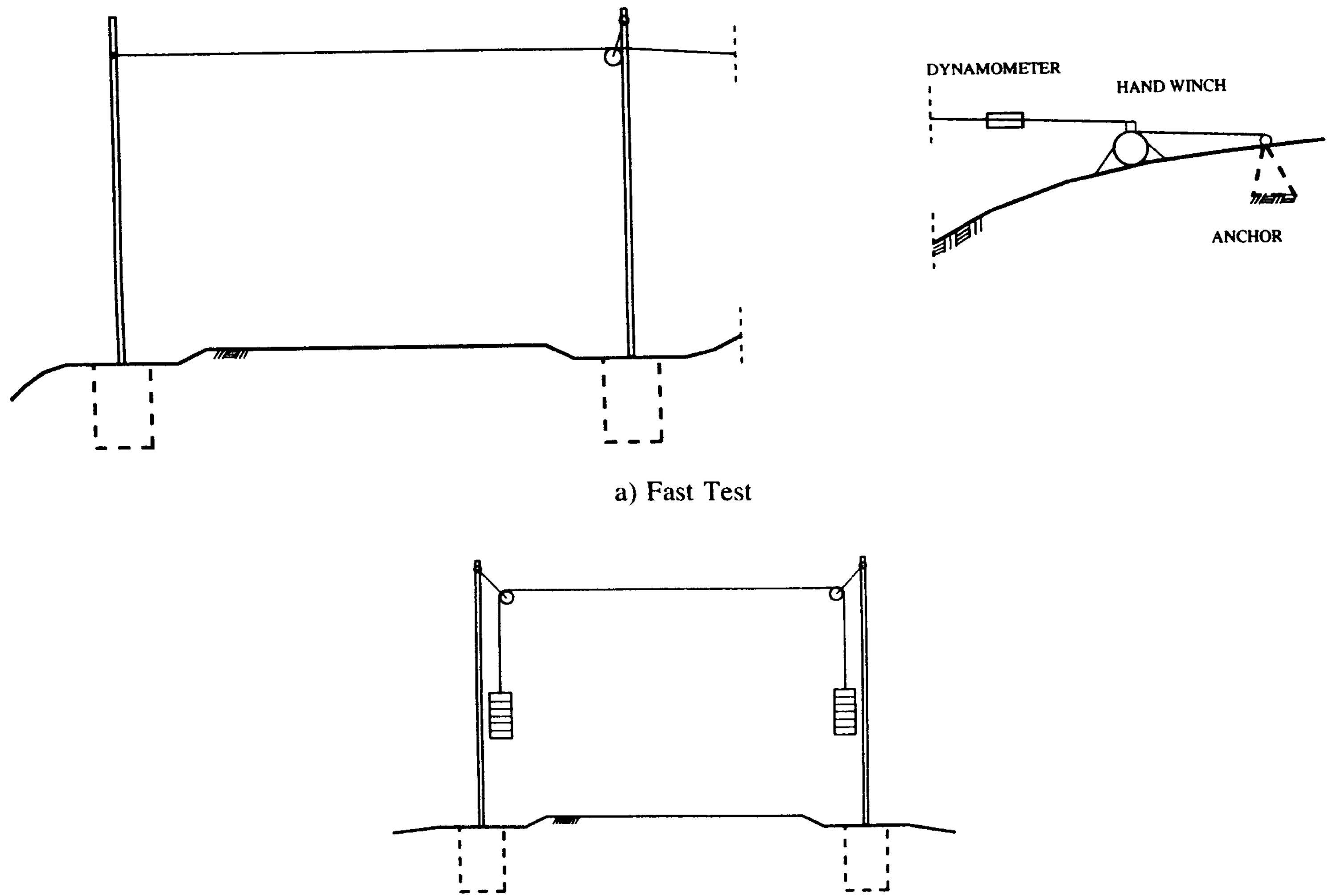

a) Fast Test

b) Slow Test

Figure 2.11 Lateral Load Application in UIC/ORE Test.

CHAPTER 3

HYPERBOLIC STRESS-STRAIN MODEL AND DETERMINATION OF PARAMETERS

3.1 Introduction

It is well known that stress-strain relationships for soil are generally non-linear. The importance of non-linearity in the analysis depends on factors such as the type of soil, the magnitude of loading compared to the ultimate value and the magnitude of the associated deformations.

In this chapter, a simplified non-linear model proposed by Duncan and Chang (1970) for the mathematical modelling of soil behaviour is briefly reviewed. In order to provide data for the numerical studies on the clay used a series of conventional triaxial compression tests were carried out to supplement the tests performed by previous research workers.

3.2 Hyperbolic Model

This model was proposed by Duncan and Chang (1970) based on the works of Kondner (1963), Kondner and Zelasco (1963) and Janbu (1963) and later modified by

Clough and Duncan (1971) and Duncan (1981). The model approximates the shape of the stress-strain relationship of a soil as a hyperbola. Figure 3.1 shows such a relation which can be expressed by the equation

$$(\sigma_1 - \sigma_3) = \frac{\epsilon}{a + b\epsilon} \tag{3.1}$$

where

σ_1 and σ_3 = major and minor principal stresses

$(\sigma_1 - \sigma_3)$ = principal stress difference (known as deviator stress)

ε = axial strain

a and b = constants.

The maximum deviator stress $(\sigma_1 - \sigma_3)_{ult}$ = 1/b is obtained at infinite strain and the initial slope at zero strain, $d(\sigma_1 - \sigma_3) / d\varepsilon = 1/a$.

By re-writing equation (3.1) as

$$\frac{\epsilon}{(\sigma_1 - \sigma_3)} = a + b\epsilon \tag{3.2}$$

a straight line relationship is obtained between variables $\varepsilon/(\sigma_1 - \sigma_3)$ and ε as shown in figure 3.2. Parameter b is the slope of the line and parameter a is the intercept at zero strain.

In practice, compressive strength or deviator stress at failure, $(\sigma_1 - \sigma_3)_f$, occurs at finite strain and is less than $(\sigma_1 - \sigma_3)_{ult}$. The values of $(\sigma_1 - \sigma_3)_{ult}$ and $(\sigma_1 - \sigma_3)_f$ are related empirically by:

$$(\sigma_1 - \sigma_3)_f = R_f (\sigma_1 - \sigma_3)_{ult} = \frac{R_f}{b} \tag{3.3}$$

where R_f is defined as the failure ratio.

R_f is found to be between 0.70 and 1.00 for different soils and is essentially independent of confining pressure.

For the triaxial stress system the axial strain is given by Hooke's Law as:

$$\begin{aligned} \epsilon &= \frac{\sigma_1}{E} - \frac{\nu}{E} 2\sigma_3 \\ &= \frac{\sigma_1 - \sigma_3}{E} + \frac{1 - 2\nu}{E} \sigma_3 \end{aligned} \tag{3.4}$$

where E is Young's modulus and ν is Poisson's ratio.

Now for incremental changes in deviator stress and axial strain at constant σ_3:

$$\frac{d\epsilon}{d (\sigma_1 - \sigma_3)} = \frac{1}{E} \tag{3.5}$$

and thus Young's modulus corresponds to values of the slope of the deviator stress-strain curve and is referred to as the tangent modulus E_t.

When equation (3.1) is differentiated and equation (3.5) substituted into the resulting expression, the tangent modulus, E_t, is obtained as:

$$E_t = \frac{a}{(a + b\epsilon)^2} \tag{3.6}$$

When $\varepsilon = 0$, this gives the initial tangent modulus as:

$$E_i = \frac{1}{a} \tag{3.7}$$

Eliminating ε from equations (3.1) and (3.6), the tangent modulus can be written in the form

$$E_t = \frac{1}{a} [1 - b(\sigma_1 - \sigma_3)]^2 \tag{3.8}$$

For all soils except fully saturated soils tested under undrained conditions, an increase in confining pressure will result in a steeper stress-strain curve and a higher strength, and the values of E_i and $(\sigma_1 - \sigma_3)_f$ therefore increase with confining pressure. This stress-dependency is taken into account by using empirical equations to represent the variations of E_i and $(\sigma_1 - \sigma_3)_f$ with confining pressure.

Janbu (1963) suggested that the relation between initial tangent modulus and cell pressure could be obtained by plotting the experimental values, from a series of compression tests at different cell pressures, on a log-log scale as shown in figure 3.3. The initial modulus can be expressed as:

$$\log\left(\frac{E_i}{p_a}\right) = \log K + n \log\left(\frac{\sigma_3}{p_a}\right) \tag{3.9a}$$

or

$$E_i = K\, p_a \left(\frac{\sigma_3}{p_a}\right)^n \tag{3.9b}$$

where,

p_a = atmospheric pressure expressed in the same units as σ_3 and E_i, and used to make K and n non-dimensional

and K = modulus number and n = modulus exponent, respectively.

$(\sigma_1 - \sigma_3)_f$ can be related to σ_3 using Mohr-Coulomb failure criterion (see figure 3.4) by the equation

$$(\sigma_1 - \sigma_3)_f = \frac{2c\cos\phi + 2\sigma_3\sin\phi}{1 - \sin\phi} \tag{3.10}$$

where c and ϕ are the apparent cohesion and apparent angle of internal friction of the soil, respectively.

From equations (3.3) and (3.10), parameter b can be expressed as:

$$b = \frac{R_f (1 - \sin\phi)}{2c \cos\phi + 2\sigma_3 \sin\phi} \qquad (3.11)$$

Substituting equations (3.7), (3.9b) and (3.11) into equation (3.8), the tangent modulus is expressed in terms of confining pressure and deviator stress without reference to strain as

$$E_t = K\, p_a \left(\frac{\sigma_3}{p_a}\right)^n \left(1 - \frac{R_f (\sigma_1 - \sigma_3)(1 - \sin\phi)}{2c \cos\phi + 2\sigma_3 \sin\phi}\right)^2 \qquad (3.12)$$

The parameters required to define this model, c, ϕ, K, n and R_f, can be determined by carrying out a series of conventional triaxial compression tests at different cell pressures and fitting empirical equations to the results.

For saturated soil tested under undrained conditions, the values of n and ϕ are zero and thus

$$E_t = K\, p_a \left(1 - \frac{R_f (\sigma_1 - \sigma_3)}{2c}\right)^2 \qquad (3.13)$$

Dickin and King (1982) defined the reciprocal of the factor of safety of a soil element, RFOS, as the ratio of the size of the current Mohr's circle to the size of the circle having the same centre which just touches the failure envelope. Hence

$$RFOS = \frac{(\sigma_1 - \sigma_3) / 2}{[\, c \cot\phi + (\sigma_1 + \sigma_3) / 2 \,] \sin\phi} \tag{3.14}$$

An unloading/reloading modulus is used for values of RFOS less than any previous maximum value. When the value of RFOS = 1 is reached, a very small value of E_t is assigned to effect failure.

Duncan and Chang (1970) found that the stress-strain behaviour of soil on unloading and reloading may be approximated with a high degree of accuracy as linearly elastic. The same value of modulus E_{ur} is used for both unloading and reloading. The value of E_{ur} is related to the confining pressure by an equation of the same form as equation (3.9b):

$$E_{ur} = K_{ur}\, p_a \left(\frac{\sigma_3}{p_a} \right)^{n_{ur}} \tag{3.15}$$

where K_{ur} is the unloading-reloading modulus number. The values of K_{ur} are typically two to three times greater than the values of K (the modulus number for primary loading). The value of exponent n_{ur} is always very similar for primary loading and unloading-reloading, and is often assumed to be the same. For saturated soil tested under undrained conditions $n_{ur} = 0$ and $E_{ur} = K_{ur}\, p_a$

3.3 Determination of Hyperbolic Model Parameters

A series of conventional and unload/reload triaxial compression tests were performed on the saturated clay to obtain hyperbolic model parameters over the range of moisture contents used in the experimental program (see Chapters 4 and 5.). Two different sample dimensions were used. First, six samples 38 mm in diameter by 76 mm in length were tested at cell pressures over the range 0 to 400 kN/m^2 in the standard triaxial test apparatus. As the soil was saturated, and the tests were carried out under undrained conditions on samples with similar moisture contents, the stress-strain curves at various confining pressures, are very similar as shown in figure 3.5. Subsequently ten larger samples, 101.6 mm in diameter by 101.6 mm in length, were tested using free end platens over the same range of cell pressures. Based on these results, hyperbolic parameters were determined as described below.

The data obtained from the triaxial tests was plotted in the form of deviator stress versus axial strain as shown in figures 3.6 (a to k). Since the values of moisture content observed in these tests varied from 16.17% to 18.39%, the cohesion values of the clay obtained from the graphs varied over the range 116.19 kN/m^2 to 51.4 kN/m^2. A plot of $\log_{10}$(cohesion) against moisture content is shown in figure 3.7. The equation of the best fit straight line can be written as;

$$\log_{10} c = 4.4344 - 0.14838\, m \tag{3.16}$$

where

c = cohesion of clay (in kN/m^2)

m = moisture content of clay (%)

The transformed axial strain/deviator stress against axial strain curves were then plotted and straight lines fitted using the least-squares approach as shown in figures

3.8 (a to k). The hyperbolic model parameters "a" and "b" were obtained from the figures and the variation of these parameters with moisture content are presented in figures 3.9 and 3.10, respectively. The straight lines shown on these graphs were obtained using the least-squares approach. The equation of the best fit straight line was obtained from figure 3.9 as;

$$a = -3.558 \times 10^{-3} + 2.446 \times 10^{-4}\, m \tag{3.17}$$

and from figure 3.10 as;

$$b = -2.780 \times 10^{-2} + 1.934 \times 10^{-3}\, m \tag{3.18}$$

where parameters "a" and "b" are in m^2/kN and "m" in %.

In the tests, unloading/reloading was performed twice for each sample, and the values of the unload/reload moduli E_{ur} were determined as indicated in figures 3.6 (a to k). These were then plotted against their corresponding values of moisture content in figure 3.11. From a straight line fitted to the data, the relationship between E_{ur} and moisture content m can be expressed as:

$$E_{ur} = 19581 - 837\, m \tag{3.19}$$

where E_{ur} is in kN/m^2 and m in %.

The clay was virtually saturated, and therefore nearly incompressible under undrained conditions, and the value of Poisson's ratio was therefore assumed to be 0.50.

A summary of all parameters required for the hyperbolic model, and the relevant equations required for their calculation for the clay at a given moisture content, is given in table 3.1.

PARAMETER	VALUE OR PROCEDURE
ϕ	0.0
n	0.0
p_a (kN/m^2)	101.3
K	Determine "a" from equation (3.17) and calculate $K = 1 / (a\ p_a)$
K_{ur}	Determine "E_{ur}" from equation (3.19) and calculate $K_{ur} = E_{ur} / p_a$
c (kN/m^2)	Determine from equation (3.16)
R_f	Determine "b" from equation (3.18) and calculate $R_f = 2\ c\ b$

Table 3.1 Summary Table for Calculation of Hyperbolic Parameter Values for Clay at a Given Moisture Content.

3.4 Conclusion

Relationships have been found which enable appropriate values of parameters, relating to the hyperbolic stress-strain model, to be assigned to the clay used over a range of moisture content.

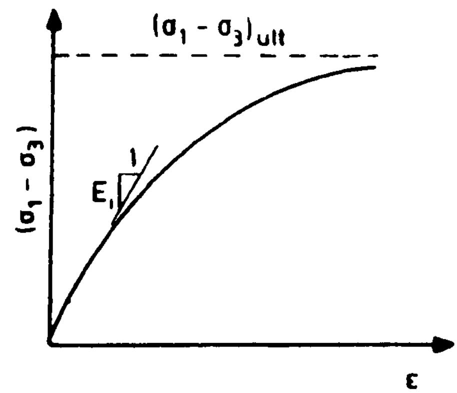

Figure 3.1 Hyperbolic Model for Non-Linear Material (Duncan, 1981).

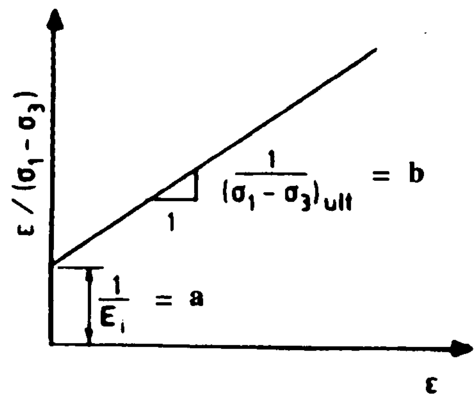

Figure 3.2 Hyperbolic Model for Transformed Axes (Duncan, 1981).

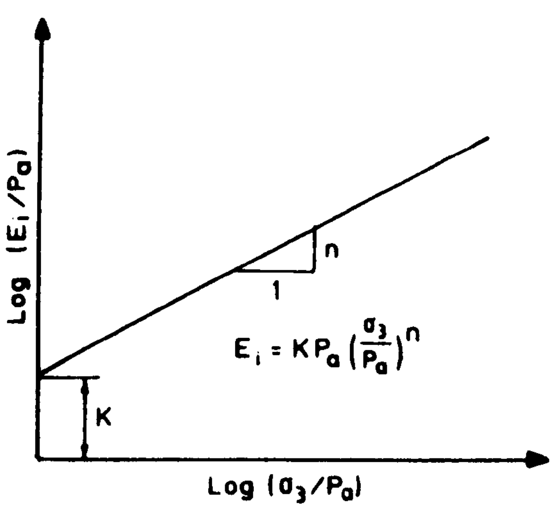

Figure 3.3 Variation of Initial Tangent Modulus with Confining Pressure (Janbu, 1981).

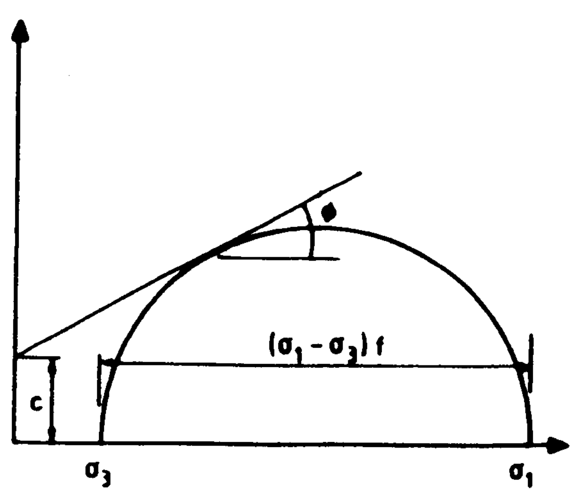

Figure 3.4 Variation of Strength with Confining Pressure.

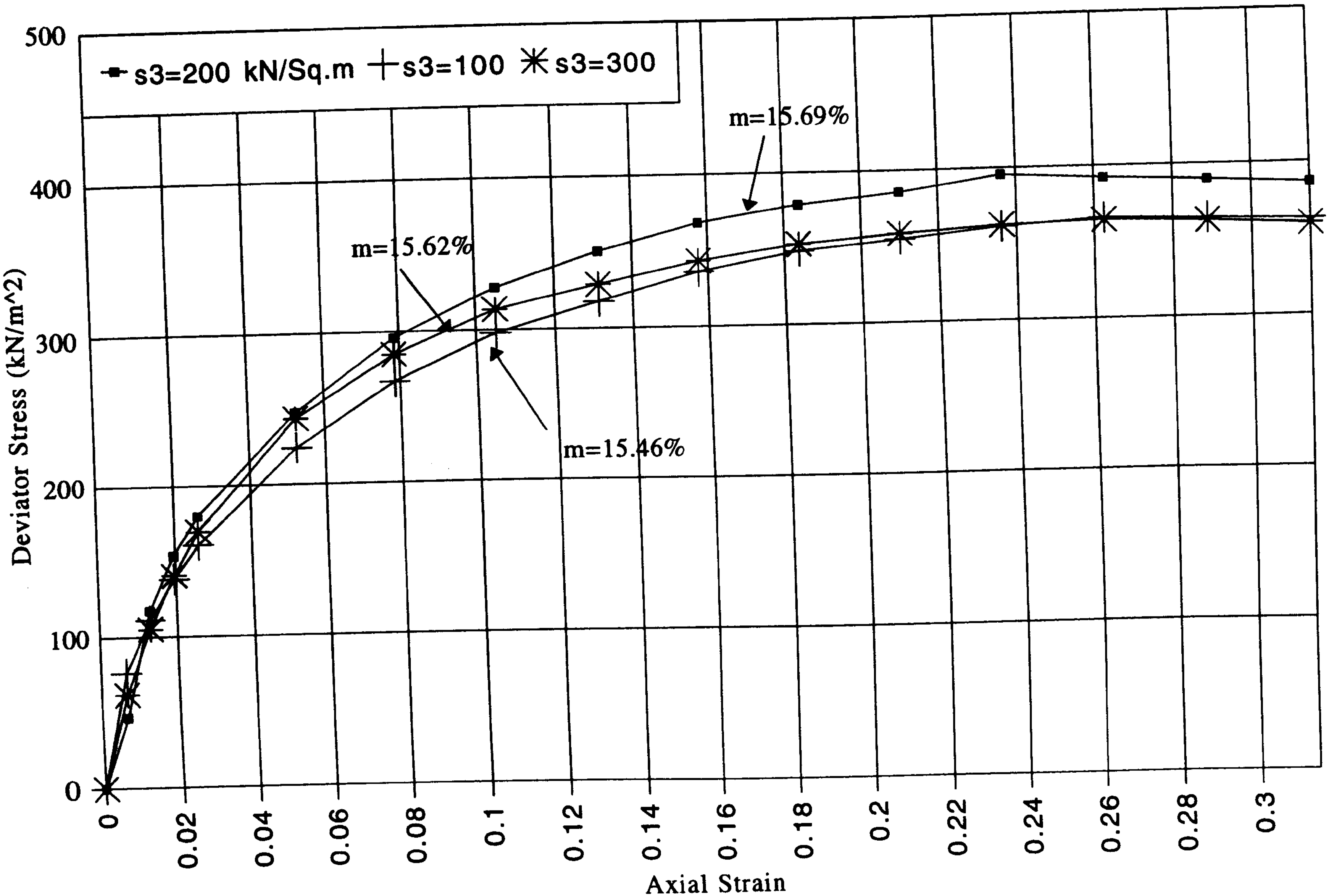

Figure 3.5 Variation of Stress-Strain Curves at Various Confining Pressures.

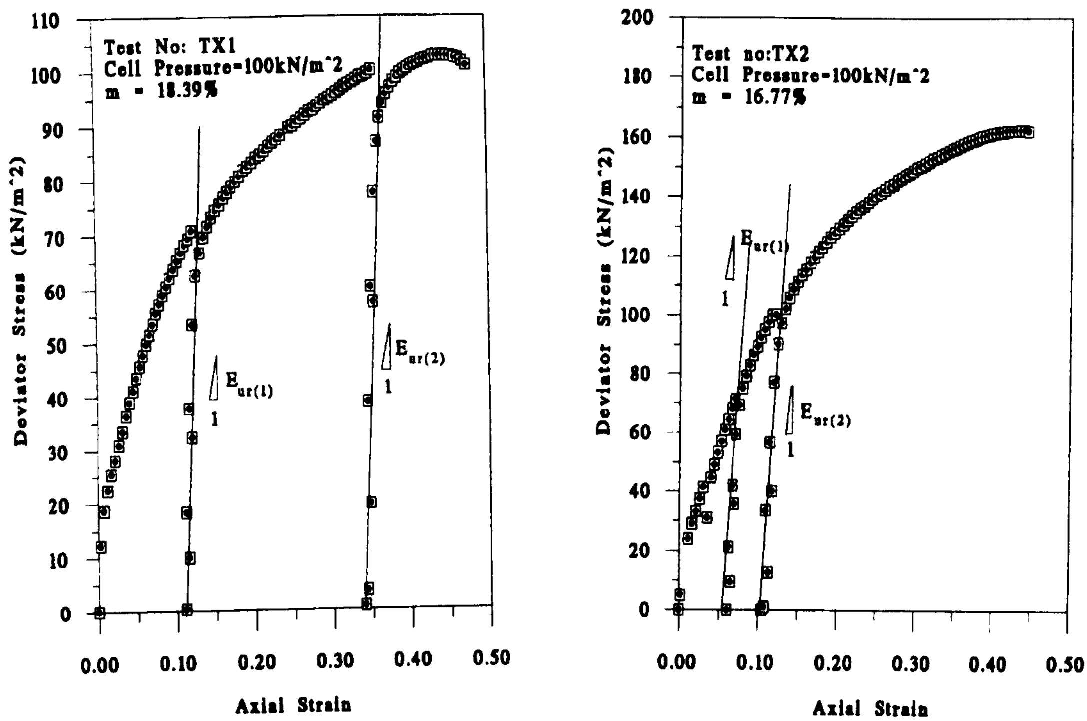

Figure 3.6 (a-b) Variation of Stress-Strain Curves for Unload/Reload Triaxial Test.

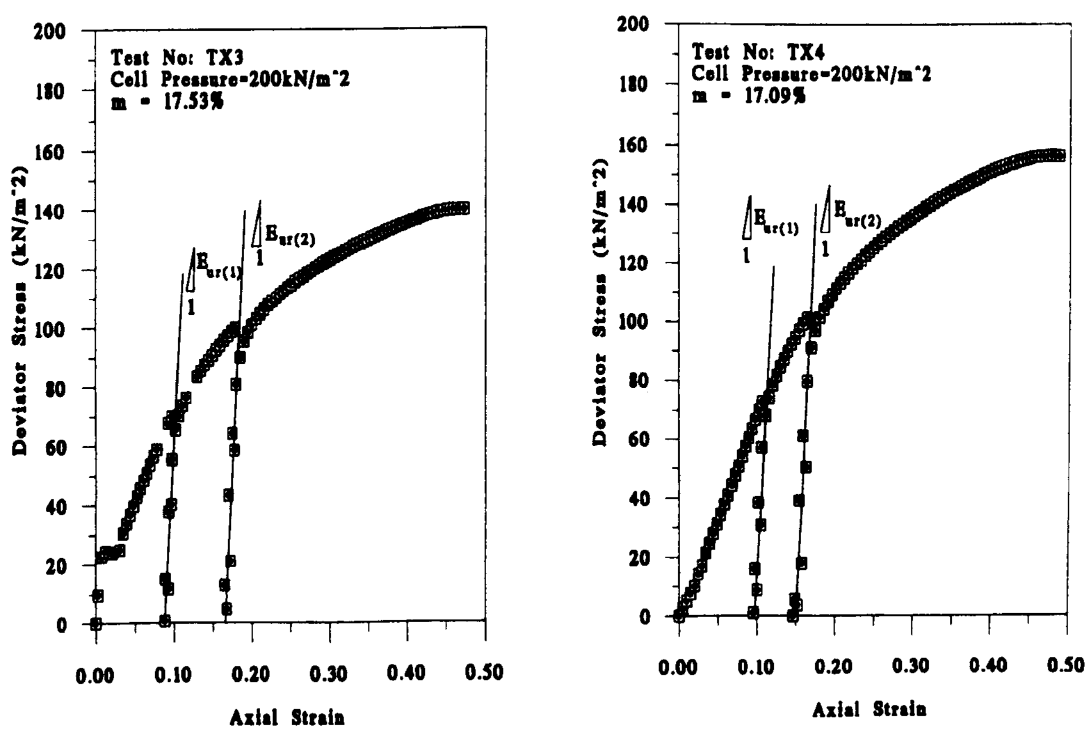

Figure 3.6 (c-d) Variation of Stress-Strain Curves for Unload/Reload Triaxial Test.

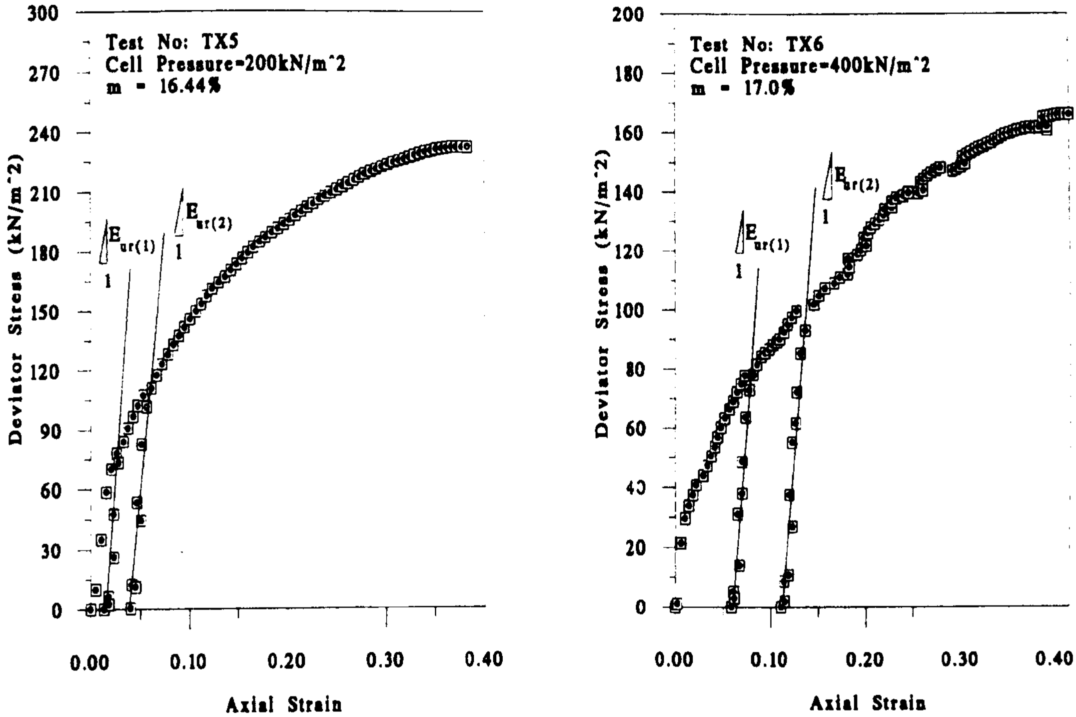

Figure 3.6 (e-f) Variation of Stress-Strain Curves for Unload/Reload Triaxial Test.

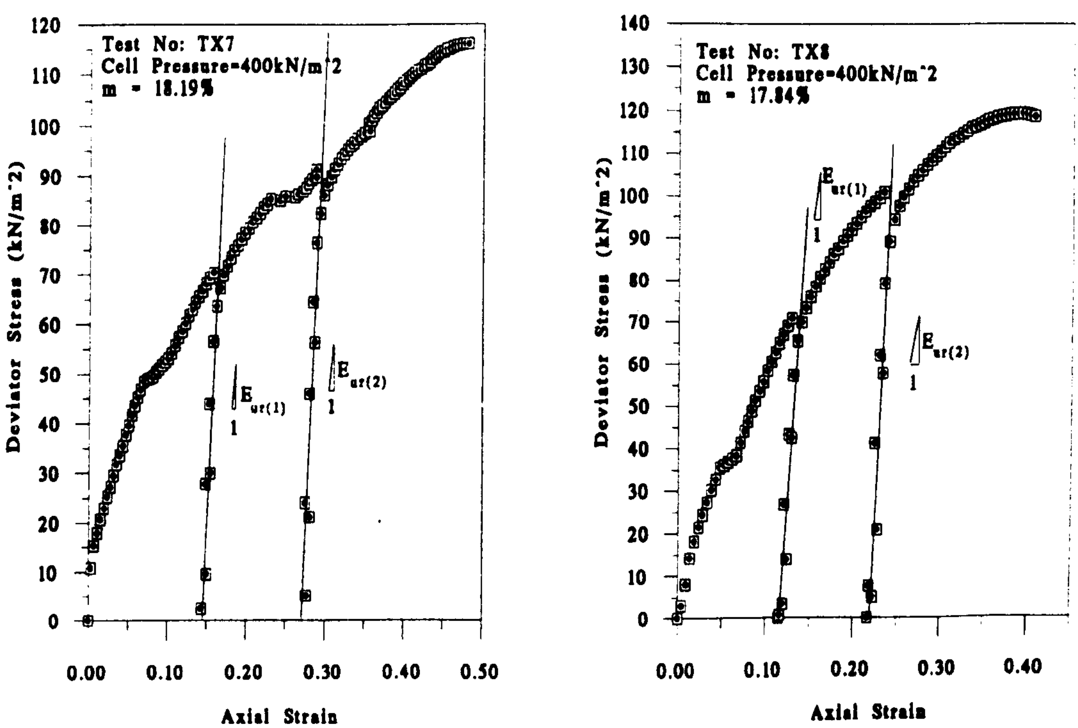

Figure 3.6 (g-h) Variation of Stress-Strain Curves for Unload/Reload Triaxial Test.

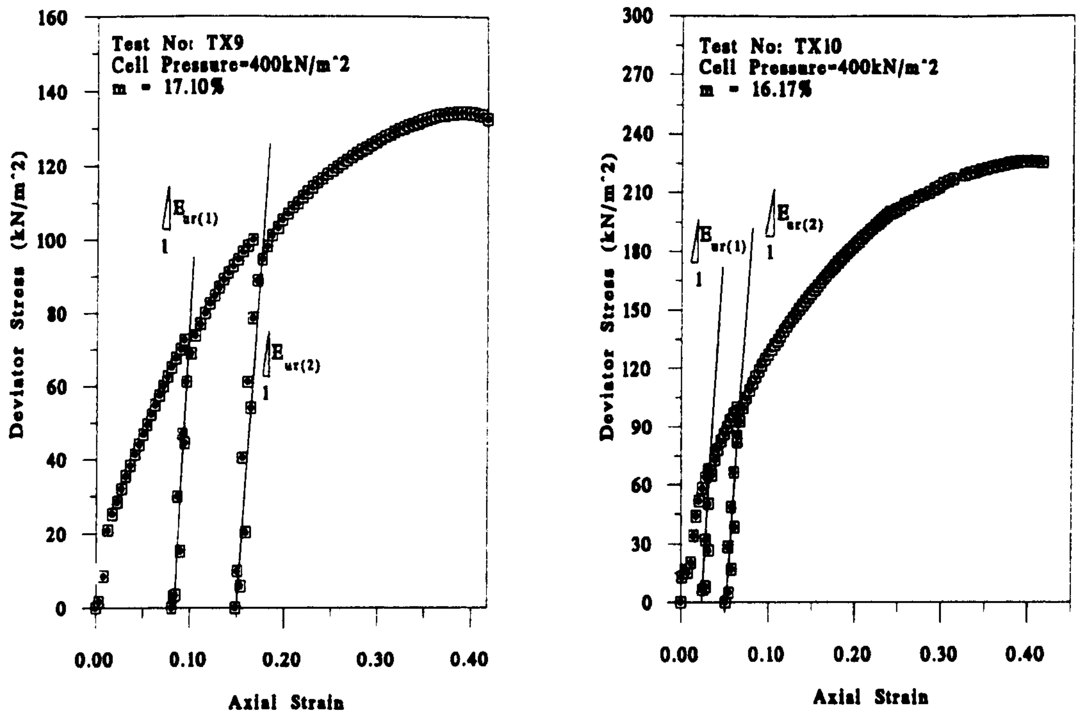

Figure 3.6 (j-k) Variation of Stress-Strain Curves for Unload/Reload Triaxial Test.

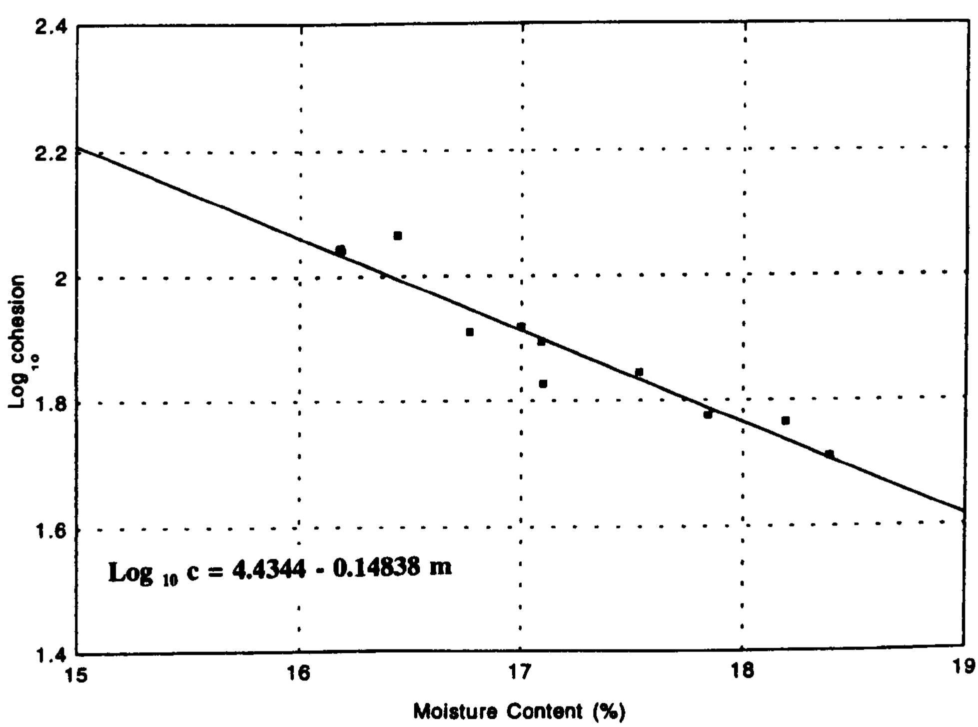

Figure 3.7 Log_{10} (cohesion) versus moisture content.

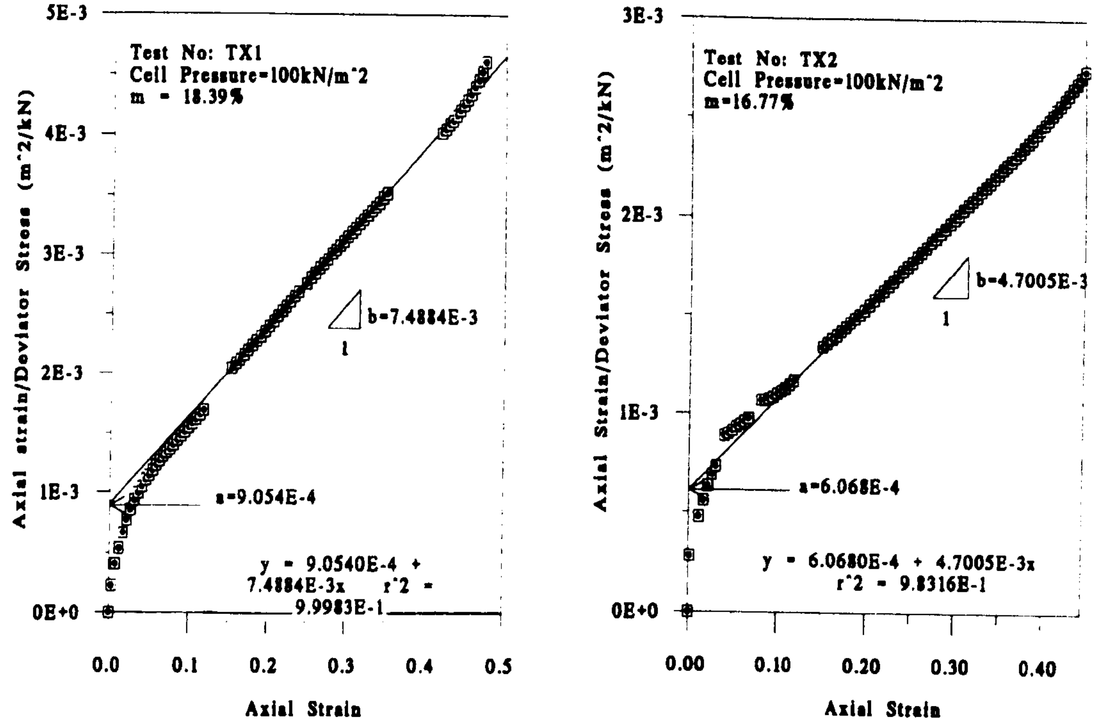

Figure 3.8 (a-b) Transformed Linear Hyperbolic Plot.

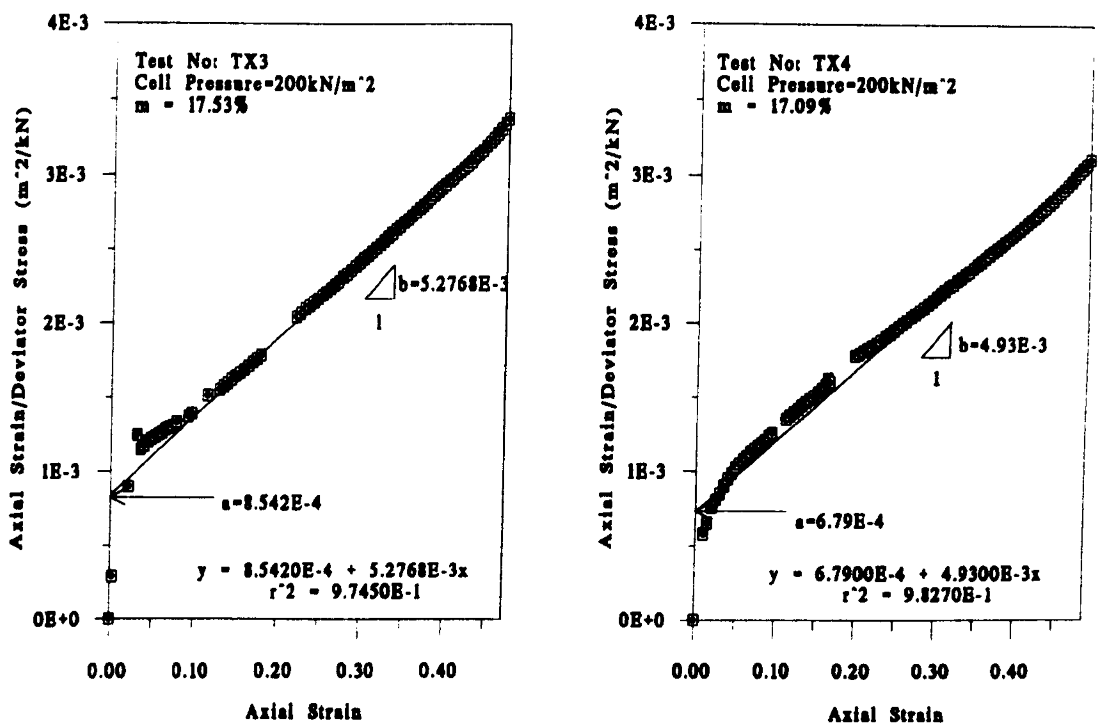

Figure 3.8 (c-d) Transformed Linear Hyperbolic Plot.

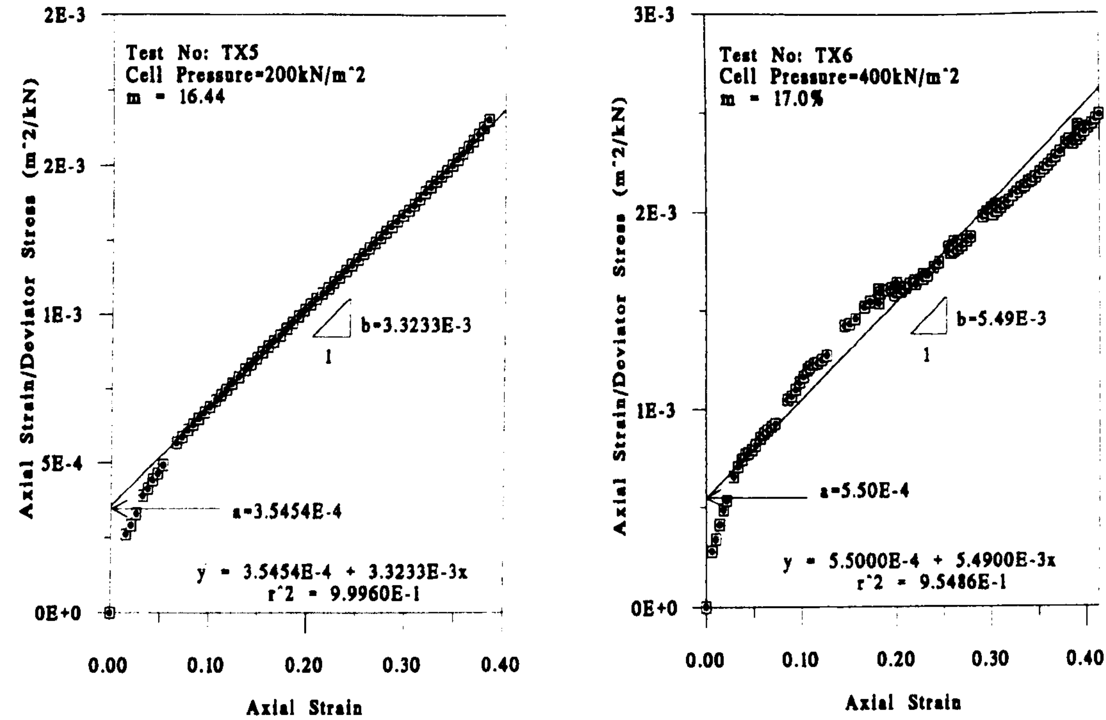

Figure 3.8 (e-f) Transformed Linear Hyperbolic Plot.

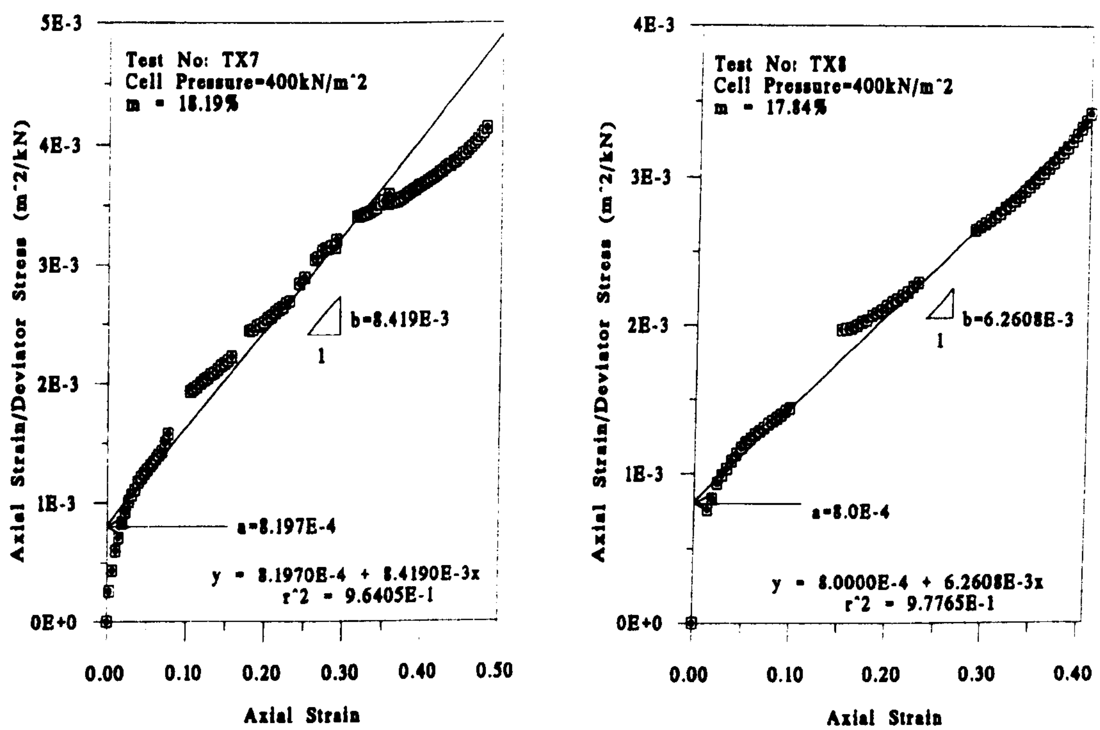

Figure 3.8 (g-h) Transformed Linear Hyperbolic Plot.

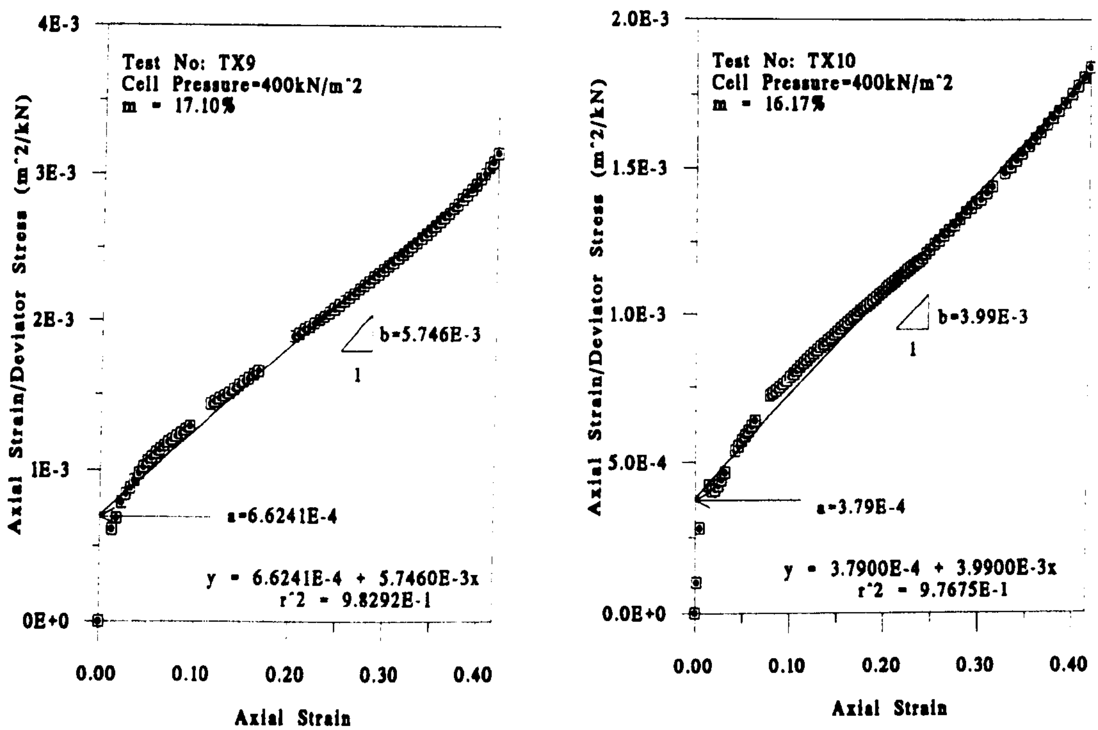

Figure 3.8 (j-k) Transformed Linear Hyperbolic Plot.

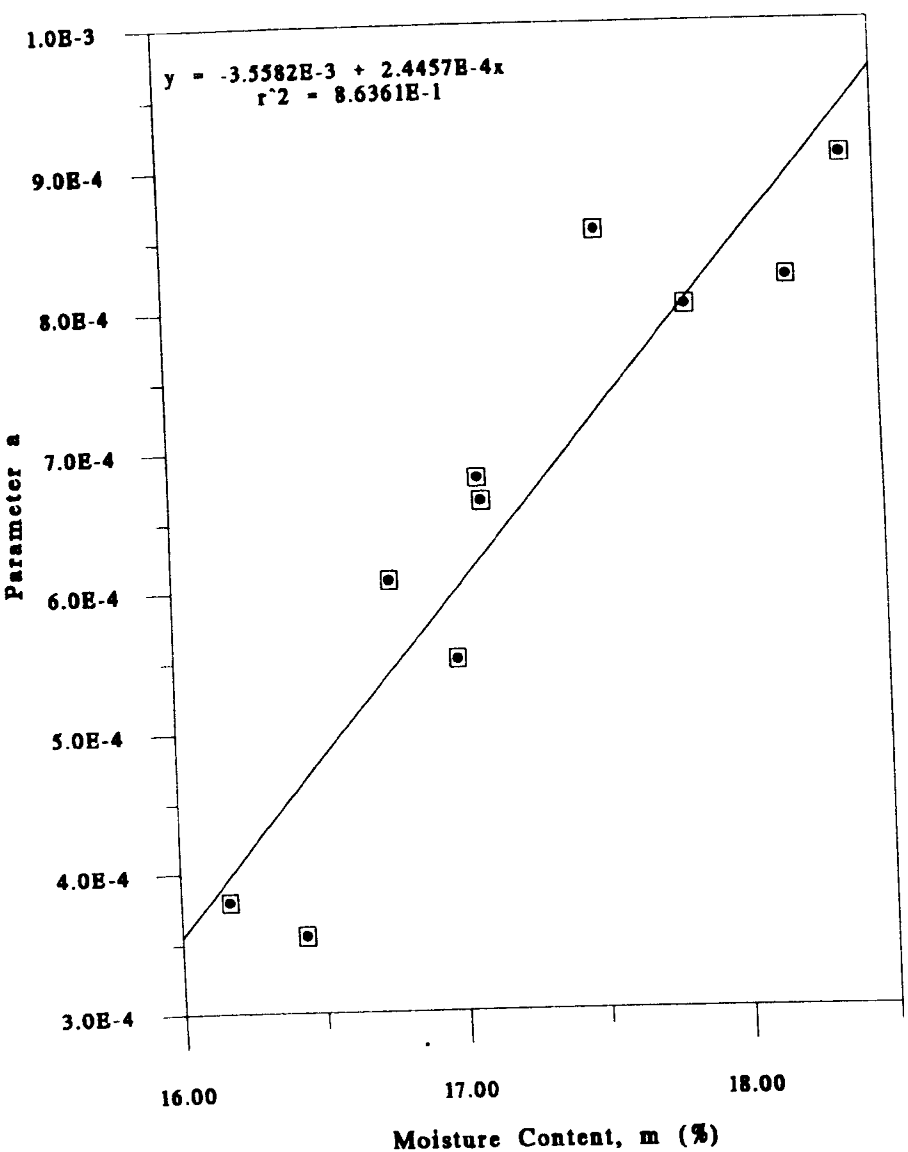

Figure 3.9 Hyperbolic Parameter "a" Against Moisture Content "m".

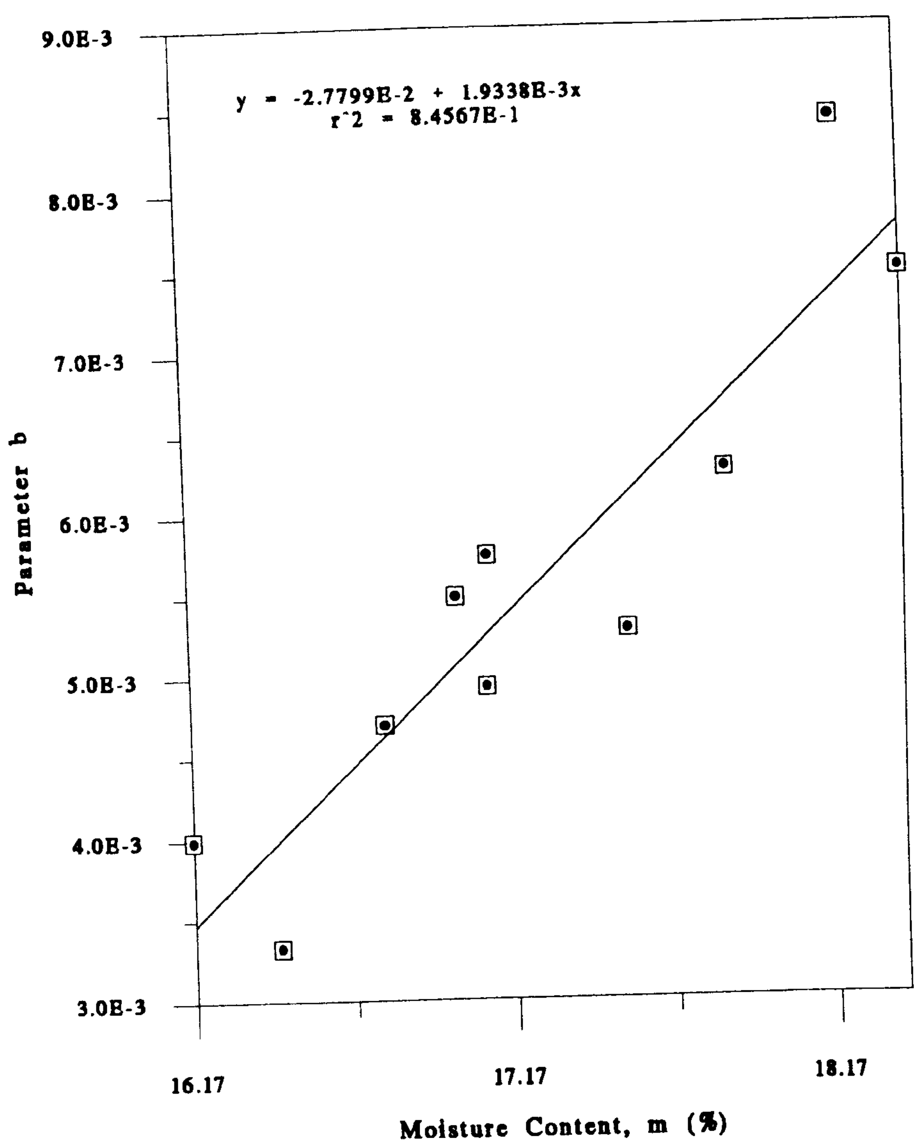

Figure 3.10 Hyperbolic Parameter "b" Against Moisture Content "m".

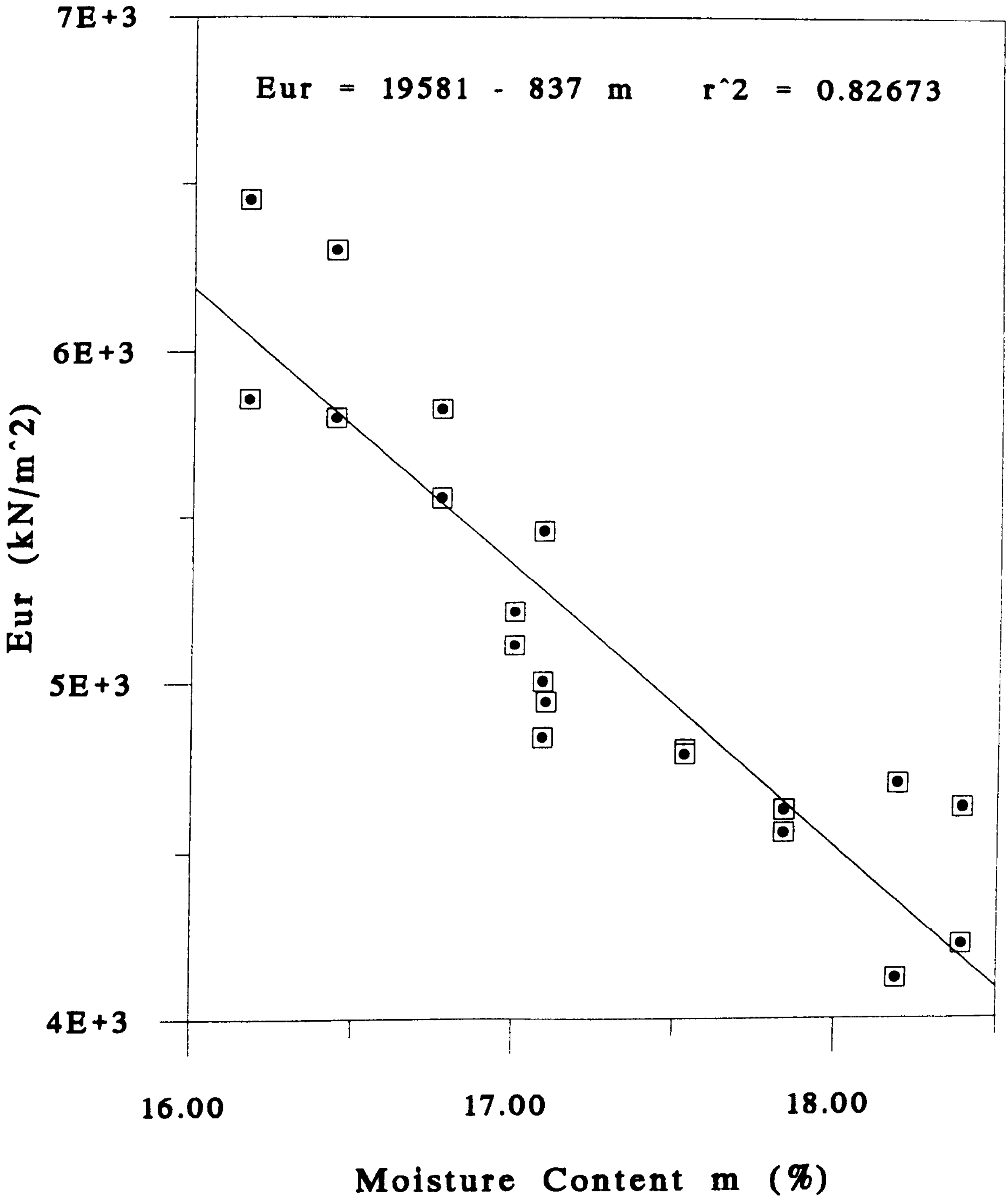

Figure 3.11 Variation of Unloading-Reloading Modulus Number with Moisture Content "m".

CHAPTER 4

CONVENTIONAL MODEL STUDIES OF SHORT PIER FOUNDATIONS IN CLAY

4.1 Introduction

Several series of conventional model tests on short, square, rigid, free-headed pier foundations in clay were carried out. Model piers with different dimensions were tested to investigate their short term response when they were subjected to large overturning moments as a result of horizontal loading applied at an appreciable height.

The experimental apparatus, soil properties and the procedure for testing the model piers are described. The results obtained from the tests are presented together with empirical relationships which have been derived between moment carrying capacity and pier geometry.

4.2 Model Piers

The model piers were notionally at 1/40th scale. Six piers of different widths and depths made from a mild steel with a bulk unit weight of 77 kN/m^3 and modulus of elasticity of 207×10^6 kN/m^2, were used. The dimensions of the piers at model and prototype scale are as listed in table 4.1.

Model No		1	2	3	4	5	6
Model (mm)	Width	20	30	40	50	60	60
	Depth	60	60	60	60	60	20
Prototy pe (m)	Width	0.80	1.20	1.60	2.00	2.40	2.40
	Depth	2.40	2.40	2.40	2.40	2.40	0.80

Table 4.1 Dimensions of the model piers tested.

The first five test piers have a depth of 60mm as shown in the table while their widths vary from 20 to 60mm. For each pier, by using different embedments, a range of effective depths was obtained. These heights varied from 20 to 60mm with a 10mm increment.

4.3 Experimental Apparatus and Procedure

4.3.1 Equipment

The tests were carried out in a wooden bin filled with saturated clay and equipped with loading and measuring devices. These are described briefly in the following sections. The general layout of the apparatus is illustrated in figure 4.1, plate 4.1 and plate 4.2.

4.3.1.1 Soil bin

A bin 570mm by 460mm in plan and 320mm high was made of wood. The walls were

20mm thick plywood and were strengthened horizontally and vertically with supports. The base plate was 20mm thick plywood and its total area was 1000mm by 800mm. The inside walls and the base of the bin were painted with a water proofing bitumen to prevent the loss of moisture from the clay throughout the testing program. Four steel bars with holes drilled at various heights were fixed vertically on both long sides of the bin so that another two angles, on which motor and gearing were fixed, could be bolted on at desired heights. The complete assembly is shown in plate 4.1.

4.3.1.2 Loading arrangement

Piers used for supporting gantries carrying the overhead power lines, electric lamp posts and signal portals are subjected to lateral loads at appreciable heights which result in large overturning moments, but to relatively low axial loads. To simulate this loading, the lateral pulling force was applied at 150mm above the level of the clay as shown in figure 4.2. This height represents 6m which is typical in the prototype.

The lateral pulling loads were applied to the model piers by means of a PARVALUX (model 21SIS) motor-gearbox system through a 250 lb SENSOTEC (model 31) load cell supplied by RDP electronics at a constant rate of displacement of 0.4mm/min. Before using the load cell, it was calibrated in tension against a standard pre-calibrated proving ring with the aid of a load frame. During the calibration, the load cell was loaded up to 1.171 kN and readings were taken from the display unit in milli-volts. The calibration factor of the load cell and the corresponding graph are given in appendix B.

In earlier tests vertical pulling rods 10mm square in cross section ranging from 160mm to 320mm in length were employed to pull the pier laterally via the pulling cable. When testing models with large widths, especially at greater depths, the pulling rods were seen to deflect under the load. This deflection had a significant effect on the results obtained. Considering this, two other rods 15mm by 25mm and 20mm by 30mm by each 300mm long were subsequently used. They were screwed into the top of the piers. The load cell and the vertical rod were connected by the pulling cable which was made of stainless steel. One end of this cable was screwed on the load cell while the other end was either screwed into the hole provided in the vertical rod or attached to a ring placed in the hole with a hook. These two different connection types are shown in plate 4.3. The latter type of connection was preferred because, with the first type, after initial displacements, the rigid end of the pulling cable caused an upwards as well as a lateral movement of the pier. The effects of both types of connections on modes of displacements are shown in figure 4.3.

4.3.1.3 Measurement of displacement

Lateral displacements of the pulling rods were measured using two conductive plastic linear potentiometers (transducers). The accuracy of these transducers was 0.001mm and they were capable of monitoring displacements up to 25mm. Prior to usage, the transducers had to be calibrated. This was effected with the aid of an inch micrometer. The readings in milli-volts for every 2.54mm increments up to 25.4mm were recorded using a data logger. Plots of the results showed linear relationships from which the calibration factors were obtained. These plots along with the relevant calculations are presented in appendix B. The transducers were placed at 50 or 100mm apart depending upon the geometry of any particular test. In earlier tests, the transducers were set behind the pulling rod and therefore recorded displacements as the rod moved away from them. On the smaller models, especially those at shallow depths, the transducer springs exerted a significant initial force to the pier even before loading. This force resulted in the load readings obtained being smaller than those which were actually causing the pier to rotate. In order to eliminate this affect, the tests were repeated with the transducer springs removed and the transducers set on the other side of the pier as shown in plate 4.1.

4.3.1.4 Data acquisition

The output from load cell and transducers was fed to an Orion data logger. The data logger was connected to a BBC Master computer for immediate processing of results. An existing computer program was modified for these experiments to accommodate one load cell and two displacement transducers and output was via an EPSON printer and a PLOTMATE plotter. Data acquisition equipment is shown in plate 4.4.

4.3.2 Soil properties

The soil used in the experiment was a remoulded silty clay from Moreton, Wirral approximately 8 miles south west of Liverpool. The properties of the clay, including grain size distribution, consolidation and strength characteristics and Atterberg limits had already been determined from standard laboratory tests by previous researchers

(Farhadi,1991). To obtain additional data in the range of moisture contents used in these tests, series of conventional and unload/reload triaxial compression tests were performed. Two different sample dimensions were used. First, six samples 38mm in diameter by 76mm in length were tested at cell pressures over the range 0 to 400 kN/m^2 in the standard triaxial test apparatus. The variation of cohesion with moisture content and the variation of the hyperbolic model parameters "a" and "b" with moisture content were obtained. Subsequently ten larger samples, 101.6mm in diameter by 101.6mm in length, were tested using free end platens over the same range of cell pressures. Interpretations of these test results with the corresponding graphs are presented in Chapter 3. The main physical properties of the clay are given in table 4.2.

Moreton Clay	
Liquid Limit, **LL**	42 %
Plastic Limit, **PL**	15 %
Plasticity Index, **PI**	27 %
Specific Gravity, S_G	2.67
Coefficient of Consolidation, C_v	0.465 m^2 /year
Range of moisture contents, **m**	15-18 %

Table 4.2 Physical properties of the clay.

The degree of saturation in the clay was found to be between 97.5% and 100%. Due to this high level of saturation, undrained shear was observed to occur with ϕ_u=0. The grain size distribution curve is given in figure 4.4. Based on these results and those of previous researchers, the soil can be classified as a brown overconsolidated inorganic silty clay of medium plasticity.

4.3.3 Experimental program

The experimental program consisted of approximately 73 tests, including the tests which were repeated if results did not fit the established pattern. All the piers were modelled at 1/40 th scale. They were tested over a range of depths and widths. A pulling height of 150mm (6m in prototype) was chosen to represent a practical height as this applies for gantries carrying the overhead power lines for the railway network.

4.3.4 Initial preparation of the soil and bin

The test bin was filled with dry Erith sand and a trial test was carried out to check the operating and recording equipment. The test bin was then emptied before being refilled with clay. The clay was cut into small pieces from the bricks provided and placed into the bin in layers of approximately 40mm thickness. Each layer was compacted using a steel tamper with a circular base, 150mm in diameter and 10mm thick, coaxially attached to the end of a rod 15mm in diameter and 500mm long. Another steel tamper with a rectangular base 20mm by 20mm in cross section and 350mm long was used to compact the clay at the corners and edges of the bin. The tampers were approximately 2 kg in weight, and were allowed to fall from a height of 300mm. Each layer was given 100 tamps. This compaction procedure was used throughout the testing program, in order to obtain a reasonably homogeneous soil. When preparation of the clay bed was completed, damp burlap was placed on its surface and then the entire bin was covered with a sheet of plastic to prevent evaporation of moisture. In order to obtain a more uniform moisture content throughout the clay, it was left to stand overnight.

4.3.5 Test procedure

The first pier model was installed into the clay during the initial packing. When a depth of 160mm was reached, the top of the clay was levelled accurately using a spirit level and then the pier was placed on it. In order to prevent any movement of the pier model while compacting the soil around it, it was fixed rigidly to the bin. (A steel bar was clamped on the soil bin and the vertical pulling rod, screwed on the pier, was attached to it.) The compaction procedure was continued layer by layer until the level of the clay was just above that required. The excess clay was then removed with a scraper, leaving the surface smooth and level. In subsequent experiments, using different piers, the previous one was excavated and replaced with the new one. The volume of clay removed with the pier was approximately 300mm by 200mm in plan and 150mm high. The clay removed was mixed up with unused clay and re-compacted around the pier. After the clay and the model had been prepared, the load cell and pulling rod were connected by means of a steel cable at the required loading height. Then, the displacement transducers were positioned in front of the pulling rod. Small pieces of double sided sticky tape were placed between the vertical pulling rod and the displacement transducers to ensure a positive contact at all times. The experimental apparatus prior to testing is shown in plate 4.5. The measured lateral displacements of two points along the rigid pulling rod are used to calculate the rotation and the lateral displacement of the pier at ground level as shown in figure 4.5.

At the beginning of a test initial readings of the load cell and displacement transducers were recorded. Lateral load was then applied to the pier. During tests, load and displacement were recorded at 20 second intervals and monitored on the screen of the BBC Master computer together with the calculated pier rotation angle. The tests were continued until the pier rotation reached about 5 degrees. Each test took 30 to 45 minutes depending upon the pier geometry and moisture content of the clay. A model at the end of a test is shown in plate 4.6. After each test, when the model was removed, a small sample of clay was taken from in front of the pier and used to determine the moisture content of the clay.

4.4 Test Results

For each test, the readings from the load cell and displacement transducers, recorded by the data logger unit, were converted to produce values of load, displacement and moment at ground level and rotation angle using a Fortran computer program on an I.B.M. PC compatible system. This procedure is explained in detail together with listing of the relevant computer programs and sample data in appendix C. 47 out of the 73 tests were used to interpret the results. The reasons for discarding some of the test results were either that they were exact duplicates or that faults had developed in the operation of the displacement transducers and application of the lateral load as described in sections 4.3.1.2 and 4.3.1.3. The model and prototype dimensions used and the moisture content values recorded are given in tables 4.3 to 4.7. Table 4.3 shows a series of tests on a model pier of 20mm breadth and using depths of embedment of 20 to 60mm in 10mm increments. Tables 4.4 to 4.7 show series of tests on model piers of 30mm to 60mm breadth using the same range of depths of embedment. In all tests, separation of the pier and the clay at the back of the pier was observed before 0.5 degrees of rotation. In order to establish the effect of the pier geometry on moment carrying capacity, moment-rotation relationships were considered for different pier geometries at prototype scale. Load - displacement relationships were also considered but these did not yield results of any consequence and are therefore not included in the thesis.

Although attempts were made, as described in section 4.3.4, to keep the moisture content of the clay constant throughout the testing program, a variation of up to 3% was observed. The relationship between cohesion and moisture content was derived in Chapter 3 as;

$$\log_{10} c = 4.4344 - 0.14838\, m \qquad (4.1)$$

where

c = cohesion of clay (in kN/m^2)

m = moisture content of clay (%)

Since the values of moisture content observed in the tests varied from 15% to 18%, the cohesion values of the clay, calculated from equation (4.1), were in the range 58 kN/m^2 to 161.7 kN/m^2. These values are also given in tables 4.3 to 4.7. Figure 4.6 shows the effect of moisture content on the moment/rotation relationships for two tests on a model pier of 30mm width and 50mm depth. However, when the ratios moment/cohesion were plotted against rotation, similar results were obtained as shown in figure 4.7. Therefore, moment values for all tests were divided by the cohesion calculated from equation (4.1) at the measured moisture content values to eliminate the effect of moisture content variation. Graphs of moment/cohesion against rotation for varying pier depths at the same pier breadths are shown in figures 4.8 to 4.12. Each set of tests was performed two or three times to check the consistency of results. When rerunning tests for the same models, different moisture content values were usually observed. However when moment/cohesion was plotted against rotation, similar results were obtained.

It can be seen that the relationships between moment/cohesion and rotation are nonlinear and do not exhibit any peak values. The k_4 concept of Rowe and Davis (1982) was tried to define failure but was not found to be satisfactory. The values of rotation obtained using this method were inconsistent and much smaller than those which would be considered unacceptable. Therefore arbitrary rotations of 0.5°, 1.0° and 1.5° were considered as alternative limiting working conditions. The moment/cohesion ratios required to cause each of these rotations were plotted against depth of pier, for different breadths of pier, as shown in figures 4.13 to 4.15. Using the least-squares approach, a series of straight lines was fitted to each of these. The equation of the best straight line can be written as;

$$\frac{M}{c} = \beta_{v1} + \beta_{v2} D \tag{4.2}$$

It is logical that in the absence of depth a negligible moment will produce rotation. Therefore these lines were constrained to pass through the origin ($\beta_{v1} = 0$). The values of slopes of these lines (β_{v2}) are given in table 4.8. The coefficients of correlation from linear regression analysis were found to be better than 0.85 for all cases. Figure 4.16 shows plots of the slopes of the straight lines against the breadth of the piers for each rotation. Best fit second order polynomial curves passing through the origin were fitted to these with correlation coefficients better than 0.98. The equation of these curves can be written as;

$$\beta_{v2} = \alpha_{v1} B + \alpha_{v2} B^2 \tag{4.3}$$

Therefore from equations (4.2) and (4.3)

$$M = c\, B\, D\, (\alpha_{v1} + \alpha_{v2} B) \tag{4.4}$$

in which

M = moment (kNm)

c = cohesion of the clay (kN/m^2)

B = breadth of the pier (m)

D = depth of the pier (m)

The values of parameters, α_{v1}, and, α_{v2}, are listed in table 4.9 at pier rotations of 0.5°, 1.0° and 1.5°. Hence the moment carrying capacities for each limiting rotation can be calculated from equation 4.4.

The location of the center of rotation during each test was calculated by dividing the lateral deflection at the ground surface by the tangent of the rotation angle for each reading. The ratio of the centre of rotation to depth of the pile was then calculated. It was zero initially, then shifted to a value of about 0.60 as tests progressed.

4.5 Conclusions

From an extensive series of conventional model tests empirical relationships have been derived between moment carrying capacity and geometry for limited rotations of short rigid piers in saturated clay.

The results presented have been scaled up to prototype size on the basis that this is usually legitimate for the immediate response of rigid structures in saturated clay. However in this problem the depth of tension zones behind the piers will be influenced by stress levels and this could have had a significant effect on the results. It was therefore decided that this study should be repeated using true scale modelling in a centrifuge.

TEST NAME	DEPTH		MOISTURE CONTENT (%)	COHESION (kN/m^2)
	MODEL SIZE (mm)	PROTOTYPE (m)		
M22RT1	20	0.80	15.79	123.45
M22RT2	20	0.80	15.43	139.60
M23RT1	30	1.20	16.16	108.79
M24RT1	40	1.60	16.01	114.51
M24RT2	40	1.60	16.30	103.71
M25RT1	50	2.00	16.46	98.19
M26RT1	60	2.40	18.05	57.03
M26RT2	60	2.40	16.70	90.46

Table 4.3 Model tests for 20mm (0.80m in prototype) breadth.

TEST NAME	DEPTH		MOISTURE CONTENT (%)	COHESION (kN/m^2)
	MODEL SIZE (mm)	PROTOTYPE (m)		
M32RT1	20	0.80	17.05	80.26
M32RT2	20	0.80	16.29	104.06
M33RT1	30	1.20	17.15	77.57
M33RT2	30	1.20	16.12	110.28
M34RT1	40	1.60	17.23	75.48
M34RT2	40	1.60	17.30	73.69
M35RT1	50	2.00	16.81	87.12
M35RT2	50	2.00	15.18	152.05
M35RT3	50	2.00	14.90	167.32
M36RT1	60	2.40	16.89	84.77
M36RT2	60	2.40	15.56	133.54
M36RT3	60	2.40	15.79	123.45

Table 4.4 Model tests for 30mm (1.20m in prototype) breadth.

TEST NAME	DEPTH		MOISTURE CONTENT (%)	COHESION (kN/m^2)
	MODEL SIZE (mm)	PROTOTYPE (m)		
M42RT1	20	0.80	16.35	101.95
M42RT2	20	0.80	16.87	85.36
M43RT1	30	1.20	16.33	102.65
M43RT2	30	1.20	15.37	142.49
M44RT1	40	1.60	15.96	116.48
M44RT2	40	1.60	15.57	133.08
M45RT1	50	2.00	16.67	91.39
M45RT2	50	2.00	15.10	156.27
M46RT1	60	2.40	16.43	99.20
M46RT2	60	2.40	15.22	149.99

Table 4.5 Model tests for 40mm (1.60m in prototype) breadth.

TEST NAME	DEPTH		MOISTURE CONTENT (%)	COHESION (kN/m^2)
	MODEL SIZE (mm)	PROTOTYPE (m)		
M52RT1	20	0.80	15.84	121.36
M52RT2	20	0.80	15.10	156.27
M53RT1	30	1.20	14.83	171.37
M54RT1	40	1.60	16.75	88.93
M54RT2	40	1.60	15.09	156.80
M55RT1	50	2.00	16.71	90.15
M55RT2	50	2.00	14.72	177.93
M56RT1	60	2.40	18.01	57.82
M56RT2	60	2.40	16.94	83.34

Table 4.6 Model tests for 50mm (2.00m in prototype) breadth.

TEST NAME	DEPTH		MOISTURE CONTENT (%)	COHESION (kN/m^2)
	MODEL SIZE (mm)	PROTOTYPE (m)		
M62RT1	20	0.80	14.85	170.20
M63RT1	30	1.20	16.52	96.20
M63RT2	30	1.20	14.91	166.75
M64RT1	40	1.60	14.86	169.62
M65RT1	50	2.00	16.78	88.02
M65RT2	50	2.00	15.02	160.60
M66RT1	60	2.40	16.37	101.26
M66RT2	60	2.40	16.06	112.57

Table 4.7 Model tests for 60mm (2.40m in prototype) breadth.

Breadth (m)	Rotation of pile from vertical axis		
	0.50°	1.00°	1.50°
0.80	0.38579	0.51180	0.62308
1.20	0.65519	0.83994	0.98112
1.60	0.88805	1.11653	1.30604
2.00	1.30810	1.54854	1.74035
2.40	1.72547	2.12531	2.41719

Table 4.8 Values of the slopes of straight lines (m^2).

Parameter	Rotation of pile from vertical axis		
	0.50°	1.00°	1.50°
α_{v1}	0.33261	0.45936	0.58004
α_{v2}	0.15922	0.16999	0.18872

Table 4.9 Values of parameters α_{v1} and α_{v2}.

4.6 Notation for Plates 4.1 to 4.6

a) Plate 4.1

(1) Soil bin
(2) Motor
(3) Steel tamper
(4) Clamp
(5) Displacement transducers
(6) Pulling Cable
(7) Pulling rod

b) Plate 4.2

(1) Pulling rods
(2) Load cell
(3) Displacement transducers
(4) Model piers

c) Plate 4.3

(1) Model piers
(2) Pulling Cable
(3) Pulling rod

d) Plate 4.4

(1) BBC MASTER computer
(2) Epson printer
(3) Plotter
(4) Data logger

e) Plate 4.5 & 4.6

(1) Motor-gearbox system
(2) Pulling cable
(3) Pulling rod
(4) Displacement transducers

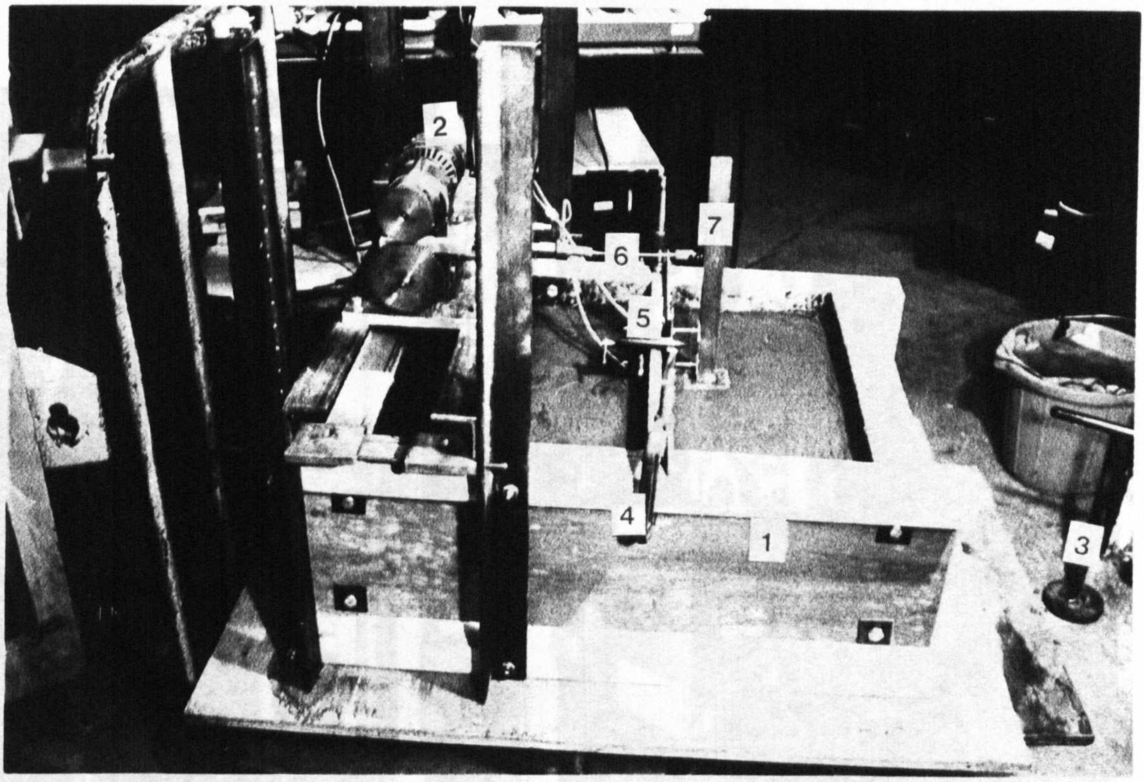

Plate 4.1 General layout of the apparatus.

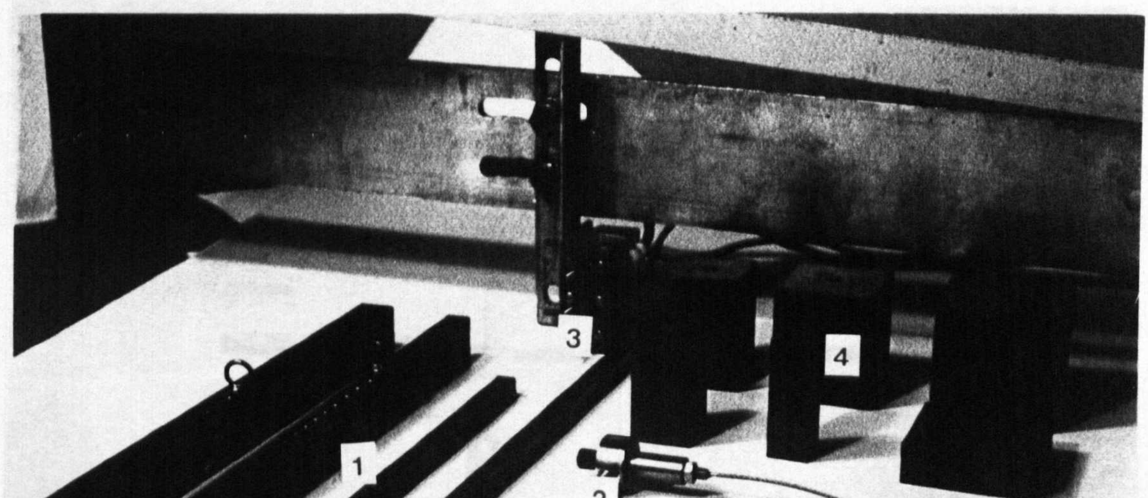

Plate 4.2 Model piers and other equipment used in the tests.

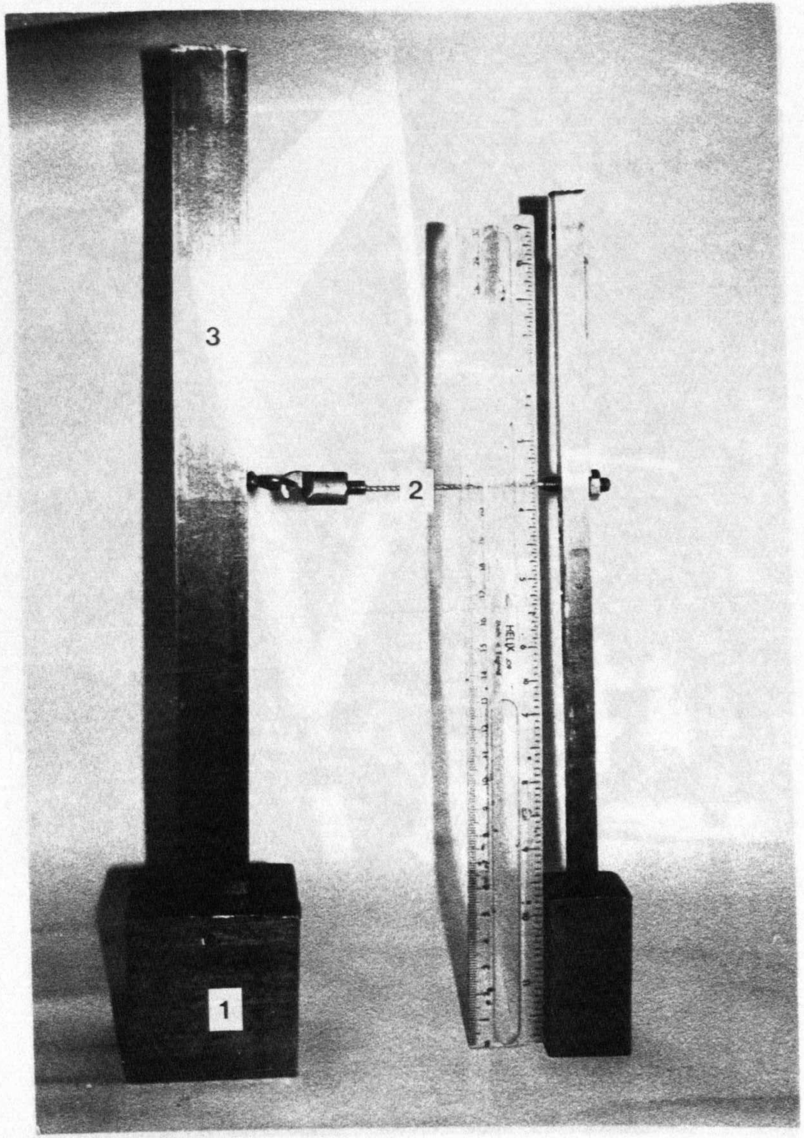

Plate 4.3 Pulling cable connection.

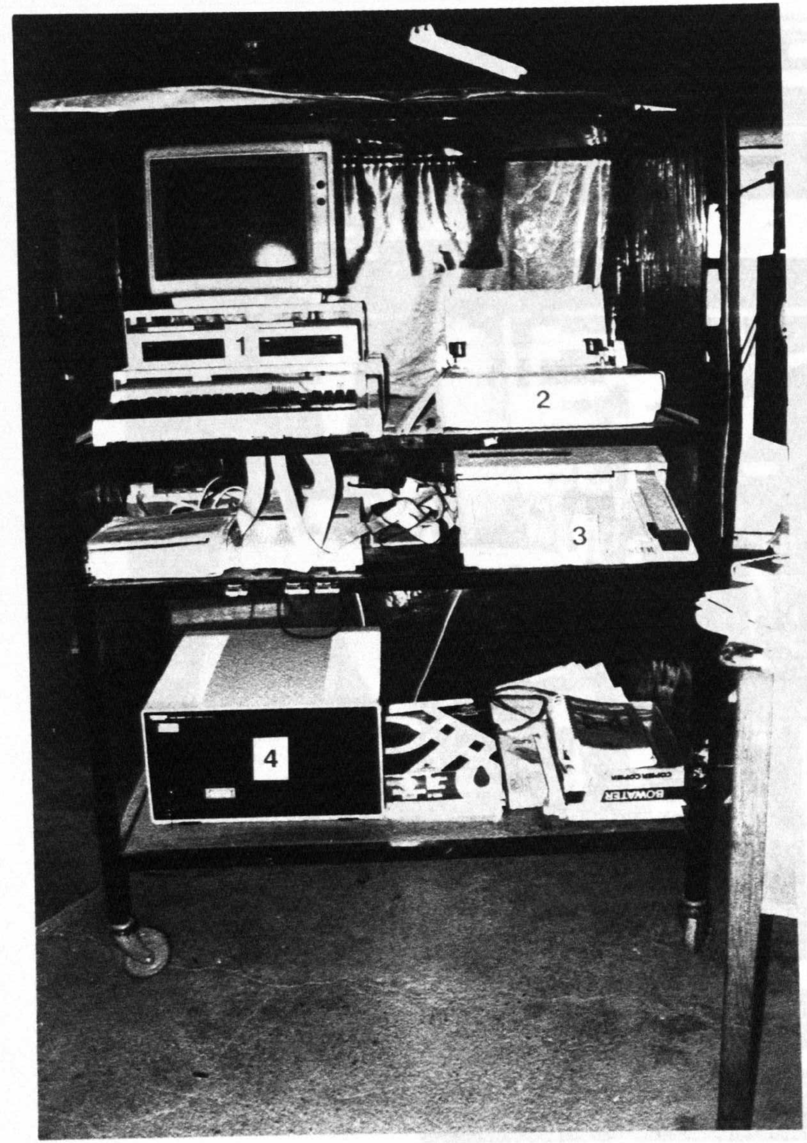

Plate 4.4 Data acquisition system.

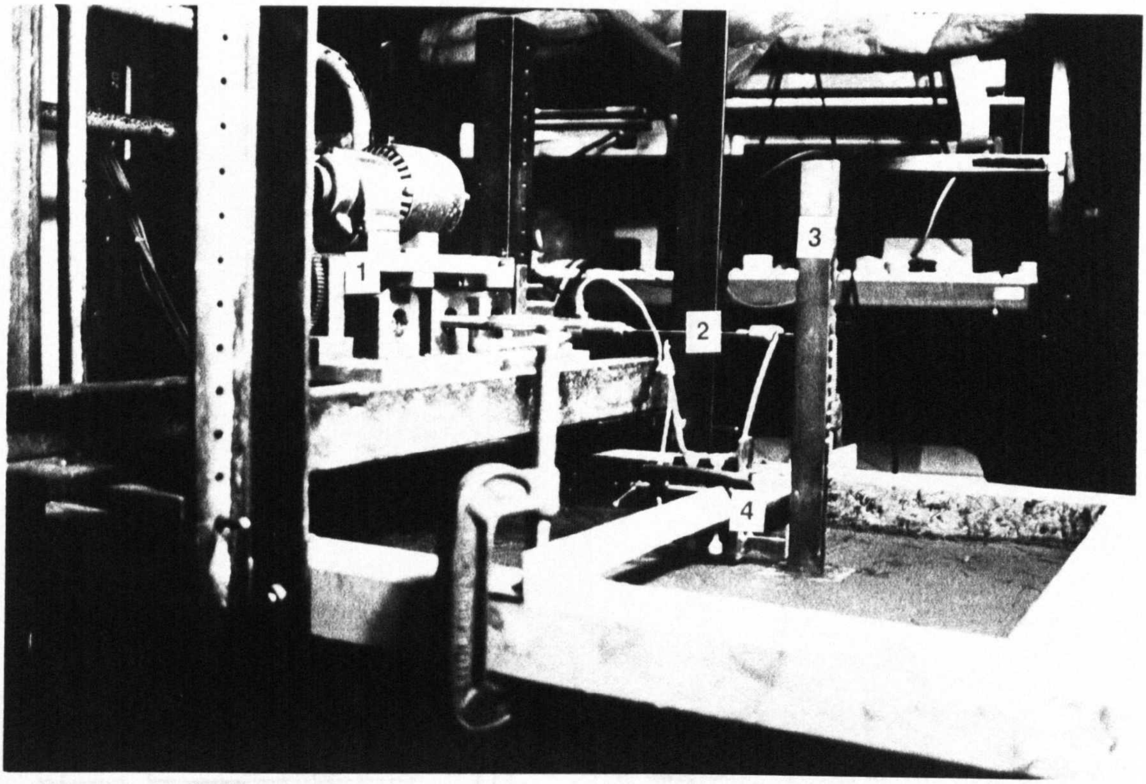

Plate 4.5 Experimental apparatus before test.

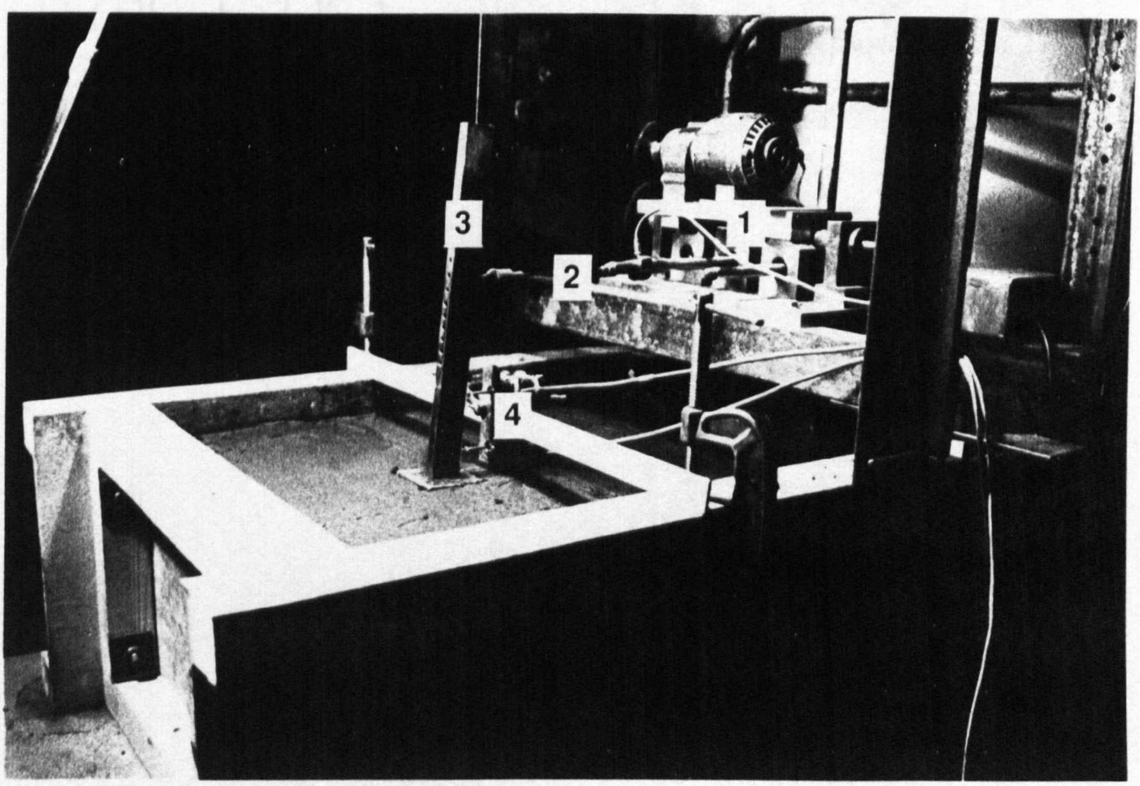

Plate 4.6 Experimental apparatus after test.

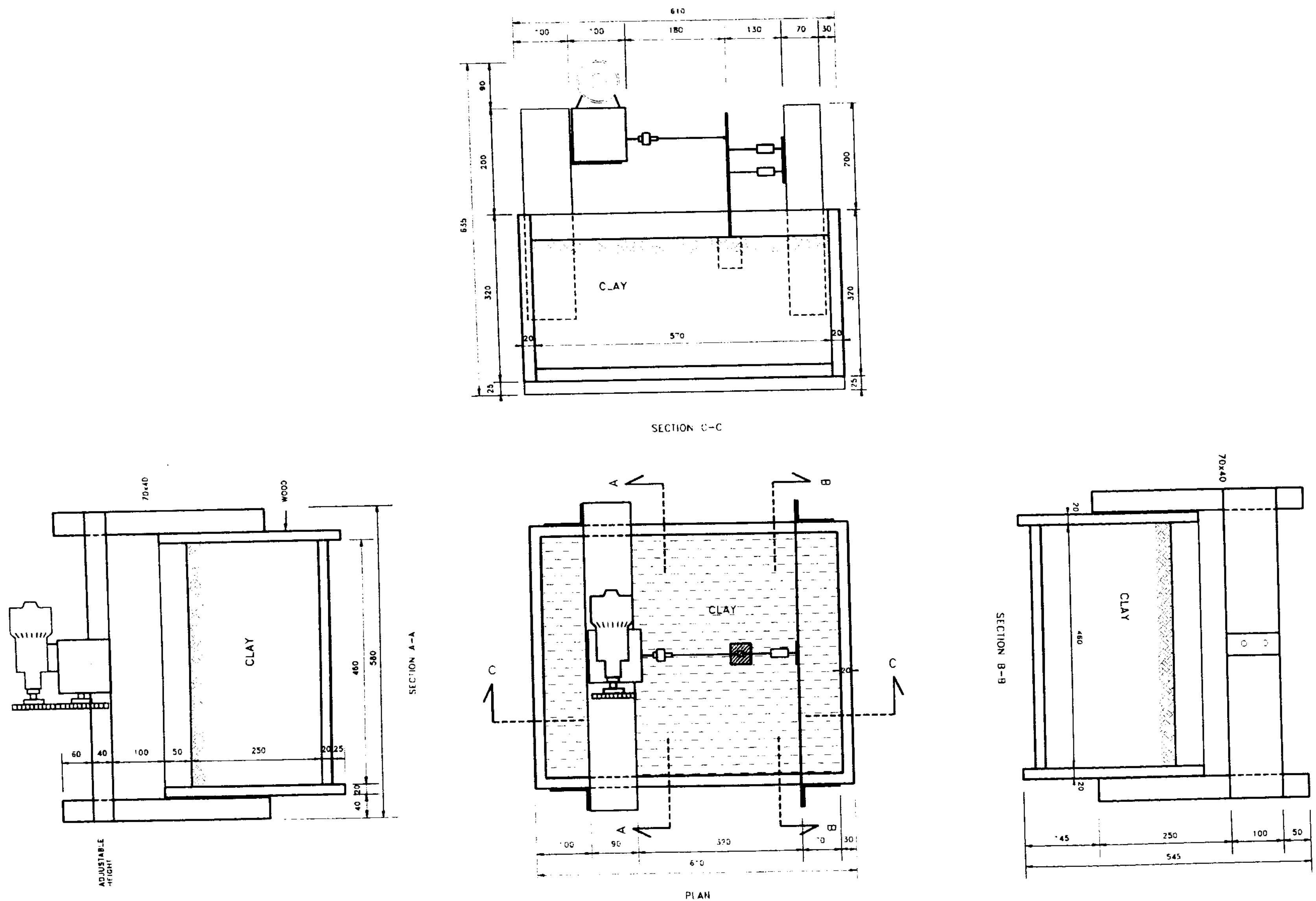

Figure 4.1 General layout of the apparatus.

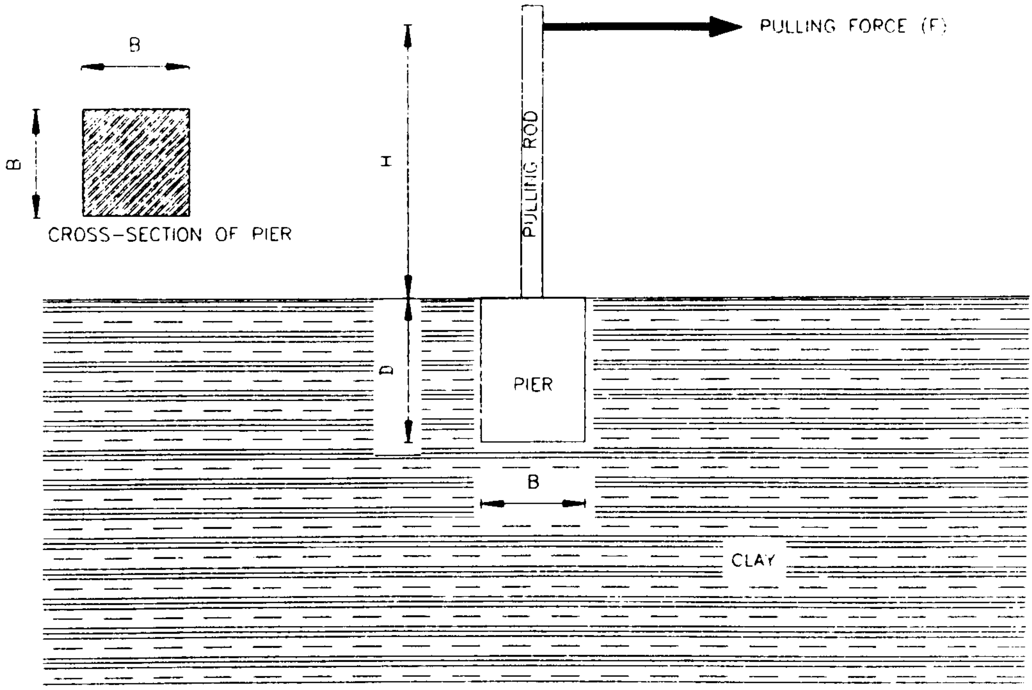

Figure 4.2 Cross section of the model pier.

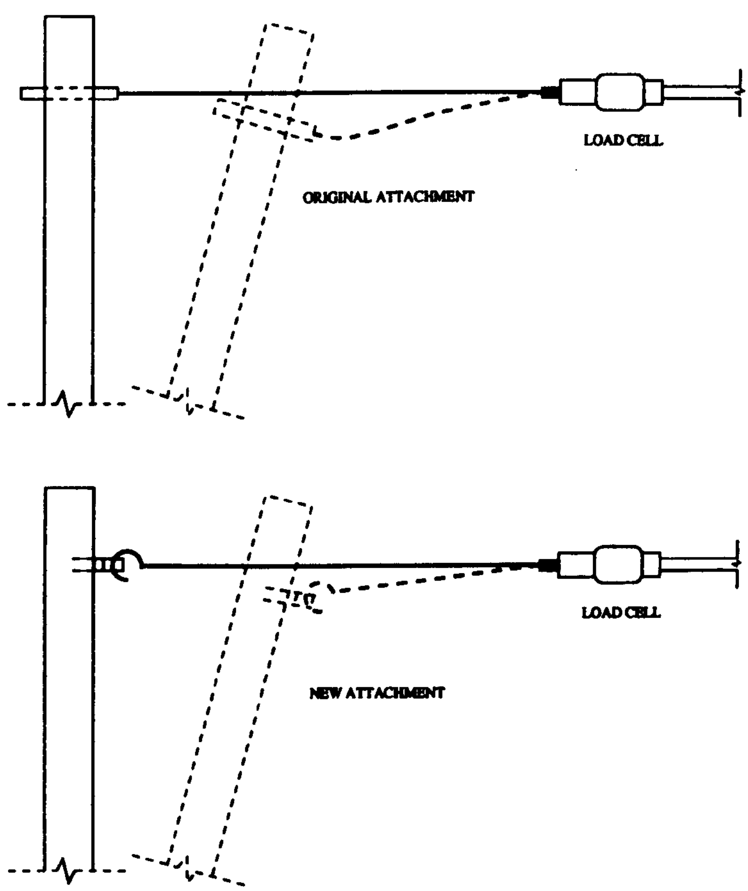

Figure 4.3 Pulling cable connection details.

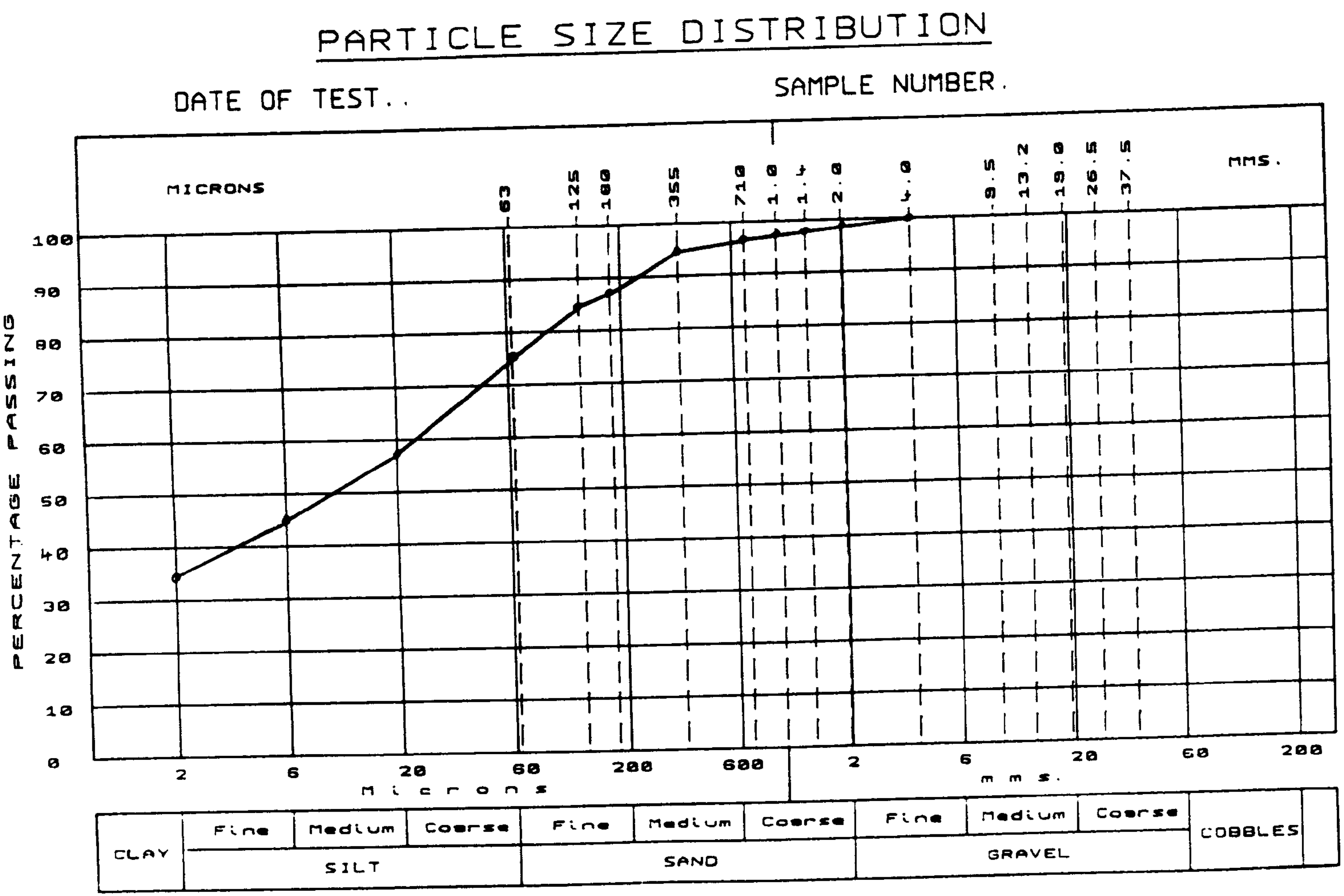

Figure 4.4 Particle size distribution curve of the clay.

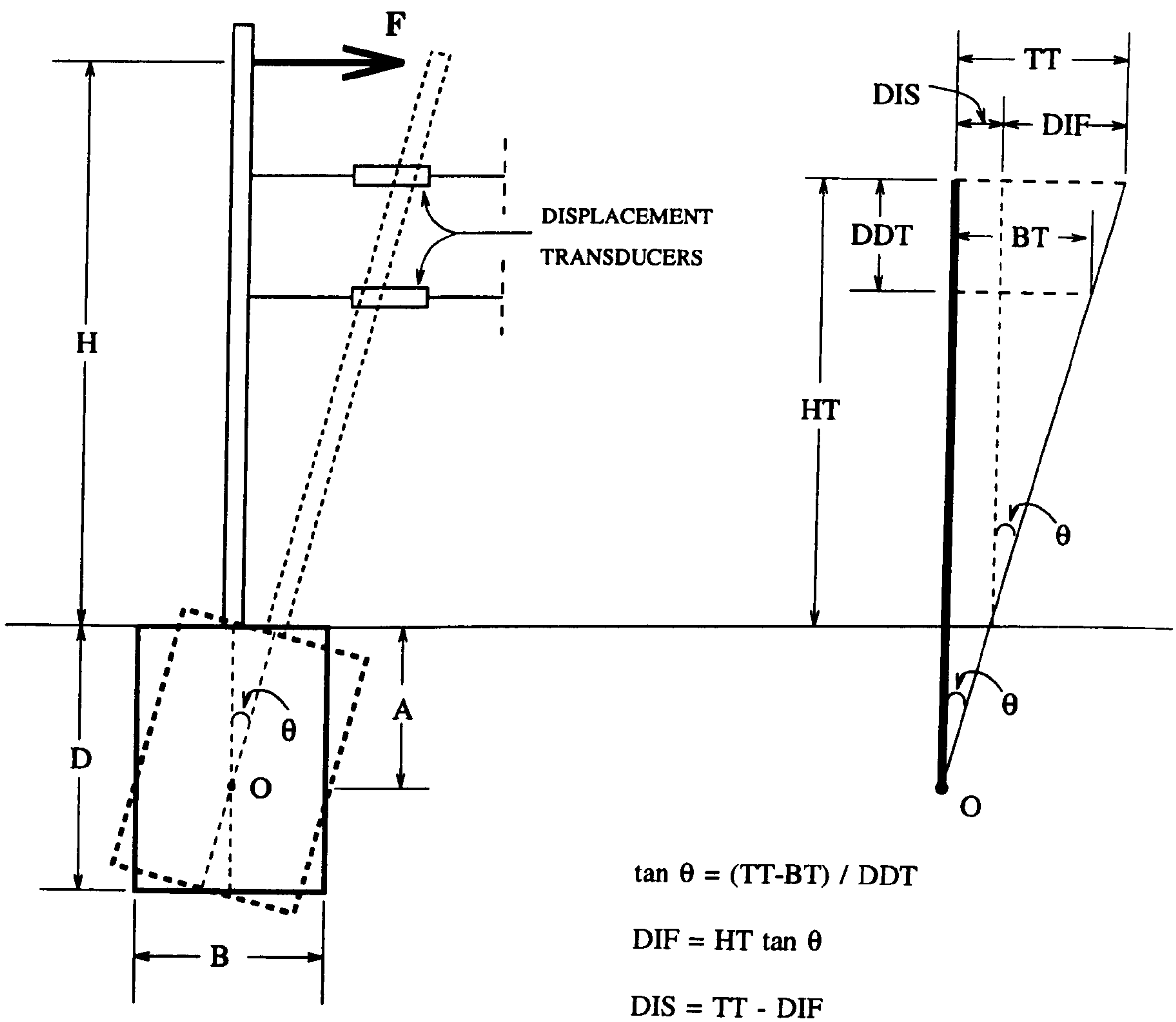

Figure 4.5 Calculation of lateral displacement at ground level and rotation.

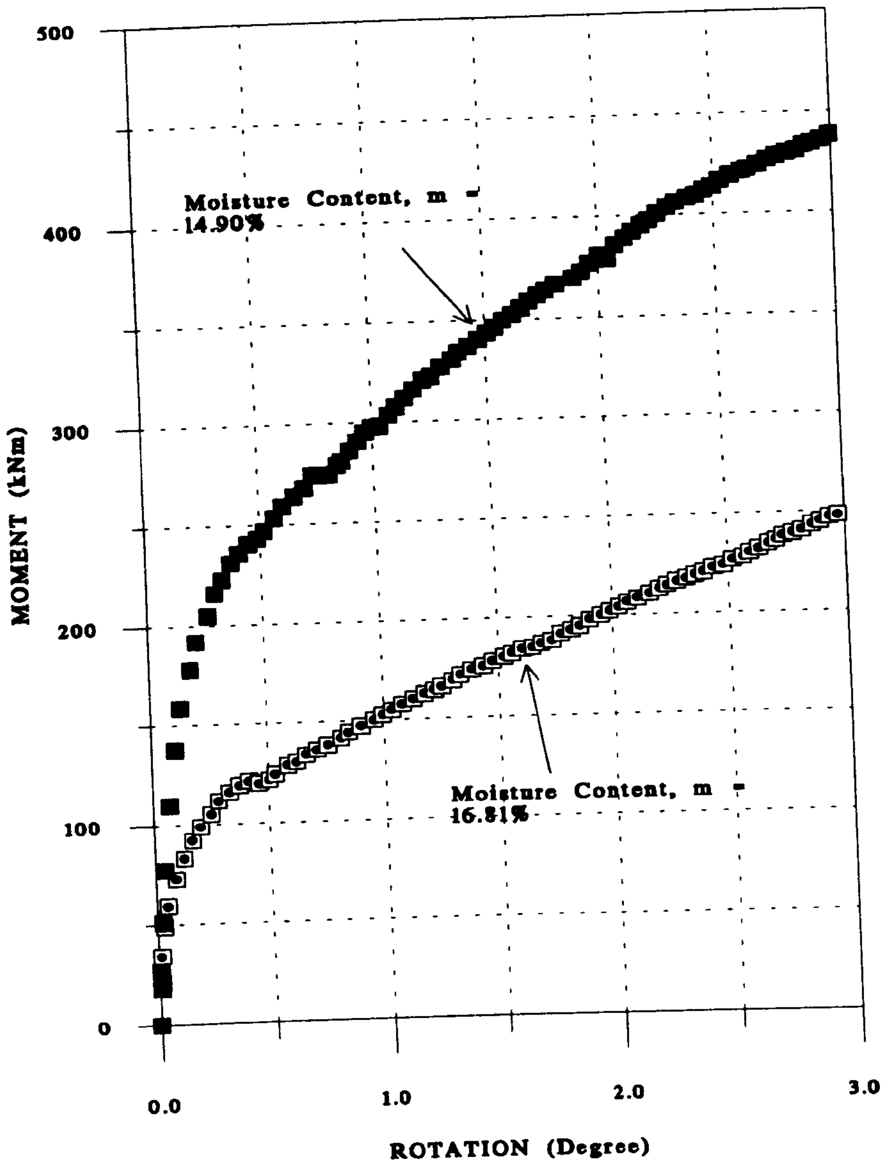

Figure 4.6 Moment against rotation (B=1.20m, D=2.0m).

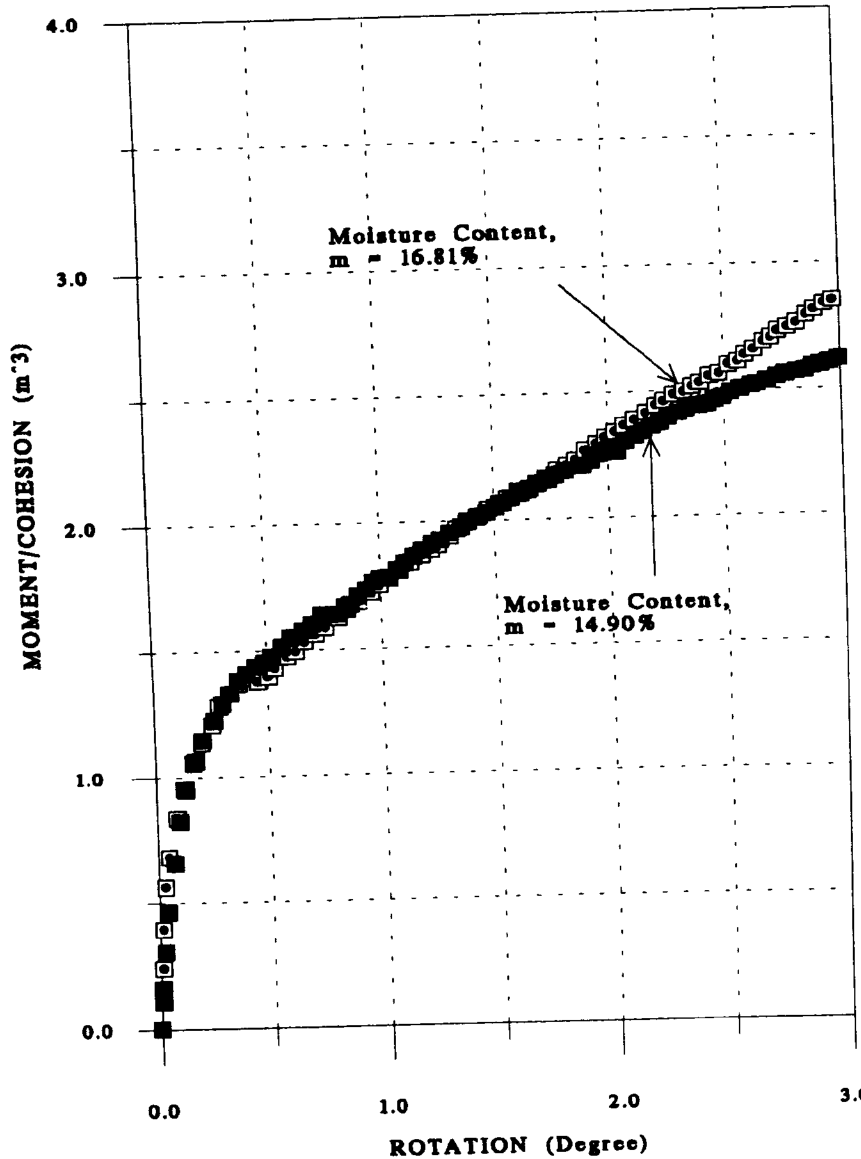

Figure 4.7 Moment/Cohesion against rotation (B=1.20m, D=2.0m).

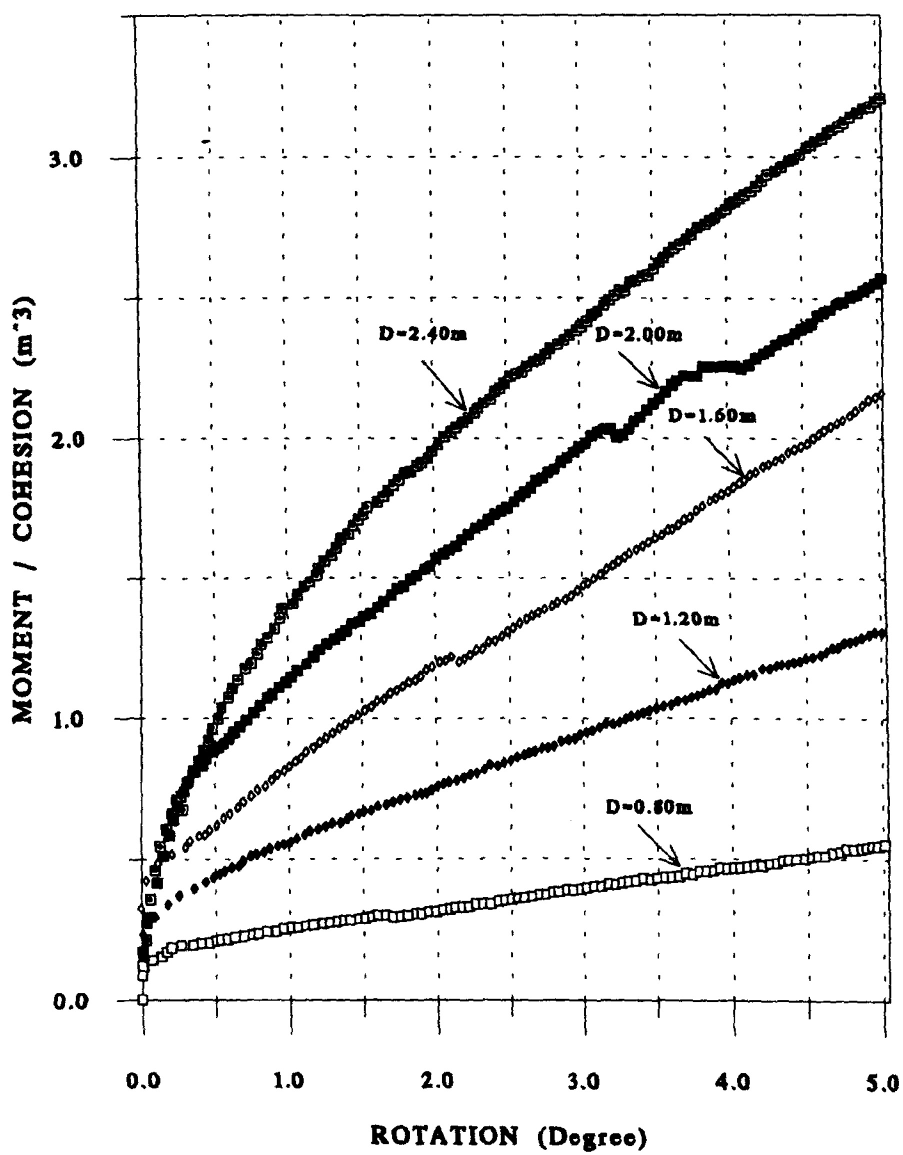

Figure 4.8 Moment/Cohesion - Rotation curves for 0.80 m prototype breadth.

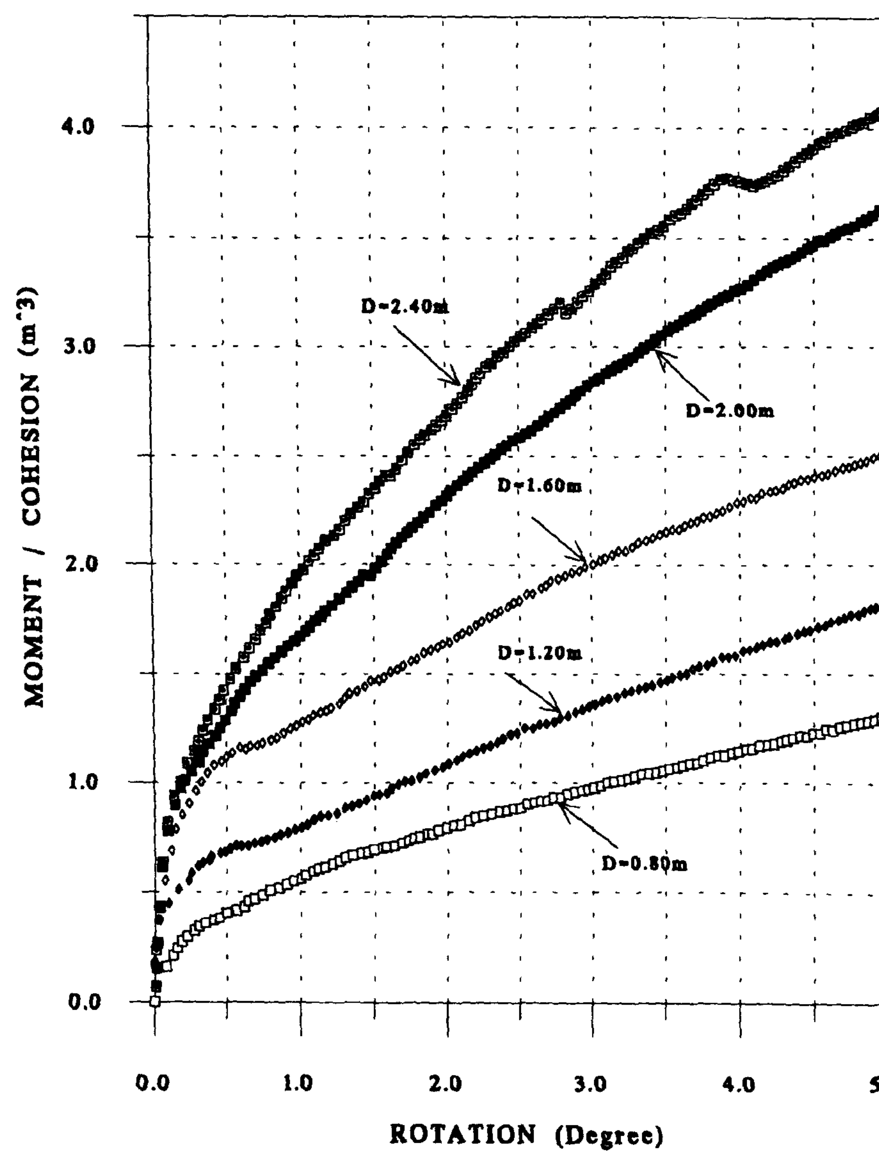

Figure 4.9 Moment/Cohesion - Rotation curves for 1.20 m prototype breadth.

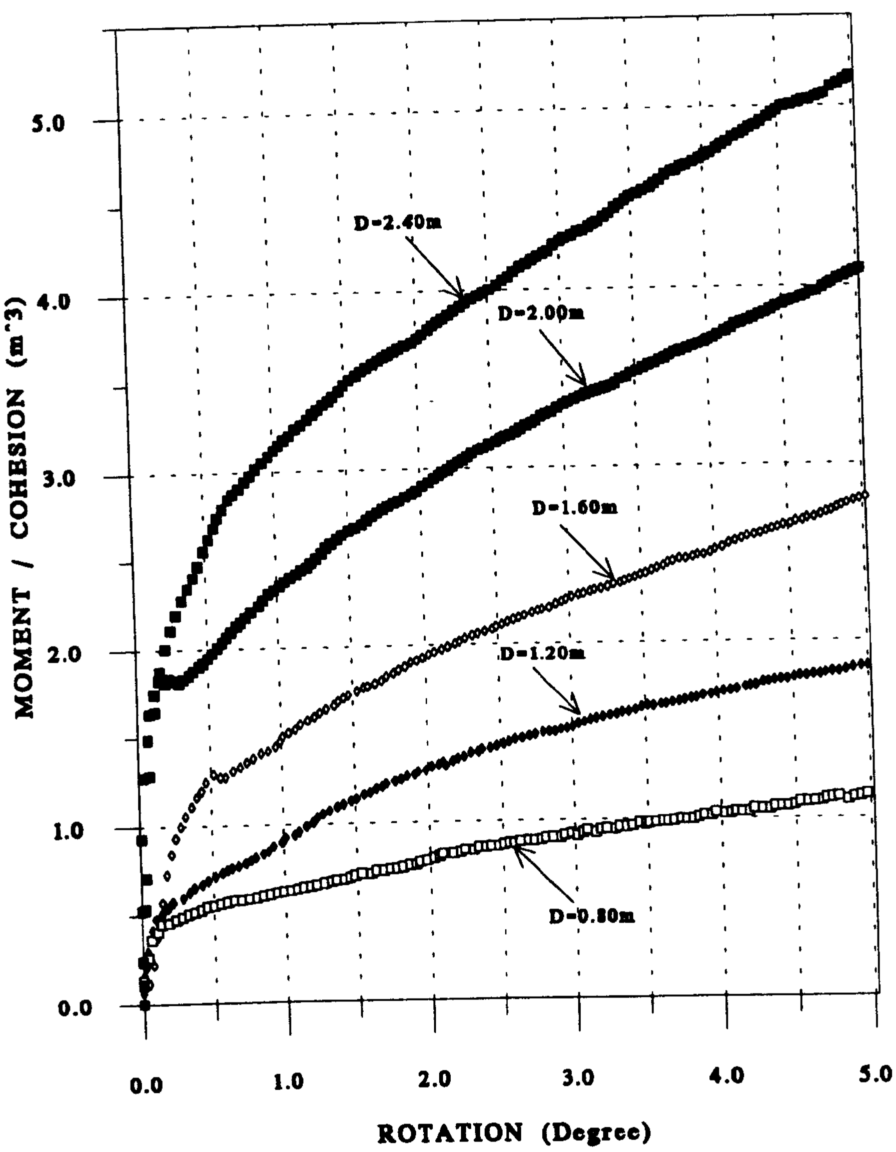

Figure 4.10 Moment/Cohesion - Rotation curves for 1.60 m prototype breadth.

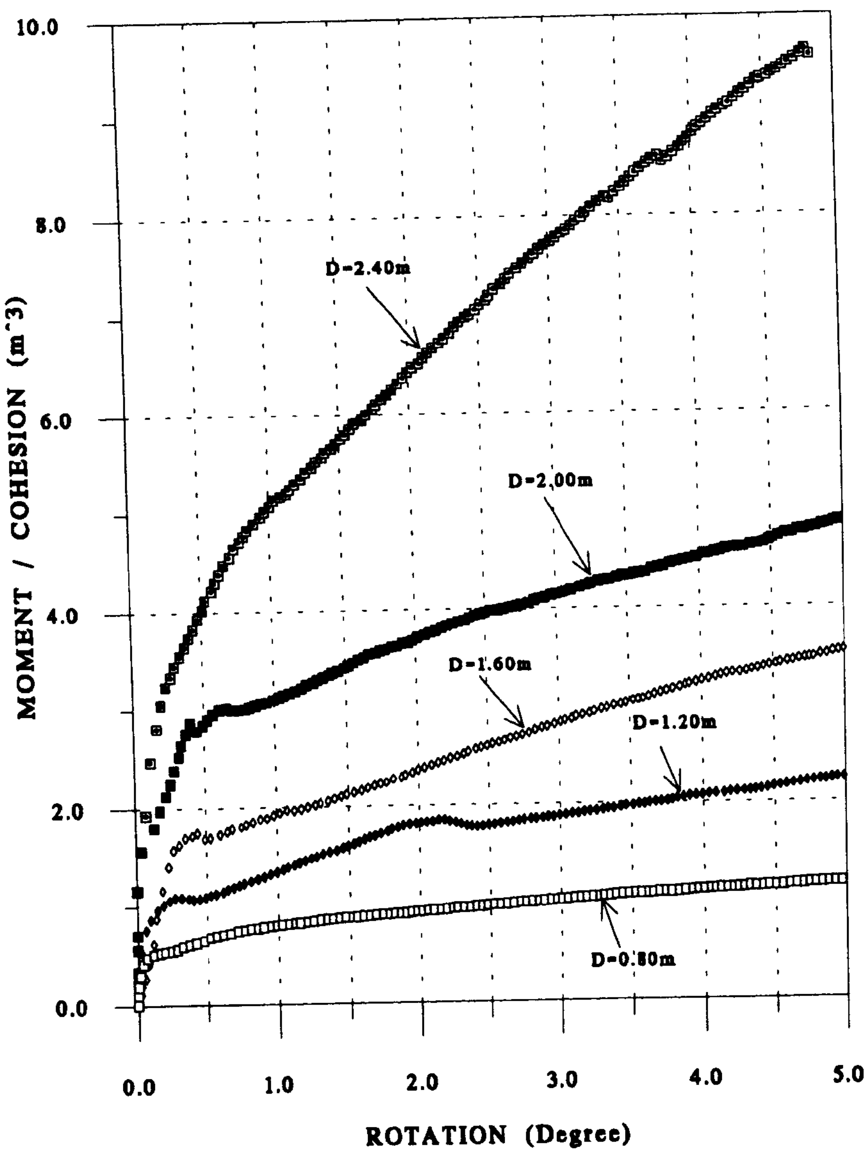

Figure 4.11 Moment/Cohesion - Rotation curves for 2.00 m prototype breadth.

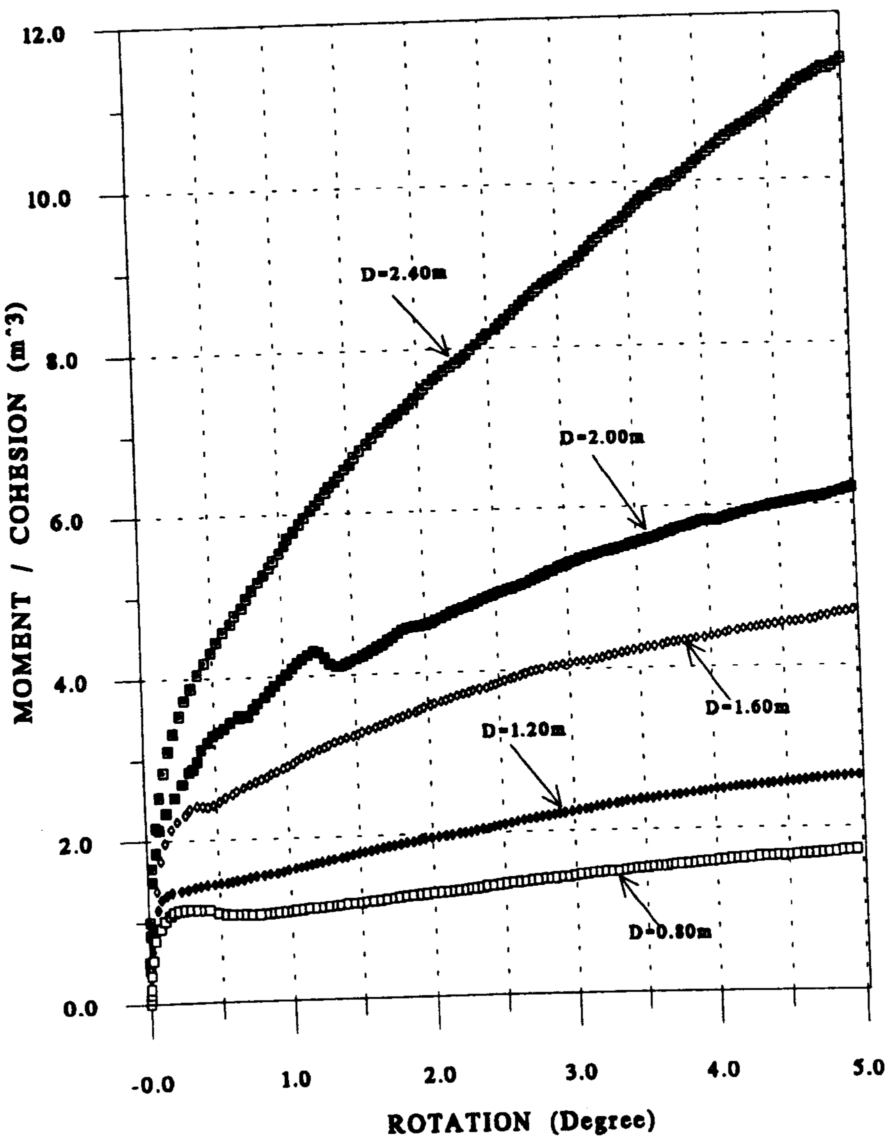

Figure 4.12 Moment/Cohesion - Rotation curves for 2.40 m prototype breadth.

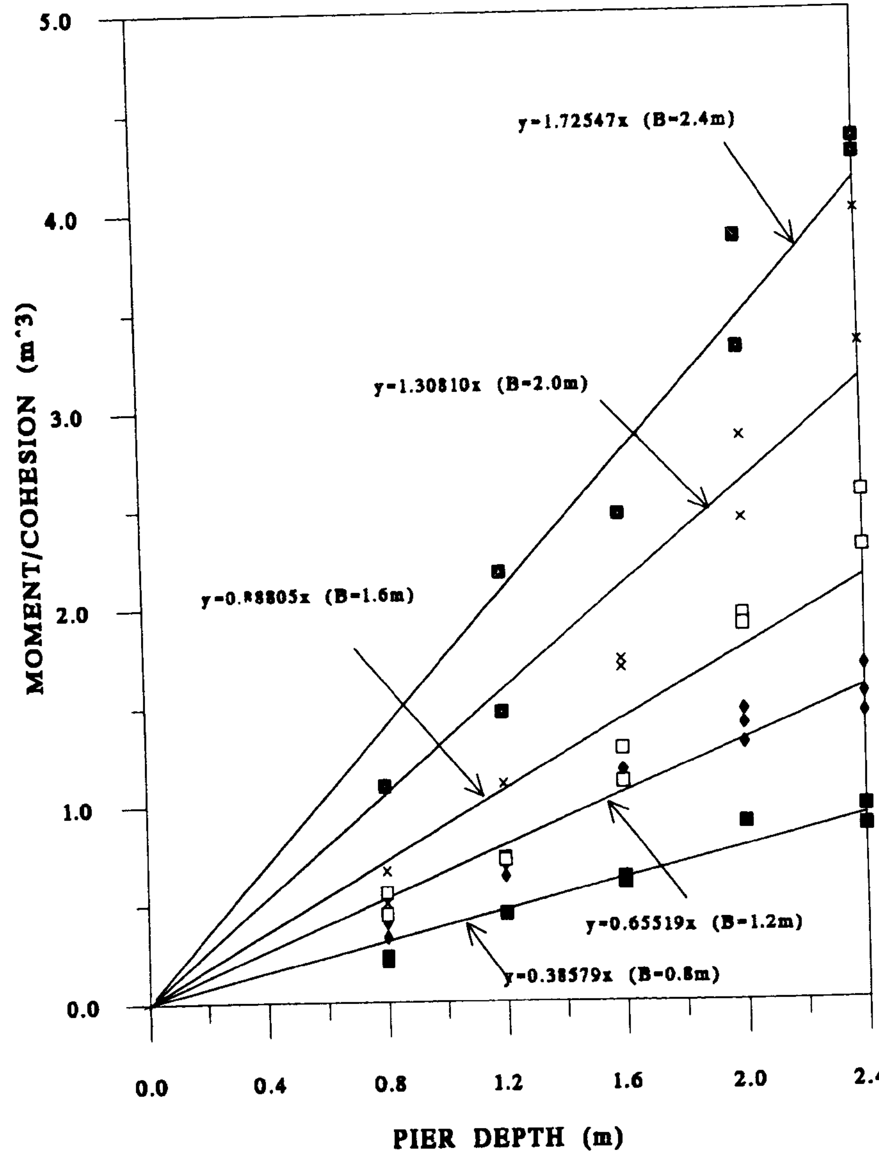

Figure 4.13 Moment/Cohesion against Pier Depth for 0.5 Degree Rotation.

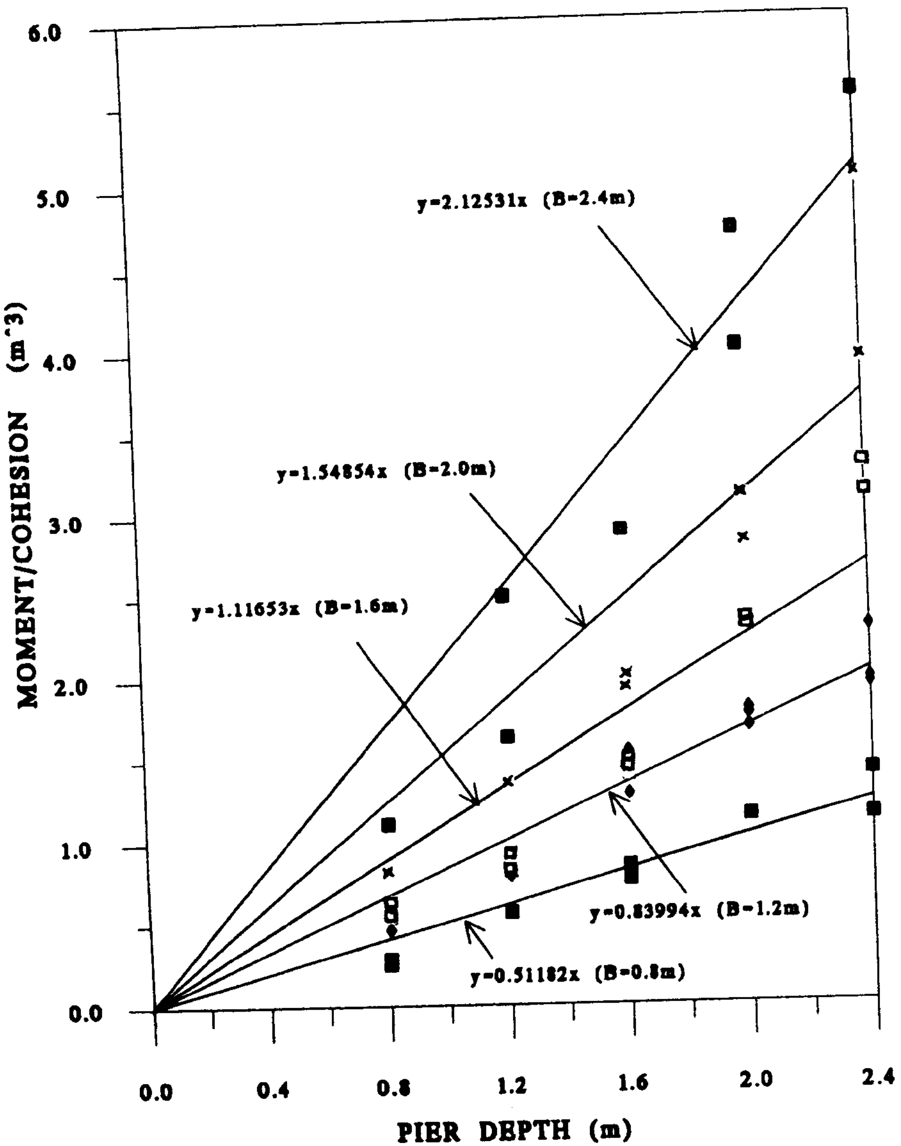

Figure 4.14 Moment/Cohesion against Pier Depth for 1.0 Degree Rotation.

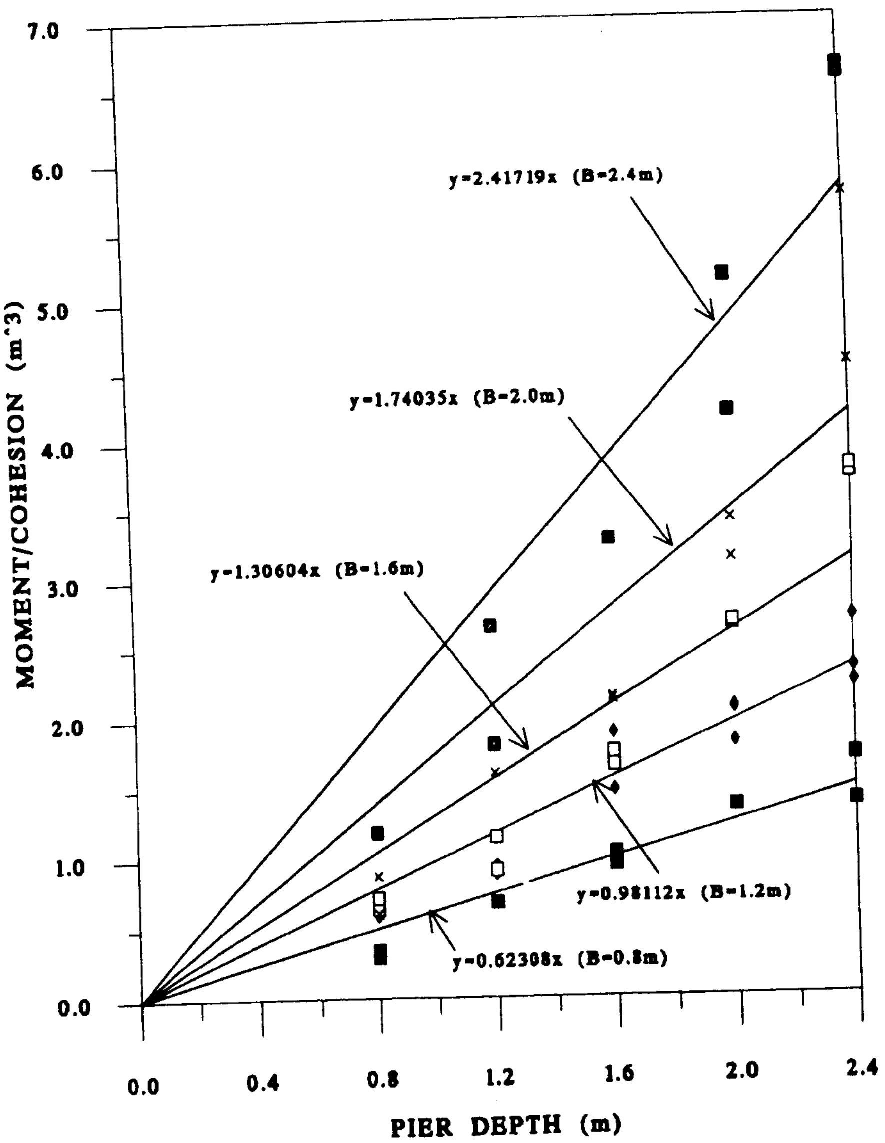

Figure 4.15 Moment/Cohesion against Pier Depth for 1.5 Degree Rotation.

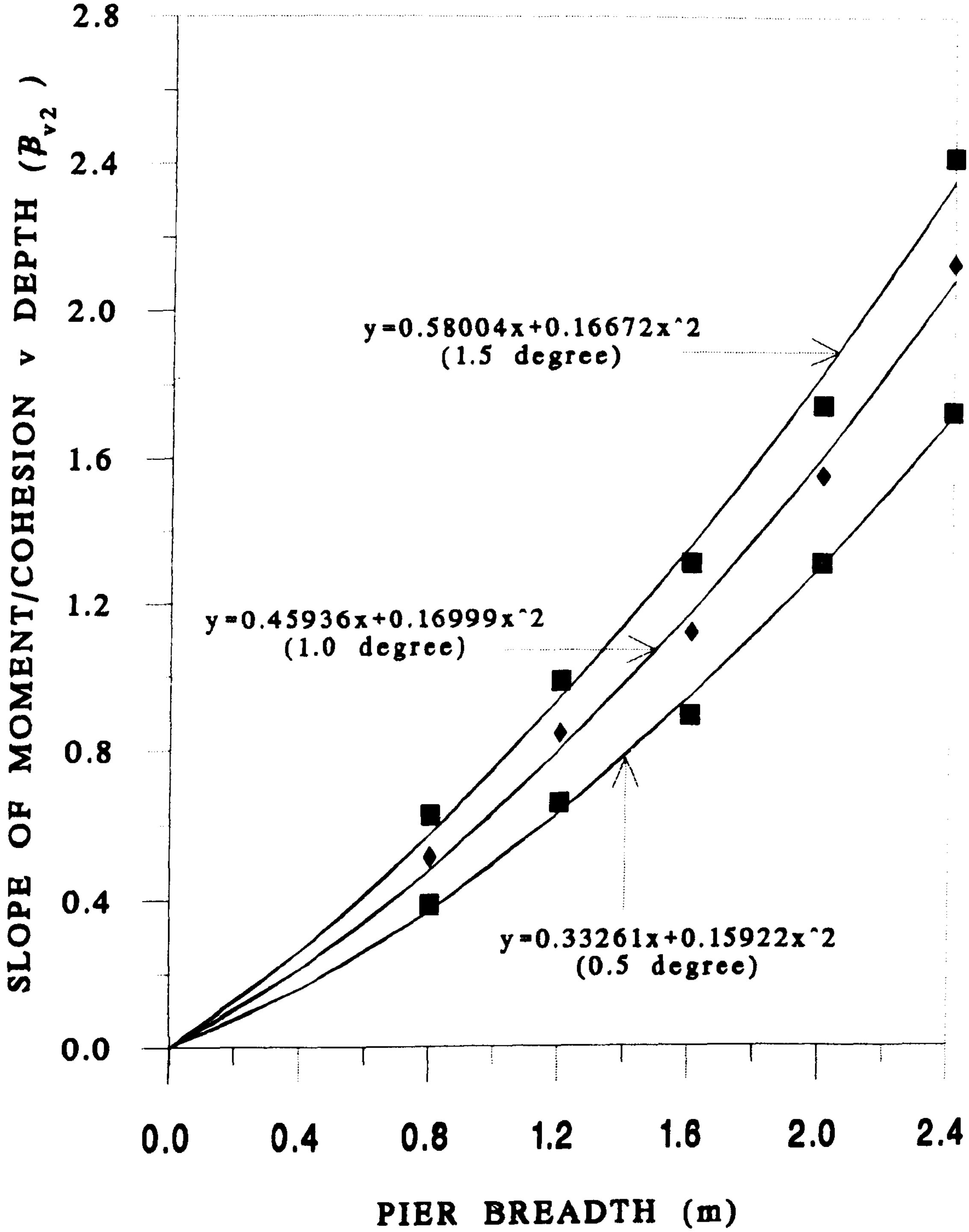

Figure 4.16 Slope of Moment/Cohesion against Pier Depth graphs against Pier Breadth.

CHAPTER 5

CENTRIFUGE MODEL STUDIES OF SHORT PIER FOUNDATIONS IN CLAY

5.1 Introduction

It is very important in soil mechanics and foundation engineering to be able to make realistic predictions of the behaviour of a prototype by using a small scale laboratory model. However, in order to make accurate predictions, models must be tested at identical stress levels to those in the field. Centrifugal modelling is one of the convenient methods to achieve this requirement.

Initially, it was expected that, for undrained behaviour of rigid foundations in saturated clay, the influence of self weight of soil would not be significant. Hence, only a few centrifugal model tests were planned to confirm this. After these tests were performed in the centrifuge, comparisons were made with the relevant conventional test data. From these comparisons, even in the range of pier depths used, it was seen that the scale effect was significant. Therefore, it was decided that an extensive series of centrifugal model tests should also be carried out.

The centrifugal model tests were carried out in the Liverpool University Geotechnical Centrifuge Laboratory. A centrifugal acceleration of 40g was employed so that stresses due to self weight of soil would be modelled correctly at 1/40th scale. As in the conventional model tests, the short, square model piers with different dimensions were tested in the saturated clay to investigate their short term response when they were subjected to a large overturning moment as a result of a horizontal loading applied at an appreciable height.

In this chapter, the basic principles and scaling laws of centrifuge modelling are outlined. The Liverpool University Centrifuge and ancillary experimental apparatus are described together with the procedure for testing the model piers. The results obtained from the tests are then presented and an alternative empirical equation, to the one obtained from the conventional model study, developed to fit the data.

5.2 Basic Principles and Scaling Laws of the Centrifuge Modelling

Body forces are very important factors in many geotechnical problems. In ordinary 1g model testing body forces are insignificant and in order to achieve similarity of behaviour between a prototype and a small scale model the body forces must be represented properly. Also the strength of many soils are dependent on stress levels. However in this study, which involves forces applied from a rigid structure to a soil whose strength is not stress dependent, centrifuge modelling was not at first thought to be necessary.

However, since the lateral stress which develops to some depth behind the pier is tensile, vertical tension cracks are likely to develop. In a cohesive soil (ϕ=0) in an active state the depth of the cracks, h_c, are given by;

$$h_c = \frac{2\,c}{\gamma} \tag{5.1}$$

This depth will therefore be influenced by the stress levels and in order to scale it correctly it was decided that the centrifugal modelling technique would be necessary.

In the centrifuge, a model of the prototype at a scale of 1/n is subjected to a gravity field of n times the earth's gravity, g, in order to achieve identical stresses at geometrically similar points in the ground. A listing of the scaling factors for centrifuge tests between the model and prototype values is shown in appendix D. The description of basic theory and the scaling laws of centrifugal modelling have been reported in detail by various workers e.g. Avgherinos and Schofield (1969), Ovesen (1979), Basset and Horner (1979), Schofield (1980, 1988).

When a centrifuge spins at angular velocity ω the acceleration at radius r is $\omega^2 r$ thus although the stress levels between model and prototype can be made similar, they will not match at all points over the depth of a model. The linear variation of acceleration with depth through the model causes a non-linear variation of stress while the correct variation in the prototype is linear. The calculation of the percentage error in the stress levels between the centrifuge modelling and prototype is presented in detail in appendix E. When an optimum scaling radius measured to 1/3 rd of the depth of the soil is used similarity of stress levels is achieved both at the soil surface where they are zero and at the 1/3 rd of the depth up from the base of soil bin. At all points between the soil surface and the layer where the correct stress occurs there is a slight pressure deficiency in the model. Below that depth there is overstress at all points. In the Liverpool centrifuge when swinging buckets are used, the maximum percentage error in stresses between model and prototype for the maximum depth of model is less than 3.5%.

5.3 The Liverpool University Geotechnical Centrifuge

The centrifuge model tests were performed by using the Liverpool University Geotechnical Centrifuge (LUGC), described in detail by King, Dickin and Lyndon (1984). The LUGC was completed in 1973. The medium-sized machine is a Model G.380.3A supplied by Triotech Inc. of California and it has been in operation since 1978. In this section, some important features of the machine are highlighted.

A general view of the centrifuge is shown in plate 5.1 and details given in figure 5.1. It consists of a cylindrical steel enclosure 3.00m in diameter by 1.70m in height which houses a 20-hp drive motor, drive shaft, rotor arm and test package carriages. A rotating arm 2.6m long, made of two steel channels, is fitted with buckets at both ends. The centrifuge had been originally used with fixed buckets but these were subsequently changed to swinging buckets to facilitate the construction and testing of models in granular soils. These swinging buckets are 570mm long, 460mm wide and 232mm deep and facilitate the construction and testing of models in any soil. With maximum depth of soil in a package, the optimum scaling radius is 1.15m. The machine can develop a maximum acceleration of 200g at 380 rpm for a package weight of less than 100kg. However the maximum permissible acceleration is limited by package weight to about 115g by the centrifugal capacity of the machine which is 25.0 g-tonnes. The acceleration and the deceleration times of the machine are completed in a very short time (e.g. 3 to 4 min.). The speed of the machine is measured by a magnetic pick-up which senses electrical impulses from a toothed wheel on the main drive shaft. Although there are two swinging soil bins located on the ends of the rotating arm, it is usual to test one only while the other, together with the additional weights, provides a counter-balance. A release mechanism is used in order to balance the rotating arm and packages statically about a horizontal pivotal shaft. The input into and the output from the centrifuge are achieved through a 60 slip ring assembly placed on the top of the steel enclosure as seen in figure 5.1 and plate 5.1. The output received from the slip ring assembly is fed to an Orion data logger. A closed circuit monochrome video camera mounted on the rotor arm close to the drive shaft allows observation of the progress of the tests on a monitor.

The LUGC has been used mainly for postgraduate research, together with third year projects, for studying a variety of problems. A number of recent and current centrifugal model studies have been published in the literature, for example, by Dickin and Leung (1983 and 1985) on anchors, by Lyndon and Pearson (1984), King and McLoughlin (1992) on retaining walls, by Chandrasekaran et al. (1984), Kulkarni et al. (1985), Fulthorpe (1986), King and Fulthorpe (1986), Dickin and Wei (1991), Dickin and Leung (1990 and 1992), Leung and Dickin (1991), and Dickin and Nazir (1992, 1993, 1994a and 1994b) on piles.

5.4 Centrifuge Model Tests

5.4.1 Model piers

The same model piers used in the conventional tests were tested in the centrifuge to enable a comparison of the results to be made. The dimensions of the model piers are presented in table 4.1 together with their equivalent prototype sizes.

5.4.2 Equipment

The apparatus may be considered as composed of four main parts which are soil bin, motor-gearbox system, displacement transducers and recording and monitoring equipment. These are described briefly in the following sections. The general layout of the apparatus is illustrated in figure 5.2, plate 5.2 and plate 5.3.

5.4.2.1 Soil bin

One of the two existing soil bins attached to the centrifuge was used in the tests while the other one was kept full with sand to provide a counter balance as shown in plate 5.4. Prior to use, the metal bin had to be isolated from the damp cohesive soil by covering its inside walls and base with waterproof cloth tape.

5.4.2.2 Loading arrangement

As in the conventional tests, lateral loads were applied at appreciable heights which results in large overturning moments. The applications of the lateral loads were through a small, low speed high torque AC PARVALUX (model 21SIS) motor and gearbox unit together with a wormdrive, worm wheel and screwjack system. The motor and gearbox unit is shown in plate 5.5. In the tests, the rate of displacement of the pulling rod at the connection point (150mm above the clay surface) was approximately 1.074mm/min. The motor was operated externally via the slip ring system. The load in the pulling rod was measured by a 1500lb (6.681kN) SENSOTEC (model 31) load cell supplied by RDP electronics. Before using the load cell, it was calibrated in tension against a standard pre-calibrated proving ring. The readings from the calibration tests and the relevant graph are given in appendix B together with the calibration values. The same vertical pulling rods were used as in the conventional tests described in section 4.3.1.3. A pulling cable which was made of stainless steel was used to connect the load cell and the vertical rod. One end of the cable was screwed on the load cell and the other end was attached to a ring fastened in a hole in the pulling rod with a hook. The detail of this connection is shown in figure 4.3.b. The output from the load cell to the data logger was by means of the slip rings.

5.4.2.3 Measurement of displacement

The lateral displacements of the pulling rods were measured via three SAKAI conductive potentiometers. They were capable of monitoring displacements up to 25mm. The calibration factors of these transducers obtained from the calibration tests are given in appendix B together with the data and relevant graphs. They were fixed at 20mm apart on a metal bar which was attached to a cross beam. In order to get a suitable height to accommodate the displacement transducers, small metal plates with holes drilled at their centres were used. The frame with the displacement transducers was placed on these plates and screwed on the soil bin. The signal from the transducers to the data logger was by the aid of the slip rings.

5.4.3 Data acquisition and monitoring equipment

Progress was monitored throughout the tests by means of a monochrome video camera and a monitor system. The output from the transducers and load cell was transmitted to an ORION data logger. A computer program "ROT2" running on a BBC micro-computer was used to control the data logger. A photograph showing the general view of the recording and monitoring equipment is shown in plate 5.3.

5.4.4 Soil properties

The same remoulded saturated silty clay was used as in the conventional tests described in Chapter 4. Its main physical properties are given in table 4.2 in section 4.3.2.

5.4.5 Initial preparation of the soil and bin

The existing unused clay was mixed with the same clay used in the conventional tests. In order to obtain a reasonably homogeneous moisture content distribution in the mixed clay, it was mixed twice using a pug-mill. Prior to use, the swinging bucket had to be divided into two parts. One part of it was for loading devices and the other part, which was 400mm long, 460mm wide and 232mm deep, was for the clay, pier and displacement transducers as shown in plate 5.2.

During the compaction of the clay, the swinging bucket was supported and the balancing lock of the central shaft was locked to protect the centrifuge shaft as shown in plate 5.6. The compaction procedure used for the clay was the same as in the conventional tests. When preparation of the clay bed was completed, damp burlap was placed on its surface and then the bucket was covered with a sheet of plastic to prevent evaporation of moisture.

5.4.6 Test procedure

After completing the compaction of the clay, to a depth of 180 mm, together with the installation of the pier, the load cell was placed in between the motor and a steel pulling cable. The pulling rod was then screwed on top of the pier. Great care was taken to make sure that the pulling cable was horizontal. Subsequently the frame carrying the displacement transducers was placed on the soil bin and secured with the aid of a long screw. Small pieces of double sided sticky tape were placed between the vertical pulling rod and the displacement transducers to ensure a positive contact at all times as in the conventional tests.

After the preparation of each test package, the precise distance "x" between clay surface and top of the soil bin was measured. An optimum scaling radius was then calculated as shown in figure 5.3. The value of speed of rotation to give an acceleration forty times the earth's gravity field (40g), obtained using this optimum scaling radius, was between 173.5 to 174.0 r.p.m. in all tests.

Prior to testing, the lock mounted at the centre of the rotating arm was released and balancing achieved by changing the weight of sand in the unused swinging bucket.

The door of the steel enclosure was then closed and locked by a key. The centrifuge motor was then only allowed to operate when the key was placed in a safety door system box which does not let the key be taken while the centrifuge is running. The machine was then spun up to the test flight speed. During this stage the progress in the test package was monitored to see if any unusual movement occurred. Initial readings of the load cell and displacement transducers were recorded. Lateral load was then applied to the pier by the motor, activated remotely via the slip ring system. During tests the output from the load cell and transducers was recorded at 20 second intervals on the data logger and monitored on the screen of the computer. The speed of the machine was continually checked and adjusted slightly if required. The tests were carried out until the pier rotation reached about 5 degrees as in the conventional tests. The computer program and the application of the lateral load were then stopped and the speed of the centrifuge slowed down to 160 rpm. At this time an immediate plot of pier load against displacement at the location of the transducers was displayed on the computer screen to indicate whether the test results were satisfactory. Once the speed was under 160 rpm, dynamic braking was applied to stop the machine quickly and securely. Each test took 13 to 18 minutes depending upon the pier geometry and moisture content of the clay. After the door of the steel enclosure was opened, the frame carrying the displacement transducers, the load cell and pier were removed. A small sample of clay was taken from in front of the pier and used to determine the moisture content of the clay. The motor gear and worm drive were disconnected and the pulling cable returned to its initial position. The volume of clay removed with the pier was approximately 300mm by 200mm in plan and 150mm high. Only this material was recompacted when another pier was installed.

5.4.7 Experimental program

The experimental program consisted of approximately 58 tests including some tests repeated to ensure consistency in the results. As in the conventional tests, the piers were tested over a range of depths and breadths and a pulling height of 150mm (6m in prototype) was used. Since the time of completion of the centrifuge test program was shorter than that of the conventional one and as the soil bin used was made of metal, moisture content variation of the clay throughout the testing program was less than in the conventional tests.

5.4.8 Test results

All output data was received by a computer program (ROT2) run on the BBC microcomputer and stored on a floppy disc. A list of the data was also printed out from the Epson printer as a back-up. Using the same procedure as described in section 4.4 for the conventional tests, the values of moments and displacements at ground level were calculated by inputting the data from the floppy disc into an I.B.M. PC compatible system. This procedure is explained in detail together with listing of the relevant computer programs and sample data in appendix C. 43 out of the 58 tests were used to interpret the results. The reasons for discarding some of the test results were either that they were exact duplicates or that faults had developed in the operation of the displacement transducers. The model and prototype dimensions used and the moisture content values recorded are given in tables 5.1 to 5.5. Table 5.1 shows a series of tests on a model pier of 20mm breadth and using depths of embedment of 20 to 60mm in 10mm increments. Tables 5.2 to 5.5 show series of tests on model piers of 30mm to 60mm breadth using the same range of depths of embedment. The values of moisture content observed in the tests varied from 15.56% to 17.77%. The strength of the clay was affected by the variation of moisture content. Since the variation of moisture content was in the range observed in the conventional tests, equation 4.1 was again used to calculate the related cohesion values. These values are also given in tables 5.1 to 5.5.

As in the conventional tests, in order to establish the effect of the pier geometry on moment carrying capacity, moment-rotation relationships were considered for different
(See Appendix D)
pier geometries at prototype scale. Graphs of moment/cohesion against rotation for varying pier depths for the 0.80m pier breadth are shown in figure 5.4. It can be seen that the data points obtained in the graphs are scattered. While the test program was continuing, the reason for this was not identified. However after the test program was completed, the maximum limit of the load cell was compared with the data obtained and it was realised that the load cell was rather insensitive. Nevertheless, as discussed

later in section 5.5, it was decided that it was acceptable to use the average values of the scattered data. Figures 5.5 to 5.8 show graphs of moment/cohesion against rotation for varying pier depths for the 1.20m to 2.40m pier breadths at 0.40m increments. It can be seen that these relationships are nonlinear and do not exhibit any peak values. As with the conventional tests, attempts were made to define failure but no reasonable and consistent method was found. Therefore arbitrary rotations of 0.50°, 1.00° and 1.50° were again considered as alternative limiting working conditions. The moment/cohesion ratios required to cause each of these rotations were plotted against the depth of the pier, for different breadths of pier, as shown in figures 5.9 to 5.11. From the figures it can be seen that the best curve that could be fitted to each set of data is a straight line and therefore linear regression analyses were carried out. The equations of the lines are of the form;

$$\frac{M}{c} = \beta_{t1} + \beta_{t2} D \qquad (5.2)$$

As explained in section 4.4 in Chapter 4, these lines were constrained to pass through the origin (β_{t1}=0). The coefficients of correlation from the linear regression analyses were found to be better than 0.93. The values of slopes of the lines (β_{t2}) are given in table 5.6. A graph of the slopes of the straight lines against the breadth of the piers for each rotation are given in figure 5.12. Best fit second order polynomial curves passing through the origin were fitted to these with correlation coefficients better than 0.99. The equation of these curves can be written as;

$$\beta_{t2} = \alpha_{t1} B + \alpha_{t2} B^2 \qquad (5.3)$$

Therefore from equations (5.2) and (5.3) the moment carrying capacities for each limiting rotation can be calculated as;

$$M = c\,B\,D\,(\,\alpha_{t1} + \alpha_{t2}\,B\,) \tag{5.4}$$

The values of parameters, α_{t1} and α_{t2} obtained are listed in table 5.7 at pier rotations of 0.5°, 1.0° and 1.5°.

From figure (5.12) it can be seen that a straight line passing through the origin could also be fitted to the set of data with correlation coefficients better than 0.97. The equation of the line is of the form;

$$\beta_{t2} = \alpha_{t3}\,B \tag{5.5}$$

Hence, from equations (5.2) and (5.5) an alternative simpler empirical equation, to equation (5.4) can be calculated as;

$$M = \alpha_{t3}\,c\,B\,D \tag{5.6}$$

The values of parameter, α_{t3} obtained are 0.9645, 1.3942 and 1.6820 at pier rotations of 0.5°, 1.0° and 1.5°, respectively.

Since the test time was short it was assumed that the recorded behaviour was essentially undrained.

5.5 Verification of the Results

After completion of the experimental program, in order to verify that the scattered data obtained from the tests was due to the insensitivity of the load cell used, two more tests were carried out on a model pier of 30mm breadth and 60mm depth. The original 1500 lb (6.681 kN) load cell was used in one and a more sensitive 250 lb (1.114kN) load cell used in the other. Figure 5.13 shows graphs of moment/cohesion against rotation obtained. It can be seen that the curve obtained using the 250 lb cell is smoother than the one obtained using the 1500 lb transducer. Since the smoother curve essentially follows the average values of the scattered data, it was decided that these average values were acceptable.

5.6 Conclusions

As for the conventional model tests, from an extensive series of centrifuge model tests empirical relationships have been derived between moment carrying capacity and geometry for limited rotations of short rigid piers in saturated clay.

The results presented have been scaled up to prototype size on the basis that this is usually legitimate for the immediate response of rigid structures in saturated clay.

TEST NAME	DEPTH		MOISTURE CONTENT (%)	COHESION (kN/m^2)
	MODEL SIZE (mm)	PROTOTYPE (m)		
M22CT1	20	0.80	15.97	116.08
M22CT2	20	0.80	16.50	96.86
M23CT1	30	1.20	16.47	97.85
M24CT1	40	1.60	16.48	97.52
M25CT1	50	2.00	17.08	79.45
M26CT1	60	2.40	17.11	78.64

Table 5.1 Model tests for 20mm (0.80m in prototype) breadth.

TEST NAME	DEPTH		MOISTURE CONTENT (%)	COHESION (kN/m²)
	MODEL SIZE (mm)	PROTOTYPE (m)		
M32CT1	20	0.80	16.24	105.85
M32CT2	20	0.80	16.57	94.57
M33CT1	30	1.20	16.45	98.53
M33CT2	30	1.20	16.58	94.25
M34CT1	40	1.60	16.62	92.97
M34CT2	40	1.60	17.34	72.69
M35CT1	50	2.00	16.83	86.53
M35CT2	50	2.00	16.82	86.83
M36CT1	60	2.40	17.25	74.96
M36CT2	60	2.40	16.68	91.08

Table 5.2 Model tests for 30mm (1.20m in prototype) breadth.

TEST NAME	DEPTH		MOISTURE CONTENT (%)	COHESION (kN/m²)
	MODEL SIZE (mm)	PROTOTYPE (m)		
M42CT1	20	0.80	15.56	133.54
M42CT2	20	0.80	16.75	88.93
M43CT1	30	1.20	16.76	88.62
M44CT1	40	1.60	16.99	81.93
M45CT1	50	2.00	17.01	81.37
M45CT2	50	2.00	16.80	87.42
M46CT1	60	2.40	17.29	73.95
M46CT2	60	2.40	17.04	80.54

Table 5.3 Model tests for 40mm (1.60m in prototype) breadth.

TEST NAME	DEPTH		MOISTURE CONTENT (%)	COHESION (kN/m^2)
	MODEL SIZE (mm)	PROTOTYPE (m)		
M52CT1	20	0.80	16.00	114.90
M52CT2	20	0.80	16.84	86.23
M52CT3	20	0.80	16.05	112.95
M53CT1	30	1.20	16.57	94.57
M53CT2	30	1.20	16.67	91.39
M54CT1	40	1.60	16.56	94.89
M55CT1	50	2.00	16.78	88.02
M55CT2	50	2.00	17.12	78.37
M56CT1	60	2.40	17.33	72.94

Table 5.4 Model tests for 50mm (2.00m in prototype) breadth.

TEST NAME	DEPTH		MOISTURE CONTENT (%)	COHESION (kN/m^2)
	MODEL SIZE (mm)	PROTOTYPE (m)		
M62CT1	20	0.80	16.50	96.86
M62CT2	20	0.80	16.62	92.97
M63CT1	30	1.20	16.57	94.57
M63CT2	30	1.20	16.86	85.65
M64CT1	40	1.60	16.24	105.85
M64CT2	40	1.60	16.80	87.42
M65CT1	50	2.00	16.48	97.52
M65CT2	50	2.00	17.72	63.84
M66CT1	60	2.40	17.77	62.76
M66CT2	60	2.40	17.11	78.64

Table 5.5 Model tests for 60mm (2.40m in prototype) breadth.

Breadth (m)	Rotation of pile from vertical axis		
	0.50°	1.00°	1.50°
0.80	0.86569	1.15970	1.36940
1.20	1.21560	1.60570	1.81983
1.60	1.39828	2.09257	2.57744
2.00	1.81338	2.75904	3.39524
2.40	2.44732	3.48138	4.17774

Table 5.6 Values of the slopes of straight lines (m^2).

Parameter	Rotation of pile from vertical axis		
	0.50°	1.00°	1.50°
α_{t1}	0.91865	1.24476	1.44832
α_{t2}	0.02345	0.07641	0.11948

Table 5.7 Values of parameters α_{t1} and α_{t2}.

5.7 <u>Notation for Plates 5.1 to 5.6</u>

a) Plate 5.1

(1) Slip ring assembly
(2) Swinging soil bin
(3) Rotating arm

b) Plate 5.2

(1) Motor-gearbox system
(2) Displacement transducer frame
(3) Displacement transducers
(4) Model pier and pulling rod

c) Plate 5.3

(1) BBC MASTER computer
(2) EPSON printer
(3) Plotter
(4) Data logger
(5) Centrifuge control system

d) Plate 5.4

(1) Swinging soil bin
(2) Counterbalance soil bin
(3) Balancing lock
(4) Monochrome video camera

e) Plate 5.5

(1) PARVALUX motor
(2) Gearbox

f) Plate 5.6

(1) Supports
(2) Swinging soil bin
(3) Displacement transducers and frame
(4) Monochrome video camera

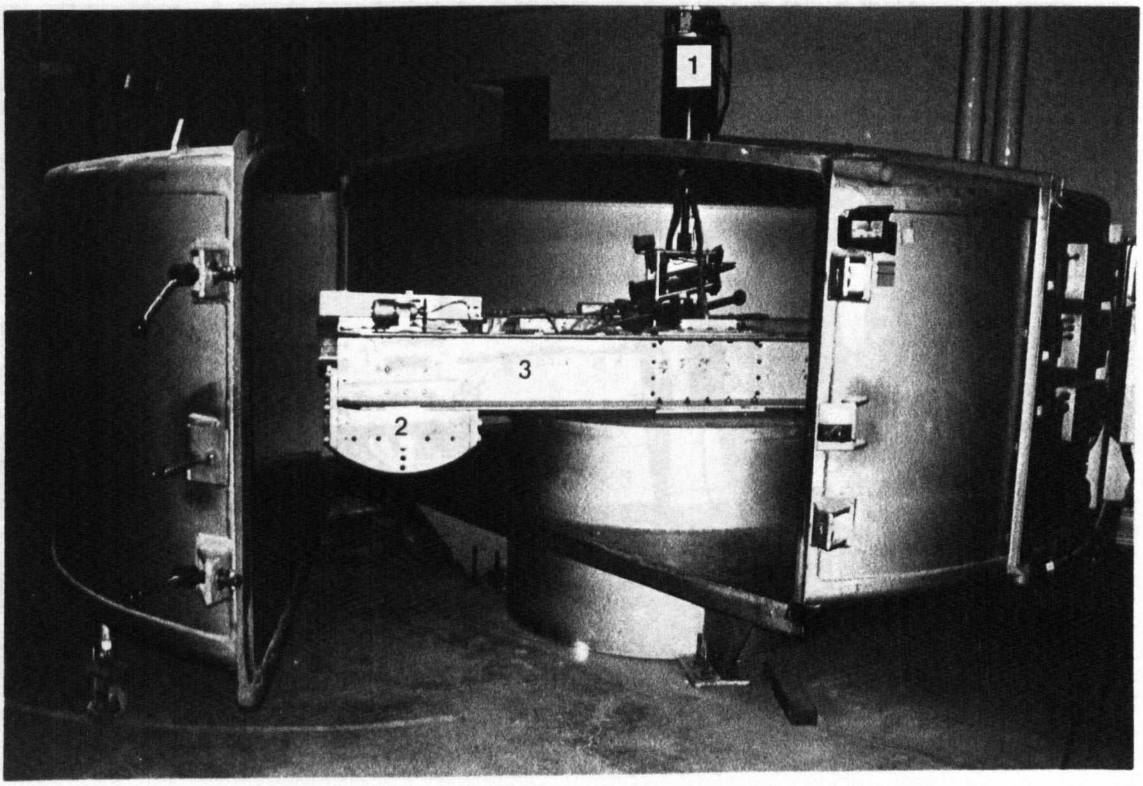

Plate 5.1 General view of the centrifuge.

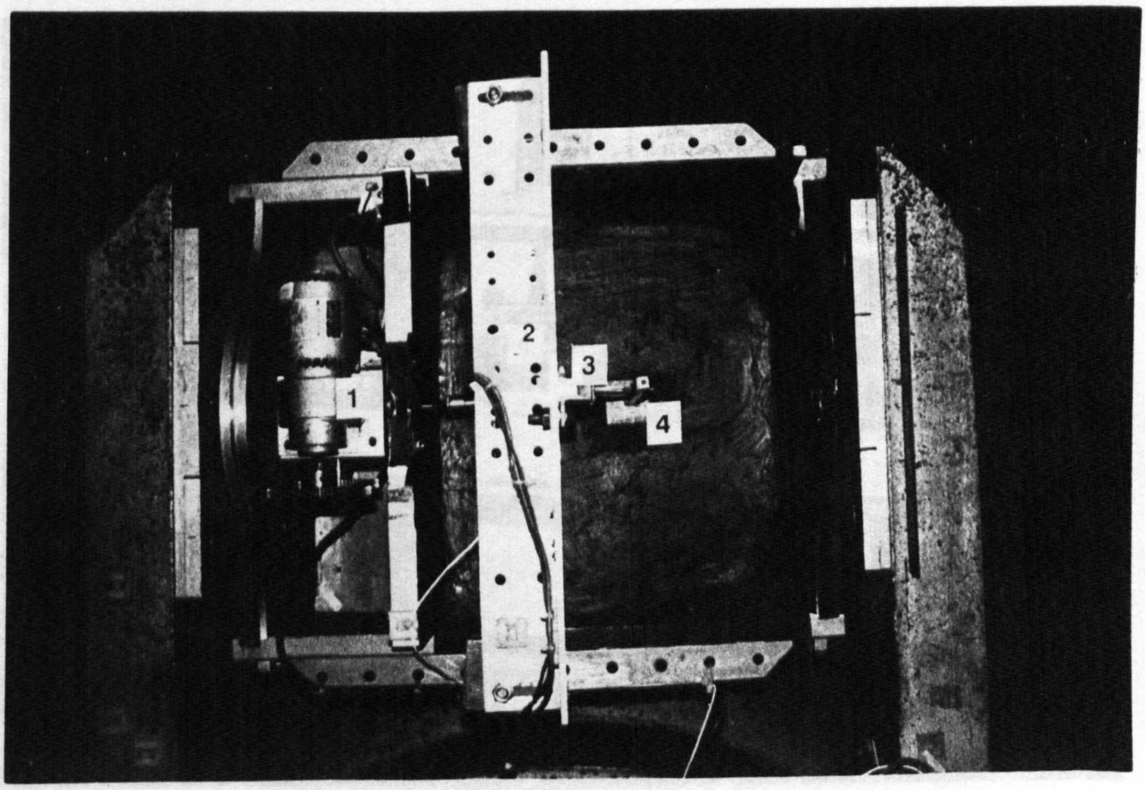

Plate 5.2 View of the package.

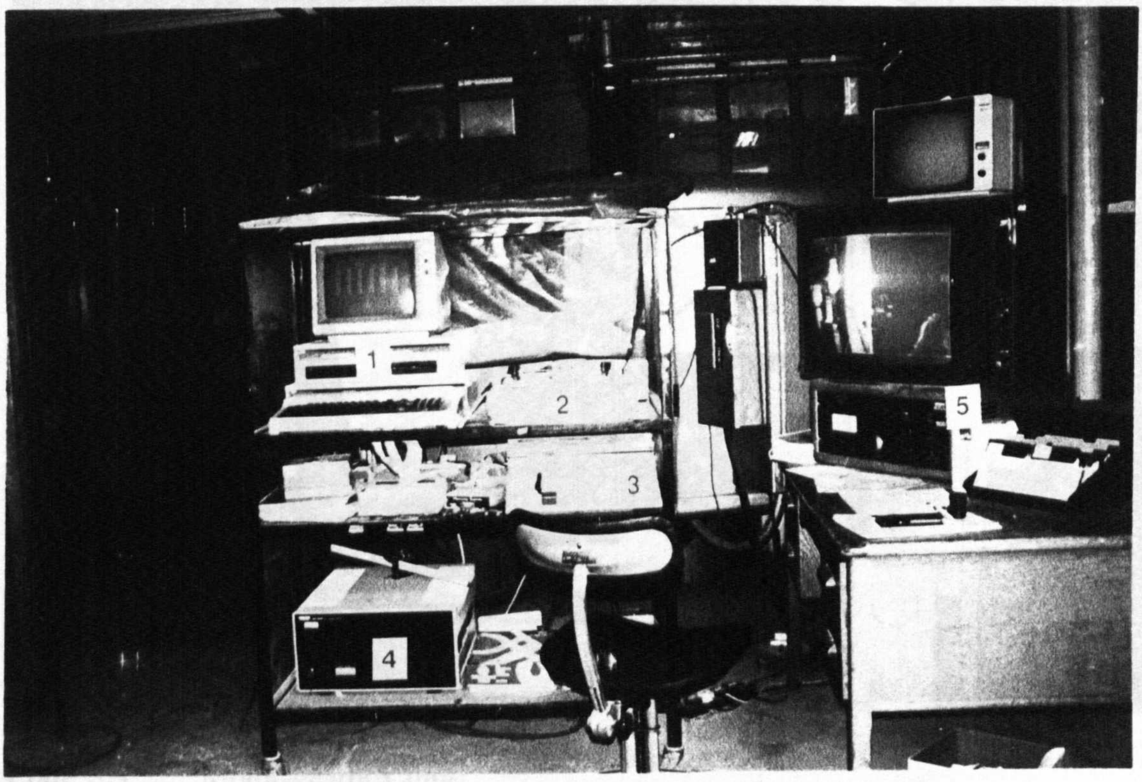

Plate 5.3 Data acquisition and monitoring equipment.

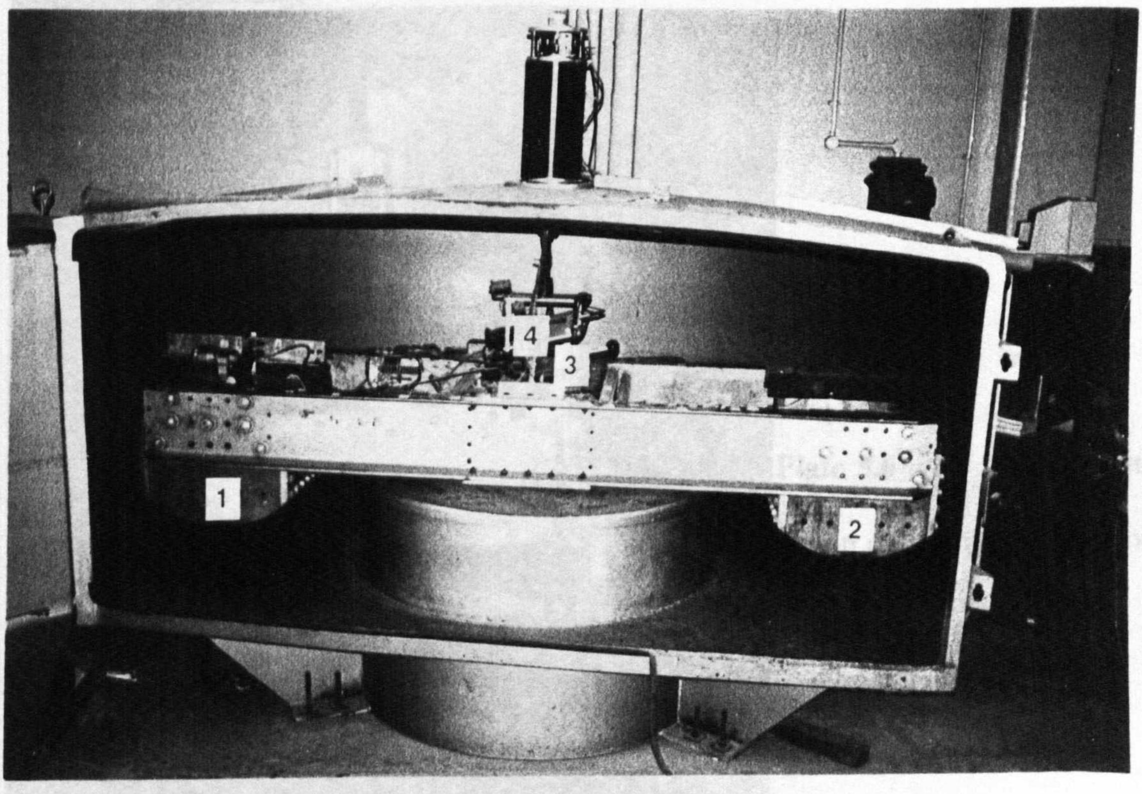

Plate 5.4 Rotating arm and swinging soil bins.

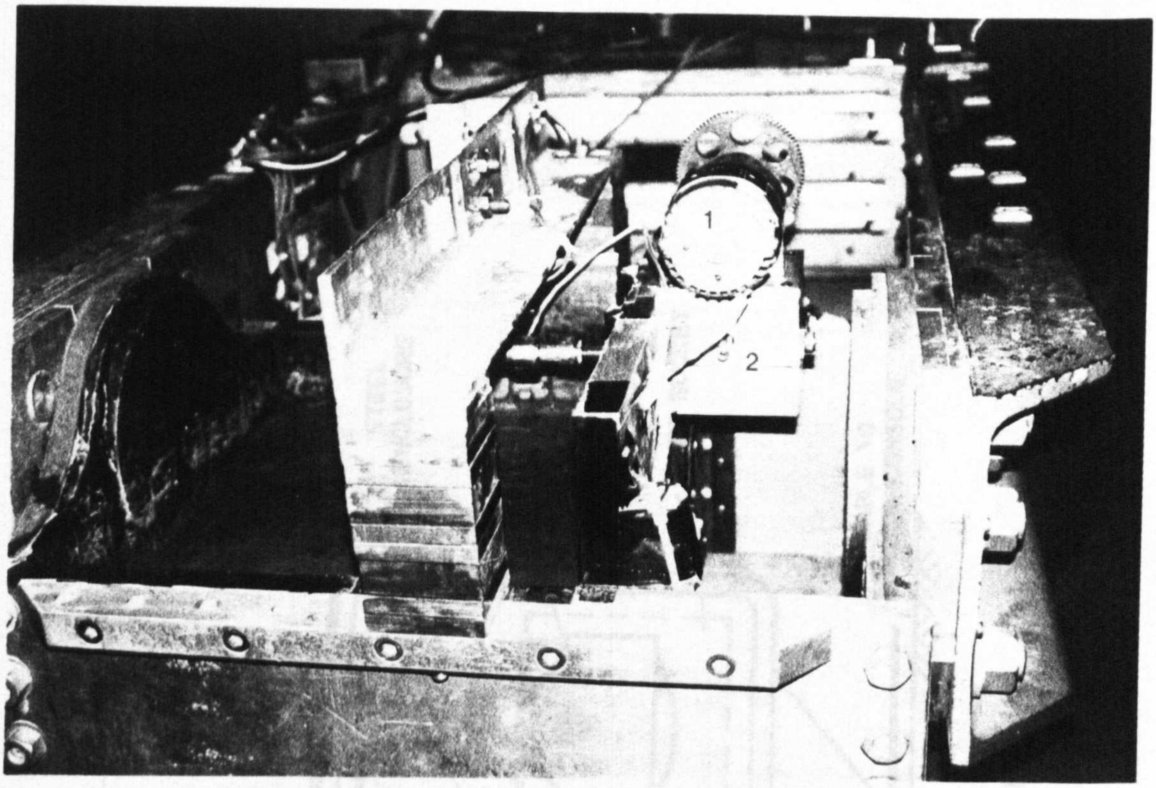

Plate 5.5 Motor-gearbox unit.

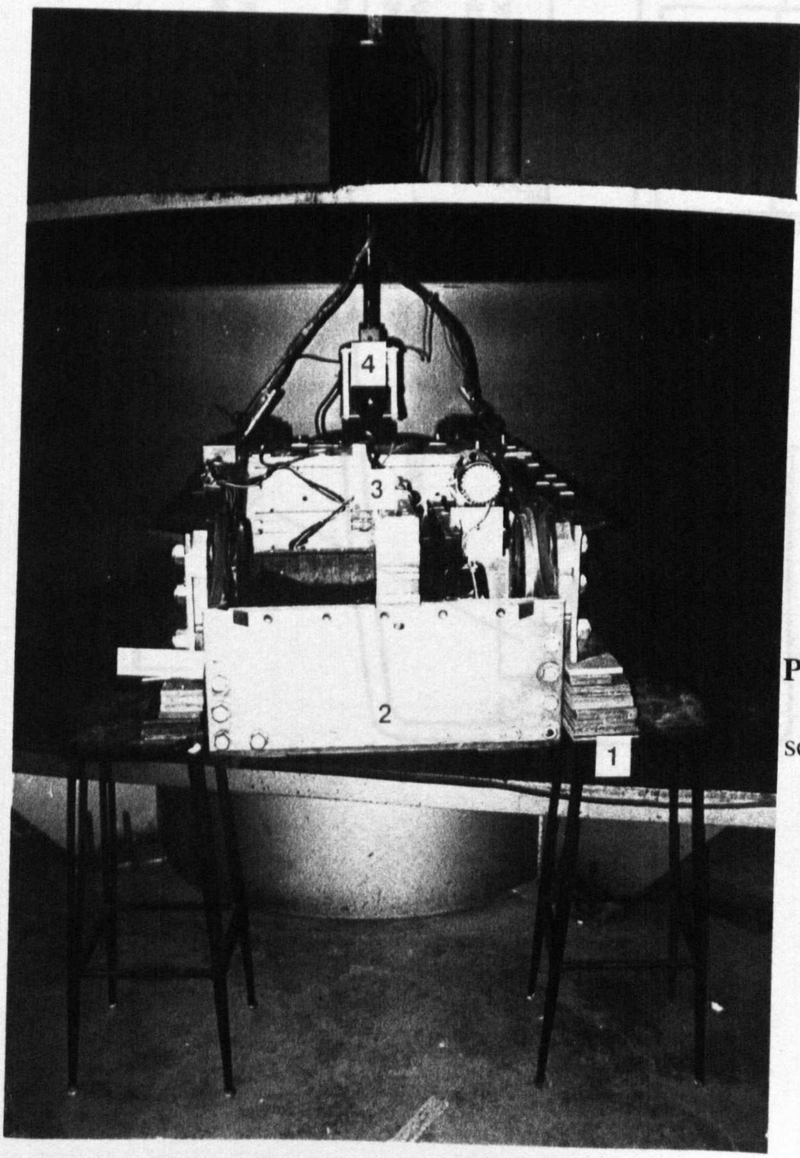

Plate 5.6 Experimental set-up during the preparation.

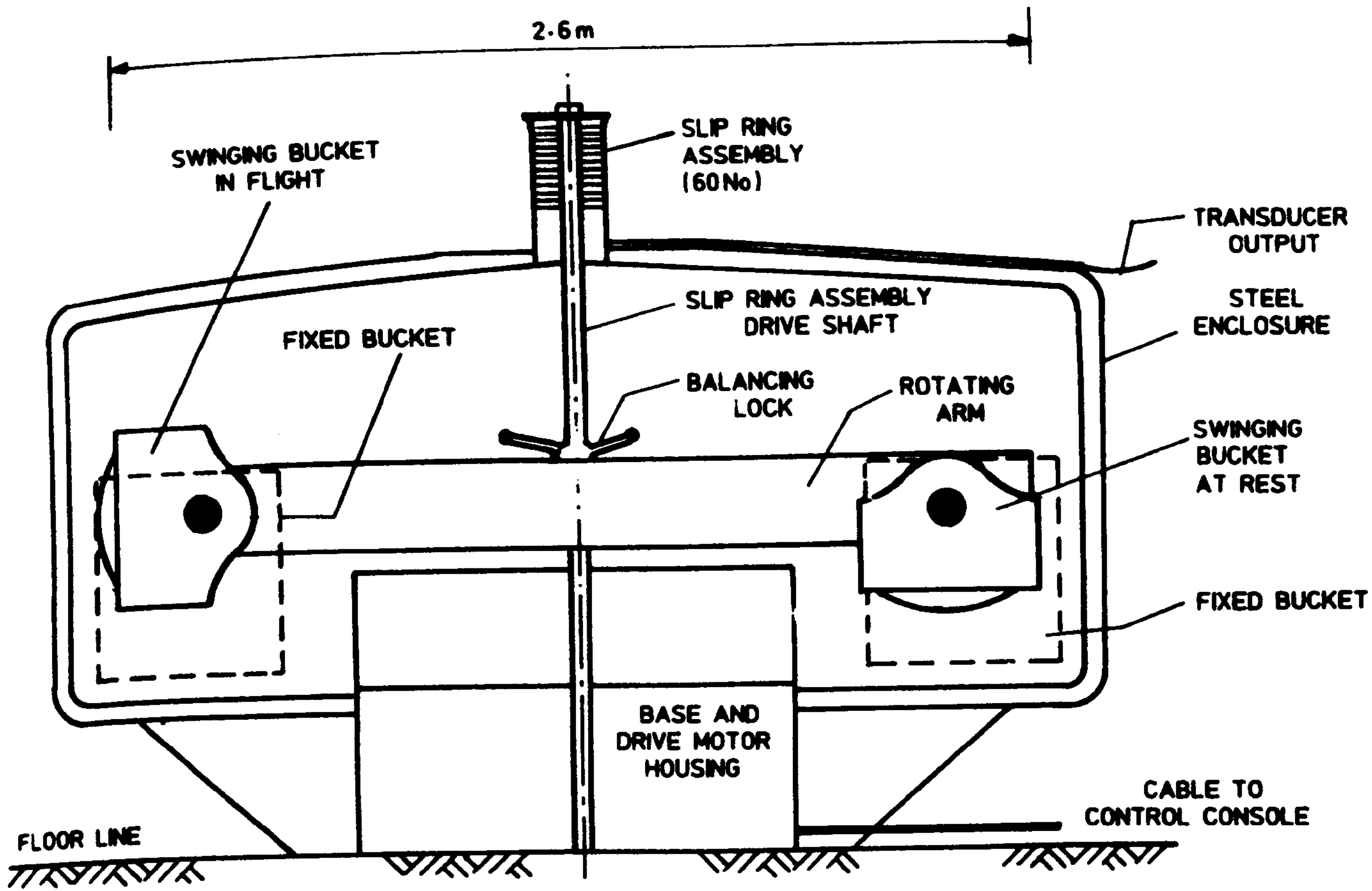

Figure 5.1 Details of the centrifuge.

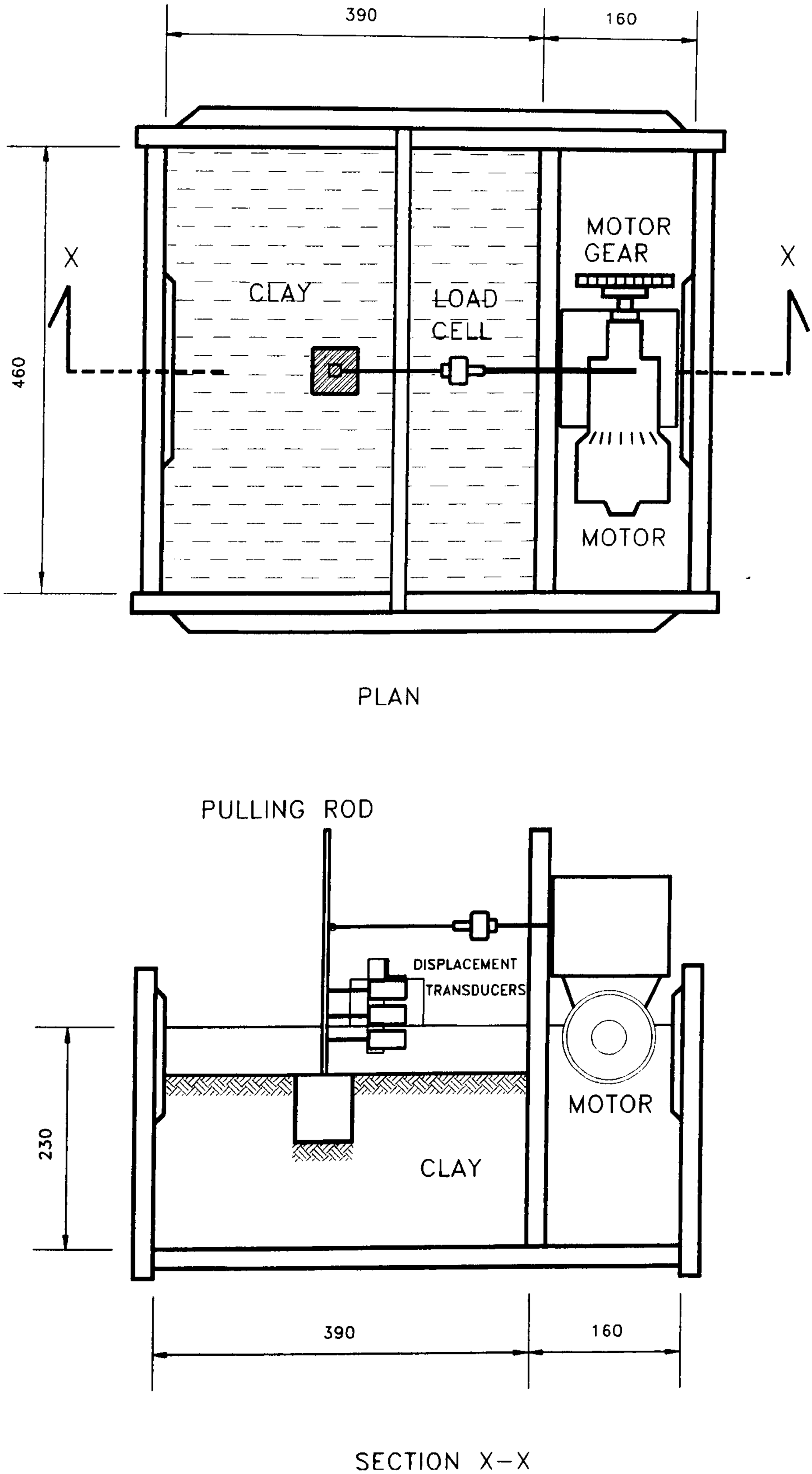

Figure 5.2 General Layout of the Package.

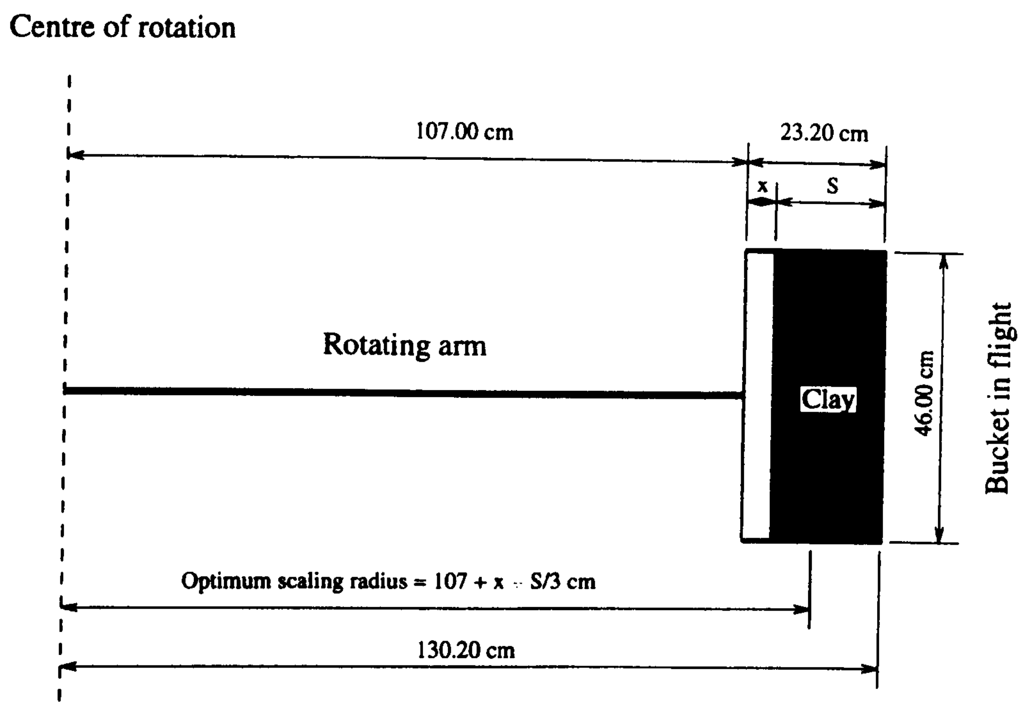

Figure 5.3 Geometry to calculate scaling radius.

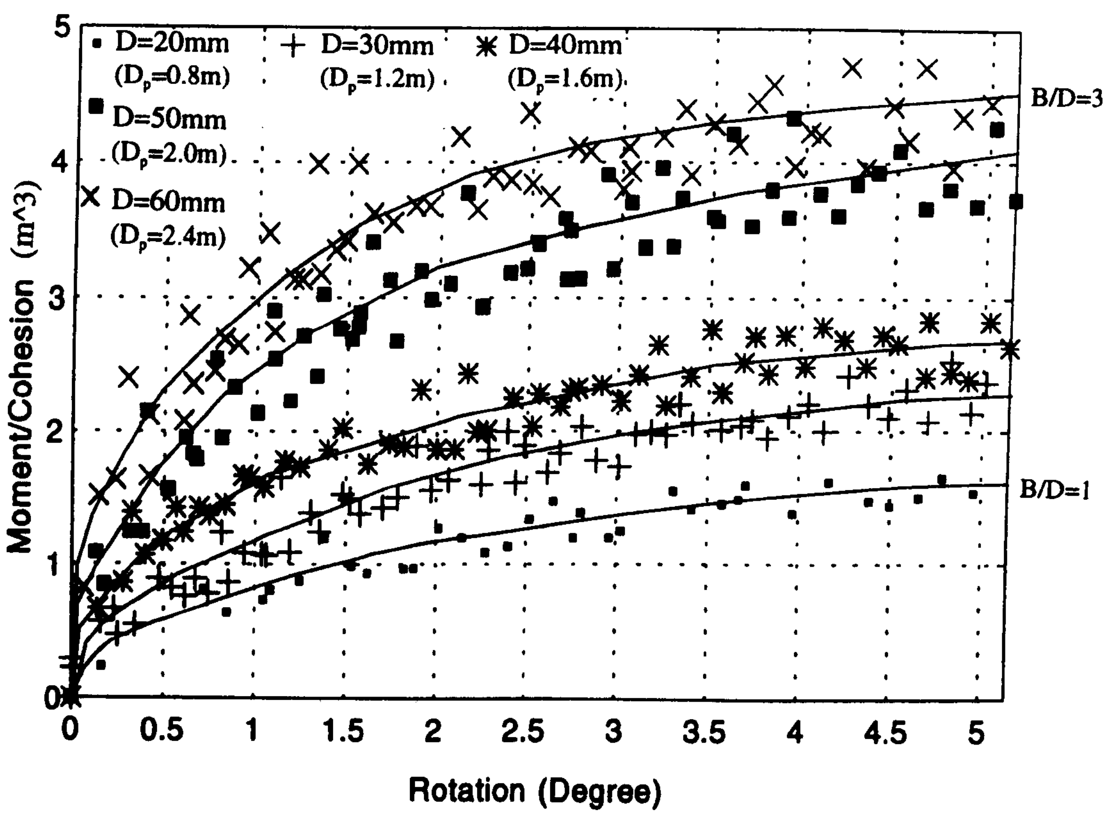

Figure 5.4 Moment/Cohesion - Rotation curves for B=0.80 m prototype breadth.

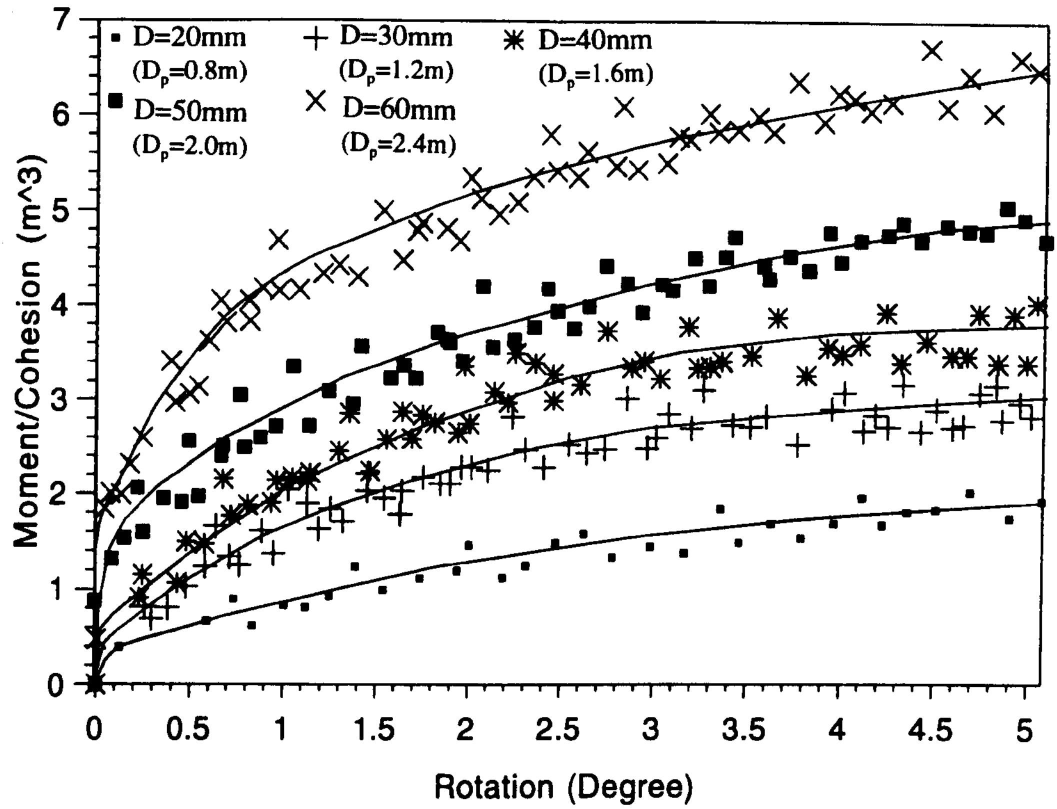

Figure 5.5 Moment/Cohesion - Rotation curves for B=1.20 m prototype breadth.

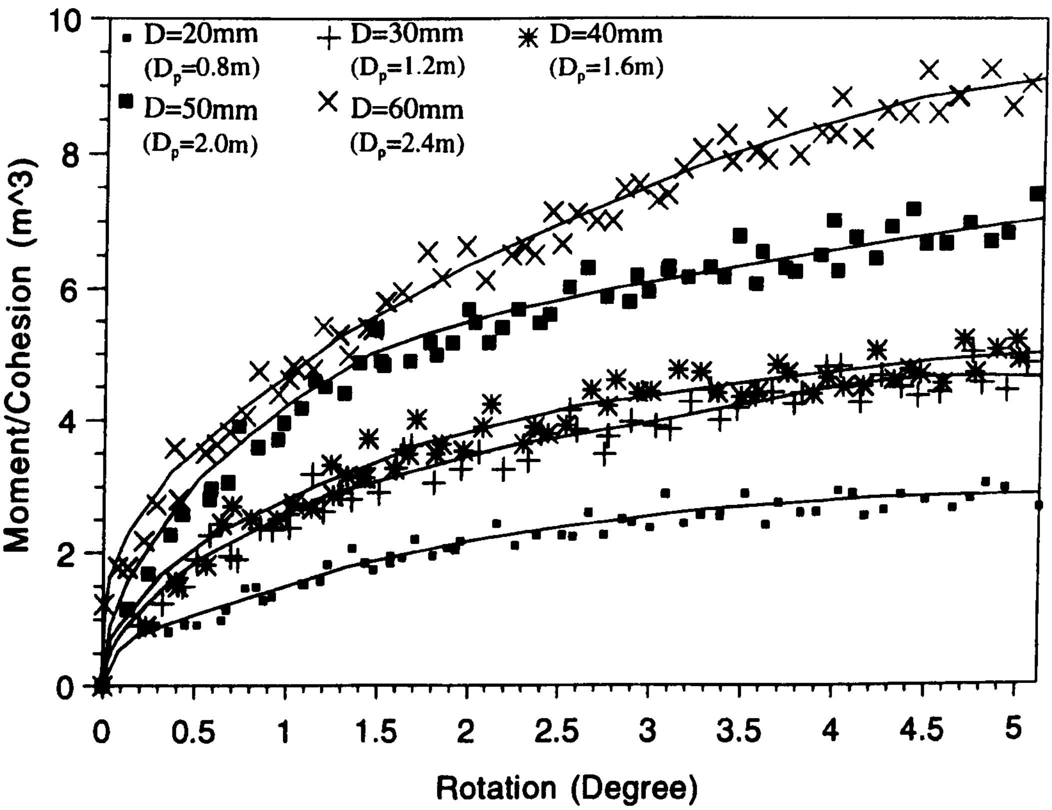

Figure 5.6 Moment/Cohesion - Rotation curves for B=1.60 m prototype breadth.

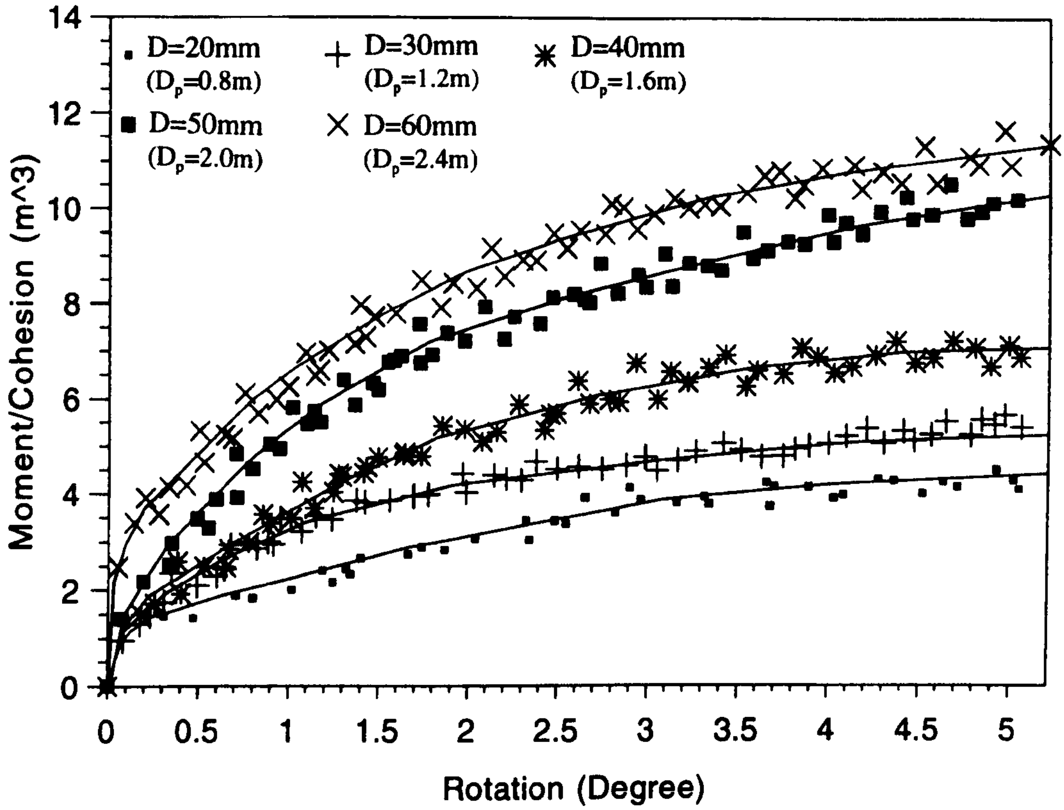

Figure 5.7 Moment/Cohesion - Rotation curves for B=2.00 m prototype breadth.

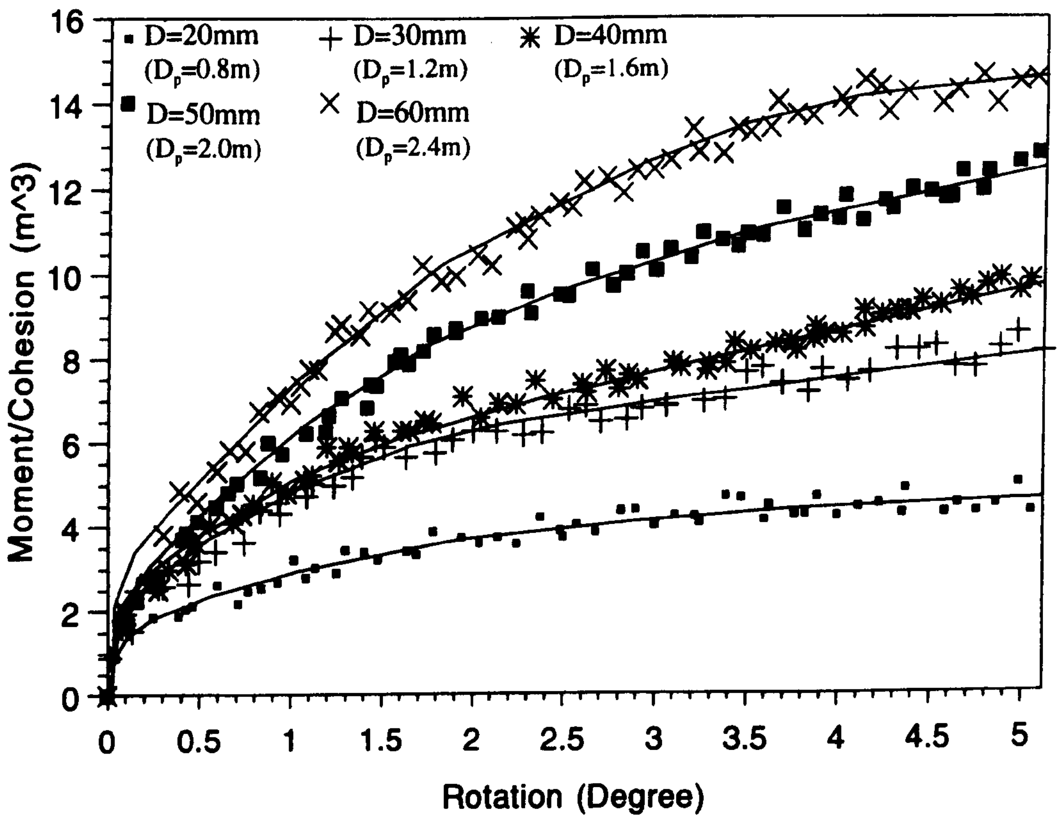

Figure 5.8 Moment/Cohesion - Rotation curves for B=2.40 m prototype breadth.

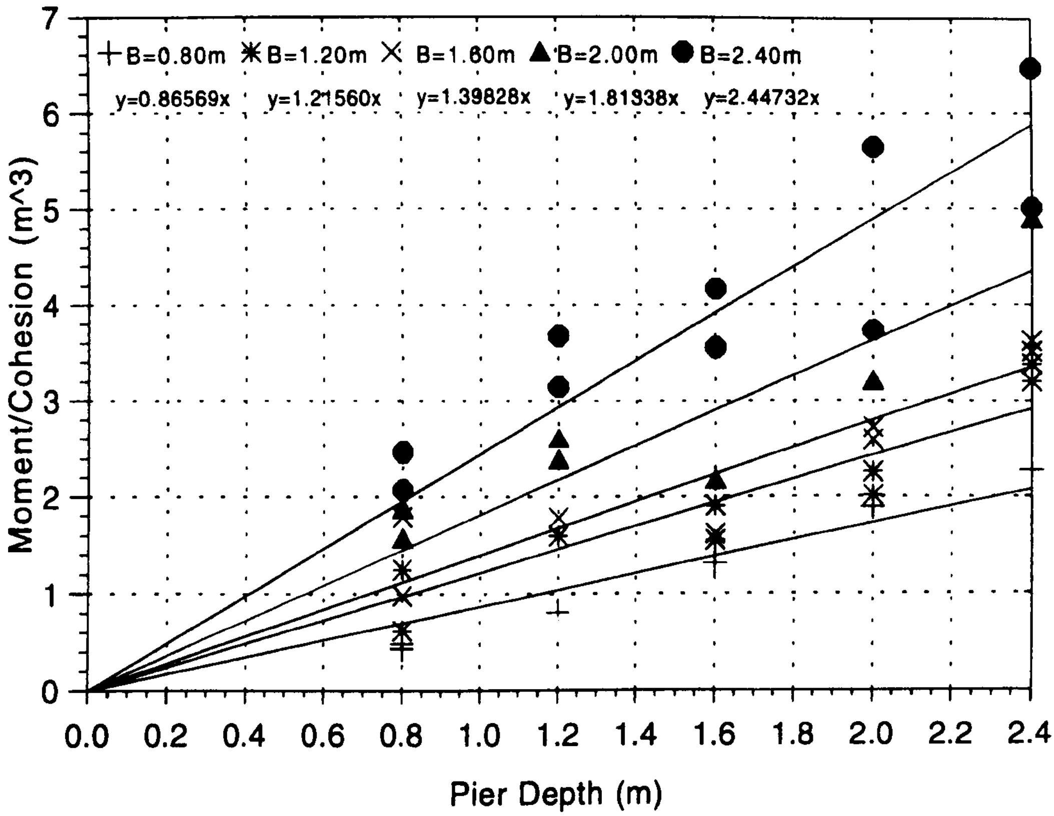

Figure 5.9 Moment/Cohesion against Pier Depth for 0.5 Degree Rotation.

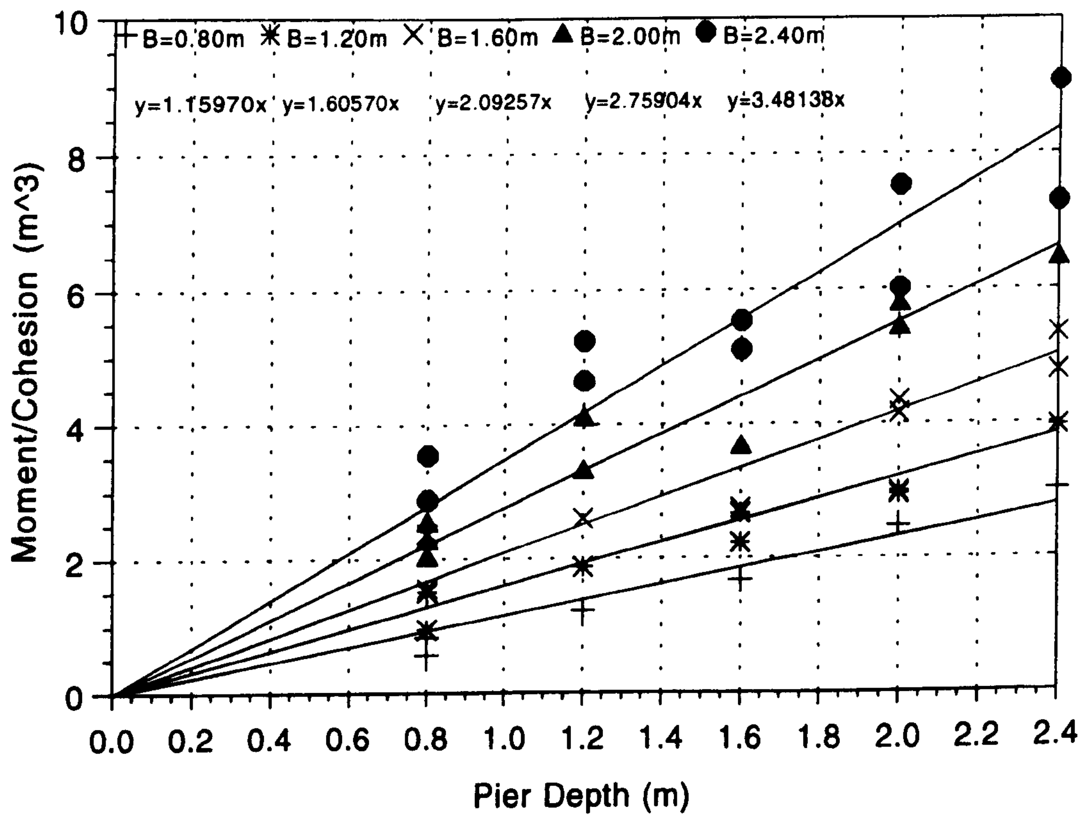

Figure 5.10 Moment/Cohesion against Pier Depth for 1.0 Degree Rotation.

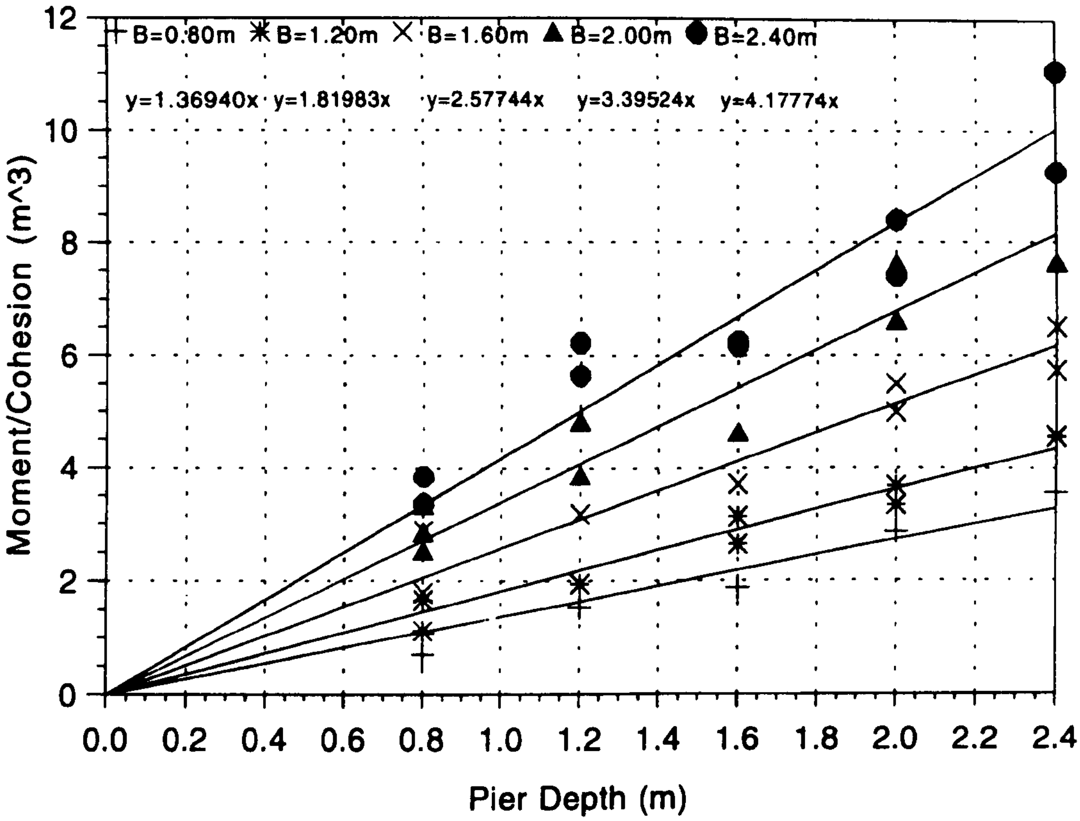

Figure 5.11 Moment/Cohesion against Pier Depth for 1.5 Degree Rotation.

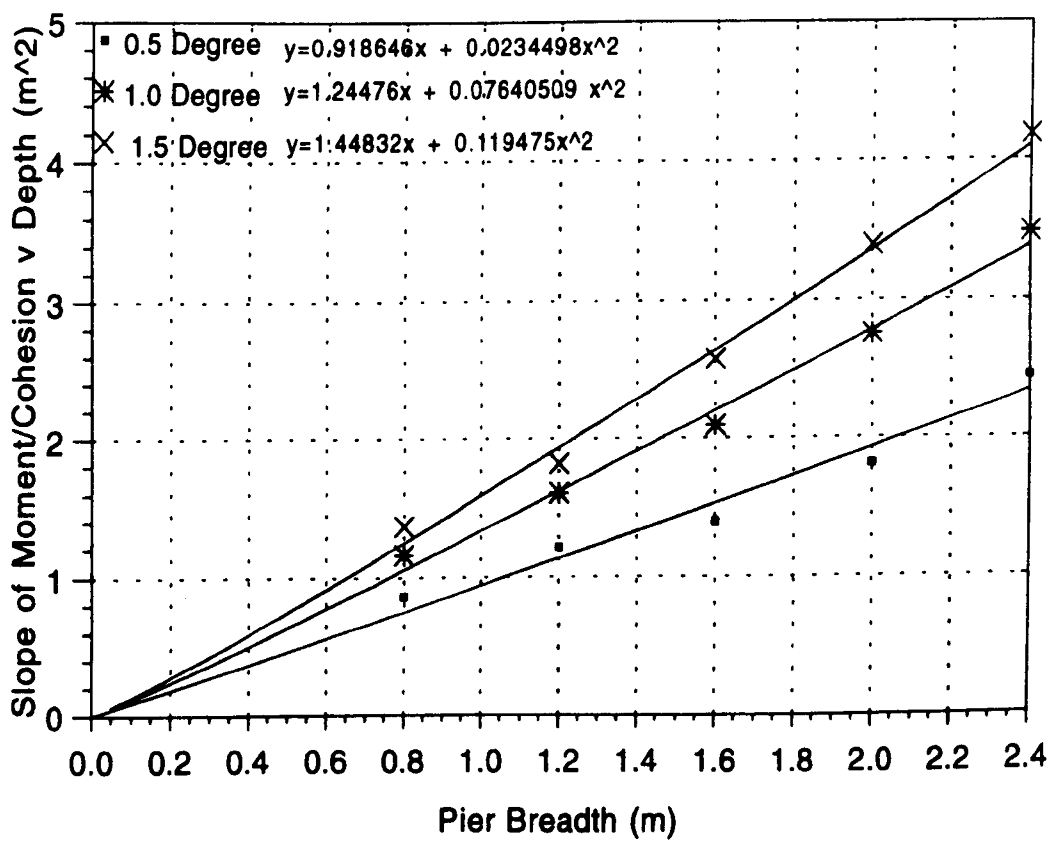

Figure 5.12 Slope of Moment/Cohesion against Pier Depth graphs against Pier Breadth.

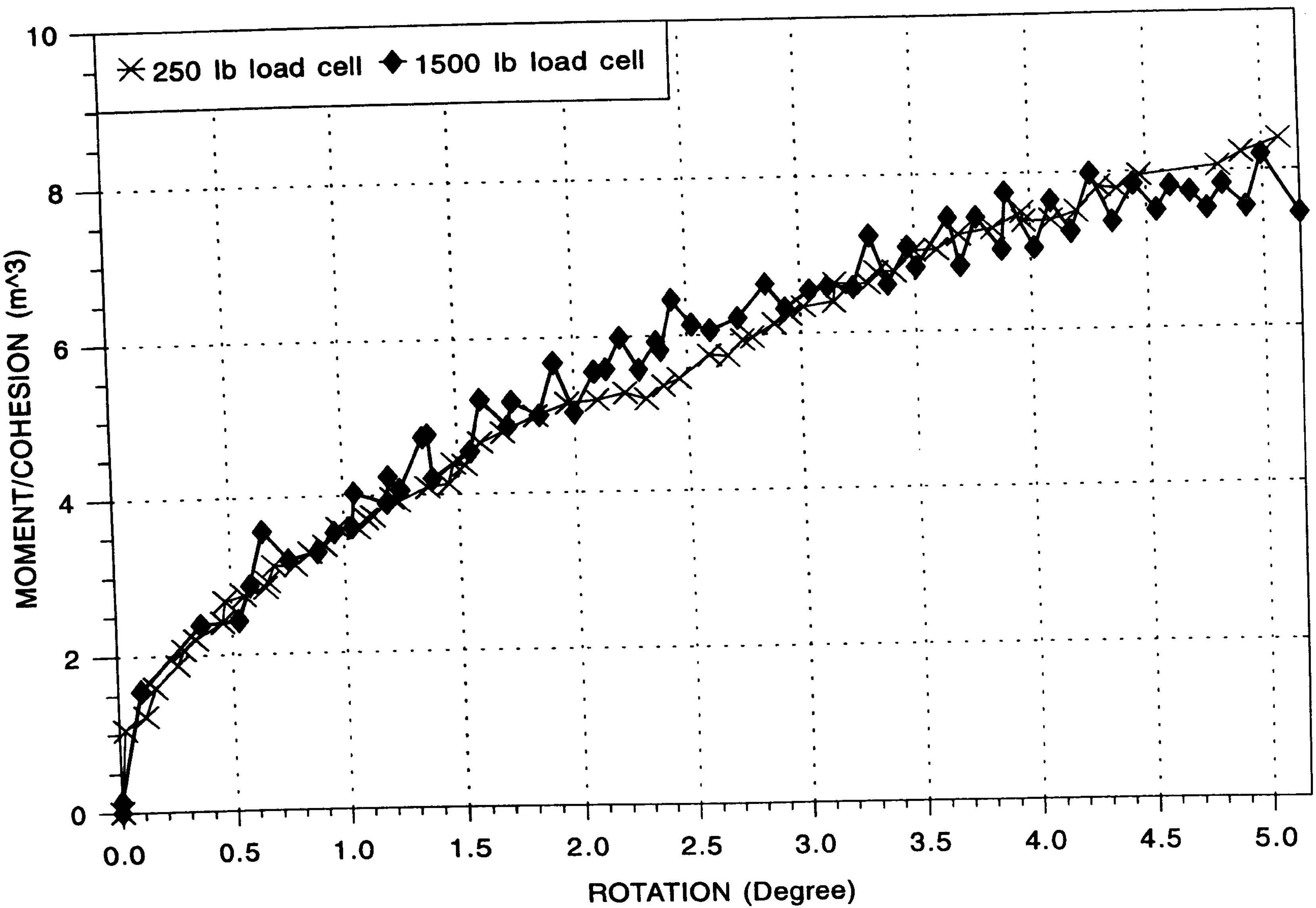

Figure 5.13 Comparison of the results using two different load cell.

CHAPTER 6

NUMERICAL PROCEDURES FOR THE ANALYSES OF SHORT PIER FOUNDATIONS USING THE FINITE ELEMENT METHOD

6.1 Introduction

The finite element method (F.E.M.) is a very powerful tool which enables numerous factors that influence the behaviour of a system to be taken into account. It has been widely used for calculating and designing all kinds of structures and foundations.

In this study, finite element analyses were carried out for comparison with the model tests which were presented in Chapters 4 and 5. Initially an existing two-dimensional (axi-symmetric) linear computer program was used and then three-dimensional linear and nonlinear computer programs were developed for the analyses of the behaviour of a short, square, rigid pier when the top of the pier is subjected to large overturning moment and relatively small vertical and horizontal forces.

In this chapter, a brief description of the F.E.M. is presented. The two-dimensional computer program is described briefly and the three-dimensional computer programs and documentation are then presented in detail.

6.2 The Finite Element Method

The F.E.M. is a very powerful, modern computational analytical technique and has received widespread attention over the last 15-20 years as more powerful computing facilities have become available. One of the earliest applications of the F.E.M. in the geotechnical field was to rocks by Zienkiewicz and Cheung (1964). They used linear triangular elements to solve a buttress dam constructed on a complex foundation. Since then, the method has been applied to the analysis of pile foundations, dams, excavations, slopes and other soil related problems. The method is well documented in the literature (see section 2.2.3.3. in Chapter 2). Hence in this section, only some important features of the method are highlighted.

The basic idea of the F.E.M. is to divide the structure and the surrounding soil being analyzed into a large number of finite elements. Hence the method uses a substitute structure whose parts are pieces of the actual structure. These elements may be one, two or three-dimensional. Points where the elements are connected to one another are called nodes.

The finite element analysis of problems in solid mechanics can be carried out using a displacement (or stiffness), force (or flexibility) or mixed procedure. Most problems in geotechnical engineering have been formulated using the displacement method. Some of the reasons for this choice are that the number and bandwidth of the final stiffness equations are smaller than those produced by other methods and it is relatively easier to establish approximation functions to satisfy compatibility requirements than it is to construct force or mixed models. The procedure outlined in this study is based on the displacement method. The displacements of the nodal points of an element are assumed to be unknown quantities, and the element equations expressing nodal forces in terms of these displacements are derived using variational procedures based on the minimum potential energy. The displacement components at any point in an element are described in terms of the nodal values by means of interpolation functions of the form

$$\{ \delta \} = [N] \{ d \}_e \tag{6.1}$$

where,

$[N]$ = a set of shape functions

and $\{d\}_e$ = nodal displacements of the element

The strains within the element can be expressed in terms of the element nodal displacements as

$$\{ \epsilon \} = [B] \{ d \}_e \tag{6.2}$$

where $[B]$ = strain matrix obtained after differentiation of the shape functions.

The stresses may be related to the strains by an elasticity matrix $[D]$

$$\{ \sigma \} = [D] \{ \epsilon \} \tag{6.3}$$

Total potential energy of the continuum will be the sum of the energy contribution of the individual elements provided that no singularity exists in the integrands of the functional.

$$\pi = \sum_e \pi_e = \frac{1}{2}\int_V \{ \sigma^T \}\{ \epsilon \}\, dV - \int_V \{ \Delta^T \}\{ b \}\, dV$$
$$- \int_S \{ \Delta^T \}\{ t \}\, dS - \{ d \}^T \{ R \} \qquad (6.4)$$

where,

π_e = total potential energy of the individual element

{b} = body force per unit volume

{t} = surface forces per unit area

{R} = concentrated forces applied at the nodes

{d} = nodal displacement vector

The first term of the right hand side of the equation represents the internal strain energy. The second, third and fourth terms are the work done by the body forces, surface forces and concentrated nodal forces, respectively. Substituting equations (6.1) to (6.3) into equation (6.4) the total potential energy for an element can be written as

$$\pi_e = \frac{1}{2} \int_{V_e} \{ d \}_e^T [B]^T [D] [B] \{ d \}_e \, dV$$

$$- \int_{V_e} \{ d \}_e^T [N]^T \{ b \} \, dV - \int_{S_e} \{ d \}_e^T [N]^T \{ t \} \, dS - \{ d \}_e^T \{ R \} \qquad (6.5)$$

By the principle of stationary value of the total potential energy (Przemieniecki, 1968)

$$\frac{\partial \pi_e}{\partial \{ d \}_e^T} = 0 \qquad (6.6)$$

and application of this yields

$$\frac{\partial \pi_e}{\partial d_e^T} = [k] \{ d \}_e - \{ f \} = 0 \qquad (6.7)$$

where

$$\{ f \} = \int_{V_e} [N]^T \{ b \} \, dV + \int_{S_e} [N]^T \{ t \} \, dS + \{ R \} \qquad (6.8)$$

and

$$[k] = \int_{V_e} [B]^T [D] [B] \, dV \qquad (6.9)$$

Equation (6.7) can be interpreted as an element stiffness relationship

$$\{f\} = [k]\{d\}_e \tag{6.10}$$

where

$\{f\}$ = an equivalent nodal force vector

and $[k]$ = element stiffness matrix

[k] and {f} are determined for each element in terms of its own local co-ordinate system and then transposed to suit the global co-ordinate system which is being used to define the geometry of the whole system.

The stiffness matrix and nodal load vector of the whole system is then obtained by superposing those for all the elements giving

$$\{F\} = [K]\{d\} \tag{6.11}$$

where,

$[K]$ = overall stiffness matrix

$\{d\}$ = nodal displacement vector of the whole system

$\{F\}$ = resultant nodal load vector of the whole system

For specified loadings, known displacements are introduced and the equations solved for the unknown nodal displacements in the vector $\{d\}_e$. With the nodal displacements determined, the element strains and stresses can then be found from the strain-displacement and the stress-strain relationships, respectively.

6.3 Two-Dimensional (axi-symmetric) Linear Analysis

The finite element method based on harmonic representation of displacements in the circumferential direction, can be used for analysing a cylindrical pier subjected to a lateral load in an homogeneous elastic continuum. A computer program using the Fortran language was developed to implement these procedures by Chandrasekaran and King (1982). It is possible to consider vertical inhomogeneity and variable flexural rigidity along the length of piers and also free-head and fixed head conditions. A lateral load and moment can be applied to a pile with a free head. The program was further modified by King in order to introduce horizontal and vertical friction elements beneath the base and sides of the piles and the continuum and an automatic mesh generation routine to generate the entire model geometry. Only the number of soil and foundation elements and the dimensions of the mesh subdivision, in each co-ordinate direction, have to be specified. For convenience the program used in this study was simplified to analyze only problems in which soil and pier are homogeneous.

A brief description of the harmonic representation, the finite element formulation and the computer program are given in the following section.

6.3.1 Harmonic Representation

In cases where the geometry and elastic properties of the continuum remain independent of the circumferential co-ordinate θ, arbitrary loadings may be accommodated by the Fourier series method. Wilson (1965) proposed the following approach which can apply to problems with axisymmetrical geometry such as the laterally loaded pier. It is assumed that the displacements at an arbitrary point (r, z, θ) in the continuum are

$$u = \bar{u} \cos n\theta$$
$$v = \bar{v} \cos n\theta \qquad (6.12)$$
$$w = \bar{w} \sin n\theta$$

where,

u = radial displacement, v = axial displacement, w = circumferential displacement and $\bar{u}$, $\bar{v}$, and $\bar{w}$ are functions of r and z.

n = an integer

It can be shown that displacements of this form will be produced by applied loadings of the same form, namely:

$$P_r = \bar{p}_r \cos n\theta$$
$$P_z = \bar{p}_z \cos n\theta \qquad (6.13)$$
$$P_\theta = \bar{p}_\theta \sin n\theta$$

where,

P_r = force in the radial direction, P_z = force in the axial direction and P_θ =

force in the circumferential direction.

Since the principle of superposition allows loadings which are more general but which still retain symmetry about the 0-π plane to be considered, the following formulae for the loads and displacements can be used:-

$$
\begin{aligned}
P_r &= \sum_{n=1}^{\infty} \overline{p_r} \cos n\theta \\
P_z &= \sum_{n=1}^{\infty} \overline{p_z} \cos n\theta \\
P_\theta &= \sum_{n=1}^{\infty} \overline{p_\theta} \sin n\theta
\end{aligned}
\qquad (6.14a)
$$

$$
\begin{aligned}
u &= \sum_{n=1}^{\infty} \overline{u} \cos n\theta \\
v &= \sum_{n=1}^{\infty} \overline{v} \cos n\theta \\
w &= \sum_{n=1}^{\infty} \overline{w} \sin n\theta
\end{aligned}
\qquad (6.14b)
$$

where n = a variable integer indicating the number of harmonics.

For most practical problems only the first 4 or 5 terms in the series need be considered. Chandrasekaran and King (1982) found that only the first harmonic n=1 needed be considered for an elastic analysis of a laterally loaded pile.

6.3.2 Finite Element Formulation and the Computer Program PIER2D

Eight-noded rectangular isoparametric elements were used to represent the pier and the soil medium while six noded rectangular isoparametric elements were used for the friction elements. The variation of displacement of any point (r, z and θ) within the element was represented by

$$u = \sum_{i=1}^{j} \sum_{n=1}^{\infty} N_i \, \overline{u_i} \cos n\theta$$
$$v = \sum_{i=1}^{j} \sum_{n=1}^{\infty} N_i \, \overline{v_i} \cos n\theta \qquad (6.15)$$
$$w = \sum_{i=1}^{j} \sum_{n=1}^{\infty} N_i \, \overline{w_i} \sin n\theta$$

where,

j = the number of nodes in each element

N_i= the shape function for the i th node in the element

The shape functions $N_i(\xi,\eta)$ for nodes i=1,8 (see figure 6.1a) are

$$N_i = \frac{1}{4}(1 + \xi\xi_i)(1 + \eta\eta_i)(\xi\xi_i + \eta\eta_i - 1) \quad for \quad i = 1,2,3,4$$
$$N_i = \frac{1}{2}(1 - \xi^2)(1 + \eta\eta_i) \quad for \quad i = 5,7 \qquad (6.16)$$
$$N_i = \frac{1}{2}(1 + \xi\xi_i)(1 - \eta^2) \quad for \quad i = 6,8$$

where,

$$\xi = \frac{r - r_c}{a}, \qquad \eta = \frac{z - z_c}{b}$$

By following the method outlined by Chandrasekaran and King (1982), the expression for the stiffness matrix is obtained as

$$k = \pi\, a\, b \int_{-1}^{+1} \int_{-1}^{+1} [\,B\,]^T [\,D\,] [\,B\,] (\,\xi a + r_c\,)\, d\xi\, d\eta \qquad (6.17)$$

where,

a, b = dimensions of element with respect to r and z

[B] = strain matrix

[D] = elasticity matrix

The pier elements and the soil continuum elements were joined by the zero width friction elements shown in figure 6.1b. For the horizontal and vertical friction elements stiffness matrices were derived by King similar to those developed by Goodman et al. (1968). The matrix is dependent on the length and the values of unit tangential (k_s) and unit normal stiffness (k_n). The unit normal resistance is set high to simulate a non-compressible interface. The value for tangential stiffness is determined from shear tests on an interface of the appropriate materials.

The computer program PIER2D was developed to analyze a vertical pier subjected to lateral load and moment, using the finite element theory described above. The accuracy of the program was verified by Chandrasekaran and King (1982). A typical finite element idealisation for analysing a short pier foundation, consisting of soil, pier and friction elements, is shown in figure 6.2.

The computer output consists of the following:-

(i) The input information, the x and y co-ordinates of the nodes and node numbers of the elements as generated in the program.

(ii) The initial stresses in elements, the load matrix and the amplitudes of radial, vertical and circumferential displacements for all nodes.

(iii) The stresses at the centre of each element in the r-z plane for which $\theta = 0$.

(iv) For all nodes on the pile centre line the node number, depth, lateral deflection, slope, bending moment, shear force, soil reaction, the ratio of soil pressure to lateral deflection and the flexural rigidity value are printed. These values of slope, bending moment, and shear force are values estimated from the nodal displacements using finite difference relationships.

The computer program listing and the data preparation are given in Appendix F1. The computer program has been used in this study for comparison with the model tests and the results will be presented in Chapter 8.

6.4 Three-Dimensional Linear and Nonlinear Analyses

6.4.1 Introduction

As mentioned in the previous section, an axisymmetric finite element analysis, was first used to investigate the behaviour of short pier foundations. It is well known that clays are not capable of holding tensile stresses. The tension behind the pier cannot be released simply by setting the normal stiffness of the friction element to zero because the axisymmetric material properties associated with Fourier series can not model this type of behaviour easily. In order to consider this and the nonlinear stress-strain behaviour of the clay, two more conventional three-dimensional finite element programmes were developed. One of these was linearly elastic and enabled anisotropy of soil to be taken into account, and the other was non-linearly elastic but isotropic.

6.4.2 Three-dimensional isoparametric formulation (Eight-node brick element)

An eight-node isoparametric brick element, which is one of the most popular three-dimensional elements, was used for both soil and pier. This element is also known as the rectangular prismatic element. It is shown in figure 6.3 and has dimensions, 2a, 2b and 2c in the x, y, and z directions, respectively. Isoparametric elements were first developed by Ergatoudis et al (1968), and are named so because the same interpolation functions are used to define position and displacements within the element. They are formulated using a normalized co-ordinate system $\xi\eta\zeta$, which is defined by the element geometry and not by the element orientation in the global co-ordinate system. There is a relation between the two systems for each element of a structure, and this relation is used in the formulation. Co-ordinates $\xi\eta\zeta$ are attached to the element and are scaled so that sides of a hexahedron are defined by $\xi = \pm 1$, $\eta = \pm 1$ and $\zeta = \pm 1$.

With origin at the centroid of the element the displacement function is that of the first member of the serendipity family, namely:

$$u = \sum_{i=1}^{i=8} N_i \, u_i$$
$$v = \sum_{i=1}^{i=8} N_i \, v_i \qquad (6.18)$$
$$w = \sum_{i=1}^{i=8} N_i \, w_i$$

where,

N_i = shape function for the i-th node in the element

u_i, v_i, and w_i = displacements of the i-th node

with the shape function in the form of,

$$N_i = \frac{1}{8} (1 + \xi\xi_i) (1 + \eta\eta_i) (1 + \zeta\zeta_i) \qquad (6.19)$$

Thus for example at node 1 where $\xi = 1$, $\eta = -1$ and $\zeta = 1$,

$$N_1 = \frac{1}{8} (1 + \xi) (1 - \eta) (1 + \zeta) \qquad (6.20)$$

The serendipity co-ordinates, $\xi\eta\zeta$, are related to the global co-ordinates by

$$\xi = \frac{x - x_0}{a} , \qquad \eta = \frac{y - y_0}{b} , \qquad \zeta = \frac{z - z_0}{c} \qquad (6.21)$$

where,

a, b, and c = element half-lengths in the x, y, and z directions, respectively

x, y, and z = global co-ordinates

and x_0, y_0, and z_0 = global co-ordinates of the centroid

This displacement functions give linearly varying displacements along the edges and therefore the compatibility requirement is met on common faces of adjacent elements.

The six strain components in three dimensions are

$$\{ \epsilon \} = [\epsilon_x , \epsilon_y , \epsilon_z , \gamma_{xy} , \gamma_{yz} , \gamma_{xz}]^T$$
$$= \left[\frac{\partial u}{\partial x} , \frac{\partial v}{\partial y} , \frac{\partial w}{\partial z} , \frac{\partial u}{\partial y} + \frac{\partial v}{\partial x} , \frac{\partial v}{\partial z} + \frac{\partial w}{\partial y} , \frac{\partial w}{\partial x} + \frac{\partial u}{\partial z} \right]^T \tag{6.22}$$

These can be related to the nodal displacements after differentiating equation (6.18). The strain-displacement or kinematic relationship for small deformations can then be written in a compact form as

$$\{ \epsilon \} = [B] \{ d \}_e \tag{6.23}$$

where,

[B] = strain matrix

and $\{d\}_e = [u_1, v_1, w_1, \text{.........}, u_8, v_8, w_8]$ is the nodal displacement vector of the element.

6.4.2.1 Stress-Strain relationship

The behaviour of the soil is assumed to be linearly elastic. To be more generally applicable the soil medium is considered to be transversely isotropic with the horizontal (x-y) plane as the plane of isotropy as shown in figure 6.4. The stress-strain relationship of a transversely isotropic body is governed by five elastic constants, E_1, ν_1, E_2, ν_2 and G_2, (Lekhnitskii, 1963) and is

$$\epsilon_x = \left[\frac{\sigma_x}{E_1} - \frac{\nu_1 \sigma_y}{E_1} - \frac{\nu_2 \sigma_z}{E_2} \right]$$

$$\epsilon_y = \left[\frac{\sigma_y}{E_1} - \frac{\nu_1 \sigma_x}{E_1} - \frac{\nu_2 \sigma_z}{E_2} \right] \qquad (6.24)$$

$$\epsilon_z = \left[\frac{\sigma_z}{E_2} - \frac{\nu_2 \sigma_x}{E_2} - \frac{\nu_2 \sigma_y}{E_2} \right]$$

$$\gamma_{xy} = \frac{2\,\tau_{xy}}{E_1(1+\nu_1)} \; ; \; \gamma_{yz} = \frac{\tau_{yz}}{G_2} \; ; \; \gamma_{xz} = \frac{\tau_{xz}}{G_2}$$

where E_1 is the modulus of elasticity in the plane of isotropy, ν_1 is Poisson's ratio in the plane of isotropy, E_2 is the modulus of elasticity in the direction perpendicular to the plane of isotropy, ν_2 is Poisson's ratio representing the strain in the plane of isotropy due to unit strain normal to it and G_2 is the shear modulus in planes perpendicular to the plane of isotropy.

Expressing the stresses in terms of strains

$$\begin{Bmatrix} \sigma_x \\ \sigma_y \\ \sigma_z \\ \tau_{xy} \\ \tau_{yz} \\ \tau_{xz} \end{Bmatrix} = \begin{bmatrix} C_1 & C_2 & C_3 & 0 & 0 & 0 \\ C_2 & C_1 & C_3 & 0 & 0 & 0 \\ C_3 & C_3 & C_4 & 0 & 0 & 0 \\ 0 & 0 & 0 & C_5 & 0 & 0 \\ 0 & 0 & 0 & 0 & C_6 & 0 \\ 0 & 0 & 0 & 0 & 0 & C_6 \end{bmatrix} \begin{Bmatrix} \epsilon_x \\ \epsilon_y \\ \epsilon_z \\ \gamma_{xy} \\ \gamma_{yz} \\ \gamma_{xz} \end{Bmatrix} \tag{6.25}$$

where,

$C_1 = \beta (1 - n \nu_2^2) E_2$

$C_2 = \beta (\nu_1 + n \nu_2^2) E_2$

$C_3 = \beta \nu_2 (1 + \nu_1) E_2$

$C_4 = \beta (1 + \nu_1) (1 - \nu_1) E_2 / n$

$C_5 = n E_2 / [2 (1 + \nu_1)]$

$C_6 = m E_2$

$\beta = n / [(1 + \nu_1) (1 - \nu_1 - 2n \nu_2^2)]$

$n = E_1 / E_2$

and $m = G_2 / E_2$

or in a compact form

$$\{ \sigma \} = [D] \{ \epsilon \} \tag{6.26}$$

where, [D] = elasticity matrix.

6.4.2.2 The element stiffness matrix

Since the eight-node linear brick element shown in figure 6.3 has three degrees of freedom at each corner, the nodal force vector {f} and the nodal displacement vector $\{d\}_e$ are given as

$$\{f\} = [f_{x1}, f_{y1}, f_{z1}, \ldots\ldots, f_{x8}, f_{y8}, f_{z8}]^T \tag{6.27a}$$

and

$$\{d\}_e = [u_1, v_1, w_1, \ldots\ldots, u_8, v_8, w_8]^T \tag{6.27b}$$

The element stiffness matrix can be evaluated as

$$[k] = \int_{V_e} [B]^T [D] [B] \, dV \tag{6.28}$$

where, V_e = volume of the hexahedron, using numerical integration.

The strain matrix [B] with respect to global co-ordinates is given by a 24 x 6 matrix consisting of eight 3 x 6 submatrices $[B_i]$ formed for i = 1 to 8 as

$$[B_i] = \begin{bmatrix} \frac{\partial N_i}{\partial x} & 0 & 0 \\ 0 & \frac{\partial N_i}{\partial y} & 0 \\ 0 & 0 & \frac{\partial N_i}{\partial z} \\ \frac{\partial N_i}{\partial y} & \frac{\partial N_i}{\partial x} & 0 \\ 0 & \frac{\partial N_i}{\partial z} & \frac{\partial N_i}{\partial y} \\ \frac{\partial N_i}{\partial z} & 0 & \frac{\partial N_i}{\partial x} \end{bmatrix} \tag{6.29}$$

The derivatives of the shape function N_i in the strain matrix [B] may be evaluated with respect to local coordinates by applying the chain rule of differentiation, as follows

$$\begin{Bmatrix} \frac{\partial N_i}{\partial \xi} \\ \frac{\partial N_i}{\partial \eta} \\ \frac{\partial N_i}{\partial \zeta} \end{Bmatrix} = \begin{bmatrix} \frac{\partial x}{\partial \xi} & \frac{\partial y}{\partial \xi} & \frac{\partial z}{\partial \xi} \\ \frac{\partial x}{\partial \eta} & \frac{\partial y}{\partial \eta} & \frac{\partial z}{\partial \eta} \\ \frac{\partial x}{\partial \zeta} & \frac{\partial y}{\partial \zeta} & \frac{\partial z}{\partial \zeta} \end{bmatrix} \begin{Bmatrix} \frac{\partial N_i}{\partial x} \\ \frac{\partial N_i}{\partial y} \\ \frac{\partial N_i}{\partial z} \end{Bmatrix} \tag{6.30}$$

The above square matrix is called the Jacobian matrix [J]. In order to find the global derivatives, the matrix [J] must be inverted.

$$\begin{Bmatrix} \dfrac{\partial N_i}{\partial x} \\ \dfrac{\partial N_i}{\partial y} \\ \dfrac{\partial N_i}{\partial z} \end{Bmatrix} = [J]^{-1} \begin{Bmatrix} \dfrac{\partial N_i}{\partial \xi} \\ \dfrac{\partial N_i}{\partial \eta} \\ \dfrac{\partial N_i}{\partial \zeta} \end{Bmatrix} \tag{6.31}$$

Since in the isoparametric formulation position in the element is expressed by the same interpolation functions as are the displacements, the Jacobian matrix may be evaluated from the geometric relationships:-

$$x = \sum_{i=1}^{i=8} N_i \, x_i \,, \qquad y = \sum_{i=1}^{i=8} N_i \, y_i \,, \qquad z = \sum_{i=1}^{i=8} N_i \, z_i \tag{6.32}$$

The Jacobian matrix may now be written in the form

$$[J] = \begin{bmatrix} \Sigma \dfrac{\partial N_i}{\partial \xi} x_i & \Sigma \dfrac{\partial N_i}{\partial \xi} y_i & \Sigma \dfrac{\partial N_i}{\partial \xi} z_i \\ \Sigma \dfrac{\partial N_i}{\partial \eta} x_i & \Sigma \dfrac{\partial N_i}{\partial \eta} y_i & \Sigma \dfrac{\partial N_i}{\partial \eta} z_i \\ \Sigma \dfrac{\partial N_i}{\partial \zeta} x_i & \Sigma \dfrac{\partial N_i}{\partial \zeta} y_i & \Sigma \dfrac{\partial N_i}{\partial \zeta} z_i \end{bmatrix} \tag{6.33}$$

The elemental volume dV = dx dy dz may be written in terms of local co-ordinates as

$$dV = dx\ dy\ dz = \det \mid J \mid d\xi\ d\eta\ d\zeta \tag{6.34}$$

Therefore, the volume integral (element stiffness matrix) may be written in the form

$$\begin{aligned} \{ k \} &= \int_{V_e} [B]^T [D] [B]\ dV \\ &= \int_{-1}^{1} \int_{-1}^{1} \int_{-1}^{1} [B]^T [D] [B] \det \mid J \mid d\xi\ d\eta\ d\zeta \end{aligned} \tag{6.35}$$

The integration is carried out by summation at Gauss points to give the 24 x 24 stiffness matrix

$$[k] = \sum_{k=1}^{p} \sum_{j=1}^{n} \sum_{i=1}^{m} w_i\ w_j\ w_k\ f (\xi_i , \eta_j , \zeta_k) \tag{6.36}$$

where,

m, n, and p = sampling points in ξ, η, and ζ directions, respectively

w_i, w_j, and w_k = weight coefficients

and $f (\xi_i, \eta_j, \zeta_k) = [B]^T [D] [B] \det [J]$

In this study 2 sampling points are used in each direction.

6.4.2.3 Prescribed boundary conditions

The equilibrium equations (6.11) are modified to account for prescribed boundary displacements. Several different methods of actually performing this operation exist. In this study this is carried out according to the procedure suggested by Zienkiewicz (1977). In this method if d_i is prescribed to be equal to α, then the diagonal term k_{ii} of [K] is multiplied by an arbitrary large number, say 10^{12}, and the corresponding term in the right hand side vector is replaced by $k_{ii} \times 10^{12} \times \alpha$.

6.4.2.4 Solution of equilibrium equations

Equation (6.11) is symmetrical and banded. The solution of this yields the unknown nodal displacements. One of several methods for solving the equations is direct Gaussian elimination in which the given system of equations is reduced to an equivalent triangular system and then, the solutions given inturn by back substitution. The method is well documented in the literature, see for example Fox (1964) and Zienkiewicz (1977).

With large systems of equations, as the matrix [K] is symmetric, it is common to store it in a compact rectangular array by retaining only terms located in the upper half of the diagonal band including the diagonal elements as shown in figure 6.5. This requires only n x UBW vector space storage where n is the number of equations and UBW is the upper band width.

The requirement for main core storage space is then kept to a minimum using peripheral storage and a blocking technique. The core storage needed using this method is only 2m x m where $m \geq UBW$. The arrangements of blocks in the core and peripheral unit are shown in figures 6.6 and 6.7.

The assembly of stiffness matrices and load vectors are carried out block by block. First all the terms from elements which contribute to the first block of equations are assembled. These equations are then modified for prescribed displacements if any. The first block of equations are then transferred to a peripheral unit (2). The bottom block of equations are then shifted to the top block locations in the core and the bottom block is initialized. After the assembly of the second block of equations is completed, it is transferred on to the peripheral unit. This is repeated until all the equations are stored peripherally in blocks.

After the completion of this stage, the first two blocks are transferred back into the main core. Elimination is carried out on the first m equations and the upper triangular form of these equations is transferred to a peripheral unit (1). The second block of equations are then shifted to the top block in the core and the third block of equations transferred from the peripheral unit to the bottom block in the core. The second block of equations are then reduced to upper triangular form and transferred to the peripheral unit. This is carried out until all the equations are reduced to upper triangular form.

Back substitution is carried out starting from the last block. The upper triangular matrix in unit (1) is transferred block by block into the core and back substitution is carried out yielding the displacement vector.

6.4.2.5 Evaluation of stresses in the medium and the pier elements

After evaluation of strains using equation (6.23), the stresses in the soil medium and the pier foundation are evaluated using equation (6.26). The three principal stresses can be evaluated by solving the following equation (see Boresi et al. (1978))

$$\sigma^3 - I_1 \sigma^2 + I_2 \sigma - I_3 = 0 \tag{6.37}$$

where,

$$I_1 = \sigma_x + \sigma_y + \sigma_z$$

$$I_2 = \sigma_x \sigma_y + \sigma_y \sigma_z + \sigma_x \sigma_z - \tau_{xy}^2 - \tau_{yz}^2 - \tau_{zx}^2$$

and $$I_3 = \sigma_x \sigma_y \sigma_z + 2 \tau_{xy} \tau_{yz} \tau_{zx} - \sigma_x \tau_{yz}^2 - \sigma_y \tau_{xz}^2 - \sigma_z \tau_{xy}^2$$

The three roots (σ_1, σ_2, σ_3) of equation (6.37) give the values of the three principal stresses. This equation was solved in this study using MATHEMATICA, the commercial mathematical package.

6.4.3 Description of the computer program PIER3DLN for linear analysis

Computer program PIER3DLN was written in FORTRAN to evaluate the effects of lateral load on the behaviour of a rigid pier foundation using the three-dimensional finite element procedure outlined above. The program can be used on an I.B.M. PC compatible system or a Unix Main Frame system. A simplified flow chart for the program is shown in figure 6.8 and the computer program listing and the data preparation instructions are given in Appendix F2. Hence in this section, only important features of the program are discussed.

An automatic mesh generation routine facility was written to generate the entire model geometry and element generation requiring only the number of nodes, number of soil and foundation elements and the co-ordinates of the nodal points along x, y and z axes. A typical finite element idealisation is shown in figure 6.9. In the automatic mesh generation the origin of the co-ordinate axes is node number 1. The numbering continues first in the z- direction, then in the y- direction and finally in the x- direction. Elements are also numbered starting from the top element at the origin and continues in the same order.

The pier and the soil medium are modelled using continuum elements. Inhomogeneity and transverse isotropy of the soil medium can be considered. The same stiffness and stress subroutines are used for both the soil medium and the pier.

The soil can be specified as transversely isotropic or isotropic while the pier will usually be considered to be isotropic. It is possible to consider vertical inhomogeneity in the soil since the properties are given layer by layer.

Force components are applied in the directions of the x, y, and z axes. Moment components must be applied by means of two equal and opposite forces, F and -F a distance M/F apart, as shown in figure 6.10. Two different types of load applications were programmed. A value of LDC = 1 indicates an arbitrary loading condition, where the user can apply the loads at any points by defining the node numbers and the values of the load components applied. However for use in this research the pier is usually divided into two elements in both the x- and y- directions, and by specifying a value of LDC = 0, the distribution of moment or/and axial and lateral loads at the nine nodes at the top of the pier is calculated and applied in the program. For the symmetric case, six nodes instead of nine are considered as shown in figure 6.11.

To account for symmetry the common nodes on the y- axis are prevented from translation. This can be done either by typing the node numbers and the relevant fixity conditions or automatically when a value of NSYM = 1 is chosen.

The computer output consists of the following. The input information, the x-, y- and z- co-ordinates of the nodes as generated in the program. This is followed by the initial stresses at the centre of each element. Then the displacements in the x-, y- and z- directions are printed for all nodes. Finally, the stresses at the centre of each element are printed.

6.4.4 Assessment of accuracy

In order to assess the accuracy of the finite element procedure, the free standing model cantilever shown in figure 6.12 was employed. The model was tested by applying separate horizontal, vertical and moment loads at the free end. With the computer program PIER3DLN the cantilever was modelled by fixing a pier at its base and setting the specific weight of the pier to zero. The length of the cantilever was equal to 10 units. The finite element mesh employed is shown in figure 6.12.

The values of displacement obtained from the finite element calculations are compared with those obtained from the conventional bending theory in table 6.1 for the vertical, horizontal and moment loads, respectively. For vertical loading the deflection was found to be same as the expected value, for lateral loading 1% less than expected and for moment loading 3% less than expected. These results are well within the accuracy of any results expected from finite element analysis.

Distance from top	Displacements from Load A		Displacements from Load B		Displacements from Load C	
	Beam Formulae	Finite Element	Beam Formulae	Finite Element	Beam Formulae	Finite Element
0	100	100	100	98.91	100	96.97
1	90	90	85.05	84.22	81	78.55
2	80	80	70.40	69.82	64	62.06
3	70	70	56.35	56.00	49	47.52
4	60	60	43.20	43.05	36	34.91
5	50	50	31.25	31.27	25	24.24
6	40	40	20.80	20.95	16	15.52
7	30	30	12.15	12.36	9	8.73
8	20	20	5.60	5.82	4	3.88
9	10	10	1.45	1.60	1	0.97
10	0	0	0	0	0	0

Table 6.1 Free standing cantilever: Comparative values of deflection.

6.4.5 <u>Description of the computer program PIER3DNL for non-linear analysis</u>

In the elastic analysis the soil and pier are assumed to be in contact at all times. However, since soil has limited ability to take tension, it is likely that separation occurs behind the pier at the top and in front of the pier at the bottom. Because of this separation and the non-linearity of the stress-strain soil behaviour, it is desirable in finite element analysis to account for this behaviour. One of the most popular methods of simulating the non-linear behaviour of soil is to use the hyperbolic stress-strain model and an incremental finite element analysis. The loading is applied in a series of small increments and a modulus for each element is selected at the beginning of each increment depending on the stresses in the element. The incremental displacements, stresses and strains are summed progressively. Hyperbolic stress-strain relationships were described in Chapter 3.

The three-dimensional linear elastic program PIER3DLN, described earlier in this chapter, was modified here to simulate non-linear behaviour and called PIER3DNL. A simplified flow chart of operation of PIER3DNL for the complete analysis of a pier foundation is shown in figure 6.13 and the program listing and data preparation are given in Appendix F3. In this section, only the different features of the program are discussed.

The two main differences for the preparation of input data for the program PIER3DNL from the program PIER3DLN are that seven hyperbolic model parameters, instead of five elastic parameters, and the number of increments have to be specified. The computer output shows similar differences. When a value of NPRNT = 1 is specified, the nodal displacements and element stresses at the end of each increment are printed but when a value of NPRNT = 0 is given, only the final results are printed.

6.4.5.1 Incremental analysis

The first stage of the analysis was to introduce the initial stresses due to unit weights, water pressures and earth pressure coefficients, in the soil and foundation elements. The horizontal stresses, σ_x and σ_y, in an element were assumed to be equal to $K_0\ \sigma_z$, in which σ_z is the vertical stress in the element and K_0 is the coefficient of lateral earth pressure at rest. Shear stresses were set equal to zero for all elements. The load was then applied in increments. Two iterations were performed for each increment. The modulus values for soil elements for the first iteration were based on the values of stress at the beginning of that increment. In the second iteration, refined values were based on the average values of stress at the beginning of that increment and at the end of first iteration of the increment and on whether an element was being subjected to first time loading, unloading or re-loading. If tensile stresses were obtained in any soil element it was assigned a small value, E_t = 1.0 kN/m^2. If an element failed in shear a small value, E_t = 0.5 kN/m^2 was assigned.

At the end of each increment, the incremental nodal displacements and element stresses in soil and foundation elements were added to the previous total values to obtain the nodal displacements and element stresses at the end of the increment.

6.5 Conclusions

The three-dimensional linear and non-linear computer programs, developed in this study, and an existing two-dimensional one can be used for both clay and sand by providing the appropriate parameters. Assessment of the accuracy of the linear 3-D program indicated that the programs are reliable. The application of the programs to predict the behaviour of piers in saturated remoulded clay, is considered in Chapter 7.

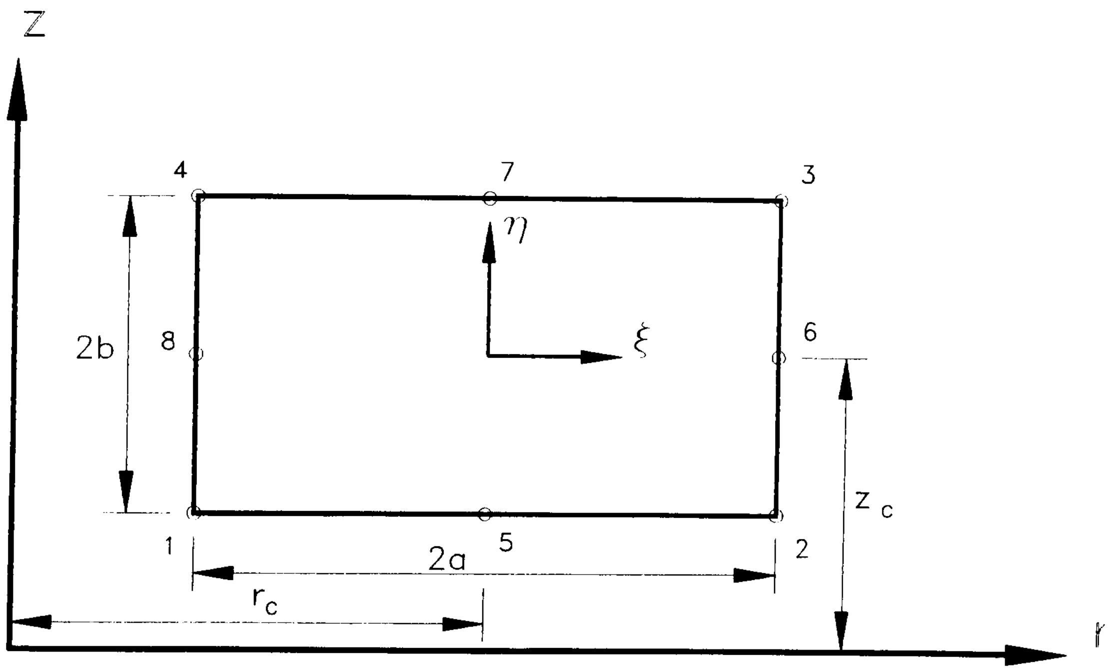

a) Eight Node Isoparametric Element

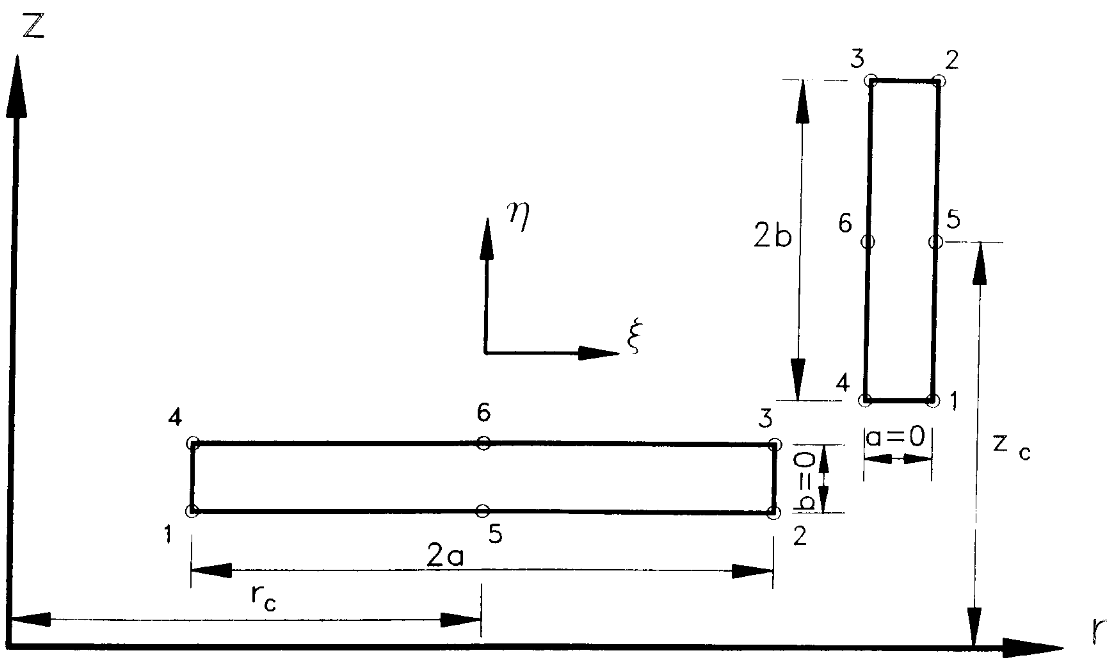

b) Six Node Isoparametric Element

Figure 6.1 Pier, Soil and Friction Elements.

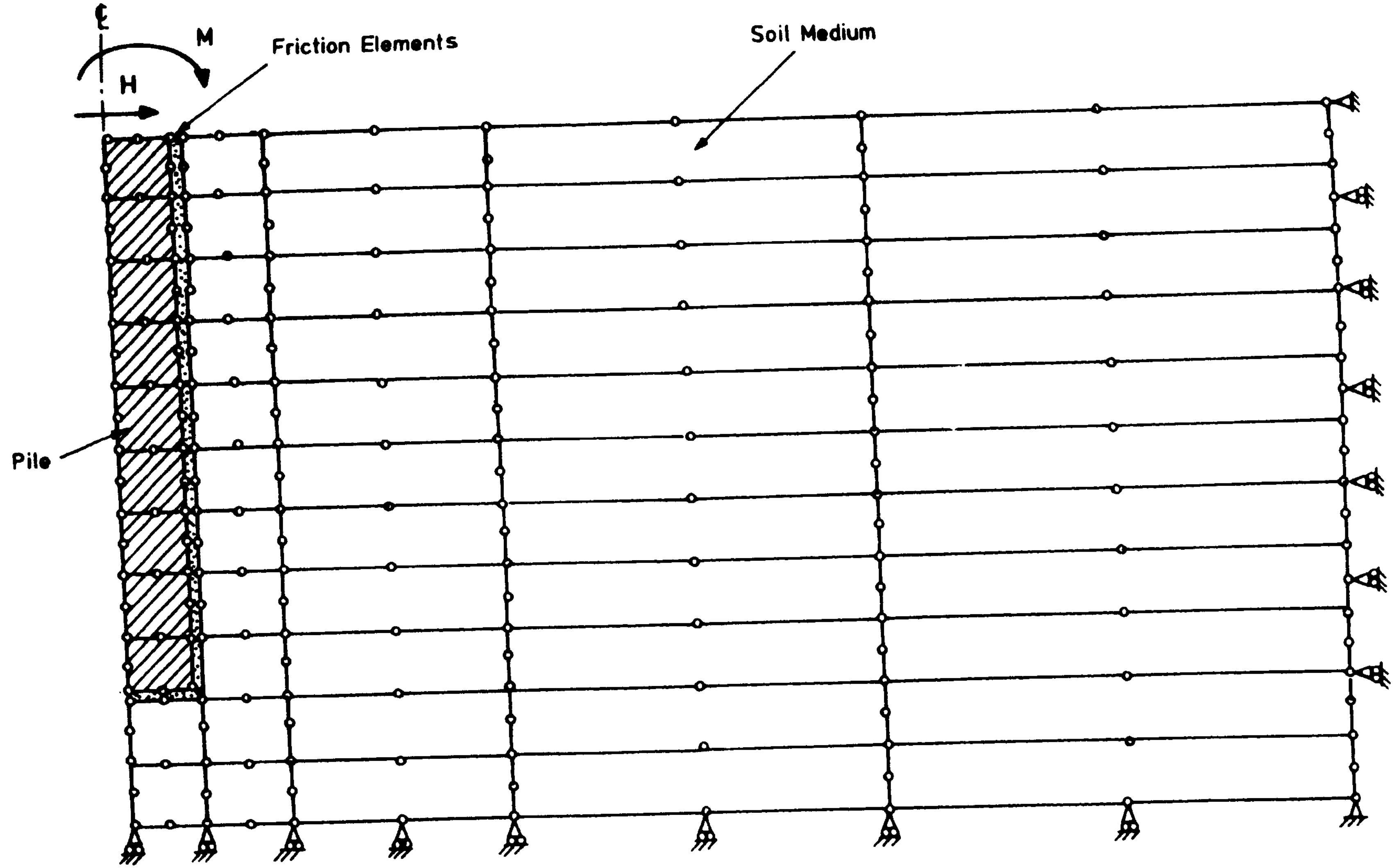

Figure 6.2 Typical Finite Element Mesh for Program PIER2D.

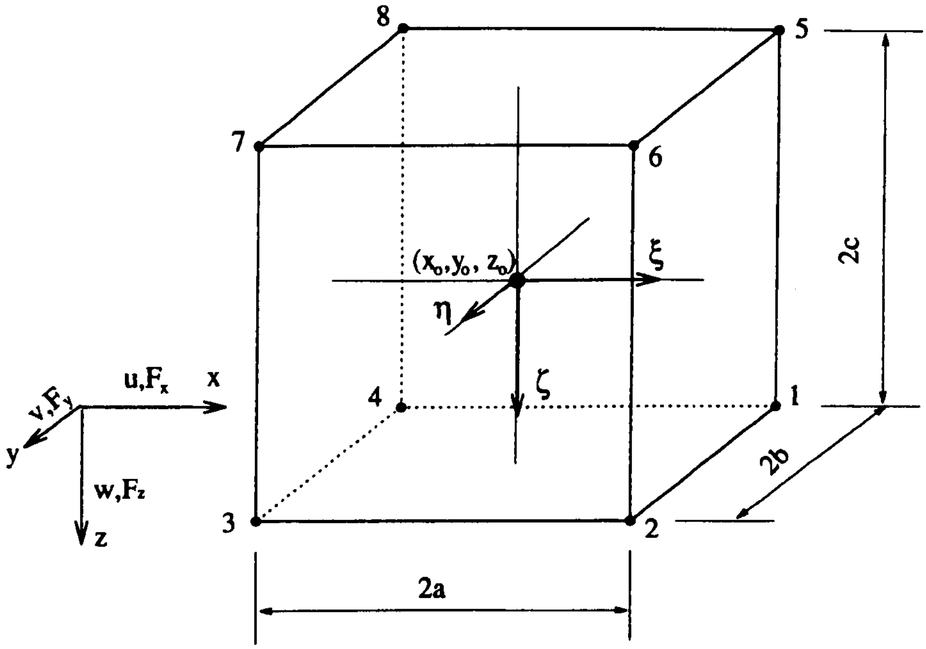

Figure 6.3 Isoparametric Eight-Node Rectangular Prismatic Element.

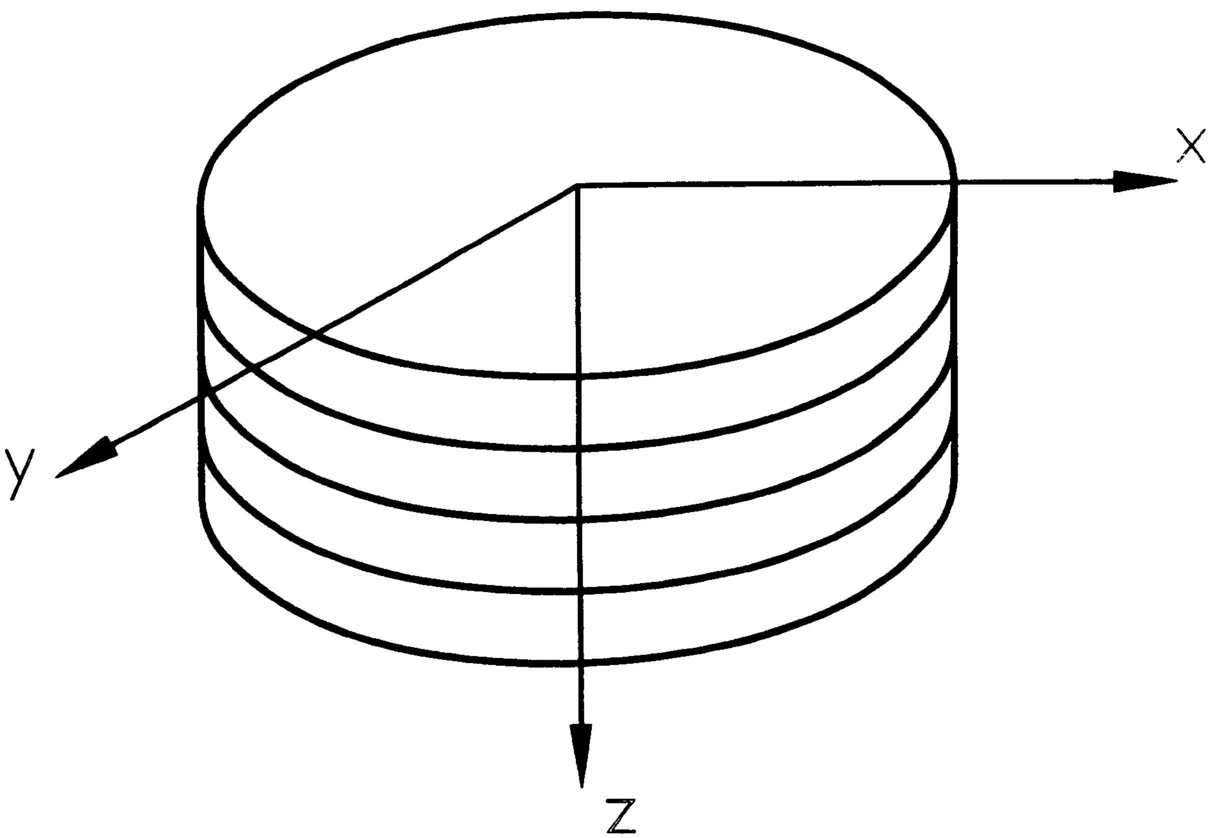

Figure 6.4 Transversely Isotropic Body.

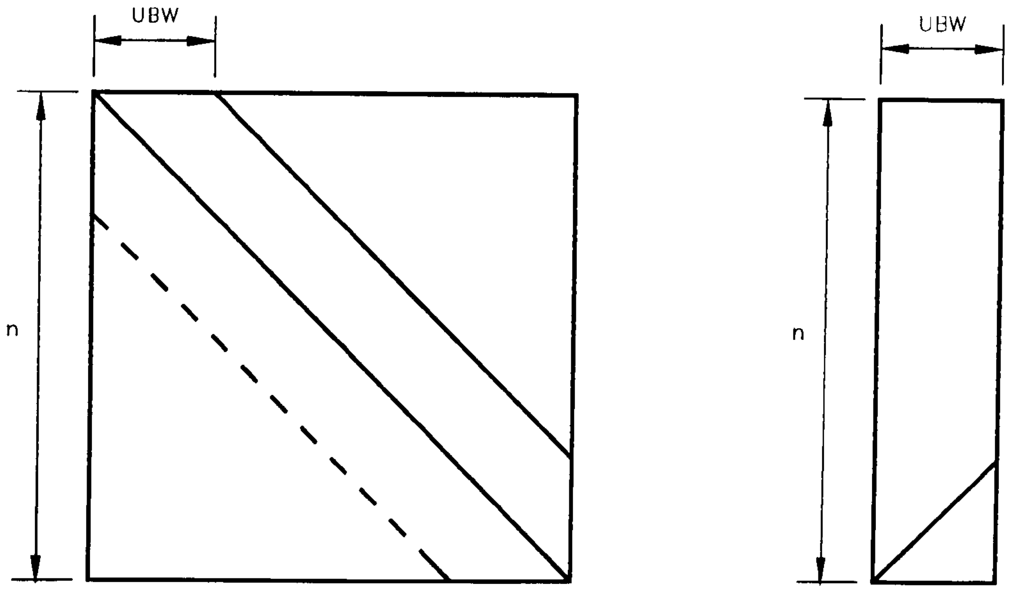

Figure 6.5 Banded Form of Stiffness Matrix.

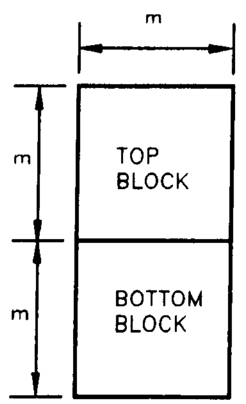

Figure 6.6 Block Arrangement in the Core.

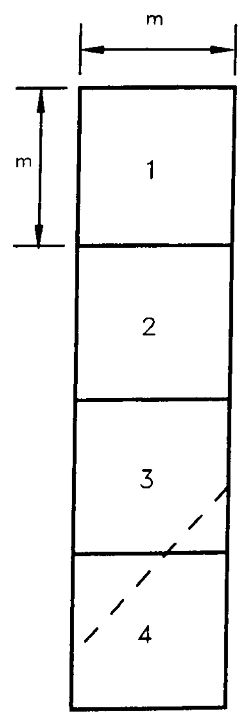

Figure 6.7 Block Arrangement in the Peripheral Unit.

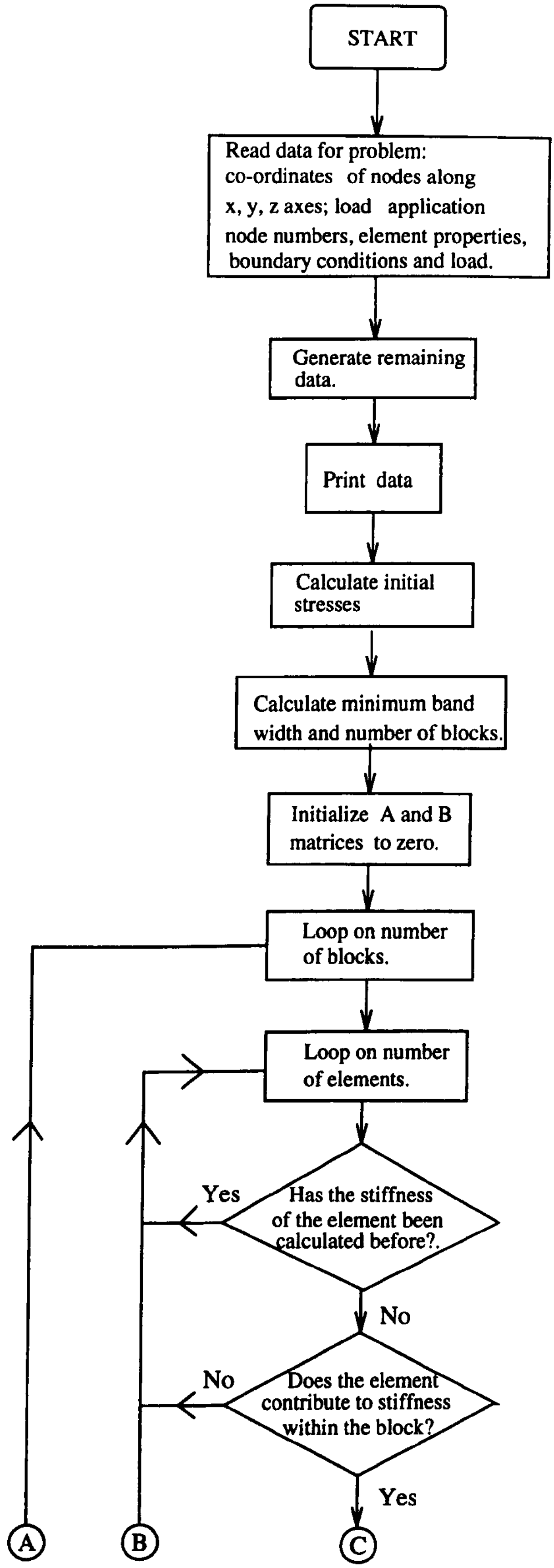
START
Read data for problem: co-ordinates of nodes along x, y, z axes; load application node numbers, element properties, boundary conditions and load.
Generate remaining data.
Print data
Calculate initial stresses
Calculate minimum band width and number of blocks.
Initialize A and B matrices to zero.
Loop on number of blocks.
Loop on number of elements.
Has the stiffness of the element been calculated before?.
Yes
No
Does the element contribute to stiffness within the block?
No
Yes
A
B
C

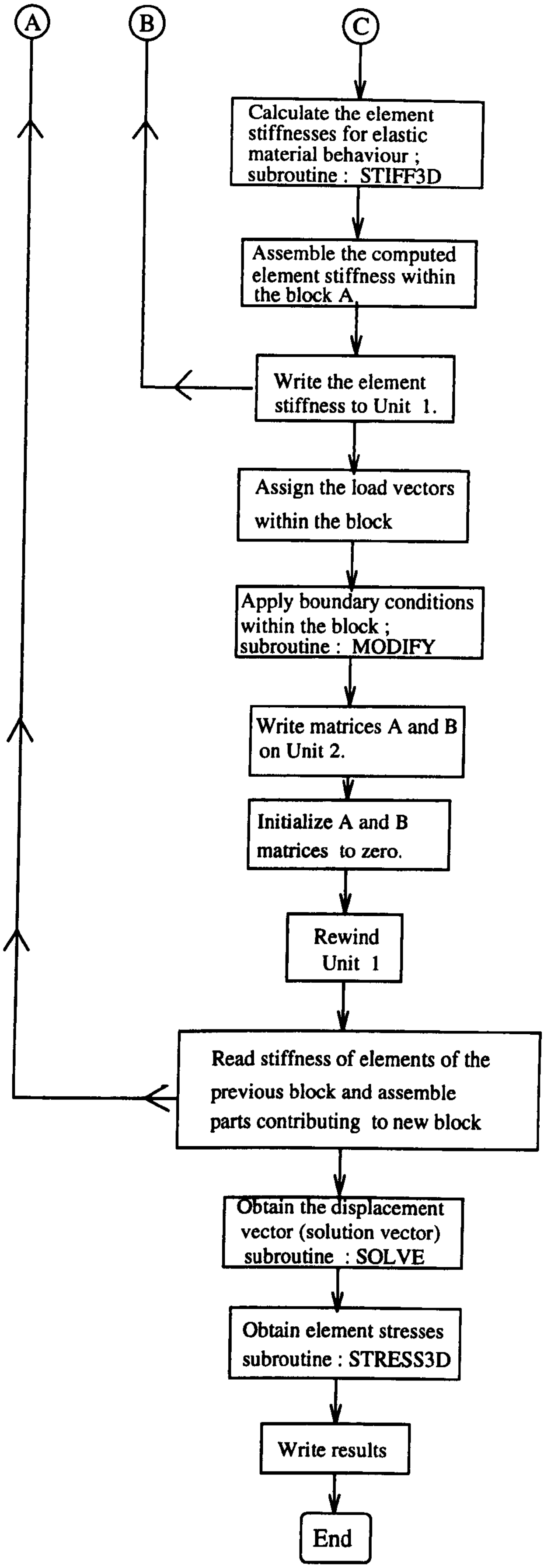

Figure 6.8 Simplified Flow Chart for Program PIER3DLN.

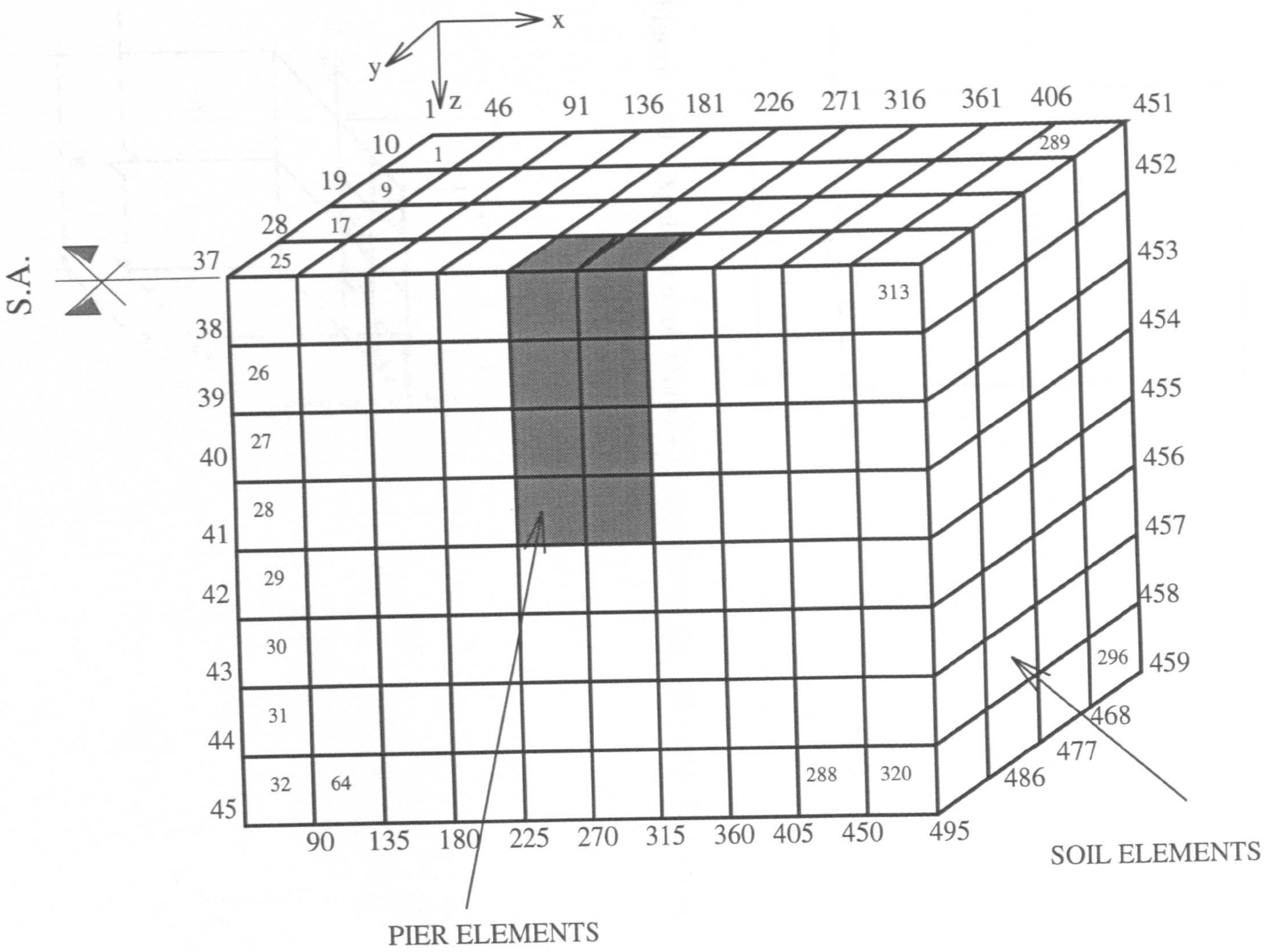

Figure 6.9 Typical Finite Element Mesh for PIER3DLN (Symmetric Case).

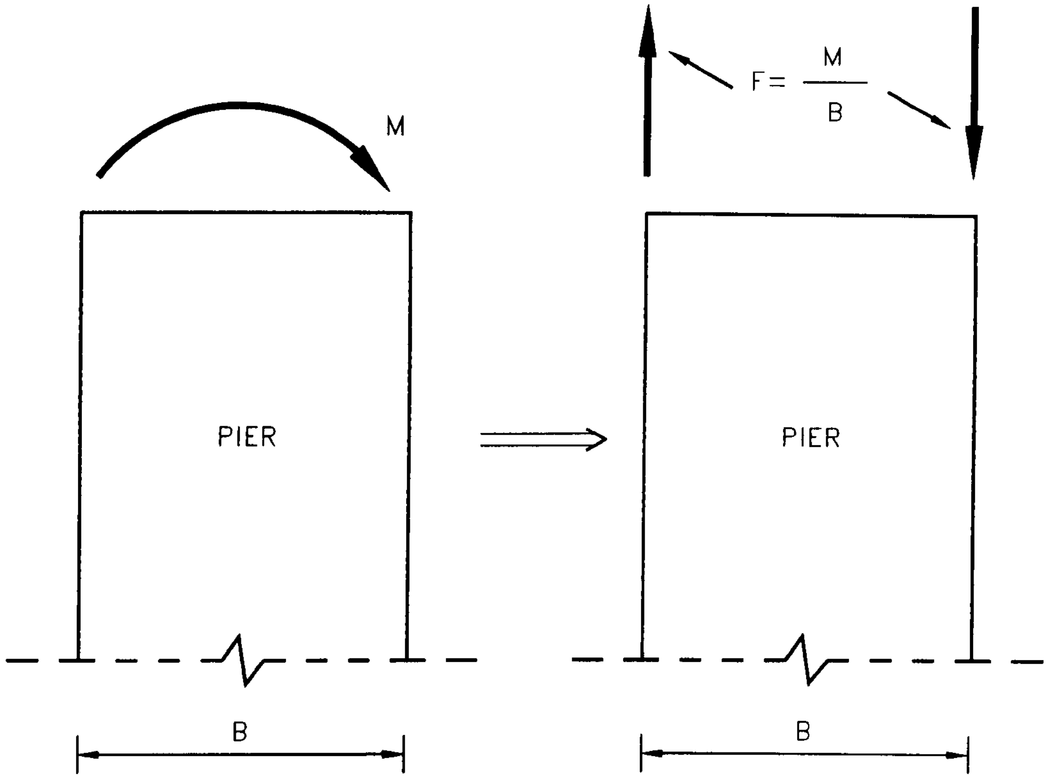

Figure 6.10 Application of Moment Using Two Equal and Opposite Forces.

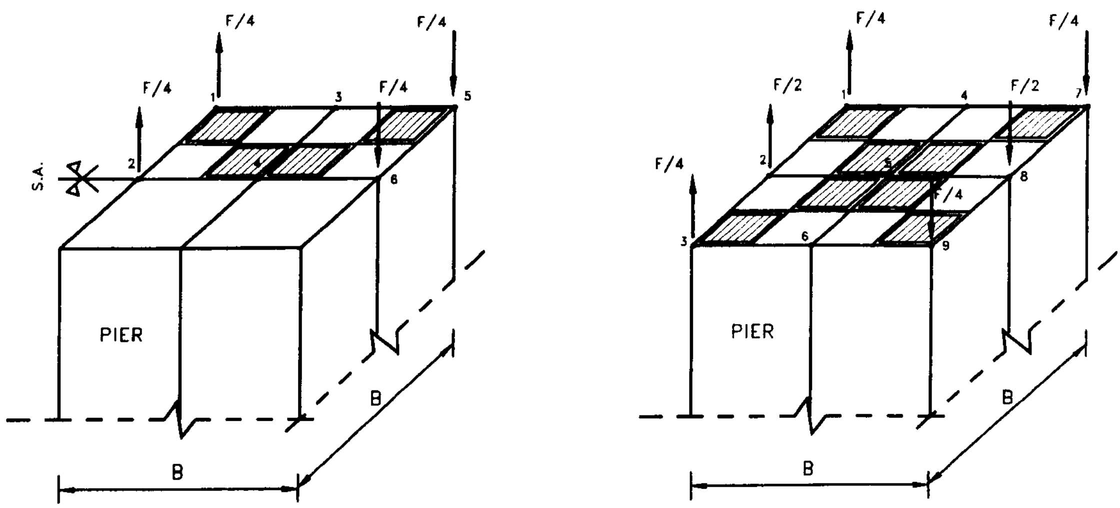

a) Symmetric Case   **b)** Non-Symmetric Case

Figure 6.11 Loading Arrangement.

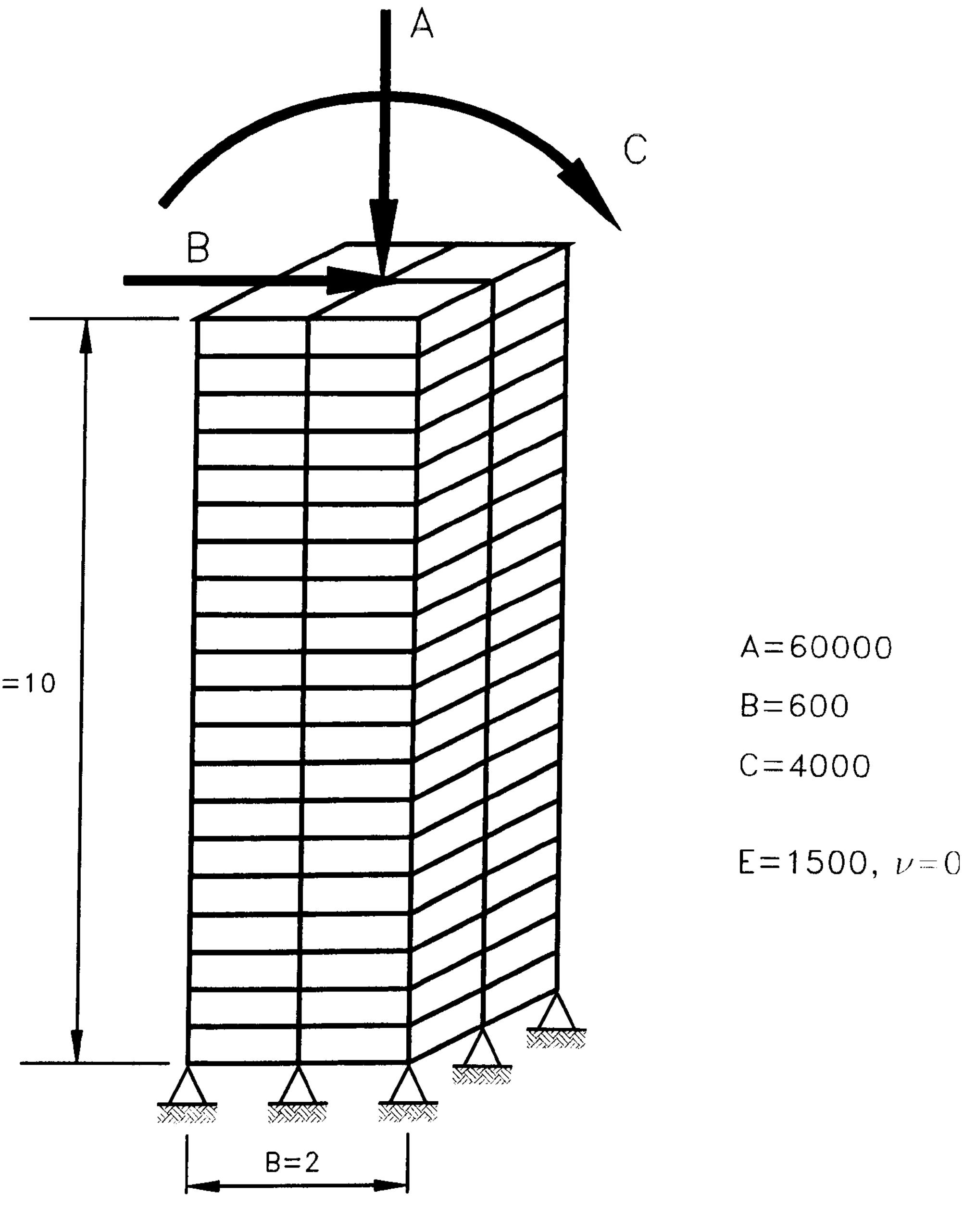

Figure 6.12 Finite Element Mesh of Free Standing Cantilever.

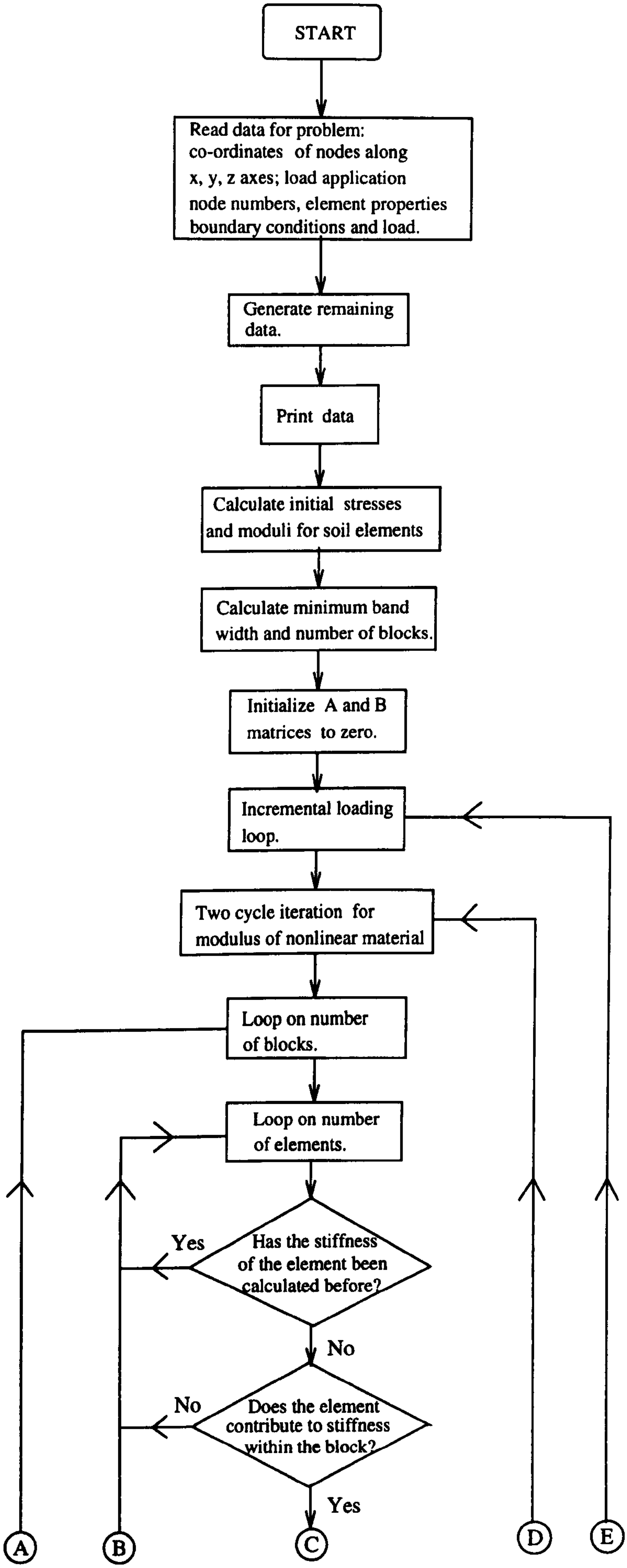
START
Read data for problem: co-ordinates of nodes along x, y, z axes; load application node numbers, element properties boundary conditions and load.
Generate remaining data.
Print data
Calculate initial stresses and moduli for soil elements
Calculate minimum band width and number of blocks.
Initialize A and B matrices to zero.
Incremental loading loop.
Two cycle iteration for modulus of nonlinear material
Loop on number of blocks.
Loop on number of elements.
Has the stiffness of the element been calculated before?
Yes
No
Does the element contribute to stiffness within the block?
No
Yes
A
B
C
D
E

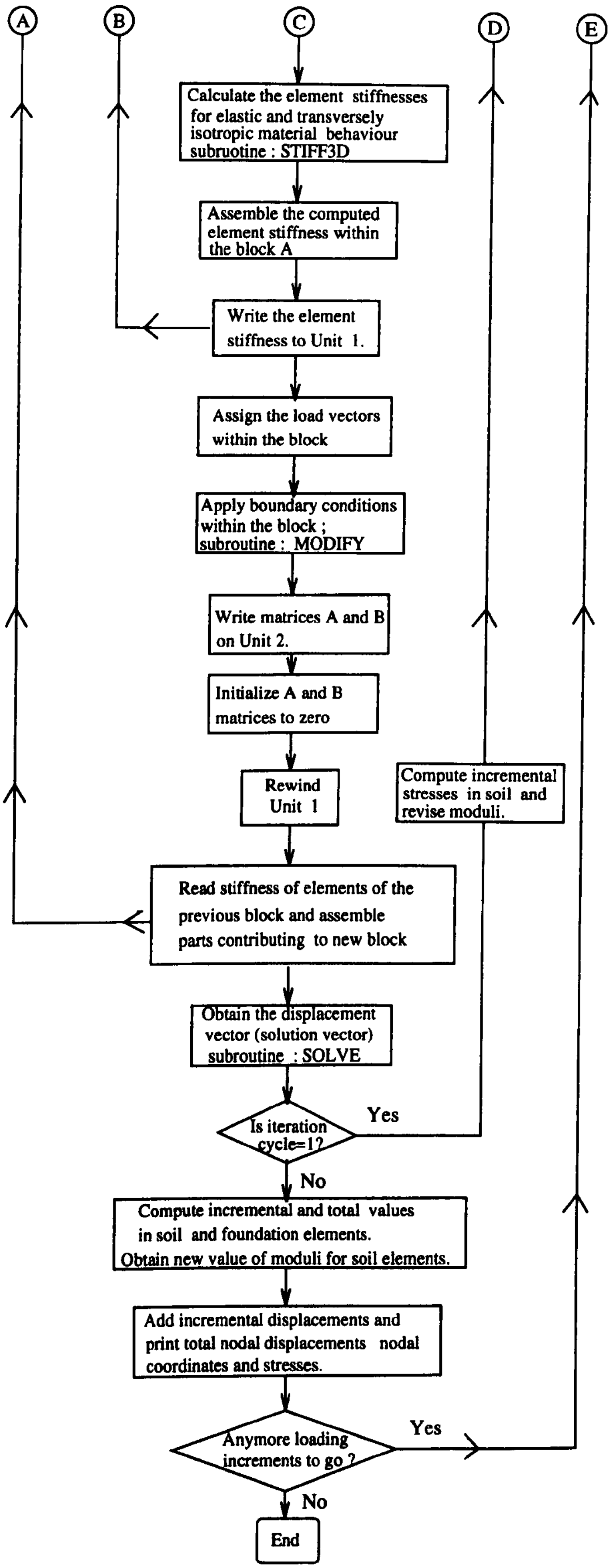

Figure 6.13 Simplified Flow Chart for Program PIER3DNL.

CHAPTER 7

RESULTS OF NUMERICAL STUDIES OF SHORT PIER FOUNDATIONS IN CLAY

7.1 Introduction

Finite element analyses were carried out to predict the moment/rotation responses of pier foundations and to compare them with those observed in the model tests. The three finite element computer programs described in Chapter 6 were used. Linear elastic properties were used for both the pier and the soil elements in the two-dimensional axi-symmetric and the three-dimensional linear analyses while the hyperbolic stress-strain model was used for the soil in the three-dimensional non-linear analysis.

In this chapter, five of the piers used in the model tests are considered. The analyses of one of these is explained in considerable detail to demonstrate how the programs should be used while the results of the remaining analyses are discussed briefly in section 7.5. A series of meshes with different dimensions are employed to develop the optimum distances between the foundation and soil boundaries in order to reduce the side effect. The values of soil properties used are those obtained from the laboratory tests described in previous chapters and both the full-scale geometry and the restricted prototype geometry modelled in the tests are used for the construction of the meshes.

The effect of the pulling height on the moment/rotation behaviour of a rigid pier foundation using the 3-D linear program is presented in section 7.2.5. Comparison of results from the three finite element programs are also discussed.

7.2 Three-Dimensional Linear Analysis

The accuracy of the three-dimensional linear computer program (PIER3DLN), developed in this study, has been assessed in Chapter 6. The program was first used to develop the most suitable mesh and boundaries for the supporting soil. In this investigation, the properties of the soil and the foundation elements were kept similar to those employed in the experimental study. The pier was subjected to a lateral load and moment applied at ground level to represent a lateral load applied at a given height above ground level. With the exception of the analyses described in section 7.2.5, this height was taken as 6 m at full-scale (150 mm at model scale).

7.2.1 Finite element meshes and boundary conditions

Five finite element meshes were employed in this study. Since the foundation and the loading are symmetrical only one-half of the foundation was analyzed. The construction of the meshes was based on the prototype size of a typical steel pier of 1.60 m (40 mm in model) square section and 2.40 m (60 mm in model) long which was used in the experimental study. For each mesh, the total number of elements and the number of elements in the x-, y- and z- directions are presented in table 7.1 together with the total number of nodes. Each mesh had 2, 1 and 4 pier elements along the x-, y- and z- directions, respectively. A typical finite element mesh composed of soil and foundation elements together with the boundary conditions used for the analyses, is shown in figure 7.1, which contains 784 elements and 1080 nodal points. The mesh patterns were so arranged that smaller elements were used near the foundation, where the displacement and stresses are expected to vary quickly and larger elements in regions away from it. By scaling the widths of the elements from the pier face to the boundary, the end boundaries of the soil stratum were located at distances of 2.5, 4, 5, 7.5, 10 and 20 times the breadth of the pier from the centre. The side boundaries were located at a distance of 5.75 times the breadth of the pier from the centre and it was assumed that the influence of these boundaries would be negligible. The nodes on the end x-z and y-z planes were restrained in the y- and x-directions, respectively, while the nodes on the bottom plane were restrained in the z-direction. Thus all boundary surfaces were considered to be smooth.

Mesh Number	Number of Elements			Total Number of elements	Total number of Nodes
	x- dir.	y- dir.	z- dir.		
1	6	3	8	144	252
2	10	5	8	400	594
3	14	7	8	784	1080
4	16	7	8	896	1224
5	20	7	8	1120	1512

Table 7.1 Description of Meshes

7.2.2 Soil and foundation properties

The soil was assumed to be homogeneous, isotropic and elastic and to have uniform properties with depth. The undrained modulus of the soil, E_s, can be determined from equations 3.7 and 3.17 (see Chapter 3) at a given moisture content. Hence for the average value of the moisture content observed in the model tests of 17% the undrained modulus, E_s, was determined as 1668 kN/m^2. Poisson's ratio for deformation without drainage is equal 0.5, and since this value cannot be used directly in finite element analyses, a value of 0.48 was used in this study for consistency in all the programs. A value of one was assumed for K_0. Young's modulus and Poisson's ratio for the piers were taken as 207.10^6 kN/m^2 and 0.25, respectively.

A summary of the parameters used is given in table 7.2.

SOIL		
Parameters		Value
Moisture Content,	m	17.0 %
Young's Modulus,	E_s	1668 kN/m^2
Bulk Unit Weight,	γ_b	21.07 kN/m^3
Poisson's Ratio,	ν_s	0.48
Coefficient of Earth Pressure at Rest,	K_o	1
FOUNDATION		
Poisson's Ratio,	ν_p	0.25
Young's Modulus,	E_p	207.0x10^6 kN/m^2

Table 7.2 The Properties of the Soil and Foundation (for Program PIER3DLN).

7.2.3 Mesh selection and analysis at full-scale geometry

The pier (B=1.6m, D=2.4m) was analyzed under a lateral load of 73.33 kN and a moment of 440.0 kNm applied at its top. These values were obtained from the centrifugal experiment, M46CT1, for 1.0° rotation.

The analysis using PIER3DLN required about 600 seconds CPU time in the Unix Main Frame System of the University of Liverpool for mesh no. 3 with 1080 nodal points. Examples of input and limited output data using mesh no. 3 are listed in Appendix G1.

The pier rotations, which were simply calculated from displacements, obtained using mesh no. 3 with a stratum depth of 5B = 8 m are presented in table 7.3 for end y-z planes at 2.5B, 4B, 5B, 7.5B, 10B and 20B, respectively. The lateral displacements at the top of the pier increased with increase in boundary distance, as would be expected, but the depth to the point of rotation also increased. As seen from the table, the values do not change significantly for end boundaries at greater distances than 7.5B.

Distance	2.5 B = 4m	4 B = 6.4m	5 B = 8m	7.5 B = 12m	10 B = 16m	20 B ≈ 31.8m
Rotation	1.01°	0.94°	0.93°	0.85°	0.83°	0.84°

Table 7.3 Calculated Rotation for Different Soil Boundaries (mesh no. 3)

The results obtained using different meshes for a boundary distance of 7.5B and stratum depth 5B are shown in table 7.4. It can be seen that, the magnitude of the calculated rotation increases with an increase in the number of elements but does not increase significantly for meshes finer than no. 3.

Mesh Number	1	2	3	4	5
Number of Elements Employed in the Mesh	144	400	784	896	1120
Rotation	0.47°	0.75°	0.85°	0.86°	0.87°

Table 7.4 Calculated Rotation for Different Meshes (7.5 B = 12 m)

In order to see the effect of the depth of stratum, it was extended from 8 m to 12.4 m using mesh no. 3 with boundaries at a distance 7.5 B. The difference in the rotation was less than 0.4 %.

Hence mesh no. 3 was selected for further studies with end boundaries at 7.5B and stratum depth 5B.

7.2.4 Analysis of the restricted prototype geometry modelled in the tests

As indicated in the previous section, some amount of side effect occurs depending on the distances of the end boundaries when they are at less than 7.5 B from the centre of the pier. Since the results obtained in this chapter will be compared with the experimental results, the construction of the meshes need to be based on the restricted prototype modelled in the centrifugal and conventional tests. The soil bin, employed in the conventional tests, was 570 mm long by 460 mm wide and the depth of soil used was about 240 mm. In the centrifuge tests, the soil bin was 400 mm long, 460 mm wide and it was filled to a depth of 180 mm. Thus in the conventional tests the side and bottom boundaries of the soil stratum were located at distances of about 7.1B, 5.75B and 6B, respectively, while they were located at distances of about 5B, 5.75B and 4.5B, in the centrifugal tests.

These two soil bin sizes were used together with mesh no. 3. The measured bulk density was used in the input data for the analysis of a conventional test while 40 times this value was used for the analysis of a centrifuge test in order to match the stress levels in that test. Model load and moment values of $73.33/40^2 = 0.045833$ kN and $440.0/40^3 = 0.006875$ kNm respectively were applied at the top of the 40 mm square by 60 mm long pier. The rotations of the pier were calculated as 0.926° for the conventional test and 0.932° for the centrifuge test.

7.2.5 Effect of Pulling Height

In both experimental and numerical studies, the lateral pulling force was usually applied at 150 mm (6 m in prototype) above the level of the clay since this is the approximate height of railway power lines. In order to investigate the effect of the pulling height on the moment carrying capacity of a short rigid pier the 3-D linear computer program, PIER3DLN, was used. A typical model pier of 40 mm square section and 60 mm long was considered, so that the ratio of the depth to breadth of the pier, D/B, was 1.5. Mesh no. 3 was used for prototype size of the model. The pulling height varied from 1 to 20 m. A moment applied at the top of the pier was

440 kNm while the lateral load varied from 22 kN to 440 kN depending on the pulling height. The values of rotations obtained are shown in table 7.5 together with the values of the pulling height, pulling height ratio, L/D, and lateral pulling force. Figure 7.2 shows the variation of the rotations with L/D. The results show that the rotation decreases with an increase in pulling height ratio and that the pulling height greatly affects the performance of the pier foundation for L/D < 2.5. Thus in the present study in which a constant pulling height was used, the pulling height ratio varied from 2.5 to 7.5 and its effect was not significant. A similar conclusion was reached by Nazir (1994). He showed that the effect of pulling height was an important parameter on the moment carrying capacity of short piles in sand especially for L/D < 2.0, contrary to UIC/ORE (1957) where it was concluded that it was only of minor importance.

Pulling Height (L), m	Pulling Height Ratio (L/D)	Lateral Load (kN)	Pier Rotation (°)
1	0.417	440.00	1.700
2	0.833	220.00	1.190
4	1.667	110.00	0.936
6	2.500	73.33	0.850
8	3.330	55.00	0.810
10	4.170	44.00	0.780
12	5.000	36.67	0.766
14	5.830	31.43	0.754
16	6.670	27.50	0.745
20	8.330	22.00	0.732

Table 7.5 Calculated Rotation for Different Pulling Height Ratio

7.3 Two-Dimensional (axi-symmetric) Linear Analysis

Two dimensional (axi-symmetric) linear analysis was carried out using the existing program, PIER2D. For convenience the program used in this study was simplified to analyze only problems in which soil and pier are homogeneous.

7.3.1 Finite element mesh and boundary conditions

The same discretisation was used as in the central x-z plane of mesh no. 3 for the three-dimensional analysis described in section 7.2.1. (Since this program takes account of axi-symmetry, only one half of the mesh is employed.) The finite element mesh composed of soil, pier and friction elements used for the analyses is shown in figure 7.3.

The nodes along the right-hand boundary were restrained to horizontal displacements, while the nodes at the bottom were restrained to vertical displacements, simulating smooth surfaces.

7.3.2 Soil medium, pier and friction element properties

In addition to the properties of the soil medium and foundation used in the three-dimensional linear analysis, the flexural and the axial rigidities of the pier are required. Since the program can only be used for analysing cylindrical piers, and in this study only square section piers were tested, a suitable equivalent diameter must be assumed. Taking equal areas, DIA = $2B / \sqrt{\pi}$ where DIA is the diameter of the circular section and B is the width of the square shaped pier. Thus the equivalent circular cross-section for a square shaped pier of 1.60 m width is 1.80 m diameter. The flexural rigidity of the circular pier was assumed to be equal to that of the square one.

For the friction elements, the stiffness factors, k_n and k_s, were set high (10^{10} kN/m^2) to ensure perfect compatibility between pier and soil elements to enable a comparison of the results to be made with those from the other two programs.

An analysis using PIER2D required about 10 seconds CPU time in the Unix Main Frame System of the University of Liverpool for the mesh with 61 elements. Examples of input and limited output data using this mesh are listed in Appendix G2.

7.3.3 Analysis at full-scale geometry

The influence of the vertical boundary of the finite element mesh was checked using different distances as in the three-dimensional case. The calculated rotations for a lateral load of 73.33 kN and a moment of 440.0 kNm applied at the top of the pier, and a depth of stratum of 8 m are shown in table 7.6.

Soil Boundaries	2.5 B = 2.22DIA = 4m	5 B = 4.44DIA = 8m	7.5 B = 6.67DIA = 12m	10 B = 8.89DIA = 16m	13 B = 11.6DIA = 20.8m	20 B ≈ 18DIA = 32m
Rotation	1.42°	1.38°	1.34°	1.33°	1.31°	1.308°

Table 7.6 Calculated Rotation for Different Soil Boundaries

As seen from the table, the calculated rotation with the side boundary at 20.8 m is considered to be sufficiently accurate since the difference between it and the one calculated with the side boundary at 32.0 m is less than 0.2%.

In order to see the effect of depth of stratum, the depth was extended to 12.4 m using the side boundary at 16 m. The difference in the rotation was less than 0.8 %.

Therefore, the distance from the side boundary was kept as 20.8 m and the depth of stratum as 8 m for subsequent analyses.

7.3.4 Analysis of the restricted prototype geometry modelled in the tests

In a similar manner to that described in section 7.2.4 the mesh shown in figure 7.3 was matched to the respective dimensions of the soil strata contained in the bins in the conventional and centrifuge model tests.

Analysis with the corresponding model loading yielded calculated rotations of 1.36° for both model tests.

7.4 Three-Dimensional Non-Linear Analysis

Three-dimensional non-linear analysis was carried out using program PIER3DNL.

7.4.1 Finite element mesh and boundary conditions

Since the foundation and the loading are symmetrical only one-half of the geometry was analyzed. Mesh no. 3, described earlier in this chapter, was used with identical dimensions and boundary conditions as used for the three-dimensional linear analysis (see section 7.2.3).

7.4.2 Soil and foundation properties

Hyperbolic stress-strain relationships for undrained behaviour of the clay used were determined from triaxial tests as described in Chapter 3. Calculation of the values of hyperbolic parameters at a given moisture content is shown in table 3.1, Chapter 3.

The pier foundation was assumed to be a linearly elastic material with Young's modulus and Poisson's ratio of 207.10^6 kN/m^2 and 0.25, respectively, as in the three-dimensional linear analyses.

A summary of the parameters used is given in table 7.7.

SOIL		
Parameters		**Value**
Moisture Content,	m	17.0 %
Angle of Internal Friction,	ϕ	0.0°
Stiffness Exponent,	n	0.0
Atmospheric Pressure,	p_a	101.3 kN/m^2
Stiffness Number, Primary Loading,	K	16.47
Stiffness Number, Unloading-Reloading,	K_{ur}	52.83
Cohesion,	c	81.65 kN/m^2
Failure Ratio,	R_f	0.83
Bulk Unit Weight,	γ_b	21.07 kN/m^3
Poisson's Ratio,	ν_s	0.48
Coefficient of Earth Pressure at Rest,	K_o	1
FOUNDATION		
Poisson's Ratio,	ν_p	0.25
Young's Modulus,	E_p	207.0x10^6 kN/m^2

Table 7.7 The Properties of the Soil and Foundation (for Program PIER3DNL).

7.4.3 Analytical procedures employed in the program

Hyperbolic stress-strain relationships and incremental finite element analysis were discussed in Chapters 3 and 6.

The soil properties are modified after each increment of load in accordance with the state of stress computed in each element. In the beginning of the analysis, initial values of the modulus of elasticity, E_i, are calculated using the initial stresses due to self weight and lateral earth pressure at rest. The values of tangent modulus, E_t, during loading are computed using equation 3.12, Chapter 3. The incremental displacements, stresses and strains are summed progressively.

7.4.4 Determination of a suitable number of increments

The CPU time required to perform this nonlinear finite element analysis depends on the number of nodal points and on the number of increments. A suitable mesh has already been selected. Therefore, further work was needed to determine a suitable number of increments for the analysis.

A large lateral load of 500 kN and corresponding moment of 3000 kNm were applied at the top of the pier. A large value was chosen to enable the trend of the moment-rotation curve to be established well past the working range. The number of increments was chosen in the range of 1 to 20 and the calculated final rotations are shown in table 7.8.

Number of Increments	1	2	5	10	20
Final Rotation	10.91°	14.64°	18.20°	18.30°	18.29°

Table 7.8 Calculated Final Rotations for Different Numbers of Increments

As observed, the calculated rotation increases with the number of increments used until 10 and then does not change significantly. Therefore, it was decided to use 10 increments in subsequent analyses. A graph of moment versus rotation for 10 increments is shown in figure 7.4., and input and limited output data for this example are listed in Appendix G3.

This analysis required about 90 minutes CPU time in the Unix Main Frame System.

7.4.5 Finite element results

Three finite element analyses were carried out using program PIER3DNL to correspond with the behaviour of a 1.6 m square, 2.4 m long pier

i) in the conventional model study.

ii) in the centrifugal model study.

and iii) at full-scale.

In the experimental part of this study the tests were carried on until the pier rotation reached about 5 to 6 degrees. In order to compare the numerical and experimental results, the pier rotations from numerical studies should be in the same range as those from experimental ones. Therefore, four times the load and moment used in the three-dimensional linear analysis were applied at the top of the pier. These were a model load of 0.183325 kN and a moment of 0.0275 kNm for the two model studies. In the analysis of the conventional one, the pier rotated a lot more than expected. Therefore, after some trials the values of the applied model load and moment were reduced to 0.041667 kN and 0.00625 kNm. For the full-scale analysis a load of 293.33 kN and a moment of 1760.0 kNm were applied. The results from these studies are presented in figures 7.5 to 7.7.

During the incremental analyses, as expected, it was observed that some soil medium elements in the vicinity of the pier failed because of tensile stresses. This was most apparent in the analysis of the conventional model where over 20 elements out of 784 failed after the first increment.

7.5 Application of the Programs for Different Pier Widths

Further results were obtained for square, 2.40 m long prototype piers, as modelled in the centrifuge, with widths of 0.80, 1.20, 2.00, and 2.40 m. In order to compare the results of these analyses with the results derived from the centrifugal model study in Chapter 5 the load and moment values applied at the top of the piers were those obtained from equation 5.4 for 1.0° rotation. Table 7.9 shows the calculated rotations obtained from all three programs.

Pier Width(m)	Moisture Content m (%)	Cohesion c (kN/m^2)	Load (kN)	Moment (kNm)	Angle of Rotations		
					2D	3D lin.	3D nonl.
0.80	17.11	78.64	32.86	197.17	1.42°	0.94°	1.13°
1.20	17.25	74.96	48.09	288.52	1.41°	0.95°	1.29°
1.60	17.29	73.95	64.70	388.20	1.22°	0.92°	1.06°
2.00	17.33	72.94	81.55	489.31	1.34°	0.96°	0.98°
2.40	17.11	78.64	107.82	646.90	1.12°	0.87°	1.03°

Table 7.9 Calculated Rotation for Different Pier Widths (2.40 m long).

In comparison with the experimental value of 1°, the calculated rotations from the 2-D linear and 3-D non-linear programs for different pier sizes tested are generally overestimated. The overestimation is in the range of 12 to 42 % from the 2-D program while it is -2 to 29 % from the 3-D non-linear program. However, overall agreement of the results of the 3-D non-linear program is better than those of the 2-D program. The calculated rotations from the 3-D linear program show that these are underestimated by 8 to 13 %. Comparison of the 3-D linear and non-linear programs shows that for the first two piers the results of the linear program are better than those of the non-linear one since its maximum difference from the observed values is only 6 % against 29 % from the non-linear program. However, for the last three piers, the results of the non-linear program are better since its maximum difference from the observed value is only 6 % against 13 % from the linear program. It is clear that the effect of nonlinearity is significant even at 1 degree of rotation since the difference between the two sets of results are in the range of 18 to 35 % except for the 2.0 m pier for which the difference is only 2%.

7.6 Conclusions

The results of numerical studies to predict the behaviour of piers in saturated remoulded clay have been obtained from the application of the two and three-dimensional programs. These show that for moments below a certain threshold, the variation of moment with rotation is almost linear and the soil shows a relatively high resistance to rotation. For higher values of moment the relationship becomes nonlinear, so that for a small increase in moment, rotation is much increased. The importance of the consideration of nonlinear behaviour of soil arises at this region. The results obtained from the analyses of conventional models were significantly different from those obtained from analyses of centrifuge models and at full-scale. The results of these three different analyses are presented together in figure 7.8. As described in Chapter 5, centrifuge modelling involves raising the bulk densities of the model materials so that the stress levels in the model and at full-scale are equal at corresponding points. As seen from the figure, the results of centrifugal model and full-scale one are in good agreement. The small difference between the two is because of the effect of the restricted prototype geometry modelled in the tests. The result for the conventional model, even with the values of the load and moment 4.4 times less than those applied in the analyses of the centrifuge model and at full-scale, shows the same order of rotation as the others. The difference between the conventional and centrifuge model and full-scale can be explained as follows;

Since the small model dimensions were given and the measured bulk density was used in the input data for the analysis of a conventional test, the initial lateral stresses, which were calculated at the centre of each element as $\sigma_z = K_o \gamma z$, were very small. After the application of each incremental load and moment, the lateral stress which develops to some depth behind and in the vicinity of the pier was tensile, so that some elements in these region were eliminated in the program by assigning a small value of Young's modulus, $E_t = 1.0$ kN/m^2. Thus in the following incremental loadings the resistance of these elements were negligible.

However in the analysis of a centrifuge model test, although the small model dimensions were given, 40 times the value of the measured bulk density was used, so that the stress levels were identical to those in the prototype. Since the initial prototype lateral stresses were considerably higher than conventional ones, tensile stresses were not observed as quickly as in conventional one. For example, in the analysis of the conventional model (using program PIER3DNL), element 329, behind the pier at ground level (see figure 7.1) had an initial stress value of 0.158 kN/m^2 at its centre while it was 6.321 kN/m^2 in the centrifuge model and at full-scale. The element failed just after the first increment in the conventional model while it failed after the fourth increment in the other two analyses for the same loading.

Comparisons of the finite element programs showed that the results of the 3-D analyses were much closer to the centrifuge experimental results than those of the 2-D analysis for small rotations.

Comparisons of these results with the experimental results will be made in Chapter 8.

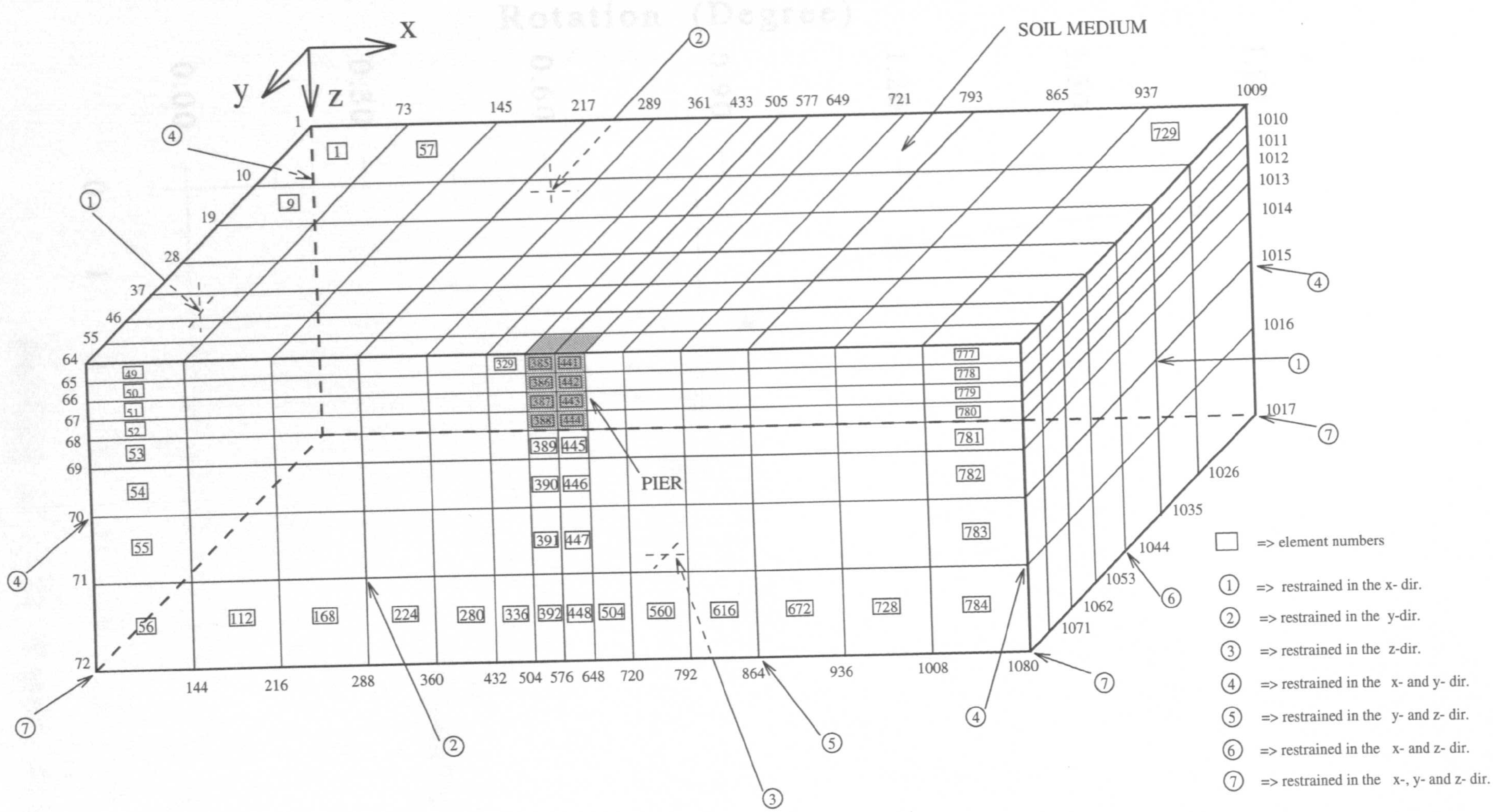

Figure 7.1 Typical Finite Element Mesh for Programs PIER3DLN and PIER3DNL.

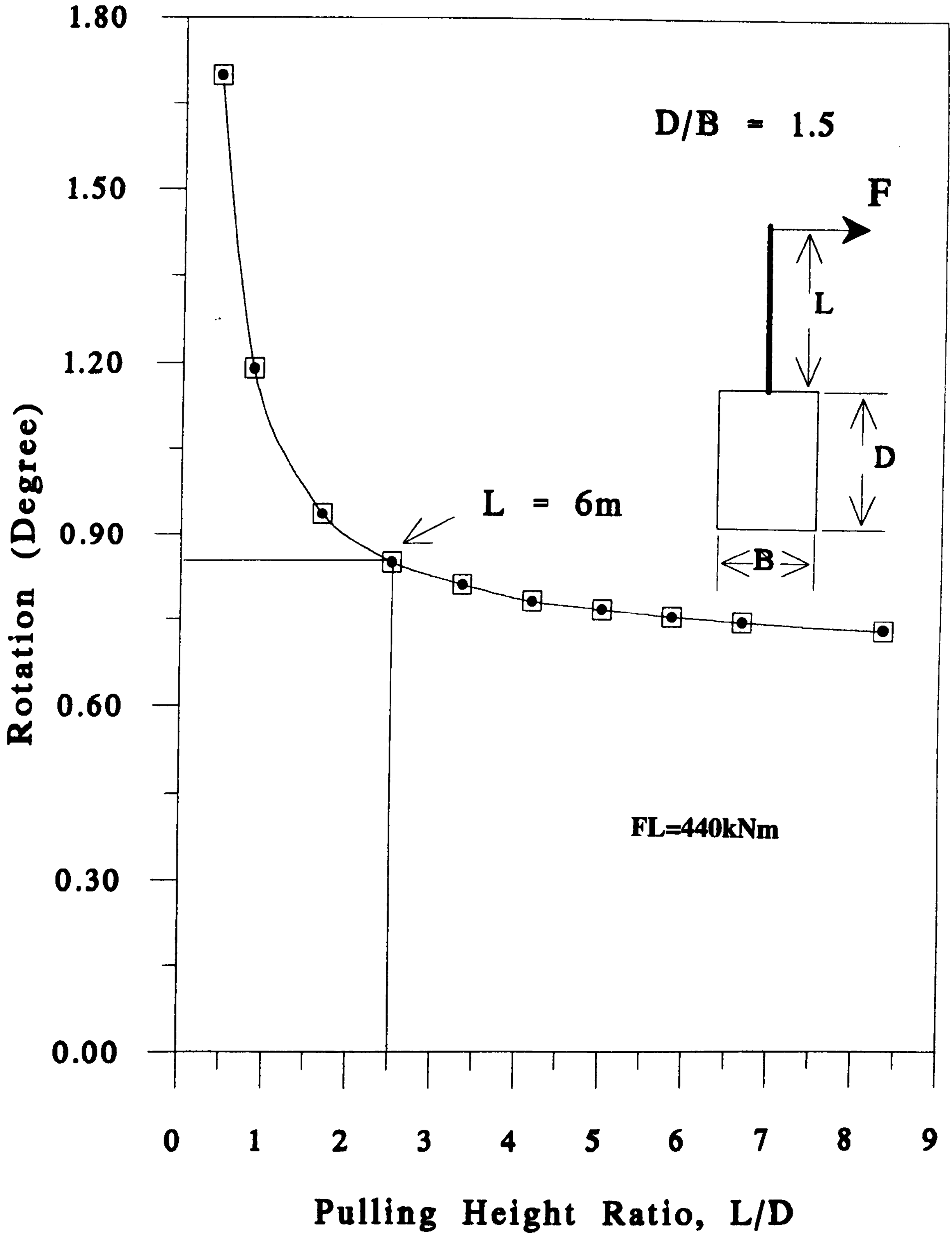

Figure 7.2 Effect of Pulling Height Ratio on Rotation.

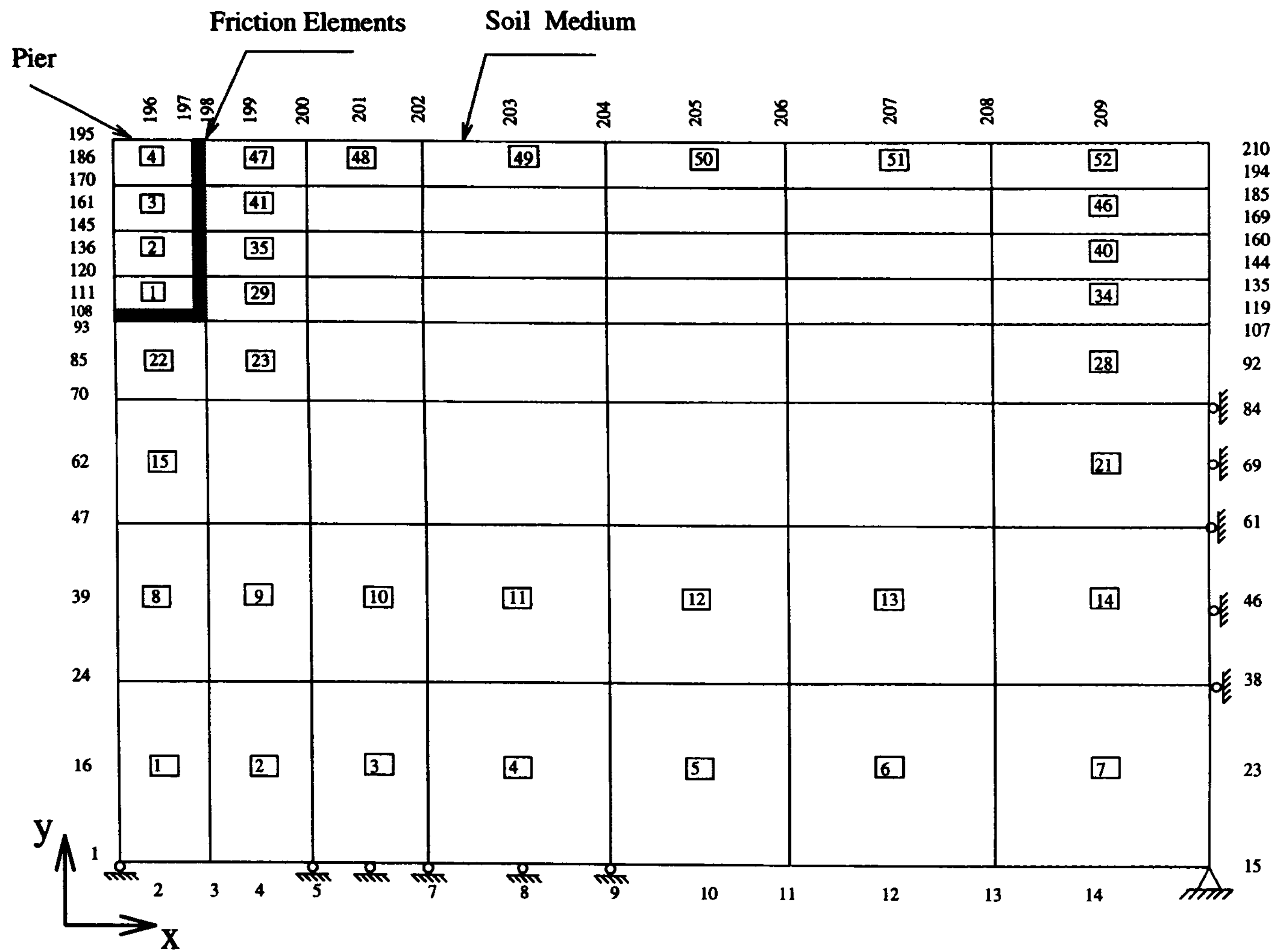

Figure 7.3 Typical Finite Element Mesh for Program PIER2D.

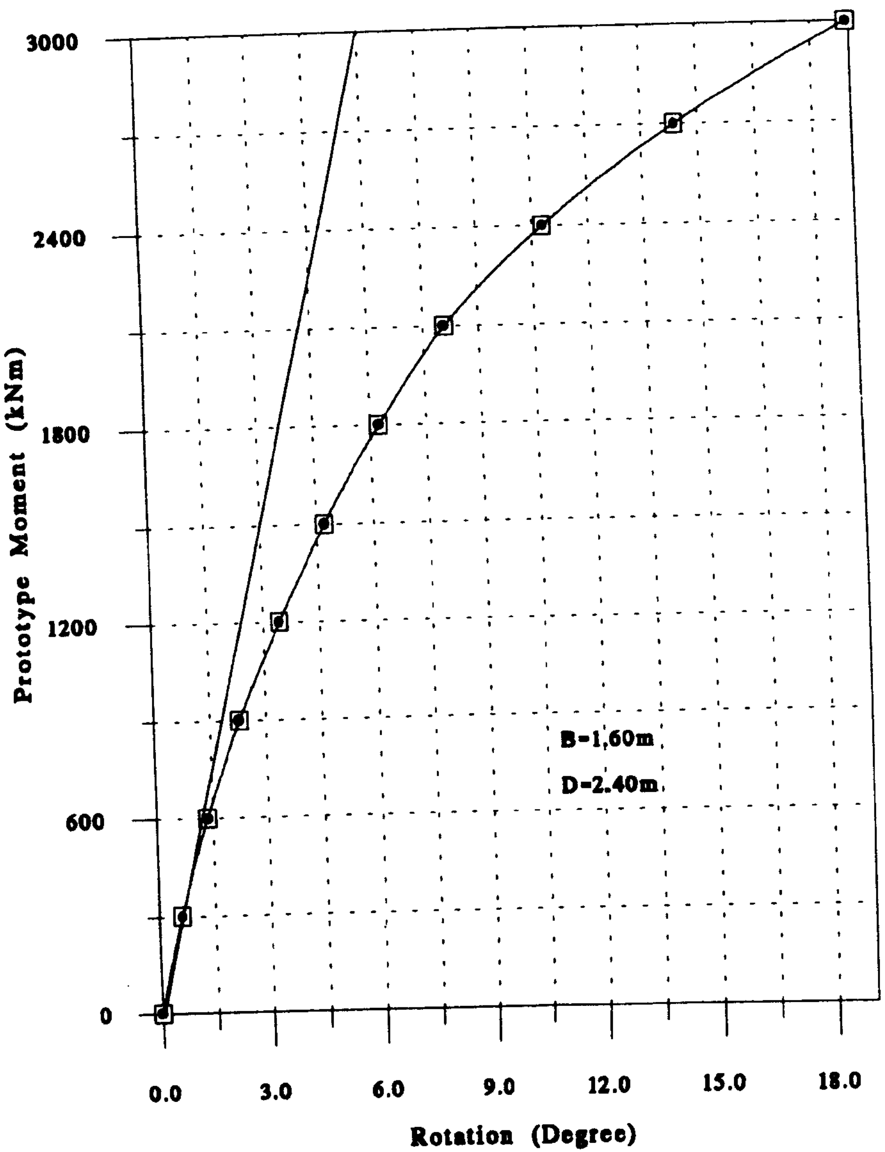

Figure 7.4 Moment - Rotation Curve for 10 Increments. (Full Scale)

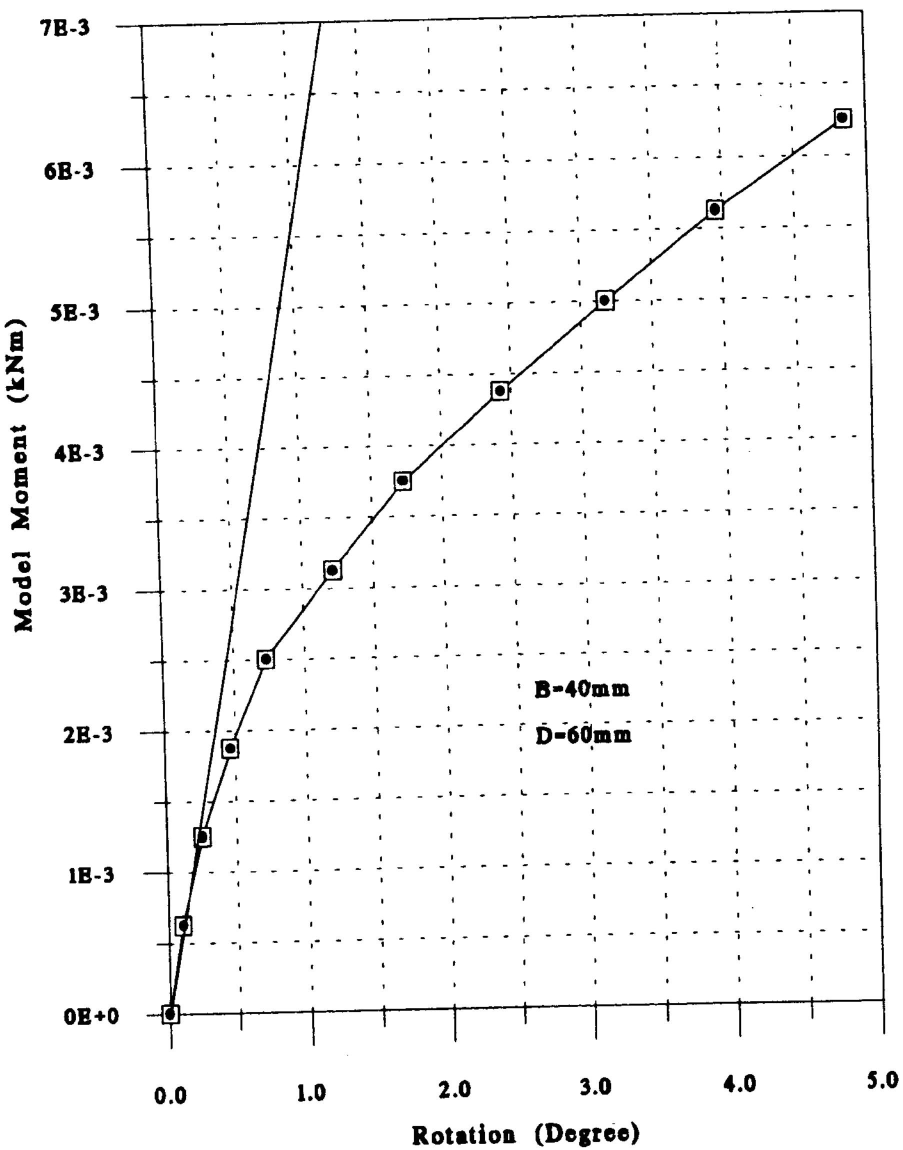

Figure 7.5 Moment - Rotation Curve for Conventional Model Study.

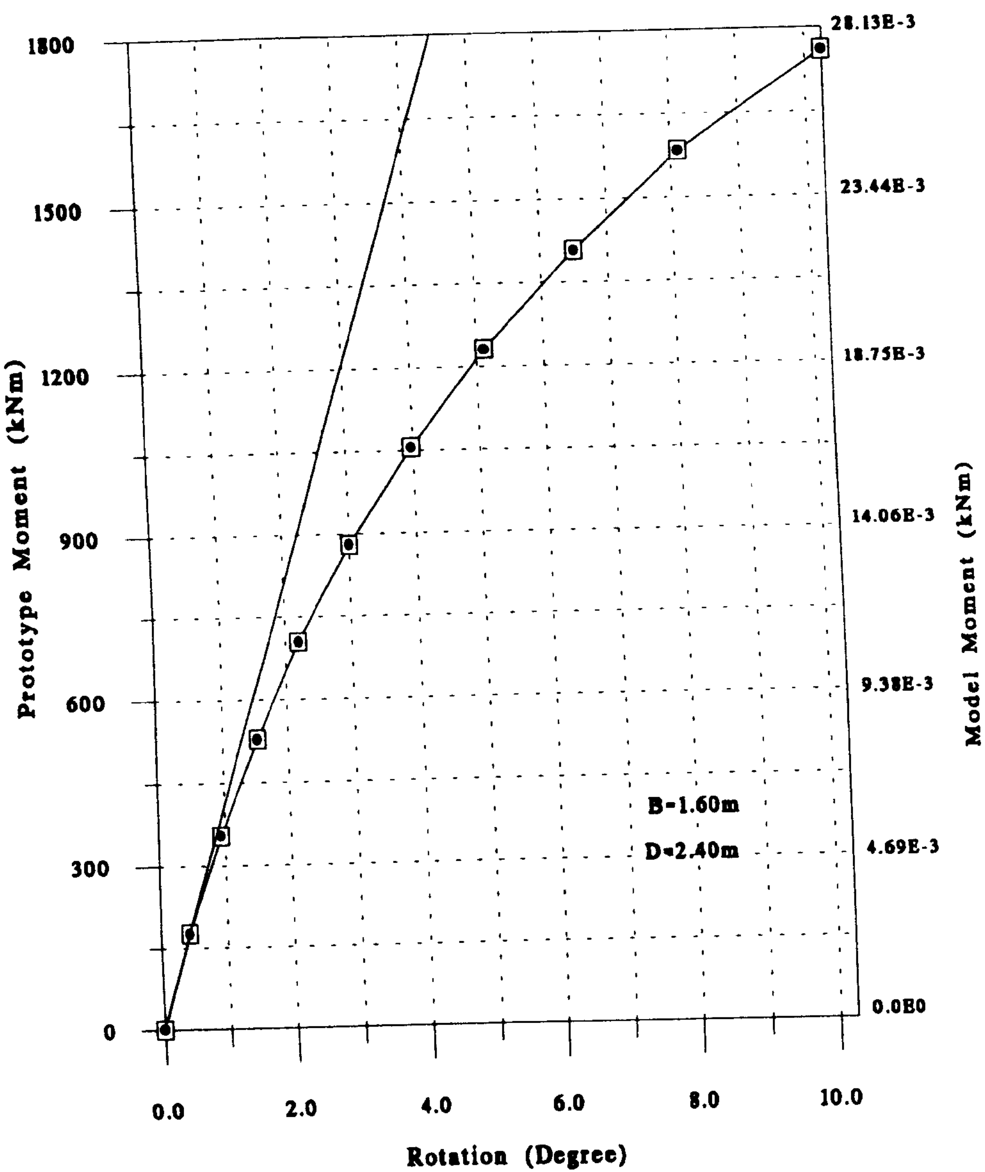

Figure 7.6 Moment - Rotation Curve for Centrifugal Model Study.

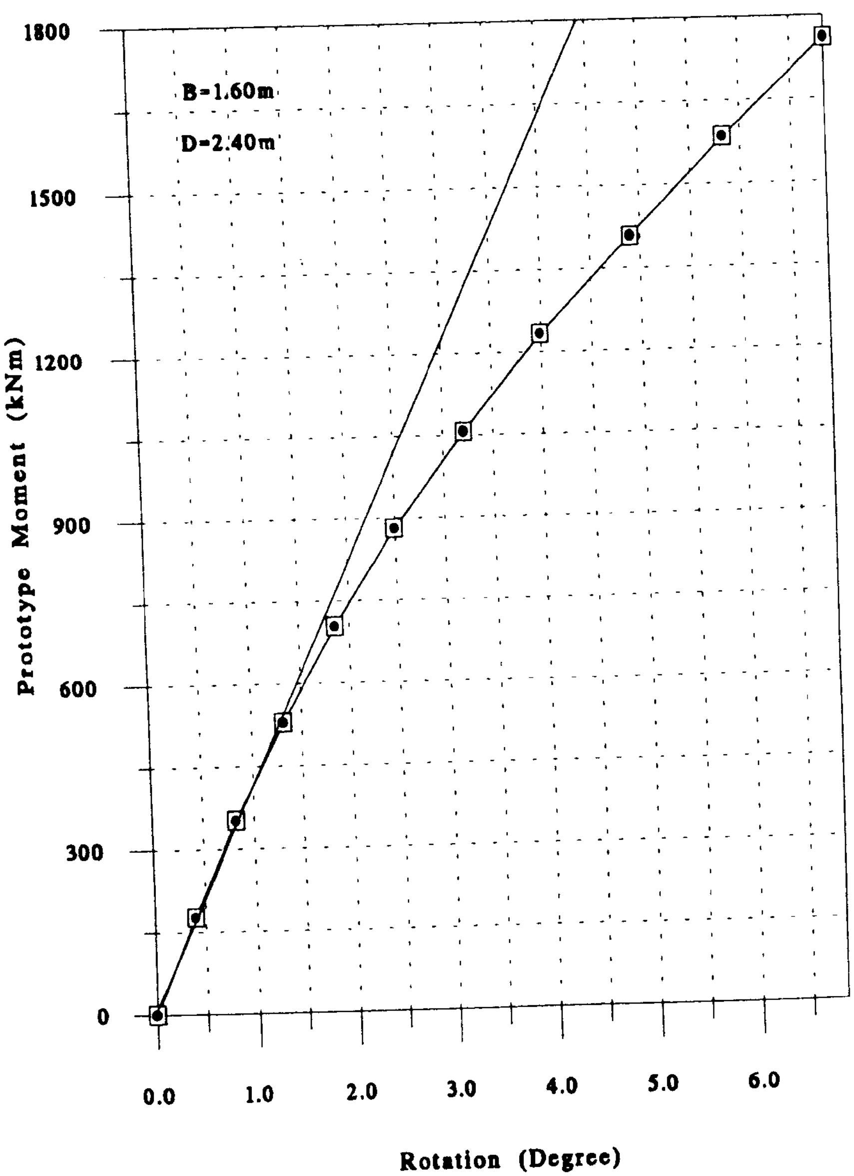

Figure 7.7 Moment - Rotation Curve for Full-Scale Study.

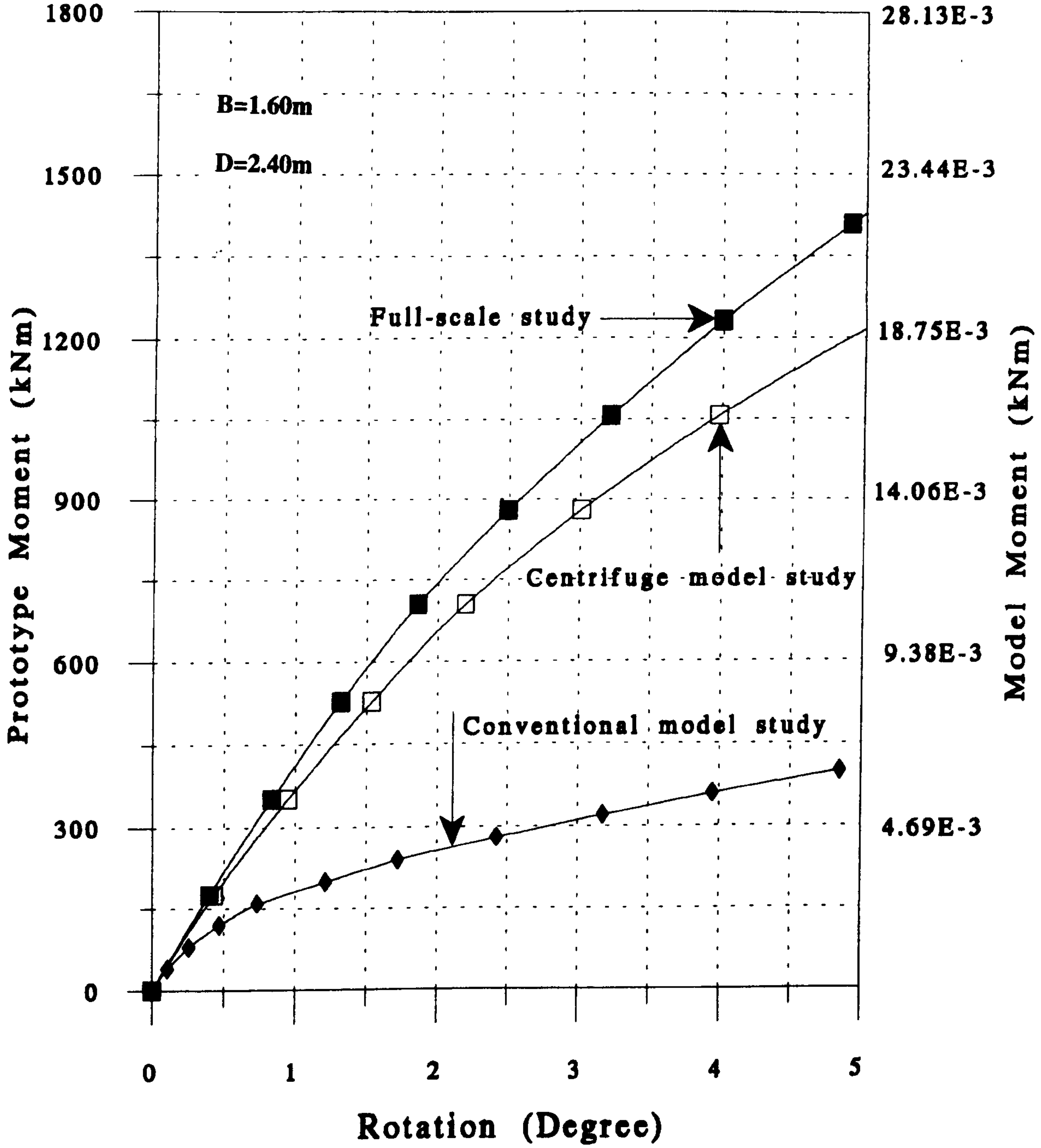

Figure 7.8 Comparison of Moment - Rotation Curves (PIER3DNL).

CHAPTER 8

COMPARISON OF THE RESULTS OF EXPERIMENTAL AND NUMERICAL STUDIES

8.1 Introduction

In this chapter, the results of moment-rotation behaviour of a typical pier observed in the conventional and centrifugal model tests, reported in Chapters 4 and 5, are compared with each other and then with those predicted by the two and three-dimensional finite element models, presented in Chapters 6 and 7. Furthermore, the closeness of fit of the empirical equations, derived in model tests, are illustrated for typical experiments. The effect of the embedment ratio on rotational stiffness of piers predicted by the 3-D non-linear program is then compared with that observed in the centrifugal model tests.

In addition, some of the existing design formulae that are frequently used in the literature for predicting the behaviour of single pile and rigid pier foundations subjected to lateral loads and moments are examined. These have been described briefly in section 2.2.1. The results of model tests and numerical analyses are used to consider the relative merits of these existing design formulae such as that of UIC/ORE (1957), and Brinch-Hansen (1961). Appropriate equations are re-called as required.

A wide range of pier sizes were tested in the experimental phase of this work. However, in order to keep the size of this thesis at a reasonable level, only some representative sizes are used to illustrate comparisons.

8.2 Comparison of Conventional and Centrifugal Model Test Results

As described in section 4.4 (Chapter 4), since a variation in the moisture content of the clay of up to 3% was observed in the tests, a relation between moisture content and cohesion was obtained in order to make allowance for the variation in strength. Therefore, moment values for all tests were divided by the cohesion values calculated from equation (4.1) at the measured moisture content values to eliminate the effect of moisture content variation. Also, the results obtained from the centrifugal and conventional tests have been scaled up to prototype size. The relationships between moment/cohesion and rotation obtained from these tests for a typical square-shaped pier of 1.60 m width and 2.40 m length is illustrated in figure 8.1. Comparisons show that the values of moment/cohesion from conventional tests are smaller than those from centrifuge model tests by a factor of at least 1.75 even for small values of rotation. This demonstrates that a scale effect does exist when a rigid pier is tested at different stress levels in saturated clay. As discussed earlier in sections 4.5, 5.2, 7.4 and 7.6, the depth of tension zones behind and in the vicinity of the piers are influenced by stress levels and this has a significant effect on the results.

8.3 The Closeness of Fit of the Empirical Equations Derived from Conventional and Centrifugal Model Tests

In Chapters 4 and 5, from an extensive series of conventional model tests empirical relationships were derived between moment carrying capacity and geometry for limited rotations of short rigid piers in saturated clay. Hence the moment carrying capacities for each limiting rotation can be calculated from equations 4.4 and 5.4. The values of parameters, α_{v1}, and α_{v2} for the conventional model tests and α_{t1}, and α_{t2} for centrifugal model tests are listed in tables 4.9 and 5.7, respectively at pier rotations of 0.5°, 1.0° and 1.5°. The equations give the results for the prototype size. As mentioned during the derivation of the equations, correlation coefficients for the best fits were always better than 0.85. In order to ascertain that they give close results for any typical pier size, an average width of the piers tested is considered. It is a pier of 1.60 m square section and 2.40 m long.

The moment-rotation relationships for the pier using the results of centrifuge and conventional model tests, (M46CT1 and M46RT1, respectively) and those obtained from the equations are shown in figure 8.2. Since the values of moisture content observed in the tests were 17.29% and 16.43%, the measured moment values were multiplied by the ratios of the corresponding cohesion values, $c_{m=17.00}/c_{m=17.29\%}$ (81.65/73.95 = 1.104) and $c_{m=17.0}/c_{m=16.43\%}$ (81.65/99.20 = 0.823), so that the results would be consistent. The results of both empirical equations show very good agreement with those observed in the tests, particularly the values associated with the centrifuge model tests.

8.4 Comparison of Numerical and Experimental Results

8.4.1 Typical moment/rotation relationships

The three-dimensional linear and non-linear computer programs, developed in this study, and an existing two-dimensional one were used in Chapter 7 to predict results for the pier sizes employed in the tests. The moment/rotation behaviour from these predictions are compared with the corresponding observed behaviour, in both the conventional and centrifugal model studies of a typical pier, in figure 8.3. The results of the numerical studies were obtained using the soil parameters at a value of the moisture content of 17%. Since the values of moisture content observed in the conventional model test, M46RT1, and in the centrifugal model test, M46CT1, were 16.43% and 17.29%, respectively, the measured moment values were multiplied by the ratios of the corresponding cohesion values, $c_{m=17.0}/c_{m=16.43\%}$ (81.65/99.20 = 0.823) and $c_{m=17.00}/c_{m=17.29\%}$ (81.65/73.95 = 1.104), so that they were consistent with the numerical results. As observed, the results of the conventional model study and 3-D non-linear finite element analysis, with the same restricted boundaries, are in good agreement. The corresponding results for the centrifugal model study are also in good agreement for pier rotations in the range of 0 to 2.5 degrees but the agreement is not as good as for the conventional one for larger rotations. However it should be considered that, for design purposes, the pier rotation will be less than 2.5 degrees and hence the disagreement between numerical and experimental results for larger rotations is not of practical importance. Another point to be considered is that, as discussed in section 7.6 (Chapter 7), the numerical results for the centrifuge model and at full-scale are in good agreement; the small difference between the two is because of the effect of the restricted prototype geometry modelled in the tests. Overall, it is clear that the difference between the results from conventional and centrifuge model studies is significant.

From the linear finite element models the results of both 2-D axi-symmetric and 3-D programs for the restricted prototype sizes of the model are in poor agreement with the non-linear curve observed in the centrifuge test. Generally, the results of the 2-D program underestimate the observed moment values until 1.5° of pier rotation and overestimate for larger values while those of the 3-D linear program are in good agreement until 1.0° rotation but overestimate for larger values.

8.4.2 Limiting moment capacity for 1° rotation

It has been observed that the embedment ratio is one of the factors which affects the limiting moment values. Therefore as a further comparison of the results of centrifuge model tests and those of numerical studies the performance of 1.6 m square piers with five different depths were evaluated. An average value of moisture content of 17%, observed in the tests, was considered. The corresponding value of cohesion was determined from equation 3.16 as 81.65 kN/m^2. Empirical equation 5.4 (see Chapter 5) obtained from the centrifugal tests was used to determine the limiting moment values required to cause 1 degree rotation of each pier. For the numerical analyses, the three-dimensional non-linear computer program, PIER3DNL, was used for identical dimensions as used in the tests. Initial trial values of lateral load and moment were obtained from the corresponding experiments. For each pier, the usage of the computer program was repeated until a rotation of 1 degree was reached. Values of limiting moment obtained for different embedment ratios, D/B, are shown in figure 8.4. From the graphs, it can be seen that the numerical and centrifuge model results are in good agreement even though the variation of the experimental results is linear while that of the numerical results is slightly non-linear.

8.5 Comparison of Experimental Results with Existing Design Formulae

There are several empirical methods for analysing or designing single pile and rigid pier foundations subjected to lateral loads. These methods, which are based on the results of conventional testing either at full-scale or on small models, have been discussed in detail in Chapter 2. Most of these studies, however, were on long piles subjected to large lateral loads and small moments. Moreover there is little published data which may be used to establish a rationale for the actual values of soil properties which should be used in these methods. Hence, a direct comparison between the results of these methods and those of the present study is difficult.

As mentioned earlier in the experimental studies (Chapters 4 and 5) the relationships between moment and rotation do not exhibit any peak values. Therefore, arbitrary rotations of 0.5°, 1.0° and 1.5° were considered as alternative limiting working conditions while in the previous studies, such as that of UIC/ORE (1957), Brinch-Hansen (1961), and Broms (1964b), equations were generally derived for ultimate moment capacities. Since no certain values for the factors of safety are recommended with these methods, the results will be compared directly.

Attempts were made to compare the results obtained using all of the existing design formulae presented in Chapter 2. However, some of these were not included here because of difficulties in assigning appropriate parameter values. Therefore, in the following sections only the design formulae of the UIC/ORE (1957) and Brinch-Hansen (1961) are considered.

Since the lateral pulling force was applied at 150 mm (6 m in prototype) above the level of the clay in the tests, the same 6 m height was kept in all of the following calculations. Typical values of moisture content, m = 17%, and cohesion, c = 81.65 kN/m^2, were considered for the clay.

8.5.1 Brinch-Hansen's method

Five prototype piers of 0.80, 1.20, 1.60, 2.00 and 2.40 m square sections and 2.40 m deep, were considered. Following the procedure described in section 2.2.1.5 in Chapter 2, the passive resistance diagram was divided into 12 horizontal elements each 0.2 m high. For each pier, the initial value of the depth of the point of rotation, a, was considered as 1.60 m (2/3 rd of the depth of the pier) and a final value of 1.5 m was determined from equation 2.11 by a process of trial and error. Values of maximum bending moment at ground level were then calculated.

For the 1.6 m square pier, a comparison between the results of the author's empirical expression (equation 5.4) at pier rotations of 0.5°, 1.0° and 1.5° and that obtained using Brinch-Hansen's method is shown in figure 8.5 together with the result of the corresponding experiment, M46CT1. Since the value of moisture content observed in the test was 17.29%, the measured moment values were multiplied by the ratio of the corresponding cohesion values, $c_{m=17.0}/c_{m=17.29\%}$ (81.65/73.95 = 1.104). Brinch-Hansen's solution is constant for all pier rotations. For a pier rotation of about 2.75° the value of moment observed in the test agrees with Brinch-Hansen's solution. However, the figure shows that the experimental curve does not exhibit any peak value and that for rotations below 2.75°, limiting moment values obtained from the author's empirical expression are lower than Brinch-Hansen's ultimate value. For all five piers the calculated moment values and the pier rotations, where the results of Brinch-Hansen's and those of the corresponding experiments coincide, are also shown in table 8.1.

Pier Width, B (m)	Calculated Moment Values (kNm)				Rotation Values (Degree) (Calculated from the intersection of the results of the two analyses)
	Author's Equation. (5.4)			Brinch-Hansen	
	0.5°	1.0°	1.5°		
0.80	146.96	204.72	242.03	341.30	3.40°
1.20	222.64	314.27	374.29	473.57	3.25°
1.60	299.79	428.61	514.04	637.82	2.75°
2.00	378.42	547.74	661.28	765.62	2.60°
2.40	458.51	671.66	816.01	873.30	2.20°

Table 8.1 Comparison of Moment/Cohesion - Rotation Curves of Centrifuge Tests with Brinch-Hansen's Ultimate Values (for 2.4 m pier depth).

8.5.2 UIC/ORE Method

The author's empirical expression (equation 5.4) at pier rotation of 1.0° and the UIC/ORE procedure described in section 2.2.1.1 were used for a whole range of pier sizes.

A bulk unit weight of 77 kN/m^3 for the mild steel piers was used to determine their weights. The values of parameters, K_1 and K_2, were determined from equations (2.2c). A constant value of 0.4 was obtained for parameter, K_1, since square section piers were considered, while the value of parameter, K_2, varied very little over the range of geometries considered (from 2.02 to 2.14) and an average value of 2.08 was used in the analyses. The value of surface profile factor, K (see equation (2.3)), was used as unity since a flat ground was considered. After the calculation of pure overturning moment, $(M_R)_p$, from equation (2.2b), the values of moment limit at ground level were determined from equation (2.3). The results of both analyses were divided by corresponding cohesion values. It was observed that the results of the UIC/ORE method were considerably higher than any ultimate values indicated by extrapolation of the experimental curves. By chance they appear to be approximately 7.5 times larger than those of this research for 1° rotation. The values of moment/cohesion obtained from both methods are given in table 8.2 together with the results of Brinch-Hansen's method for the piers considered in the previous section. The actual values obtained from the UIC/ORE method are given next to those obtained from Brinch-Hansen's method while those obtained by dividing them by a factor of 7.5 are given next to author's values. It is clearly shown that the results of the UIC/ORE method also overestimates the results in comparison with Brinch-Hansen's method. The author's values and the factored UIC/ORE values are presented graphically for comparison in figure 8.6.

Pier Width, B (m)	Pier Depth, D (m)	Moment/Cohesion (m^3)			
		Brinch-Hansen	UIC/ORE	Author's Eq. 5.4	$\frac{\text{UIC/ORE}}{7.5}$
0.80	0.80	-	6.053	0.836	0.807
0.80	1.20	-	8.385	1.254	1.118
0.80	1.60	-	11.96	1.672	1.595
0.80	2.00	-	16.79	2.089	2.238
0.80	2.40	4.18	22.83	2.507	3.044
1.20	0.80	-	8.970	1.283	1.196
1.20	1.20	-	12.57	1.924	1.676
1.20	1.60	-	17.16	2.566	2.288
1.20	2.00	-	23.58	3.207	3.144
1.20	2.40	5.80	31.55	3.849	4.207
1.60	0.80	-	12.52	1.750	1.669
1.60	1.20	-	17.03	2.625	2.270
1.60	1.60	-	23.19	3.500	3.092
1.60	2.00	-	31.14	4.374	4.152
1.60	2.40	7.812	40.91	5.249	5.454
2.00	0.80	-	16.81	2.236	2.241
2.00	1.20	-	22.70	3.354	3.027
2.00	1.60	-	30.30	4.472	4.040
2.00	2.00	-	39.80	5.590	5.307
2.00	2.40	9.377	51.33	6.708	6.844
2.40	0.80	-	21.91	2.742	2.921
2.40	1.20	-	29.43	4.113	3.924
2.40	1.60	-	38.61	5.484	5.148
2.40	2.00	-	49.77	6.855	6.636
2.40	2.40	10.696	63.08	8.226	8.410

Table 8.2 Calculated Moment/Cohesion Values from Empirical Equation 5.4 (for 1° rotation), and from the Brinch-Hansen and UIC/ORE Methods.

8.6 Conclusions

1. A significant difference between the conventional and the centrifugal test results was obtained in both the results of the numerical and experimental studies. From the comparisons it was concluded that the results of centrifuge model tests were more reliable than those of conventional ones. This shows that the extrapolation of an observed data from a 1/N th scale model at 1g in the laboratory to a full-scale prototype is unreliable principally with respect to tensile stress changes. Therefore instead of full-scale testing which is usually undesirable for economic reasons, the results produced from centrifugal modelling can be considered as an accurate and realistic measurement of pier-soil interaction.

2. Assessment of the accuracy of equations (4.4) and (5.4) derived from the experimental results for pier rotations of 0.5°, 1.0° and 1.5° indicated that they are reliable.

3. From the comparisons between experimental and numerical analyses, it was shown that three-dimensional finite element analysis, using a hyperbolic stress-strain model for the soil, provided satisfactory predictions of observed moment-rotation behaviour and working moment limits.

4. The methods of Brinch-Hansen and UIC/ORE have been applied to the model pier foundations. Brinch-Hansen's method underestimates the results of tests observed in this study and the rotation values obtained from the intersection of the results varied

from 2.20° to 3.40° (an average value of 2.80°). It was observed that the UIC/ORE method overestimates the ultimate moment carrying capacity in comparison with the results of the present study and with Brinch-Hansen's method but gives values approximately 7.5 times larger than the results of this research for 1° rotation.

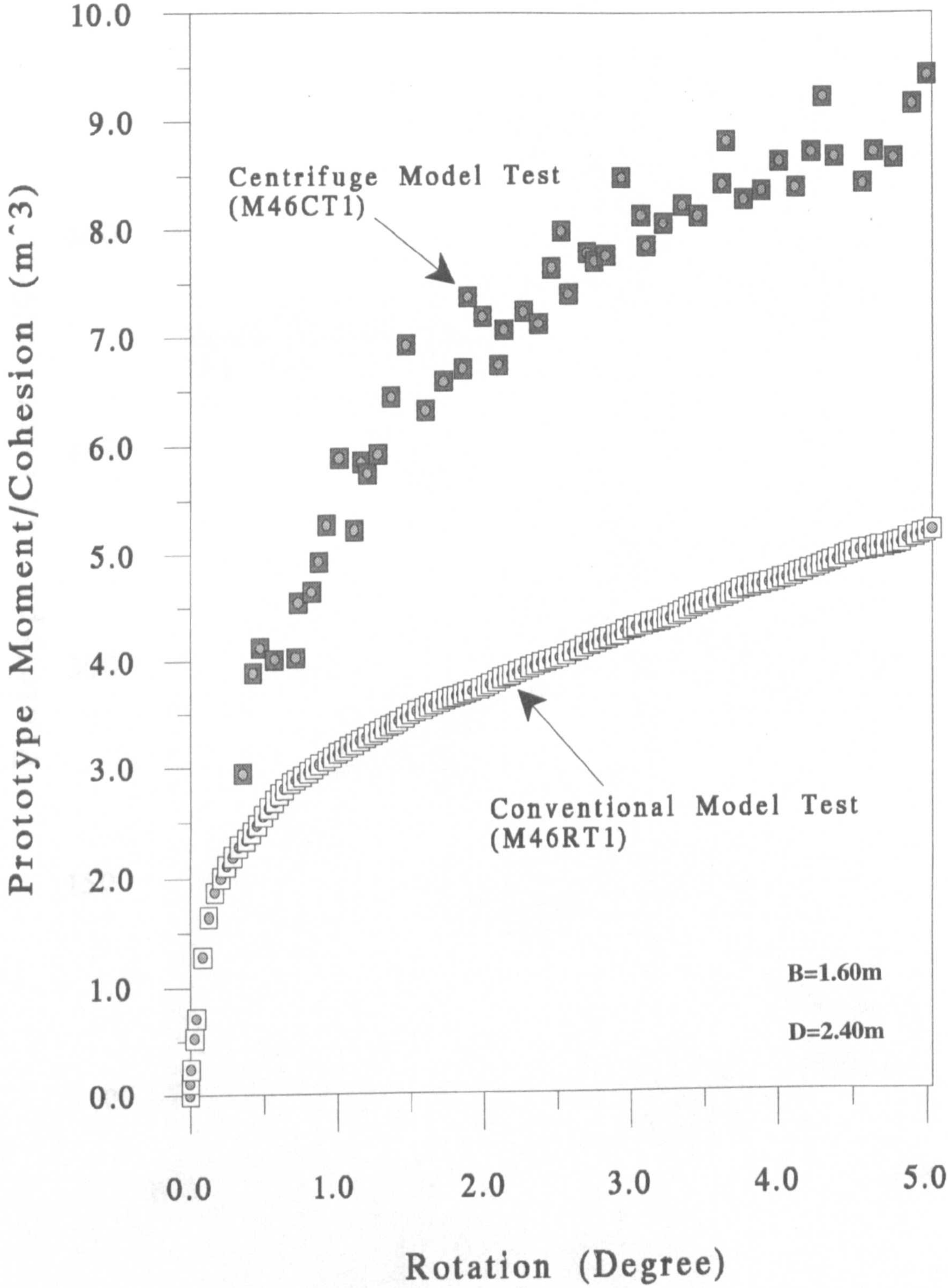

Figure 8.1 Comparison of Conventional and Centrifugal Moment/Cohesion - Rotation Curves.

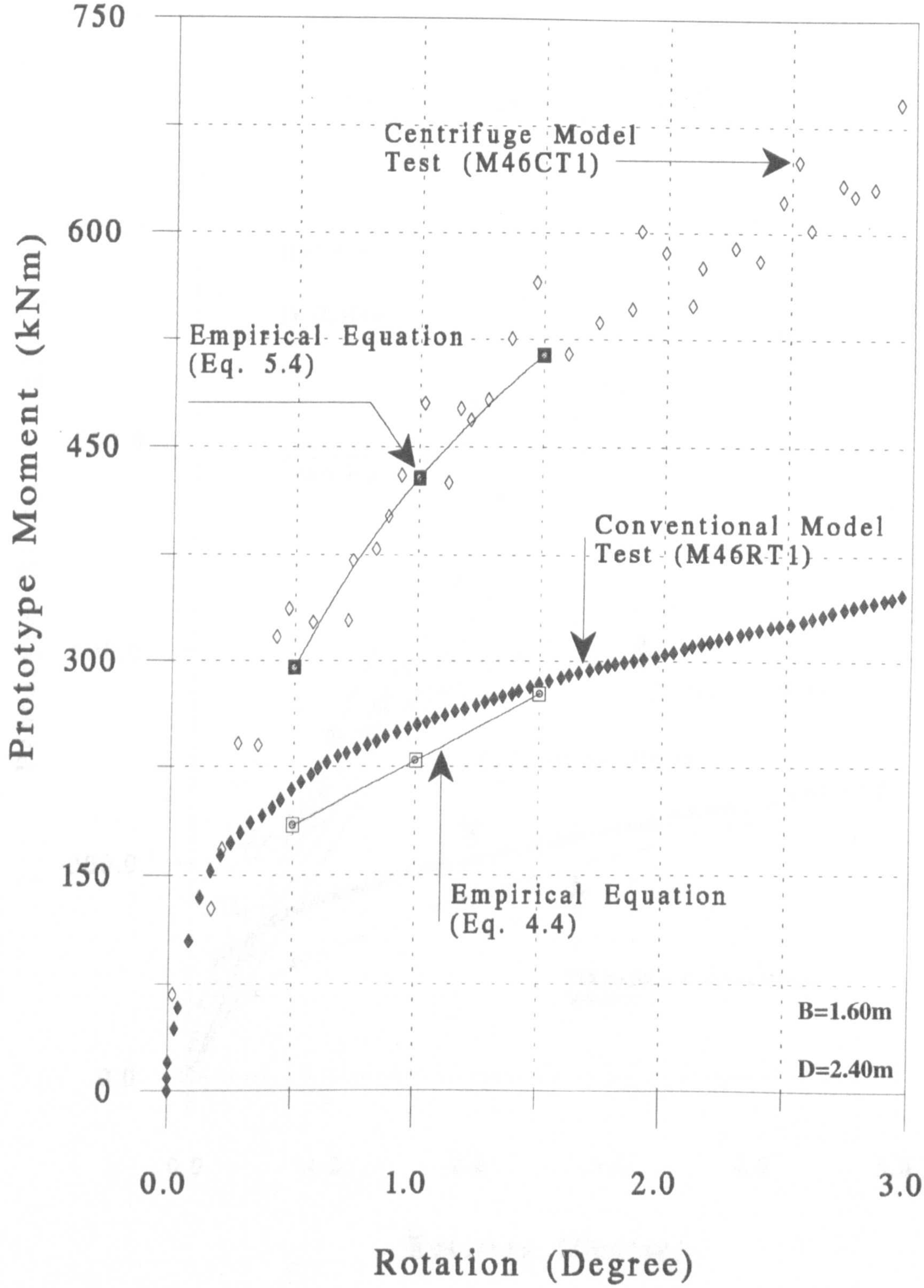

Figure 8.2 Comparison of Moment - Rotation Curves of Experiments with the Results of Derived Equations.

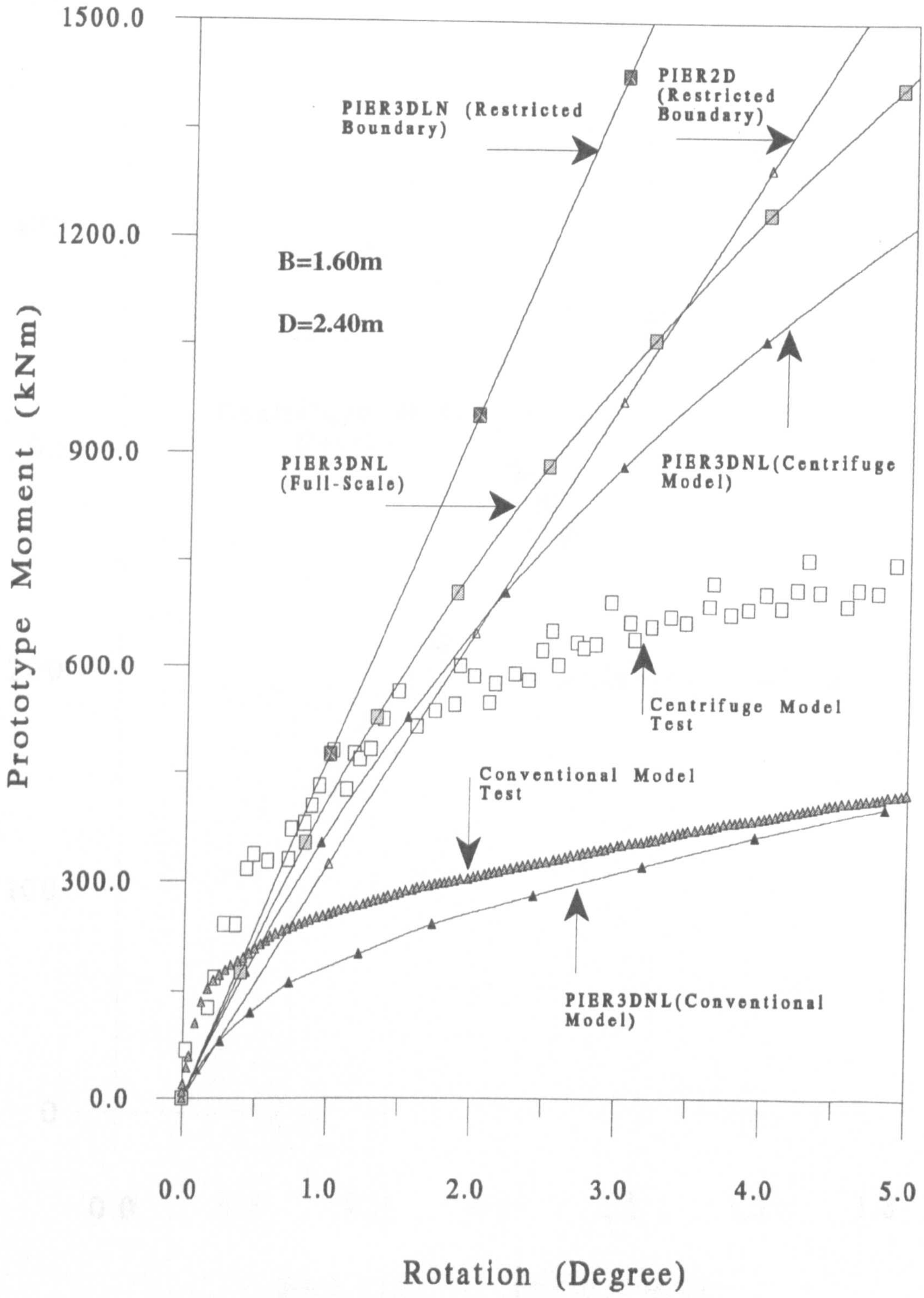

Figure 8.3 Comparison of Experimental and Numerical Moment - Rotation Curves.

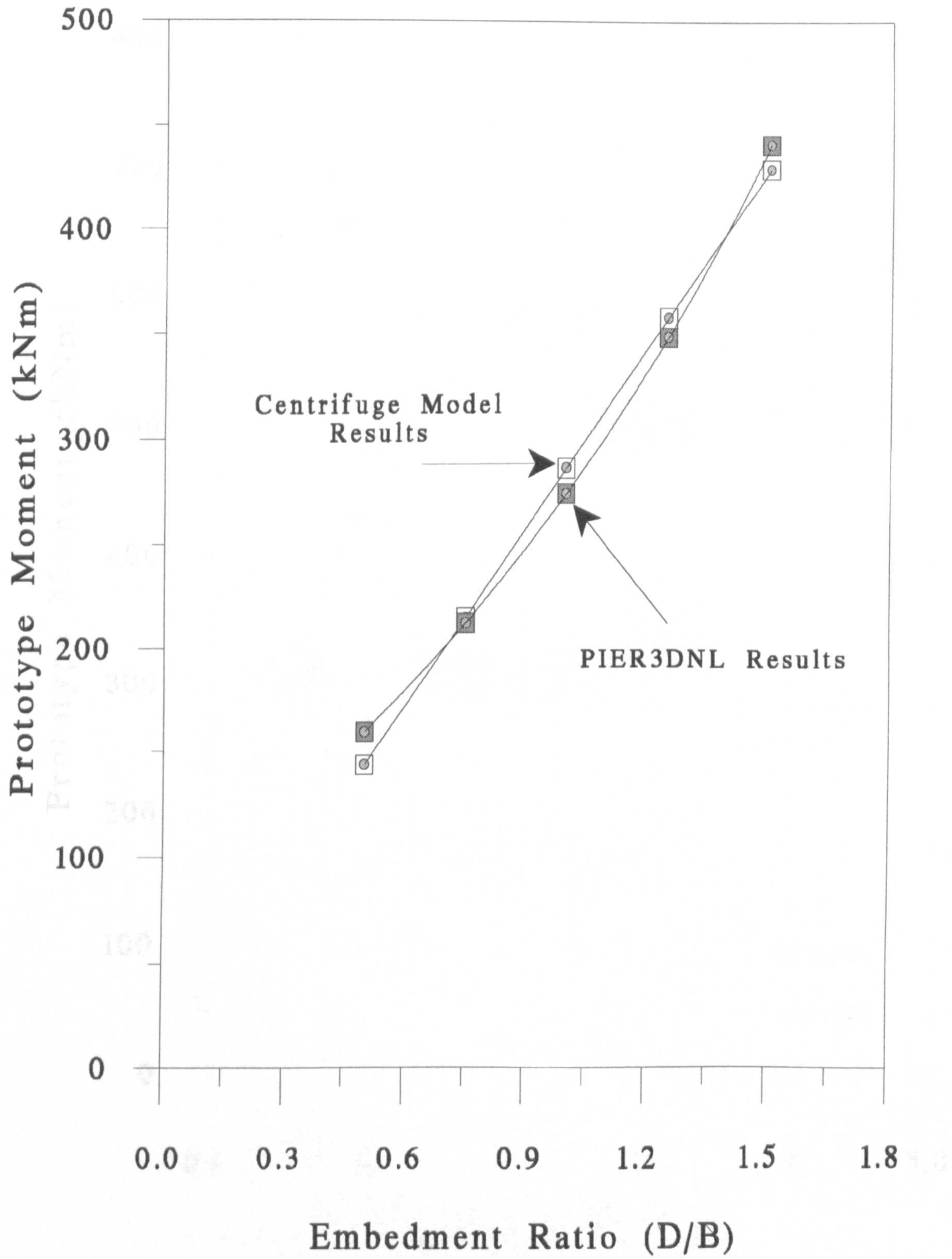

Figure 8.4 Effect of Embedment Ratio on Limiting Moment for 1° Rotation.

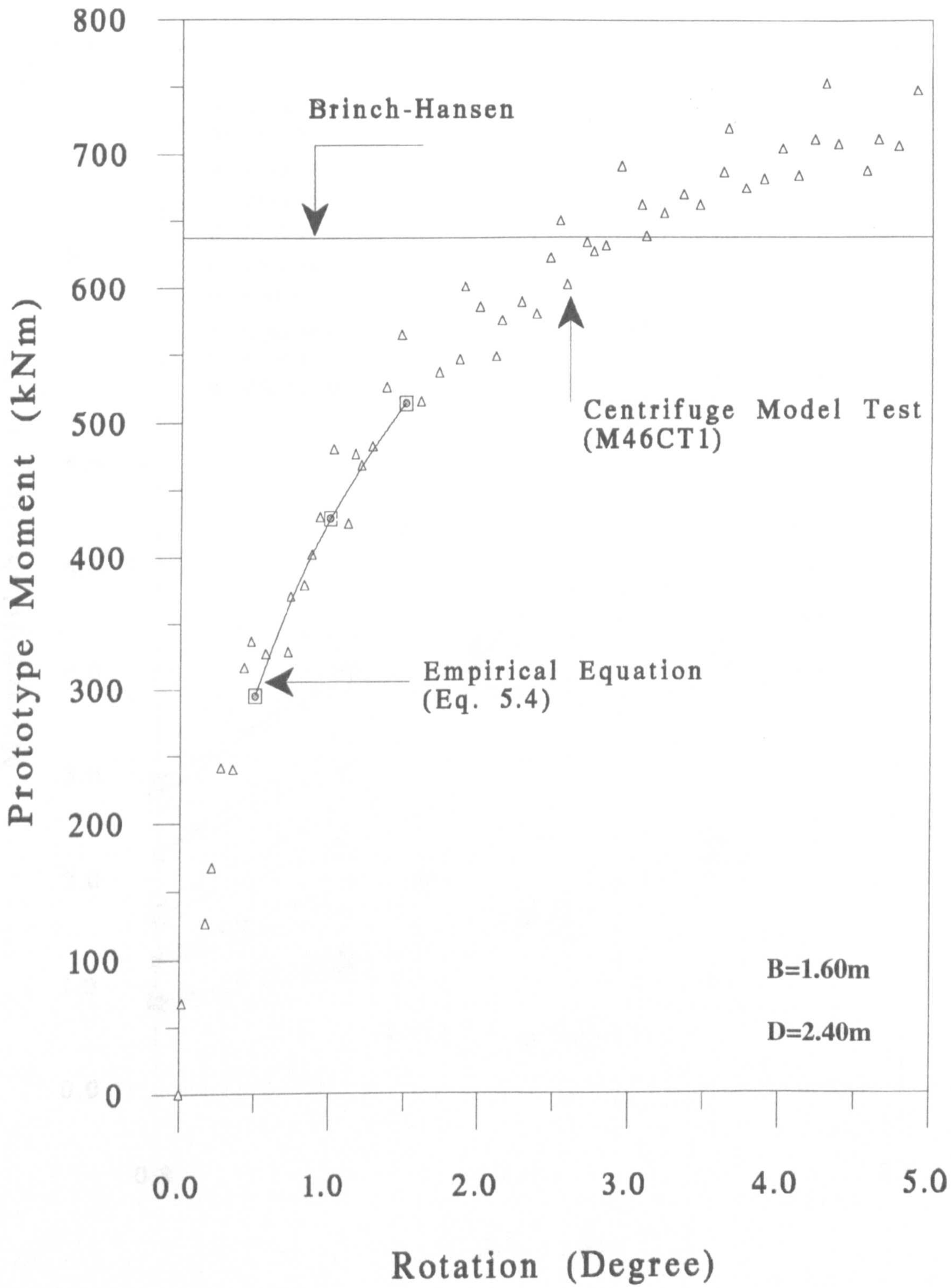

Figure 8.5 Comparison of Moment - Rotation Curves of Centrifuge Tests with Brinch-Hansen's Ultimate Values.

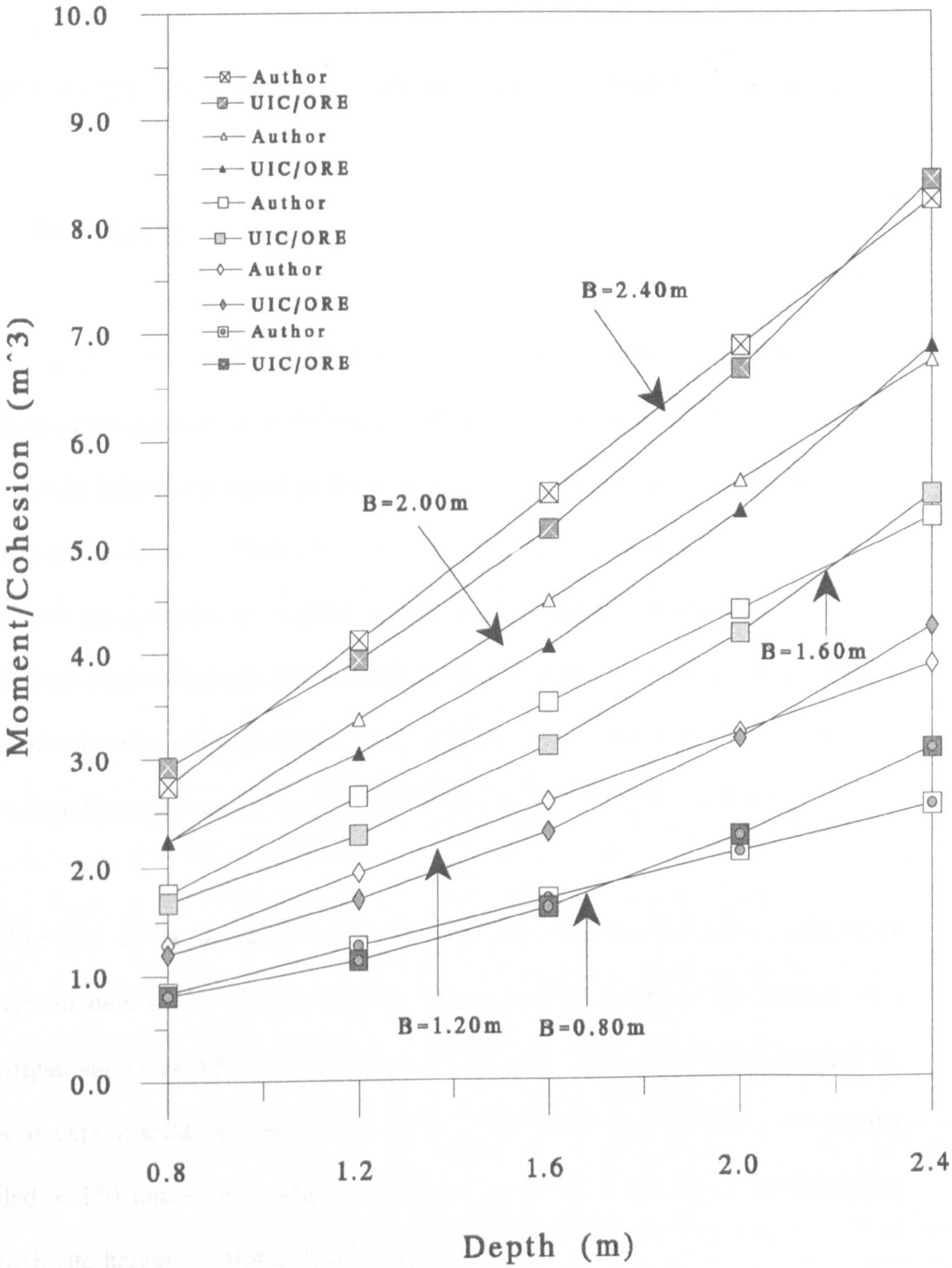

Figure 8.6 Comparison of Limiting Moment Values of Equation (5.4) (for 1° Rotation) with those of (UIC/ORE)/7.5.

CHAPTER 9

CONCLUSIONS AND SUGGESTIONS FOR FURTHER RESEARCH

9.1 Introduction

The work presented in this thesis represents a comprehensive investigation on the moment carrying capacity of rigid pier foundations in saturated clay soil. The study was mainly laboratory based and was performed with the aid of conventional and centrifugal model tests. First, conventional model tests were employed to study the moment-rotation behaviour of piers based on the assumption that scale effect would not be important with respect to immediate stability. Centrifugal model tests, however, were subsequently employed since a preliminary comparison test showed that there was a significant difference between the results of the two types of testing.

Another aim of the research was to simulate the behaviour of piers using finite element models and to validate both the model and the results of the experimental investigations. Three different finite element programs were used for this investigation. In both experimental and numerical studies, the lateral pulling force was usually applied at 150 mm (6 m in prototype) above the level of the clay since this is the approximate height of railway power lines.

In addition to the experimental and numerical works, a comprehensive literature survey of laterally loaded pile and pier foundations in clay soils was carried out.

In this chapter, the major conclusions drawn from the work are presented. Since some aspects of the problem were not studied and also some new questions have arisen from this study, much scope remains for further work using both numerical and experimental techniques. Recommendations for further research are therefore discussed at the end of this chapter concerning clarifications needed, and directions which may be undertaken, as a continuation of the current research.

9.2 General Conclusions

The main conclusions, drawn from the present study, are summarised as follows:

From the literature survey, it was concluded that although a considerable amount of research has been carried out on the ultimate load capacity of long piles subjected to large lateral loads and small moments, the research conducted for short piles and piers subjected to large lateral loads and moments is inadequate. Therefore, the techniques for the analyses of short pier foundations are not as advanced and as well understood as those for the long piles.

Experimental Studies

1) From undrained triaxial tests, relationships have been found which enable appropriate values of parameters, relating to a hyperbolic stress-strain model, to be assigned to the clay used over a small range of moisture contents. It was found that

the procedures developed for calculating the parameters were reliable in the range of moisture content for Moreton clay.

2) Experimental studies showed that the relationships between moment/cohesion against rotation are non-linear but do not exhibit any peak values. All results presented have been scaled up to prototype size on the basis that this is usually legitimate even for conventional model tests for the immediate response of rigid structures in saturated clay.

3) A small variation of the values of moisture content of clay had a significant effect on the moment carrying capacity of pier foundations and it was found that the behaviour of laterally loaded piers in saturated clay was directly dependent on undrained shear strength.

4) From extensive series of conventional model tests and centrifuge model tests empirical relationships have been derived between moment carrying capacity and geometry for limited rotations of 0.5°, 1.0° and 1.5° of short rigid piers in saturated clay. A very close fit was found between the moment-rotation values using these empirical equations and the observed data obtained from the model tests. The only material property involved in these equations is the apparent cohesion of the clay.

5) Both series of experimental results showed that the moment carrying capacity increased with increases in pier length and width. The variation was linear with pier length and slightly non-linear with pier width.

6) From comparisons of the results of centrifugal and conventional model tests, it was observed that for the same pier rotations, the moment carrying capacities from centrifugal model tests were significantly (1.5 to 2 times) larger than those from conventional model tests.

Numerical Studies

7) The three-dimensional linear and non-linear computer programs, developed in this study, and an existing axi-symmetric two-dimensional one can be used for both clay and sand by providing the appropriate parameters. Assessment of the accuracy of the linear three-dimensional computer programs indicated that they were reliable.

8) From analyses to test the optimum distances between a foundation of breadth B and depth $\leq$ 1.5 B and the soil boundaries, using the three-dimensional linear program, PIER3DLN, it was found that boundary effects was insignificant when the sides were at more than 7.5B from the centre of the pier and the stratum depth was more than 5B.

9) In incremental analyses, using the three-dimensional non-linear finite element computer program, PIER3DNL, it was found that 10 load increments were sufficient to give consistent results.

10) Predictions of the immediate behaviour of piers in saturated clay were obtained from the application of the two and three-dimensional programs. These showed that for moments below a certain threshold, the variation of moment with rotation is almost

linear and the soil shows relatively a high resistance to rotation. For higher moment values, the relationship becomes nonlinear, so that for equal increases in moment, subsequent rotations are increased. Peak values were not reached within a reasonable rotation. (The limit of the displacement transducers was reached at less than 7° rotation.)

11) As was the case with the experiments, the results of the computer analyses of conventional models were significantly different from those of the centrifuge models and those at full-scale. For example, even with load and moment values, in the analyses of conventional models, 4.4 times less than those applied in the analyses of centrifuge models and in full-scale analyses, the same order of rotations were obtained. It was also found that an element which failed just after the first load increment in the conventional model failed after the fourth load increment in the other two analyses for the same loading.

12) From the three-dimensional linear finite element analyses, using program PIER3DLN, it was found that the pulling height affected the moment/rotation performance of pier foundations for L/D (pulling height/pier depth) < 2.5.

13) It was found that the results of analyses of centrifuge models and those at full-scale were in good agreement. This confirms that centrifuge modelling, which involves raising the bulk densities of the model materials so that the stress levels in the model and at full-scale are equal at corresponding points, can be considered as an accurate and realistic method for measuring pier-soil interaction. Small differences can be attributed to the boundary restrictions of the centrifuge bucket since the side and bottom boundaries of the soil stratum were located at distances of only 5B, 5.75B and 4.5B, respectively.

14) Comparisons showed that for small rotations the results of the three-dimensional linear and non-linear analyses were much closer to the experimental results than those of the 2-D analysis. Overall, the results of the three-dimensional finite element analysis, using the hyperbolic stress-strain model for soil, provided the most satisfactory predictions of observed moment-rotation behaviour.

Comparisons of the Results of Experiments, Numerical Studies and Existing Design Formulae

15) The results of the conventional model tests were in very good agreement with those of the corresponding three-dimensional non-linear computer analyses. Also, the results of the centrifuge model tests were in good agreement with those of the corresponding three-dimensional non-linear computer analyses for pier rotations in the range of 0 to 2.5 degrees.

16) A comparison of the results of empirical equation (5.4), derived from the centrifuge model tests, and those of numerical analyses for the limiting moment values required to cause 1 degree rotation of piers showed a good agreement even though the variation of the experimental results was linear while that of the numerical results was slightly non-linear.

17) Existing analytical solutions for predicting the behaviour of laterally loaded pile and pier foundations were considered. The methods of Brinch-Hansen and UIC/ORE have been applied to the model pier foundations. Brinch-Hansen's method underestimated the results of tests observed in this study and the rotation values obtained from the intersection of the results varied from 2.20° to 3.40° (an average value of 2.80°). It was observed that the UIC/ORE method overestimated the ultimate moment carrying capacity in comparison with the results of the present study and with Brinch-Hansen's method but gave values approximately 7.5 times larger than the results of this research for 1° rotation.

9.3 Suggestions for Further Research

The present research has provided answers to various questions relating to short pier foundations subjected to lateral load and moment. However, many aspects have not been explored herein and therefore further suggestions are put forward for the continuation of this project:-

(i). The three-dimensional computer programs developed and used in this study could be modified by introducing friction elements for the side faces and the pier base to allow for slippage between its faces and the soil and to consider different shear and normal stiffnesses depending on stress conditions.

(ii). In this study, since for large rotation values (>2.5°), a significant difference was observed between the results of centrifuge model tests and those of its corresponding three-dimensional non-linear computer program, a more sophisticated model to represent the stress-strain relationship of clay (such as an elasto-plastic stress-strain relationship) could be employed instead of hyperbolic model in the three-dimensional computer program, PIER3DNL.

(iii). For more general application in practice, the pulling height could be varied in the tests to examine its effect on the moment-rotation behaviour. (This was considered in a limited way in the numerical phase of this study.)

(iv). Similar tests to the ones undertaken in this program of work could be carried out on pier foundations located close to either a cutting or an embankment since these occur commonly in practice.

(v). A more appropriate replicas of a typical prototypes, such as concrete models, could be used instead of the mild steel ones tested here.

(vi). More parametric studies could be done using the three-dimensional computer programs.

(vii). Similar experimental work could be carried out on the long-term behaviour of short pier foundations in clay.

REFERENCES

Avgherinos, P.J., and Schofield, A.N., (1969), "Drawdown Failures of Centrifuged Models." Proceedings of the 7th International Conference of SMFE, Mexico, Vol. 2, pp. 497-505.

Balfour Beatty Construction Ltd., (1986), "Report on Foundation Design for Overhead Catenary System", Tuen Mun LRT Interim report, BBPCL.

Banerjee, P.K., and Davies, T.G., (1978), "The Behaviour of Axially and Laterally Loaded Single Piles Embedded in Nonhomogeneous Soils." Geotechnique, Vol. 28, No.3, pp. 309-326.

Banerjee, P.K., and Davies, T.G., (1980), "Analysis of Some Reported Case Histories of Laterally Loaded Pile Groups." Proc. Int. Conf. Num. Methods in Offshore Piling, London, U.K., pp. 101-108.

Banerjee, P.K., and Driscoll, R.M.C., (1975), "Program for the Analysis of Pile Groups of any Geometry Subjected to Horizontal and Vertical Loads and Moments." HECB/B/7-PGROUP, DoT, Highway Engineering Computer Branch.

Banerjee, P.K., and Driscoll, R.M.C., (1976), "Three Dimensional Analysis of Raked Pile Groups." Instn. Civil Engnr., Part 2.61, pp. 653-671.

Bartolomey, A.A., (1977), "Experimental Analysis of Pile Groups Under Lateral Load." Proc. of the Special Session 10 of the 9th Int. Conf. on Soil Mechanics and Found. Eng., Tokyo, pp. 101-108.

Bassett, R.H and Craig, W.H (1988), "The Development of Geotechnical Centrifuge in U.K 1965-1985", Centrifuges in Soil Mechanics - ed. Craig, W.H, James, R.G and Schofield, A.N. Balkema, Rotterdam, pp 35-60.

Basset, R.H., and Horner, J., (1979), "Prototype Deformations from Centrifugal Model Tests." Design Parameters in Geotechnical Engineering, BGS London, Vol. 2, pp. 1-9.

Bathe, K.J., (1982), "Finite Element Procedures in Engineering Analysis." Prentice-Hall Inc. Englewood Cliffs, New Jersey.

Bhushan, K., Haley, S.C., and Fong, P.T., (1979), "Lateral Load Tests on Drilled Piers in Stiff Clays." Journal of Geotechnical Engineering, Vol. 105, No GT8, pp. 969-985.

Boresi, A.P., Sidebottom, O.M., Seely, F.B., and Smith, J.O., (1978), "Advanced Mechanics of Materials." John Wiley and Sons, New York.

Brinch Hansen, J., (1961), "The Ultimate Resistance of Rigid Piles Against Transversal Forces." The Danish Geotechnical Institute Bulletin, Bulletin No. 12, pp. 5-9.

Broms, B.B., (1964a), "Lateral Resistance of Piles in Cohesionless Soils." Journal of the Soil Mechanics and Foundation Division, Proceedings of ASCE, Vol. 90, No. SM3. pp. 123-149.

Broms, B.B., (1964b), "Lateral Resistance of Piles in Cohesive Soils." Journal of Soil Mechanics and Foundation Division, Proceedings of ASCE, Vol. 90, No. SM2. pp. 27-63.

Broms, B.B., (1965), "Design of Laterally Loaded Piles." Journal of Soil Mechanics and Foundation Division, Proceedings of ASCE, Vol. 91, No. SM3. pp. 79-99.

Broms, B.B., (1981), "Precast Piling Practice." Thomas Telford Ltd., London, pp. 68-79.

Bucky, P.B., (1931), "Use of Models for the Study of Mining Problems." Am. Inst. Min. and Met. Eng., Tech. Pub., pp. 425-428.

Budhu, M., and Davies, T.G., (1988), "Analysis of Laterally Loaded Piles in Soft Clay." Journal of Geotechnical Engineering, ASCE, Vol. 114, No. 1, pp. 21-39.

Burnett, D.S., (1987), "Finite Element Analysis." Addison-Wesley, Reading.

Chandrasekaran, V.S., and King, G.J.W., (1982), "Laterally Loaded Piles: Finite Element Analysis and Design and Pilot Centrifugal Model Studies." Internal Report, The University of Liverpool.

Chandrasekaran, V.S., Kulkarni, K.R. and King, G.J.W., (1984), "Analytical and Laterally Loaded Single Piles: Pro. Symp. Recent Advances in Geotechnical Centrifuge Modelling." University of California, pp. 116-135.

Cheney, J.A., (1988), "American Literature on Geotechnical Centrifuge Modelling 1931-1984." Centrifuges in Soil Mechanics, Balkema, Rotterdam, Brookfield, pp. 77-80.

Clough, G.W., and Duncan, J.M., (1971), "Finite Element Analysis of Retaining Wall Behaviour." Journal of the Soil Mechanics and Foundation Division, Proceedings of the ASCE, Vol. 97, No. SM12, pp. 1657-1674.

Craig, W.H., (1985), "Modelling Pile Installation in Centrifuge Experiments." Proceedings of the 11th International Conference of SMFE, San Fransisco, Vol. 2, pp. 1101-1104.

Craig, W.H, (1988), "Centrifugal models in Marine and Costal Engineering", Centrifugal Models in Marine and Coastal geotechnical design, University of Manchester, pp. 440-445.

Craig, W.H., (1989a), "Edouard Phillips (1821-1889) and the Idea of Centrifuge Modelling." Geotechnique, The Institution of Civil Engineers, London, Vol. 39, No. 4. pp. 697-700.

Craig, W.H., (1989b), "The Use of Centrifuge in Geotechnical Engineering Education." Geotechnical Testing Journal, GTJODJ, Vol. 12, No. 4. pp. 288-291.

Craig, W.H., James, R.G., and Schofield, A.N., (1988), "Centrifuges in Soil Mechanics." Balkema, Rotterdam, Brookfield.

Czerniak, E., (1957), "Resistance to Overturning of Single Short Piles." Journal of Structural Division, Proceedings of ASCE, Vol. 83. No. ST2. pp.1-25.

Davidenkov, N.N., (1933), "The New Method of the Application of Models to the Study of the Equilibrium of Soils." J. Tech. Physics, Moscow, Vol. 3, pp. 131-136.

Davies, T.G., and Budhu, M., (1986), "Non-linear Analysis of Laterally Loaded Piles in Heavily Overconsolidated Clays." Geotechnique, Vol. 36, No.4, pp. 527-538.

Davisson, M.T., (1960), "Behaviour of Flexible Piles Subjected to Moment, Shear and Axial Load, PhD Thesis. University of Illinois.

Davisson, M.T., and Gill, H.L., (1963), "Laterally Loaded Piles in a Layered Soil System." Journal of the Soil Mechanics and Foundation Division, Proceedings of the ASCE, Vol. 96, No. SM5, pp. 1605-1627.

Desai, C.S., and Abel, J.F., (1972), "Introduction to the Finite Element Method." Van Nostrand Reinhold Company, New York.

Desai, C.S., and Kuppusamy, T., (1980), "Application of a Numerical Procedure for Laterally Loaded Structures." Numerical Methods in Offshore Piling, ICE, pp. 93-99.

Desai, I.D., and Chandrasekaran, V.S., (1980), "Displacements of Laterally Loaded Circular Wells." Conference in Geotechnical Engineering, Geotech 80, Bombay, pp. 165-170.

Dickin, E.A., and King, G.J.W., (1982), "The Behaviour of Hyperbolic Stress-Strain Models in Triaxial and Plane Strain Compression." International Symposium on Numerical Models in Geomechanics, Zurich, pp. 303-311.

Dickin, E.A., and Leung, C.F., (1983), "Centrifugal Model Tests on Vertical Anchor Plates", Journal of Geotechnical Engineering, Proc. of the ASCE, No. GT12, Vol.109, pp. 1503-1525.

Dickin, E.A., and Leung, C.F., (1985), "Evaluation of Design Methods for Vertical Anchor Plates." Journal of Geotechnical Engineering, ASCE, Vol. 111, No. 4, pp. 500-520.

Dickin, E.A., and Leung, C.F., (1990), "Performance of Piles with Enlarged Bases in Sand", Canadian Geotechnical Journal, No. 5, Vol. 27, pp. 546-556.

Dickin, E.A., and Leung, C.F., (1992), "The Influence of Foundation Geometry on the Uplift Behaviour of Piles with Enlarged Bases in Sand", Canadian Geotechnical Journal, No. 3, Vol. 29, pp. 498-505.

Dickin, E.A., and Nazir, R., (1992), "Overturning Resistance of Short Piled Foundations in Sand", GEOTROPIKA '92, International Conference on Geotechnical Engineering, Malaysia.

Dickin, E.A., and Nazir, R., (1993), "Centrifugal Modelling of Side-Bearing Foundations in Sand", Dept. of Civil Engineering, University of Liverpool, Report No. CE/26/93.

Dickin E.A., and Nazir, R., (1994a), "Appraisal of Design Methods for Laterally Loaded Short Piles in Sand", GEOTROPIKA '94, International Conference on Geotechnical Engineering, Malaysia.

Dickin, E.A., and Nazir, R., (1994b), "Geometric Factors Influencing the Behaviour of Side-Bearing Foundations in Sand", Proc. International Conference Centrifuge '94, Singapore, (Eds. Leung, C.F., Lee, F.H. and Tan, T.S., Publ. A.A. Balkema Rotterdam), pp. 527-532.

Dickin, E.A., and Wei, M.J., (1991), "Moment Carrying Capacity of Short Piles in Sand", Centrifuge 91, Proc. International Conference Geotechnical Centrifuge Modelling, Colorado, Balkema, Rotterdam.

Douglas, D.J., and Davis, E.H., (1964), "The Movement of Buried Footings Due to Moment and Horizontal Load and the Movement of Anchor Plates." Geotechnique, Vol. 14, pp. 115-132.

Duncan, J.M., and Chang, C.Y., (1970), "Nonlinear Analysis of Stress and Strain in Soils." Journal of the Soil Mechanics and Foundation Division, ASCE, Vol. 96, No. SM5, pp. 1629-1653.

Duncan, J.M., (1981), "Hyperbolic Stress-Strain Relationship." Limit Equilibrium Plasticity and Generalised Stress-Strain in Geotechnical Engineering, ASCE Workshop, Montreal, pp. 443-460.

Edwards, L.W., (1979), "Non-Linear Finite Element Analysis of Embankments." Engineering Software Proceedings, pp. 599-613.

Ergatoudis, I., Irons, B.M., and Zienkiewicz, D.C., (1968), "Curved Isoparametric, Quadrilateral Elements for Finite Element Analysis." Journal of the Solids Struct., Vol. 4, pp. 31-42.

Farhadi, A., (1991), "The Immediate Settlement of Pier Foundation in Saturated Clay." Ph.D Thesis, University of Liverpool.

Fox, L., (1964), "An introduction to numerical linear Algebra." Clarendon Press, Oxford.

Fulthorpe, J.N., (1986), "The Response of Vertical Piles to Lateral Loading and Moment." Ph.D Thesis, University of Liverpool.

Gabr, M.A., and Borden, R.H., (1990), "Lateral Analysis of Piers Constructed on Slopes." Journal of Geotechnical Engineering, ASCE, Vol. 116, No 12, pp. 1831-1850.

Gabr, M.A., Lunne, T., and Powell, J.J., (1994), "P-y Analysis of Laterally Loaded Piles in Clay Using DMT." Journal of Geotechnical Engineering, ASCE, Vol. 120, No 5, pp. 816-837.

Gallagher, R.H., (1975), "Finite Element Analysis." Prentice-Hall, New Jersey.

Georgiadis, M., Anagnostopoulos, C., and Saflekou, S., (1992), "Cyclic Lateral Loading of Piles in Soft Clay." Geotechnical Engineering, Vol. 23, pp. 47-60.

Georgiadis, M., and Butterfield, R., (1982), "Laterally Loaded Pile Behaviour." Journal of the Geotechnical Engineering, ASCE, Vol. 108, No. GT1, pp. 155-165.

Goodman, R.E., Taylor, R.L., and Brekke, T.L., (1968), "A Model for the Mechanics of Jointed Rock." Journal of Soil Mechanics and Foundation Div., ASCE, Vol. 96, pp. 1367-1370.

Hamilton, J.M., and Phillips, R., (1991), "Centrifuge Study of Laterally Loaded Behaviour in Clay." Centrifuge 1991, Balkema, Rotterdam, pp. 285-292.

Hetenyi, M., (1946), "Beams on Elastic Foundations." University of Michigan Press.

Hinton, E., and Owen, D.R.J., (1979), "Finite Element Programming." Academic Press, London.

Huebner, K.H., (1975), "Finite Element Method for Engineers." Wiley, New York.

Ismael, N.F., and Klym, T.W., (1978), "Behaviour of Rigid Piers in Layered Cohesive Soils." Journal of Geotechnical Engineering, ASCE, Vol. 104, No. GT8, pp. 1061-1074.

Janbu, N., (1963), "Soil Compressibility as Determined by Oedometer and Triaxial Tests." European Conference on Soil Mechanics and Foundation Engineering, Wiesbaden, Germany, Vol. 1, pp. 19-25.

King, G.J.W., (1977), "An Introduction to Superstructure/Raft/Soil Interaction." Proc. Int. Symp. on Soil-Structure Interaction, Roorkee, India, pp. 453-466.

King, G.J.W., (1984), "Some Applications of the Finite Element Method in Soil Mechanics." Ph.D Thesis, University of Liverpool.

King, G.J.W., Dickin, E.A., and Lyndon, A., (1984), "The Development of a Medium-Size Centrifugal Testing Facility." Symposium of Applications of Centrifuge Modelling in Geotechnical Design, Manchester, pp. 25-46.

King, G.J.W., and Fulthorpe, J.N., (1986), "Centrifuge Model Tests on Laterally Loaded Single Piles", Proc. 3rd Indian Conf. on Ocean Eng., Bombay, pp BB1-BB11.

King, G.J.W., (1989), "Centrifuge Model Studies on Piles and Pile Groups Subjected to Lateral Loads." Dep. of Civil Engn. Univ. of Liverpool, Int. Report No. CE/4/89.

King, G.J.W., and McLoughlin, J.P., (1992), "Centrifuge Model Studies of a Cantilever Retaining Wall in Sand." Proc. I.C.E. Int. Conf. on Retaining Structures, Cambridge University.

Kondner, R.L., (1963), "Hyperbolic Stress-Strain Response: Cohesive Soils." Journal of the Soil Mechanics and Foundation Division, ASCE, Vol. 89, No. SM1. pp. 115-143.

Kondner, R.L., Zelasco, J.S., (1963), "A Hyperbolic Stress-Strain Formulation for Sands." Proceedings of 2nd Pan-American Conference on Soil Mechanics and Foundation Engineering, Brazil, Vol. 1, pp. 289-324.

Kramer, S.L., (1992), "Use of Air Bag System for Instrumentation of Lateral Load Tests on Previously Installed Pipe Piles." Geotechnical Testing Journal, GTJODJ, Vol. 15, No. 4, pp. 399-403.

Kulkarni, K.R., Chandrasekaran, V.S., and King, G.J.W., (1985), "Centrifugal Model Studies on Laterally Loaded Pile Groups in Sand", Proc. of the 11th, ICSMFE, San Francisco, Vol. 2, pp. 1113-1116.

Lekhnitskii, S.G. (1963), "Theory of Elasticity of an Anisotropic Elastic Body." Holden-Day, San-Fransisco.

Leung, C.F., and Dickin, E.A., (1991), "Uplift Capacity of Foundations", Recent Advances in Geotechnical Engineering III, Singapore, pp. 20-24.

Lyndon, A., and Pearson, R.A., (1984), "Pressure Distribution on a Rigid Retaining Wall in Cohesionless Material." AA Balkema, Rotterdam, pp 271-281.

Martin, H.C., and Carey, G., (1973), "Introduction to Finite Element Analysis." McGraw-Hill, New York.

Matlock, H., and Reese, L.C., (1960), "Generalised Solutions for Laterally Loaded Piles." Journal of the Soil Mechanics and Foundations Division, Proceedings of the ASCE, Vol. 86, No. SM5. pp.63-91.

Matlock, H., and Reese, L.C., (1961), "Foundation Analysis of Offshore Pile-Supported Structures." Proceedings of the 5th International Conference ISSMFE, Paris, Vol. 2, pp. 91-97.

Matlock, H., (1970), "Correlations for Design of Laterally Loaded Piles in Soft Clay." Proceedings of the Offshore Technology Conference, 2nd Conf., Houston, Texas, Paper OTC1204, pp. 577-594.

McCorkle, B.L., (1969), "Side-Bearing Pier Foundations." Civil Engineering., ASCE, pp. 65-66.

McClelland, B., and Focht, J.A., (1956), "Soil Modulus for Laterally Loaded Piles." Journal of the Soil Mechanics and Foundations Division, ASCE, Vol. 82, No. SM 4, Proc. Paper 1081, pp. 1-22.

Meyerhof, G.G., Yalcin, A.S., and Mathur, S.K., (1983), "Ultimate Pile Capacity for Eccentric Inclined Load." Journal of Geotechnical Engineering, ASCE, Vol. 109, No. 3, pp. 408-423.

Meyerhof, G.G., (1981), "The Bearing Capacity of Short Rigid Piles and Pile Groups Under Inclined Load in Clay." Canadian Geotechnical Journal, Vol. 18, pp. 297-300.

Meyerhof, G.G., and Sastry, V.V.R.N., (1985), "Bearing Capacity of Rigid Piles Under Eccentric and Inclined Loads." Canadian Geotechnical Journal, Vol. 22(3), pp. 267-276.

Meyerhof, G.G., and Yalcin, A.S., (1984), "Pile Capacity for Eccentric Inclined Load in Clay." Canadian Geotechnical Journal, Vol. 21, pp. 389-396.

Meyerhof, G.G., Sastry, V.V.R.N., and Yalcin, A.S., (1988), "Lateral Resistance and Deflection of Flexible Piles." Canadian Geotechnical Journal, Vol. 25, pp. 511-522.

Mindlin, R.D., (1936), "Force at a Point in the Interior of a Semi-Infinite Solid." Physics, 7, pp. 195-202.

Murf, J.D., and Hamilton, J.M., (1993), "P-Ultimate for Undrained Analysis of Laterally Loaded Piles." Journal of Geotechnical Engineering, Vol. 119, No. 1, pp. 91-107.

Nazir, R.B., (1994), "The Moment Carrying Capacity of Short Piles in Sand." Ph.D. Thesis, University of Liverpool.

Ovesen, N.K., (1979), "The Use of Physical Models in Design: The Scaling Law Relationship", Proc. 7th. European Conference Soil Mechanics and Foundation Engineering, Brighton, Vol.4, pp. 318-323.

Palmer, L.A., and Thompson, J.B., (1948), "The Earth Pressure and Deflection Along the Embedded Length of Piles Subjected to Lateral Thrust", Proc. of the 2nd. ICSMFE Rotterdam, Vol.5, pp 156-161.

Pise, P.J., (1984), "Lateral Response of Free-Head Pile." Journal of Geotechnical Engineering, ASCE, Vol. 110, No. 12, pp. 1805-1809.

Pokrovsky, G.Y., (1933), "On the Application of Centrifugal Force for Modelling Earth Works in Clay." J. Tech. Physics, Moscow, Vol. 3, pp. 537-539.

Pokrovsky, G.Y., and Fedorov, I.S., (1936), "Studies of Soil Pressures and Deformations by Means of a Centrifuge." Proc. of the 1st ICSMFE, Harvard University, Vol. 1, No. 70.

Poulos, H.G., (1971), "Behaviour of Laterally Loaded Piles: I. Single Piles." Journal of Soil Mechanics and Foundations Division, Proc. of the ASCE, No. SM5, Vol. 97, pp 711-731.

Poulos, H.G., (1979), "Settlement of Single Piles in Nonhomogeneous Soil." Journal of Geotechnical Engineering Division, ASCE, Vol. 105, No. GT5, pp 627-641.

Poulos, H.G., and Davis, E.H., (1980), "Pile Foundation Analysis and Design." John Wiley and Sons Inc. New York.

Przemieniecki, J.S., (1968), "Theory of Matrix Structural Analysis." McGraw-Hill.

Pyke, R., and Beikae, M., (1984), "A New Solutions for the Resistance of Single Piles to Lateral Loading." Laterally Loaded Deep Foundations: Analysis and Performance, ASTM STP835, Eds., Langer, J.A., Mosley, E.T., and Thompson, C.D., pp. 3-20.

Ramelot, C., and Vandeperre, L., (1950), "Les Foundations de Pylones Electriques: Leur Resistance au Renversement, Leur Stabilitè, Leur Calcul Ètude Experimentale." Comptes Rendus de Recherces de, l'Institut Pour Encouragement de la Recherche Scientifique dans l'Industrie et l'Agriculture, No.2.

Randolph, M.F., (1981), "The Response of Flexible Piles to Lateral Loading." Geotechnique, Vol. 31, No. 2, pp. 247-259.

Reese, L.C., (1958), "Discussion of Soil Modulus for Laterally Loaded Piles by B. McClelland and J. A. Focht." Jr. Trans. Am. Soc. Civ. Engrs. Vol. 123, pp. 1071-1074.

Reese, L.C., and Welch, R.C., (1975), "Lateral Loading of Deep Foundations in Stiff Clay." Journal of the Geotechnical Engineering Division, ASCE, Vol. 101, No. GT7, pp. 633-649.

Reese, L.C., and Desai, C.S., (1977), "Laterally Loaded Piles." Numerical Methods in Geotechnical Engineering, Mc Graw-Hill Book Company, Edited by Chandrasekaran, S.D., and John, T.C., Chapter 9, pp. 297-325.

Rowe, R.K., and Davis, E.H., (1982), "The Behaviour of Anchor Plates in Clay." Geotechnique, The Institution of Civil Engineers, London, Vol. 32, No. 1, pp. 9-23.

Sastry, V.V.R.N., and Meyerhof, G.G., (1986), "Lateral Soil Pressures and Displacements of Rigid Piles in Homogeneous Soils Under Eccentric and Inclined Loads." Canadian Geotechnical Journal, Vol. 23, pp. 281-286.

Sastry, V.V.R.N., Meyerhof, G.G., and Koumoto, T., (1986), "Behaviour of Rigid Piles in Layered Soils Under Eccentric and Inclined Loads." Canadian Geotechnical Journal, Vol. 23, pp. 451-457.

Sastry, V.V.R.N., and Meyerhof, G.G., (1987), "Influence of Installation Method on the Behaviour of Rigid Piles in Clay Subjected to Moment and Horizontal Load." Canadian Geotechnical Journal, Vol. 24, pp. 145-149.

Schofield, A.N., (1980), "Cambridge Geotechnical Centrifuge Operations." Geotechnique, The Institute of Civil Engineers, London Vol. 30, No. 4, pp. 227-268.

Schofield, A.N., (1988), "An Introduction to Centrifuge Modelling", Centrifuge in Soil Mechanics - ed. Craig, W.H, James, R.G and Schofield, A.N, Balkema, Rotterdam, pp. 1-9.

Scott, R.F., (1981), " Pile Testing in a Centrifuge." Proceedings of the 10th ICSMFE, Stockholm, Vol. 2, pp. 839-842.

Selby, A.R., and Arta, M.R., (1991), "Three-Dimensional Finite Element Anlaysis of Pile Groups Under Lateral Loading." Computers and Structures, Vol. 40, No. 5, pp. 1329-1336.

Shilts, W.L., Graves, L.D., and Driscoll, C.G., (1948), "A Report of Field and Laboratory Tests on the Stability of Posts Against Lateral Load."Proceedings of the 2nd ICSMFE, Rotterdam, Vol. 5, pp. 107-112.

Smith, I.M., (1980), "Numerical Methods in Offshore Piling." Institution of Civil Engineers, London.

Smith, T.D., (1987), "Pile Horizontal Soil Modulus Values." Journal of Geotechnical Engineering, ASCE, Vol. 113, No. 9, pp. 1040-1043.

Sun, K., and Pires, J.A., (1993), "Simplified Approach for Pile and Foundation Interaction Analysis." Journal of Geotechnical Engineering, ASCE, Vol. 119, No. 9. pp. 1462-1479.

Terzaghi, K., (1955), "The Evaluation of Coefficients of Subgrade Reaction." Geotechnique, Vol. 5, No. 4, pp. 297-326.

Trochanis, A.M., Bielak, J., and Christiano, P., (1991a), "Three-Dimensional Nonlinear Study of Piles." Journal of Geotechnical Engineering, Vol. 117, No. 3, pp. 429-447.

Trochanis, A.M., Bielak, J., and Christiano, P., (1991b), "Simplified Model for Analysis of One or Two Piles." Journal of Geotechnical Engineering, Vol. 117, No. 3, pp. 448-466.

UIC/ORE, (1957), "Calculation of Cetenary Masts and Foundations." Interim Report No. 1, International Union of Railways/Office for Research and Experiments, Utrecht.

Vallabhan, C.V.G., and Alikhanlou, F., (1982), "Short Rigid Piers in Clays." Journal of the Geotechnical Engineering Division, ASCE, Vol. 108, No. GT10, pp. 1255-1272.

Verruijt, A., and Kooijman, A.P., (1989), "Laterally Loaded Piles in a Layered Elastic Medium." Geotechnique, Vol. 39, No. 1, pp. 39-46.

Wilson, E.L., (1965), "Structural Analysis of Axisymmetric Solids." AIAA, Vol. 3, No. 12, pp. 2269-2274.

Wood, L.A., (1979), "Lawpile - A Program for the Analysis of Laterally Loaded Pile Groups and Propped Sheetpile and Diaphragm Walls." Proc. 1st Int. Conf. on Engineering Software, Southampton University, Vol. 1.4, pp. 614-632.

Yokoyama, Y., (1985), "A Non-Linear Analysis of Pile Structures." Soils and Foundations, Japanese Society of Soil Mechanics and Foundation Engineering, Vol. 25, No. 4, pp. 92-102.

Zienkiewicz, O.C., and Cheng, Y.K., (1964), "Buttress Dams on Complex Rock Foundations." Water Power, Vol. 16, p. 193.

Zienkiewicz, O.C., (1977), "The Finite Element Method in Engineering Science." McGraw-Hill, London.

ADDITIONAL BIBLIOGRAPHY

Abduljauwad, S.N., Al-Sulaimani, G.J., and Basunbul, I.A., (1990), "Model Piles Embedded in Submerged Sand and Subjected to Static and Cyclic Lateral Loadings." Geotechnical Engineering, Vol. 21, pp. 161-175.

Abendroth, R.E., and Greimann, L.F., (1989), "Rational Design Approach for Integral Abutment Bridge Piles." Transportation Research Record, No. 1223, pp. 12-23.

Abendroth, R.E., and Greimann, L.F., (1990), "Pile Behaviour Established from Model Test." Journal of Geotechnical Engineering, Vol. 116, No. 4, pp. 571-588.

Almeida, M.S.S., Britto, A.M., and Parry, R.H.G., (1986), "Numerical Modelling of a Centrifuged Embankment on Soft Clay." Canadian Geotechnical Journal,Vol. 23, pp. 103-114.

Anagnostopoulos, C., and Georgiadis, M., (1993), "Interaction of Axial and Lateral Pile Responses." Journal of Geotechnical Engineering, Vol. 119, No. 4, pp. 793-798.

Bloomquist, D.G., Davidson, J.L., and Townsend, F.C., (1984), "Platform Orientation and Start up Time During Centrifuge Testing." Geotechnical Testing Journal, GTJODJ, Vol. 7, No. 4. pp. 195-199.

Banerjee, P.K., and Driscoll, R.M.C., (1976), "Three Dimensional Analysis of Raked Pile Groups." Instn. Civil Engnr., Part 2.61, pp. 653-671.

Chow, Y.K., (1987a), "Axial and Lateral Response of Pile Groups Embedded in Nonhomogeneous Soils." International Journal for Numerical and Analytical Methods in Geomechanics, Vol. 11, pp. 621-638.

Chow, Y.K., (1987b), "Three-Dimensional Analysis of Pile Groups." Journal of Geotechnical Engineering, ASCE, Vol. 113, No. 6, pp. 637-651.

Clegg, D.P., (1981), "Model Piles in Stiff Clay." Cambridge, PhD Thesis.

Craig, W.H., (1983), "Simulation of Foundations for Offshore Structure Using Centrifuge Modelling." Development in Soil Mechanics and Foundation Engineering, Model Studies, Vol. 1, pp. 1-25.

Craig, W.H., and Rowe, P.W., (1981), "Operation of a Geotechnical Centrifuge from 1970 to 1979." Geotechnical Testing Journal, GTJODJ, Vol. 4, No. 1. pp. 19-25.

Davisson, M.T., and Salley, J.R., (1970), "Model Study of Laterally Loaded Piles." Journal of the Soil Mechanics and Foundation Division, Proceedings of the ASCE, Vol. 96, No. SM5, pp. 1605-1627.

Desai, C.S., (1976), "Design-Analysis of Deep Pile Foundations Using Finite Element Method." In: Analysis and Design of Building Foundations, Ed. Hsai-Yang Fang. Envo Publishingo Co. pp. 583-609.

Desai, C.S., and Christian, J.T., (1977), "Numerical Methods in Geotechnical Engineering." McGraw-Hill Book Company, New York.

Drumm, E.C., Bennett, R.M., and Oakley, G.J., (1990), "Probabilistic Response of Laterally Loaded Piers by Three-Point Approximation." International Journal for Numerical and Analytical Methods in Geomechanics, Vol. 14, pp. 499-507.

El Sharnouby, B., and Novak, M., (1986), "Flexibility Coefficients and Interaction Factors for Pile Group Analysis." Canadian Geotechnical Journal, Vol. 23, pp. 441-450.

Feda, J., (1993), "Service Load of Short Large-Diameter Bored Piles." Journal of Geotechnical Engineering, ASCE, Vol. 119, No. 9. pp. 1482-1489.

Franke, E., and Muth, G., (1985), "Scale Effect in 1g-Model Tests on Horizontally Loaded Piles." Proc. of the 11th. ICSMFE San Francisco, Vol.2, pp. 1011-1014.

Gabr, M.A., (1986), "Influence the Base Resistance on the Lateral Load Deflection Behaviour of Rigid Pier." Proc. Int. Conf. on Soil-Struct. Interaction, Paris, pp. 219-226.

Hoadley, P.J., Barton, Y.O., and Parry, R.H.G., (1981), "Cyclic Lateral Load on Model Pile in a Centrifuge." Proceedings of the 10th ICSMFE, Stockholm, Vol. 1, pp. 621-625.

Irons, B.M., (1971), "Quadrature Rules for Brick Based Finite Elements." Int. Journal for Numerical Methods in Engineering, Vol. 3, pp. 293-294.

Jain, N.K., Ranjan, G., and Ramasamy, G., (1987), "Effect of Vertical Load on Flexural Behaviour of Piles." Geotechnical Engineering, Vol. 18, pp. 185-204.

Jewel, R.A., (1989), "Direct Shear Test on Sand." Geotechnique, The Institution of Civil Engineers, London, Vol. 39, No. 2. pp. 309-322.

Ko, H.Y., (1988), "Summary of the State-of-the-art in Centrifuge Model Testing"; Centrifuge 88, Proc. International Conference Geotechnical Centrifuge Modelling, Paris, Balkema, Rotterdam, pp. 11-18.

Kubo, K., (1965), "Experimental Study of the Behaviour of Laterally Loaded Piles." Proc. of the 6th. ICSMFE, Montreal, Vol. 2, pp. 275-279.

Kueh, G.C., (1989), "The Design of Pile Foundations Subjected to the Large Moments." M.Sc.(Eng) Dissertation, University of Liverpool.

Lee, C.Y., (1993), "Settlement of Pile Groups." Journal of Geotechnical Engineering, ASCE, Vol. 119, No. 9. pp. 1449-1461.

Leung, C.F., (1981), "The Effect of Shape, Size and Embedment on the Load-Displacement Behaviour of Vertical Anchors in Sand." Ph.D Thesis, University of Liverpool.

Leung, C.F., and Dickin, E.A., (1984), "Scale Error of Conventional Model Tests."Proc. Int.Symposium on Geotechnical Centrifuge Model Testing, Japanese Society for Soil Mechanics and Foundation Engineering, pp. 133-138.

Liem, D.H.W., (1988), "Appraisal of Lade's Elasto-Plastic Soil Models and Their Application to Vertical Anchors in Sand." Ph.D Thesis, University of Liverpool.

Meyerhof, G.G., Sastry, V.V.R.N., and Yalcin, A.S., (1988), "Lateral Resistance and Deflection of Flexible Piles." Canadian Geotechnical Journal, Vol. 25, pp. 511-522.

Muqtadir, A., and Desai, C.S., (1986), "Three-Dimensional Analysis of a Pile-Group Foundation." International Journal for Numerical and Analytical Methods in Geomechanics, Vol. 10, No. 1. pp.41-58.

Parikh, S.K., and Pal, S.C., (1979), "Parametric Analysis of Axially Loaded Concrete Piles in Non-Homogeneous Cohesive and Cohesionless Soil Deposits." Third Int. Conference on Numerical Methods in Geomechanics, Aachen, pp. 1531-1538.

Poulos, H.G., (1971b), "Behaviour of Laterally Loaded Piles: II. Pile Groups." Journal of Soil Mechanics and Foundations Division, Proc. of the ASCE, No. SM5, Vol. 97, pp 733-737.

Poulos, H.G., (1980), "An Approach for the Analyses of Offshore Pile Groups." Proc. Int. Conf. Numerical Methods in Offshore Piling, London, U.K., pp. 119-126.

Raes, P.E., (1936), "Theory of Lateral Bearing Capacity of Piles", Proc. of the 1st ICSMFE Harvard University, Vol.3, pp 166-169.

Rajani, B., and Morgenstern, N., (1993), "Pipelines and Laterally Loaded Piles in Elastoplastic Medium." Journal of Geotechnical Engineering, ASCE, Vol. 119, No. 9. pp. 1431-1448.

Reese, L.C., and Matlock, H., (1956), "Non-dimensional Solutions for Laterally Loaded Piles with Soil Modulus Assumed Proportional to Depth." Proc. 8th Conf. on Soil Mechanics and Foundation Engineering, Austin, Texas, pp. 27-41.

Robertson, P.K., Campanella, R.G., and Brown, P.T., (1985), "Design of Axially and Laterally Loaded Piles Using in situ Tests: A Case History." Canadian Geotechnical Journal, Vol. 22, pp. 518-527.

Rojas, E., (1993), "Static Behaviour of Model Friction Piles." Ground Engnr, pp. 26-29.

Roscoe, K. H., (1957), "A Comparison of Tied and Free Pier Foundations." Proceedings of the 4th ICSMFE London, Vol. 1, pp. 419-423.

Roscoe, K. H., and Schofield, A.N., (1956), "The Stability of Short Pier Foundations in Sand." Symposium on the Plastic Theory of Structures, Cambridge, British Welding Journal, Vol. 3, No. 8. pp. 343-354.

Rowe, P.W., (1956), "The Single Pile Subject to Horizontal Force." Geotechnique, The Institution of Civil Engineers, London, Vol. 6, No. 2, pp. 70-85.

Saglamer, A., and Parry, R.H.G., (1979), "Model Study of Laterally Loaded Single Piles." Proc. 7th European Conf. on Soil Mechanics and Foundation Engineering. British Geotechnique Society, Vol. 2, pp. 115-120.

Santamarina, J.C. and Godding, D.J., (1989), "Centrifuge Modelling: A Study of Similarity." Geotechnical Testing Journal, GTJODJ, Vol. 12, No. 2, pp. 163-166.

Sastry, V.V.R.N., and Meyerhof, G.G., (1990), "Behaviour of Flexible Piles Under Inclined Loads." Canadian Geotechnical Journal, Vol. 27, pp. 19-28.

Sharnouby, B.E., and Novak, M., (1986), "Flexibility Coefficients and Interaction Factors for Pile Group Analysis." Canadian Geotechnical Journal, Vol. 23, pp. 441-450.

Shen, C.K., Bang, S., Desalvatore, M., and Poran, C.J., (1988), "Laterally loaded Cast-in-Drilled-Hole Piles." Transportation Research Record, No. 1191, pp. 155-165.

Spillers, W.R., and Stoll, R.D., (1964), "Lateral Response of Piles." Journal of the Soil Mechanics and Foundations Division, Vol. 90, No. SM6, pp. 1-9.

Steenfelt, J.S.S., (1989), "Centrifugal Modelling and Limit Analysis-Reciprocity or Adversity?" Proceedings of the 12th International Conference of SMFE, Rio de Jeneiro, Vol. 2, pp. 987-990.

Terashi, M., Kitazume, M., and Kawabata, K., (1989), "Centrifuge Modelling of a Laterally Loaded Pile." Proceedings of the 12th International Conference of SMFE, Rio de Jenerio, Vol. 2, pp. 991-994.

Tuen Mun LRT, (1986), "Report on Foundation Design for Overhead Catenary System." Interim Report, BBPCL.

Vaziri, H., and Han, Y., (1993), "Impedance Functions of Piles in Inhomogeneous Media." Journal of Geotechnical Engineering, ASCE, Vol. 119, No. 9. pp. 1414-1430.

Wang, M., and Liao, W.P., (1987), "Active Length of Laterally Loaded Piles." Journal of Geotechnical Engineering, ASCE, Vol. 113, No. 9, pp. 1044-1048.

Yuanxun, F., and Sijing, W., (1979), "On the Application of an Interpolation Matrix for Computation of Stresses in Finite Elements." Third Int. Conference on Numerical Methods in Geomechanics, Aachen, pp. 1273-1280.

Yukio Yoshii et al, (1989), "Prediction of Horizontal Behaviour of Pier Foundations." Proceedings of the International Symposium on Computer and Physical Modelling in Geotechnical Engineering, Bangkok, pp. 149-159.

APPENDIX A

A CONSTANT MODULUS APPROACH FOR A LATERALLY LOADED SHORT RIGID PIER IN CLAY

In this approach tensile stresses on the front and back of the pier are neglected on the assumption that the depth of pier is smaller than the height of tension cracks. It is assumed however that its weight is sufficient to prevent tension on the underside.

Figure A.1 shows corner displacement components due to the rotation of pier.

For small rotations, the displacement components of point O are

$$\Delta x_O = r_O \, \Theta \sin \alpha_O = (1 - \epsilon) \, D \, \Theta$$

$$\Delta y_O = r_O \, \Theta \cos \alpha_O = \frac{B}{2} \, \Theta$$

Similarly

$$\Delta x_P = (1 - \epsilon) \, D \, \Theta$$

$$\Delta y_P = \frac{B}{2} \, \Theta$$

and

$$\Delta x_Q = \Delta x_R = \epsilon \, D \, \Theta$$

$$\Delta y_Q = \Delta y_R = \frac{B}{2} \, \Theta$$

where

D = depth of pier

B = breadth of pier

ε = ratio of the depth of pivot point from ground level to pier depth

Θ = rotation angle

For a constant modulus of subgrade reaction, the forces and soil reactions on the pier are as shown in figure A.2.

To satisfy moment equilibrium about the point of rotation C:-

$$\frac{1}{3}\left(\epsilon^3 D^3 k \Theta + (1 - \epsilon)^3 D^3 k \Theta\right) + \frac{2}{3}\left(\frac{B}{2}\right)^3 k \Theta = F(L + \epsilon D)$$

∴

$$k \Theta \left(\frac{1}{3}(1 - 3\epsilon + 3\epsilon^2) D^3 + \frac{2}{3}\left(\frac{B}{2}\right)^3 \right) = F(L + \epsilon D) \qquad \text{(A.1)}$$

where k = Kb

K = soil modulus (in units of force/length^3)

b = width of pier perpendicular to B

F = lateral load

L = height of load above ground

To satisfy horizontal equilibrium:-

$$\frac{1}{2}\left(\epsilon^2 D^2 - (1-\epsilon)^2 D^2\right) k\,\Theta = F$$

$\therefore$

$$\frac{1}{2}(2\epsilon - 1) D^2 k\,\Theta = F \qquad \text{(A.2)}$$

Multiplying equation (A.2) by εD and subtracting it from equation (A.1):-

$$\begin{aligned} \frac{F L}{k\,\Theta} &= \left(\frac{1}{3}(1 - 3\epsilon + 3\epsilon^2) - \frac{1}{2}(2\epsilon^2 - \epsilon)\right) D^3 + \frac{2}{3}\left(\frac{B}{2}\right)^3 \\ &= \left(\frac{1}{3} - \frac{\epsilon}{2}\right) D^3 + \frac{2}{3}\left(\frac{B}{2}\right)^3 \end{aligned} \qquad \text{(A.3)}$$

From equations (A.2) and (A.3):-

$$\frac{1}{2}(2\epsilon - 1) L D^2 = \left(\frac{1}{3} - \frac{\epsilon}{2}\right) D^3 + \frac{2}{3}\left(\frac{B}{2}\right)^3$$

$$\therefore \qquad (6\epsilon - 3)\frac{L}{D} - (2 - 3\epsilon) = \frac{1}{2}\left(\frac{B}{D}\right)^3$$

$\therefore$

$$\epsilon = \frac{\left(\frac{B}{D}\right)^3 + 6\left(\frac{L}{D}\right) + 4}{12\left(\frac{L}{D}\right) + 6} \qquad \text{(A.4)}$$

When B=0, equation (A.4) gives

$$\epsilon = \frac{3\left(\frac{L}{D}\right) + 2}{6\left(\frac{L}{D}\right) + 3}$$

From equations (A.2) and (A.4)

$$\frac{F\,L}{k\,\Theta} = \frac{1}{2}\,(\,2\epsilon - 1\,)\,L\,D^2$$

$$= \frac{1}{2}\left(2\left(\frac{\left(\frac{B}{D}\right)^3 + 6\left(\frac{L}{D}\right) + 4}{12\left(\frac{L}{D}\right) + 6}\right) - 1\right)L\,D^2$$

Hence the moment at ground level, M = F L, is given by

$$\frac{M}{k\,\Theta} = \frac{B^3 + D^3}{12 + 6\,(D/L)} \qquad \text{(A.5)}$$

Over a practical range of D from 0 to 2.4m, with L=6m, the denominator varies from 12 to 14.4. Therefore this model indicates that the moment for a given rotation should increase with the cube of B or D.

(When B=0, equation (A.5) gives

$$\frac{M}{k\,\Theta} = \frac{D^3}{12 + 6\,(D/L)}$$

which when L/D is large becomes

$$\frac{M}{k\,\Theta} = \frac{D^3}{12} \quad)$$

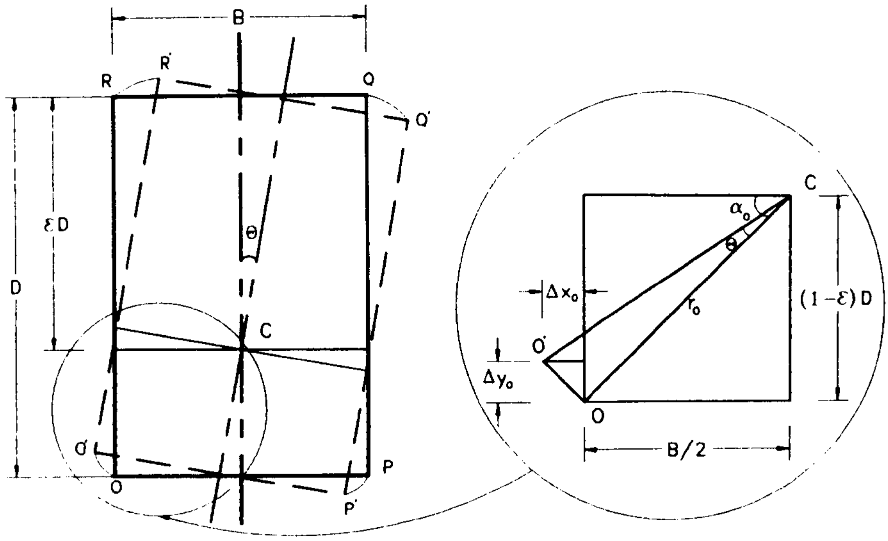

Figure A.1 Corner Displacement Components due to Rotation of a Pier.

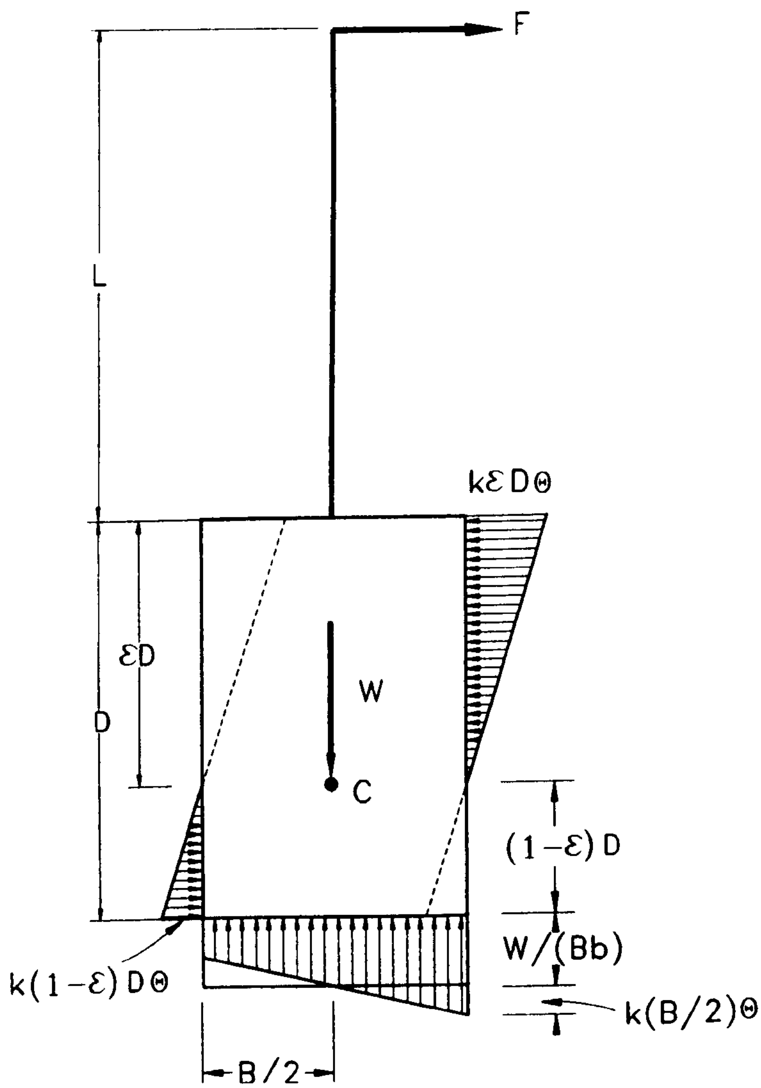

Figure A.2 Forces and soil reactions on pier

APPENDIX B

CALIBRATIONS FOR LOAD CELLS AND DISPLACEMENT TRANSDUCERS

A total number of two load cells and five conductive plastic linear potentiometers (transducers), with different load and displacement capacities were used in the tests (conventional and centrifugal model tests).

B.1 Load Cell Calibrations for the Conventional Tests

A 250 lb SENSOTEC (model 31) load cell was used to obtain readings in conventional tests. The load cell was calibrated in tension against a standard pre-calibrated proving ring with the aid of a load frame. The calibration factor of the proving ring was 1 div. = 5.854 N. During the calibration, the load cell was loaded up to about 1.171kN (=200 division of the proving ring) and readings were taken from the display unit in milli-volts. Two sets of readings were taken, one during loading and one during un-loading of the load cell and the average values of the readings were used in calculations. These are shown in table B.1 together with the corresponding load values. The proving ring readings were then plotted against the load cell readings to obtain the calibration value of the load cell as shown in figure B.1. The value of calibration factor was obtained as $1.84\text{x}10^{-2}$ kN/mV.

Division of Proving Ring	Load (kN)	Average Reading (mV)
0	0.000	0.333
20	0.117	6.441
40	0.234	12.690
60	0.351	19.076
80	0.468	25.320
100	0.585	31.583
120	0.702	38.365
140	0.820	44.752
160	0.937	51.243
180	1.054	57.393
200	1.171	63.599

Table B.1 Calibration Readings of a 250 lb Capacity Load Cell.

B.2 Calibration of Displacement Transducers for the Conventional Tests

Two SAKAI conductive plastic linear potentiometers (transducers) were used in this work to determine the rotation of the pier. These were calibrated independently with the aid of an inch micrometer. The readings in milli-volts for every 2.54mm increments up to 25.4mm were recorded using a data logger. The first 10 readings of each linear potentiometer were recorded during the increasing movement of the micrometer screw gauge while the second set of readings were taken when the micrometer was unscrewed back to the normal position. The average values of readings are shown in table B.2. Plots of the results showed linear relationships from which the calibration factors were obtained. These plots are shown in figure B.2. The values of calibration factors were obtained as 1.489×10^{-3} and 1.483×10^{-3} mm/mV. for top and bottom displacement transducers, respectively.

Distance Travel (ins)	Distance Travel (mm)	Average Reading (mV)	
		Bottom Transd.	Top Transd.
0.0	0.00	18802.0	18446.0
0.1	2.54	17089.0	16709.0
0.2	5.08	15341.0	14946.9
0.3	7.62	13599.0	13201.1
0.4	10.16	11864.6	11486.6
0.5	12.70	10167.4	9803.3
0.6	15.24	8488.6	8126.7
0.7	17.78	6775.1	6436.1
0.8	20.32	5071.9	4726.2
0.9	22.86	3369.8	3033.0
1.0	25.40	1665.34	1374.2

Table B.2 Calibration Readings of Displacement Transducers for Conventional Tests.

B.3 Load Cell Calibrations for the Centrifuge Tests

A 1500 lb SENSOTEC load cell was used to obtain readings in centrifuge tests. The calibration of this load cell was carried out in a similar manner to the calibration of the load cell used in the conventional test. However, load cell readings were recorded here for every 50 division of the proving ring up to the value of 500 division. The readings from the calibration tests are given in table B.3 together with the corresponding load values. The proving ring readings were plotted against the load cell readings to obtain the calibration value of the load cell. This plot is shown in figure B.3. The value of calibration factor was obtained as 0.109929 kN/mV.

Division of Proving Ring	Load (kN)	Average Reading (mV)
0	0.000	-0.227
50	0.293	2.321
100	0.585	4.987
150	0.878	7.673
200	1.171	10.368
250	1.464	12.975
300	1.756	15.523
350	2.049	18.209
400	2.342	20.905
450	2.634	23.729
500	2.927	26.424

Table B.3 Calibration Readings of a 1500 lb Capacity Load Cell.

B.4 Calibration of Displacement Transducers for the Centrifuge Tests

Three SAKAI conductive plastic linear potentiometers (transducers) were used in the centrifuge model tests. These were calibrated following the procedure described in section B.2. The average values of readings are shown in table B.4. Plots of the results showed linear relationships from which the calibration factors were obtained. These plots are shown in figure B.4. The values of calibration factors were obtained as 1.475×10^{-3}, 1.479×10^{-3} and 1.481×10^{-3} kN/mV. for top, middle and bottom displacement transducers, respectively.

Distance Travel (ins)	Distance Travel (mm)	Average Reading (mV)		
		Top Transd.	Middle Transd.	Bottom Transd.
0.0	0.00	19291.0	19309.5	19315.0
0.1	2.54	17638.0	17679.5	17637.5
0.2	5.08	15998.8	16022.8	15917.5
0.3	7.62	14301.2	14304.0	14152.6
0.4	10.16	12607.9	12537.2	12465.7
0.5	12.70	10855.0	10785.4	10705.8
0.6	15.24	9139.4	9029.3	8939.3
0.7	17.78	7370.0	7313.1	7213.6
0.8	20.32	5593.4	5596.6	5516.5
0.9	22.86	3831.6	3863.8	3835.1
1.0	25.40	2074.8	2132.4	2161.6

Table B.4 Calibration Readings of Displacement Transducers for Centrifuge Tests.

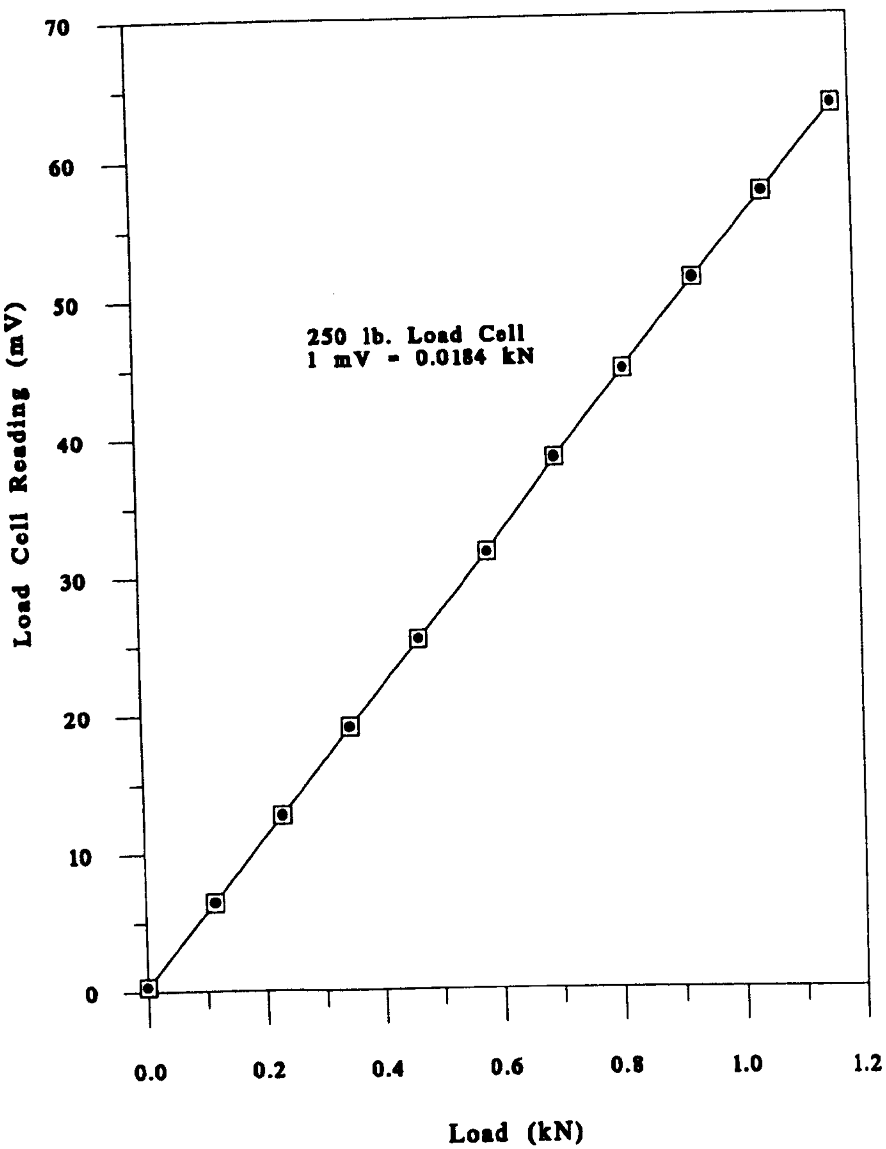

Figure B.1 Calibration of Load Cell for Conventional Tests.

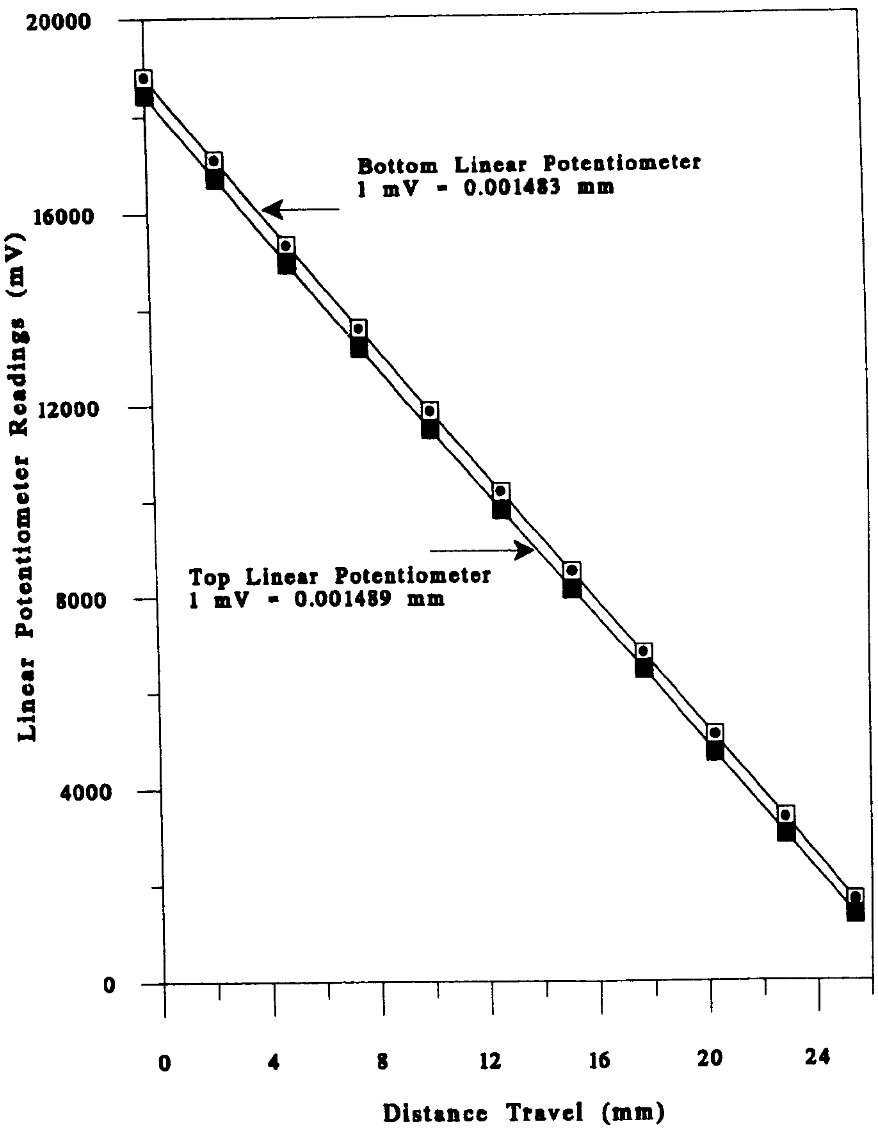

Figure B.2 Calibrations of Displacement Transducers for Conventional Tests.

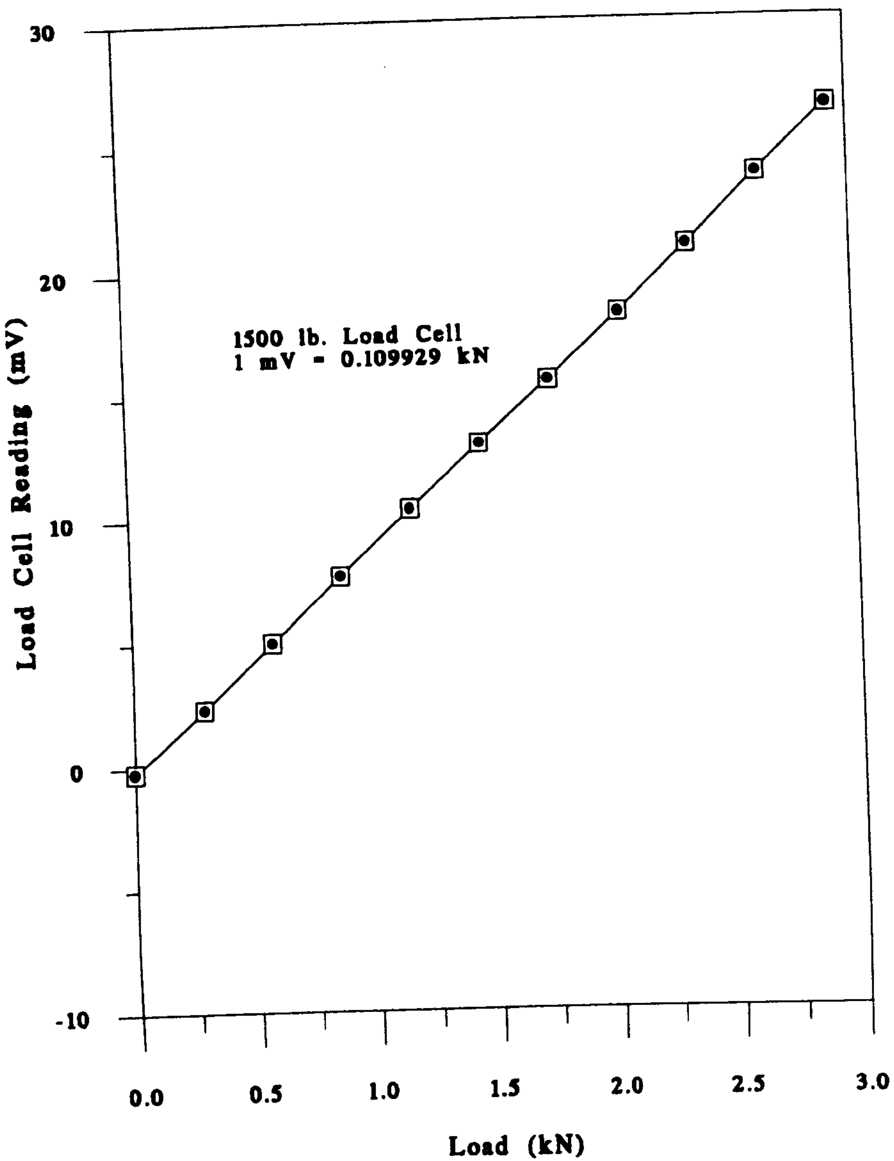

Figure B.3 Calibration of Load Cell for Centrifugal Tests.

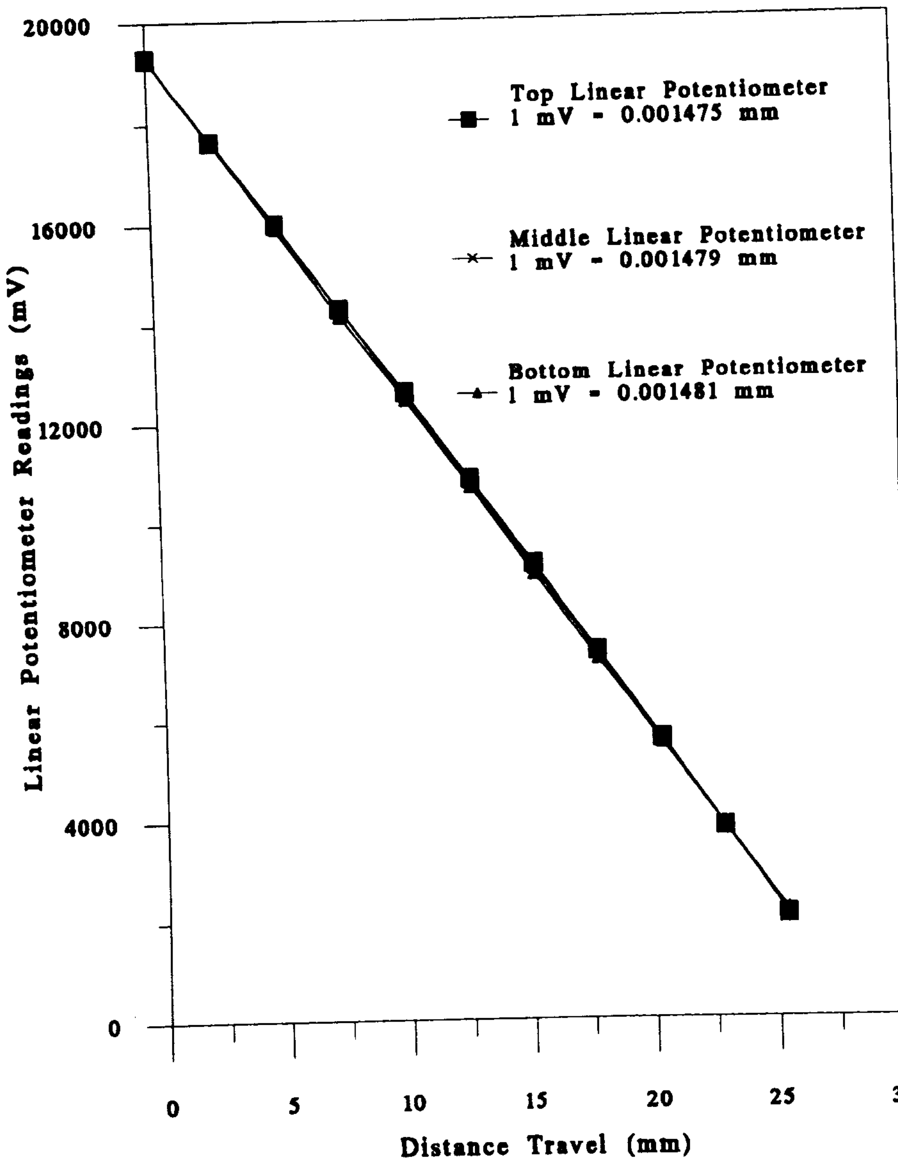

Figure B.4 Calibrations of Displacement Transducers for Centrifugal Tests.

APPENDIX C

COMPUTER PROGRAMS TO RUN THE TESTS AND PROCESS THE RESULTS

Computer programs to read data from data logger during the tests (ROT2), subsequently to convert these data to ASCII format (MODEL1) and finally to analyze them (LAM2) were used in this study. Listing of the computer programs is presented together with sample data.

C.1 Program ROT2

This program was used for the centrifugal tests as listed in the following section. In order to use it for the conventional tests some alterations were made. Lines 211, 220, 230, 921, 930, 940, 1151, 1451, 1581, 1590, 1600, 1781, 2321, 2330 and 2340 were deleted and lines 100, 440, 650, 710, 720, 730, 740, 1190, 1200, 1280, 2500 and 2560 were changed to the following:

```
100 DIMZ(200,4),x1(200),x3(200),x4(200),y(200),sload(200),temp(200):ZZ=1:length=215
440 PRINT"    CELL     TOP        BOTTOM         ROTATION"
650 PRINTload"   "top_deflection"   "bottom_deflection"        "rotation"     "count
710 DATA "CH 41 SE 645"
720 DATA "CH 43-45 SE 685"
730 DATA "TA 1 OP ME TR TI DE 0 CO * RE IN IN 20"
740 DATA "TA 1 CH 41,43,45 AT F LO EV FO CO MA VA TO GP"
1190 PRINT"    MODEL     TOP     BOTTOM       TOTAL       TOP      BOTTOM"
1200 PRINT"     LOAD     DEF.    DEF.         RESISTANCE    DISP.    DISP. "
1280 PRINTload,top_deflection,bottom_deflection, rotation"        "STR$(I)
2500 resistance=load*g*g:top_displacement=top_deflection*g:bottom_displacement=bottom_deflection*g
2560 INPUT#ZO%,width,piledepht,DA$,LCAL,D1CAL,D3CAL,datum,spacing,position
```

Program list

```
10 REM***************************************************************************************
20 REM************** MOMENT CARRYING CAPACITY OF SHORT PIER FOUNDATIONS ******************
40 REM***************************************************************************************
50 ON ERROR GOTO1810
60 CLOSE#0
70 *INITIALISE
```

```
80 MODE128
90 @%=&2030A
100 DIMZ(200,4),x1(200),x2(200),x3(200),y(200),sload(200),temp(200):ZZ=1:length=215
110 *STYLE CL
120 PROCInitialise
130 IF FF=1 THEN T=1000:GOTO860
140 DA$=TIME$
150 PROCTest_no
160 PO%=OPENOUT(TN$)
170 PRINT#PO%,width
180 PRINT#PO%,piledepht
190 PRINT#PO%,DA$
200 PRINT#PO%,LCAL
210 PRINT#PO%,D1CAL
211 PRINT#PO%,D2CAL
212 PRINT#PO%,D3CAL
213 PRINT#PO%,datum
214 PRINT#PO%,spacing
215 PRINT#PO%,position
220 PRINT#PO%,SPEED
230 PRINT#PO%,g
255 :
260 *IEEE
270 T=0:CO=0
280 cmd%=OPENIN("COMMAND")
290 data%=OPENIN("DATA")
300 PRINT#cmd%,"BBC DEVICE NO",0
310 PRINT#cmd%,"CLEAR"
320 Endtime=TIME + 400
330 REPEAT UNTIL TIME>Endtime
340 PRINT#cmd%,"REMOTE ENABLE"
350 PRINT#cmd%,"LOCAL LOCKOUT"
360 PRINT#cmd%,"END OF STRING",CHR$(13)
370 orion%=OPENIN("16")
380 PRINT#cmd%,"UNLISTEN"
390 PRINT#cmd%,"LISTEN",orion%,"EXECUTE"
400 RESTORE700
405 :
410 CLS
420 DA$=TIME$:PRINTTIME$:PRINT:PRINT"TEST NO. "TN$:PRINT
430 PRINT"     LOAD              DEFLECTION"
440 PRINT"     CELL      TOP       MIDDLE       BOTTOM"
450 PRINT"-------------------------------------------"
460 VDU28,0,26,79,5
470 READ task$
480 IF task$="END"THEN 510
490 PRINT#data%,task$
500 GOTO470
510 PRINT#cmd%,"UNLISTEN"
520 IF INKEY(-33)THENPROCSend_command
530 IF INKEY(-117)THENSOUND1,-15,53,2:GOTO390
540 IF INKEY(-120)THENSOUND1,-15,53,2:PROCTerminate:GOTO850
550 PRINT#cmd%,"STATUS"
560 INPUT#cmd%,state%
570 IF (state% AND 32)<>32 THEN GOTO670
580 PROCSerial_poll
590 IF (ASC(orionstatus$)AND 64)<>64 THEN690
600 PROCCollect_data
610 IF LEFT$(oriondata$,1)<>"C"  THEN 520
620 OD$=MID$(oriondata$,6,8)+MID$(oriondata$,26,8)+MID$(oriondata$,46,8)+MID$ (oriondata$,66,8)
630 reading$=OD$
640 T=T+1:count=T:I=T:PROCCrunch
650 PRINTload"  "top_deflection"  "middle_deflection"        "bottom_deflection"  "count
660 PROCDump
670 GOTO520
680 :
690 PRINT"Request not from ORION":PROCTerminate
```

```
700 DATA "HA"
710 DATA "CH 1 SE 645"
720 DATA "CH 21-25 SE 685"
730 DATA "TA 1 OP ME TR TI DE 0 CO * RE IN IN 15"
740 DATA "TA 1 CH 1,21,23,25 AT F LO EV FO CO MA VA TO GP"
750 DATA "MO OF"
760 DATA "RU"
770 DATA "END"
780 :
790 DEFPROCDump
800 *ADFS
810 PRINT#PO%,reading$
820 *IEEE
830 ENDPROC
840 :
850 *ADFS
860 CLOSE#0:ZO%=OPENIN(TN$)
870 VDU26
880 INPUT#ZO%,width:DM$=STR$(width)
890 INPUT#ZO%,piledepht:pw$=STR$(piledepht)
900 INPUT#ZO%,DA$
910 INPUT#ZO%,LCAL:L$=STR$(LCAL)
920 INPUT#ZO%,D1CAL:D1$=STR$(D1CAL)
921 INPUT#ZO%,D2CAL:D2$=STR$(D2CAL)
922 INPUT#ZO%,D3CAL:D3$=STR$(D3CAL)
923 INPUT#ZO%,datum
924 INPUT#ZO%,spacing
925 INPUT#ZO%,position
930 INPUT#ZO%,SPEED
940 INPUT#ZO%,g
970 PROCCheck
980 :
990 VDU2
995 PRINT
1000 PRINT"DATE OF TEST    = ";DA$;
1010 PRINT "        TEST NO.  = ";
1020 *STYLE N
1030 PRINTTN$
1040 *STYLE XN
1050 PRINT STRING$(96,"-")
1060 PRINT
1090 PRINT"                                   PILE          WIDTH       = ";Width
1100 PRINT"                                  DEPTH    OF     PILE        = ";piledepht
1110 PRINT"                               SPEED OF          ROTATION      = ";SPEED
1120 PRINT"                             GRAVITATIONAL       FORCE       = ";g
1122 PRINT"           SPACING OF DISPLACENT TRANSDUCERS       (mms.)                =";spacing
1123 PRINT"     POSITION OF LOAD CELL (ABOVE CLAY LEVEL)      (mms.)                  =";datum
1124 PRINT"        BOTTOM DISP. TRANS. FROM DATUM LEVEL       (mms.)                ="position
1130 PRINT:PRINT
1140 PRINT"             LOAD CELL CALIBRATION FACTOR (         KN/DIV )       = "L$
1150 PRINT"   TOP DISPLACEMENT TRANSDUCER CAL.  FACTOR         (mm/DIV)              ="D1$
1151 PRINT"MIDDLE DISPLACEMENT TRANSDUCER CAL.  FACTOR         (mm/DIV)             ="D2$
1152 PRINT"BOTTOM DISPLACEMENT TRANSDUCER CAL.  FACTOR         (mm/DIV)            = "D3$
1160 PRINT:PRINT
1170 @%=&2030C
1180 PRINT"                 MODEL TEST RESULTS
PROTOTYPE TEST RESULTS":PRINT
1190 PRINT"     MODEL     TOP      MIDDLE      BOTTOM       TOTAL       TOP      MIDDLE        BOTTOM"
1200 PRINT"      LOAD        DEF.       DEF.       DEF.      RESISTANCE   DISP.       DISP.      DISP. "
1210 *UNDERLINE ON
1220 PRINT"       KN.            mms.          KN.          mms.                  "
1230 *UNDERLINE OFF
1240 Z$="":X=0:Z=0
1250 v=0
1260 FORI=1TOT
1270 INPUT#ZO%,A$:reading$=A$:PROCCrunch:PROCPrototype
1280 PRINTload,top_deflection,middle_deflection,bottom_         deflection ,"
```

```
",resistance,top_displacement,middle_      displacement,bottom_displacement"          "STR$(I)
1290 NEXTI
1300 PRINT
1310 CLOSE#ZO%
1320 *PCODE 12
1330 *INITIALISE
1340 VDU3
1350 PROCGraph
1360 *PCODE 12
1370 PROCPlotmate
1380 END
1390 :
1400 DEFPROCCheck
1410 CLS:PRINT"HERE ARE THE LIST OF CALIBRATIONS:"
1420 PRINT"1. WIDTH OF PILE                                            = ";DM$
1430 PRINT"2. DEPTH OF PILE                                             = ";pw$
1440 PRINT"3. LOAD CELL CALIBRATION                          =        ";L$
1450 PRINT"4. TOP DISPLACEMENT TRANSDUCER CALIBRATION        =        ";D1$
1451 PRINT"5. MIDDLE DISPLACEMENT TRANSDUCER CALIBRATION     =        ";D2$
1452 PRINT"6. BOTTOM DISPLACEMENT TRANSDUCER CALIBRATION     =        ";D3$
1453 PRINT"7. SPACING OF DISPLACEMENT TRANSDUCERS            =        ";spacing
1454 PRINT"8. POSITION OF LOAD CELL (ABOVE CLAY LEVEL)      (mms.) = ";datum
1455 PRINT"9. BOTTOM DISP. TRANS. FROM DATUM LEVEL ( mms.)      =       ";position
1460 PRINT"10.SPEED OF ROTATION (r.p.m.)                       =       ";SPEED
1470 PRINT"11.GRAVITY FIELD                                    =       ";g
1500 PRINT:PRINT:PRINT"ARE THESE O.K ?";:INPUT A$
1510 IFA$="Y"THENGOTO1630
1520 INPUT "ENTER THE LINE NO. TO BE ALTERED";N
1530 IFN>12 OR N<0 THEN 1520
1540 ON N GOTO 1550,1560,1570,1580,1581,1582,1583,1584,1585,1590,1600,1610
1550 INPUT"WIDTH OF PILE =                 ";width:DM$=STR$(width): GOTO1410
1560 INPUT"DEPTH OF PILE + TIE BAR =    ";piledepht:pw$=STR$(piledepht):GOTO1410
1570 INPUT"LOAD CELL CALIBRATION =";LCAL:L$=STR$(LCAL): GOTO1410
1580 INPUT"TOP DISPLACEMENT TRANSDUCER CALIBRATION =
";D1CAL:D1$=STR$(D1CAL):GOTO1410
1581 INPUT"MIDDLE DISPLACEMENT TRANSDUCER CALIBRATION =
";D2CAL:D2$=STR$(D2CAL):GOTO1410
1582 INPUT"BOTTOM DISPLACEMENT TRANSDUCER CALIBRATION =
";D3CAL:D3$=STR$(D3CAL):GOTO1410
1583 INPUT" SPACING OF DISPLACEMENT TRANSDUCERS                 =
";spacing:GOTO1410
1584 INPUT" POSITION OF LOAD CELL (ABOVE CLAY LEVEL) (mms.)      =
";datum:GOTO1410
1585 INPUT" BOTTOM DISP. TRANS. FROM DATUM LEVEL ( mms.)        =
";position:GOTO1410
1590 INPUT"SPEED OF ROTATION (r.p.m.)                 =          ";SPEED: GOTO1410
1600 INPUT"GRAVITY FIELD                              =          ";g:GOTO1410
1623 GOTO1410
1630 CLS:ENDPROC
1640 :
1650 DEFPROCInitialise
1660 CLS:PRINT"Do you wish to read an existing test file          (Y/N)";:INPUT A$
1670 IFA$="Y"THENFF=1:GOTO1680 ELSE FF=0:GOTO1700
1680 *CAT
1690 PRINT"INPUT TEST NO.";:INPUT TN$
1700 ENDPROC
1710 :
1720 DEFPROCCrunch
1730 Q=1
1740 FORY=1TO4:Z(I,Y)=VAL(MID$(reading$,Q,8))
1750   Q=Q+8
1760 NEXTY
1770 load=(Z(I,1)-Z(1,1))*VAL(L$):y(I)=load
1780 top_deflection=(Z(I,2)-Z(1,2))*VAL(D1$)*-1:x1(I)= top_      deflection
1781 middle_deflection=(Z(I,3)-Z(1,3))*VAL(D2$)*-1:x2(I)=mi       ddle_deflection
1782 bottom_deflection=(Z(I,4)-Z(1,4))*VAL(D3$)*-1:x3(I)=bo       ttom_deflection
1790 ENDPROC
```

```
1800 :
1810 IF ERR =6 THEN count=I-1:GOTO1300
1820 PRINT"ERROR NO. =";ERR;" AT LINE NO. ";ERL
1830 VDU3:END
1840 :
1970 DEF PROCSerial_poll
1980 PRINT#cmd%,"SERIAL POLL",orion%,1
1990 INPUT#cmd%,orionstatus$
2000 ENDPROC
2010 :
2020 DEF PROCCollect_data
2030 PRINT#cmd%,"TALK",orion%
2040 INPUT#data%,oriondata$
2050 PRINT#cmd%,"UNTALK"
2060 length=LEN(oriondata$)
2070 oriondata$=LEFT$(oriondata$,length-1)
2080 ENDPROC
2090 :
2100 DEF PROCSend_command
2110 SOUND1,-15,53,2
2120 INPUT LINE "Enter Command : "command$
2130 IF command$=""THEN910
2140 PRINT#cmd%,"LISTEN",orion%,"EXECUTE"
2150 PRINT#data%,command$
2160 PRINT#cmd%,"UNLISTEN"
2170 ENDPROC
2180 :
2190 DEF PROCTerminate
2200 PRINT"Prog terminated"
2210 PRINT#cmd%,"LISTEN",orion%,"EXECUTE"
2220 PRINT#data%,"HA"
2230 PRINT#cmd%,"UNLISTEN"
2240 PRINT#cmd%,"REMOTE DISABLE"
2250 ENDPROC
2260 :
2270 DEF PROCTest_no
2280 CLS:INPUT "TEST NO = ";TN$
2290 INPUT"WIDTH OF PILE                              =          ";width:DM$=STR$(width)
2300 INPUT"DEPTH OF PILE                                =        ";piledepht:pw$=STR$(piledepht)
2310 INPUT"LOAD CELL CALIBRATION                        =                 ";LCAL:L$=STR$(LCAL)
2320 INPUT"TOP DISPLACEMENT TRANSDUCER CALIBRATION =                           ";D1CAL:D1$=STR$(D1CAL)
2321 INPUT"MIDDLE DISPLACEMENT TRANSDUCER CALIBRATION =                        ";D2CAL:D2$=STR$(D2CAL)
2322 INPUT"BOTTOM DISPLACEMENT TRANSDUCER CALIBRATION =                        ";D3CAL:D3$=STR$(D3CAL)
2323 INPUT"SPACING OF DISPLACENT TRANSDUCERS (mms.) =          ";spacing
2324 INPUT"POSITION OF LOAD CELL (ABOVE CLAY LEVEL) (mms.)      = ";datum
2325 INPUT"BOTTOM DISP. TRANS. FROM DATUM LEVEL ( mms.) =       "position
2330 INPUT"SPEED OF ROTATION (r.p.m.)               = ";SPEED
2340 INPUT"GRAVITY FIELD                            = ";g
2370 PROCCheck
2380 ENDPROC
2390 :
2400 DEF PROCSort
2410 Q=1
2420 FORY=1TO8:Z(I,Y)=VAL(MID$(A$,Q,8)):PRINTZ(I,Y);
2430   Q=Q+8
2440 NEXTY
2450 PRINT
2460 A$=""
2470 ENDPROC
2480 :
2490 DEFPROCPrototype
2500   resistance=load*g*g:top_displacement=top_deflection*g:middle_displacement
middle_deflection*g:bottom_displacement=bottom_deflection*g
2510 ENDPROC
2520 :
2530 DEFPROCRaw
2540 INPUT"TEST NO. = ";TN$
```

```
2550 ZO%=OPENIN(TN$)
2560 INPUT#ZO%,width,piledepht,DA$,LCAL,D1CAL,D2CAL,D3CAL,datum,spacing,position,          SPEED,g
2570 VDU2
2580 PRINTTN$,DA$:PRINT
2590 FORX=1TO1000
2600   INPUT#ZO%,A$
2610   PRINTSTR$(X),A$
2620 NEXTX
2630 CLOSE#0:*PCODE12:VDU3
2640 ENDPROC
2650 :
2660 DEFPROCGraph
2670 VDU23,1,0;0;0;0;:REM CURSOR OFF
2680 PROCChar
2690 X%=50:Y%=100
2700 CLS
2710 VDU29,150;150;
2720 MOVE0,800:DRAW0,0:DRAW1100,0:DRAW1100,800:DRAW0,800
2730 FORX=0TO1100 STEP50:MOVEX,8:DRAWX,0:NEXT
2740 FORX=0TO800 STEP50:MOVEX,800:DRAWX,792:NEXT
2750 MOVE800,800:DRAW800,700:DRAW1100,700
2760 VDU5:FORX=0TO1100STEP100:MOVEX-20,-30:X$=STR$(INT          (10*X/X%+.5)/10)
2770   IFLENX$<2 THENX$=X$+".0"
2780 PRINTX$:NEXT
2790 MOVE850,760:PRINTTN$
2800  FORY=0TO800  STEP  80:MOVE0,Y:DRAW  8,Y:MOVE-80,Y+10:PRINTLEFT$(STR$(INT
((1000*Y/Y%)*10+.5)/10),5):NEXT
2810 FORY=0TO640  STEP 80:MOVE1100,Y:DRAW 1092,Y:NEXT
2820 PRINT TAB(0,6):FORI=LEN(T$) TO 1 STEP-1:PRINTMID$          (T$,I,1):NEXT
2830 MOVE 400,-100:PRINT"PILE DISPLACEMENT mms."
2840 IFA$="M" THEN PROCSmooth ELSE PROCCurve
2850 A$=GET$:IFA$=""THEN 2850
2860 IFA$="D" THEN X%=X%*2:IF X%>200 THEN X%=X%/2:GOTO2700
2870 IFA$="D" THEN 2700
2880 IFA$="U" THEN X%=X%/2:IF X%<50  THEN X%=X%*2:GOTO2700
2890 IFA$="U" THEN 2700
2900 IFA$="L" THEN Y%=Y%*2:GOTO2700
2910 IFA$="S" THEN Y%=Y%/2:GOTO2700
2920 IFA$="M" THEN 2700
2930 IFA$="P"THENVDU2:PRINT:PRINT:PRINT:VDU3:*GDUMP 1 1 3       1 20
2940 VDU4
2950 VDU23,1,1;0;0;0;
2960 ENDPROC
2970 :
2980 DEFPROCChar
2990 VDU23,224,0,56,124,198,130,254,254,0: REM "D" SIDEWAYS
3000 VDU23,225,0,130,146,146,146,254,254,0:REM "E" SIDEWAYS
3010 VDU23,226,254,254,64,48,64,254,254,0: REM "M" SIDEWAYS
3020 VDU23,227,0,6,6,6,6,254,254,0:REM "L" SIDEWAYS
3030 VDU23,228,0,126,254,144,144,254,126,0:REM "A" SIDEWAYS
3040 VDU23,230,0,124,254,130,130,254,124,0:REM "O" SIDEWAYS
3050 VDU23,234,0,0,130,198,124,56,0,0:    REM "("  SIDEWAYS
3060 VDU23,235,0,34,54,28,8,254,254,0:    REM "k"  SIDEWAYS
3070 VDU23,236,0,30,62,32,32,62,62,0:    REM "n"  SIDEWAYS
3080 VDU23,240,0,0,0,3,3,0,0,0     :    REM "."  SIDEWAYS
3090 VDU23,231,0,254,254,28,112,254,254,0: REM "N" SIDEWAYS
3100 VDU23,242,0,0,56,124,198,130,0,0:    REM ")"  SIDEWAYS
3110 T$=CHR$(226)+CHR$(230)+CHR$(224)+CHR$(225)+CHR$(227)+" "
3120 T$=T$+CHR$(227)+CHR$(230)+CHR$(228)+CHR$(224)+" "
3130 T$=T$+CHR$(234)+CHR$(231)+CHR$(242)
3140 ENDPROC
3150 :
3160 DEFPROCCurve
3170 MOVE0,0
3180 FORX=1TOcount
3190   DRAWx1(X)*X%,y(X)*Y%
3200 NEXT
```

```
3201 MOVE0,0
3202 FORX=1TOcount
3203   DRAWx2(X)*X%,y(X)*Y%
3204 NEXT
3205 MOVE0,0
3206 FORX =1 TO count
3207   DRAWx3(X)*X%,y(X)*Y%
3208 NEXT
3210 ENDPROC
3220 :
3230 DEFPROCPlotmate
3240 CLS:PRINT"DO YOU WANT A PLOT OF PROTOTYPE LOAD AGAINST DISPLACEMENT(Y/N)"
3250 A$=GET$:IFA$=""THEN3250
3260 IFA$="N" THEN 3570
3270 IFA$="Y"THEN3300
3280 GOTO3250
3290 PRINT
3300 PRINT"PLEASE INSERT PEN AND PAPER INTO PLOTMATE AND PRESS RETURN WHEN        READY"
3310 A$=GET$:IFA$<>CHR$(13) THEN 3310
3320 PROCScales
3330 *PLTMATE
3340 VDU 23,255,0,0,0,0,0,0,0,64
3350 VDU29,500;200;
3360 MOVE0,0:DRAW0,1600:DRAW2000,1600:DRAW2000,0:DRAW0,0
3370 FORX=0TO2000 STEP100:MOVEX,10:DRAWX,0:NEXT
3380 FORX=0TO2000 STEP 200:MOVEX-40,-30:VDU5:PRINTSTR$(INT(X*X%/2000)):VDU4:         NEXT
3390 FORX=0TO1600 STEP100:MOVEX,1600:DRAWX,1590:NEXT
3400 MOVE1600,1600:DRAW1600,1400:DRAW2000,1400
3410 MOVE1700,1520:VDU5:PRINTTN$:VDU4
3420   FORY=0TO1600   STEP200:MOVE0,Y:DRAW   10,Y:MOVE-130,Y+15:VDU5:PRINTSTR$(INT
(Y*Y%/1600)):VDU4:NEXT
3430 FORY=0TO1600 STEP200:MOVE2000,Y:DRAW 1990,Y:NEXT
3440 MOVE 700,-100:VDU5:PRINT"PILE DISPLACEMENT mms.":VDU4
3450 MOVE -250,400:VDU5
3460 VDU23,255,5,6,0,2,0,0,0,64
3470 PRINT"PROTOTYPE LOAD kns."
3480 VDU 23,255,0,0,0,0,0,0,0,64
3490 VDU4
3500 MOVE0,0
3510 FORX=1TO count:
3520   DRAWg*x1(X)*2000/X%,g*g*y(X)*1600/Y%
3530 NEXT
3531 MOVE0,0
3532 FORX=1TO count:
3533   DRAWg*x2(X)*2000/X%,g*g*y(X)*1600/Y%
3534 NEXT
3535 MOVE0,0
3536 FORX=1TO count:
3537   DRAWg*x3(X)*2000/X%,g*g*y(X)*1600/Y%
3538 NEXT
3540 MOVE2000,0
3550 *PARK
3560 *OFFMATE
3570 ENDPROC
3580 :
3590 DEFPROCScales
3600 CLS:PRINT"CHOOSE MAXIMUM LOAD IN UNITS OF 800 ";:INPUT Y%
3610 PRINT:PRINT"CHOOSE MAXIMUM DISPLACEMENT IN UNITS OF 200";:INPUTX%
3620 CLS:PRINT"HERE ARE YOUR CHOSEN VALUES:":PRINT
3630 PRINT"         MAXIMUM LOAD ="Y%
3640 PRINT"MAXIMUM DISPLACEMENT ="X%
3650 PRINT:PRINT"ARE THESE OK?"
3660 A$=GET$:IFA$<>"Y"ANDA$<>"N"THEN3660
3670 IFA$="N" THEN 3600
3680 ENDPROC
3685 :
3690 DEFPROCSmooth
```

```
3700 FOR X =1 TO count:temp(X)=y(X):NEXT
3710 ZZ=1
3720 IF ZZ>=6 THEN 3790
3730 FORI=3 TO count-2
3740 sload(I)=.6*temp(I)+.15*(temp(I-1)+temp(I+1))+.05*(temp(I-2)+temp(I+2))
3750 NEXTI
3760 sload(1)=temp(1):sload(2)=temp(2):sload(count)=temp(count):sload(count-1)=        temp (count-1)
3770 FORX=1TO count:temp(X)=sload(X):NEXT
3780 ZZ=ZZ+1:GOTO3720
3790 MOVE0,0
3800 FORX= 1 TO count
3810   DRAWx(X)*X%,sload(X)*Y%
3820 NEXT
3830 ENDPROC
3835 :
3840 REM ENTER THE FOLLOWING LINES FOR DOTTED PRINT-OUT
3850 REM 965 GOTO1220
3860 REM 1250 REM
3870 REM 3100PLOT 69,x(X)*X%,y(X)*Y%
3880 REM 3430PLOT69,g*x(X)*2000/X%,g*g*y(X)*1600/Y%
3890 REM 1290REM
```

C.2 Program MODEL1

```
10  CLOSE#0
20  *INITIALISE
30  @%=&4040A
40  MODE128
50  DIM Z(200,4),TX(200),BX(200),LD(200),RT(200),DIF(200)
60  *STYLE CL
70  PROCName
80  PROCInput
90  PROCCrunch
100  PROCTransfer
110  END
120 :
130 DEFPROCName
160  *CAT
170  PRINT
180  INPUT"TEST NO. = ";TN$
190  INPUT"NUMBERS OF DATA";T
200  TT$="M"+TN$
210  PRINT"OUTPUT-FILE = ";TT$
220 ENDPROC
230 :
240 DEFPROCInput
250  ZO%=OPENIN(TN$)
260  INPUT#ZO%,width,piledepht,DA$,LCAL,D1CAL,D3CAL,datum,spacing,position,SPEED
270  FOR I=1 TO T
280       INPUT#ZO%,A$
290       Q=1
300       FOR Y=1 TO 4
310            Z(I,Y)=VAL(MID$(A$,Q,8))
320            Q=Q+8
330       NEXT Y
340  NEXT I
350  CLOSE#ZO%
360 ENDPROC
370 :
380 DEFPROCCrunch
390  FOR I=1 TO T
400       LD(I)=(Z(I,1)-Z(1,1))*LCAL
410       TX(I)=(Z(I,2)-Z(1,2))*D1CAL*(-1)
420       BX(I)=(Z(I,3)-Z(1,3))*D3CAL*(-1)
```

```
430        DIF(I)=TX(I)-BX(I)
440        RT(I)=DEG(ATN(DIF(I)/(spacing)))
450  NEXT I
460 ENDPROC
470 :
480 DEFPROCTransfer
500  PO%=OPENOUT(TT$)
510     L=37
520     :
530     WORD$="TEST NO."
540     PROCPrint
550     PROCSpace
560     WORD$="MODEL:" +TN$
570     PROCPrint
580     PROCReturn
590     :
600     WORD$="DATE OF TEST"
610     PROCPrint
620     PROCSpace
630     DA$=MID$(DA$,1,3)+"."+MID$(DA$,5,20)
640     WORD$=DA$
650     PROCPrint
660     PROCReturn
670     :
680     WORD$="WIDTH"
690     PROCPrint
700     PROCSpace
710     WORD$=STR$(width)
720     PROCPrint
730     PROCReturn
740     :
750 WORD$="PILE DEPTH"
760 PROCPrint
770 PROCSpace
780 WORD$=STR$(piledepht)
790 PROCPrint
800 PROCReturn
810 :
820     WORD$="POSITION OF LOAD CELL (ABOVE CLAY)"
830     PROCPrint
840     PROCSpace
850     WORD$=STR$(datum)
860     PROCPrint
870     PROCReturn
880     :
890     WORD$="BOTTOM DISP. TRANS. ABOVE LOAD CELL"
900     PROCPrint
910     PROCSpace
920     WORD$=STR$(position)
930     PROCPrint
940     PROCReturn
950     :
960     WORD$="SPACING OF TRANSDUCERS"
970     PROCPrint
980     PROCSpace
990     WORD$=STR$(spacing)
1000     PROCPrint
1010     PROCReturn
1020     :
1030     WORD$="SPEED OF ROTATION"
1040     PROCPrint
1050     PROCSpace
1060     WORD$=STR$(SPEED)
1070     PROCPrint
1080     PROCReturn
1090     :
1100     WORD$="LOAD CELL CAL. FACTOR (KN/DIV)"
```

```
1110     PROCPrint
1120     PROCSpace
1130     WORD$=STR$(LCAL)
1140     PROCPrint
1150     PROCReturn
1160     :
1170     WORD$="TOP TRANS. CAL. FACTOR (mm/DIV)"
1180     PROCPrint
1190     PROCSpace
1200     WORD$=STR$(D1CAL)
1210     PROCPrint
1220     PROCReturn
1230     :
1240     WORD$="BOT. TRANS. CAL. FACTOR (mm/DIV)"
1250     PROCPrint
1260     PROCSpace
1270     WORD$=STR$(D3CAL)
1280     PROCPrint
1290     PROCReturn
1300     :
1310  FOR I=1 TO T
1320        L=4   : WORD$=STR$(I)
1330        PROCPrint
1340        PROCSpace
1350        :
1360     L=16 : WORD$=STR$(RT(I))
1370     PROCPrint
1380     PROCSpace
1390     :
1400        WORD$=STR$(LD(I))
1410        PROCPrint
1420        PROCSpace
1430        :
1440        WORD$=STR$(TX(I))
1450        PROCPrint
1460        PROCSpace
1470        :
1480        WORD$=STR$(BX(I))
1490        PROCPrint
1500     PROCSpace
1510        :
1520        PROCReturn
1530        :
1540  NEXT I
1550  CLOSE#PO%
1560 ENDPROC
1570 :
1580 DEFPROCPrint
1590  FOR J=1 TO L
1600        NUMS=ASC(MID$(WORD$,J,1))
1610        IF ( NUMS = -1 ) THEN NUMS=32
1620        BPUT#PO%,NUMS
1630  NEXT J
1640 ENDPROC
1650 :
1660 DEFPROCSpace
1670      BPUT#PO%,32
1680      BPUT#PO%,32
1690 ENDPROC
1700 :
1710 DEFPROCReturn
1720  BPUT#PO%,10
1730  BPUT#PO%,13
1740 ENDPROC
1750 :
```

C.3 Program LAM2

```
C       PJ=PILE EMBEDDED LENGTH
C       PT=POINT OF ROTATION
        DIMENSION Y(200),THETA(200),DIFF(200)
        DIMENSION X(200),AD(200),PT(200)
        DIMENSION TX(200),REC(200),DISP(200),BX(200),MX(200),ox(200)
        DIMENSION YD(200),THETAD(200),DIFFD(200)
        DIMENSION XD(200),ALD(200),PTD(200),MM(200)
        DIMENSION TXD(200),RECD(200),DISPD(200),BXD(200),MXD(200)
        CHARACTER*72 DATAFN,OUTPF
        CHARACTER TITLE*72
        REAL TX,Y,X,DIFF,DISP,THETA
        REAL AD,PT,BX,MX,MM,ACI,ox
        REAL ALD,PTD,BXD,MXD
        REAL TXD,YD,XD,DIFFD,DISPD,THETAD
        INTEGER REC,RECD
        print *, 'ENTER THE NAME OF DATA FILE WITH PATH'
        read '(a)',DATAFN
        print *, 'ENTER THE NAME OF OUTPUT FILE WITH PATH'
        read '(a)',OUTPF
        open(5,file=datafn,status='old')
        open(6,file=outpf,status='new')
        READ (5,'(72A)')TITLE
        READ(5,*)E,BH,N,PJ,DDT
        TG=E+BH
        H=TG+DDT
c       WRITE(6,*)TITLE
c       WRITE(6,*)'==========='
        WRITE(6,*)
        WRITE(6,*)'        DEGREE  LOAD(KN)  MOM(KN.M)   DISPLACE(mm)    RATIO    (A/D)'
        DO 67 I=1,N
        READ(5,*)REC(I),X(I),Y(I),TX(I),ox(i),BX(I)
        THETA(I)=X(I)*3.141593/180
        MM(I)=Y(I)*E/1000
C*******************************************************************************************
C*************CALCULATION OF MOMENT, DISPLACEMENT AND PIVOT POINT DEPTH OF PIER***********
C*******************************************************************************************
         DIFF(I)=H*TAN(THETA(I))
C       IF(THETA(I).EQ.0.0)THETA(I)=1E-40
        DISP(I)=TX(I)-DIFF(I)
        ACI=TAN(THETA(I))
        IF(ACI.EQ.0.0)ACI=1E-30
        PT(I)=DISP(I)
        PT(I)=PT(I)/ACI
        AD(I)=PT(I)/PJ
        J=I
        WRITE(6,11)J,X(I),Y(I),MM(I),DISP(I),AD(I)
 11     FORMAT(i3,9X,F9.7,9X,F9.7,9X,F9.7,9X,F9.7,9X,F9.7,9X,F9.7)
 67      CONTINUE
C       WRITE(6,12)RECD(J),XD(J),YD(J),DISPD(J),ALD(J)
C12     FORMAT(1X,I5,2X,F12.7,3X,F12.7,3X,F12.7,2X,F12.7)
C68      CONTINUE
        STOP
        END
```

C.4 A Typical Output from Program MODEL1

```
TEST NO.                             MODEL:56RT2
DATE OF TEST                         Thu.11 Mar 1993.14:50:35
WIDTH                                50
PILE DEPTH                           60
POSITION OF LOAD CELL (ABOVE CLAY)     150
```

BOTTOM DISP. TRANS. ABOVE LOAD CELL	-110
SPACING OF TRANSDUCERS	50
LOAD CELL CAL. FACTOR (KN/DIV)	1.84E-2
TOP TRANS. CAL. FACTOR (mm/DIV)	1.489E-3
BOT. TRANS. CAL. FACTOR (mm/DIV)	1.483E-3

	Rotation	Load Cell	top_deflection	middle_deflection
1	0	0	0	0
2	0	1.913600001E-3	0	0
3	3.412484557E-4	4.857600004E-3	2.977954559E-4	0
4	9.213851416E-3	1.012E-2	8.040602272E-3	0
5	7.371762075E-2	1.672560001E-2	6.581379546E-2	1.483E-3
6	0.115999848	2.14544E-2	0.1323721023	3.1143E-2
7	0.1653257056	2.438E-2	0.2154582955	7.1184E-2
8	0.1971113664	2.647760001E-2	0.2906527955	0.11864
9	0.2333331418	2.809680001E-2	0.3697187046	0.166096
10	0.2755265215	2.894320001E-2	0.4539961023	0.213552
11	0.3028755022	2.98632E-2	0.5253191988	0.261008
12	0.3409597214	3.07832E-2	0.603045	0.305498
13	0.3771668219	3.159280002E-2	0.6791328979	0.349988
14	0.4072451231	3.242080001E-2	0.7528383979	0.397444
15	0.4408786563	3.313840002E-2	0.8237148013	0.438968
16	0.4774123365	3.404E-2	0.8971225002	0.480492
17	0.5126013495	3.490480001E-2	0.9738060001	0.5264649999
18	0.537246434	3.57144E-2	1.048702699	0.5798529999
19	0.5879052286	3.65424E-2	1.127024102	0.613962
20	0.610645493	3.72968E-2	1.194326898	0.661418
21	0.6449798753	3.80328E-2	1.270265898	0.7073910001
22	0.6753830533	3.88424E-2	1.341291199	0.7518809999
23	0.718417163	3.950480001E-2	1.424824102	0.797854
24	0.7524156873	4.027760001E-2	1.501954301	0.84531
25	0.7908422619	4.08664E-2	1.581466898	0.8912830001
26	0.8199337185	4.13632E-2	1.663213	0.9476369999
27	0.8471138943	4.19336E-2	1.735876199	0.996576
28	0.8944091159	4.2504E-2	1.823131603	1.042549
29	0.9408227131	4.305599999E-2	1.9036865	1.08259
30	0.9707303513	4.355279999E-2	1.978732103	1.131529
31	1.005584118	4.39944E-2	2.058095802	1.180468
32	1.032413428	4.45648E-2	2.128972199	1.227924
33	1.082923638	4.489599999E-2	2.214589699	1.269448
34	1.128649604	4.51168E-2	2.294549	1.309489
35	1.150046388	4.55216E-2	2.366616603	1.362877
36	1.187283799	4.59632E-2	2.448064898	1.411816
37	1.230994182	4.642320001E-2	2.533682398	1.459272
38	1.264818508	4.699359999E-2	2.612152699	1.508211
39	1.308185238	4.741679999E-2	2.697472398	1.555667
40	1.334524652	4.79504E-2	2.773858103	1.609055
41	1.381790472	4.830000001E-2	2.8581355	1.652062
42	1.401491576	4.875999999E-2	2.931692103	1.708416
43	1.449109492	4.91096E-2	3.019245301	1.754389
44	1.479858484	4.949599999E-2	3.095035398	1.803328
45	1.513362239	4.993759999E-2	3.179163898	1.858199
46	1.547342117	5.03056E-2	3.256294102	1.905655
47	1.581348384	5.08024E-2	3.339380302	1.959043
48	1.60767453	5.128079999E-2	3.414277	2.010948
49	1.662280014	5.15384E-2	3.509424102	2.058404
50	1.695757248	5.20536E-2	3.589085603	2.108826
51	1.741281762	5.253199999E-2	3.667407	2.147384
52	1.766806242	5.293680001E	3.753471199	2.211153
53	1.807084357	5.34336E-2	3.836110699	2.258609

54	1.841797651	5.382E-2	3.9272375	2.319412
55	1.879672468	5.428000001E-2	4.004814398	2.363902
56	1.921131658	5.47768E-2	4.0870072	2.409875
57	1.961395843	5.53104E-2	4.168157699	2.455848
58	1.992994167	5.58072E-2	4.247670302	2.507753
59	2.029880953	5.62304E-2	4.333287802	2.561141
60	2.076785547	5.656159999E-2	4.420245398	2.607114
61	2.106845782	5.70952E-2	4.498417899	2.659019
62	2.139317771	5.750000001E-2	4.584631002	2.716856
63	2.174473296	5.794160001E-2	4.664292501	2.765795
64	2.221539476	5.83832E-2	4.751399001	2.811768
65	2.254837738	5.87328E-2	4.833889604	2.865156
66	2.297483329	5.92296E-2	4.920102699	2.914095
67	2.332829081	5.978159999E-2	5.005869104	2.968966
68	2.363049235	6.0168E-2	5.084190501	3.020871
69	2.40857695	6.06096E-2	5.171445899	3.068327
70	2.439495641	6.08488E-2	5.254829898	3.124681
71	2.484173551	6.12352E-2	5.342829801	3.17362
72	2.517799773	6.16768E-2	5.4256182	3.227008
73	2.561096335	6.206319999E-2	5.509448899	3.272981
74	2.57841977	6.24864E-2	5.588365899	3.33675
75	2.616767517	6.305679999E-2	5.666389501	3.38124
76	2.66549873	6.347999998E-2	5.753496001	3.42573
77	2.698427469	6.39216E-2	5.834199801	3.477635
78	2.729509223	6.443680002E-2	5.919221699	3.535472
79	2.778074899	6.487840001E-2	6.009157302	3.582928
80	2.820352422	6.532000002E-2	6.096561603	3.63335
81	2.864526513	6.576159998E-2	6.191559803	3.689704
82	2.90203241	6.611119999E-2	6.274794899	3.740126
83	2.937847756	6.653440002E-2	6.359519001	3.793514
84	2.970271154	6.6884E-2	6.444243103	3.849868
85	3.013548408	6.719680002E-2	6.531051802	3.898807
86	3.050030225	6.754640001E-2	6.614882501	3.950712
87	3.091089404	6.795120001E-2	6.699755501	3.999651
88	3.127048713	6.819039999E-2	6.7816505	4.050073
89	3.162148163	6.854000001E-2	6.861312	4.099012
90	3.194870741	6.899999999E-2	6.940377899	4.149434
91	3.237095401	6.931279998E-2	7.023315201	4.195406999
92	3.264051257	6.969920002E-2	7.101785501	4.250278
93	3.30341337	7.01592E-2	7.189636501	4.303665999
94	3.34768999	7.0656E-2	7.278827604	4.354087999
95	3.396539674	7.107919999E-2	7.369061001	4.401543999
96	3.435564805	7.091360001E-2	7.459592201	4.457898
97	3.472029884	7.148399999E-2	7.546400899	4.512769001
98	3.514088023	7.190720001E-2	7.635145303	4.564673999
99	3.545610923	7.234879999E-2	7.716146899	4.618062001
100	3.580863996	7.275359999E-2	7.798935302	4.669966999
101	3.615271457	7.315839999E-2	7.882468199	4.723355001
102	3.650859008	7.354479999E-2	7.965554399	4.77526
103	3.693043238	7.396799998E-2	8.048491701	4.821233001
104	3.7237247	7.426240001E-2	8.133215804	4.879070001
105	3.772541353	7.455679998E-2	8.224938199	4.928009
106	3.807103834	7.41152E-2	8.308620002	4.981396999
107	3.846236071	7.444640002E-2	8.393344104	5.031819001
108	3.882137673	7.4888E-2	8.475239102	5.082241001
109	3.923973398	7.531119999E-2	8.560856603	5.13118
110	3.951079036	7.57712E-2	8.643942803	5.1905
111	3.980362998	7.6084E-2	8.7230087	5.243888
112	4.0181139	7.661760002E-2	8.805052605	5.292827001

113	4.047583371	7.705919998E-2	8.8887344	5.350663999
114	4.087399354	7.739039999E-2	8.980010103	5.407018
115	4.123789148	7.77768E-2	9.062351804	5.45744
116	4.159680098	7.820000002E-2	9.147224803	5.510828
117	4.193877477	7.851279998E-2	9.232097801	5.565699
118	4.237045318	7.888080002E-2	9.320395503	5.616121
119	4.272416813	7.912000001E-2	9.404821802	5.669508999
120	4.309325695	7.952480001E-2	9.4935662	5.725863
121	4.347906958	7.996639999E-2	9.579332605	5.777767999
122	4.385134066	8.027919999E-2	9.665396802	5.831156
123	4.422364302	8.068399999E-2	9.752950002	5.886027001
124	4.460269181	8.110720001E-2	9.841098804	5.940897999
125	4.493082788	8.125439999E-2	9.924780603	5.995769
126	4.541631838	8.147519999E-2	10.0156096	6.0439665
127	4.572576536	8.178800001E-2	10.098398	6.099579001
128	4.610457521	8.20088E-2	10.18476	6.152670398
129	4.65205265	8.23216E-2	10.2720154	6.203389
130	4.685012721	8.265280002E-2	10.3546549	6.257073602
131	4.728618292	8.298400001E-2	10.4405702	6.304677898
132	4.770558041	8.337039998E-2	10.5324415	6.359697202
133	4.804696945	8.372000002E-2	10.6170167	6.414271601
134	4.838822881	8.404160002E-2	10.6995073	6.466769798
135	4.877887832	8.437999998E-2	10.7928676	6.525793202
136	4.904738808	8.470079999E-2	10.8723802	6.581702298
137	4.942414574	8.5032E-2	10.9587422	6.634942001
138	4.976032771	8.538719999E-2	11.043913	6.6905545
139	5.011669202	8.5724E-2	11.12863711	6.743942499

C.5 A Typical Output from Program LAM2

	DEGREE	LOAD(KN)	MOM(KN.M)	DISPLACE(mm)	RATIO(A/D)
1	0.0000000	0.0000000	0.0000000	0.0000000	0.0000000
2	0.0003412	0.0048576	0.0007286	-.0002382	-.6666669
3	0.0092139	0.0101200	0.0015180	-.0064325	-.6666668
4	0.0737176	0.0167256	0.0025088	-.0499817	-.6474562
5	0.1159998	0.0214544	0.0032182	-.0498403	-.4102930
6	0.1653257	0.0243800	0.0036570	-.0442355	-.2555055
7	0.1971114	0.0264776	0.0039716	-.0189703	-.0919034
8	0.2333331	0.0280968	0.0042145	0.0031978	0.0130871
9	0.2755265	0.0289432	0.0043415	0.0211967	0.0734636
10	0.3028755	0.0298632	0.0044795	0.0495591	0.1562522
11	0.3409597	0.0307832	0.0046175	0.0674603	0.1889345
12	0.3771668	0.0315928	0.0047389	0.0866721	0.2194375
13	0.4072451	0.0324208	0.0048631	0.1131284	0.2652648
14	0.4408787	0.0331384	0.0049708	0.1311705	0.2841056
15	0.4774123	0.0340400	0.0051060	0.1471875	0.2944006
16	0.5126014	0.0349048	0.0052357	0.1685921	0.3140633
17	0.5372464	0.0357144	0.0053572	0.2047732	0.3639639
18	0.5879052	0.0365424	0.0054814	0.2035122	0.3305516
19	0.6106455	0.0372968	0.0055945	0.2350908	0.3676219
20	0.6449799	0.0380328	0.0057049	0.2570910	0.3806219
21	0.6753830	0.0388424	0.0058264	0.2803528	0.3963748
22	0.7184172	0.0395048	0.0059257	0.2962779	0.3937958
23	0.7524157	0.0402776	0.0060416	0.3199944	0.4060981
24	0.7908422	0.0408664	0.0061300	0.3391358	0.4094751
25	0.8199337	0.0413632	0.0062045	0.3751761	0.4369161
26	0.8471139	0.0419336	0.0062900	0.4051356	0.4566656

27	0.8944091	0.0425040	0.0063756	0.4180827	0.4463361
28	0.9408227	0.0430560	0.0064584	0.4257127	0.4320571
29	0.9707304	0.0435528	0.0065329	0.4537663	0.4463376
30	1.0055841	0.0439944	0.0065992	0.4783655	0.4542221
31	1.0324135	0.0445648	0.0066847	0.5070852	0.4689771
32	1.0829237	0.0448960	0.0067344	0.5133344	0.4526080
33	1.1286496	0.0451168	0.0067675	0.5214409	0.4411244
34	1.1500463	0.0455216	0.0068282	0.5598851	0.4648327
35	1.1872838	0.0459632	0.0068945	0.5828166	0.4686909
36	1.2309942	0.0464232	0.0069635	0.5997434	0.4651724
37	1.2648185	0.0469936	0.0070490	0.6250575	0.4718375
38	1.3081852	0.0474168	0.0071125	0.6422224	0.4687185
39	1.3345246	0.0479504	0.0071926	0.6772125	0.4844971
40	1.3817905	0.0483000	0.0072450	0.6872027	0.4748208
41	1.4014915	0.0487600	0.0073140	0.7297950	0.4971588
42	1.4491094	0.0491096	0.0073664	0.7425039	0.4891886
43	1.4798585	0.0494960	0.0074244	0.7699616	0.4967337
44	1.5133623	0.0499376	0.0074906	0.8014269	0.5055817
45	1.5473421	0.0503056	0.0075458	0.8251436	0.5091068
46	1.5813484	0.0508024	0.0076204	0.8547728	0.5160410
47	1.6076745	0.0512808	0.0076921	0.8882847	0.5274866
48	1.6622800	0.0515384	0.0077308	0.8975878	0.5154923
49	1.6957573	0.0520536	0.0078080	0.9246180	0.5205269
50	1.7412817	0.0525320	0.0078798	0.9313655	0.5106093
51	1.7668062	0.0529368	0.0079405	0.9772980	0.5280460
52	1.8070843	0.0534336	0.0080150	0.9966073	0.5264692
53	1.8417977	0.0538200	0.0080730	1.0331514	0.5354806
54	1.8796725	0.0542800	0.0081420	1.0511718	0.5338349
55	1.9211316	0.0547768	0.0082165	1.0681689	0.5307516
56	1.9613959	0.0553104	0.0082966	1.0860000	0.5285259
57	1.9929942	0.0558072	0.0083711	1.1158187	0.5344213
58	2.0298810	0.0562304	0.0084346	1.1434231	0.5376825
59	2.0767856	0.0565616	0.0084842	1.1566081	0.5315886
60	2.1068459	0.0570952	0.0085643	1.1874993	0.5379924
61	2.1393178	0.0575000	0.0086250	1.2226357	0.5454956
62	2.1744733	0.0579416	0.0086912	1.2469964	0.5473611
63	2.2215395	0.0583832	0.0087575	1.2600629	0.5413670
64	2.2548378	0.0587328	0.0088099	1.2901685	0.5461075
65	2.2974834	0.0592296	0.0088844	1.3092880	0.5439028
66	2.3328290	0.0597816	0.0089672	1.3394430	0.5479899
67	2.3630493	0.0601680	0.0090252	1.3702149	0.5534022
68	2.4085770	0.0606096	0.0090914	1.3858314	0.5491174
69	2.4394956	0.0608488	0.0091273	1.4205618	0.5557365
70	2.4841735	0.0612352	0.0091853	1.4382517	0.5525252
71	2.5177999	0.0616768	0.0092515	1.4681194	0.5564573
72	2.5610964	0.0620632	0.0093095	1.4838061	0.5528830
73	2.5784197	0.0624864	0.0093730	1.5354571	0.5682797
74	2.6167674	0.0630568	0.0094585	1.5531201	0.5663816
75	2.6654987	0.0634800	0.0095220	1.5635171	0.5597344
76	2.6984274	0.0639216	0.0095882	1.5923829	0.5631016
77	2.7295091	0.0644368	0.0096655	1.6284719	0.5692962
78	2.7780750	0.0648784	0.0097318	1.6419439	0.5639560
79	2.8203523	0.0653200	0.0097980	1.6627803	0.5625380
80	2.8645265	0.0657616	0.0098642	1.6882186	0.5623220
81	2.9020324	0.0661112	0.0099167	1.7123904	0.5629894
82	2.9378479	0.0665344	0.0099802	1.7407093	0.5653111
83	2.9702711	0.0668840	0.0100326	1.7743673	0.5699404
84	3.0135484	0.0671968	0.0100795	1.7930107	0.5676430
85	3.0500302	0.0675464	0.0101320	1.8193750	0.5690873

86	3.0910895	0.0679512	0.0101927	1.8395667	0.5677454
87	3.1270487	0.0681904	0.0102286	1.8648105	0.5689051
88	3.1621482	0.0685400	0.0102810	1.8891711	0.5699269
89	3.1948707	0.0690000	0.0103500	1.9166780	0.5722907
90	3.2370954	0.0693128	0.0103969	1.9330802	0.5696437
91	3.2640512	0.0696992	0.0104549	1.9690719	0.5754476
92	3.3034134	0.0701592	0.0105239	1.9948893	0.5760307
93	3.3476901	0.0706560	0.0105984	2.0142956	0.5739244
94	3.3965397	0.0710792	0.0106619	2.0275302	0.5693677
95	3.4355648	0.0709136	0.0106370	2.0565424	0.5709393
96	3.4720299	0.0714840	0.0107226	2.0858631	0.5729828
97	3.5140879	0.0719072	0.0107861	2.1082964	0.5721967
98	3.5456109	0.0723488	0.0108523	2.1395936	0.5755150
99	3.5808640	0.0727536	0.0109130	2.1667919	0.5770783
100	3.6152716	0.0731584	0.0109738	2.1960635	0.5792932
101	3.6508591	0.0735448	0.0110317	2.2230234	0.5806735
102	3.6930432	0.0739680	0.0110952	2.2394252	0.5782578
103	3.7237246	0.0742624	0.0111394	2.2757535	0.5827831
104	3.7725413	0.0745568	0.0111835	2.2904649	0.5789388
105	3.8071039	0.0741152	0.0111173	2.3196182	0.5809695
106	3.8462360	0.0744464	0.0111670	2.3425984	0.5807379
107	3.8821378	0.0748880	0.0112332	2.3678412	0.5815508
108	3.9239733	0.0753112	0.0112967	2.3874388	0.5800933
109	3.9510791	0.0757712	0.0113657	2.4277449	0.5858271
110	3.9803629	0.0760840	0.0114126	2.4605918	0.5893710
111	4.0181141	0.0766176	0.0114926	2.4830456	0.5891434
112	4.0475836	0.0770592	0.0115589	2.5202069	0.5935925
113	4.0873995	0.0773904	0.0116086	2.5486236	0.5944185
114	4.1237893	0.0777768	0.0116665	2.5735097	0.5949081
115	4.1596799	0.0782000	0.0117300	2.6017098	0.5962197
116	4.1938777	0.0785128	0.0117769	2.6325784	0.5983569
117	4.2370453	0.0788808	0.0118321	2.6527009	0.5967657
118	4.2724166	0.0791200	0.0118680	2.6812582	0.5981780
119	4.3093257	0.0795248	0.0119287	2.7117004	0.5997686
120	4.3479071	0.0799664	0.0119950	2.7365150	0.5998659
121	4.3851342	0.0802792	0.0120419	2.7637625	0.6006756
122	4.4223642	0.0806840	0.0121026	2.7924876	0.6017892
123	4.4602690	0.0811072	0.0121661	2.8207369	0.6026905
124	4.4930830	0.0812544	0.0121882	2.8525591	0.6050205
125	4.5416317	0.0814752	0.0122213	2.8666515	0.6014831
126	4.5725765	0.0817880	0.0122682	2.9005237	0.6044542
127	4.6104574	0.0820088	0.0123013	2.9269981	0.6049382
128	4.6520529	0.0823216	0.0123482	2.9484868	0.6039069
129	4.6850128	0.0826528	0.0123979	2.9790082	0.6058468
130	4.7286181	0.0829840	0.0124476	2.9959636	0.6036512
131	4.7705579	0.0833704	0.0125056	3.0215006	0.6034199
132	4.8046970	0.0837200	0.0125580	3.0520749	0.6051748
133	4.8388228	0.0840416	0.0126062	3.0805798	0.6064987
134	4.8778877	0.0843799	0.0126570	3.1121335	0.6077805
135	4.9047389	0.0847008	0.0127051	3.1491594	0.6116281
136	4.9424148	0.0850320	0.0127548	3.1759005	0.6120965
137	4.9760327	0.0853872	0.0128080	3.2078671	0.6140597
138	5.0116692	0.0857240	0.0128586	3.2361865	0.6150535

APPENDIX D

SCALING FACTORS IN CENTRIFUGE TESTS (3D)

QUANTITY	PROTOTYPE	MODEL
Specific Weight	$\gamma_p = \varrho g$	$\gamma_m = N\varrho g = N\gamma_p$ (fact)
Length	L_p	$L_m = L_p/N$ (from choice)
Pressure	$P_p = \gamma_p L_p$	$P_m = \gamma_m L_m = N\gamma_p(L_p/N)$ $= P_p$
Force	$F_p \equiv P_p L_p^2$	$F_m \equiv P_m L_m^2 = P_p(L_p^2/N^2)$ $= F_p/N^2$
Moment	$M_p = F_p L_p$	$M_m = F_m L_m =$ $(F_p/N^2)(L_p/N) = M_p/N^3$
Second Moment of area	$I_p \equiv L_p^4$	$I_m \equiv L_m^4 = (L_p^4/N^4)$ $= I_p/N^4$
Deflection in extension or compression	$\delta_p = \sigma_p L_p/E$	$\delta_m = \sigma_m L_m/E =$ $(\sigma_p/E)(L_p/N) = \delta_p/N$
Deflection in bending	$\delta_p \propto F_p L_p^3/(EI)_p$	$\delta_m \propto F_m L_m^3/(EI)_m =$ $(F_p L_p^3/N^5)(N^4/(EI)_p) = \delta_p/N$

(If E values are different, EI is modelled. If cross sections are not similar, the fibre stresses will be different).

APPENDIX E

OPTIMUM SCALING RADIUS IN CENTRIFUGE TESTS

As discussed in detail by King (1989), when a model of the prototype of a scale of 1/n is subjected to a gravity field of n times the earth gravity, g, its vertical stress distribution will not match at all points with those of prototype since the linear variation of acceleration with depth through the model causes a non-linear variation of stress while the correct variation in the prototype is linear.

Referring to the figure E.1, when a soil model of height s (S in prototype) is spun at angular velocity ω, the vertical stress at radius r in the model will be

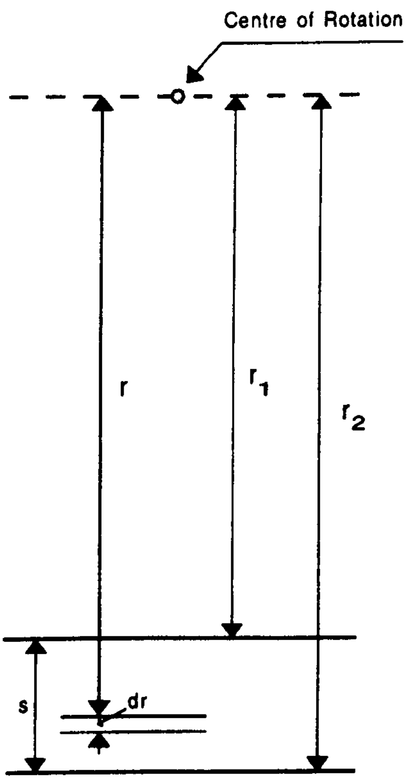

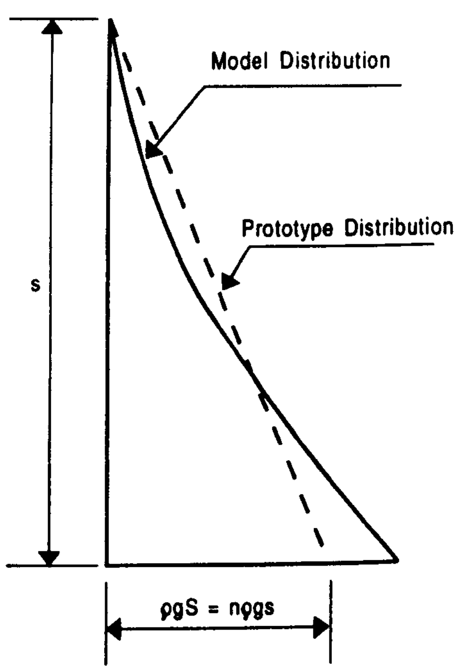

Figure E.1 Model of Soil Stratum. **Figure E.2** Vertical Stress Distribution in Model.

$$\sigma_{vm} = \rho\ \omega^2 \int_{r_1}^{r} r\ dr = \frac{\rho\ \omega^2}{2} (r^2 - r_1^2) \qquad \text{(E.1)}$$

and thus similarity of stress levels between model and prototype is achieved both at soil surface where they are zero and at one other position $r = r_o$ (see figure E.2).

For equal stresses at r_o,

$$\rho\ \frac{\omega^2}{2} (r_o^2 - r_1^2) = \rho g n\ (r_o - r_1)$$

Therefore

$$\omega^2 = \frac{2ng}{(r_o + r_1)} \qquad \text{(E.2)}$$

The error at other positions is given by

$$\begin{aligned} \epsilon &= n\rho g\ (r - r_1) - \frac{\rho\omega^2}{2} (r^2 - r_1^2) \\ &= n\rho g\ (r - r_1) - n\rho g\ \frac{(r^2 - r_1^2)}{(r_o + r_1)} \end{aligned}$$

For a mathematical maximum $d\varepsilon/dr = 0$ and therefore $r = (r_o + r_1)/2$, and for another practical maximum $r = r_2$.

It may be considered that the best overall approximation is obtained when the maximum percentage errors are equal therefore

$$\frac{\left[\left[\frac{(r_o + r_1)}{2} - r_1\right] n\rho g - \left[\left[\frac{r_o + r_1}{2}\right]^2 - r_1^2\right] \frac{n\rho g}{r_o + r_1}\right]}{\left[\frac{(r_o + r_1)}{2} - r_1\right] n\rho g}$$

$$= \frac{\left[(r_2{}^2 - r_1^2)\,\frac{n\rho g}{r_o + r_1} - (r_2 - r_1)\, n\rho g\right]}{(r_2 - r_1)\, n\rho g}$$

Therefore

$$1 - \frac{\frac{(r_o + r_1)}{2} + r_1}{(r_o + r_1)} = \frac{(r_2 + r_1)}{(r_o + r_1)} - 1$$

Therefore

$$r_o = r_1 + \frac{2}{3}(r_2 - r_1) \qquad \text{(E.3)}$$

This is optimum radius at which model and field stresses are equal.

The maximum errors are

$$\bar{\epsilon} = \frac{r_2 - r_o}{r_o + r_1} = \frac{h/3}{2\bar{r}} = \frac{h}{6\bar{r}} \qquad \text{(E.4)}$$

Now from equations (E.2) and (E.3), the optimum scaling radius

$$\bar{r} = \frac{ng}{\omega^2} = \frac{r_o + r_1}{2} = r_1 + h/3 \qquad \text{(E.5)}$$

(For example, in the Liverpool University centrifuge with an optimum scaling radius of 114.73 cm and the model of maximum depth of 23.2 cm, the maximum deviation between prototype and model in percentage terms will be 3.4%. In this study the soil bin was filled to an average depth of 18.0 cm, therefore the error was about 2.5 %).

Thus the optimum scaling radius is at the 1/3 rd point from the top and this is the radius which should be used in conjunction with the geometrical scaling factor n to determine the optimum angular velocity.

$$\bar{\omega} = \sqrt{\frac{ng}{r_1 + h/3}} \qquad \text{(E.6)}$$

APPENDIX F1

DATA PREPARATION AND PROGRAM LISTING FOR PROGRAM PIER2D

F1.1 DATA PREPARATION

---

1. NAME

10 unit alpha-numeric identification of problems (eg. TRIAL1, EXAMPLE1)

---

2. NPX, NPY, NEXP, NEYP, NPFP, NPFF

NPX = Number of nodal points in the x- direction
NPY = Number of nodal points in the y- direction
NEXP = Number of elements in the pier in the x- direction
NEYP = Number of elements in the pier in the y- direction
NPFP = First pier element node number (bottom left of the pier)
NPFF = First friction element node number (bottom left of the friction element)

---

3. XX(N), N = 1, NPX

XX = x- co-ordinates of nodal points along x- axis

---

4. YY(N), N = 1, NPY

YY = y- co-ordinates of nodal points along y- axis

---

5. NUGP, HKO, RO, RO1, HT, HT1

NUGP = Number of gauss points (4 or 9)
HKO = Coefficient of lateral earth pressure at rest (K_0)
RO = Specific weight of soil above water table
RO1 = Specific weight of soil below water table
HT = Total height of soil
HT1 = Height of water table (0.0 if no water table)

---

6. YMM, PRM, PRP, FRP, ARP, SN, SS

YMM = Soil modulus
PRM = Poisson's ratio for soil
PRP = Poisson's ratio for pier
FRP = Flexural rigidity of pier (EI)
ARP = Axial rigidity of pier (EA)
SN = Normal stiffness of friction element
SS = Shear stiffness of friction element

---

7. HLOAD, CLOAD

HLOAD = Horizontal load applied on pier head
CLOAD = Moment load applied on pier head

---

8. NHAR, THETA

NHAR = Number of harmonics (This is set equal to 1)
THETA = Angle around pier

---

9. NUMBC

NUMBC = Number of boundary conditions

---

10. NPB(L), NFIX(L), L = 1, NUMBC

NPB = The node number at which displacement is set equal to zero

NFIX = Code prescribing the degrees of freedom in which displacements are prescribed equal to zero

- = 0 radial, vertical and circumferential displacements are equal to zero
- = 1 radial and vertical displacements are equal to zero
- = 2 radial and circumferential displacements are equal to zero
- = 3 vertical and circumferential displacements are equal to zero
- = 4 radial displacements are equal to zero
- = 5 vertical displacements are equal to zero
- = 6 circumferential displacements are equal to zero

---

11. ICODE

ICODE = 0 if pier head is fixed
= 1 if pier head is free

F1.2 PROGRAM LISTING

```
      PROGRAM PIER2D
      IMPLICIT REAL*8 (A-H,O-Z)
      DIMENSION NPM(60,8),NPF(20,6),NPP(60,8)
      DIMENSION NMMM(900),NFFF(900),NPPP(900)
      DIMENSION XX(25),YY(40),XORD(300),YORD(300)
      DIMENSION YCP(100,9),BTOT(900),B(900)
      DIMENSION GS(3),GSWT(3),XG(9),YG(9),XD(3),YD(3)
      DIMENSION SIGIMX(60,9),SIGIMY(60,9),SIGIMZ(60,9)
      DIMENSION SIGMX(60,9),SIGMY(60,9),SIGMZ(60,9)
     1,SIGMXY(60,9),SIGMXZ(60,9),SIGMYZ(60,9)
      DIMENSION SIGIFN(20,9)
      DIMENSION SIGFN(20,9),SIGFSX(20,9),SIGFSY(20,9)
      DIMENSION SIGIPX(20,9),SIGIPY(20,9),SIGIPZ(20,9)
      DIMENSION SIGPX(20,9),SIGPY(20,9),SIGPZ(20,9)
     1,SIGPXY(20,9),SIGPXZ(20,9),SIGPYZ(20,9)
      DIMENSION YDM(60,9),YDM1(60,9),XDM(60,9),YDF(20,9)
     1,YDF1(20,9),XDF(20,9),YDP(20,9),YDP1(20,9),XDP(20,9)
      DIMENSION PROPM(60,2),PROPP(20,4),STN(20),STS(20)
      DIMENSION A(900,80),S(24,24),LM(24),LF(18),LP(24)
      DIMENSION NPB(60),NFIX(60)
      DIMENSION NCPP(60)
      COMMON/FIRST/NUGP,NHAR,THETA1,S,XORD,YORD,GSWT,GS
      COMMON/SECOND/NPM,PROPM
      COMMON/THIRD/NPF,STN,STS,NEXP
      COMMON/FOURTH/NPP,PROPP
      COMMON/FIFTH/A,B,NBAND,NT
      COMMON/SIXTH/BTOT

 COMMON/SEVENTH/SIGMX,SIGMY,SIGMZ,SIGMXY,SIGMXZ,SIGMYZ
      COMMON/EIGHTH/SIGFN,SIGFSX,SIGFSY
      COMMON/NINTH/SIGPX,SIGPY,SIGPZ,SIGPXY,SIGPXZ,SIGPYZ
      CHARACTER*72 DATAFN,OUTPF
      CHARACTER NAME*10
      PRINT *, 'ENTER THE NAME OF DATA FILE WITH PATH'
      READ '(A)',DATAFN
      print *, 'ENTER THE NAME OF OUTPUT FILE WITH PATH'
      READ '(A)',OUTPF
      OPEN(5,FILE=DATAFN,STATUS='OLD')
      OPEN(6,FILE=OUTPF,STATUS='UNKNOWN')
      READ(5,100) NAME
  100 FORMAT(A10)
      READ(5,*) NPX,NPY,NEXP,NEYP,NPFP,NPFF
C
C     GENERATION OF NODE NUMBERS FOR MEDIUM ELEMENTS
C
      NOX=(NPX-1)/2
      NOY=(NPY-1)/2
      NUMEL=NOX*NOY-NEXP*NEYP
      NUFEL=NEXP+NEYP
      NUPEL=NEXP*NEYP
      I=0
      MM=NPX-2
      DO 300 N=1,NOY
      NN=0
      DO 300 M=1,MM,2
      I=I+1
      NPM(I,1)=(N-1)*(2*NPX-NOX)+M
      IF(NPM(I,1).EQ.NPFF)GO TO 500
      NPM(I,2)=NPM(I,1)+2
      NPM(I,3)=NPM(I,2)+(2*NPX-NOX)
      NPM(I,4)=NPM(I,3)-2
      NPM(I,5)=NPM(I,1)+1
      NPM(I,6)=NPM(I,3)-NOX-NN-2
      NPM(I,7)=NPM(I,4)+1
      NPM(I,8)=NPM(I,6)-1
      NN=NN+1
  300 CONTINUE
      GO TO 3010
  500 MM=NPX-2*NEXP-2
      NNPX=NPX-2*NEXP
      NNOX=NOX-NEXP
      N1=NPFF+2*NEXP-1
      DO 301 N=1,NEYP
      IF(N.EQ.1)N2=0
      IF(N.GT.1)N2=2*NEXP+1
      IF(N.EQ.1)N3=2*NEXP+1
      IF(N.GT.1)N3=0
      NN=0
      DO 301 M=1,MM,2
      NPM(I,1)=N1+(N-1)*(3*NNOX+3*NEXP+4)+N2+M
      NPM(I,2)=NPM(I,1)+2
      NPM(I,3)=NPM(I,2)+3*NNOX+3*NEXP+4+N3
      NPM(I,4)=NPM(I,3)-2
      NPM(I,5)=NPM(I,1)+1
      NPM(I,6)=NPM(I,3)-NNOX-NN-2*NEXP-3
      NPM(I,7)=NPM(I,3)-1
      NPM(I,8)=NPM(I,6)-1
      NN=NN+1
      I=I+1
  301 CONTINUE
 3010 CONTINUE
      WRITE(6,209)
  209 FORMAT(1H1)
      WRITE(6,211)
  211 FORMAT(//'   NPX     NPY     NEXP     NEYP     NPFP     NPFF')
      WRITE(6,212) NPX,NPY,NEXP,NEYP,NPFP,NPFF
  212 FORMAT(//6(I6,2X))
      WRITE(6,213)
  213 FORMAT(//'    ELEMENT AND NODE NUMBERS FOR MEDIUM
ELEMENTS')
      WRITE(6,210)
  210 FORMAT(//,'  I    1    2    3    4    5    6    7    8')
      WRITE(6,215)(I,(NPM(I,J),J=1,8),I=1,NUMEL)
  215 FORMAT(//9(2X,I4))
```

```
C
C    GENERATION OF NODE NUMBERS FOR FRICTION ELEMENTS
C
      I=0
      NPFF1=NPFF-1
      MM=2*NEXP-1
      DO 302 M=1,MM,2
      I=I+1
      NPF(I,1)=NPFF1+M
      NPF(I,2)=NPF(I,1)+2
      NPF(I,3)=NPF(I,2)+2*NEXP+2*NNOX+1
      NPF(I,4)=NPF(I,3)-2
      NPF(I,5)=NPF(I,1)+1
      NPF(I,6)=NPF(I,3)-1
      IF(I.EQ.NEXP)GO TO 501
  302 CONTINUE
      GO TO 3030
  501 DO 303 N=1,NEYP
      I=I+1
      IF(N.GT.1)N2=0
      IF(N.EQ.1)N2=2*NEXP+1
      NPF(I,1)=NPF((I-1),2)
      NPF(I,2)=NPF(I,1)+3*NNOX+N2+3*NEXP+4
      NPF(I,3)=NPF(I,2)-1
      NPF(I,4)=NPF((I-1),3)
      NPF(I,5)=NPF(I,1)+2*NNOX+N2+NEXP+2
      NPF(I,6)=NPF(I,5)-1
  303 CONTINUE
 3030 CONTINUE
      WRITE(6,217)
  217 FORMAT(//'    ELEMENT AND NODE NUMBERS FOR FRICTION
ELEMENTS')
      WRITE(6,216)
  216 FORMAT(//,'   I    1    2    3    4    5    6  ')
      WRITE(6,220)(I,(NPF(I,J),J=1,6),I=1,NUFEL)
  220 FORMAT(//7(2X,I4))
C
C    GENERATION OF NODE NUMBERS FOR PILE ELEMENTS
C
      I=0
      MM=2*NEXP-1
      NPFP1=NPFP-1
      DO 304 N=1,NEYP
      IF(N.EQ.1)N3=0
      IF(N.GT.1)N3=2*NEXP+1
      IF(N.EQ.1)N4=0
      IF(N.GT.1)N4=NEXP+NNOX+2
      IF(N.LE.2)N5=0
      IF(N.GT.2)N5=1
      IF(N.EQ.1)N6=0
      IF(N.GT.1)N6=1
      NN=0
      DO 304 M=1,MM,2
      I=I+1
      NPP(I,1)=NPFP1+M+N3+N4+N5*(N-2)*(3*NEXP+3*NNOX+4)
      NPP(I,2)=NPP(I,1)+2
      NPP(I,3)=NPP(I,2)+3*NEXP+NNOX+3+(2*NNOX+1)*N6
      NPP(I,4)=NPP(I,3)-2
      NPP(I,5)=NPP(I,1)+1
      NPP(I,6)=NPP(I,3)-NEXP-NN-NNOX-3
      NPP(I,7)=NPP(I,3)-1
      NPP(I,8)=NPP(I,6)-1
      NN=NN+1
  304 CONTINUE
      WRITE(6,222)
  222 FORMAT(//'    ELEMENT AND NODE NUMBERS FOR PILE
ELEMENTS')
      WRITE(6,221)
  221 FORMAT(//,'   I    1    2    3    4    5    6    7    8')
      WRITE(6,225)(I,(NPP(I,J),J=1,8),I=1,NUPEL)
  225 FORMAT(//9(2X,I4))
C
C    GENERATION OF NODE COORDINATES
C
      READ(5,*) (XX(N),N=1,NPX)
      READ(5,*) (YY(N),N=1,NPY)
      L=1
      TH=YY(NPY)
      NNOY=NOY-NEYP
      K=0
      K1=0
      K2=0
      K3=0
      DO 307 J=1,NPY,2
      K=((J-2*K3-1)*(2*NPX-NOX+K1))/2+1+K2
      KK=K
      DO 307 I=1,NPX
      XORD(K)=XX(I)
      YORD(K)=YY(J)
      IF(K.EQ.(KK+2*NEXP).AND.K.GT.(NPFP+2*NEXP))GO TO 503
      K=K+1
      IF(K.EQ.NPFP)GO TO 502
      GO TO 307
  502 NPPX=2*NEXP+1
      DO 306 II=1,NPPX
      XORD(K)=XX(II)
      YORD(K)=YY(J)
      K=K+1
  306 CONTINUE
      K1=2
      K2=NNOY*(2*NPX-NOX)+2*NEXP
      K3=NNOY
      GO TO 307
  503 K=K+1
      XORD(K)=XX(I)
      YORD(K)=YY(J)
      K=K+1
  307 CONTINUE
      MM=NPY-2
      DO 308 M=1,MM,2
```

```
      J=M+1
      K=((M-1)*(2*NPX-NOX))/2+(NPX+1)
      DO 308 I=1,NPX,2
      IF(K.EQ.NPFP)GO TO 505
      XORD(K)=XX(I)
      YORD(K)=YY(J)
      K=K+1
      IF(K.EQ.NPFF)GO TO 505
      GO TO 308
  505 MMM=2*NEYP-1
      NNOY=NOY-NEYP
      DO 309 MI=1,MMM,2
      J=2*NNOY+1+MI
      K=NPFP+2*NEXP+1+((MI-1)*(2*NPX-NOX+2))/2
      KK=K
      DO 309 II=1,NPX,2
      XORD(K)=XX(II)
      YORD(K)=YY(J)
      IF(K.EQ.(KK+NEXP).AND.K.GT.(NPFP+2*NEXP))GO TO 506
      K=K+1
      GO TO 309
  506 K=K+1
      XORD(K)=XX(II)
      YORD(K)=YY(J)
      K=K+1
  309 CONTINUE
      GO TO 405
  308 CONTINUE
  405 LL=NPM(NUMEL,3)
      WRITE(6,227) (XX(N),N=1,NPX)
  227 FORMAT(//'    XX',10F10.4,/,6X,10F10.4,/,6X,10F10.4)
      WRITE(6,228) (YY(N),N=1,NPY)
  228 FORMAT(//'    YY',10F10.4,/,6X,10F10.4,/,6X,10F10.4)
      WRITE(6,229)
  229 FORMAT(//'    COORDINATES OF ALL THE NODES')
      WRITE(6,226)
  226 FORMAT(//'  NP     XORD     YORD      NP     XORD      ',
     1'YORD      NP     XORD     YORD')
      WRITE(6,230) (K,XORD(K),YORD(K),K=1,LL)
  230 FORMAT(//1(I6,2F10.4,I10,2F10.4,I10,2F10.4))
C
C     INITIALISE FORCES IN THE PILE
C
      DO 310 I=1,NUPEL
      DO 310 J=1,6
      YCP(I,J)=0.0
  310 CONTINUE
C
C     INITAILISE TOTAL DISPLACEMENTS
C
      NT=3*LL
      DO 311 I=1,NT
      BTOT(I)=0.0
  311 CONTINUE
C
C                 ****INITIALISE STRESSES****
C
C
C     CALCULATION OF GAUSS POINTS
C
      READ(5,*) NUGP,HK0,R0,R01,HT,HT1
      READ(5,*) YMM,PRM,PRP,FRP,ARP,SN,SS
      PI=3.14159265359
      YMP=4.*FRP/PI/XX(3)**4
      IF(NUGP.EQ.9)GO TO 507
      GS(1)=-(1.0/SQRT(3.0))
      GS(2)=-GS(1)
      GSWT(1)=1.0
      GSWT(2)=1.0
      GO TO 400
  507 GS(1)=-(1.0/SQRT(5.0/3.0))
      GS(2)=0.0
      GS(3)=-GS(1)
      GSWT(1)=5.0/9.0
      GSWT(2)=8.0/9.0
      GSWT(3)=GSWT(1)
C
C     INITIALISE STRESSES IN THE SOIL MEDIUM
C
  400 DO 316 N=1,NUMEL
      I=NPM(N,5)
      J=NPM(N,8)
      I1=NPM(N,2)
      J1=NPM(N,4)
      XC=XORD(I)
      YC=YORD(J)
      XD(1)=XC-XORD(J)
      YD(1)=YC-YORD(I)
      IF(NUGP.EQ.9)GO TO 508
      XD(2)=XORD(I1)-XC
      YD(2)=YORD(J1)-YC
      GO TO 401
  508 XD(2)=0.0
      YD(2)=0.0
      XD(3)=XORD(I1)-XC
      YD(3)=YORD(J1)-YC
  401 M=0
      IF(NUGP.EQ.9)L1=3
      IF(NUGP.EQ.4)L1=2
      DO 312 K=1,L1
      M=M+1
      XG(M)=XC+GS(K)*XD(K)
      YG(M)=YC+GS(1)*YD(1)
  312 CONTINUE
      IF(NUGP.EQ.4)GO TO 313
      DO 313 K=1,L1
      M=M+1
      XG(M)=XC+GS(K)*XD(K)
      YG(M)=YC+GS(2)*YD(2)
  313 CONTINUE
```

```
    DO 314 K=1,L1
    M=M+1
    XG(M)=XC+GS(K)*XD(K)
    YG(M)=YC+GS(L1)*YD(L1)
  314 CONTINUE
    DO 315 M=1,NUGP
    IF(YG(M).LE.HT1)GO TO 509
    SIGIMY(N,M)=-R0*(HT-YG(M))
    SIGIMX(N,M)=HK0*SIGIMY(N,M)
    YDM(N,M)=HT-YG(M)
    XDM(N,M)=XG(M)
    GO TO 315
  509 SIGIMY(N,M)=-R0*(HT-HT1)-R01*(HT1-YG(M))
    SIGIMX(N,M)=HK0*SIGIMY(N,M)
    YDM(N,M)=HT-YG(M)
    YDM1(N,M)=HT1-YG(M)
    XDM(N,M)=XG(M)
  315 CONTINUE
cc   PROPM(N,1)=YMM*((TH-YY(L))-(YY(L+2)-YY(L))/2)
    IF(NPM(N+1,1).NE.NPM(N,2)) L=L+2
C
C   MEDIUM ELEMENT PROPERTIES
C
    PROPM(N,1)=YMM
    PROPM(N,2)=PRM
  316 CONTINUE
    WRITE(6,238) NUGP,HK0,R0,R01,HT,HT1
  238 FORMAT(//'   NO.GAUSS POINTS=',I2,/'   KO VALUE=',F7.4,/
   *       '  BULK DENSITY=',F7.4,/'   SUBMERGED
DENSITY=',F7.4,/
   *       '  FULL HEIGHT=',F7.4,/'   HEIGHT OF WATER
TABLE=',F7.4)
    WRITE(6,239) YMM,PRM,YMP,PRP,FRP,ARP,SN,SS
  239 FORMAT(//'   SOIL MODULUS=',E13.6,/
   * '   POISSON RATIO FOR SOIL=',F7.4,/
   * '   PILE MODULUS=',E13.6,/
   * '   PIOSSON RATIO FOR PILE=',F7.4,/
   * '   FLEXURAL RIGIDITY OF PILE=',E13.6,/
   * '   AXIAL RIGIDITY OF PILE=',E13.6,/
   * '   NORMAL STIFFNESS OF FRICTION ELEMENT=',E13.6,/
   * '   SHEAR STIFFNESS OF FRICTION ELEMENT=',E13.6)
    WRITE(6,233)
  233 FORMAT(//'   INITIAL STRESSES IN MEDIUM ELEMENTS')
    IF(HT1.GT.0.0)GO TO 510
    WRITE(6,231)
  231 FORMAT(//'   I   GPNU    DEPTH    HORZ.DIST      SIGIMZ',
   1'        SIGIMR          ET          PR')
    DO 318 N=1,NUMEL
    WRITE(6,232)
  232 FORMAT(/)
    DO 318 M=1,NUGP
    WRITE(6,235)
N,M,YDM(N,M),XDM(N,M),SIGIMY(N,M),SIGIMX(N,M)
    1,PROPM(N,1),PROPM(N,2)
  235 FORMAT(1(I6,2X,I3,4X,F7.4,4X,F7.4,4X,E13.6,2X,E13.6
    1,2X,E13.6,2X,F7.4))
    GO TO 318
  510 WRITE(6,236)
  236 FORMAT(//'   I   GPNU    DEPTH    DEPTH.BL.WT   HORZ.DIST
SIG',
   1'IM        SIGIMR          ET          PR')
    DO 317 K=1,NUMEL
    WRITE(6,237)
  237 FORMAT(/)
    DO 317 J=1,NUGP
    WRITE(6,240) K,J,YDM(K,J),YDM1(K,J),XDM(K,J),SIGIMY(K,J),
   1SIGIMX(K,J),PROPM(K,1),PROPM(K,2)
  240 FORMAT(1(I6,2X,I3,4X,F7.4,4X,F7.4,4X,F7.4,4X,E13.6,2X,E13.6
   1,2X,E13.6,2X,F7.4))
  317 CONTINUE
  318 CONTINUE
C
C   INITIALISE STRESSES IN THE FRICTION ELEMENTS
C
C
C   IN THE HORIZONTAL FRICTION ELEMENTS
C
    DO 323 N=1,NEXP
    I=NPF(N,5)
    J=NPF(N,4)
    I1=NPF(N,2)
    XC=XORD(I)
    YC=YORD(J)
    XD(1)=XC-XORD(J)
    YD(1)=0.0
    IF(NUGP.EQ.9)GO TO 511
    XD(2)=XORD(I1)-XC
    YD(2)=0.0
    GO TO 402
  511 XD(2)=0.0
    YD(2)=0.0
    XD(3)=XORD(I1)-XC
    YD(3)=0.0
  402 M=0
    DO 319 K=1,L1
    M=M+1
    XG(M)=XC+GS(K)*XD(K)
    YG(M)=YC
  319 CONTINUE
    IF(NUGP.EQ.4)GO TO 320
    DO 320 K=1,L1
    M=M+1
    XG(M)=XC+GS(K)*XD(K)
    YG(M)=YC
  320 CONTINUE
    DO 321 K=1,L1
    M=M+1
    XG(M)=XC+GS(K)*XD(K)
    YG(M)=YC
  321 CONTINUE
```

```
      DO 322 M=1,NUGP
      IF(YG(M).LE.HT1)GO TO 512
      SIGIFN(N,M)=-R0*(HT-YG(M))
      YDF(N,M)=HT-YG(M)
      XDF(N,M)=XG(M)
      GO TO 322
  512 SIGIFN(N,M)=-R0*(HT-HT1)-R01*(HT1-YG(M))
      YDF(N,M)=HT-YG(M)
      YDF1(N,M)=HT1-YG(M)
      XDF(N,M)=XG(M)
  322 CONTINUE
C
C     HORIZONTAL FRICTION ELEMENT PROPERTIES
C
      STN(N)=SN
      STS(N)=SS
  323 CONTINUE
      WRITE(6,243)
  243 FORMAT(//'    INITIAL STRESSES IN HORIZONTAL FRICTION
ELEMENTS')
      IF(HT1.GT.0.0)GO TO 513
      WRITE(6,241)
  241 FORMAT(//'    I   GPNU    DEPTH    HORZ.DIST      SIGIFN
',
     1'  SN              SS')
      DO 325 N=1,NEXP
      WRITE(6,242)
  242 FORMAT(/)
      DO 325 M=1,NUGP
      WRITE(6,245) N,M,YDF(N,M),XDF(N,M),SIGIFN(N,M)
     1,STN(N),STS(N)
  245 FORMAT(1(I6,2X,I3,4X,F7.4,4X,F7.4,4X,E13.6,2X,E13.6
     1,2X,E13.6))
      GO TO 325
  513 WRITE(6,246)
  246 FORMAT(//'    I   GPNU    DEPTH    DEPTH.BL.WT   HORZ.DIST
SIG',
     1'IF          SN              SS')
      DO 324 K=1,NEXP
      WRITE(6,247)
  247 FORMAT(/)
      DO 324 J=1,NUGP
      WRITE(6,250) K,J,YDF(K,J),YDF1(K,J),XDF(K,J),SIGIFN(K,J)
     1,STN(K),STS(K)
  250 FORMAT(1(I6,2X,I3,4X,F7.4,4X,F7.4,4X,F7.4,4X,E13.6,2X,E13.6
     1,2X,E13.6))
  324 CONTINUE
  325 CONTINUE
C
C     IN VERTICAL FRICTION ELEMENTS
C
      NEXP1=NEXP+1
      DO 330 N=NEXP1,NUFEL
      J=NPF(N,5)
      I=NPF(N,4)
      I1=NPF(N,2)
      XC=XORD(I)
      YC=YORD(J)
      XD(1)=0.0
      YD(1)=YC-YORD(I)
      IF(NUGP.EQ.9)GO TO 514
      XD(2)=0.0
      YD(2)=YORD(I1)-YC
      GO TO 403
  514 XD(2)=0.0
      YD(2)=0.0
      XD(3)=0.0
      YD(3)=YORD(I1)-YC
  403 M=0
      DO 326 K=1,L1
      M=M+1
      XG(M)=XC
      YG(M)=YC+GS(1)*YD(1)
  326 CONTINUE
      IF(NUGP.EQ.4)GO TO 327
      DO 327 K=1,L1
      M=M+1
      XG(M)=XC
      YG(M)=YC+GS(2)*YD(2)
  327 CONTINUE
      DO 328 K=1,L1
      M=M+1
      XG(M)=XC
      YG(M)=YC+GS(L1)*YD(L1)
  328 CONTINUE
      DO 329 M=1,NUGP
      IF(YG(M).LE.HT1)GO TO 515
      SIGIFN(N,M)=-R0*HK0*(HT-YG(M))
      YDF(N,M)=HT-YG(M)
      XDF(N,M)=XG(M)
      GO TO 329
  515 SIGIFN(N,M)=-R0*HK0*(HT-HT1)-R01*HK0*(HT1-YG(M))
      YDF(N,M)=HT-YG(M)
      YDF1(N,M)=HT1-YG(M)
      XDF(N,M)=XG(M)
  329 CONTINUE
C
C     VERTICAL FRICTION ELEMENT PROPERTIES
C
      STN(N)=SN
      STS(N)=SS
  330 CONTINUE
      WRITE(6,253)
  253 FORMAT(//'    INITIAL STRESSES IN VERTICAL FRICTION
ELEMENTS')
      IF(HT1.GT.0.0)GO TO 516
      WRITE(6,251)
  251 FORMAT(//'    I   GPNU    DEPTH    HORZ.DIST      SIGIFN
',
     1'  SN              SS')
```

```
      DO 332 N=NEXP1,NUFEL
      WRITE(6,252)
  252 FORMAT(/)
      DO 332 M=1,NUGP
      WRITE(6,255) N,M,YDF(N,M),XDF(N,M),SIGIFN(N,M)
     1,STN(N),STS(N)
  255 FORMAT(1(I6,2X,I3,4X,F7.4,4X,F7.4,4X,E13.6,2X,E13.6
     1,2X,E13.6))
      GO TO 332
  516 WRITE(6,256)
  256 FORMAT(//'   I   GPNU    DEPTH    DEPTH.BL.WT  HORZ.DIST
 SIG',
     1'IF          SN            SS')
      DO 331 K=NEXP1,NUFEL
      WRITE(6,257)
  257 FORMAT(/)
      DO 331 J=1,NUGP
      WRITE(6,260) K,J,YDF(K,J),YDF1(K,J),XDF(K,J),SIGIFN(K,J)
     1,STN(K),STS(K)
  260 FORMAT(1(I6,2X,I3,4X,F7.4,4X,F7.4,4X,F7.4,4X,E13.6,2X,E13.6
     1,2X,E13.6))
  331 CONTINUE
  332 CONTINUE
C
C     INITIALISE STRESSES IN THE PILE ELEMENTS
C
      DO 337 N=1,NUPEL
      I=NPP(N,5)
      J=NPP(N,8)
      I1=NPP(N,2)
      J1=NPP(N,4)
      XC=XORD(I)
      YC=YORD(J)
      XD(1)=XC-XORD(J)
      YD(1)=YC-YORD(I)
      IF(NUGP.EQ.9)GO TO 517
      XD(2)=XORD(I1)-XC
      YD(2)=YORD(J1)-YC
      GO TO 404
  517 XD(2)=0.0
      YD(2)=0.0
      XD(3)=XORD(I1)-XC
      YD(3)=YORD(J1)-YC
  404 M=0
      DO 333 K=1,L1
      M=M+1
      XG(M)=XC+GS(K)*XD(K)
      YG(M)=YC+GS(1)*YD(1)
  333 CONTINUE
      IF(NUPG.EQ.4)GO TO 334
      DO 334 K=1,L1
      M=M+1
      XG(M)=XC+GS(K)*XD(K)
      YG(M)=YC+GS(2)*YD(2)
  334 CONTINUE
      DO 335 K=1,L1
      M=M+1
      XG(M)=XC+GS(K)*XD(K)
      YG(M)=YC+GS(L1)*YD(L1)
  335 CONTINUE
      DO 336 M=1,NUGP
      IF(YG(M).LE.HT1)GO TO 518
      SIGIPY(N,M)=-R0*(HT-YG(M))
      SIGIPX(N,M)=HK0*SIGIPY(N,M)
      YDP(N,M)=HT-YG(M)
      XDP(N,M)=XG(M)
      GO TO 336
  518 SIGIPY(N,M)=-R0*(HT-HT1)-R01*(HT1-YG(M))
      SIGIPX(N,M)=HK0*SIGIPY(N,M)
      YDP(N,M)=HT-YG(M)
      YDP1(N,M)=HT1-YG(M)
      XDP(N,M)=XG(M)
  336 CONTINUE
C
C     PILE ELEMENT PROPERTIES
C
      PROPP(N,1)=YMP
      PROPP(N,2)=PRP
      PROPP(N,3)=FRP
      PROPP(N,4)=ARP
  337 CONTINUE
      WRITE(6,263)
  263 FORMAT(//'   INITIAL STRESSES IN PILE ELEMENTS')
      IF(HT1.GT.0.0)GO TO 519
      WRITE(6,261)
  261 FORMAT(//'   I   GPNU    DEPTH    HORZ.DIST      SIGIPZ
',
     1'  SIGIPR         ET          PR          FRP          ARP')
      DO 339 N=1,NUPEL
      WRITE(6,262)
  262 FORMAT(/)
      DO 339 M=1,NUGP
      WRITE(6,265) N,M,YDP(N,M),XDP(N,M),SIGIPY(N,M),SIGIPX(N,M)
     1,PROPP(N,1),PROPP(N,2),PROPP(N,3),PROPP(N,4)
  265 FORMAT(1(I6,2X,I3,4X,F7.4,4X,F7.4,4X,E13.6,2X,E13.6
     1,2X,E13.6,2X,F7.4,2X,E13.6,2X,E13.6))
      GO TO 339
  519 WRITE(6,266)
  266 FORMAT(//'   I  GPNU  DEPTH   DTH.B.WT  HORZ.DT    SIGIPZ
     ',
     1'  SIGIPR         ET          PR          FRP          ARP')
      DO 338 K=1,NUPEL
      WRITE(6,267)
  267 FORMAT(/)
      DO 338 J=1,NUGP
      WRITE(6,270) K,J,YDP(K,J),YDP1(K,J),XDP(K,J),SIGIPY(K,J)
     1,SIGIPX(K,J),PROPP(K,1),PROPP(K,2),PROPP(K,3),PROPP(K,4)
  270 FORMAT(1(I6,2X,I2,2X,F7.4,2X,F7.4,2X,F7.4,2X,E13.6,2X,E13.6
     1,2X,E13.6,2X,F6.4,2X,E13.6,2X,E13.6))
  338 CONTINUE
```

```
  339 CONTINUE
C
C    BANDWIDTH CALCULATION
C
      N=NOX*NNOY+1
      NBAND=(NPM(N,3)-NPM(N,1)+1)*3
      WRITE(6,275) NBAND
  275 FORMAT(//'    BANDWIDTH=',I5)
C
C    ASSIGNMENT OF THE NODAL LOADS
C
      READ(5,*) NLC,NINC
      WRITE(6,276) NLC,NINC
  276 FORMAT(//'    NO.LOADING CASES=',I3,/'
 NO.INCREMENTS=',I3)
      READ(5,*) HLOAD,CLOAD
      DO 340 L=1,NT
      B(L)=0.0
  340 CONTINUE
      I=3*NPP(NUPEL,3)-2
      DIA=2*(XX(3)-XX(1))
      II=I
      B(II-6)=HLOAD/60.
      B(II-5)=2.*CLOAD/(15.*DIA)
      B(II-4)=-HLOAD/180.
      B(II-3)=14.*HLOAD/45.
      B(II-2)=-8.*CLOAD/(5.*DIA)
      B(II-1)=-2.*HLOAD/5.
      B(II)=4.*HLOAD/45.
      B(II+1)=-6.*CLOAD/(5.*DIA)
      B(II+2)=-8.*HLOAD/45.
      WRITE(6,280)
  280 FORMAT(//'    LOAD MATRIX')
      WRITE(6,285)
  285 FORMAT(//'    NP   RADIAL    AXIAL    CIRCUMF       NP
 RADIA',
     1'L    AXIAL    CIRCUMF       NP   RADIAL    AXIAL
 CIRCUMF')
      WRITE(6,290) (N,B(3*N-2),B(3*N-1),B(3*N),N=1,LL)
  290 FORMAT(//1(I6,3F10.4,I10,3F10.4,I10,3F10.4))
C
C    ****ASSEMBLY OF STIFFNESS****
C
C
C    INITIALISE A-MATRIX
C
      NPL=NPM(NUMEL,3)*3
      DO 341 I=1,NPL
      DO 341 J=1,NBAND
      A(I,J)=0.0
  341 CONTINUE
C
C    MEDIUM ELEMENTS
C
      READ(5,*) NHAR,THETA1
      WRITE(6,295) NHAR,THETA1
  295 FORMAT(//'    NUMBER OF HARMONICS=',I3,/'    ANGLE
 AROUND PILE='
     1,F4.1)
      DO 344 N=1,NUMEL
      CALL STIFFM(N)
      I=1
      DO 342 II=1,8
      LM(I)=3*NPM(N,II)-2
      LM(I+1)=LM(I)+1
      LM(I+2)=LM(I)+2
      I=I+3
  342 CONTINUE
      DO 343 J=1,24
      JJ=LM(J)
      DO 343 K=1,24
      KK=LM(K)
      IF(KK.LT.JJ)GO TO 343
      KK=KK-JJ+1
      A(JJ,KK)=A(JJ,KK)+S(J,K)
  343 CONTINUE
  344 CONTINUE
C
C    FRICTION ELEMENTS
C
      DO 347 N=1,NUFEL
      CALL STIFFF(N)
      I=1
      DO 345 II=1,6
      LF(I)=3*NPF(N,II)-2
      LF(I+1)=LF(I)+1
      LF(I+2)=LF(I)+2
      I=I+3
  345 CONTINUE
      DO 346 J=1,18
      JJ=LF(J)
      DO 346 K=1,18
      KK=LF(K)
      IF(KK.LT.JJ)GO TO 346
      KK=KK-JJ+1
      A(JJ,KK)=A(JJ,KK)+S(J,K)
  346 CONTINUE
  347 CONTINUE
C
C    PILE ELEMENTS
C
      DO 350 N=1,NUPEL
      CALL STIFFP(N)
      I=1
      DO 348 II=1,8
      LP(I)=3*NPP(N,II)-2
      LP(I+1)=LP(I)+1
      LP(I+2)=LP(I)+2
      I=I+3
  348 CONTINUE
```

```
      DO 349 J=1,24
      JJ=LP(J)
      DO 349 K=1,24
      KK=LP(K)
      IF(KK.LT.JJ)GO TO 349
      KK=KK-JJ+1
      A(JJ,KK)=A(JJ,KK)+S(J,K)
  349 CONTINUE
  350 CONTINUE
C
C     BOUNDARY CONDITIONS WITHIN THE BLOCK
C
C     NFIX = 0 RADIAL,VERTICAL AND CIRCUMFRENTIAL
DISPLACMENTS = 0
C     NFIX = 1 RADIAL AND VERTICAL DISPLACEMENTS = 0
C     NFIX = 2 RADIAL AND CIRCUMFRENTIAL DISPLACEMENTS =
0
C     NFIX = 3 VERTICAL AND CIRCUMFRENTAL DISPLACEMENTS
= 0
C     NFIX = 4 RADIAL DISPLACEMENTS = 0
C     NFIX = 5 VERTICAL DISPLACEMENTS = 0
C     NFIX = 6 CIRCUMFRENTIAL DISPLACEMENTS = 0
C
      READ(5,*) NUMBC
      READ(5,*) (NPB(L),NFIX(L),L=1,NUMBC)
      WRITE(6,2000)
 2000 FORMAT(//'    NODE NUMBER AND BOUNDARY CONDITION')
      WRITE(6,2001)
 2001 FORMAT(//'    NPB  NFIX  NPB  NFIX  NPB  NFIX  NPB  NFIX
NPB  N',
     1'FIX  NPB  NFIX  NPB  NFIX'//)
      WRITE (6,2002) (NPB(L),NFIX(L),L=1,NUMBC)
 2002 FORMAT(1(4X,I3,3X,I2,3X,I3,3X,I2,3X,I3,3X,I2,3X,I3,3X,I2
     1,3X,I3,3X,I2,3X,I3,3X,I2,3X,I3,3X,I2))
      NT=3*NPM(NUMEL,3)
      DO 351 L=1,NUMBC
      M=NPB(L)
      IF(NFIX(L).EQ.3)GO TO 520
      IF(NFIX(L).EQ.5)GO TO 520
      IF(NFIX(L).EQ.6)GO TO 521
      N=3*M-2
      CALL MODIFY(N)
      IF(NFIX(L).EQ.2)GO TO 521
      IF(NFIX(L).EQ.4)GO TO 351
  520 N=3*M-1
      CALL MODIFY(N)
      IF(NFIX(L).EQ.1)GO TO 351
      IF(NFIX(L).EQ.5)GO TO 351
  521 N=3*M
      CALL MODIFY(N)
  351 CONTINUE
C
C     SOLVE FOR DISPLACEMENTS
C
      CALL SOLVE
      DO 352 N=1,NT
      BTOT(N)=BTOT(N)+B(N)
  352 CONTINUE
      WRITE(6,2010)
 2010 FORMAT(//'    AMPLITUDES OF DISPLACEMENTS FOR
MEDIUM ELEMENTS')
      WRITE(6,2011)
 2011 FORMAT(//'    NP     RADIAL        AXIAL         CIRCUMF
',
     1'    NP      RADIAL        AXIAL         CIRCUMF'//)
      NTL=0
      DO 354 NE=1,NUMEL
      DO 354 NP=1,8
      N=NPM(NE,NP)
      DO 353 I=1,NE
      DO 353 J=1,8
      IF(I.EQ.NE.AND.J.EQ.NP)GO TO 524
      IF(N.EQ.NPM(I,J))GO TO 354
  353 CONTINUE
  524 NTL=NTL+1
      NMMM(NTL)=N
  354 CONTINUE
C
C     CALL NAG FILE SUBROUTINE FOR SORTING A MATRIX
C
      IFAIL=0
      CALL M01CBF(NMMM,1,NTL,'A',IFAIL)
      IF(IFAIL.NE.0)GO TO 522
      GO TO 523
  522 WRITE(6,2016)
 2016 FORMAT(//'    IFAIL NOT EQUAL TO ZERO'/'    IFAIL=',I3)
      STOP
  523 WRITE(6,2012)
(NMMM(N),BTOT(3*NMMM(N)-2),BTOT(3*NMMM(N)-1)
     1,BTOT(3*NMMM(N)),N=1,NTL)
 2012 FORMAT(1(I6,2X,E13.6,2X,E13.6,2X,E13.6,I10,4X,E13.6,2X,E13.6,2X
     1,E13.6))
      WRITE(6,2014)
 2014 FORMAT(//'    AMPLITUDES OF DISPLACEMENTS FOR
FRICTION ELEMENTS')
      WRITE(6,2011)
      NTL=0
      DO 356 NE=1,NUFEL
      DO 356 NP=1,6
      N=NPF(NE,NP)
      DO 355 I=1,NE
      DO 355 J=1,6
      IF(I.EQ.NE.AND.J.EQ.NP)GO TO 525
      IF(N.EQ.NPF(I,J))GO TO 356
  355 CONTINUE
  525 NTL=NTL+1
      NFFF(NTL)=N
  356 CONTINUE
C
C     CALL NAG FILE SUBROUTINE
```

```
C
      CALL M01CBF(NFFF,1,NTL,'A',IFAIL)
      IF(IFAIL.NE.0)GO TO 522
      WRITE(6,2012) (NFFF(N),BTOT(3*NFFF(N)-2),BTOT(3*NFFF(N)-1)
     1,BTOT(3*NFFF(N))),N=1,NTL)
      WRITE(6,2015)
 2015 FORMAT(//'    AMPLITUDES OF DISPLACEMENTS FOR PILE
ELEMENTS')
      WRITE(6,2011)
      NTL=0
      DO 358 NE=1,NUPEL
      DO 358 NP=1,8
      N=NPP(NE,NP)
      DO 357 I=1,NE
      DO 357 J=1,8
      IF(I.EQ.NE.AND.J.EQ.NP)GO TO 526
      IF(N.EQ.NPP(I,J))GO TO 358
  357 CONTINUE
  526 NTL=NTL+1
      NPPP(NTL)=N
  358 CONTINUE
C
C     CALL NAG FILE SUBROUTINE
C
      CALL M01CBF(NPPP,1,NTL,'A',IFAIL)
      IF(IFAIL.NE.0)GO TO 522
      WRITE(6,2012) (NPPP(N),BTOT(3*NPPP(N)-2),BTOT(3*NPPP(N)-1)
     1,BTOT(3*NPPP(N))),N=1,NTL)
C
C     COMPUTATION OF STRESSES IN MEDIUM ELEMENTS
C
      DO 359 N=1,NUMEL
      CALL STRESSM(N)
  359 CONTINUE
      WRITE(6,2020)
 2020 FORMAT(//'    STRESSES DUE TO APPLIED LOADS IN MEDIUM
ELEMENTS')
      WRITE(6,2021)
 2021 FORMAT(//'   I   GPNU    SIGMX        SIGMY        SIGMZ
',
     1'      SIGMXY       SIGMXZ       SIGMYZ')
      DO 360 N=1,NUMEL
      WRITE(6,2023)
 2023 FORMAT(/)
      DO 360 M=1,NUGP
      WRITE(6,2022)
N,M,SIGMX(N,M),SIGMY(N,M),SIGMZ(N,M),SIGMXY(N,M)
     1,SIGMXZ(N,M),SIGMYZ(N,M)
 2022 FORMAT(1(I6,2X,I3,3X,E13.6,2X,E13.6,2X,E13.6,2X,E13.6,2X,E13.6
     1,2X,E13.6))
  360 CONTINUE
      WRITE(6,2030)
 2030 FORMAT(//'    RESULTANT OF INITIAL AND APPLIED
STRESSES IN MEDIU',
     1'M ELEMENTS')
      WRITE(6,2021)
      DO 361 N=1,NUMEL
      WRITE(6,2023)
      DO 361 M=1,NUGP
      SIGMX(N,M)=SIGMX(N,M)+SIGIMX(N,M)
      SIGMY(N,M)=SIGMY(N,M)+SIGIMY(N,M)
      SIGMZ(N,M)=SIGMZ(N,M)+SIGIMZ(N,M)
      WRITE(6,2022)
N,M,SIGMX(N,M),SIGMY(N,M),SIGMZ(N,M),SIGMXY(N,M)
     1,SIGMXZ(N,M),SIGMYZ(N,M)
  361 CONTINUE
C
C     COMPUTATION OF STRESSES IN FRICTION ELEMENTS
C
      DO 362 N=1,NUFEL
      CALL STRESSF(N)
  362 CONTINUE
      WRITE(6,2040)
 2040 FORMAT(//'    STRESSES DUE TO APPLIED LOADS ')
      WRITE(6,2041)
 2041 FORMAT(//'   IN HORIZONTAL FRICTION ELEMENTS')
      WRITE(6,2042)
 2042 FORMAT(//'   I   GPNU    SIGFNZ       SIGFSR       SIGFSC')
      IF(NUGP.EQ.4)NN=2
      IF(NUGP.EQ.9)NN=3
      DO 363 N=1,NEXP
      WRITE(6,2044)
 2044 FORMAT(/)
      DO 363 M=1,NUGP
      WRITE(6,2043) N,M,SIGFN(N,M),SIGFSX(N,M),SIGFSY(N,M)
 2043 FORMAT(1(I6,2X,I3,3X,E13.6,2X,E13.6,2X,E13.6))
  363 CONTINUE
      WRITE(6,2050)
 2050 FORMAT(//'   IN VERTICAL FRICTION ELEMENTS')
      WRITE(6,2051)
 2051 FORMAT(//'   I   GPNU    SIGFNR       SIGFSZ       SIGFC')
      NEXP1=NEXP+1
      DO 364 N=NEXP1,NUFEL
      WRITE(6,2044)
      DO 364 M=1,NUGP
      WRITE(6,2043) N,M,SIGFN(N,M),SIGFSX(N,M),SIGFSY(N,M)
  364 CONTINUE
      DO 365 N=1,NUFEL
      DO 365 M=1,NUGP
      SIGFN(N,M)=SIGFN(N,M)+SIGIFN(N,M)
  365 CONTINUE
      WRITE(6,2060)
 2060 FORMAT(//'    RESULTANT OF INITIAL AND APPLIED
STRESSES')
      WRITE(6,2061)
 2061 FORMAT(//'   IN HORIZONTIAL FRICTION ELEMENTS')
      WRITE(6,2042)
      DO 366 N=1,NEXP
      WRITE(6,2044)
      DO 366 M=1,NUGP
```

```
      WRITE(6,2043) N,M,SIGFN(N,M),SIGFSX(N,M),SIGFSY(N,M)
  366 CONTINUE
      WRITE(6,2070)
 2070 FORMAT(//'    IN VERTICAL FRICTION ELEMENTS')
      WRITE(6,2051)
      DO 367 N=NEXP1,NUFEL
      WRITE(6,2044)
      DO 367 M=1,NUGP
      WRITE(6,2043) N,M,SIGFN(N,M),SIGFSX(N,M),SIGFSY(N,M)
  367 CONTINUE
C
C     COMPUTATION OF STRESSES IN PILE ELEMENTS
C
      DO 368 N=1,NUPEL
      CALL STRESSP(N)
  368 CONTINUE
      WRITE(6,2080)
 2080 FORMAT(//'    STRESSES DUE TO APPLIED LOADS IN PILE
ELEMENTS')
      WRITE(6,2081)
 2081 FORMAT(//'    I    GPNU    SIGPX        SIGPY        SIGPZ  ',
     1'       SIGPXY      SIGPXZ       SIGPYZ')
      DO 369 N=1,NUPEL
      WRITE(6,2083)
 2083 FORMAT(/)
      DO 369 M=1,NUGP
      WRITE(6,2082)
N,M,SIGPX(N,M),SIGPY(N,M),SIGPZ(N,M),SIGPXY(N,M)
     1,SIGPXZ(N,M),SIGPYZ(N,M)
 2082 FORMAT(1(I6,2X,I3,3X,E13.6,2X,E13.6,2X,E13.6,2X,E13.6,2X,E13.6
     1,2X,E13.6))
  369 CONTINUE
      WRITE(6,2090)
 2090 FORMAT(//'    RESULTANT OF INITIAL AND APPLIED
STRESSES IN PILE ',
     1'  ELEMENTS')
      WRITE(6,2081)
      DO 370 N=1,NUPEL
      WRITE(6,2083)
      DO 370 M=1,NUGP
      SIGPX(N,M)=SIGPX(N,M)+SIGIPX(N,M)
      SIGPY(N,M)=SIGPY(N,M)+SIGIPY(N,M)
      SIGPZ(N,M)=SIGPZ(N,M)+SIGIPZ(N,M)
      WRITE(6,2082)
N,M,SIGPX(N,M),SIGPY(N,M),SIGPZ(N,M),SIGPXY(N,M)
     1,SIGPXZ(N,M),SIGPYZ(N,M)
  370 CONTINUE
C
C     NODES AT CENTRE OF PILE
C
      NCTL=0
      DO 371 N=1,NUPEL,NEXP
      NCTL=NCTL+1
      NCPP(NCTL)=NPP(N,1)
      NCPP(NCTL+1)=NPP(N,8)
```

```
      NCTL=NCTL+1
  371 CONTINUE
      NCTL=NCTL+1
      NEXPC=NEXP*NEYP-NEXP+1
      NCPP(NCTL)=NPP(NEXPC,4)
C
C     DISPLACEMEMT OF CENTRE OF PILE
C
      DO 372 N=1,NCTL
      NCP=(3*NCPP(N)-2)
      YCP(N,1)=BTOT(NCP)
  372 CONTINUE
C
C     COMPUTATION OF SLOPE,BENDING MOMENT,SHEAR AND
SOIL-PRESSURE
C
      READ(5,*) ICODE
C
C     ICODE=0 FIXED HEAD
C     ICODE NE 0 FREE HEAD
C
      WRITE(6,2100)
 2100 FORMAT(//'    FORCES CALCULATED USING DISPLACEMENTS
AT THE CENT',
     1'RE  OF THE PILE')
      WRITE(6,2101)
 2101 FORMAT(//'   NP    DEPTH   DISPLACEMENT     SLOPE
MOMEN',
     1'T        SHEAR        PRESSURE       SGRM          FRP'//)
      DO 373 I=2,(NCTL-1)
      K=NCPP(I)
      K1=NCPP(I-1)
      K2=NCPP(I+1)
      H=YORD(K)-YORD(K1)
      AH=YORD(K2)-YORD(K)
      ALP=AH/H
      YCP(I,2)=(YCP((I-1),1)/(ALP*(1.0+ALP))+(1.0-1.0/ALP)*YCP(I,1)
     1-ALP*YCP((I+1),1)/(1.0+ALP))/H
      YCP(I,3)=(2.0*YCP((I-1),1)/(ALP*(1.0+ALP))-2.0*YCP(I,1)/ALP
     1+2.0*YCP((I+1),1)/(1.0+ALP))/(H**2)
      YCP(I,3)=YCP(I,3)*PROPP(1,3)
  373 CONTINUE
      DO 374 I=2,(NCTL-1)
      K=NCPP(I)
      K1=NCPP(I-1)
      K2=NCPP(I+1)
      H=YORD(K)-YORD(K1)
      AH=YORD(K2)-YORD(K)
      ALP=AH/H
      YCP(I,4)=(YCP((I-1),3)/(ALP*(1.0+ALP))+(1.0-1.0/ALP)*YCP(I,3)
     1-ALP*YCP((I+1),3)/(1.0+ALP))/H
      YCP(I,5)=-(2.0*YCP((I-1),3)/(ALP*(1.0+ALP))-2.0*YCP(I,3)/ALP
     1+2.0*YCP((I+1),3)/(1.0+ALP))/(H**2)
  374 CONTINUE
      K=NCPP(1)
```

```
      K1=NCPP(2)
      H=YORD(K)-YORD(K1)
      YF=2.0*YCP(1,1)-YCP(2,1)
      YCP(1,2)=(YF-YCP(1,1))/(2.0*H)
      YCP(1,3)=0.0
      YCP(1,4)=0.0
      YCP(1,5)=2.0*YCP(2,5)/(H**2)
      K=NCPP(NCTL)
      K1=NCPP(NCTL-1)
      H=YORD(K)-YORD(K1)
      IF(ICODE.EQ.0)GO TO 528
      YF=CLOAD*H**2/PROPP(1,3)+2.0*YCP(NCTL,1)
     1-YCP((NCTL-1),1)
      YCP(NCTL,2)=(YCP((NCTL-1),1)-YF)/(2.0*H)
      YCP(NCTL,3)=CLOAD
      GO TO 529
  528 CONTINUE
C 528 YCP(NCTL,2)=0.0
      YCP(NCTL,2)=0.0

 YCP(NCTL,3)=2.0*PROPP(1,3)*(YCP((NCTL-1),1)-YCP(NCTL,1))/(H**2)
  529 CONTINUE
C 529 YCP(NCTL,4)=HLOAD
      YCP(NCTL,4)=HLOAD
      YF2=YCP((NCTL-1),3)-HLOAD*2.0*H
      YCP(NCTL,5)=(YCP((NCTL-1),3)-2.0*YCP(NCTL,3)+YF2)/(H**2.0)
      J=NCPP(NCTL)
      DO 375 I=1,NCTL
      K=NCPP(I)
      DEPTH=YORD(J)-YORD(K)
      SM=YCP(I,5)/YCP(I,1)
      WRITE(6,2110) NCPP(I),DEPTH,YCP(I,1),YCP(I,2),YCP(I,3),YCP(I,4)
     1,YCP(I,5),SM,PROPP(1,3)
 2110 FORMAT(1(I6,2X,F6.3,2X,E13.6,2X,E13.6,2X,E13.6,2X,E13.6,2X
     1,E13.6,2X,E13.6,2X,E13.6))
  375 CONTINUE
C
C     NEW LINES IN HERE
C
      STOP
      END
      SUBROUTINE STIFFM(N)
C
C     STIFFNESS OF MEDIUM ELEMENTS
C
      IMPLICIT REAL*8 (A-H,O-Z)

COMMON/FIRST/NUGP,NHAR,THETA1,S(24,24),XORD(300),YORD(300),
GSWT(3)
     1,GS(3)
      COMMON/SECOND/NPM(60,8),PROPM(60,2)
      DIMENSION D(6,6),B(6,24),DB(6,24),BTDB(24,24)
      PI=3.14159265359
      IJ=NPM(N,1)
      I1=NPM(N,5)
      I2=NPM(N,2)
      J1=NPM(N,8)
      J2=NPM(N,4)
      AA=(XORD(I2)-XORD(IJ))/2.0
      BB=(YORD(J2)-YORD(IJ))/2.0
      XC=XORD(I1)
      YC=YORD(J1)
      DO 3440 I=1,24
      DO 3440 J=1,24
      S(I,J)=0.0
 3440 CONTINUE
      IF(NUGP.EQ.4)NN=2
      IF(NUGP.EQ.9)NN=3
      DO 3446 IN=1,NN
      X=GS(IN)
      DO 3446 JN=1,NN
      Y=GS(JN)
      ET=PROPM(N,1)
      PR=PROPM(N,2)
      COM=ET*(1.0-PR)/((1.0+PR)*(1.0-2.0*PR))
      DO 3441 I=1,6
      DO 3441 J=1,6
      D(I,J)=0.0
 3441 CONTINUE
      D(1,1)=COM
      D(1,2)=COM*PR/(1.0-PR)
      D(1,3)=D(1,2)
      D(2,1)=D(1,2)
      D(2,2)=COM
      D(2,3)=D(1,2)
      D(3,1)=D(1,2)
      D(3,2)=D(1,2)
      D(3,3)=COM
      D(4,4)=COM*(0.5-PR)/(1.0-PR)
      D(5,5)=D(4,4)
      D(6,6)=D(4,4)
      DO 3442 I=1,6
      DO 3442 J=1,24
      B(I,J)=0.0
 3442 CONTINUE
      AN1=(X**2+Y**2-1.0-X**2*Y-Y**2*X+X*Y)/4.0
      AN2=(X**2+Y**2-1.0-X**2*Y+Y**2*X-X*Y)/4.0
      AN3=(X**2+Y**2-1.0+X**2*Y+Y**2*X+X*Y)/4.0
      AN4=(X**2+Y**2-1.0+X**2*Y-Y**2*X-X*Y)/4.0
      AN5=(1.0-X**2)*(1.0-Y)/2.0
      AN6=(1.0+X)*(1.0-Y**2)/2.0
      AN7=(1.0-X**2)*(1.0+Y)/2.0
      AN8=(1.0-X)*(1.0-Y**2)/2.0
      CC=(AA*X+XC)
      B(1,1)=(2.0*X+Y-2.0*X*Y-Y**2)/(4.0*AA)
      B(1,4)=(2.0*X-Y-2.0*X*Y+Y**2)/(4.0*AA)
      B(1,7)=(2.0*X+Y+2.0*X*Y+Y**2)/(4.0*AA)
      B(1,10)=(2.0*X-Y+2.0*X*Y-Y**2)/(4.0*AA)
      B(1,13)=(X*Y-X)/AA
      B(1,16)=(1.0-Y**2)/(2.0*AA)
```

```
      B(1,19)=(-X*Y-X)/AA
      B(1,22)=(Y**2-1.0)/(2.0*AA)
      B(2,2)=(2.0*Y+X-2.0*X*Y-X**2)/(4.0*BB)
      B(2,5)=(2.0*Y-X+2.0*X*Y-X**2)/(4.0*BB)
      B(2,8)=(2.0*Y+X+2.0*X*Y+X**2)/(4.0*BB)
      B(2,11)=(2.0*Y-X-2.0*X*Y+X**2)/(4.0*BB)
      B(2,14)=(X**2-1.0)/(2.0*BB)
      B(2,17)=(-X*Y-Y)/BB
      B(2,20)=(1.0-X**2)/(2.0*BB)
      B(2,23)=(X*Y-Y)/BB
      B(3,1)=AN1/CC
      B(3,3)=AN1*NHAR/CC
      B(3,4)=AN2/CC
      B(3,6)=AN2*NHAR/CC
      B(3,7)=AN3/CC
      B(3,9)=AN3*NHAR/CC
      B(3,10)=AN4/CC
      B(3,12)=AN4*NHAR/CC
      B(3,13)=AN5/CC
      B(3,15)=AN5*NHAR/CC
      B(3,16)=AN6/CC
      B(3,18)=AN6*NHAR/CC
      B(3,19)=AN7/CC
      B(3,21)=AN7*NHAR/CC
      B(3,22)=AN8/CC
      B(3,24)=AN8*NHAR/CC
      B(4,1)=B(2,2)
      B(4,2)=B(1,1)
      B(4,4)=B(2,5)
      B(4,5)=B(1,4)
      B(4,7)=B(2,8)
      B(4,8)=B(1,7)
      B(4,10)=B(2,11)
      B(4,11)=B(1,10)
      B(4,13)=B(2,14)
      B(4,14)=B(1,13)
      B(4,16)=B(2,17)
      B(4,17)=B(1,16)
      B(4,19)=B(2,20)
      B(4,20)=B(1,19)
      B(4,22)=B(2,23)
      B(4,23)=B(1,22)
      B(5,1)=-B(3,3)
      B(5,3)=B(1,1)-B(3,1)
      B(5,4)=-B(3,6)
      B(5,6)=B(1,4)-B(3,4)
      B(5,7)=-B(3,9)
      B(5,9)=B(1,7)-B(3,7)
      B(5,10)=-B(3,12)
      B(5,12)=B(1,10)-B(3,10)
      B(5,13)=-B(3,15)
      B(5,15)=B(1,13)-B(3,13)
      B(5,16)=-B(3,18)
      B(5,18)=B(1,16)-B(3,16)
      B(5,19)=-B(3,21)
      B(5,21)=B(1,19)-B(3,19)
      B(5,22)=-B(3,24)
      B(5,24)=B(1,22)-B(3,22)
      B(6,2)=B(5,1)
      B(6,3)=B(4,1)
      B(6,5)=B(5,4)
      B(6,6)=B(4,4)
      B(6,8)=B(5,7)
      B(6,9)=B(4,7)
      B(6,11)=B(5,10)
      B(6,12)=B(4,10)
      B(6,14)=B(5,13)
      B(6,15)=B(4,13)
      B(6,17)=B(5,16)
      B(6,18)=B(4,16)
      B(6,20)=B(5,19)
      B(6,21)=B(4,19)
      B(6,23)=B(5,22)
      B(6,24)=B(4,22)
      DO 3443 J=1,24
      DO 3443 I=1,6
      DB(I,J)=0.0
      DO 3443 K=1,6
      DB(I,J)=DB(I,J)+D(I,K)*B(K,J)
 3443 CONTINUE
      DO 3444 J=1,24
      DO 3444 I=1,24
      BTDB(I,J)=0.0
      DO 3444 K=1,6
      BTDB(I,J)=BTDB(I,J)+B(K,I)*DB(K,J)
 3444 CONTINUE
      DO 3445 I=1,24
      DO 3445 J=1,24
      BTDB(I,J)=(AA*X+XC)*BTDB(I,J)*GSWT(IN)*GSWT(JN)
      S(I,J)=S(I,J)+BTDB(I,J)
 3445 CONTINUE
 3446 CONTINUE
      CONST=PI*AA*BB
      DO 3447 I=1,24
      DO 3447 J=1,24
      S(I,J)=CONST*S(I,J)
 3447 CONTINUE
      RETURN
      END
      SUBROUTINE STIFFF(N)
C
C     STIFFNESS OF FRITION ELEMENTS
C
      IMPLICIT REAL*8 (A-H,O-Z)

COMMON/FIRST/NUGP,NHAR,THETA1,S(24,24),XORD(300),YORD(300),
GSWT(3)
     1,GS(3)
      COMMON/THIRD/NPF(20,6),STN(20),STS(20),NEXP
      DIMENSION D(3,3),B(3,18),DB(3,18),BTDB(18,18)
```

```
      PI=3.14159265359
      IJ=NPF(N,1)
      I2=NPF(N,5)
      I3=NPF(N,2)
      AA=(XORD(I3)-XORD(IJ))/2.0
      BB=(YORD(I3)-YORD(IJ))/2.0
      IF(N.LE.NEXP)AB=AA
      IF(N.GT.NEXP)AB=BB
      XC=XORD(I2)
      YC=YORD(I2)
      DO 3470 I=1,18
      DO 3470 J=1,18
      S(I,J)=0.0
 3470 CONTINUE
      IF(NUGP.EQ.4)NN=2
      IF(NUGP.EQ.9)NN=3
      DO 3477 IN=1,NN
      Z=GS(IN)
      SSN=STN(N)
      STT=STS(N)
      DO 3471 I=1,3
      DO 3471 J=1,3
      D(I,J)=0.0
 3471 CONTINUE
      IF(N.GT.NEXP)GO TO 5470
      D(1,1)=STT
      D(2,2)=SSN
      D(3,3)=STT
      GO TO 5471
 5470 D(1,1)=SSN
      D(2,2)=STT
      D(3,3)=STT
 5471 CONTINUE
      DO 3472 I=1,3
      DO 3472 J=1,18
      B(I,J)=0.0
 3472 CONTINUE
      AN1=Z*(Z-1.0)/2
      AN2=Z*(Z+1.0)/2
      AN3=(1.0-Z**2)
      B(1,1)=AN1
      B(1,4)=AN2
      B(1,7)=-AN2
      B(1,10)=-AN1
      B(1,13)=AN3
      B(1,16)=-AN3
      B(2,2)=AN1
      B(2,5)=AN2
      B(2,8)=-AN2
      B(2,11)=-AN1
      B(2,14)=AN3
      B(2,17)=-AN3
      B(3,3)=AN1
      B(3,6)=AN2
      B(3,9)=-AN2
      B(3,12)=-AN1
      B(3,15)=AN3
      B(3,18)=-AN3
      IF(N.LE.NEXP)CCH=-1.0
      IF(N.GT.NEXP)CCH=1.0
      DO 3473 I=1,3
      DO 3473 J=1,18
      B(I,J)=B(I,J)*CCH
 3473 CONTINUE
      DO 3474 J=1,18
      DO 3474 I=1,3
      DB(I,J)=0.0
      DO 3474 K=1,3
      DB(I,J)=DB(I,J)+D(I,K)*B(K,J)
 3474 CONTINUE
      DO 3475 J=1,18
      DO 3475 I=1,18
      BTDB(I,J)=0.0
      DO 3475 K=1,3
      BTDB(I,J)=BTDB(I,J)+B(K,I)*DB(K,J)
 3475 CONTINUE
      CC=AA*Z+XC
      IF(N.LE.NEXP)CH=CC
      IF(N.GT.NEXP)CH=1.0
      DO 3476 I=1,18
      DO 3476 J=1,18
      BTDB(I,J)=CH*BTDB(I,J)*GSWT(IN)
      S(I,J)=S(I,J)+BTDB(I,J)
 3476 CONTINUE
 3477 CONTINUE
      IF(N.LE.NEXP)CONST=PI*AA
      IF(N.GT.NEXP)CONST=PI*BB*XC
      DO 3478 I=1,18
      DO 3478 J=1,18
      S(I,J)=CONST*S(I,J)
 3478 CONTINUE
      RETURN
      END
      SUBROUTINE STIFFP(N)
C
C     STIFFNESS OF PILE ELEMENTS
C
      IMPLICIT REAL*8 (A-H,O-Z)

COMMON/FIRST/NUGP,NHAR,THETA1,S(24,24),XORD(300),YORD(300),
GSWT(3)
     1,GS(3)
      COMMON/FOURTH/NPP(60,8),PROPP(20,4)
      DIMENSION D(6,6),B(6,24),DB(6,24),BTDB(24,24)
      PI=3.14159265359
      IJ=NPP(N,1)
      I1=NPP(N,5)
      I2=NPP(N,2)
      J1=NPP(N,8)
      J2=NPP(N,4)
```

```
      AA=(XORD(I2)-XORD(IJ))/2.0
      BB=(YORD(J2)-YORD(IJ))/2.0
      XC=XORD(I1)
      YC=YORD(J1)
      DO 3500 I=1,24
      DO 3500 J=1,24
      S(I,J)=0.0
 3500 CONTINUE
      IF(NUGP.EQ.4)NN=2
      IF(NUGP.EQ.9)NN=3
      DO 3506 IN=1,NN
      X=GS(IN)
      DO 3506 JN=1,NN
      Y=GS(JN)
      ET=PROPP(N,1)
      PR=PROPP(N,2)
      COM=ET*(1.0-PR)/((1.0+PR)*(1.0-2.0*PR))
      DO 3501 I=1,6
      DO 3501 J=1,6
      D(I,J)=0.0
 3501 CONTINUE
      D(1,1)=COM
      D(1,2)=COM*PR/(1.0-PR)
      D(1,3)=D(1,2)
      D(2,1)=D(1,2)
      D(2,2)=COM
      D(2,3)=D(1,2)
      D(3,1)=D(1,2)
      D(3,2)=D(1,2)
      D(3,3)=COM
      D(4,4)=COM*(0.5-PR)/(1.0-PR)
      D(5,5)=D(4,4)
      D(6,6)=D(4,4)
      DO 3502 I=1,6
      DO 3502 J=1,24
      B(I,J)=0.0
 3502 CONTINUE
      AN1=(X**2+Y**2-1.0-X**2*Y-Y**2*X+X*Y)/4.0
      AN2=(X**2+Y**2-1.0-X**2*Y+Y**2*X-X*Y)/4.0
      AN3=(X**2+Y**2-1.0+X**2*Y+Y**2*X+X*Y)/4.0
      AN4=(X**2+Y**2-1.0+X**2*Y-Y**2*X-X*Y)/4.0
      AN5=(1.0-X**2)*(1.0-Y)/2.0
      AN6=(1.0+X)*(1.0-Y**2)/2.0
      AN7=(1.0-X**2)*(1.0+Y)/2.0
      AN8=(1.0-X)*(1.0-Y**2)/2.0
      CC=(AA*X+XC)
      B(1,1)=(2.0*X+Y-2.0*X*Y-Y**2)/(4.0*AA)
      B(1,4)=(2.0*X-Y-2.0*X*Y+Y**2)/(4.0*AA)
      B(1,7)=(2.0*X+Y+2.0*X*Y+Y**2)/(4.0*AA)
      B(1,10)=(2.0*X-Y+2.0*X*Y-Y**2)/(4.0*AA)
      B(1,13)=(X*Y-X)/AA
      B(1,16)=(1.0-Y**2)/(2.0*AA)
      B(1,19)=(-X*Y-X)/AA
      B(1,22)=(Y**2-1.0)/(2.0*AA)
      B(2,2)=(2.0*Y+X-2.0*X*Y-X**2)/(4.0*BB)
      B(2,5)=(2.0*Y-X+2.0*X*Y-X**2)/(4.0*BB)
      B(2,8)=(2.0*Y+X+2.0*X*Y+X**2)/(4.0*BB)
      B(2,11)=(2.0*Y-X-2.0*X*Y+X**2)/(4.0*BB)
      B(2,14)=(X**2-1.0)/(2.0*BB)
      B(2,17)=(-X*Y-Y)/BB
      B(2,20)=(1.0-X**2)/(2.0*BB)
      B(2,23)=(X*Y-Y)/BB
      B(3,1)=AN1/CC
      B(3,3)=AN1*NHAR/CC
      B(3,4)=AN2/CC
      B(3,6)=AN2*NHAR/CC
      B(3,7)=AN3/CC
      B(3,9)=AN3*NHAR/CC
      B(3,10)=AN4/CC
      B(3,12)=AN4*NHAR/CC
      B(3,13)=AN5/CC
      B(3,15)=AN5*NHAR/CC
      B(3,16)=AN6/CC
      B(3,18)=AN6*NHAR/CC
      B(3,19)=AN7/CC
      B(3,21)=AN7*NHAR/CC
      B(3,22)=AN8/CC
      B(3,24)=AN8*NHAR/CC
      B(4,1)=B(2,2)
      B(4,2)=B(1,1)
      B(4,4)=B(2,5)
      B(4,5)=B(1,4)
      B(4,7)=B(2,8)
      B(4,8)=B(1,7)
      B(4,10)=B(2,11)
      B(4,11)=B(1,10)
      B(4,13)=B(2,14)
      B(4,14)=B(1,13)
      B(4,16)=B(2,17)
      B(4,17)=B(1,16)
      B(4,19)=B(2,20)
      B(4,20)=B(1,19)
      B(4,22)=B(2,23)
      B(4,23)=B(1,22)
      B(5,1)=-B(3,3)
      B(5,3)=B(1,1)-B(3,1)
      B(5,4)=-B(3,6)
      B(5,6)=B(1,4)-B(3,4)
      B(5,7)=-B(3,9)
      B(5,9)=B(1,7)-B(3,7)
      B(5,10)=-B(3,12)
      B(5,12)=B(1,10)-B(3,10)
      B(5,13)=-B(3,15)
      B(5,15)=B(1,13)-B(3,13)
      B(5,16)=-B(3,18)
      B(5,18)=B(1,16)-B(3,16)
      B(5,19)=-B(3,21)
      B(5,21)=B(1,19)-B(3,19)
      B(5,22)=-B(3,24)
      B(5,24)=B(1,22)-B(3,22)
```

```
      B(6,2)=B(5,1)
      B(6,3)=B(4,1)
      B(6,5)=B(5,4)
      B(6,6)=B(4,4)
      B(6,8)=B(5,7)
      B(6,9)=B(4,7)
      B(6,11)=B(5,10)
      B(6,12)=B(4,10)
      B(6,14)=B(5,13)
      B(6,15)=B(4,13)
      B(6,17)=B(5,16)
      B(6,18)=B(4,16)
      B(6,20)=B(5,19)
      B(6,21)=B(4,19)
      B(6,23)=B(5,22)
      B(6,24)=B(4,22)
      DO 3503 J=1,24
      DO 3503 I=1,6
      DB(I,J)=0.0
      DO 3503 K=1,6
      DB(I,J)=DB(I,J)+D(I,K)*B(K,J)
 3503 CONTINUE
      DO 3504 J=1,24
      DO 3504 I=1,24
      BTDB(I,J)=0.0
      DO 3504 K=1,6
      BTDB(I,J)=BTDB(I,J)+B(K,I)*DB(K,J)
 3504 CONTINUE
      DO 3505 I=1,24
      DO 3505 J=1,24
      BTDB(I,J)=(AA*X+XC)*BTDB(I,J)*GSWT(IN)*GSWT(JN)
      S(I,J)=S(I,J)+BTDB(I,J)
 3505 CONTINUE
 3506 CONTINUE
      CONST=PI*AA*BB
      DO 3507 I=1,24
      DO 3507 J=1,24
      S(I,J)=CONST*S(I,J)
 3507 CONTINUE
      RETURN
      END
      SUBROUTINE MODIFY(N)
C
C     BOUNDARY CONDITION WITIN THE BLOCK
C
      IMPLICIT REAL*8 (A-H,O-Z)
      COMMON/FIFTH/A(900,80),B(900),NBAND,NT
      DO 3351 M=2,NBAND
      K=N-M+1
      IF(K) 5511,5511,5510
5510 A(K,M)=0.0
5511 K=N+M-1
      IF(NT.LT.K)GO TO 3351
      A(N,M)=0.0
3351 CONTINUE
```

```
      A(N,1)=1.0
      B(N)=0.0
      RETURN
      END
      SUBROUTINE SOLVE
C
C     SOLVE FOR DISPLACEMENTS
C
      IMPLICIT REAL*8 (A-H,O-Z)
      COMMON/FIFTH/A(900,80),B(900),NBAND,NT
      DO 3522 N=1,NT
      IF(A(N,1).EQ.0.0)GO TO 3522
      B(N)=B(N)/A(N,1)
      DO 3521 L=2,NBAND
      IF(A(N,L).EQ.0.0)GO TO 3521
      C=A(N,L)/A(N,1)
      I=N+L-1
      IF(I.GT.NT)GO TO 9522
      J=0
      DO 3520 K=L,NBAND
      J=J+1
      A(I,J)=A(I,J)-A(N,K)*C
 3520 CONTINUE
      B(I)=B(I)-A(N,L)*B(N)
      A(N,L)=C
 3521 CONTINUE
 9522 CONTINUE
 3522 CONTINUE
      DO 3523 M=1,NT
      N=NT+1-M
      DO 3523 K=2,NBAND
      L=N+K-1
      IF(L.GT.NT)GO TO 3523
      B(N)=B(N)-A(N,K)*B(L)
 3523 CONTINUE
      RETURN
      END
      SUBROUTINE STRESSM(N)
C
C     COMPUTATION OF STRESS IN MEDIUM ELEMENTS
C
      IMPLICIT REAL*8 (A-H,O-Z)

COMMON/FIRST/NUGP,NHAR,THETA1,S(24,24),XORD(300),YORD(300)
     1,GSWT(3),GS(3)
      COMMON/SECOND/NPM(60,8),PROPM(60,2)
      COMMON/SIXTH/BTOT(900)

COMMON/SEVENTH/SIGMX(60,9),SIGMY(60,9),SIGMZ(60,9),SIGMXY(6
0,9)
     1,SIGMXZ(60,9),SIGMYZ(60,9)
      DIMENSION D(6,6),B(6,24),DB(6,24),U(24)
      PI=3.14159265359
      I=NPM(N,1)
      J=NPM(N,2)
```

```
      K=NPM(N,3)
      L=NPM(N,4)
      II=NPM(N,5)
      JJ=NPM(N,6)
      KK=NPM(N,7)
      LL=NPM(N,8)
      AA=(XORD(J)-XORD(I))/2.0
      BB=(YORD(K)-YORD(J))/2.0
      XC=XORD(II)
      YC=YORD(LL)
      THETA1=THETA1*PI/180
      ST=SIN(THETA1)
      CT=COS(THETA1)
      U(1)=BTOT(3*I-2)
      U(2)=BTOT(3*I-1)
      U(3)=BTOT(3*I)
      U(4)=BTOT(3*J-2)
      U(5)=BTOT(3*J-1)
      U(6)=BTOT(3*J)
      U(7)=BTOT(3*K-2)
      U(8)=BTOT(3*K-1)
      U(9)=BTOT(3*K)
      U(10)=BTOT(3*L-2)
      U(11)=BTOT(3*L-1)
      U(12)=BTOT(3*L)
      U(13)=BTOT(3*II-2)
      U(14)=BTOT(3*II-1)
      U(15)=BTOT(3*II)
      U(16)=BTOT(3*JJ-2)
      U(17)=BTOT(3*JJ-1)
      U(18)=BTOT(3*JJ)
      U(19)=BTOT(3*KK-2)
      U(20)=BTOT(3*KK-1)
      U(21)=BTOT(3*KK)
      U(22)=BTOT(3*LL-2)
      U(23)=BTOT(3*LL-1)
      U(24)=BTOT(3*LL)
      IF(NUGP.EQ.4)NN=2
      IF(NUGP.EQ.9)NN=3
      NN1=0
      DO 3594 IN=1,NN
      X=GS(IN)
      DO 3594 JN=1,NN
      Y=GS(JN)
      NN1=NN1+1
      ET=PROPM(N,1)
      PR=PROPM(N,2)
      COM=ET*(1.0-PR)/((1.0+PR)*(1.0-2.0*PR))
      DO 3590 I=1,6
      DO 3590 J=1,6
      D(I,J)=0.0
3590 CONTINUE
      D(1,1)=COM
      D(1,2)=COM*PR/(1.0-PR)
      D(1,3)=D(1,2)
      D(2,1)=D(1,2)
      D(2,2)=COM
      D(2,3)=D(1,2)
      D(3,1)=D(1,2)
      D(3,2)=D(1,2)
      D(3,3)=COM
      D(4,4)=COM*(0.5-PR)/(1.0-PR)
      D(5,5)=D(4,4)
      D(6,6)=D(4,4)
      DO 3591 I=1,6
      DO 3591 J=1,24
      B(I,J)=0.0
3591 CONTINUE
      AN1=(X**2+Y**2-1.0-X**2*Y-Y**2*X+X*Y)/4.0
      AN2=(X**2+Y**2-1.0-X**2*Y+Y**2*X-X*Y)/4.0
      AN3=(X**2+Y**2-1.0+X**2*Y+Y**2*X+X*Y)/4.0
      AN4=(X**2+Y**2-1.0+X**2*Y-Y**2*X-X*Y)/4.0
      AN5=(1.0-X**2)*(1.0-Y)/2.0
      AN6=(1.0+X)*(1.0-Y**2)/2.0
      AN7=(1.0-X**2)*(1.0+Y)/2.0
      AN8=(1.0-X)*(1.0-Y**2)/2.0
      CC=(AA*X+XC)
      B(1,1)=(2.0*X+Y-2.0*X*Y-Y**2)*CT/(4.0*AA)
      B(1,4)=(2.0*X-Y-2.0*X*Y+Y**2)*CT/(4.0*AA)
      B(1,7)=(2.0*X+Y+2.0*X*Y+Y**2)*CT/(4.0*AA)
      B(1,10)=(2.0*X-Y+2.0*X*Y-Y**2)*CT/(4.0*AA)
      B(1,13)=(X*Y-X)*CT/AA
      B(1,16)=(1.0-Y**2)*CT/(2.0*AA)
      B(1,19)=(-X*Y-X)*CT/AA
      B(1,22)=(Y**2-1.0)*CT/(2.0*AA)
      B(2,2)=(2.0*Y+X-2.0*X*Y-X**2)*CT/(4.0*BB)
      B(2,5)=(2.0*Y-X+2.0*X*Y-X**2)*CT/(4.0*BB)
      B(2,8)=(2.0*Y+X+2.0*X*Y+X**2)*CT/(4.0*BB)
      B(2,11)=(2.0*Y-X-2.0*X*Y+X**2)*CT/(4.0*BB)
      B(2,14)=(X**2-1.0)*CT/(2.0*BB)
      B(2,17)=(-X*Y-Y)*CT/BB
      B(2,20)=(1.0-X**2)*CT/(2.0*BB)
      B(2,23)=(X*Y-Y)*CT/BB
      B(3,1)=AN1*CT/CC
      B(3,3)=AN1*NHAR*CT/CC
      B(3,4)=AN2*CT/CC
      B(3,6)=AN2*NHAR*CT/CC
      B(3,7)=AN3*CT/CC
      B(3,9)=AN3*NHAR*CT/CC
      B(3,10)=AN4*CT/CC
      B(3,12)=AN4*NHAR*CT/CC
      B(3,13)=AN5*CT/CC
      B(3,15)=AN5*NHAR*CT/CC
      B(3,16)=AN6*CT/CC
      B(3,18)=AN6*NHAR*CT/CC
      B(3,19)=AN7*CT/CC
      B(3,21)=AN7*NHAR*CT/CC
      B(3,22)=AN8*CT/CC
      B(3,24)=AN8*NHAR*CT/CC
      B(4,1)=B(2,2)
```

```
      B(4,2)=B(1,1)
      B(4,4)=B(2,5)
      B(4,5)=B(1,4)
      B(4,7)=B(2,8)
      B(4,8)=B(1,7)
      B(4,10)=B(2,11)
      B(4,11)=B(1,10)
      B(4,13)=B(2,14)
      B(4,14)=B(1,13)
      B(4,16)=B(2,17)
      B(4,17)=B(1,16)
      B(4,19)=B(2,20)
      B(4,20)=B(1,19)
      B(4,22)=B(2,23)
      B(4,23)=B(1,22)
      B(5,1)=-B(3,3)*ST/CT
      B(5,3)=(B(1,1)-B(3,1))*ST/CT
      B(5,4)=-B(3,6)*ST/CT
      B(5,6)=(B(1,4)-B(3,4))*ST/CT
      B(5,7)=-B(3,9)*ST/CT
      B(5,9)=(B(1,7)-B(3,7))*ST/CT
      B(5,10)=-B(3,12)*ST/CT
      B(5,12)=(B(1,10)-B(3,10))*ST/CT
      B(5,13)=-B(3,15)*ST/CT
      B(5,15)=(B(1,13)-B(3,13))*ST/CT
      B(5,16)=-B(3,18)*ST/CT
      B(5,18)=(B(1,16)-B(3,16))*ST/CT
      B(5,19)=-B(3,21)*ST/CT
      B(5,21)=(B(1,19)-B(3,19))*ST/CT
      B(5,22)=-B(3,24)*ST/CT
      B(5,24)=(B(1,22)-B(3,22))*ST/CT
      B(6,2)=B(5,1)
      B(6,3)=B(4,1)*ST/CT
      B(6,5)=B(5,4)
      B(6,6)=B(4,4)*ST/CT
      B(6,8)=B(5,7)
      B(6,9)=B(4,7)*ST/CT
      B(6,11)=B(5,10)
      B(6,12)=B(4,10)*ST/CT
      B(6,14)=B(5,13)
      B(6,15)=B(4,13)*ST/CT
      B(6,17)=B(5,16)
      B(6,18)=B(4,16)*ST/CT
      B(6,20)=B(5,19)
      B(6,21)=B(4,19)*ST/CT
      B(6,23)=B(5,22)
      B(6,24)=B(4,22)*ST/CT
      DO 3592 J=1,24
      DO 3592 I=1,6
      DB(I,J)=0.0
      DO 3592 K=1,6
      DB(I,J)=DB(I,J)+D(I,K)*B(K,J)
 3592 CONTINUE
      SIGMX(N,NN1)=0.0
      SIGMY(N,NN1)=0.0
```

```
      SIGMZ(N,NN1)=0.0
      SIGMXY(N,NN1)=0.0
      SIGMXZ(N,NN1)=0.0
      SIGMYZ(N,NN1)=0.0
      DO 3593 J=1,24
      SIGMX(N,NN1)=SIGMX(N,NN1)+DB(1,J)*U(J)
      SIGMY(N,NN1)=SIGMY(N,NN1)+DB(2,J)*U(J)
      SIGMZ(N,NN1)=SIGMZ(N,NN1)+DB(3,J)*U(J)
      SIGMXY(N,NN1)=SIGMXY(N,NN1)+DB(4,J)*U(J)
      SIGMXZ(N,NN1)=SIGMXZ(N,NN1)+DB(5,J)*U(J)
      SIGMYZ(N,NN1)=SIGMYZ(N,NN1)+DB(6,J)*U(J)
 3593 CONTINUE
 3594 CONTINUE
      RETURN
      END
      SUBROUTINE STRESSF(N)
C
C     COMPUTATION OF STRESSES IN FRICTION ELEMENTS
C
      IMPLICIT REAL*8 (A-H,O-Z)
COMMON/FIRST/NUGP,NHAR,THETA1,S(24,24),XORD(300),YORD(300)
     1,GSWT(3),GS(3)
      COMMON/THIRD/NPF(20,6),STN(20),STS(20),NEXP
      COMMON/SIXTH/BTOT(900)
      COMMON/EIGHTH/SIGFN(20,9),SIGFSX(20,9),SIGFSY(20,9)
      DIMENSION D(3,3),B(3,18),DB(3,18),U(18)
      PI=3.14159265359
      I=NPF(N,1)
      J=NPF(N,2)
      K=NPF(N,3)
      L=NPF(N,4)
      II=NPF(N,5)
      JJ=NPF(N,6)
      AA=(XORD(J)-XORD(I))/2.0
      BB=(YORD(J)-YORD(I))/2.0
      THETA1=THETA1*PI
      ST=SIN(THETA1)
      CT=COS(THETA1)
      IF(N.LE.NEXP)AB=AA
      IF(N.GT.NEXP)AB=BB
      XC=XORD(II)
      YC=YORD(II)
      U(1)=BTOT(3*I-2)
      U(2)=BTOT(3*I-1)
      U(3)=BTOT(3*I)
      U(4)=BTOT(3*J-2)
      U(5)=BTOT(3*J-1)
      U(6)=BTOT(3*J)
      U(7)=BTOT(3*K-2)
      U(8)=BTOT(3*K-1)
      U(9)=BTOT(3*K)
      U(10)=BTOT(3*L-2)
      U(11)=BTOT(3*L-1)
      U(12)=BTOT(3*L)
```

```
      U(13)=BTOT(3*II-2)
      U(14)=BTOT(3*II-1)
      U(15)=BTOT(3*II)
      U(16)=BTOT(3*JJ-2)
      U(17)=BTOT(3*JJ-1)
      U(18)=BTOT(3*JJ)
      IF(NUGP.EQ.4)NN=2
      IF(NUGP.EQ.9)NN=3
      NN1=0
      DO 3625 JN=1,NN
      DO 3625 IN=1,NN
      Z=GS(IN)
      SSN=STN(N)
      STT=STS(N)
      NN1=NN1+1
      DO 3620 I=1,3
      DO 3620 J=1,3
      D(I,J)=0.0
3620 CONTINUE
      IF(N.GT.NEXP)GO TO 5620
      D(1,1)=STT
      D(2,2)=SSN
      D(3,3)=STT
      GO TO 5621
5620 D(1,1)=SSN
      D(2,2)=STT
      D(3,3)=STT
5621 DO 3621 I=1,3
      DO 3621 J=1,18
      B(I,J)=0.0
3621 CONTINUE
      AN1=(2.0*Z-1.0)
      AN2=-4.0*Z
      AN3=(2.0*Z+1.0)
      B(1,1)=AN1*CT
      B(1,4)=AN2*CT
      B(1,7)=AN3*CT
      B(1,10)=-AN1*CT
      B(1,13)=-AN2*CT
      B(1,16)=-AN3*CT
      B(2,2)=AN1*CT
      B(2,5)=AN2*CT
      B(2,8)=AN3*CT
      B(2,11)=-AN1*CT
      B(2,14)=-AN2*CT
      B(2,17)=-AN3*CT
      B(3,3)=AN1*ST
      B(3,6)=AN2*ST
      B(3,9)=AN3*ST
      B(3,12)=-AN1*ST
      B(3,15)=-AN2*ST
      B(3,18)=-AN3*ST
      DO 3622 I=1,3
      DO 3622 J=1,18
      B(I,J)=B(I,J)/(2.0*AB)
3622 CONTINUE
      DO 3623 J=1,18
      DO 3623 I=1,3
      DB(I,J)=0.0
      DO 3623 K=1,3
      DB(I,J)=DB(I,J)+D(I,K)*B(K,J)
3623 CONTINUE
      SIGFN(N,NN1)=0.0
      SIGFSX(N,NN1)=0.0
      SIGFSY(N,NN1)=0.0
      DO 3624 J=1,18
      SIGFN(N,NN1)=SIGFN(N,NN1)+DB(1,J)*U(J)
      SIGFSX(N,NN1)=SIGFSX(N,NN1)+DB(2,J)*U(J)
      SIGFSY(N,NN1)=SIGFSY(N,NN1)+DB(3,J)*U(J)
3624 CONTINUE
3625 CONTINUE
      RETURN
      END
      SUBROUTINE STRESSP(N)
C
C     COMPUTATION OF STRESS IN PILE ELEMENTS
C
      IMPLICIT REAL*8 (A-H,O-Z)
COMMON/FIRST/NUGP,NHAR,THETA1,S(24,24),XORD(300),YORD(300)
     1,GSWT(3),GS(3)
      COMMON/FOURTH/NPP(60,8),PROPP(20,4)
      COMMON/SIXTH/BTOT(900)
COMMON/NINTH/SIGPX(20,9),SIGPY(20,9),SIGPZ(20,9),SIGPXY(20,9)
     1,SIGPXZ(20,9),SIGPYZ(20,9)
      DIMENSION D(6,6),B(6,24),DB(6,24),U(24)
      PI=3.14159265359
      I=NPP(N,1)
      J=NPP(N,2)
      K=NPP(N,3)
      L=NPP(N,4)
      II=NPP(N,5)
      JJ=NPP(N,6)
      KK=NPP(N,7)
      LL=NPP(N,8)
      AA=(XORD(J)-XORD(I))/2.0
      BB=(YORD(K)-YORD(J))/2.0
      XC=XORD(II)
      YC=YORD(LL)
      THETA1=THETA1*PI/180
      ST=SIN(THETA1)
      CT=COS(THETA1)
      U(1)=BTOT(3*I-2)
      U(2)=BTOT(3*I-1)
      U(3)=BTOT(3*I)
      U(4)=BTOT(3*J-2)
      U(5)=BTOT(3*J-1)
      U(6)=BTOT(3*J)
      U(7)=BTOT(3*K-2)
```

```
      U(8)=BTOT(3*K-1)
      U(9)=BTOT(3*K)
      U(10)=BTOT(3*L-2)
      U(11)=BTOT(3*L-1)
      U(12)=BTOT(3*L)
      U(13)=BTOT(3*II-2)
      U(14)=BTOT(3*II-1)
      U(15)=BTOT(3*II)
      U(16)=BTOT(3*JJ-2)
      U(17)=BTOT(3*JJ-1)
      U(18)=BTOT(3*JJ)
      U(19)=BTOT(3*KK-2)
      U(20)=BTOT(3*KK-1)
      U(21)=BTOT(3*KK)
      U(22)=BTOT(3*LL-2)
      U(23)=BTOT(3*LL-1)
      U(24)=BTOT(3*LL)
      IF(NUGP.EQ.4)NN=2
      IF(NUGP.EQ.9)NN=3
      NN1=0
      DO 3684 IN=1,NN
      X=GS(IN)
      DO 3684 JN=1,NN
      Y=GS(JN)
      NN1=NN1+1
      ET=PROPP(N,1)
      PR=PROPP(N,2)
      COM=ET*(1.0-PR)/((1.0+PR)*(1.0-2.0*PR))
      DO 3680 I=1,6
      DO 3680 J=1,6
      D(I,J)=0.0
 3680 CONTINUE
      D(1,1)=COM
      D(1,2)=COM*PR/(1.0-PR)
      D(1,3)=D(1,2)
      D(2,1)=D(1,2)
      D(2,2)=COM
      D(2,3)=D(1,2)
      D(3,1)=D(1,2)
      D(3,2)=D(1,2)
      D(3,3)=COM
      D(4,4)=COM*(0.5-PR)/(1.0-PR)
      D(5,5)=D(4,4)
      D(6,6)=D(4,4)
      DO 3681 I=1,6
      DO 3681 J=1,24
      B(I,J)=0.0
 3681 CONTINUE
      AN1=(X**2+Y**2-1.0-X**2*Y-Y**2*X+X*Y)/4.0
      AN2=(X**2+Y**2-1.0-X**2*Y+Y**2*X-X*Y)/4.0
      AN3=(X**2+Y**2-1.0+X**2*Y+Y**2*X+X*Y)/4.0
      AN4=(X**2+Y**2-1.0+X**2*Y-Y**2*X-X*Y)/4.0
      AN5=(1.0-X**2)*(1.0-Y)/2.0
      AN6=(1.0+X)*(1.0-Y**2)/2.0
      AN7=(1.0-X**2)*(1.0+Y)/2.0
      AN8=(1.0-X)*(1.0-Y**2)/2.0
      CC=(AA*X+XC)
      B(1,1)=(2.0*X+Y-2.0*X*Y-Y**2)*CT/(4.0*AA)
      B(1,4)=(2.0*X-Y-2.0*X*Y+Y**2)*CT/(4.0*AA)
      B(1,7)=(2.0*X+Y+2.0*X*Y+Y**2)*CT/(4.0*AA)
      B(1,10)=(2.0*X-Y+2.0*X*Y-Y**2)*CT/(4.0*AA)
      B(1,13)=(X*Y-X)*CT/AA
      B(1,16)=(1.0-Y**2)*CT/(2.0*AA)
      B(1,19)=(-X*Y-X)*CT/AA
      B(1,22)=(Y**2-1.0)*CT/(2.0*AA)
      B(2,2)=(2.0*Y+X-2.0*X*Y-X**2)*CT/(4.0*BB)
      B(2,5)=(2.0*Y-X+2.0*X*Y-X**2)*CT/(4.0*BB)
      B(2,8)=(2.0*Y+X+2.0*X*Y+X**2)*CT/(4.0*BB)
      B(2,11)=(2.0*Y-X-2.0*X*Y+X**2)*CT/(4.0*BB)
      B(2,14)=(X**2-1.0)*CT/(2.0*BB)
      B(2,17)=(-X*Y-Y)*CT/BB
      B(2,20)=(1.0-X**2)*CT/(2.0*BB)
      B(2,23)=(X*Y-Y)*CT/BB
      B(3,1)=AN1*CT/CC
      B(3,3)=AN1*NHAR*CT/CC
      B(3,4)=AN2*CT/CC
      B(3,6)=AN2*NHAR*CT/CC
      B(3,7)=AN3*CT/CC
      B(3,9)=AN3*NHAR*CT/CC
      B(3,10)=AN4*CT/CC
      B(3,12)=AN4*NHAR*CT/CC
      B(3,13)=AN5*CT/CC
      B(3,15)=AN5*NHAR*CT/CC
      B(3,16)=AN6*CT/CC
      B(3,18)=AN6*NHAR*CT/CC
      B(3,19)=AN7*CT/CC
      B(3,21)=AN7*NHAR*CT/CC
      B(3,22)=AN8*CT/CC
      B(3,24)=AN8*NHAR*CT/CC
      B(4,1)=B(2,2)
      B(4,2)=B(1,1)
      B(4,4)=B(2,5)
      B(4,5)=B(1,4)
      B(4,7)=B(2,8)
      B(4,8)=B(1,7)
      B(4,10)=B(2,11)
      B(4,11)=B(1,10)
      B(4,13)=B(2,14)
      B(4,14)=B(1,13)
      B(4,16)=B(2,17)
      B(4,17)=B(1,16)
      B(4,19)=B(2,20)
      B(4,20)=B(1,19)
      B(4,22)=B(2,23)
      B(4,23)=B(1,22)
      B(5,1)=-B(3,3)*ST/CT
      B(5,3)=(B(1,1)-B(3,1))*ST/CT
      B(5,4)=-B(3,6)*ST/CT
      B(5,6)=(B(1,4)-B(3,4))*ST/CT
      B(5,7)=-B(3,9)*ST/CT
```

```
      B(5,9)=(B(1,7)-B(3,7))*ST/CT
      B(5,10)=-B(3,12)*ST/CT
      B(5,12)=(B(1,10)-B(3,10))*ST/CT
      B(5,13)=-B(3,15)*ST/CT
      B(5,15)=(B(1,13)-B(3,13))*ST/CT
      B(5,16)=-B(3,18)*ST/CT
      B(5,18)=(B(1,16)-B(3,16))*ST/CT
      B(5,19)=-B(3,21)*ST/CT
      B(5,21)=(B(1,19)-B(3,19))*ST/CT
      B(5,22)=-B(3,24)*ST/CT
      B(5,24)=(B(1,22)-B(3,22))*ST/CT
      B(6,2)=B(5,1)
      B(6,3)=B(4,1)*ST/CT
      B(6,5)=B(5,4)
      B(6,6)=B(4,4)*ST/CT
      B(6,8)=B(5,7)
      B(6,9)=B(4,7)*ST/CT
      B(6,11)=B(5,10)
      B(6,12)=B(4,10)*ST/CT
      B(6,14)=B(5,13)
      B(6,15)=B(4,13)*ST/CT
      B(6,17)=B(5,16)
      B(6,18)=B(4,16)*ST/CT
      B(6,20)=B(5,19)
      B(6,21)=B(4,19)*ST/CT
      B(6,23)=B(5,22)
      B(6,24)=B(4,22)*ST/CT
      DO 3682 J=1,24
      DO 3682 I=1,6
      DB(I,J)=0.0
      DO 3682 K=1,6
      DB(I,J)=DB(I,J)+D(I,K)*B(K,J)
 3682 CONTINUE
      SIGPX(N,NN1)=0.0
      SIGPY(N,NN1)=0.0
      SIGPZ(N,NN1)=0.0
      SIGPXY(N,NN1)=0.0
      SIGPXZ(N,NN1)=0.0
      SIGPYZ(N,NN1)=0.0
      DO 3683 J=1,24
      SIGPX(N,NN1)=SIGPX(N,NN1)+DB(1,J)*U(J)
      SIGPY(N,NN1)=SIGPY(N,NN1)+DB(2,J)*U(J)
      SIGPZ(N,NN1)=SIGPZ(N,NN1)+DB(3,J)*U(J)
      SIGPXY(N,NN1)=SIGPXY(N,NN1)+DB(4,J)*U(J)
      SIGPXZ(N,NN1)=SIGPXZ(N,NN1)+DB(5,J)*U(J)
      SIGPYZ(N,NN1)=SIGPYZ(N,NN1)+DB(6,J)*U(J)
 3683 CONTINUE
 3684 CONTINUE
      RETURN
      END
```

APPENDIX F2

DATA PREPARATION AND PROGRAM LISTING FOR PROGRAM PIER3DLN

F2.1 DATA PREPARATION

---

1. NAME

10 unit alpha-numeric identification of problems (eg. TRIAL1, EXAMPLE1)

---

2. NSYM, LDC

NSYM	= 1 For symmetric case.
	= 0 For non-symmetric case.
LDC	= 1 If pier element is divided into two elements both in the x- and y-directions with standard loading.
	= 0 For pier with other sub-divisions or loadings.

---

3. NTNEL, NPE, NUMNP, NOLN, NPX, NPY, NPZ, NUMBC

NTNEL	= Total number of elements in the mesh
NPE	= Number of pier elements
NUMNP	= Number of nodal points
NOLN	= Number of nodes at which loads are applied
	(NOLN=9 for LDC=1 if NSYM=0, NOLN=6 for LDC=1 if NSYM=1)
NPX	= Number of nodes along x- axis
NPY	= Number of nodes along y- axis
NPZ	= Number of nodes along z- axis
NUMBC	= Number of boundary conditions

4. NELP(I), I = 1, NPE

NELP = Element numbers of pier elements

---

5. NNLN(N), N = 1, NOLN Omit if LDC = 0

NNLN = Node number at which load is applied

---

6. NPB(L), NFIX(L), L = 1, NUMBC

NPB	= Boundary node number	
NFIX	= Boundary condition code	
	= 1	x- displacement = 0
	= 2	y- displacement = 0
	= 3	z- displacement = 0
	= 4	x- and y- displacements = 0
	= 5	y- and z- displacements = 0
	= 6	x- and z- displacements = 0
	= 7	x-, y- and z- displacements = 0

---

7. XX(I), I = 1, NPX

XX = Co-ordinates of nodal points along x- axis

---

8. YY(I), I = 1, NPY

YY = Co-ordinates of nodal points along y- axis

---

9. ZZ(I), I = 1, NPZ

ZZ = Co-ordinates of nodal points along z- axis

---

10. WX, WY Omit if LDC = 0

WX = Pier breadth along x- axis
WY = Pier breadth along y- axis

---

11. HT1, HKO, RO, RO1

HT1 = Height of soil below water table
HKO = Coefficient of lateral earth pressure at rest (K_0)
RO = Specific weight of soil above water table
RO1 = Specific weight of soil below water table

---

12. PROPM(I,J), J = 1, 5 I = 1, NELZ

PROPM = Soil elastic constants (for a transversely isotropic body)
NELZ = Number of elements in z-direction

Properties of I-th layer from top are as follows

PROPM(I,1) = E_2
PROPM(I,2) = ν_2
PROPM(I,3) = ν_1
PROPM(I,4) = $n = E_1 / E_2$
PROPM(I,5) = $m = G_2 / E_2$

---

13. PROPP(J), J = 1, 2

PROPP = Pier elastic constants, E and ν (for a linear isotropic body)

PROPP(1) = E
PROPP(2) = ν

14. VLOAD, XHLOAD, YHLOAD, XMLOAD, YMLOAD

VLOAD	= Load in z- direction at the top of the pier
XHLOAD	= Load in x- direction at the top of the pier
YHLOAD	= Load in y- direction at the top of the pier
XMLOAD	= Moment in x- direction at the top of the pier
YMLOAD	= Moment in y- direction at the top of the pier

15. NNLN(II), XXF(II), YYF(II), ZZF(II), N = 1, NOLN Omit if LDC = 1

NNLN	= Node number at which load is applied
XXF	= Nodal load in x-direction
YYF	= Nodal load in y-direction
ZZF	= Nodal load in z-direction

F2.2 PROGRAM LISTING

```
      PROGRAM UCB
      IMPLICIT REAL*8 (A-H,O-Z)
      COMMON/FIRST/A(400,400),B(6000)
      COMMON/SECOND/MM,NT
 COMMON/THIRD/SGMX(2000),SGMY(2000),SGMZ(2000),SGMXY(2000)
     *,SGMYZ(2000),SGMXZ(2000)
      CHARACTER*72 DATAFN,OUTPF
      CHARACTER NAME*10
      DIMENSION
 NNLN(100),NPB(2000),NFIX(2000),XX(25),YY(20),ZZ(40)
      DIMENSION PROPM(40,5),NP(2000,8),LM(24),KM(2),S(24,24)
      DIMENSION
 NUME(2000),PROPP(2),XXF(100),YYF(100),ZZF(100),NELP(80)
      DIMENSION NTYPE(1100),COORD(2000,3)
      PRINT *,'ENTER DATA FILE NAME WITH PATH'
      READ '(A)',DATAFN
      PRINT *,'ENTER OUTPUT FILE NAME WITH PATH'
      READ '(A)',OUTPF
      OPEN(5,FILE=DATAFN,STATUS='OLD')
      OPEN(6,FILE=OUTPF,STATUS='NEW')
      OPEN(1,FILE='UNIT1.DAT',FORM='UNFORMATTED')
      OPEN(2,FILE='UNIT2.DAT',FORM='UNFORMATTED')
      OPEN(3,FILE='UNIT3.DAT',FORM='UNFORMATTED')
C
C     READ DATA
C
      READ (5,1) NAME
      READ (5,*) NSYM,LDC
      READ (5,*) NTNEL,NPE,NUMNP,NOLN,NPX,NPY,NPZ,NUMBC
      READ (5,*) (NELP(I),I=1,NPE)
      IF(LDC.EQ.1) THEN
      READ (5,*) (NNLN(N),N=1,NOLN)
      ENDIF
      READ (5,*) (NPB(L),NFIX(L),L=1,NUMBC)
      READ (5,*) (XX(I),I=1,NPX)
      READ (5,*) (YY(I),I=1,NPY)
      READ (5,*) (ZZ(I),I=1,NPZ)
      IF(LDC.EQ.1) THEN
      READ (5,*) WX,WY
      ENDIF
      READ (5,*) HT1,HKO,RO,RO1
      IF(NSYM.EQ.0) GO TO 1111
      L=1
C
C     SYMMETRIC CASE
C
      NNYZ=NPY*NPZ
      DO 220 I=NPZ,NUMNP,NPZ
      NPB(L)=I
      NFIX(L)=7
  220 L=L+1
      DO 221 I=1,NPZ-1
      NPB(L)=I
      NFIX(L)=4
  221 L=L+1
      N=NNYZ-NPZ+1
      DO 222 I=N,NNYZ-1
      NPB(L)=I
      NFIX(L)=4
  222 L=L+1
      N1=NUMNP-NNYZ+1
      N2=N1+NPZ-2
      DO 223 I=N1,N2
      NPB(L)=I
      NFIX(L)=4
  223 L=L+1
      N1=NUMNP-NPZ+1
      N2=NUMNP-1
      DO 224 I=N1,N2
      NPB(L)=I
      NFIX(L)=4
  224 L=L+1
      K=NPZ
      DO 225 M=1,2
      DO 226 J=1,NPY-2
      DO 227 I=1,NPZ-1
      K=K+1
      NPB(L)=K
      NFIX(L)=1
  227 L=L+1
  226 K=K+1
  225 K=NUMNP-NNYZ+NPZ
      K=NNYZ
      DO 228 N=1,2
      DO 229 J=1,NPX-2
      DO 230 I=1,NPZ-1
      K=K+1
      NPB(L)=K
      NFIX(L)=2
  230 L=L+1
  229 K=K+NNYZ-NPZ+1
  228 K=2*NNYZ-NPZ
 1111 NT=3*NUMNP
      MM=3*(NPZ*(NPY+1)+2)
      NUMBLK=(NT-1)/MM+1
      NELX=NPX-1
      NELY=NPY-1
      NELZ=NPZ-1
      NELYZ=NELY*NELZ
      READ (5,*) ((PROPM(I,J),J=1,5),I=1,NELZ)
      READ (5,*) (PROPP(J),J=1,2)
      IF(LDC.EQ.1) THEN
      READ (5,*) VLOAD,XHLOAD,YHLOAD,XMLOAD,YMLOAD
```

```
      ENDIF
      IF(LDC.EQ.0) THEN
      READ(5,*) (NNLN(II),XXF(II),YYF(II),ZZF(II),II=1,NOLN)
      END IF
C
C     GENERATION OF NODE CO-ORDINATES
C
      NPXY=NPX*NPY
      NPXZ=NPX*NPZ
      NPYZ=NPY*NPZ
      K=1
      DO 514 L1=1,NPX
       DO 514 J1=1,NPYZ
             COORD(K,1)=XX(L1)
 514         K=K+1
      K=1
      DO 525 L2=1,NPY
      N=K
       DO 526 M1=1,NPX
       DO 527 I1=1,NPZ
             COORD(K,2)=YY(L2)
 527         K=K+1
 526  K=NPYZ*M1+N
 525  K=NPZ*L2+1
      DO 535 L3=1,NPZ
       K=L3
      DO 535 J3=1,NPXY
             COORD(K,3)=ZZ(L3)
 535         K=K+NPZ
      DO 333 I1=1,NTNEL
 333  NTYPE(I1)=1
      DO 334 I2=1,NPE
 334  NTYPE(NELP(I2))=2
C
C     GENERATION OF NODE NUMBERS FOR ELEMENTS
C
      DO 122 N=1,NTNEL
      NXE=(N-1)/NELYZ+1
      NYE=(N-(NXE-1)*NELYZ-1)/NELZ+1
      NZE=N-(NXE-1)*NELYZ-(NYE-1)*NELZ
      NP(N,1)=NXE*NPYZ+(NYE-1)*NPZ+NZE+1
      NP(N,2)=NP(N,1)+NPZ
      NP(N,3)=NP(N,2)-NPYZ
      NP(N,4)=NP(N,3)-NPZ
      NP(N,5)=NP(N,1)-1
      NP(N,6)=NP(N,2)-1
      NP(N,7)=NP(N,3)-1
      NP(N,8)=NP(N,4)-1
 122  CONTINUE
C
C     PRINT DATA
C
      WRITE (6,*) NAME
      WRITE (6,610)
      WRITE (6,615) NTNEL,NPE,NUMNP,NOLN,NPX,NPY,NPZ,NUMBC
```

```
      WRITE (6,*)
      WRITE(6,213)
      WRITE(6,212)
      WRITE(6,215)(I,(NP(I,J),J=1,8),I=1,NTNEL)
      WRITE (6,201)
      WRITE (6,625) (NELP(I),I=1,NPE)
      WRITE (6,645)
      WRITE (6,650)
      WRITE (6,655) (XX(I),I=1,NPX)
      WRITE (6,660)
      WRITE (6,655) (YY(I),I=1,NPY)
      WRITE (6,665)
      WRITE (6,655) (ZZ(I),I=1,NPZ)
      WRITE(6,935)
      WRITE(6,940)
      DO 951 IP=1,NUMNP,2
      WRITE(6,950) IP,(COORD(IP,IDIM),IDIM=1,3),IP+1,(COORD((IP+1),
     *IDIM),IDIM=1,3)
 951  CONTINUE
      WRITE(6,238) HT1,HKO,RO,RO1
      WRITE (6,620)
      WRITE (6,625) (NNLN(N),N=1,NOLN)
      WRITE (6,630)
      WRITE (6,635)
      WRITE (6,640) (NPB(L),NFIX(L),L=1,NUMBC)
      WRITE (6,3001)
      WRITE (6,670)
      WRITE (6,675) ((PROPM(I,J),J=1,5),I=1,NELZ)
      WRITE (6,3002)
      WRITE (6,671)
      WRITE (6,675) (PROPP(J),J=1,2)
      WRITE (6,522)
      IF(LDC.EQ.1) THEN
      WRITE (6,523)
      WRITE (6,521) VLOAD,XHLOAD,YHLOAD,XMLOAD,YMLOAD
      END IF
      IF(LDC.EQ.0) THEN
      WRITE (6,3901)
      WRITE (6,3902) (NNLN(II),XXF(II),YYF(II),ZZF(II),II=1,NOLN)
      END IF
      WRITE (6,*)
      WRITE (6,680) MM
      DO 315 I=1,NTNEL
 315  NUME(I)=I
      NF=1
      NL=MM
      DO 325 J=1,MM
      DO 325 I=1,MM
 325  A(I,J)=0.0
      DO 320 I=1,MM
 320  B(I)=0.0
C
C     INITIALISE STRESSES
C
      HT=ZZ(NPZ)
```

```
      WRITE(6,3006)
      WRITE(6,3007)
      DO 265 N=1,NTNEL
      NXE=(N-1)/NELYZ+1
      NYE=(N-(NXE-1)*NELYZ-1)/NELZ+1
      NZE=N-(NXE-1)*NELYZ-(NYE-1)*NELZ
      I=NZE+1
      L=NZE
      Z=(ZZ(I)+ZZ(L))/2.
      HT2=HT-HT1
      IF(Z.GT.HT2)GOTO 261
      SGMZ(N)=-RO*(Z)
      GOTO 262
  261 SGMZ(N)=-RO*(HT2)-RO1*(Z-HT2)
  262 CONTINUE
      SGMX(N)=HKO*SGMZ(N)
      SGMY(N)=HKO*SGMZ(N)
      WRITE(6,3005)N,SGMX(N),SGMY(N),SGMZ(N)
      SGMXY(N)=0.0
      SGMYZ(N)=0.0
  265 SGMXZ(N)=0.0
      DO 710 NB=1,NUMBLK
      NC=0
      REWIND 1
C
C     COMPUTE STIFFNESS OF ELEMENTS CONTRIBUTING TO THE
CURRENT
C     BLOCK
C
      DO 720 N=1,NTNEL
      IF(NUME(N).LT.0)GO TO 720
      NXE=(N-1)/NELYZ+1
      NYE=(N-(NXE-1)*NELYZ-1)/NELZ+1
      NZE=N-(NXE-1)*NELYZ-(NYE-1)*NELZ
      KM(1)=3*(NXE*NPYZ+NYE*NPZ+NZE+1)
      KM(2)=KM(1)-MM+1
      DO 730 I=1,2
      IF(KM(I).LT.NF)GO TO 730
      IF(KM(I).GT.NL)GO TO 730
      GO TO 740
  730 CONTINUE
      GO TO 720
  740 NC=NC+1
      NUME(N)=-NUME(N)
      MTYPE=NZE
      IF(NTYPE(N).EQ.2)GO TO 142
      P1=PROPM(MTYPE,1)
      P2=PROPM(MTYPE,2)
      P3=PROPM(MTYPE,3)
      P4=PROPM(MTYPE,4)
      P5=PROPM(MTYPE,5)
      CALL STIF3D (N,NP,COORD,P1,P2,P3,P4,P5,S)
      GO TO 143
  142 P1=PROPP(1)
      P2=PROPP(2)
      P3=P2
      P4=1.0
      P5=0.5/(1+P2)
      CALL STIF3D (N,NP,COORD,P1,P2,P3,P4,P5,S)
C
C     ASSEMBLE THE COMPUTED STIFFNESSES
C
  143 DO 900 I=1,8
      DO 900 J=1,3
      JJ=3*I-3+J
  900 LM(JJ)=3*NP(N,I)-3+J
      DO 260 I=1,24
      IF(LM(I).LT.NF)GO TO 260
      IF(LM(I).GT.NL) GO TO 260
      II=LM(I)
      I1=II-NF+1
      DO 250 J=1,24
      JJ=LM(J)
      IF(JJ.LT.II)GO TO 250
      JJ=JJ-II+1
      A(I1,JJ)=A(I1,JJ)+S(I,J)
  250 CONTINUE
  260 CONTINUE
      IF(NB.EQ.NUMBLK)GO TO 720
C
C     WRITE THE COMPUTED STIFFNESSES TO UNIT 1
C
      WRITE (1) (LM(I),I=1,24),((S(I,J),J=1,24),I=1,24)
  720 CONTINUE
C
C     ASSIGN LOAD VECTORS WITHIN THE BLOCK
C
      IF(LDC.EQ.1) THEN
      FX=YMLOAD/WX
      FY=XMLOAD/WY
      DO 150 N=1,NOLN
      JM=3*NNLN(N)
      IF(JM.LT.NF)GO TO 150
      IF(JM.GT.NL)GO TO 150
      I1=JM-NF+1
      IF(NSYM.EQ.1)THEN
      IF(N.EQ.1)THEN
      B(I1-2)=XHLOAD/16
      B(I1-1)=YHLOAD/16
      B(I1)=VLOAD/16+(FX/4)+(-FY/4)
      ELSEIF(N.EQ.2)THEN
      B(I1-2)=XHLOAD/8/2
      B(I1-1)=YHLOAD/8/2
      B(I1)=(VLOAD/8+(FX/2))/2
      ELSEIF(N.EQ.3)THEN
      B(I1-2)=XHLOAD/8
      B(I1-1)=YHLOAD/8
      B(I1)=VLOAD/8+(-FY/2)
      ELSEIF(N.EQ.4)THEN
      B(I1-2)=XHLOAD/4/2
```

```
      B(I1-1)=YHLOAD/4/2
      B(I1)=VLOAD/4/2
      ELSEIF(N.EQ.5)THEN
      B(I1-2)=XHLOAD/16
      B(I1-1)=YHLOAD/16
      B(I1)=VLOAD/16+(-FX/4)+(-FY/4)
      ELSEIF(N.EQ.6)THEN
      B(I1-2)=XHLOAD/8/2
      B(I1-1)=YHLOAD/8/2
      B(I1)=(VLOAD/8+(-FX/2))/2
      ENDIF
      ELSEIF(N.EQ.1)THEN
      B(I1-2)=XHLOAD/16
      B(I1-1)=YHLOAD/16
      B(I1)=VLOAD/16+(FX/4)+(-FY/4)
      ELSEIF(N.EQ.2)THEN
      B(I1-2)=XHLOAD/8
      B(I1-1)=YHLOAD/8
      B(I1)=VLOAD/8+(FX/2)
      ELSEIF(N.EQ.3)THEN
      B(I1-2)=XHLOAD/16
      B(I1-1)=YHLOAD/16
      B(I1)=VLOAD/16+(FX/4)+(FY/4)
      ELSEIF(N.EQ.4)THEN
      B(I1-2)=XHLOAD/8
      B(I1-1)=YHLOAD/8
      B(I1)=VLOAD/8+(-FY/2)
      ELSEIF(N.EQ.5)THEN
      B(I1-2)=XHLOAD/4
      B(I1-1)=YHLOAD/4
      B(I1)=VLOAD/4
      ELSEIF(N.EQ.6)THEN
      B(I1-2)=XHLOAD/8
      B(I1-1)=YHLOAD/8
      B(I1)=VLOAD/8+(FY/2)
      ELSEIF(N.EQ.7)THEN
      B(I1-2)=XHLOAD/16
      B(I1-1)=YHLOAD/16
      B(I1)=VLOAD/16+(-FX/4)+(-FY/4)
      ELSEIF(N.EQ.8)THEN
      B(I1-2)=XHLOAD/8
      B(I1-1)=YHLOAD/8
      B(I1)=VLOAD/8+(-FX/2)
      ELSEIF(N.EQ.9)THEN
      B(I1-2)=XHLOAD/16
      B(I1-1)=YHLOAD/16
      B(I1)=VLOAD/16+(-FX/4)+(FY/4)
      ENDIF
150   CONTINUE
      ENDIF
      IF(LDC.EQ.0) THEN
      DO 1222 N=1,NOLN
      JM=3*NNLN(N)
      IF(JM.LT.NF)GO TO 1222
      IF(JM.GT.NL)GO TO 1222
      I1=JM-NF+1
      B(I1-2)=XXF(N)
      B(I1-1)=YYF(N)
      B(I1-0)=ZZF(N)
1222  CONTINUE
      ENDIF
C
C     IMPOSE BOUNDARY CONDITIONS WITHIN THE BLOCK
C
      DO 200 L=1,NUMBC
      IF(NPB(L).LT.0)GO TO 200
      M=NPB(L)
      JM1=3*M-2
      JM2=JM1+1
      JM3=JM2+1
      IF(JM1.GT.NL)GO TO 200
      IF(JM3.LT.NF)GO TO 200
      NPB(L)=-NPB(L)
      IF(NFIX(L).NE.1)GO TO 170
      CALL MODIFY(JM1,NF)
      GO TO 200
170   IF(NFIX(L).NE.2)GO TO 175
      CALL MODIFY(JM2,NF)
      GO TO 200
175   IF(NFIX(L).NE.3)GO TO 180
      CALL MODIFY(JM3,NF)
      GO TO 200
180   IF(NFIX(L).NE.4)GO TO 185
      CALL MODIFY(JM1,NF)
      CALL MODIFY(JM2,NF)
      GO TO 200
185   IF(NFIX(L).NE.5)GO TO 190
      CALL MODIFY(JM2,NF)
      CALL MODIFY(JM3,NF)
      GO TO 200
190   IF(NFIX(L).NE.6)GO TO 195
      CALL MODIFY(JM1,NF)
      CALL MODIFY(JM3,NF)
      GO TO 200
195   IF(NFIX(L).NE.7) GO TO 200
      CALL MODIFY(JM1,NF)
      CALL MODIFY(JM2,NF)
      CALL MODIFY(JM3,NF)
200   CONTINUE
C
C     WRITE THE RESULTING BLOCK STIFFNESS AND LOAD
VECTORS TO UNIT 2
C
      DO 210 I=1,MM
210   WRITE (2) (A(I,J),J=1,MM),(B(I))
C
C     INITIALIZE A AND B MATRICES
C
      REWIND 1
      DO 750 I=1,MM
```

```
      DO 755 J=1,MM
  755 A(I,J)=0.0
  750 B(I)=0.0
      IF(NB.EQ.NUMBLK) GO TO 710
C
C    COMPUTE NEW BLOCK PARAMETERS
C
      NF=NF+MM
      NL=NL+MM
C
C    ASSEMBLE THE COMPUTED STIFFNESSES IN THE NEW
BLOCK
C
      DO 760 NCC=1,NC
      READ(1) (LM(I),I=1,24),((S(I,J),J=1,24),I=1,24)
      DO 770 I=1,24
      IF(LM(I).LT.NF) GO TO 770
      IF(LM(I).GT.NL)GO TO 770
      II=LM(I)
      I1=II-NF+1
      DO 780 J=1,24
      JJ=LM(J)
      IF(JJ.LT.II)GO TO 780
      JJ=JJ-II+1
      A(I1,JJ)=A(I1,JJ)+S(I,J)
  780 CONTINUE
  770 CONTINUE
  760 CONTINUE
  710 CONTINUE
C
C    SOLVE FOR NODAL DISPLACEMENTS
C
      CALL SOLVE2
      WRITE(6,38)
      WRITE(6,39)
      REWIND 3
      DO 555 N=NT,1,-1
  555 READ(3) B(N)
C
C    PRINT OF DISPLACEMENTS
C
      DO 101 J=1,NT,3
  101 WRITE (6,691) J,B(J),J+1,B(J+1),J+2,B(J+2)
      WRITE(6,33)
C
C    PRINT OF STRESSES
C
      WRITE (6,37)
      DO 850 N=1,NTNEL
      NXE=(N-1)/NELYZ+1
      NYE=(N-(NXE-1)*NELYZ-1)/NELZ+1
      NZE=N-(NXE-1)*NELYZ-(NYE-1)*NELZ
      DO 145 I=1,NPE
      IF(N.EQ.NELP(I))GO TO 146
      P1=PROPM(MTYPE,1)
      P2=PROPM(MTYPE,2)
      P3=PROPM(MTYPE,3)
      P4=PROPM(MTYPE,4)
      P5=PROPM(MTYPE,5)
  145 CONTINUE
      CALL STRESS
(N,P1,P2,P3,P4,P5,NPYZ,NPZ,LM,NP,ZZ,XX,YY,NXE,NYE,NZE)
      GO TO 850
  146 P1=PROPP(1)
      P2=PROPP(2)
      P3=P2
      P4=1.0
      P5=0.5/(1+P2)
      CALL STRESS
(N,P1,P2,P3,P4,P5,NPYZ,NPZ,LM,NP,ZZ,XX,YY,NXE,NYE,NZE)
  850 CONTINUE
      IF(NSYM.EQ.1)GO TO 1131
      JY=NELY/2-1
      GO TO 1142
 1131 JY=NELY-1
 1142 N=JY*NELZ+1
    1 FORMAT(A10)
   33 FORMAT(1H ,//,27H              ELEMENT STRESSES)
   37 FORMAT(/5HEL NO,5X,5H SIGX,5X,5H SIGY,5X,5H SIGZ,5X,6H
SIGXY,5X,
     *6H SIGYZ,5X,6H SIGXZ /)
   38 FORMAT(//,21H NODAL DISPLACEMENTS )
   39 FORMAT(/9X,6HX-DISP,10X,6HY-DISP,11X,6HZ-DISP,5X/)
  201 FORMAT(//,21H PIER ELEMENT NUMBERS,/)
  212 FORMAT(//,'   I   1   2   3   4   5   6   7   8')
  215 FORMAT(/9(2X,I4))
  213 FORMAT(//'   ELEMENT AND NODE NUMBERS FOR
ELEMENTS')
  238 FORMAT(//,'   HEIGHT OF WATER TABLE=',F7.4,/'   KO
VALUE='
     *,F7.4,/'   BULK DENSITY=',F7.4,/'   SUBMERGED
DENSITY=',F7.4)
  691 FORMAT(3(I4,1X,E12.4,2X))
  521 FORMAT(5F10.3)
  522 FORMAT(//,20H    APPLIED LOADING,/)
  523
FORMAT(5X,5HVLOAD,5X,6HXHLOAD,3X,6HYHLOAD,4X,6HXMLOAD
,4X,         6HYMLOAD,    ./)
  615 FORMAT (I6,7I9)
  610 FORMAT (//,70H NTNEL     NPE         NUMNP       NOLN
NPX       NP
     *Y    NPZ   NUMBC,/)
  620 FORMAT (//,31H NODES AT WHICH LOAD IS APPLIED,/)
  625 FORMAT (10I6)
  630 FORMAT(//,20H BOUNDARY CONDITIONS)
  635 FORMAT (/,5(11H  NPB  CODE),/)
  640 FORMAT (5(I5,I6))
  645 FORMAT (//,10H MESH DATA)
  650 FORMAT (/,25H COORDINATES ALONG X-AXIS,/)
  655 FORMAT(8F10.4)
```

```
  660 FORMAT (//,25H COORDINATES ALONG Y-AXIS,/)
  665 FORMAT (//,25H COORDINATES ALONG Z-AXIS,/)
  670 FORMAT (/,65H    E2              PR2       PR1
           E1/E2     *      G2/E2 ,/)
  671 FORMAT (/,33H  PIER MODULUS   POISSON RATIO   ,/)
  675 FORMAT (5E14.5)
  680 FORMAT (/,13H BAND WIDTH =,I5,/)
  935 FORMAT(//25H  NODAL POINT COORDINATES,/)
  940 FORMAT(5H NODE,5X,1HX,8X,1HY,8X,1HZ,8X,6H
 NODE,5X,1HX,8X,1HY,8X,
    *1HZ,/)
  950 FORMAT(I4,2X,3F9.5,5X,i4,2X,3F9.5)
 3001 FORMAT(1H ,//,27H    SOIL ELEMENT PROPERTIES)
 3002 FORMAT(1H ,//,27H    PIER ELEMENT PROPERTIES)
 3005 FORMAT(1H ,I6,3(3X,E13.6))
 3006 FORMAT(1H ,/,27H                          INITIAL STRESSES,/)
 3007 FORMAT(/8H   EL NO,4X,8H                SIGX,4X,10H
 SIGY,7X,
    *10H     SIGZ /)
 3901 FORMAT(7H  NODES,5X,6H  XXF ,6X,6H  YYF ,6X,6H  ZZF ,/)
 3902 FORMAT (I6,2X,F9.3,3X,F9.3,3X,F9.3)
      STOP
      END

      SUBROUTINE STIF3D(N,NP,COORD,P1,P2,P3,P4,P5,S)
      IMPLICIT REAL*8 (A-H,O-Z)
      DIMENSION S(24,24),DM(6,6),POSGP(3),WEIGP(3)
     .,COORD(2000,3),SHAPE(8),DERIV(3,8),CARTD(3,8),BMI(6,3)
     .,BMJ(6,3),NP(2000,8)
C
C***  INITIALIZE THE ELEMENT STIFFNESS MATRIX (S)
C
      DO 10 IE=1,24
      DO 10 JE=1,24
   10 S(IE,JE)=0.0
C
C***  INITIALIZE AND EVALUATE THE MATRIX OF ELASTIC
RIGIDITIES (DM)
C
      DO 5 ISIZE=1,6
      DO 5 JSIZE=1,6
    5 DM(ISIZE,JSIZE)=0.0
      COM=P4*P1/((1+P3)*(1-P3-2*P4*P2*P2))
      DM(1,1)=(1-P4*P2*P2)*COM
      DM(1,2)=(P3+P4*P2*P2)*COM
      DM(1,3)=P2*(1+P3)*COM
      DM(2,1)=DM(1,2)
      DM(2,2)=DM(1,1)
      DM(2,3)=DM(1,3)
      DM(3,1)=DM(1,3)
      DM(3,2)=DM(1,3)
      DM(3,3)=(1+P3)*(1-P3)*COM/P4
      DM(4,4)=(1-P3-2*P4*P2*P2)*COM/2
      DM(5,5)=P5*(1+P3)*(1-P3-2*P4*P2*P2)*COM/P4
      DM(6,6)=DM(5,5)
C
C***  EVALUATE THE COORDINATES OF NODES
C
      KGASP=0
C
C***  ENTER LOOPS FOR VOLUME NUMERICAL INTEGRATION
C***  SET UP GAUSSIAN INTEGRATION CONSTANTS
C
cc    POSGP(1)=-0.774596669241483
cc    POSGP(2)=0.0
cc    POSGP(3)=0.774596669241483
cc    WEIGP(1)=0.555555555555556
cc    WEIGP(2)=0.888888888888889
cc    WEIGP(3)=0.555555555555556
      POSGP(1)=-0.577350269189626
      POSGP(2)=0.577350269189626
      WEIGP(1)=1.0
      WEIGP(2)=1.0
cc    DO 30 IGAUS=1,3
      DO 30 IGAUS=1,2
      XI=POSGP(IGAUS)
cc    DO 30 JGAUS=1,3
      DO 30 JGAUS=1,2
      ET=POSGP(JGAUS)
cc    DO 30 KGAUS=1,3
      DO 30 KGAUS=1,2
      KGASP=KGASP+1
C     WRITE (6,*) 'KGASP',KGASP
      ZT=POSGP(KGAUS)
C
C***  EVALUATE THE SHAPE FUNCTIONS AND ELEMENTAL
VOLUME
C
      CALL SFUNC (DERIV,XI,ET,ZT,SHAPE)
      CALL JACOB (N,NP,COORD,CARTD,DERIV,DJACB,IELEM,SHAPE)

DVOLUM=DJACB*WEIGP(IGAUS)*WEIGP(JGAUS)*WEIGP(KGAUS)
C
C***  EVALUATE THE B AND DB MATRICES
C
      DO 20 INODE=1,8
      CALL BMATB (BMI,CARTD,INODE)
      DO 20 JNODE=INODE,8
      CALL BMATB (BMJ,CARTD,JNODE)
   20 CALL SUBPB (BMI,BMJ,DVOLUM,DM,S,INODE,JNODE)
   30 CONTINUE
      RETURN
      END

      SUBROUTINE SFUNC (DERIV,XI,ET,ZT,SHAPE)
      IMPLICIT REAL*8 (A-H,O-Z)
C
C***  EVALUATES SHAPE FUNCTIONS AND THEIR DERIVATIVES
FOR 8 NODED
C***  HEXAHEDRAL ISOPARAMETRIC ELEMENT
```

```
C
      DIMENSION DERIV(3,8),SHAPE(8)
C
C***  SHAPE FUNCTIONS
C
      SHAPE(1)=((1-XI)*(1+ET)*(1-ZT))/8
      SHAPE(2)=((1+XI)*(1+ET)*(1-ZT))/8
      SHAPE(3)=((1+XI)*(1-ET)*(1-ZT))/8
      SHAPE(4)=((1-XI)*(1-ET)*(1-ZT))/8
      SHAPE(5)=((1-XI)*(1+ET)*(1+ZT))/8
      SHAPE(6)=((1+XI)*(1+ET)*(1+ZT))/8
      SHAPE(7)=((1+XI)*(1-ET)*(1+ZT))/8
      SHAPE(8)=((1-XI)*(1-ET)*(1+ZT))/8
C
C***  SHAPE FUNCTIONS DERIVATIVES
C
      DERIV(1,1)=-((1+ET)*(1-ZT))/8
      DERIV(1,2)=((1+ET)*(1-ZT))/8
      DERIV(1,3)=((1-ET)*(1-ZT))/8
      DERIV(1,4)=-((1-ET)*(1-ZT))/8
      DERIV(1,5)=-((1+ET)*(1+ZT))/8
      DERIV(1,6)=((1+ET)*(1+ZT))/8
      DERIV(1,7)=((1-ET)*(1+ZT))/8
      DERIV(1,8)=-((1-ET)*(1+ZT))/8
      DERIV(2,1)=((1-XI)*(1-ZT))/8
      DERIV(2,2)=((1+XI)*(1-ZT))/8
      DERIV(2,3)=-((1+XI)*(1-ZT))/8
      DERIV(2,4)=-((1-XI)*(1-ZT))/8
      DERIV(2,5)=((1-XI)*(1+ZT))/8
      DERIV(2,6)=((1+XI)*(1+ZT))/8
      DERIV(2,7)=-((1+XI)*(1+ZT))/8
      DERIV(2,8)=-((1-XI)*(1+ZT))/8
      DERIV(3,1)=-((1-XI)*(1+ET))/8
      DERIV(3,2)=-((1+XI)*(1+ET))/8
      DERIV(3,3)=-((1+XI)*(1-ET))/8
      DERIV(3,4)=-((1-XI)*(1-ET))/8
      DERIV(3,5)=((1-XI)*(1+ET))/8
      DERIV(3,6)=((1+XI)*(1+ET))/8
      DERIV(3,7)=((1+XI)*(1-ET))/8
      DERIV(3,8)=((1-XI)*(1-ET))/8
      RETURN
      END

      SUBROUTINE JACOB
(N,NP,COORD,CARTD,DERIV,DJACB,IELEM,SHAPE)
      IMPLICIT REAL*8 (A-H,O-Z)
C
C***  EVALUATES JACOBIAN MATRIX AND ITS INVERSE
C***  CARTESIAN SHAPE FUNCTION DERIVATIVES AT PRESENT
SAMPLING POINT
C
      DIMENSION
CARTD(3,8),DERIV(3,8),SHAPE(8),COORD(2000,3),XJM(3,3)
     .,XJACI(3,3),NP(2000,8)
C
C***  CREATE JACOBIAN MATRIX  (XJM)
C
      DO 35 ID=1,3
      DO 35 JD=1,3
      XJM(ID,JD)=0.0
      DO 35 INODE=1,8
      NUM=NP(N,INODE)
   35 XJM(ID,JD)=XJM(ID,JD)+DERIV(ID,INODE)*COORD(NUM,JD)
C
C***  CALCULATE DETERMINANT AND INVERSE OF JACOBIAN
MATRIX
C

DJACB=XJM(1,1)*XJM(2,2)*XJM(3,3)+XJM(1,2)*XJM(2,3)*XJM(3,1)+
     .XJM(1,3)*XJM(2,1)*XJM(3,2)-(XJM(1,3)*XJM(2,2)*XJM(3,1)+
     .XJM(1,1)*XJM(2,3)*XJM(3,2)+XJM(1,2)*XJM(2,1)*XJM(3,3))
      IF(DJACB) 6,6,8
    6 WRITE (6,901) IELEM
      STOP
    8 CONTINUE
      XJACI(1,1)=(XJM(2,2)*XJM(3,3)-XJM(2,3)*XJM(3,2))/DJACB
      XJACI(1,2)=(XJM(1,3)*XJM(3,2)-XJM(1,2)*XJM(3,3))/DJACB
      XJACI(1,3)=(XJM(1,2)*XJM(2,3)-XJM(1,3)*XJM(2,2))/DJACB
      XJACI(2,1)=(XJM(2,3)*XJM(3,1)-XJM(2,1)*XJM(3,3))/DJACB
      XJACI(2,2)=(XJM(1,1)*XJM(3,3)-XJM(1,3)*XJM(3,1))/DJACB
      XJACI(2,3)=(XJM(1,3)*XJM(2,1)-XJM(1,1)*XJM(2,3))/DJACB
      XJACI(3,1)=(XJM(2,1)*XJM(3,2)-XJM(3,1)*XJM(2,2))/DJACB
      XJACI(3,2)=(XJM(1,2)*XJM(3,1)-XJM(1,1)*XJM(3,2))/DJACB
      XJACI(3,3)=(XJM(1,1)*XJM(2,2)-XJM(1,2)*XJM(2,1))/DJACB
C
C***  CALCULATE CARTESIAN DERIVATIVES
C
      DO 40 ID=1,3
      DO 40 INODE=1,8
      CARTD(ID,INODE)=0.0
      DO 40 JD=1,3

CARTD(ID,INODE)=CARTD(ID,INODE)+XJACI(ID,JD)*DERIV(JD,INOD
E)
   40 CONTINUE
  901 FORMAT(//,36H PROGRAM HALTED IN SUBROUTINE
JACOB,/,11X,24H ZERO OR
     . NEGATIVE VOLUME,10X,16H ELEMENT NUMBER ,I5)
      RETURN
      END


      SUBROUTINE BMATB (BMX,CARTD,KNODE)
      IMPLICIT REAL*8 (A-H,O-Z)
C
C***  EVALUATES STRAIN-DISPLACEMENT MATRIX
C
      DIMENSION BMX(6,3),CARTD(3,8)
      DNKDX=CARTD(1,KNODE)
      DNKDY=CARTD(2,KNODE)
```

```
      DNKDZ=CARTD(3,KNODE)
C
C***  INITIALIZE AND FORM B MATRIX  (BMX)
C
      DO 40 IS=1,6
      DO 40 JS=1,3
   40 BMX(IS,JS)=0.0
      BMX(1,1)=DNKDX
      BMX(2,2)=DNKDY
      BMX(3,3)=DNKDZ
      BMX(4,1)=DNKDY
      BMX(4,2)=DNKDX
      BMX(5,2)=DNKDZ
      BMX(5,3)=DNKDY
      BMX(6,1)=DNKDZ
      BMX(6,3)=DNKDX
      RETURN
      END

      SUBROUTINE SUBPB
(BIMAT,BJMAT,DVOLUM,DMATX,S,INODE,JNODE)
      IMPLICIT REAL*8 (A-H,O-Z)
      DIMENSION
BIMAT(6,3),BJMAT(6,3),DBMAT(6,3),DMATX(6,6),SBSTF(3,3),
     .S(24,24)
C
C***  EVALUATE D*B MATRIX (DBMAT)
C
      DO 45 J1=1,3
      DO 45 I1=1,6
      DBMAT(I1,J1)=0.0
      DO 45 K1=1,6
   45 DBMAT(I1,J1)=DBMAT(I1,J1)+DMATX(I1,K1)*BJMAT(K1,J1)
C
C***  EVALUATE BT*(D*B) MATRIX (SBSTF)
C
      DO 50 J2=1,3
      DO 50 I2=1,3
      SBSTF(I2,J2)=0.0
      DO 50 K2=1,6
   50 SBSTF(I2,J2)=SBSTF(I2,J2)+BIMAT(K2,I2)*DBMAT(K2,J2)
C
C***  ASSEMBLE SBSTF INTO ELEMENT STIFFNESS MATRIX
C
      IFROW=0
      JFCOL=0
      IFROW=(INODE-1)*3+IFROW
      JFCOL=(JNODE-1)*3+JFCOL
      DO 55 I3=1,3
      IRSUB=IFROW+I3
      DO 55 J3=1,3
      JCSUB=JFCOL+J3
   55 S(IRSUB,JCSUB)=S(IRSUB,JCSUB)+SBSTF(I3,J3)*DVOLUM
      DO 110 J=1,24
      DO 110 I=1,24
      S(I,J)=S(J,I)
  110 CONTINUE
      RETURN
      END

      SUBROUTINE MODIFY (N,NF)
      IMPLICIT REAL*8 (A-H,O-Z)
      COMMON/FIRST/A(400,400),B(6000)
      COMMON/SECOND/MM,NT
      N1=N-NF+1
      A(N1,1)=A(N1,1)*.1E+12
      B(N1)=0.0
      RETURN
      END

      SUBROUTINE SOLVE2
      IMPLICIT REAL*8 (A-H,O-Z)
      COMMON/FIRST/A(400,400),B(6000)
      COMMON/SECOND/MM,NT
      REWIND 2
      REWIND 1
      REWIND 3
      IC=1
      NC=MM+1
      NB=1
      DO 50 I=1,MM
      READ(2) (A(I,M),M=1,MM),B(I)
   50 CONTINUE
  200 N=IC
      B(N)=B(N)/A(N,1)
      DO 270 L=2,MM
      IF(A(N,L).EQ.0.0)GO TO 270
      C=A(N,L)/A(N,1)
      I=N+L-1
      IF(I.GT.MM)I=I-MM
      J=0
      DO 290 K=L,MM
      J=J+1
  290 A(I,J)=A(I,J)-C*A(N,K)
      B(I)=B(I)-A(N,L)*B(N)
      A(N,L)=C
  270 CONTINUE
      WRITE (1) (A(N,M),M=2,MM),(B(N))
      DO 100 M=1,MM
  100 A(N,M)=0.0
      B(N)=0.0
      IF(NB.EQ.NT)GO TO 300
      IF(NC.GT.NT)GO TO 210
      READ (2) (A(N,M),M=1,MM),B(N)
  210 NC=NC+1
      NB=NB+1
      IC=IC+1
      IF(IC.GT.MM)IC=1
      IF(IC.NE.1) GO TO 200
      GO TO 200
```

```
 300 CONTINUE
     DO 400 K=1,MM
     N=MM-K+1
     BACKSPACE 1
     READ(1)  (A(N,M),M=2,MM),B(N)
     BACKSPACE 1
 400 CONTINUE
     IC=MM
     NC=MM+1
     NB=1
 410 N=IC
     DO 430 M=2,MM
     K=N-M+1
     IF(K.LT.1)K=MM+K
     B(K)=B(K)-A(K,M)*B(N)
 430 CONTINUE
     WRITE(3) (B(N))
     B(N)=0.0
     DO 450 J=1,MM
 450 A(N,J)=0.0
     IF(NB.EQ.NT)GO TO 500
     IF(NC.GT.NT)GO TO 480
     BACKSPACE 1
     READ(1)  (A(N,J),J=2,MM),B(N)
     BACK SPACE 1
 480 NC=NC+1
     NB=NB+1
     IC=IC-1
     IF(IC.EQ.0)IC=MM
     IF(IC.NE.MM) GO TO 410
     GO TO 410
 500 CONTINUE
     RETURN
     END

     SUBROUTINE STRESS
(N,P1,P2,P3,P4,P5,NPYZ,NPZ,LM,NP,ZZ,XX,YY,NXE,
    *NYE,NZE)
     IMPLICIT REAL*8 (A-H,O-Z)
     COMMON/FIRST/A(400,400),B(6000)
     COMMON/SECOND/MM,NT
COMMON/THIRD/SGMX(2000),SGMY(2000),SGMZ(2000),SGMXY(2000)
    *,SGMYZ(2000),SGMXZ(2000)
     DIMENSION XX(25),YY(20),ZZ(40)
     DIMENSION NP(2000,8),LM(24)
     X=0.0
     Y=0.0
     Z=0.0
     XY=0.0
     YZ=0.0
     XZ=0.0
     AA=ABS(XX(NXE+1)-XX(NXE))/2.
     BB=ABS(YY(NYE+1)-YY(NYE))/2.
     CC=ABS(ZZ(NZE+1)-ZZ(NZE))/2.
     DO 901 I=1,8
     DO 901 J=1,3
     JJ=3*I-3+J
 901 LM(JJ)=3*NP(N,I)-3+J
     U1=(B(LM(1))+B(LM(4))-B(LM(7))-B(LM(10))+B(LM(13))
    *+B(LM(16))-B(LM(19))-B(LM(22)))/AA
     V1=(-B(LM(2))+B(LM(5))+B(LM(8))-B(LM(11))-B(LM(14))
    *+B(LM(17))+B(LM(20))-B(LM(23)))/BB
     W1=(B(LM(3))+B(LM(6))+B(LM(9))+B(LM(12))-B(LM(15))
    *-B(LM(18))-B(LM(21))-B(LM(24)))/CC
     U2=(-B(LM(1))+B(LM(4))+B(LM(7))-B(LM(10))-B(LM(13))
    *+B(LM(16))+B(LM(19))-B(LM(22)))/BB
     V2=(B(LM(2))+B(LM(5))-B(LM(8))-B(LM(11))+B(LM(14))
    *+B(LM(17))-B(LM(20))-B(LM(23)))/AA
     V3=(B(LM(2))+B(LM(5))+B(LM(8))+B(LM(11))-B(LM(14))
    *-B(LM(17))-B(LM(20))-B(LM(23)))/CC
     W2=(-B(LM(3))+B(LM(6))+B(LM(9))-B(LM(12))-B(LM(15))
    *+B(LM(18))+B(LM(21))-B(LM(24)))/BB
     U3=(B(LM(1))+B(LM(4))+B(LM(7))+B(LM(10))-B(LM(13))
    *-B(LM(16))-B(LM(19))-B(LM(22)))/CC
     W3=(B(LM(3))+B(LM(6))-B(LM(9))-B(LM(12))+B(LM(15))
    *+B(LM(18))-B(LM(21))-B(LM(24)))/AA
     BETA=P4/((1.+P3)*(1.-P3-2.*P4*P2**2.))
     C1=BETA*(1.-P4*P2**2.)*P1
     C2=BETA*(P3+P4*P2**2.)*P1
     C3=BETA*P2*(1+P3)*P1
     C4=BETA*(1+P3)*(1-P3)*P1/P4
     C5=P4*P1/(2*(1+P3))
     C6=P5*P1
     X=(C1*U1+C2*V1+C3*W1)/8.
     Y=(C2*U1+C1*V1+C3*W1)/8.
     Z=(C3*U1+C3*V1+C4*W1)/8.
     XY=(C5*(U2+V2))/8.
     YZ=(C6*(V3+W2))/8.
     XZ=(C6*(U3+W3))/8.
     SGMX(N)=SGMX(N)+X
     SGMY(N)=SGMY(N)+Y
     SGMZ(N)=SGMZ(N)+Z
     SGMXY(N)=SGMXY(N)+XY
     SGMYZ(N)=SGMYZ(N)+YZ
     SGMXZ(N)=SGMXZ(N)+XZ
     WRITE
(6,35)N,SGMX(N),SGMY(N),SGMZ(N),SGMXY(N),SGMYZ(N),SGMXZ(N)
  35 FORMAT(1H ,I3,6(2X,E9.3))
     RETURN
     END
```

APPENDIX F3

DATA PREPARATION AND PROGRAM LISTING FOR PROGRAM PIER3DNL

F3.1 DATA PREPARATION

---

1. NAME

10 unit alpha-numeric identification of problems (eg. TRIAL1, EXAMPLE1)

---

2. NSYM, LDC, NPRNT

NSYM	= 1 For symmetric case.
	= 0 For non-symmetric case.
LDC	= 1 If pier element is divided into two elements both in the x- and y- directions.
	= 0 For pier with other sub-divisions or loadings.
NPRNT	= 1 For full output
	= 0 For restricted output

---

3. NTNEL, NPE, NUMNP, NOLN, NPX, NPY, NPZ, NUMBC

NTNEL	= Total number of elements in the mesh
NPE	= Number of pier elements
NUMNP	= Number of nodal points
NOLN	= Number of nodes at which loads are applied
	(NOLN=9 for LDC=1 if NSYM=0, NOLN=6 for LDC=1 if NSYM=1)
NPX	= Number of nodes along x- axis
NPY	= Number of nodes along y- axis

NPZ = Number of nodes along z- axis

NUMBC = Number of boundary conditions

---

4. NELP(I), I = 1, NPE

NELP = Element numbers of pier elements

---

5. NNLN(N), N = 1, NOLN Omit if LDC = 0

NNLN = Node number at which load is applied

---

6. NPB(L), NFIX(L), L = 1, NUMBC

NPB = Boundary node number

NFIX = Boundary condition code

	= 1	x- displacement = 0
	= 2	y- displacement = 0
	= 3	z- displacement = 0
	= 4	x- and y- displacements = 0
	= 5	y- and z- displacements = 0
	= 6	x- and z- displacements = 0
	= 7	x-, y- and z- displacements = 0

---

7. XX(I), I = 1, NPX

XX = Co-ordinates of nodal points along x- axis

---

8. YY(I), I = 1, NPY

YY = Co-ordinates of nodal points along y- axis

9. ZZ(I), I = 1, NPZ

ZZ = Co-ordinates of nodal points along z- axis

---

10. WX, WY Omit if LDC = 0

WX = Pier breadth along x- axis
WY = Pier breadth along y- axis

---

11. HT1, HKO, RO, RO1

HT1 = Height of soil below water table
HKO = Coefficient of lateral earth pressure at rest (K_0)
RO = Specific weight of soil above water table
RO1 = Specific weight of soil below water table

---

12. PM1, PM2, PM3, PM4, PM5, PM6, PM7

Soil properties and parameters used in hyperbolic model.

PM1 = c = Cohesion
PM2 = ϕ = Angle of shearing resistance
PM3 = R_f = Friction angle
PM4 = K = Stiffness no (primary loading)
PM5 = n = Stiffness exponent
PM6 = p = Atmosferic pressure (101.3 kN/m^2)
PM7 = K_{ur} = Unloading-reloading stiffness no

---

13. SOILPR, PROPP(J), J = 1, 2

SOILPR = Soil Poisson ratio

PROPP = Pier elastic constants, E and ν (for a linear isotropic body)

PROPP(1) = E

PROPP(2) = ν

---

14. NINC

NINC = Number of increments in which loads to be applied

---

15. VLOAD, XHLOAD, YHLOAD, XMLOAD, YMLOAD

VLOAD = Load in z- direction at the top of the pier

XHLOAD = Load in x- direction at the top of the pier

YHLOAD = Load in y- direction at the top of the pier

XMLOAD = Moment in x- direction at the top of the pier

YMLOAD = Moment in y- direction at the top of the pier

---

16. NNLN(II), XXF(II), YYF(II), ZZF(II), N = 1, NOLN Omit if LDC = 1

NNLN = Node number at which load is applied

XXF = Nodal load in x-direction

YYF = Nodal load in y-direction

ZZF = Nodal load in z-direction

F3.2 PROGRAM LISTING

```
      PROGRAM PIER3DNL
      COMMON/FIRST/A(400,400),B(4000),B2(4000),BT(4000)
      COMMON/SECOND/MM,NT

COMMON/THIRD/SGMX(2000),SGMY(2000),SGMZ(2000),SGMXY(2000)
     *,SGMYZ(2000),SGMXZ(2000),RFOS(2000),ETM(2000),SIGMA1(2000)
     *,SIGMA3(2000)
      CHARACTER*72 DATAFN,OUTPF
      CHARACTER NAME*10
      DIMENSION
NPB(2000),NFIX(2000),XX(25),YY(20),ZZ(40),NNLN(100)
      DIMENSION NP(2000,8),LM(24),KM(2),S(24,24),NELP(200)
      DIMENSION NUME(2000),PROPP(2),COORD(2000,3),NTYPE(1100)
      DIMENSION XXF(100),YYF(100),ZZF(100)
      PRINT *,'ENTER DATA FILE NAME WITH PATH'
      READ '(A)',DATAFN
      PRINT *,'ENTER OUTPUT FILE NAME WITH PATH'
      READ '(A)',OUTPF
      OPEN(5,FILE=DATAFN,STATUS='OLD')
      OPEN(6,FILE=OUTPF,STATUS='NEW')
      OPEN(1,FILE='UNIT1.DAT',FORM='UNFORMATTED')
      OPEN(2,FILE='UNIT2.DAT',FORM='UNFORMATTED')
      OPEN(3,FILE='UNIT3.DAT',FORM='UNFORMATTED')
C
C     READ DATA
C
      READ (5,1) NAME
      READ (5,*) NSYM,LDC,NPRNT
      READ (5,*) NTNEL,NPE,NUMNP,NOLN,NPX,NPY,NPZ,NUMBC
      READ (5,*) (NELP(I),I=1,NPE)
      IF(LDC.EQ.1) THEN
      READ (5,*) (NNLN(N),N=1,NOLN)
      ENDIF
      READ (5,*) (NPB(L),NFIX(L),L=1,NUMBC)
      READ (5,*) (XX(I),I=1,NPX)
      READ (5,*) (YY(I),I=1,NPY)
      READ (5,*) (ZZ(I),I=1,NPZ)
      IF(LDC.EQ.1) THEN
      READ (5,*) WX,WY
      ENDIF
      READ (5,*) HT1,HKO,RO,RO1
      IF(NSYM.EQ.0) GO TO 1111
      L=1
C
C     SYMMETRIC CASE
C
      NNYZ=NPY*NPZ
      DO 220 I=NPZ,NUMNP,NPZ
      NPB(L)=I
      NFIX(L)=7
  220 L=L+1
      DO 221 I=1,NPZ-1
      NPB(L)=I
      NFIX(L)=4
  221 L=L+1
      N=NNYZ-NPZ+1
      DO 222 I=N,NNYZ-1
      NPB(L)=I
      NFIX(L)=4
  222 L=L+1
      N1=NUMNP-NNYZ+1
      N2=N1+NPZ-2
      DO 223 I=N1,N2
      NPB(L)=I
      NFIX(L)=4
  223 L=L+1
      N1=NUMNP-NPZ+1
      N2=NUMNP-1
      DO 224 I=N1,N2
      NPB(L)=I
      NFIX(L)=4
  224 L=L+1
      K=NPZ
      DO 225 M=1,2
      DO 226 J=1,NPY-2
      DO 227 I=1,NPZ-1
      K=K+1
      NPB(L)=K
      NFIX(L)=1
  227 L=L+1
  226 K=K+1
  225 K=NUMNP-NNYZ+NPZ
      K=NNYZ
      DO 228 N=1,2
      DO 229 J=1,NPX-2
      DO 230 I=1,NPZ-1
      K=K+1
      NPB(L)=K
      NFIX(L)=2
  230 L=L+1
  229 K=K+NNYZ-NPZ+1
  228 K=2*NNYZ-NPZ
 1111 NT=3*NUMNP
      MM=3*(NPZ*(NPY+1)+2)
      NUMBLK=(NT-1)/MM+1
      NELX=NPX-1
      NELY=NPY-1
      NELZ=NPZ-1
      NELYZ=NELY*NELZ
      READ (5,*) PM1,PM2,PM3,PM4,PM5,PM6,PM7
      READ (5,*) SOILPR,(PROPP(J),J=1,2)
      READ (5,*) NINC
      IF(LDC.EQ.1) THEN
      READ (5,*) VLOAD,XHLOAD,YHLOAD,XMLOAD,YMLOAD
```

```
      ENDIF
      IF(LDC.EQ.0) THEN
      READ(5,*) (NNLN(II),XXF(II),YYF(II),ZZF(II),II=1,NOLN)
      END IF
C
C     GENERATION OF NODE CO-ORDINATES
C
      NPXY=NPX*NPY
      NPXZ=NPX*NPZ
      NPYZ=NPY*NPZ
      K=1
      DO 514 L1=1,NPX
       DO 514 J1=1,NPYZ
              COORD(K,1)=XX(L1)
  514         K=K+1
      K=1
      DO 525 L2=1,NPY
      N=K
       DO 526 M1=1,NPX
       DO 527 I1=1,NPZ
              COORD(K,2)=YY(L2)
  527         K=K+1
  526 K=NPYZ*M1+N
  525 K=NPZ*L2+1
      DO 535 L3=1,NPZ
      K=L3
      DO 535 J3=1,NPXY
              COORD(K,3)=ZZ(L3)
  535         K=K+NPZ
      DO 333 I1=1,NTNEL
  333 NTYPE(I1)=1
      DO 334 I2=1,NPE
  334 NTYPE(NELP(I2))=2
C
C     GENERATION OF NODE NUMBERS FOR ELEMENTS
C
      DO 122 N=1,NTNEL
      NXE=(N-1)/NELYZ+1
      NYE=(N-(NXE-1)*NELYZ-1)/NELZ+1
      NZE=N-(NXE-1)*NELYZ-(NYE-1)*NELZ
      NP(N,1)=NXE*NPYZ+(NYE-1)*NPZ+NZE+1
      NP(N,2)=NP(N,1)+NPZ
      NP(N,3)=NP(N,2)-NPYZ
      NP(N,4)=NP(N,3)-NPZ
      NP(N,5)=NP(N,1)-1
      NP(N,6)=NP(N,2)-1
      NP(N,7)=NP(N,3)-1
      NP(N,8)=NP(N,4)-1
  122 CONTINUE
C
C     PRINT DATA
C
      WRITE (6,*) NAME
      WRITE (6,610)
      WRITE (6,615) NTNEL,NPE,NUMNP,NOLN,NPX,NPY,NPZ,NUMBC
```

```
      WRITE (6,*)
      WRITE(6,213)
      WRITE(6,212)
      WRITE(6,215)(I,(NP(I,J),J=1,8),I=1,NTNEL)
      WRITE (6,201)
      WRITE (6,625) (NELP(I),I=1,NPE)
      WRITE (6,645)
      WRITE (6,650)
      WRITE (6,655) (XX(I),I=1,NPX)
      WRITE (6,660)
      WRITE (6,655) (YY(I),I=1,NPY)
      WRITE (6,665)
      WRITE (6,655) (ZZ(I),I=1,NPZ)
      WRITE(6,935)
      WRITE(6,940)
      DO 951 IP=1,NUMNP,2
      WRITE(6,950) IP,(COORD(IP,IDIM),IDIM=1,3),IP+1,(COORD((IP+1),
     *IDIM),IDIM=1,3)
  951 CONTINUE
      WRITE(6,238) HT1,HKO,RO,RO1
      WRITE (6,620)
      WRITE (6,625) (NNLN(N),N=1,NOLN)
      WRITE (6,630)
      WRITE (6,635)
      WRITE (6,640) (NPB(L),NFIX(L),L=1,NUMBC)
      WRITE (6,445)
      WRITE (6,446)
      WRITE (6,444) PM1,PM2,PM3,PM4,PM5,PM6,PM7
      WRITE (6,3002)
      WRITE (6,671)
      WRITE (6,675) SOILPR,(PROPP(J),J=1,2)
      WRITE (6,522)
      IF(LDC.EQ.1) THEN
      WRITE (6,523)
      WRITE (6,521) VLOAD,XHLOAD,YHLOAD,XMLOAD,YMLOAD
      END IF
      IF(LDC.EQ.0) THEN
      WRITE (6,3901)
      WRITE (6,3902) (NNLN(II),XXF(II),YYF(II),ZZF(II),II=1,NOLN)
      END IF
      WRITE (6,*)
      WRITE (6,680) MM
      DO 315 I=1,NTNEL
  315 NUME(I)=I
      NF=1
      NL=MM
      DO 325 J=1,MM
      DO 325 I=1,MM
  325 A(I,J)=0.0
      DO 320 I=1,MM
      BT(I)=0.0
  320 B(I)=0.0
C
C     INITIALISE STRESSES
C
```

```
      HT=ZZ(NPZ)
      WRITE (6,3006)
      WRITE (6,3007)
      DO 265 N=1,NTNEL
      NXE=(N-1)/NELYZ+1
      NYE=(N-(NXE-1)*NELYZ-1)/NELZ+1
      NZE=N-(NXE-1)*NELYZ-(NYE-1)*NELZ
      I=NZE+1
      L=NZE
      Z=(ZZ(I)+ZZ(L))/2.
      HT2=HT-HT1
      IF(Z.GT.HT2)GOTO 261
      SGMZ(N)=-RO*(Z)
      GOTO 262
  261 SGMZ(N)=-RO*(HT2)-RO1*(Z-HT2)
  262 CONTINUE
      SGMX(N)=HKO*SGMZ(N)
      SGMY(N)=HKO*SGMZ(N)
      Z=-SGMZ(N)
      X=-SGMX(N)
      CP2=COS(PM2)
      SP2=SIN(PM2)
      IF(X.GT.Z) GOTO 266
      S1=Z
      S3=X
      GOTO 267
  266 S1=X
      S3=Z
  267 R1=(S1-S3)/2
      IF(S3.EQ.0.0)S3=PM6/3
      C1=(S1+S3)/2
      R2=PM1*CP2+C1*SP2
      PR=SOILPR
      RFOS(N)=R1/R2
      SS1=PM3*(1.0-SP2)*(S1-S3)
      SS2=2.0*PM1*CP2+2.0*S3*SP2
      SS3=PM4*PM6*(S3/PM6)**Pm5
      SS4=(1.0-SS1/SS2)**2
      ETM(N)=SS3*SS4
      SGMXY(N)=0.0
      SGMYZ(N)=0.0
      SGMXZ(N)=0.0
  265 WRITE
(6,3005)N,SGMX(N),SGMY(N),SGMZ(N),ETM(N),PR,RFOS(N)
C
C     LOOP ON LOADING
C
      DO 1400 INCN=1,NINC
C
C     TWO CYCLE ITERATION FOR MODULUS OF NON-LINEAR
MATERIAL
C
            NCYCLE=0
C
c     INITIALIZE B-MATRIX
```

```
C
  725 CONTINUE
      DO 700 I=1,NT
  700 B(I)=0.0
      REWIND 2
      NCYCLE=NCYCLE+1
      DO 710 NB=1,NUMBLK
      NC=0
      REWIND 1
C
C     COMPUTE STIFFNESS OF ELEMENTS CONTRIBUTING TO THE
CURRENT
C     BLOCK
C
      DO 720 N=1,NTNEL
      IF(NUME(N).LT.0)GO TO 720
      NXE=(N-1)/NELYZ+1
      NYE=(N-(NXE-1)*NELYZ-1)/NELZ+1
      NZE=N-(NXE-1)*NELYZ-(NYE-1)*NELZ
      KM(1)=3*(NXE*NPYZ+NYE*NPZ+NZE+1)
      KM(2)=KM(1)-MM+1
      DO 730 I=1,2
      IF(KM(I).LT.NF)GO TO 730
      IF(KM(I).GT.NL)GO TO 730
      GO TO 740
  730 CONTINUE
      GO TO 720
  740 NC=NC+1
      NUME(N)=-NUME(N)
      MTYPE=NZE
      IF(NTYPE(N).EQ.2)GO TO 142
      P1=ETM(N)
      P2=SOILPR
      CALL STIF3D (N,NP,COORD,P1,P2,S)
      GO TO 143
  142 P1=PROPP(1)
      P2=PROPP(2)
      CALL STIF3D (N,NP,COORD,P1,P2,S)
C
C     ASSEMBLE THE COMPUTED STIFFNESSES
C
  143 DO 900 I=1,8
      DO 900 J=1,3
      JJ=3*I-3+J
  900 LM(JJ)=3*NP(N,I)-3+J
      DO 260 I=1,24
      IF(LM(I).LT.NF)GO TO 260
      IF(LM(I).GT.NL) GO TO 260
      II=LM(I)
      I1=II-NF+1
      DO 250 J=1,24
      JJ=LM(J)
      IF(JJ.LT.II)GO TO 250
      JJ=JJ-II+1
      A(I1,JJ)=A(I1,JJ)+S(I,J)
```

```
  250 CONTINUE
  260 CONTINUE
      IF(NB.EQ.NUMBLK)GO TO 720
C
C     WRITE THE COMPUTED STIFFNESSES TO UNIT 1
C
      WRITE(1) (LM(I),I=1,24),((S(I,J),J=1,24),I=1,24)
  720 CONTINUE
C
C     ASSIGN LOAD VECTORS WITHIN THE BLOCK
C
      IF(LDC.EQ.1) THEN
      XHLOAD=XHLOAD/NINC
      YHLOAD=YHLOAD/NINC
      VLOAD=VLOAD/NINC
      FX=YMLOAD/WX/NINC
      FY=XMLOAD/WY/NINC
      DO 150 N=1,NOLN
      JM=3*NNLN(N)
      IF(JM.LT.NF)GO TO 150
      IF(JM.GT.NL)GO TO 150
      I1=JM-NF+1
      IF(NSYM.EQ.1)THEN
      IF(N.EQ.1)THEN
      B(I1-2)=XHLOAD/16
      B(I1-1)=YHLOAD/16
      B(I1)=VLOAD/16+(FX/4)+(-FY/4)
      ELSEIF(N.EQ.2)THEN
      B(I1-2)=XHLOAD/8/2
      B(I1-1)=YHLOAD/8/2
      B(I1)=(VLOAD/8+(FX/2))/2
      ELSEIF(N.EQ.3)THEN
      B(I1-2)=XHLOAD/8
      B(I1-1)=YHLOAD/8
      B(I1)=VLOAD/8+(-FY/2)
      ELSEIF(N.EQ.4)THEN
      B(I1-2)=XHLOAD/4/2
      B(I1-1)=YHLOAD/4/2
      B(I1)=VLOAD/4/2
      ELSEIF(N.EQ.5)THEN
      B(I1-2)=XHLOAD/16
      B(I1-1)=YHLOAD/16
      B(I1)=VLOAD/16+(-FX/4)+(-FY/4)
      ELSEIF(N.EQ.6)THEN
      B(I1-2)=XHLOAD/8/2
      B(I1-1)=YHLOAD/8/2
      B(I1)=(VLOAD/8+(-FX/2))/2
      ENDIF
      ELSEIF(N.EQ.1)THEN
      B(I1-2)=XHLOAD/16
      B(I1-1)=YHLOAD/16
      B(I1)=VLOAD/16+(FX/4)+(-FY/4)
      ELSEIF(N.EQ.2)THEN
      B(I1-2)=XHLOAD/8
      B(I1-1)=YHLOAD/8
      B(I1)=VLOAD/8+(FX/2)
      ELSEIF(N.EQ.3)THEN
      B(I1-2)=XHLOAD/16
      B(I1-1)=YHLOAD/16
      B(I1)=VLOAD/16+(FX/4)+(FY/4)
      ELSEIF(N.EQ.4)THEN
      B(I1-2)=XHLOAD/8
      B(I1-1)=YHLOAD/8
      B(I1)=VLOAD/8+(-FY/2)
      ELSEIF(N.EQ.5)THEN
      B(I1-2)=XHLOAD/4
      B(I1-1)=YHLOAD/4
      B(I1)=VLOAD/4
      ELSEIF(N.EQ.6)THEN
      B(I1-2)=XHLOAD/8
      B(I1-1)=YHLOAD/8
      B(I1)=VLOAD/8+(FY/2)
      ELSEIF(N.EQ.7)THEN
      B(I1-2)=XHLOAD/16
      B(I1-1)=YHLOAD/16
      B(I1)=VLOAD/16+(-FX/4)+(-FY/4)
      ELSEIF(N.EQ.8)THEN
      B(I1-2)=XHLOAD/8
      B(I1-1)=YHLOAD/8
      B(I1)=VLOAD/8+(-FX/2)
      ELSEIF(N.EQ.9)THEN
      B(I1-2)=XHLOAD/16
      B(I1-1)=YHLOAD/16
      B(I1)=VLOAD/16+(-FX/4)+(FY/4)
      ENDIF
  150 CONTINUE
      ENDIF
      IF(LDC.EQ.0) THEN
      DO 1222 N=1,NOLN
      JM=3*NNLN(N)
      IF(JM.LT.NF)GO TO 1222
      IF(JM.GT.NL)GO TO 1222
      I1=JM-NF+1
      B(I1-2)=XXF(N)/NINC
      B(I1-1)=YYF(N)/NINC
      B(I1-0)=ZZF(N)/NINC
 1222 CONTINUE
      ENDIF
C
C     IMPOSE BOUNDARY CONDITIONS WITHIN THE BLOCK
C
      DO 200 L=1,NUMBC
      IF(NPB(L).LT.0)GO TO 200
      M=NPB(L)
      JM1=3*M-2
      JM2=JM1+1
      JM3=JM2+1
      IF(JM1.GT.NL)GO TO 200
      IF(JM3.LT.NF)GO TO 200
      NPB(L)=-NPB(L)
```

```
      IF(NFIX(L).NE.1)GO TO 170
      CALL MODIFY(JM1,NF)
      GO TO 200
  170 IF(NFIX(L).NE.2)GO TO 175
      CALL MODIFY(JM2,NF)
      GO TO 200
  175 IF(NFIX(L).NE.3)GO TO 180
      CALL MODIFY(JM3,NF)
      GO TO 200
  180 IF(NFIX(L).NE.4)GO TO 185
      CALL MODIFY(JM1,NF)
      CALL MODIFY(JM2,NF)
      GO TO 200
  185 IF(NFIX(L).NE.5)GO TO 190
      CALL MODIFY(JM2,NF)
      CALL MODIFY(JM3,NF)
      GO TO 200
  190 IF(NFIX(L).NE.6)GO TO 195
      CALL MODIFY(JM1,NF)
      CALL MODIFY(JM3,NF)
      GO TO 200
  195 IF(NFIX(L).NE.7) GO TO 200
      CALL MODIFY(JM1,NF)
      CALL MODIFY(JM2,NF)
      CALL MODIFY(JM3,NF)
  200 CONTINUE
C
C     WRITE THE RESULTING BLOCK STIFFNESS AND LOAD
VECTORS TO UNIT 2
C
      DO 210 I=1,MM
  210 WRITE(2) (A(I,J),J=1,MM),(B(I))
C
C     INITIALIZE A AND B MATRICES
C
      REWIND 1
      DO 750 I=1,MM
      DO 755 J=1,MM
  755 A(I,J)=0.0
  750 B(I)=0.0
      IF(NB.EQ.NUMBLK) GO TO 710
C
C     COMPUTE NEW BLOCK PARAMETERS
C
      NF=NF+MM
      NL=NL+MM
C
C     ASSEMBLE THE COMPUTED STIFFNESSES IN THE NEW
BLOCK
C
      DO 760 NCC=1,NC
      READ(1) (LM(I),I=1,24),((S(I,J),J=1,24),I=1,24)
      DO 770 I=1,24
      IF(LM(I).LT.NF) GO TO 770
      IF(LM(I).GT.NL)GO TO 770
      II=LM(I)
      I1=II-NF+1
      DO 780 J=1,24
      JJ=LM(J)
      IF(JJ.LT.II)GO TO 780
      JJ=JJ-II+1
      A(I1,JJ)=A(I1,JJ)+S(I,J)
  780 CONTINUE
  770 CONTINUE
  760 CONTINUE
  710 CONTINUE
C
C     SOLVE FOR NODAL DISPLACEMENTS
C
      DO 1966 KK=1,NTNEL
 1966 NUME(KK)=-NUME(KK)
      NF=1
      NL=MM
      DO 231 L=1,NUMBC
  231  NPB(L)=-NPB(L)
      CALL SOLVE2
c     WRITE(6,388)
c     WRITE(6,39)
      REWIND 3
      DO 555 N=NT,1,-1
  555 READ(3) B(N)
C
C     PRINT OF DISPLACEMENTS
C
      IF(NCYCLE.EQ.1) GOTO 38
      WRITE (6,309) INCN
      CONTINUE
C
C     PRINT OF STRESSES
C
      IF(INCN.NE.NINC) GOTO 38
   37 FORMAT(//5HEL NO,5X,5H SIGX,5X,5H SIGY,5X,5H SIGZ,5X,6H
SIGXY,5X,
     *6H SIGYZ,5X,6H SIGXZ,5x,6hSIGMA1,5x,6hSIGMA3,5x,6h   ETM/)
   38 CONTINUE
      DO 850 N=1,NTNEL
      NXE=(N-1)/NELYZ+1
      NYE=(N-(NXE-1)*NELYZ-1)/NELZ+1
      NZE=N-(NXE-1)*NELYZ-(NYE-1)*NELZ
      IF(NTYPE(N).EQ.2)GO TO 146
      P1=ETM(N)
      P2=SOILPR
      CALL STRESS
(N,P1,P2,NPYZ,NPZ,LM,NP,ZZ,XX,YY,NXE,NYE,NZE,
     *PM1,PM2,PM3,PM4,PM5,PM6,PM7,ncycle,npe,incn,ninc,nelp,ntype)
      GO TO 850
  146 P1=PROPP(1)
      P2=PROPP(2)
      CALL STRESS
(N,P1,P2,NPYZ,NPZ,LM,NP,ZZ,XX,YY,NXE,NYE,NZE,
```

```
      *PM1,PM2,PM3,PM4,PM5,PM6,PM7,ncycle,npe,incn,ninc,nelp,ntype)
  850 CONTINUE
C
C     END OF FIRST ITERATION
C
      IF(NCYCLE.EQ.1)GO TO 725
C
C     ADD  INCREMENTAL        DISPLACEMENTS  AND  PRINT
C
      KK=1
      DO 211 IK=1,NUMNP
      DO 211 JK=1,3
      COORD(IK,JK)=COORD(IK,JK)+B(KK)
  211 KK=KK+1
      DO 402 I=1,NT
  402 BT(I)=BT(I)+B(I)
      IF(NPRNT.EQ.1) THEN
      WRITE (6,388)
      WRITE (6,39)
      DO 107 J=1,NT,3
  107 WRITE (6,691) J,BT(J),J+1,BT(J+1),J+2,BT(J+2)
      WRITE(6,935)
      WRITE(6,940)
      DO 952 IP=1,NUMNP,2
      WRITE(6,950) IP,(COORD(IP,IDIM),IDIM=1,3),IP+1,(COORD((IP+1),
     *IDIM),IDIM=1,3)
  952 CONTINUE
      WRITE(6,33)
      WRITE(6,37)
      DO 9001 N=1,NTNEL
      WRITE (6,90)
N,SGMX(N),SGMY(N),SGMZ(N),SGMXY(N),SGMYZ(N),SGMXZ(N)
     *,SIGMA1(N),SIGMA3(N),ETM(n)
 9001 CONTINUE
      ENDIF
      IF(NPRNT.EQ.1) GOTO  1400
      IF(INCN.EQ.NINC) THEN
      WRITE (6,388)
      WRITE (6,39)
      DO 9107 J=1,NT,3
 9107 WRITE (6,691) J,BT(J),J+1,BT(J+1),J+2,BT(J+2)
c     WRITE(6,935)
c     WRITE(6,940)
c     DO 9952 IP=1,NUMNP,2
c     WRITE(6,950) IP,(COORD(IP,IDIM),IDIM=1,3),IP+1,(COORD((IP+1),
c    *IDIM),IDIM=1,3)
c9952 CONTINUE
      WRITE(6,33)
      WRITE(6,37)
      DO 9011 N=1,NTNEL
      WRITE (6,90)
N,SGMX(N),SGMY(N),SGMZ(N),SGMXY(N),SGMYZ(N),SGMXZ(N)
     *,SIGMA1(N),SIGMA3(N),ETM(N)
 9011 CONTINUE
      ENDIF
 1400 CONTINUE
    1 FORMAT(A10)
   33 FORMAT(1H ,//,27H              ELEMENT STRESSES)
   39 FORMAT(/9X,6HX-DISP,10X,6HY-DISP,11X,6HZ-DISP,5X/)
   90 FORMAT(I5,9(2X,E9.3))
  201 FORMAT(//,21H PIER ELEMENT NUMBERS,/)
  212 FORMAT(//,'   I    1    2    3    4    5    6    7    8')
  215 FORMAT(/9(2X,I4))
  213 FORMAT(//'   ELEMENT AND NODE NUMBERS FOR
ELEMENTS')
  238 FORMAT(//,'    HEIGHT OF WATER TABLE=',F7.4,/'    KO
VALUE='
     *,F7.4,/'    BULK DENSITY=',F7.4,/'    SUBMERGED
DENSITY=',F7.4)
  309 FORMAT(//,3X,'INCN.NO.=',I5,/)
  388 FORMAT(//,21H NODAL DISPLACEMENTS )
  444 FORMAT(7F12.3)
  445 FORMAT(//,1H ,'      SOIL PARAMETERS - HYPERBOLIC
MODEL')
  446 FORMAT(/'    COHESION  FRICT.ANGLE  FAIL.RATIO',
     *'  STIFFN.NO  STIFFN.EXP  ATMOS.PRESS  U/R STIFFN.NO'/)
  691 FORMAT(3(I4,1X,E12.4,2X))
  521 FORMAT(5F10.3)
  522 FORMAT(//,20H    APPLIED LOADING,/)
  523 FORMAT(7H
VLOAD,8X,6HXHLOAD,3X,6HYHLOAD,4X,6HXMLOAD,4X,6HYMLOA
D)
  615 FORMAT (I6,7I9)
  610 FORMAT (//,70H NTNEL      NPE          NUMNP       NOLN
NPX          NP    *Y      NPZ    NUMBC,/)
  620 FORMAT (//,31H NODES AT WHICH LOAD IS APPLIED,/)
  625 FORMAT (10I6)
  630 FORMAT(//,20H BOUNDARY CONDITIONS)
  635 FORMAT (/,5(11H  NPB  CODE),/)
  640 FORMAT (5(I5,I6))
  645 FORMAT (//,10H MESH DATA)
  650 FORMAT (/,25H COORDINATES ALONG X-AXIS,/)
  655 FORMAT(8F10.4)
  660 FORMAT (//,25H COORDINATES ALONG Y-AXIS,/)
  665 FORMAT (//,25H COORDINATES ALONG Z-AXIS,/)
  671 FORMAT (/,50H SOIL POISSON RATIO    PIER MODULUS
POISSON   RATIO ,/)
  675 FORMAT (E14.5,6X,2E14.5)
  680 FORMAT (/,13H BAND WIDTH =,I5,/)
  935 FORMAT(//25H  NODAL POINT COORDINATES,/)
  940 FORMAT(5H NODE,5X,1HX,8X,1HY,8X,1HZ,8X,6H
NODE,5X,1HX,8X,1HY,8X,
     *1HZ,/)
  950 FORMAT(I4,2X,3F9.5,5X,i4,2X,3F9.5)
 3002 FORMAT(1H ,//,36H    PIER AND SOIL ELEMENT PROPERTIES)
 3005 FORMAT(1H ,I6,6(3X,E13.6))
 3006 FORMAT(1H ,/,27H                         INITIAL STRESSES,/)
 3007 FORMAT(/8H   EL NO,4X,8H              SIGX,4X,10H
SIGY,7X,
     *10H     SIGZ ,5X,10H     ETM  ,5X,9H     PR ,7X,9H     RFOS/)
```

```
 3901 FORMAT(7H  NODES,5X,6H  XXF ,6X,6H  YYF ,6X,6H  ZZF ,/)
 3902 FORMAT (I6,2X,F9.3,3X,F9.3,3X,F9.3)
      STOP
      END

      SUBROUTINE STIF3D(N,NP,COORD,P1,P2,S)
      DIMENSION S(24,24),DM(6,6),POSGP(3),WEIGP(3)
     .,COORD(2000,3),SHAPE(8),DERIV(3,8),CARTD(3,8),BMI(6,3)
     .,BMJ(6,3),NP(2000,8)
C
C***  INITIALIZE THE ELEMENT STIFFNESS MATRIX (S)
C
      DO 10 IE=1,24
      DO 10 JE=1,24
   10 S(IE,JE)=0.0
C
C***  INITIALIZE AND EVALUATE THE MATRIX OF ELASTIC
RIGIDITIES (DM)
C
      DO 5 ISIZE=1,6
      DO 5 JSIZE=1,6
    5 DM(ISIZE,JSIZE)=0.0
      COM=P1*(1.-P2)/((1+P2)*(1-2.*P2))
      DM(1,1)=COM
      DM(1,2)=COM*P2/(1.-P2)
      DM(1,3)=DM(1,2)
      DM(2,1)=DM(1,2)
      DM(2,2)=DM(1,1)
      DM(2,3)=DM(1,2)
      DM(3,1)=DM(1,2)
      DM(3,2)=DM(1,2)
      DM(3,3)=DM(1,1)
      DM(4,4)=COM*(1.-2.*P2)/(2.*(1.-P2))
      DM(5,5)=DM(4,4)
      DM(6,6)=DM(4,4)
C
C***  EVALUATE THE COORDINATES OF NODES
C
      KGASP=0
C
C***  ENTER LOOPS FOR VOLUME NUMERICAL INTEGRATION
C***  SET UP GAUSSIAN INTEGRATION CONSTANTS
C
      POSGP(1)=-0.577350269189626
      POSGP(2)=0.577350269189626
      WEIGP(1)=1.0
      WEIGP(2)=1.0
      DO 30 IGAUS=1,2
      XI=POSGP(IGAUS)
      DO 30 JGAUS=1,2
      ET=POSGP(JGAUS)
      DO 30 KGAUS=1,2
      KGASP=KGASP+1
      ZT=POSGP(KGAUS)
C
C***  EVALUATE THE SHAPE FUNCTIONS AND ELEMENTAL
VOLUME
C
      CALL SFUNC (DERIV,XI,ET,ZT,SHAPE)
      CALL JACOB (N,NP,COORD,CARTD,DERIV,DJACB,IELEM,SHAPE)

DVOLUM=DJACB*WEIGP(IGAUS)*WEIGP(JGAUS)*WEIGP(KGAUS)
C
C***  EVALUATE THE B AND DB MATRICES
C
      DO 20 INODE=1,8
      CALL BMATB (BMI,CARTD,INODE)
      DO 20 JNODE=INODE,8
      CALL BMATB (BMJ,CARTD,JNODE)
   20 CALL SUBPB (BMI,BMJ,DVOLUM,DM,S,INODE,JNODE)
   30 CONTINUE
      RETURN
      END

      SUBROUTINE SFUNC (DERIV,XI,ET,ZT,SHAPE)
C
C***  EVALUATES SHAPE FUNCTIONS AND THEIR DERIVATIVES
FOR 8 NODED
C***  HEXAHEDRAL ISOPARAMETRIC ELEMENT
C
      DIMENSION DERIV(3,8),SHAPE(8)
C
C***  SHAPE FUNCTIONS
C
      SHAPE(1)=((1+XI)*(1-ET)*(1+ZT))/8
      SHAPE(2)=((1+XI)*(1+ET)*(1+ZT))/8
      SHAPE(3)=((1-XI)*(1+ET)*(1+ZT))/8
      SHAPE(4)=((1-XI)*(1-ET)*(1+ZT))/8
      SHAPE(5)=((1+XI)*(1-ET)*(1-ZT))/8
      SHAPE(6)=((1+XI)*(1+ET)*(1-ZT))/8
      SHAPE(7)=((1-XI)*(1+ET)*(1-ZT))/8
      SHAPE(8)=((1-XI)*(1-ET)*(1-ZT))/8
C
C***  SHAPE FUNCTIONS DERIVATIVES
C
      DERIV(1,1)=((1-ET)*(1+ZT))/8
      DERIV(1,2)=((1+ET)*(1+ZT))/8
      DERIV(1,3)=-((1+ET)*(1+ZT))/8
      DERIV(1,4)=-((1-ET)*(1+ZT))/8
      DERIV(1,5)=((1-ET)*(1-ZT))/8
      DERIV(1,6)=((1+ET)*(1-ZT))/8
      DERIV(1,7)=-((1+ET)*(1-ZT))/8
      DERIV(1,8)=-((1-ET)*(1-ZT))/8
      DERIV(2,1)=-((1+XI)*(1+ZT))/8
      DERIV(2,2)=((1+XI)*(1+ZT))/8
      DERIV(2,3)=((1-XI)*(1+ZT))/8
      DERIV(2,4)=-((1-XI)*(1+ZT))/8
      DERIV(2,5)=-((1+XI)*(1-ZT))/8
      DERIV(2,6)=((1+XI)*(1-ZT))/8
      DERIV(2,7)=((1-XI)*(1-ZT))/8
```

```
      DERIV(2,8)=-((1-XI)*(1-ZT))/8
      DERIV(3,1)=((1+XI)*(1-ET))/8
      DERIV(3,2)=((1+XI)*(1+ET))/8
      DERIV(3,3)=((1-XI)*(1+ET))/8
      DERIV(3,4)=((1-XI)*(1-ET))/8
      DERIV(3,5)=-((1+XI)*(1-ET))/8
      DERIV(3,6)=-((1+XI)*(1+ET))/8
      DERIV(3,7)=-((1-XI)*(1+ET))/8
      DERIV(3,8)=-((1-XI)*(1-ET))/8
      RETURN
      END

      SUBROUTINE JACOB
(N,NP,COORD,CARTD,DERIV,DJACB,IELEM,SHAPE)
C
C***  EVALUATES JACOBIAN MATRIX AND ITS INVERSE
C***  CARTESIAN SHAPE FUNCTION DERIVATIVES AT PRESENT
SAMPLING POINT
C
c     IMPLICIT REAL*8 (A-H,O-Z)
      DIMENSION
CARTD(3,8),DERIV(3,8),SHAPE(8),COORD(2000,3),XJM(3,3)
     .,XJACI(3,3),NP(2000,8)
C
C***  CREATE JACOBIAN MATRIX  (XJM)
C
      DO 35 ID=1,3
      DO 35 JD=1,3
      XJM(ID,JD)=0.0
      DO 35 INODE=1,8
      num=np(n,inode)
   35 XJM(ID,JD)=XJM(ID,JD)+DERIV(ID,INODE)*COORD(NUM,JD)
C
C***  CALCULATE DETERMINANT AND INVERSE OF JACOBIAN
MATRIX
C

DJACB=XJM(1,1)*XJM(2,2)*XJM(3,3)+XJM(1,2)*XJM(2,3)*XJM(3,1)+
     .XJM(1,3)*XJM(2,1)*XJM(3,2)-(XJM(1,3)*XJM(2,2)*XJM(3,1)+
     .XJM(1,1)*XJM(2,3)*XJM(3,2)+XJM(1,2)*XJM(2,1)*XJM(3,3))
      IF(DJACB) 6,6,8
    6 WRITE (6,901) IELEM
      STOP
    8 CONTINUE
      XJACI(1,1)=(XJM(2,2)*XJM(3,3)-XJM(2,3)*XJM(3,2))/DJACB
      XJACI(1,2)=(XJM(1,3)*XJM(3,2)-XJM(1,2)*XJM(3,3))/DJACB
      XJACI(1,3)=(XJM(1,2)*XJM(2,3)-XJM(1,3)*XJM(2,2))/DJACB
      XJACI(2,1)=(XJM(2,3)*XJM(3,1)-XJM(2,1)*XJM(3,3))/DJACB
      XJACI(2,2)=(XJM(1,1)*XJM(3,3)-XJM(1,3)*XJM(3,1))/DJACB
      XJACI(2,3)=(XJM(1,3)*XJM(2,1)-XJM(1,1)*XJM(2,3))/DJACB
      XJACI(3,1)=(XJM(2,1)*XJM(3,2)-XJM(3,1)*XJM(2,2))/DJACB
      XJACI(3,2)=(XJM(1,2)*XJM(3,1)-XJM(1,1)*XJM(3,2))/DJACB
      XJACI(3,3)=(XJM(1,1)*XJM(2,2)-XJM(1,2)*XJM(2,1))/DJACB
C
C***  CALCULATE CARTESIAN DERIVATIVES
C
      DO 40 ID=1,3
      DO 40 INODE=1,8
      CARTD(ID,INODE)=0.0
      DO 40 JD=1,3

CARTD(ID,INODE)=CARTD(ID,INODE)+XJACI(ID,JD)*DERIV(JD,INOD
E)
   40 CONTINUE
  901 FORMAT(//,36H PROGRAM HALTED IN SUBROUTINE
JACOB,/,11X,24H ZERO OR
     . NEGATIVE VOLUME,10X,16H ELEMENT NUMBER ,I5)
      RETURN
      END

      SUBROUTINE BMATB (BMX,CARTD,KNODE)
C
C***  EVALUATES STRAIN-DISPLACEMENT MATRIX
C
c     IMPLICIT REAL*8 (A-H,O-Z)
      DIMENSION BMX(6,3),CARTD(3,8)
      DNKDX=CARTD(1,KNODE)
      DNKDY=CARTD(2,KNODE)
      DNKDZ=CARTD(3,KNODE)
C
C***  INITIALIZE AND FORM B MATRIX  (BMX)
C
      DO 40 IS=1,6
      DO 40 JS=1,3
   40 BMX(IS,JS)=0.0
      BMX(1,1)=DNKDX
      BMX(2,2)=DNKDY
      BMX(3,3)=DNKDZ
      BMX(4,1)=DNKDY
      BMX(4,2)=DNKDX
      BMX(5,2)=DNKDZ
      BMX(5,3)=DNKDY
      BMX(6,1)=DNKDZ
      BMX(6,3)=DNKDX
      RETURN
      END

      SUBROUTINE SUBPB
(BIMAT,BJMAT,DVOLUM,DMATX,S,INODE,JNODE)
      DIMENSION
BIMAT(6,3),BJMAT(6,3),DBMAT(6,3),DMATX(6,6),SBSTF(3,3),
     .S(24,24)
C
C***  EVALUATE D*B MATRIX (DBMAT)
C
      DO 45 J1=1,3
      DO 45 I1=1,6
      DBMAT(I1,J1)=0.0
      DO 45 K1=1,6
   45 DBMAT(I1,J1)=DBMAT(I1,J1)+DMATX(I1,K1)*BJMAT(K1,J1)
```

```
C
C***  EVALUATE BT*(D*B) MATRIX (SBSTF)
C
      DO 50 J2=1,3
      DO 50 I2=1,3
      SBSTF(I2,J2)=0.0
      DO 50 K2=1,6
   50 SBSTF(I2,J2)=SBSTF(I2,J2)+BIMAT(K2,I2)*DBMAT(K2,J2)
C
C***  ASSEMBLE SBSTF INTO ELEMENT STIFFNESS MATRIX
C
      IFROW=0
      JFCOL=0
      IFROW=(INODE-1)*3+IFROW
      JFCOL=(JNODE-1)*3+JFCOL
      DO 55 I3=1,3
      IRSUB=IFROW+I3
      DO 55 J3=1,3
      JCSUB=JFCOL+J3
   55 S(IRSUB,JCSUB)=S(IRSUB,JCSUB)+SBSTF(I3,J3)*DVOLUM
      DO 110 J=1,24
      DO 110 I=1,24
      S(I,J)=S(J,I)
  110 CONTINUE
      RETURN
      END

      SUBROUTINE MODIFY (N,NF)
      COMMON/FIRST/A(400,400),B(4000),B2(4000),BT(4000)
      COMMON/SECOND/MM,NT
      N1=N-NF+1
      A(N1,1)=A(N1,1)*.1E+12
      B(N1)=0.0
      RETURN
      END

      SUBROUTINE SOLVE2
      COMMON/FIRST/A(400,400),B(4000),B2(4000),BT(4000)
      COMMON/SECOND/MM,NT
      REWIND 2
      REWIND 1
      REWIND 3
      IC=1
      NC=MM+1
      NB=1
      DO 50 I=1,MM
      READ(2) (A(I,M),M=1,MM),B(I)
   50 CONTINUE
  200 N=IC
      B(N)=B(N)/A(N,1)
      DO 270 L=2,MM
      IF(A(N,L).EQ.0.0)GO TO 270
      C=A(N,L)/A(N,1)
      I=N+L-1
      IF(I.GT.MM)I=I-MM
      J=0
      DO 290 K=L,MM
      J=J+1
  290 A(I,J)=A(I,J)-C*A(N,K)
      B(I)=B(I)-A(N,L)*B(N)
      A(N,L)=C
  270 CONTINUE
      WRITE(1) (A(N,M),M=2,MM),(B(N))
      DO 100 M=1,MM
  100 A(N,M)=0.0
      B(N)=0.0
      IF(NB.EQ.NT)GO TO 300
      IF(NC.GT.NT)GO TO 210
      READ(2) (A(N,M),M=1,MM),B(N)
  210 NC=NC+1
      NB=NB+1
      IC=IC+1
      IF(IC.GT.MM)IC=1
      IF(IC.NE.1) GO TO 200
      GO TO 200
  300 CONTINUE
      DO 400 K=1,MM
      N=MM-K+1
      BACKSPACE 1
      READ(1)  (A(N,M),M=2,MM),B(N)
      BACKSPACE 1
  400 CONTINUE
      IC=MM
      NC=MM+1
      NB=1
  410 N=IC
      DO 430 M=2,MM
      K=N-M+1
      IF(K.LT.1)K=MM+K
      B(K)=B(K)-A(K,M)*B(N)
  430 CONTINUE
      WRITE(3)(B(N))
      B(N)=0.0
      DO 450 J=1,MM
  450 A(N,J)=0.0
      IF(NB.EQ.NT)GO TO 500
      IF(NC.GT.NT)GO TO 480
      BACKSPACE 1
      READ(1)  (A(N,J),J=2,MM),B(N)
      BACK SPACE 1
  480 NC=NC+1
      NB=NB+1
      IC=IC-1
      IF(IC.EQ.0)IC=MM
      IF(IC.NE.MM) GO TO 410
      GO TO 410
  500 CONTINUE
      RETURN
      END
```

```
      SUBROUTINE STRESS (N,P1,P2,NPYZ,NPZ,LM,NP,ZZ,XX,YY,NXE,
     *NYE,NZE,PM1,PM2,PM3,PM4,PM5,PM6,PM7,ncycle,npe,incn,ninc,nelp,
     *ntype)
      COMMON/FIRST/A(400,400),B(4000),B2(4000),BT(4000)
      COMMON/SECOND/MM,NT
      COMMON/THIRD/SGMX(2000),SGMY(2000),SGMZ(2000),SGMXY(2000)
     *,SGMYZ(2000),SGMXZ(2000),RFOS(2000),ETM(2000),SIGMA1(2000)
     *,SIGMA3(2000)
      DIMENSION XX(25),YY(20),ZZ(40),ntype(1100)
      DIMENSION NP(2000,8),LM(24),NELP(200)
      AA=ABS(XX(NXE+1)-XX(NXE))/2.
      BB=ABS(YY(NYE+1)-YY(NYE))/2.
      CC=ABS(ZZ(NZE+1)-ZZ(NZE))/2.
      DO 901 I=1,8
      DO 901 J=1,3
      JJ=3*I-3+J
  901 LM(JJ)=3*NP(N,I)-3+J
      U1=(B(LM(1))+B(LM(4))-B(LM(7))-B(LM(10))+B(LM(13))
     *+B(LM(16))-B(LM(19))-B(LM(22)))/AA
      V1=(-B(LM(2))+B(LM(5))+B(LM(8))-B(LM(11))-B(LM(14))
     *+B(LM(17))+B(LM(20))-B(LM(23)))/BB
      W1=(B(LM(3))+B(LM(6))+B(LM(9))+B(LM(12))-B(LM(15))
     *-B(LM(18))-B(LM(21))-B(LM(24)))/CC
      U2=(-B(LM(1))+B(LM(4))+B(LM(7))-B(LM(10))-B(LM(13))
     *+B(LM(16))+B(LM(19))-B(LM(22)))/BB
      V2=(B(LM(2))+B(LM(5))-B(LM(8))-B(LM(11))+B(LM(14))
     *+B(LM(17))-B(LM(20))-B(LM(23)))/AA
      V3=(B(LM(2))+B(LM(5))+B(LM(8))+B(LM(11))-B(LM(14))
     *-B(LM(17))-B(LM(20))-B(LM(23)))/CC
      W2=(-B(LM(3))+B(LM(6))+B(LM(9))-B(LM(12))-B(LM(15))
     *+B(LM(18))+B(LM(21))-B(LM(24)))/BB
      U3=(B(LM(1))+B(LM(4))+B(LM(7))+B(LM(10))-B(LM(13))
     *-B(LM(16))-B(LM(19))-B(LM(22)))/CC
      W3=(B(LM(3))+B(LM(6))-B(LM(9))-B(LM(12))+B(LM(15))
     *+B(LM(18))-B(LM(21))-B(LM(24)))/AA
      P3=P2
      P4=1.0
      P5=0.5/(1.0+P2)
      BETA=P4/((1.+P3)*(1.-P3-2.*P4*P2**2.))
      C1=BETA*(1.-P4*P2**2.)*P1
      C2=BETA*(P3+P4*P2**2.)*P1
      C3=BETA*P2*(1+P3)*P1
      C4=BETA*(1+P3)*(1-P3)*P1/P4
      C5=P4*P1/(2*(1+P3))
      C6=P5*P1
      X=(C1*U1+C2*V1+C3*W1)/8.
      Y=(C2*U1+C1*V1+C3*W1)/8.
      Z=(C3*U1+C3*V1+C4*W1)/8.
      XY=(C5*(U2+V2))/8.
      YZ=(C6*(V3+W2))/8.
      XZ=(C6*(U3+W3))/8.
      SX=SGMX(N)+X/2
      SY=SGMY(N)+Y/2
      SZ=SGMZ(N)+Z/2
      SXY=SGMXY(N)+XY/2
      SYZ=SGMYZ(N)+YZ/2
      SXZ=SGMXZ(N)+XZ/2
      IF(NCYCLE.EQ.1)GOTO 112
      SX=SX+X/2
      SY=SY+Y/2
      SZ=SZ+Z/2
      SXY=SXY+XY/2
      SYZ=SYZ+YZ/2
      SXZ=SXZ+XZ/2
  112 continue
      call RR(SX,SY,SZ,SXY,SYZ,SXZ,SIG1,SIG3)
      IF(Ntype(n).EQ.2)GO TO 161
C     NOTE: PRINCIPAL STRESSES COMPN. POSTIVE
      r1=(sig1-sig3)/2
      CP2=COS(PM2)
      SP2=SIN(PM2)
      R2=PM1*CP2+C1*SP2
C     TENSION?
      IF(0.0.LT.SIG3)GO TO 120
      ETM(N)=1.0
C     TENSILE FAILURE VALUE
      GO TO 115
  120 RFS=R1/R2
C     FIRST LOADING?
      IF(RFS.LT.RFOS(N)) GO TO 125
      IF(NCYCLE.EQ.1) GO TO 127
      RFOS(N)=RFS
  127 SS1=PM3*(1.0-SP2)*(SIG1-SIG3)
      SS2=2.0*PM1*CP2+2.0*SIG3*SP2
      SS3=PM4*PM6
      IF(PM5.EQ.0.0)GOTO 130
      SS3=SS3*(SIG3/PM6)**PM5
  130 SS4=(1.0-SS1/SS2)**2
C     FAILURE?
      IF(R2.LT.R1)GOTO 135
      ETM(N)=SS3*SS4
      GO TO 115
  125 EUR=PM7*PM6
      IF(PM5.EQ.0.0)GOTO 140
      EUR=EUR*(SIG3/PM6)**PM5
C     FAILURE?
  140 IF(R2.LT.R1)GOTO 135
      ETM(N)=EUR
      GO TO 115
  135 ETM(N)=0.5
C     SHEAR FAILURE VALUE
  115 CONTINUE
  161 IF(NCYCLE.EQ.1)GOTO 160
      IF(SZ.EQ.SX)GOTO 145
      PA=28.65*ATAN(2.*SXZ/(SX-SZ))
      IF(SX.GT.SZ)GOTO 150
      IF(PA.LT.0.0)PAA=PA+90.0
      IF(PA.GT.0.0)PAA=PA-90.0
```

```
      PA=PAA
      GO TO 150
  145 PA=45.0
C     PA IS INCLN. OF MAJOR PR.PL. TO HORIZ.
  150 CONTINUE
C     STORE STRESSES
      SGMX(N)=SX
      SGMY(N)=SY
      SGMZ(N)=SZ
      SGMXY(N)=SXY
      SGMYZ(N)=SYZ
      SGMXZ(N)=SXZ
  160 CONTINUE
      SIGMA1(N)=SIG1
      SIGMA3(N)=SIG3
      RETURN
      END

      subroutine RR (sx,sy,sz,txy,tyz,txz,Sig1,Sig3)
      complex s1,s2,s3,a,b,c,r,r1,r2,r3,r4
c     complex sx,sy,sz,txy,tyz,txz
      a=-(sx+sy+sz)
      b=sx*sy+sy*sz+sx*sz-txy**2-tyz**2-txz**2
      c=-(sx*sy*sz+2*txy*tyz*txz-sx*tyz**2-sy*txz**2-sz*txy**2)
      r=-3.
      r2=-(a**2)/9.
      r1=Sqrt((r2+b/3.)**3+(-(a**3)/27.+a*b/6.-c/2.)**2)
      r3=(-(a**3)/27.+a*b/6.+r1-c/2.)**(1./3.)
      r4=(r2+b/3.)/r3
C  PRINCIPAL STRESSES
      s1= -a/3.-r4+r3
      s2= -a/3.-(-((r2+b/3)/(-(a**3)/27+a*b/6+r1-c/2)**(1./3.))
     #+ r3 )/2. + Sqrt(r)*(( r2 + b/3)/ r3 + r3)/2
      s3=-a/3.-(-(r4)+r3)/2-Sqrt(r)*(r4+ r3)/2
      SS1=REAL(-S1)
      SS2=REAL(-S2)
      SS3=REAL(-S3)
      sig1=MAX(ss1,ss2,ss3)
      sig3=MIN(ss1,ss2,ss3)
      return
      end
```

APPENDIX G1

INPUT AND OUTPUT DATA (USING PROGRAM PIER3DLN)

G1.1 INPUT DATA

```
BR16DP24
   1    1
 784    8 1080    6   15    8    9  456
 385  386  387  388  441  442  443  444
 487  496  559  568  631  640
  10    1   11    1   12    1   13    1   14    1   15    1   16    1   17    1
  19    1   20    1   21    1   22    1   23    1   24    1   25    1   26    1
  28    1   29    1   30    1   31    1   32    1   33    1   34    1   35    1
  37    1   38    1   39    1   40    1   41    1   42    1   43    1   44    1
  46    1   47    1   48    1   49    1   50    1   51    1   52    1   53    1
  55    1   56    1   57    1   58    1   59    1   60    1   61    1   62    1
1018    1 1019    1 1020    1 1021    1 1022    1 1023    1 1024    1 1025    1
1027    1 1028    1 1029    1 1030    1 1031    1 1032    1 1033    1 1034    1
1036    1 1037    1 1038    1 1039    1 1040    1 1041    1 1042    1 1043    1
1045    1 1046    1 1047    1 1048    1 1049    1 1050    1 1051    1 1052    1
1054    1 1055    1 1056    1 1057    1 1058    1 1059    1 1060    1 1061    1
1063    1 1064    1 1065    1 1066    1 1067    1 1068    1 1069    1 1070    1
  73    2   74    2   75    2   76    2   77    2   78    2   79    2   80    2
 145    2  146    2  147    2  148    2  149    2  150    2  151    2  152    2
 217    2  218    2  219    2  220    2  221    2  222    2  223    2  224    2
 289    2  290    2  291    2  292    2  293    2  294    2  295    2  296    2
 361    2  362    2  363    2  364    2  365    2  366    2  367    2  368    2
 433    2  434    2  435    2  436    2  437    2  438    2  439    2  440    2
 505    2  506    2  507    2  508    2  509    2  510    2  511    2  512    2
 577    2  578    2  579    2  580    2  581    2  582    2  583    2  584    2
 649    2  650    2  651    2  652    2  653    2  654    2  655    2  656    2
 721    2  722    2  723    2  724    2  725    2  726    2  727    2  728    2
 793    2  794    2  795    2  796    2  797    2  798    2  799    2  800    2
 865    2  866    2  867    2  868    2  869    2  870    2  871    2  872    2
 937    2  938    2  939    2  940    2  941    2  942    2  943    2  944    2
 136    2  137    2  138    2  139    2  140    2  141    2  142    2  143    2
 208    2  209    2  210    2  211    2  212    2  213    2  214    2  215    2
 280    2  281    2  282    2  283    2  284    2  285    2  286    2  287    2
 352    2  353    2  354    2  355    2  356    2  357    2  358    2  359    2
 424    2  425    2  426    2  427    2  428    2  429    2  430    2  431    2
 496    2  497    2  498    2  499    2  500    2  501    2  502    2  503    2
 568    2  569    2  570    2  571    2  572    2  573    2  574    2  575    2
 640    2  641    2  642    2  643    2  644    2  645    2  646    2  647    2
 712    2  713    2  714    2  715    2  716    2  717    2  718    2  719    2
 784    2  785    2  786    2  787    2  788    2  789    2  790    2  791    2
 856    2  857    2  858    2  859    2  860    2  861    2  862    2  863    2
 928    2  929    2  930    2  931    2  932    2  933    2  934    2  935    2
1000    2 1001    2 1002    2 1003    2 1004    2 1005    2 1006    2 1007    2
   1    4    2    4    3    4    4    4    5    4    6    4    7    4    8    4
  64    4   65    4   66    4   67    4   68    4   69    4   70    4   71    4
1009    4 1010    4 1011    4 1012    4 1013    4 1014    4 1015    4 1016    4
1072    4 1073    4 1074    4 1075    4 1076    4 1077    4 1078    4 1079    4
   9    7   18    6   27    6   36    6   45    6   54    6   63    6   72    7
  81    5   90    3   99    3  108    3  117    3  126    3  135    3  144    5
 153    5  162    3  171    3  180    3  189    3  198    3  207    3  216    5
 225    5  234    3  243    3  252    3  261    3  270    3  279    3  288    5
 297    5  306    3  315    3  324    3  333    3  342    3  351    3  360    5
 369    5  378    3  387    3  396    3  405    3  414    3  423    3  432    5
 441    5  450    3  459    3  468    3  477    3  486    3  495    3  504    5
 513    5  522    3  531    3  540    3  549    3  558    3  567    3  576    5
 585    5  594    3  603    3  612    3  621    3  630    3  639    3  648    5
 657    5  666    3  675    3  684    3  693    3  702    3  711    3  720    5
 729    5  738    3  747    3  756    3  765    3  774    3  783    3  792    5
 801    5  810    3  819    3  828    3  837    3  846    3  855    3  864    5
 873    5  882    3  891    3  900    3  909    3  918    3  927    3  936    5
 945    5  954    3  963    3  972    3  981    3  990    3  999    3 1008    5
1017    7 1026    6 1035    6 1044    6 1053    6 1062    6 1071    6 1080    7
0.0  2.3  4.5  6.6  8.6 10.0 11.2 12.0 12.8 14.0 15.4 17.4 19.5 21.7 24.0
0.0  2.3  4.5  6.6  8.6 10.0 11.2 12.0
0.0  0.6  1.2  1.8  2.4  3.2  4.4  6.0  8.0
```

1.6	0.8			
0.0	1.0	21.07	0.0	
1668.08	0.48	0.48	1.0	0.33784
1668.08	0.48	0.48	1.0	0.33784
1668.08	0.48	0.48	1.0	0.33784
1668.08	0.48	0.48	1.0	0.33784
1668.08	0.48	0.48	1.0	0.33784
1668.08	0.48	0.48	1.0	0.33784
1668.08	0.48	0.48	1.0	0.33784
1668.08	0.48	0.48	1.0	0.33784
207.0E6	0.25			
0.0	73.333	0.0	0.0	-440.00

G1.2 LIMITED OUTPUT DATA

BR16DP24

NTNEL	NPE	NUMNP	NOLN	NPX	NPY	NPZ	NUMBC
784	8	1080	6	15	8	9	456

ELEMENT AND NODE NUMBERS FOR ELEMENTS

I	1	2	3	4	5	6	7	8
1	74	83	11	2	73	82	10	1
2	75	84	12	3	74	83	11	2
3	76	85	13	4	75	84	12	3
4	77	86	14	5	76	85	13	4
5	78	87	15	6	77	86	14	5
6	79	88	16	7	78	87	15	6
7	80	89	17	8	79	88	16	7
8	81	90	18	9	80	89	17	8
9	83	92	20	11	82	91	19	10
10	84	93	21	12	83	92	20	11
381	555	564	492	483	554	563	491	482
382	556	565	493	484	555	564	492	483
383	557	566	494	485	556	565	493	484
384	558	567	495	486	557	566	494	485
385	560	569	497	488	559	568	496	487
386	561	570	498	489	560	569	497	488
387	562	571	499	490	561	570	498	489
388	563	572	500	491	562	571	499	490
389	564	573	501	492	563	572	500	491
390	565	574	502	493	564	573	501	492
775	1061	1070	998	989	1060	1069	997	988
776	1062	1071	999	990	1061	1070	998	989
777	1064	1073	1001	992	1063	1072	1000	991
778	1065	1074	1002	993	1064	1073	1001	992
779	1066	1075	1003	994	1065	1074	1002	993
780	1067	1076	1004	995	1066	1075	1003	994
781	1068	1077	1005	996	1067	1076	1004	995
782	1069	1078	1006	997	1068	1077	1005	996
783	1070	1079	1007	998	1069	1078	1006	997
784	1071	1080	1008	999	1070	1079	1007	998

PIER ELEMENT NUMBERS

385 386 387 388 441 442 443 444

MESH DATA

COORDINATES ALONG X-AXIS

0.0000 2.3000 4.5000 6.6000 8.6000 10.0000 11.2000 12.0000
12.8000 14.0000 15.4000 17.4000 19.5000 21.7000 24.0000

COORDINATES ALONG Y-AXIS

0.0000 2.3000 4.5000 6.6000 8.6000 10.0000 11.2000 12.0000

COORDINATES ALONG Z-AXIS

0.0000 0.6000 1.2000 1.8000 2.4000 3.2000 4.4000 6.0000
8.0000

NODAL POINT COORDINATES

NODE	X	Y	Z	NODE	X	Y	Z

1	0.00000	0.00000	0.00000	2	0.00000	0.00000	0.60000
3	0.00000	0.00000	1.20000	4	0.00000	0.00000	1.80000
5	0.00000	0.00000	2.40000	6	0.00000	0.00000	3.20000
7	0.00000	0.00000	4.40000	8	0.00000	0.00000	6.00000
9	0.00000	0.00000	8.00000	10	0.00000	2.30000	0.00000
11	0.00000	2.30000	0.60000	12	0.00000	2.30000	1.20000
13	0.00000	2.30000	1.80000	14	0.00000	2.30000	2.40000
15	0.00000	2.30000	3.20000	16	0.00000	2.30000	4.40000
17	0.00000	2.30000	6.00000	18	0.00000	2.30000	8.00000
19	0.00000	4.50000	0.00000	20	0.00000	4.50000	0.60000
21	0.00000	4.50000	1.20000	22	0.00000	4.50000	1.80000
23	0.00000	4.50000	2.40000	24	0.00000	4.50000	3.20000
25	0.00000	4.50000	4.40000	26	0.00000	4.50000	6.00000

501	11.20000	12.00000	3.20000	502	11.20000	12.00000	4.40000
503	11.20000	12.00000	6.00000	504	11.20000	12.00000	8.00000
505	12.00000	0.00000	0.00000	506	12.00000	0.00000	0.60000
507	12.00000	0.00000	1.20000	508	12.00000	0.00000	1.80000
509	12.00000	0.00000	2.40000	510	12.00000	0.00000	3.20000
511	12.00000	0.00000	4.40000	512	12.00000	0.00000	6.00000
513	12.00000	0.00000	8.00000	514	12.00000	2.30000	0.00000
515	12.00000	2.30000	0.60000	516	12.00000	2.30000	1.20000
517	12.00000	2.30000	1.80000	518	12.00000	2.30000	2.40000
519	12.00000	2.30000	3.20000	520	12.00000	2.30000	4.40000
521	12.00000	2.30000	6.00000	522	12.00000	2.30000	8.00000
523	12.00000	4.50000	0.00000	524	12.00000	4.50000	0.60000
525	12.00000	4.50000	1.20000	526	12.00000	4.50000	1.80000

1057	24.00000	10.00000	1.80000	1058	24.00000	10.00000	2.40000
1059	24.00000	10.00000	3.20000	1060	24.00000	10.00000	4.40000
1061	24.00000	10.00000	6.00000	1062	24.00000	10.00000	8.00000
1063	24.00000	11.20000	0.00000	1064	24.00000	11.20000	0.60000
1065	24.00000	11.20000	1.20000	1066	24.00000	11.20000	1.80000
1067	24.00000	11.20000	2.40000	1068	24.00000	11.20000	3.20000
1069	24.00000	11.20000	4.40000	1070	24.00000	11.20000	6.00000
1071	24.00000	11.20000	8.00000	1072	24.00000	12.00000	0.00000
1073	24.00000	12.00000	0.60000	1074	24.00000	12.00000	1.20000
1075	24.00000	12.00000	1.80000	1076	24.00000	12.00000	2.40000
1077	24.00000	12.00000	3.20000	1078	24.00000	12.00000	4.40000
1079	24.00000	12.00000	6.00000	1080	24.00000	12.00000	8.00000

HEIGHT OF WATER TABLE= 0.0000
KO VALUE= 1.0000
BULK DENSITY=21.0700
SUBMERGED DENSITY= 0.0000

NODES AT WHICH LOAD IS APPLIED

487 496 559 568 631 640

BOUNDARY CONDITIONS

NPB	CODE	NPB	CODE	NPB	CODE	NPB	CODE	NPB	CODE
10	1	11	1	12	1	13	1	14	1
15	1	16	1	17	1	19	1	20	1
21	1	22	1	23	1	24	1	25	1
26	1	28	1	29	1	30	1	31	1
32	1	33	1	34	1	35	1	37	1
38	1	39	1	40	1	41	1	42	1
43	1	44	1	46	1	47	1	48	1
49	1	50	1	51	1	52	1	53	1
55	1	56	1	57	1	58	1	59	1
60	1	61	1	62	1	1018	1	1019	1
1020	1	1021	1	1022	1	1023	1	1024	1
1025	1	1027	1	1028	1	1029	1	1030	1
1031	1	1032	1	1033	1	1034	1	1036	1
1037	1	1038	1	1039	1	1040	1	1041	1
1042	1	1043	1	1045	1	1046	1	1047	1
1048	1	1049	1	1050	1	1051	1	1052	1
1054	1	1055	1	1056	1	1057	1	1058	1
1059	1	1060	1	1061	1	1063	1	1064	1
1065	1	1066	1	1067	1	1068	1	1069	1
1070	1	73	2	74	2	75	2	76	2
77	2	78	2	79	2	80	2	145	2
146	2	147	2	148	2	149	2	150	2
151	2	152	2	217	2	218	2	219	2
220	2	221	2	222	2	223	2	224	2
289	2	290	2	291	2	292	2	293	2
294	2	295	2	296	2	361	2	362	2
363	2	364	2	365	2	366	2	367	2
368	2	433	2	434	2	435	2	436	2
437	2	438	2	439	2	440	2	505	2
506	2	507	2	508	2	509	2	510	2
511	2	512	2	577	2	578	2	579	2
580	2	581	2	582	2	583	2	584	2
649	2	650	2	651	2	652	2	653	2
654	2	655	2	656	2	721	2	722	2
723	2	724	2	725	2	726	2	727	2
728	2	793	2	794	2	795	2	796	2
797	2	798	2	799	2	800	2	865	2
866	2	867	2	868	2	869	2	870	2
871	2	872	2	937	2	938	2	939	2
940	2	941	2	942	2	943	2	944	2
136	2	137	2	138	2	139	2	140	2
141	2	142	2	143	2	208	2	209	2

210	2	211	2	212	2	213	2	214	2
215	2	280	2	281	2	282	2	283	2
284	2	285	2	286	2	287	2	352	2
353	2	354	2	355	2	356	2	357	2
358	2	359	2	424	2	425	2	426	2
427	2	428	2	429	2	430	2	431	2
496	2	497	2	498	2	499	2	500	2
501	2	502	2	503	2	568	2	569	2
570	2	571	2	572	2	573	2	574	2
575	2	640	2	641	2	642	2	643	2
644	2	645	2	646	2	647	2	712	2
713	2	714	2	715	2	716	2	717	2
718	2	719	2	784	2	785	2	786	2
787	2	788	2	789	2	790	2	791	2
856	2	857	2	858	2	859	2	860	2
861	2	862	2	863	2	928	2	929	2
930	2	931	2	932	2	933	2	934	2
935	2	1000	2	1001	2	1002	2	1003	2
1004	2	1005	2	1006	2	1007	2	1	4
2	4	3	4	4	4	5	4	6	4
7	4	8	4	64	4	65	4	66	4
67	4	68	4	69	4	70	4	71	4
1009	4	1010	4	1011	4	1012	4	1013	4
1014	4	1015	4	1016	4	1072	4	1073	4
1074	4	1075	4	1076	4	1077	4	1078	4
1079	4	9	7	18	6	27	6	36	6
45	6	54	6	63	6	72	7	81	5
90	3	99	3	108	3	117	3	126	3
135	3	144	5	153	5	162	3	171	3
180	3	189	3	198	3	207	3	216	5
225	5	234	3	243	3	252	3	261	3
270	3	279	3	288	5	297	5	306	3
315	3	324	3	333	3	342	3	351	3
360	5	369	5	378	3	387	3	396	3
405	3	414	3	423	3	432	5	441	5
450	3	459	3	468	3	477	3	486	3
495	3	504	5	513	5	522	3	531	3
540	3	549	3	558	3	567	3	576	5
585	5	594	3	603	3	612	3	621	3
630	3	639	3	648	5	657	5	666	3
675	3	684	3	693	3	702	3	711	3
720	5	729	5	738	3	747	3	756	3
765	3	774	3	783	3	792	5	801	5
810	3	819	3	828	3	837	3	846	3
855	3	864	5	873	5	882	3	891	3
900	3	909	3	918	3	927	3	936	5
945	5	954	3	963	3	972	3	981	3
990	3	999	3	1008	5	1017	7	1026	6
1035	6	1044	6	1053	6	1062	6	1071	6
1080	7								

SOIL ELEMENT PROPERTIES

E2	PR2	PR1	E1/E2	G2/E2
0.16681E+04	0.48000E+00	0.48000E+00	0.10000E+01	0.33784E+00
0.16681E+04	0.48000E+00	0.48000E+00	0.10000E+01	0.33784E+00
0.16681E+04	0.48000E+00	0.48000E+00	0.10000E+01	0.33784E+00
0.16681E+04	0.48000E+00	0.48000E+00	0.10000E+01	0.33784E+00
0.16681E+04	0.48000E+00	0.48000E+00	0.10000E+01	0.33784E+00
0.16681E+04	0.48000E+00	0.48000E+00	0.10000E+01	0.33784E+00
0.16681E+04	0.48000E+00	0.48000E+00	0.10000E+01	0.33784E+00
0.16681E+04	0.48000E+00	0.48000E+00	0.10000E+01	0.33784E+00

PIER ELEMENT PROPERTIES

PIER MODULUS	POISSON RATIO
0.20700E+09	0.25000E+00

APPLIED LOADING,

VLOAD	XHLOAD	YHLOAD	XMLOAD	YMLOAD
0.000	73.333	0.000	0.000	-440.000

BAND WIDTH = 249

INITIAL STRESSES

EL NO	SIGX	SIGY	SIGZ
1	-0.632100E+01	-0.632100E+01	-0.632100E+01
2	-0.189630E+02	-0.189630E+02	-0.189630E+02
3	-0.316050E+02	-0.316050E+02	-0.316050E+02
4	-0.442470E+02	-0.442470E+02	-0.442470E+02
5	-0.589960E+02	-0.589960E+02	-0.589960E+02
6	-0.800660E+02	-0.800660E+02	-0.800660E+02
7	-0.109564E+03	-0.109564E+03	-0.109564E+03
8	-0.147490E+03	-0.147490E+03	-0.147490E+03
9	-0.632100E+01	-0.632100E+01	-0.632100E+01
10	-0.189630E+02	-0.189630E+02	-0.189630E+02
11	-0.316050E+02	-0.316050E+02	-0.316050E+02

12	-0.442470E+02	-0.442470E+02	-0.442470E+02
13	-0.589960E+02	-0.589960E+02	-0.589960E+02
14	-0.800660E+02	-0.800660E+02	-0.800660E+02
15	-0.109564E+03	-0.109564E+03	-0.109564E+03

471	-0.109564E+03	-0.109564E+03	-0.109564E+03
472	-0.147490E+03	-0.147490E+03	-0.147490E+03
473	-0.632100E+01	-0.632100E+01	-0.632100E+01
474	-0.189630E+02	-0.189630E+02	-0.189630E+02
475	-0.316050E+02	-0.316050E+02	-0.316050E+02
476	-0.442470E+02	-0.442470E+02	-0.442470E+02
477	-0.589960E+02	-0.589960E+02	-0.589960E+02
478	-0.800660E+02	-0.800660E+02	-0.800660E+02
479	-0.109564E+03	-0.109564E+03	-0.109564E+03
480	-0.147490E+03	-0.147490E+03	-0.147490E+03
481	-0.632100E+01	-0.632100E+01	-0.632100E+01
482	-0.189630E+02	-0.189630E+02	-0.189630E+02
483	-0.316050E+02	-0.316050E+02	-0.316050E+02
484	-0.442470E+02	-0.442470E+02	-0.442470E+02
485	-0.589960E+02	-0.589960E+02	-0.589960E+02

773	-0.589960E+02	-0.589960E+02	-0.589960E+02
774	-0.800660E+02	-0.800660E+02	-0.800660E+02
775	-0.109564E+03	-0.109564E+03	-0.109564E+03
776	-0.147490E+03	-0.147490E+03	-0.147490E+03
777	-0.632100E+01	-0.632100E+01	-0.632100E+01
778	-0.189630E+02	-0.189630E+02	-0.189630E+02
779	-0.316050E+02	-0.316050E+02	-0.316050E+02
780	-0.442470E+02	-0.442470E+02	-0.442470E+02
781	-0.589960E+02	-0.589960E+02	-0.589960E+02
782	-0.800660E+02	-0.800660E+02	-0.800660E+02
783	-0.109564E+03	-0.109564E+03	-0.109564E+03
784	-0.147490E+03	-0.147490E+03	-0.147490E+03

NODAL DISPLACEMENTS

	X-DISP		Y-DISP		Z-DISP
1	-0.5671E-17	2	0.3364E-15	3	0.3455E-03
4	0.3323E-16	5	0.3785E-15	6	0.3213E-03
7	0.4844E-16	8	0.3959E-15	9	0.2952E-03
10	0.6117E-16	11	0.4089E-15	12	0.2674E-03
13	0.8071E-16	14	0.4600E-15	15	0.2385E-03
16	0.1193E-15	17	0.5589E-15	18	0.1993E-03
19	0.1379E-15	20	0.6130E-15	21	0.1422E-03
22	0.1174E-15	23	0.6035E-15	24	0.7406E-04
25	0.8994E-16	26	0.5774E-15	27	-0.9433E-16
601	0.1472E-02	602	0.1962E-03	603	-0.5271E-03
604	0.1503E-02	605	0.1958E-03	606	-0.6691E-03
607	0.1395E-02	608	0.1858E-03	609	-0.7607E-03
610	0.1082E-02	611	0.1598E-03	612	-0.7764E-03
613	0.6340E-03	614	0.1306E-03	615	-0.6606E-03
616	0.2862E-03	617	0.1179E-03	618	-0.3924E-03
619	0.1550E-03	620	0.1118E-03	621	-0.1195E-14
622	0.1149E-02	623	-0.8066E-16	624	-0.1977E-03
625	0.1332E-02	626	-0.1382E-15	627	-0.3682E-03
1000	0.4500E-02	1001	0.1449E-02	1002	-0.2226E-02
1003	0.4300E-02	1004	0.1446E-02	1005	-0.2750E-02
1006	0.3427E-02	1007	0.1076E-02	1008	-0.3054E-02
1009	0.2288E-02	1010	0.6275E-03	1011	-0.3110E-02
1012	0.1235E-02	1013	0.3951E-03	1014	-0.2916E-02
1015	0.4092E-03	1016	0.4333E-03	1017	-0.2496E-02
1018	-0.1838E-03	1019	0.4266E-03	1020	-0.1795E-02
1021	-0.5031E-03	1022	0.3737E-03	1023	-0.9452E-03
1024	-0.6178E-03	1025	0.3588E-03	1026	-0.2077E-14
1501	-0.4519E-02	1502	-0.5369E-14	1503	-0.8190E-02
1504	-0.2697E-02	1505	-0.2455E-14	1506	-0.3695E-02
1507	-0.1835E-02	1508	-0.7462E-15	1509	-0.1139E-02
1510	-0.1626E-02	1511	-0.3199E-15	1512	-0.1777E-15
1513	-0.6484E-03	1514	-0.8908E-26	1515	0.5431E-13
1516	-0.6199E-03	1517	0.2770E-26	1518	0.5563E-13
1519	-0.6037E-03	1520	0.7126E-26	1521	0.5587E-13
1522	-0.5975E-03	1523	0.1287E-25	1524	0.5496E-13
1525	-0.6005E-03	1526	0.1992E-25	1527	0.5282E-13
1702	0.2762E-01	1703	0.6216E-28	1704	-0.8282E-12
1705	0.1871E-01	1706	-0.1599E-28	1707	-0.8282E-12
1708	0.9793E-02	1709	-0.3989E-28	1710	-0.8282E-12
1711	0.8804E-03	1712	0.2607E-29	1713	-0.8282E-12
1714	-0.8032E-02	1715	0.1308E-27	1716	-0.8282E-12
1717	-0.6044E-02	1718	-0.1343E-24	1719	-0.7608E-12
1720	-0.3253E-02	1721	-0.3805E-25	1722	-0.5254E-12
1723	-0.2084E-02	1724	-0.1469E-25	1725	-0.2570E-12
1726	-0.1741E-02	1727	-0.1176E-25	1728	-0.3446E-24
2002	-0.2221E-03	2003	-0.3425E-03	2004	-0.1760E-04
2005	-0.2374E-03	2006	-0.3795E-03	2007	0.1501E-04
2008	-0.2663E-03	2009	-0.4022E-03	2010	0.4629E-04
2011	-0.3045E-03	2012	-0.3996E-03	2013	0.6661E-04
2014	-0.3653E-03	2015	-0.3686E-03	2016	0.8085E-04
2017	-0.4603E-03	2018	-0.3255E-03	2019	0.8081E-04
2020	-0.5621E-03	2021	-0.2958E-03	2022	0.5306E-04
2023	-0.6107E-03	2024	-0.2820E-03	2025	0.3418E-15
2500	0.5748E-03	2501	-0.5570E-03	2502	0.9788E-03

2503	0.2143E-03	2504	-0.4906E-03	2505	0.7872E-03
2506	-0.7411E-04	2507	-0.4492E-03	2508	0.4553E-03
2509	-0.1829E-03	2510	-0.4322E-03	2511	0.1332E-14
2512	0.2443E-02	2513	-0.7475E-03	2514	0.9527E-03
2515	0.2526E-02	2516	-0.7817E-03	2517	0.1310E-02
2518	0.2272E-02	2519	-0.7110E-03	2520	0.1574E-02
2521	0.1843E-02	2522	-0.5978E-03	2523	0.1687E-02
2524	0.1393E-02	2525	-0.4861E-03	2526	0.1663E-02

3001	0.5028E-03	3002	-0.3598E-16	3003	-0.1893E-03
3004	0.5956E-03	3005	0.1216E-17	3006	-0.1155E-03
3007	0.6658E-03	3008	0.2785E-16	3009	-0.2593E-04
3010	0.6889E-03	3011	0.7255E-16	3012	0.6367E-04
3013	0.6209E-03	3014	0.8402E-16	3015	0.1562E-03
3016	0.4249E-03	3017	0.3720E-16	3018	0.2081E-03
3019	0.2334E-03	3020	0.1269E-16	3021	0.1553E-03
3022	0.1580E-03	3023	-0.1580E-17	3024	0.7530E-15
3025	-0.5671E-17	3026	-0.3364E-15	3027	-0.3455E-03

3208	0.1061E-14	3209	-0.9514E-04	3210	0.6531E-04
3211	0.9144E-15	3212	-0.8934E-04	3213	0.6920E-15
3214	0.1354E-15	3215	-0.1536E-15	3216	-0.3842E-03
3217	0.3867E-15	3218	-0.6717E-16	3219	-0.3486E-03
3220	0.4858E-15	3221	-0.2717E-16	3222	-0.2952E-03
3223	0.6118E-15	3224	0.5908E-17	3225	-0.2265E-03
3226	0.8769E-15	3227	0.5055E-16	3228	-0.1479E-03
3229	0.1246E-14	3230	0.9333E-16	3231	-0.4895E-04
3232	0.1215E-14	3233	0.4931E-16	3234	0.4664E-04
3235	0.9620E-15	3236	0.1110E-16	3237	0.6737E-04
3238	0.8222E-15	3239	-0.8446E-17	3240	0.6238E-15

ELEMENT STRESSES

EL NO	SIGX	SIGY	SIGZ	SIGXY	SIGYZ	SIGXZ
1	-.629E+01	-.615E+01	-.629E+01	0.420E-02	-.325E-03	0.203E-03
2	-.189E+02	-.188E+02	-.189E+02	0.468E-02	-.153E-02	-.160E-03
3	-.316E+02	-.314E+02	-.316E+02	0.484E-02	-.260E-02	-.758E-03
4	-.442E+02	-.441E+02	-.442E+02	0.476E-02	-.340E-02	-.145E-02
5	-.589E+02	-.588E+02	-.590E+02	0.445E-02	-.430E-02	-.229E-02
6	-.800E+02	-.799E+02	-.800E+02	0.384E-02	-.546E-02	-.312E-02
7	-.110E+03	-.109E+03	-.110E+03	0.308E-02	-.519E-02	-.277E-02
8	-.147E+03	-.147E+03	-.147E+03	0.256E-02	-.228E-02	-.106E-02
9	-.626E+01	-.616E+01	-.629E+01	0.138E-01	-.174E-02	-.101E-02
10	-.189E+02	-.188E+02	-.189E+02	0.154E-01	-.452E-02	-.336E-02
11	-.315E+02	-.314E+02	-.316E+02	0.158E-01	-.699E-02	-.539E-02
12	-.442E+02	-.441E+02	-.442E+02	0.153E-01	-.928E-02	-.685E-02
13	-.589E+02	-.588E+02	-.589E+02	0.141E-01	-.123E-01	-.806E-02
14	-.800E+02	-.799E+02	-.800E+02	0.119E-01	-.162E-01	-.847E-02
15	-.109E+03	-.109E+03	-.109E+03	0.931E-02	-.154E-01	-.653E-02
16	-.147E+03	-.147E+03	-.147E+03	0.756E-02	-.667E-02	-.245E-02
17	-.619E+01	-.619E+01	-.629E+01	0.271E-01	-.574E-03	-.379E-02
18	-.188E+02	-.188E+02	-.189E+02	0.298E-01	-.190E-02	-.106E-01
19	-.314E+02	-.315E+02	-.316E+02	0.300E-01	-.559E-02	-.159E-01
20	-.441E+02	-.441E+02	-.442E+02	0.286E-01	-.102E-01	-.192E-01
21	-.588E+02	-.588E+02	-.589E+02	0.256E-01	-.168E-01	-.212E-01
22	-.799E+02	-.799E+02	-.800E+02	0.208E-01	-.246E-01	-.205E-01
23	-.109E+03	-.109E+03	-.109E+03	0.156E-01	-.238E-01	-.150E-01
24	-.147E+03	-.147E+03	-.147E+03	0.124E-01	-.101E-01	-.555E-02
25	-.614E+01	-.630E+01	-.636E+01	0.394E-01	0.135E-01	-.669E-02
26	-.187E+02	-.189E+02	-.190E+02	0.430E-01	0.132E-01	-.194E-01
27	-.313E+02	-.315E+02	-.316E+02	0.441E-01	0.691E-02	-.302E-01
28	-.440E+02	-.441E+02	-.442E+02	0.428E-01	-.180E-02	-.375E-01
29	-.587E+02	-.589E+02	-.589E+02	0.384E-01	-.138E-01	-.423E-01
30	-.798E+02	-.799E+02	-.799E+02	0.304E-01	-.276E-01	-.404E-01
31	-.109E+03	-.109E+03	-.109E+03	0.216E-01	-.278E-01	-.289E-01
32	-.147E+03	-.147E+03	-.147E+03	0.164E-01	-.117E-01	-.104E-01
33	-.615E+01	-.645E+01	-.646E+01	0.277E-01	0.330E-02	-.539E-02
34	-.187E+02	-.190E+02	-.191E+02	0.342E-01	0.895E-02	-.190E-01
35	-.313E+02	-.316E+02	-.317E+02	0.412E-01	0.740E-02	-.346E-01
36	-.439E+02	-.442E+02	-.442E+02	0.454E-01	-.226E-04	-.493E-01
37	-.586E+02	-.589E+02	-.589E+02	0.434E-01	-.125E-01	-.626E-01
38	-.797E+02	-.799E+02	-.799E+02	0.338E-01	-.276E-01	-.629E-01
39	-.109E+03	-.109E+03	-.109E+03	0.222E-01	-.270E-01	-.446E-01
40	-.147E+03	-.147E+03	-.147E+03	0.155E-01	-.109E-01	-.156E-01
41	-.616E+01	-.651E+01	-.648E+01	0.787E-02	0.251E-02	-.109E-03
42	-.187E+02	-.191E+02	-.191E+02	0.144E-01	0.811E-02	-.779E-02
43	-.313E+02	-.317E+02	-.317E+02	0.229E-01	0.945E-02	-.246E-01
44	-.439E+02	-.443E+02	-.443E+02	0.299E-01	0.484E-02	-.470E-01
45	-.585E+02	-.590E+02	-.590E+02	0.317E-01	-.470E-02	-.727E-01
46	-.796E+02	-.800E+02	-.799E+02	0.253E-01	-.172E-01	-.806E-01
47	-.109E+03	-.109E+03	-.109E+03	0.155E-01	-.174E-01	-.569E-01
48	-.147E+03	-.147E+03	-.147E+03	0.101E-01	-.701E-02	-.194E-01
49	-.614E+01	-.651E+01	-.646E+01	-.791E-03	-.295E-02	0.332E-02
50	-.187E+02	-.191E+02	-.191E+02	0.186E-02	0.168E-03	0.492E-03
101	-.584E+02	-.588E+02	-.587E+02	0.105E+00	-.495E-01	-.279E+00
102	-.796E+02	-.799E+02	-.797E+02	0.723E-01	-.503E-01	-.260E+00
103	-.109E+03	-.109E+03	-.109E+03	0.409E-01	-.337E-01	-.168E+00
104	-.147E+03	-.147E+03	-.147E+03	0.264E-01	-.122E-01	-.557E-01
105	-.614E+01	-.675E+01	-.676E+01	0.164E-03	-.610E-02	-.520E-02
106	-.186E+02	-.193E+02	-.193E+02	0.124E-01	-.275E-02	-.422E-01
107	-.311E+02	-.317E+02	-.317E+02	0.286E-01	-.491E-02	-.120E+00
108	-.436E+02	-.442E+02	-.442E+02	0.378E-01	-.987E-02	-.222E+00
109	-.583E+02	-.588E+02	-.587E+02	0.352E-01	-.152E-01	-.310E+00
110	-.795E+02	-.799E+02	-.797E+02	0.231E-01	-.151E-01	-.295E+00
111	-.109E+03	-.109E+03	-.109E+03	0.118E-01	-.969E-02	-.186E+00
112	-.147E+03	-.147E+03	-.147E+03	0.743E-02	-.358E-02	-.606E-01

113	-.635E+01	-.617E+01	-.632E+01	0.164E-01	-.339E-03	0.182E-02
114	-.190E+02	-.188E+02	-.190E+02	0.173E-01	-.314E-02	0.666E-04
115	-.316E+02	-.314E+02	-.316E+02	0.177E-01	-.630E-02	-.313E-02
116	-.442E+02	-.440E+02	-.442E+02	0.173E-01	-.899E-02	-.671E-02
117	-.590E+02	-.588E+02	-.590E+02	0.160E-01	-.115E-01	-.105E-01
118	-.800E+02	-.798E+02	-.800E+02	0.132E-01	-.125E-01	-.132E-01
119	-.110E+03	-.109E+03	-.109E+03	0.989E-02	-.978E-02	-.111E-01
120	-.147E+03	-.147E+03	-.147E+03	0.754E-02	-.369E-02	-.421E-02
121	-.630E+01	-.615E+01	-.631E+01	0.591E-01	-.495E-02	-.270E-02
122	-.189E+02	-.188E+02	-.189E+02	0.623E-01	-.185E-01	-.112E-01
123	-.316E+02	-.314E+02	-.316E+02	0.620E-01	-.301E-01	-.196E-01
124	-.442E+02	-.440E+02	-.442E+02	0.587E-01	-.378E-01	-.261E-01
125	-.589E+02	-.588E+02	-.589E+02	0.523E-01	-.434E-01	-.310E-01
126	-.800E+02	-.799E+02	-.800E+02	0.421E-01	-.433E-01	-.319E-01
127	-.110E+03	-.109E+03	-.109E+03	0.303E-01	-.320E-01	-.246E-01
128	-.147E+03	-.147E+03	-.147E+03	0.221E-01	-.117E-01	-.940E-02
129	-.616E+01	-.608E+01	-.628E+01	0.133E+00	-.230E-01	-.195E-01
130	-.188E+02	-.187E+02	-.189E+02	0.138E+00	-.585E-01	-.508E-01
131	-.314E+02	-.314E+02	-.315E+02	0.131E+00	-.821E-01	-.729E-01
132	-.441E+02	-.440E+02	-.441E+02	0.117E+00	-.928E-01	-.848E-01
133	-.589E+02	-.588E+02	-.589E+02	0.982E-01	-.952E-01	-.896E-01
134	-.800E+02	-.799E+02	-.799E+02	0.740E-01	-.870E-01	-.827E-01
135	-.109E+03	-.109E+03	-.109E+03	0.494E-01	-.605E-01	-.609E-01
136	-.147E+03	-.147E+03	-.147E+03	0.337E-01	-.218E-01	-.223E-01
137	-.582E+01	-.595E+01	-.618E+01	0.266E+00	-.461E-01	-.635E-01
138	-.185E+02	-.186E+02	-.188E+02	0.267E+00	-.114E+00	-.151E+00
139	-.312E+02	-.313E+02	-.314E+02	0.237E+00	-.155E+00	-.207E+00
140	-.439E+02	-.440E+02	-.441E+02	0.195E+00	-.168E+00	-.228E+00
141	-.588E+02	-.588E+02	-.588E+02	0.150E+00	-.162E+00	-.221E+00
142	-.799E+02	-.799E+02	-.798E+02	0.103E+00	-.134E+00	-.191E+00
143	-.109E+03	-.109E+03	-.109E+03	0.641E-01	-.880E-01	-.128E+00
144	-.147E+03	-.147E+03	-.147E+03	0.442E-01	-.310E-01	-.436E-01
145	-.544E+01	-.601E+01	-.630E+01	0.391E+00	-.571E-01	-.121E+00
146	-.181E+02	-.186E+02	-.188E+02	0.378E+00	-.159E+00	-.305E+00
147	-.309E+02	-.313E+02	-.314E+02	0.320E+00	-.217E+00	-.414E+00
148	-.437E+02	-.440E+02	-.439E+02	0.249E+00	-.227E+00	-.443E+00
149	-.586E+02	-.588E+02	-.586E+02	0.177E+00	-.207E+00	-.410E+00
150	-.798E+02	-.799E+02	-.796E+02	0.113E+00	-.150E+00	-.327E+00
200	-.148E+03	-.147E+03	-.147E+03	0.132E-01	-.494E-01	-.417E-01
201	-.423E+01	-.486E+01	-.553E+01	0.893E+00	-.263E+00	-.294E+00
202	-.174E+02	-.179E+02	-.183E+02	0.770E+00	-.539E+00	-.632E+00
203	-.307E+02	-.311E+02	-.311E+02	0.520E+00	-.633E+00	-.786E+00
204	-.439E+02	-.441E+02	-.438E+02	0.279E+00	-.560E+00	-.774E+00
205	-.589E+02	-.589E+02	-.585E+02	0.126E+00	-.398E+00	-.587E+00
206	-.800E+02	-.799E+02	-.794E+02	0.592E-01	-.279E+00	-.406E+00
207	-.110E+03	-.109E+03	-.109E+03	0.347E-01	-.170E+00	-.219E+00
208	-.148E+03	-.147E+03	-.147E+03	0.240E-01	-.558E-01	-.669E-01
209	-.353E+01	-.586E+01	-.682E+01	0.118E+01	-.176E+00	-.600E+00
210	-.166E+02	-.184E+02	-.189E+02	0.931E+00	-.581E+00	-.140E+01
211	-.297E+02	-.307E+02	-.305E+02	0.521E+00	-.711E+00	-.167E+01
212	-.433E+02	-.436E+02	-.429E+02	0.172E+00	-.574E+00	-.146E+01
213	-.586E+02	-.585E+02	-.576E+02	0.364E-01	-.332E+00	-.905E+00
214	-.801E+02	-.799E+02	-.791E+02	0.394E-01	-.203E+00	-.529E+00
215	-.110E+03	-.110E+03	-.109E+03	0.356E-01	-.123E+00	-.284E+00
216	-.148E+03	-.147E+03	-.147E+03	0.201E-01	-.402E-01	-.893E-01
217	-.314E+01	-.701E+01	-.812E+01	0.503E+00	-.106E+00	-.801E+00
218	-.161E+02	-.190E+02	-.195E+02	0.380E+00	-.215E+00	-.201E+01
219	-.289E+02	-.303E+02	-.299E+02	0.174E+00	-.243E+00	-.234E+01
220	-.428E+02	-.429E+02	-.420E+02	0.328E-01	-.187E+00	-.190E+01
221	-.582E+02	-.579E+02	-.567E+02	-.111E-01	-.992E-01	-.106E+01
222	-.801E+02	-.799E+02	-.789E+02	0.145E-02	-.577E-01	-.559E+00
223	-.110E+03	-.110E+03	-.109E+03	0.131E-01	-.294E-01	-.313E+00
224	-.148E+03	-.147E+03	-.147E+03	0.506E-02	-.854E-02	-.100E+00
225	-.639E+01	-.624E+01	-.635E+01	0.619E-02	0.215E-02	-.967E-02
226	-.190E+02	-.189E+02	-.190E+02	0.398E-02	0.223E-02	-.178E-01
227	-.317E+02	-.315E+02	-.316E+02	0.191E-02	-.267E-03	-.223E-01
228	-.443E+02	-.441E+02	-.443E+02	-.936E-04	-.478E-02	-.248E-01
229	-.590E+02	-.589E+02	-.590E+02	-.247E-02	-.104E-01	-.254E-01
230	-.801E+02	-.799E+02	-.800E+02	-.536E-02	-.127E-01	-.222E-01
231	-.110E+03	-.109E+03	-.110E+03	-.825E-02	-.907E-02	-.153E-01
232	-.148E+03	-.147E+03	-.147E+03	-.103E-01	-.320E-02	-.535E-02
233	-.640E+01	-.623E+01	-.639E+01	0.333E-01	0.292E-02	-.903E-02
234	-.190E+02	-.188E+02	-.190E+02	0.254E-01	-.535E-02	-.164E-01
235	-.316E+02	-.314E+02	-.316E+02	0.196E-01	-.194E-01	-.230E-01
236	-.442E+02	-.440E+02	-.442E+02	0.132E-01	-.357E-01	-.283E-01
237	-.590E+02	-.588E+02	-.589E+02	0.407E-02	-.490E-01	-.310E-01
238	-.801E+02	-.799E+02	-.800E+02	-.810E-02	-.478E-01	-.297E-01
239	-.110E+03	-.109E+03	-.109E+03	-.211E-01	-.322E-01	-.229E-01
240	-.148E+03	-.147E+03	-.147E+03	-.307E-01	-.114E-01	-.875E-02
241	-.632E+01	-.610E+01	-.640E+01	0.121E+00	-.204E-01	-.486E-02
242	-.190E+02	-.187E+02	-.190E+02	0.104E+00	-.840E-01	-.240E-01
243	-.315E+02	-.313E+02	-.315E+02	0.860E-01	-.129E+00	-.378E-01
244	-.441E+02	-.439E+02	-.441E+02	0.679E-01	-.143E+00	-.489E-01
245	-.589E+02	-.587E+02	-.588E+02	0.439E-01	-.139E+00	-.582E-01
246	-.800E+02	-.798E+02	-.799E+02	0.110E-01	-.110E+00	-.557E-01
247	-.110E+03	-.109E+03	-.109E+03	-.262E-01	-.734E-01	-.435E-01
248	-.147E+03	-.147E+03	-.147E+03	-.534E-01	-.274E-01	-.147E-01
249	-.578E+01	-.561E+01	-.627E+01	0.406E+00	-.155E+00	-.539E-01
250	-.184E+02	-.182E+02	-.186E+02	0.357E+00	-.392E+00	-.138E+00
351	-.110E+03	-.110E+03	-.110E+03	-.655E-01	-.525E-02	-.154E-01
352	-.147E+03	-.147E+03	-.147E+03	-.751E-01	-.205E-02	-.498E-02
353	-.624E+01	-.618E+01	-.627E+01	0.144E-01	0.721E-03	-.982E-02
354	-.189E+02	-.189E+02	-.189E+02	-.236E-01	-.640E-02	-.634E-02
355	-.316E+02	-.315E+02	-.316E+02	-.564E-01	-.201E-01	-.442E-02
356	-.443E+02	-.442E+02	-.442E+02	-.706E-01	-.307E-01	-.270E-02
357	-.591E+02	-.590E+02	-.590E+02	-.813E-01	-.305E-01	-.240E-01
358	-.801E+02	-.800E+02	-.801E+02	-.114E+00	-.204E-01	-.216E-01

359	-.110E+03	-.110E+03	-.110E+03	-.144E+00	-.180E-01	-.234E-02
360	-.147E+03	-.147E+03	-.147E+03	-.152E+00	-.784E-02	0.344E-02
361	-.683E+01	-.665E+01	-.686E+01	0.154E+00	-.347E-01	-.122E-01
362	-.192E+02	-.190E+02	-.192E+02	0.679E-01	-.118E+00	0.745E-01
363	-.313E+02	-.313E+02	-.313E+02	0.555E-01	-.125E+00	0.519E-01
364	-.440E+02	-.439E+02	-.439E+02	-.192E-01	-.823E-01	-.636E-01
365	-.589E+02	-.587E+02	-.588E+02	-.193E+00	-.314E-01	-.656E-01
366	-.804E+02	-.802E+02	-.803E+02	-.339E+00	-.607E-01	0.241E-01
367	-.110E+03	-.109E+03	-.109E+03	-.333E+00	-.684E-01	0.106E+00
368	-.148E+03	-.147E+03	-.147E+03	-.265E+00	-.249E-01	0.535E-01
369	-.290E+01	-.318E+01	-.373E+01	0.111E+01	-.203E+00	0.332E+00
370	-.171E+02	-.172E+02	-.174E+02	0.870E+00	-.482E+00	-.141E+00
371	-.316E+02	-.317E+02	-.314E+02	0.446E+00	-.478E+00	-.273E+00
372	-.446E+02	-.446E+02	-.442E+02	0.653E-01	-.127E+00	0.530E-02
373	-.601E+02	-.598E+02	-.599E+02	-.614E+00	0.565E-01	-.307E+00
374	-.793E+02	-.789E+02	-.790E+02	-.980E+00	-.236E+00	0.447E+00
375	-.109E+03	-.109E+03	-.109E+03	-.607E+00	-.184E+00	0.460E+00
376	-.148E+03	-.147E+03	-.147E+03	-.322E+00	-.520E-01	0.174E+00
377	-.979E+01	-.109E+02	-.106E+02	0.732E+01	-.238E+01	0.340E+00
378	-.217E+02	-.223E+02	-.220E+02	0.385E+01	-.243E+01	-.213E+00
379	-.319E+02	-.320E+02	-.318E+02	0.902E+00	-.244E+01	-.321E+00
380	-.442E+02	-.441E+02	-.438E+02	-.244E+01	-.230E+01	0.768E-01
381	-.534E+02	-.528E+02	-.511E+02	-.341E+01	-.157E+01	0.434E+01
382	-.813E+02	-.805E+02	-.793E+02	-.179E+01	-.107E+01	0.280E+01
383	-.110E+03	-.110E+03	-.109E+03	-.725E+00	-.382E+00	0.131E+01
384	-.148E+03	-.148E+03	-.147E+03	-.262E+00	-.673E-01	0.353E+00
385	0.345E+02	-.330E+02	0.222E+03	0.179E+02	-.115E+02	0.128E+02
386	-.430E+01	-.382E+02	0.196E+03	0.498E+01	-.839E+01	0.435E+02
387	-.251E+02	-.286E+02	0.128E+03	0.569E+01	-.111E+02	0.552E+02
388	-.953E+02	-.513E+02	0.728E+02	-.158E+02	-.190E+02	0.485E+02
389	-.452E+02	-.444E+02	-.412E+02	-.382E+00	0.877E-01	0.910E+01
390	-.832E+02	-.822E+02	-.795E+02	-.552E+00	-.205E+00	0.503E+01
391	-.110E+03	-.110E+03	-.109E+03	-.224E+00	-.101E+00	0.198E+01
392	-.148E+03	-.148E+03	-.148E+03	-.746E-01	-.152E-01	0.466E+00
393	-.632E+01	-.635E+01	-.633E+01	-.161E-02	-.601E-03	-.411E-02
394	-.189E+02	-.190E+02	-.190E+02	-.553E-02	-.574E-03	-.162E-01
395	-.316E+02	-.316E+02	-.316E+02	-.103E-01	-.163E-03	-.239E-01
396	-.442E+02	-.443E+02	-.442E+02	-.142E-01	0.451E-03	-.263E-01
397	-.590E+02	-.590E+02	-.590E+02	-.167E-01	0.192E-02	-.258E-01
398	-.801E+02	-.801E+02	-.801E+02	-.180E-01	0.265E-02	-.205E-01
399	-.110E+03	-.110E+03	-.110E+03	-.199E-01	0.145E-02	-.145E-01
400	-.147E+03	-.148E+03	-.147E+03	-.226E-01	0.441E-03	-.515E-02

500	-.271E+02	-.300E+02	-.317E+02	-.838E-01	0.431E+00	-.824E+01
501	-.555E+02	-.591E+02	-.635E+02	-.152E+00	0.988E-01	-.288E+00
502	-.796E+02	-.809E+02	-.844E+02	-.118E+00	0.362E+00	-.491E+00
503	-.108E+03	-.109E+03	-.110E+03	-.168E-01	0.169E+00	0.357E-01
504	-.147E+03	-.147E+03	-.148E+03	-.301E-01	0.347E-01	0.769E-01
505	-.625E+01	-.640E+01	-.629E+01	0.619E-02	-.215E-02	-.967E-02
506	-.189E+02	-.191E+02	-.189E+02	0.398E-02	-.223E-02	-.178E-01
507	-.315E+02	-.317E+02	-.316E+02	0.191E-02	0.267E-03	-.223E-01
508	-.442E+02	-.444E+02	-.442E+02	-.936E-04	0.478E-02	-.248E-01
509	-.590E+02	-.591E+02	-.590E+02	-.247E-02	0.104E-01	-.254E-01
510	-.800E+02	-.802E+02	-.801E+02	-.536E-02	0.127E-01	-.222E-01
511	-.110E+03	-.110E+03	-.110E+03	-.825E-02	0.907E-02	-.153E-01
512	-.147E+03	-.148E+03	-.148E+03	-.103E-01	0.320E-02	-.535E-02
513	-.624E+01	-.641E+01	-.625E+01	0.333E-01	-.292E-02	-.903E-02
514	-.189E+02	-.191E+02	-.189E+02	0.254E-01	0.535E-02	-.164E-01
515	-.316E+02	-.318E+02	-.316E+02	0.196E-01	0.194E-01	-.230E-01
516	-.442E+02	-.444E+02	-.443E+02	0.132E-01	0.357E-01	-.283E-01
517	-.590E+02	-.592E+02	-.590E+02	0.407E-02	0.490E-01	-.310E-01
518	-.801E+02	-.802E+02	-.801E+02	-.810E-02	0.478E-01	-.297E-01
519	-.110E+03	-.110E+03	-.110E+03	-.211E-01	0.322E-01	-.229E-01
520	-.147E+03	-.148E+03	-.148E+03	-.307E-01	0.114E-01	-.875E-02
521	-.633E+01	-.654E+01	-.624E+01	0.121E+00	0.204E-01	-.486E-02
522	-.190E+02	-.192E+02	-.189E+02	0.104E+00	0.840E-01	-.240E-01
523	-.317E+02	-.320E+02	-.317E+02	0.860E-01	0.129E+00	-.378E-01
524	-.444E+02	-.446E+02	-.444E+02	0.679E-01	0.143E+00	-.489E-01
525	-.591E+02	-.593E+02	-.592E+02	0.439E-01	0.139E+00	-.582E-01
526	-.801E+02	-.803E+02	-.802E+02	0.110E-01	0.110E+00	-.557E-01
527	-.110E+03	-.110E+03	-.110E+03	-.262E-01	0.734E-01	-.435E-01
528	-.147E+03	-.148E+03	-.148E+03	-.534E-01	0.274E-01	-.147E-01
529	-.686E+01	-.703E+01	-.638E+01	0.406E+00	0.155E+00	-.539E-01
530	-.196E+02	-.198E+02	-.193E+02	0.357E+00	0.392E+00	-.138E+00
531	-.319E+02	-.320E+02	-.318E+02	0.272E+00	0.480E+00	-.201E+00
532	-.446E+02	-.447E+02	-.447E+02	0.178E+00	0.436E+00	-.222E+00
533	-.593E+02	-.593E+02	-.595E+02	0.980E-01	0.309E+00	-.182E+00
534	-.801E+02	-.803E+02	-.805E+02	0.202E-01	0.230E+00	-.146E+00
535	-.110E+03	-.110E+03	-.110E+03	-.457E-01	0.166E+00	-.652E-01
536	-.147E+03	-.148E+03	-.148E+03	-.751E-01	0.602E-01	-.151E-01
537	-.901E+01	-.865E+01	-.772E+01	0.122E+01	0.738E+00	-.444E+00
538	-.204E+02	-.201E+02	-.196E+02	0.101E+01	0.103E+01	-.850E+00
539	-.327E+02	-.325E+02	-.325E+02	0.651E+00	0.114E+01	-.101E+01
540	-.440E+02	-.438E+02	-.443E+02	0.220E+00	0.113E+01	-.963E+00
541	-.586E+02	-.586E+02	-.594E+02	-.907E-01	0.601E+00	-.700E+00
542	-.798E+02	-.801E+02	-.808E+02	-.133E+00	0.463E+00	-.320E+00
543	-.109E+03	-.110E+03	-.110E+03	-.735E-01	0.278E+00	-.106E+00
544	-.147E+03	-.148E+03	-.148E+03	-.552E-01	0.905E-01	-.227E-01
545	-.135E+02	-.952E+01	-.717E+01	0.332E+01	0.598E+00	-.168E+01
546	-.247E+02	-.221E+02	-.212E+02	0.216E+01	0.143E+01	-.332E+01
547	-.328E+02	-.320E+02	-.325E+02	0.718E+00	0.170E+01	-.359E+01
548	-.444E+02	-.450E+02	-.466E+02	-.521E+00	0.153E+01	-.266E+01
549	-.578E+02	-.588E+02	-.604E+02	-.638E+00	0.448E+00	-.770E+00
550	-.796E+02	-.802E+02	-.814E+02	-.136E+00	0.317E+00	-.408E+00

735	-.110E+03	-.110E+03	-.110E+03	0.308E-02	0.519E-02	-.277E-02
736	-.148E+03	-.148E+03	-.148E+03	0.256E-02	0.228E-02	-.106E-02
737	-.639E+01	-.648E+01	-.635E+01	0.138E-01	0.174E-02	-.101E-02
738	-.190E+02	-.191E+02	-.190E+02	0.154E-01	0.452E-02	-.336E-02

739	-.317E+02	-.318E+02	-.316E+02	0.158E-01	0.699E-02	-.539E-02
740	-.443E+02	-.444E+02	-.443E+02	0.153E-01	0.928E-02	-.685E-02
741	-.591E+02	-.592E+02	-.590E+02	0.141E-01	0.123E-01	-.806E-02
742	-.802E+02	-.803E+02	-.801E+02	0.119E-01	0.162E-01	-.847E-02
743	-.110E+03	-.110E+03	-.110E+03	0.931E-02	0.154E-01	-.653E-02
744	-.148E+03	-.148E+03	-.148E+03	0.756E-02	0.667E-02	-.245E-02
745	-.646E+01	-.645E+01	-.635E+01	0.271E-01	0.574E-03	-.379E-02
746	-.191E+02	-.191E+02	-.190E+02	0.298E-01	0.190E-02	-.106E-01
747	-.318E+02	-.318E+02	-.316E+02	0.300E-01	0.559E-02	-.159E-01
748	-.444E+02	-.444E+02	-.443E+02	0.286E-01	0.102E-01	-.192E-01
749	-.592E+02	-.592E+02	-.591E+02	0.256E-01	0.168E-01	-.212E-01
750	-.802E+02	-.802E+02	-.802E+02	0.208E-01	0.246E-01	-.205E-01
751	-.110E+03	-.110E+03	-.110E+03	0.156E-01	0.238E-01	-.150E-01
752	-.148E+03	-.148E+03	-.148E+03	0.124E-01	0.101E-01	-.555E-02
753	-.650E+01	-.634E+01	-.628E+01	0.394E-01	-.135E-01	-.669E-02
754	-.192E+02	-.190E+02	-.189E+02	0.430E-01	-.132E-01	-.194E-01
755	-.319E+02	-.317E+02	-.316E+02	0.441E-01	-.691E-02	-.302E-01
756	-.445E+02	-.444E+02	-.443E+02	0.428E-01	0.180E-02	-.375E-01
757	-.593E+02	-.591E+02	-.591E+02	0.384E-01	0.138E-01	-.423E-01
758	-.803E+02	-.802E+02	-.802E+02	0.304E-01	0.276E-01	-.404E-01
759	-.110E+03	-.110E+03	-.110E+03	0.216E-01	0.278E-01	-.289E-01
760	-.148E+03	-.148E+03	-.148E+03	0.164E-01	0.117E-01	-.104E-01
761	-.649E+01	-.619E+01	-.618E+01	0.277E-01	-.330E-02	-.539E-02
762	-.192E+02	-.189E+02	-.189E+02	0.342E-01	-.895E-02	-.190E-01
763	-.319E+02	-.316E+02	-.315E+02	0.412E-01	-.740E-02	-.346E-01
764	-.446E+02	-.443E+02	-.442E+02	0.454E-01	0.226E-04	-.493E-01
765	-.594E+02	-.591E+02	-.591E+02	0.434E-01	0.125E-01	-.626E-01
766	-.804E+02	-.802E+02	-.802E+02	0.338E-01	0.276E-01	-.629E-01
767	-.110E+03	-.110E+03	-.110E+03	0.222E-01	0.270E-01	-.446E-01
768	-.148E+03	-.148E+03	-.148E+03	0.155E-01	0.109E-01	-.156E-01
769	-.649E+01	-.613E+01	-.616E+01	0.787E-02	-.251E-02	-.109E-03
770	-.192E+02	-.188E+02	-.188E+02	0.144E-01	-.811E-02	-.779E-02
771	-.319E+02	-.315E+02	-.315E+02	0.229E-01	-.945E-02	-.246E-01
772	-.446E+02	-.442E+02	-.442E+02	0.299E-01	-.484E-02	-.470E-01
773	-.594E+02	-.590E+02	-.590E+02	0.317E-01	0.470E-02	-.727E-01
774	-.805E+02	-.802E+02	-.802E+02	0.253E-01	0.172E-01	-.806E-01
775	-.110E+03	-.110E+03	-.110E+03	0.155E-01	0.174E-01	-.569E-01
776	-.148E+03	-.148E+03	-.148E+03	0.101E-01	0.701E-02	-.194E-01
777	-.650E+01	-.613E+01	-.618E+01	-.791E-03	0.295E-02	0.332E-02
778	-.192E+02	-.188E+02	-.188E+02	0.186E-02	-.168E-03	0.492E-03
779	-.319E+02	-.314E+02	-.314E+02	0.515E-02	-.178E-02	-.156E-01
780	-.446E+02	-.441E+02	-.441E+02	0.829E-02	-.104E-02	-.413E-01
781	-.595E+02	-.590E+02	-.590E+02	0.966E-02	0.149E-02	-.749E-01
782	-.806E+02	-.801E+02	-.802E+02	0.786E-02	0.513E-02	-.894E-01
783	-.110E+03	-.110E+03	-.110E+03	0.460E-02	0.496E-02	-.631E-01
784	-.148E+03	-.148E+03	-.148E+03	0.287E-02	0.193E-02	-.211E-01

APPENDIX G2

INPUT AND OUTPUT DATA (USING PROGRAM PIER2D)

G2.1 INPUT DATA

```
BR16DP24
15   17    1    4   108   93
0.00   0.45   0.90   1.45   2.00   3.00   4.00   5.25
6.50   7.75   9.00  10.50  12.00  14.00  16.00
0.00   1.00   2.00   2.80   3.60   4.20   4.80   5.20   5.60
5.90   6.20   6.50   6.80   7.10   7.40   7.70   8.00
  4     1.0     21.07     0.0     8.0     0.0
 1668.08    0.48    0.25    1.1305E8   5.2992E8   10.E9   10.E9
  73.333    440.0
 1    0.0
 31
 1   5   2   5   3   5   4   5   5   5   6   5   7   5   8   5
 9   5  10   5  11   5  12   5  13   5  14   5  15   1  23   4
38   4  46   4  61   4  69   4  84   4  92   4 107   4 119   4
135  4 144   4 160   4 169   4 185   4 194   4 210   4
1
```

G2.2 LIMITED OUTPUT DATA

BR16DP24

NPX	NPY	NEXP	NEYP	NPFP	NPFF
15	17	1	4	108	93

ELEMENT AND NODE NUMBERS FOR MEDIUM ELEMENTS

I	1	2	3	4	5	6	7	8
1	1	3	26	24	2	17	25	16
2	3	5	28	26	4	18	27	17
3	5	7	30	28	6	19	29	18
4	7	9	32	30	8	20	31	19
5	9	11	34	32	10	21	33	20
6	11	13	36	34	12	22	35	21
7	13	15	38	36	14	23	37	22
8	24	26	49	47	25	40	48	39
9	26	28	51	49	27	41	50	40
10	28	30	53	51	29	42	52	41
21	59	61	84	82	60	69	83	68
22	70	72	95	93	71	86	94	85
23	72	74	97	95	73	87	96	86
24	74	76	99	97	75	88	98	87
25	76	78	101	99	77	89	100	88
26	78	80	103	101	79	90	102	89
27	80	82	105	103	81	91	104	90
28	82	84	107	105	83	92	106	91
29	95	97	125	123	96	114	124	113
30	97	99	127	125	98	115	126	114
42	150	152	177	175	151	165	176	164
43	152	154	179	177	153	166	178	165
44	154	156	181	179	155	167	180	166
45	156	158	183	181	157	168	182	167
46	158	160	185	183	159	169	184	168
47	173	175	200	198	174	189	199	188
48	175	177	202	200	176	190	201	189
49	177	179	204	202	178	191	203	190
50	179	181	206	204	180	192	205	191

51	181	183	208	206	182	193	207	192
52	183	185	210	208	184	194	209	193

ELEMENT AND NODE NUMBERS FOR FRICTION ELEMENTS

I	1	2	3	4	5	6
1	93	95	110	108	94	109
2	95	123	122	110	113	112
3	123	148	147	122	138	137
4	148	173	172	147	163	162
5	173	198	197	172	188	187

ELEMENT AND NODE NUMBERS FOR PILE ELEMENTS

I	1	2	3	4	5	6	7	8
1	108	110	122	120	109	112	121	111
2	120	122	147	145	121	137	146	136
3	145	147	172	170	146	162	171	161
4	170	172	197	195	171	187	196	186

XX	0.0000	0.4500	0.9000	1.4500	2.0000	3.0000	4.0000	5.2500	6.5000	7.7500
	9.0000	10.5000	12.0000	14.0000	16.0000					
YY	0.0000	1.0000	2.0000	2.8000	3.6000	4.2000	4.8000	5.2000	5.6000	5.9000
	6.2000	6.5000	6.8000	7.1000	7.4000	7.7000	8.0000			

COORDINATES OF ALL THE NODES

NP	XORD	YORD	NP	XORD	YORD	NP	XORD	YORD
1	0.0000	0.0000	2	0.4500	0.0000	3	0.9000	0.0000
4	1.4500	0.0000	5	2.0000	0.0000	6	3.0000	0.0000
7	4.0000	0.0000	8	5.2500	0.0000	9	6.5000	0.0000
10	7.7500	0.0000	11	9.0000	0.0000	12	10.5000	0.0000
13	12.0000	0.0000	14	14.0000	0.0000	15	16.0000	0.0000
16	0.0000	1.0000	17	0.9000	1.0000	18	2.0000	1.0000
19	4.0000	1.0000	20	6.5000	1.0000	21	9.0000	1.0000
-------	-------	-------	-------	-------	-------	-------	-------	-------
184	14.0000	7.4000	185	16.0000	7.4000	186	0.0000	7.7000
187	0.9000	7.7000	188	0.9000	7.7000	189	2.0000	7.7000
190	4.0000	7.7000	191	6.5000	7.7000	192	9.0000	7.7000
193	12.0000	7.7000	194	16.0000	7.7000	195	0.0000	8.0000
196	0.4500	8.0000	197	0.9000	8.0000	198	0.9000	8.0000
199	1.4500	8.0000	200	2.0000	8.0000	201	3.0000	8.0000
202	4.0000	8.0000	203	5.2500	8.0000	204	6.5000	8.0000
205	7.7500	8.0000	206	9.0000	8.0000	207	10.5000	8.0000
208	12.0000	8.0000	209	14.0000	8.0000	210	16.0000	8.0000

NO.GAUSS POINTS= 4
KO VALUE= 1.0000
BULK DENSITY=21.0700
SUBMERGED DENSITY= 0.0000
FULL HEIGHT= 8.0000
HEIGHT OF WATER TABLE= 0.0000

SOIL MODULUS= 0.166808E+04
POISSON RATIO FOR SOIL= 0.4800
PILE MODULUS= 0.219387E+09
PIOSSON RATIO FOR PILE= 0.2500
FLEXURAL RIGIDITY OF PILE= 0.113050E+09
AXIAL RIGIDITY OF PILE= 0.529920E+09
NORMAL STIFFNESS OF FRICTION ELEMENT= 0.100000E+11
SHEAR STIFFNESS OF FRICTION ELEMENT= 0.100000E+11

INITIAL STRESSES IN MEDIUM ELEMENTS

I	GPNU	DEPTH	HORZ.DIST	SIGIMZ	SIGIMR	ET	PR
1	1	7.5774	0.1902	-0.159655E+03	-0.159655E+03	0.166808E+04	0.4800
1	2	7.5774	0.7098	-0.159655E+03	-0.159655E+03	0.166808E+04	0.4800
1	3	6.4226	0.1902	-0.135325E+03	-0.135325E+03	0.166808E+04	0.4800
1	4	6.4226	0.7098	-0.135325E+03	-0.135325E+03	0.166808E+04	0.4800
2	1	7.5774	1.1325	-0.159655E+03	-0.159655E+03	0.166808E+04	0.4800
2	2	7.5774	1.7675	-0.159655E+03	-0.159655E+03	0.166808E+04	0.4800
2	3	6.4226	1.1325	-0.135325E+03	-0.135325E+03	0.166808E+04	0.4800
2	4	6.4226	1.7675	-0.135325E+03	-0.135325E+03	0.166808E+04	0.4800

3	1	7.5774	2.4226	-0.159655E+03	-0.159655E+03	0.166808E+04	0.4800
3	2	7.5774	3.5774	-0.159655E+03	-0.159655E+03	0.166808E+04	0.4800
3	3	6.4226	2.4226	-0.135325E+03	-0.135325E+03	0.166808E+04	0.4800
3	4	6.4226	3.5774	-0.135325E+03	-0.135325E+03	0.166808E+04	0.4800
4	1	7.5774	4.5283	-0.159655E+03	-0.159655E+03	0.166808E+04	0.4800
4	2	7.5774	5.9717	-0.159655E+03	-0.159655E+03	0.166808E+04	0.4800
4	3	6.4226	4.5283	-0.135325E+03	-0.135325E+03	0.166808E+04	0.4800
4	4	6.4226	5.9717	-0.135325E+03	-0.135325E+03	0.166808E+04	0.4800
5	1	7.5774	7.0283	-0.159655E+03	-0.159655E+03	0.166808E+04	0.4800
5	2	7.5774	8.4717	-0.159655E+03	-0.159655E+03	0.166808E+04	0.4800
5	3	6.4226	7.0283	-0.135325E+03	-0.135325E+03	0.166808E+04	0.4800
5	4	6.4226	8.4717	-0.135325E+03	-0.135325E+03	0.166808E+04	0.4800
6	1	7.5774	9.6340	-0.159655E+03	-0.159655E+03	0.166808E+04	0.4800
6	2	7.5774	11.3660	-0.159655E+03	-0.159655E+03	0.166808E+04	0.4800
6	3	6.4226	9.6340	-0.135325E+03	-0.135325E+03	0.166808E+04	0.4800
6	4	6.4226	11.3660	-0.135325E+03	-0.135325E+03	0.166808E+04	0.4800
7	1	7.5774	12.8453	-0.159655E+03	-0.159655E+03	0.166808E+04	0.4800
7	2	7.5774	15.1547	-0.159655E+03	-0.159655E+03	0.166808E+04	0.4800
7	3	6.4226	12.8453	-0.135325E+03	-0.135325E+03	0.166808E+04	0.4800
7	4	6.4226	15.1547	-0.135325E+03	-0.135325E+03	0.166808E+04	0.4800
8	1	5.6619	0.1902	-0.119296E+03	-0.119296E+03	0.166808E+04	0.4800
8	2	5.6619	0.7098	-0.119296E+03	-0.119296E+03	0.166808E+04	0.4800
8	3	4.7381	0.1902	-0.998322E+02	-0.998322E+02	0.166808E+04	0.4800
8	4	4.7381	0.7098	-0.998322E+02	-0.998322E+02	0.166808E+04	0.4800

45	1	1.0732	9.6340	-0.226124E+02	-0.226124E+02	0.166808E+04	0.4800
45	2	1.0732	11.3660	-0.226124E+02	-0.226124E+02	0.166808E+04	0.4800
45	3	0.7268	9.6340	-0.153136E+02	-0.153136E+02	0.166808E+04	0.4800
45	4	0.7268	11.3660	-0.153136E+02	-0.153136E+02	0.166808E+04	0.4800
46	1	1.0732	12.8453	-0.226124E+02	-0.226124E+02	0.166808E+04	0.4800
46	2	1.0732	15.1547	-0.226124E+02	-0.226124E+02	0.166808E+04	0.4800
46	3	0.7268	12.8453	-0.153136E+02	-0.153136E+02	0.166808E+04	0.4800
46	4	0.7268	15.1547	-0.153136E+02	-0.153136E+02	0.166808E+04	0.4800
47	1	0.4732	1.1325	-0.997043E+01	-0.997043E+01	0.166808E+04	0.4800
47	2	0.4732	1.7675	-0.997043E+01	-0.997043E+01	0.166808E+04	0.4800
47	3	0.1268	1.1325	-0.267157E+01	-0.267157E+01	0.166808E+04	0.4800
47	4	0.1268	1.7675	-0.267157E+01	-0.267157E+01	0.166808E+04	0.4800
48	1	0.4732	2.4226	-0.997043E+01	-0.997043E+01	0.166808E+04	0.4800
48	2	0.4732	3.5774	-0.997043E+01	-0.997043E+01	0.166808E+04	0.4800
48	3	0.1268	2.4226	-0.267157E+01	-0.267157E+01	0.166808E+04	0.4800
48	4	0.1268	3.5774	-0.267157E+01	-0.267157E+01	0.166808E+04	0.4800
49	1	0.4732	4.5283	-0.997043E+01	-0.997043E+01	0.166808E+04	0.4800
49	2	0.4732	5.9717	-0.997043E+01	-0.997043E+01	0.166808E+04	0.4800
49	3	0.1268	4.5283	-0.267157E+01	-0.267157E+01	0.166808E+04	0.4800
49	4	0.1268	5.9717	-0.267157E+01	-0.267157E+01	0.166808E+04	0.4800
50	1	0.4732	7.0283	-0.997043E+01	-0.997043E+01	0.166808E+04	0.4800
50	2	0.4732	8.4717	-0.997043E+01	-0.997043E+01	0.166808E+04	0.4800
50	3	0.1268	7.0283	-0.267157E+01	-0.267157E+01	0.166808E+04	0.4800
50	4	0.1268	8.4717	-0.267157E+01	-0.267157E+01	0.166808E+04	0.4800
51	1	0.4732	9.6340	-0.997043E+01	-0.997043E+01	0.166808E+04	0.4800
51	2	0.4732	11.3660	-0.997043E+01	-0.997043E+01	0.166808E+04	0.4800
51	3	0.1268	9.6340	-0.267157E+01	-0.267157E+01	0.166808E+04	0.4800
51	4	0.1268	11.3660	-0.267157E+01	-0.267157E+01	0.166808E+04	0.4800
52	1	0.4732	12.8453	-0.997043E+01	-0.997043E+01	0.166808E+04	0.4800
52	2	0.4732	15.1547	-0.997043E+01	-0.997043E+01	0.166808E+04	0.4800
52	3	0.1268	12.8453	-0.267157E+01	-0.267157E+01	0.166808E+04	0.4800
52	4	0.1268	15.1547	-0.267157E+01	-0.267157E+01	0.166808E+04	0.4800

INITIAL STRESSES IN HORIZONTAL FRICTION ELEMENTS

I	GPNU	DEPTH	HORZ.DIST	SIGIFN	SN	SS
1	1	2.4000	0.1902	-0.505680E+02	0.100000E+11	0.100000E+11
1	2	2.4000	0.7098	-0.505680E+02	0.100000E+11	0.100000E+11
1	3	2.4000	0.1902	-0.505680E+02	0.100000E+11	0.100000E+11
1	4	2.4000	0.7098	-0.505680E+02	0.100000E+11	0.100000E+11

INITIAL STRESSES IN VERTICAL FRICTION ELEMENTS

I	GPNU	DEPTH	HORZ.DIST	SIGIFN	SN	SS
2	1	2.2732	0.9000	-0.478964E+02	0.100000E+11	0.100000E+11
2	2	2.2732	0.9000	-0.478964E+02	0.100000E+11	0.100000E+11
2	3	1.9268	0.9000	-0.405976E+02	0.100000E+11	0.100000E+11
2	4	1.9268	0.9000	-0.405976E+02	0.100000E+11	0.100000E+11
3	1	1.6732	0.9000	-0.352544E+02	0.100000E+11	0.100000E+11
3	2	1.6732	0.9000	-0.352544E+02	0.100000E+11	0.100000E+11
3	3	1.3268	0.9000	-0.279556E+02	0.100000E+11	0.100000E+11
3	4	1.3268	0.9000	-0.279556E+02	0.100000E+11	0.100000E+11
4	1	1.0732	0.9000	-0.226124E+02	0.100000E+11	0.100000E+11
4	2	1.0732	0.9000	-0.226124E+02	0.100000E+11	0.100000E+11
4	3	0.7268	0.9000	-0.153136E+02	0.100000E+11	0.100000E+11
4	4	0.7268	0.9000	-0.153136E+02	0.100000E+11	0.100000E+11
5	1	0.4732	0.9000	-0.997043E+01	0.100000E+11	0.100000E+11
5	2	0.4732	0.9000	-0.997043E+01	0.100000E+11	0.100000E+11
5	3	0.1268	0.9000	-0.267157E+01	0.100000E+11	0.100000E+11
5	4	0.1268	0.9000	-0.267157E+01	0.100000E+11	0.100000E+11

INITIAL STRESSES IN PILE ELEMENTS

I	GPNU	DEPTH	HORZ.DIST	SIGIPZ	SIGIPR	ET	PR	FRP	ARP
1	1	2.2732	0.1902	-0.478964E+02	-0.478964E+02	0.219387E+09	0.2500	0.113050E+09	0.529920E+09
1	2	2.2732	0.7098	-0.478964E+02	-0.478964E+02	0.219387E+09	0.2500	0.113050E+09	0.529920E+09
1	3	1.9268	0.1902	-0.405976E+02	-0.405976E+02	0.219387E+09	0.2500	0.113050E+09	0.529920E+09
1	4	1.9268	0.7098	-0.405976E+02	-0.405976E+02	0.219387E+09	0.2500	0.113050E+09	0.529920E+09
2	1	1.6732	0.1902	-0.352544E+02	-0.352544E+02	0.219387E+09	0.2500	0.113050E+09	0.529920E+09
2	2	1.6732	0.7098	-0.352544E+02	-0.352544E+02	0.219387E+09	0.2500	0.113050E+09	0.529920E+09
2	3	1.3268	0.1902	-0.279556E+02	-0.279556E+02	0.219387E+09	0.2500	0.113050E+09	0.529920E+09
2	4	1.3268	0.7098	-0.279556E+02	-0.279556E+02	0.219387E+09	0.2500	0.113050E+09	0.529920E+09
3	1	1.0732	0.1902	-0.226124E+02	-0.226124E+02	0.219387E+09	0.2500	0.113050E+09	0.529920E+09
3	2	1.0732	0.7098	-0.226124E+02	-0.226124E+02	0.219387E+09	0.2500	0.113050E+09	0.529920E+09
3	3	0.7268	0.1902	-0.153136E+02	-0.153136E+02	0.219387E+09	0.2500	0.113050E+09	0.529920E+09
3	4	0.7268	0.7098	-0.153136E+02	-0.153136E+02	0.219387E+09	0.2500	0.113050E+09	0.529920E+09
4	1	0.4732	0.1902	-0.997043E+01	-0.997043E+01	0.219387E+09	0.2500	0.113050E+09	0.529920E+09
4	2	0.4732	0.7098	-0.997043E+01	-0.997043E+01	0.219387E+09	0.2500	0.113050E+09	0.529920E+09
4	3	0.1268	0.1902	-0.267157E+01	-0.267157E+01	0.219387E+09	0.2500	0.113050E+09	0.529920E+09
4	4	0.1268	0.7098	-0.267157E+01	-0.267157E+01	0.219387E+09	0.2500	0.113050E+09	0.529920E+09

BANDWIDTH= 93

LOAD MATRIX

NP	RADIAL	AXIAL	CIRCUMF	NP	RADIAL	AXIAL	CIRCUMF	NP	RADIAL	AXIAL	CIRCUMF
1	0.0000	0.0000	0.0000	2	0.0000	0.0000	0.0000	3	0.0000	0.0000	0.0000
4	0.0000	0.0000	0.0000	5	0.0000	0.0000	0.0000	6	0.0000	0.0000	0.0000
7	0.0000	0.0000	0.0000	8	0.0000	0.0000	0.0000	9	0.0000	0.0000	0.0000
10	0.0000	0.0000	0.0000	11	0.0000	0.0000	0.0000	12	0.0000	0.0000	0.0000
13	0.0000	0.0000	0.0000	14	0.0000	0.0000	0.0000	15	0.0000	0.0000	0.0000
16	0.0000	0.0000	0.0000	17	0.0000	0.0000	0.0000	18	0.0000	0.0000	0.0000

187	0.0000	0.0000	0.0000	188	0.0000	0.0000	0.0000	189	0.0000	0.0000	0.0000
190	0.0000	0.0000	0.0000	191	0.0000	0.0000	0.0000	192	0.0000	0.0000	0.0000
193	0.0000	0.0000	0.0000	194	0.0000	0.0000	0.0000	195	0.0000	0.0000	0.0000
196	0.0000	0.0000	0.0000	197	36.6665	-488.8889	-36.6665	198	0.0000	0.0000	0.0000
199	0.0000	0.0000	0.0000	200	0.0000	0.0000	0.0000	201	0.0000	0.0000	0.0000
202	0.0000	0.0000	0.0000	203	0.0000	0.0000	0.0000	204	0.0000	0.0000	0.0000
205	0.0000	0.0000	0.0000	206	0.0000	0.0000	0.0000	207	0.0000	0.0000	0.0000
208	0.0000	0.0000	0.0000	209	0.0000	0.0000	0.0000	210	0.0000	0.0000	0.0000

NUMBER OF HARMONICS= 1
ANGLE AROUND PILE= 0.0

NODE NUMBER AND BOUNDARY CONDITION

NPB	NFIX	NPB	NFIX	NPB	NFIX	NPB	NFIX	NPB	NFIX	NPB	NFIX	NPB	NFIX
1	5	2	5	3	5	4	5	5	5	6	5	7	5
8	5	9	5	10	5	11	5	12	5	13	5	14	5
15	1	23	4	38	4	46	4	61	4	69	4	84	4

92	4	107	4	119	4	135	4	144	4	160	4	169	4
185	4	194	4	210	4								

AMPLITUDES OF DISPLACEMENTS FOR MEDIUM ELEMENTS

NP	RADIAL	AXIAL	CIRCUMF	NP	RADIAL	AXIAL	CIRCUMF
1	-0.259360E-03	0.000000E+00	0.163157E-02	2	-0.742931E-03	0.000000E+00	0.131206E-02
3	-0.121448E-02	0.000000E+00	0.100920E-02	4	-0.958826E-03	0.000000E+00	0.979318E-03
5	-0.655107E-03	0.000000E+00	0.967910E-03	6	-0.324780E-03	0.000000E+00	0.842630E-03
7	0.124461E-04	0.000000E+00	0.732164E-03	8	0.372477E-03	0.000000E+00	0.652727E-03
9	0.620639E-03	0.000000E+00	0.625766E-03	10	0.725924E-03	0.000000E+00	0.645865E-03
11	0.722971E-03	0.000000E+00	0.697988E-03	12	0.630012E-03	0.000000E+00	0.786714E-03
13	0.474394E-03	0.000000E+00	0.891861E-03	14	0.237513E-03	0.000000E+00	0.104007E-02
15	0.000000E+00	0.000000E+00	0.119053E-02	16	-0.158662E-02	-0.367923E-05	0.901341E-03
17	-0.958858E-03	-0.262017E-03	0.115063E-02	18	-0.751548E-03	-0.487087E-03	0.985929E-03
19	0.634688E-04	-0.551355E-03	0.730995E-03	20	0.667260E-03	-0.340292E-03	0.612084E-03
21	0.749587E-03	-0.126783E-03	0.689628E-03	22	0.481742E-03	-0.622276E-07	0.888372E-03
23	0.000000E+00	0.397342E-04	0.118875E-02	24	-0.620680E-03	-0.122118E-03	0.206637E-02
25	-0.111342E-02	-0.385651E-03	0.172631E-02	26	-0.149384E-02	-0.684709E-03	0.130160E-02
27	-0.110380E-02	-0.904811E-03	0.124309E-02	28	-0.687105E-03	-0.109084E-02	0.110737E-02
29	-0.223881E-03	-0.121829E-02	0.883224E-03	30	0.206683E-03	-0.115560E-02	0.690699E-03
31	0.608658E-03	-0.937060E-03	0.589800E-03	32	0.822031E-03	-0.667471E-03	0.568160E-03
33	0.874371E-03	-0.442433E-03	0.601415E-03	34	0.817519E-03	-0.238098E-03	0.666248E-03
35	0.680483E-03	-0.106235E-03	0.767370E-03	36	0.497706E-03	0.528353E-05	0.880163E-03
37	0.243794E-03	0.460975E-04	0.103422E-02	38	0.000000E+00	0.800105E-04	0.118547E-02
39	-0.243842E-02	0.234790E-03	0.164062E-02	40	-0.156521E-02	-0.113417E-02	0.188521E-02

- -

183	0.517984E-03	0.379556E-03	0.826614E-03	184	0.232610E-03	0.167087E-03	0.102401E-02
185	0.000000E+00	0.464519E-03	0.118853E-02	188	0.339201E-01	-0.211968E-01	-0.340657E-01
189	0.168005E-01	-0.973926E-02	-0.928836E-02	190	0.540508E-02	-0.319527E-02	-0.215508E-02
191	0.225038E-02	-0.953525E-03	-0.300216E-03	192	0.113349E-02	-0.116994E-03	0.390090E-03
193	0.502110E-03	0.203731E-03	0.827328E-03	194	0.000000E+00	0.287325E-03	0.119143E-02
198	0.417524E-01	-0.205012E-01	-0.414579E-01	199	0.289071E-01	-0.745659E-02	-0.177076E-01
200	0.169574E-01	-0.835411E-02	-0.105200E-01	201	0.886028E-02	-0.406571E-02	-0.458501E-02
202	0.510579E-02	-0.320875E-02	-0.243332E-02	203	0.335838E-02	-0.131535E-02	-0.100107E-02
204	0.213103E-02	-0.109191E-02	-0.351534E-03	205	0.152649E-02	-0.248278E-03	0.980516E-04
206	0.107121E-02	-0.292996E-03	0.380613E-03	207	0.764591E-03	0.211436E-03	0.641953E-03
208	0.485434E-03	0.281040E-04	0.829852E-03	209	0.221759E-03	0.372244E-03	0.103565E-02
210	0.000000E+00	0.108751E-03	0.119475E-02				

AMPLITUDES OF DISPLACEMENTS FOR FRICTION ELEMENTS

NP	RADIAL	AXIAL	CIRCUMF	NP	RADIAL	AXIAL	CIRCUMF
93	-0.141431E-01	0.468037E-03	0.144327E-01	94	-0.149819E-01	-0.107130E-01	0.148371E-01
95	-0.141407E-01	-0.204889E-01	0.144323E-01	108	-0.147032E-01	0.102519E-05	0.147025E-01
109	-0.147018E-01	-0.104795E-01	0.147022E-01	110	-0.147008E-01	-0.209560E-01	0.147021E-01
112	-0.771655E-02	-0.209571E-01	0.771648E-02	113	-0.799658E-02	-0.211906E-01	0.785136E-02
122	-0.730564E-03	-0.209582E-01	0.730728E-03	123	-0.170522E-03	-0.204913E-01	0.460962E-03
137	0.625537E-02	-0.209587E-01	-0.625495E-02	138	0.597536E-02	-0.211921E-01	-0.612007E-02
147	0.132416E-01	-0.209594E-01	-0.132408E-01	148	0.138016E-01	-0.204924E-01	-0.135105E-01
162	0.202281E-01	-0.209591E-01	-0.202272E-01	163	0.199482E-01	-0.211926E-01	-0.200923E-01
172	0.272142E-01	-0.209592E-01	-0.272138E-01	173	0.277742E-01	-0.204922E-01	-0.274836E-01
187	0.342001E-01	-0.209633E-01	-0.342006E-01	188	0.339201E-01	-0.211968E-01	-0.340657E-01
197	0.411924E-01	-0.209682E-01	-0.411882E-01	198	0.417524E-01	-0.205012E-01	-0.414579E-01

AMPLITUDES OF DISPLACEMENTS FOR PILE ELEMENTS

NP	RADIAL	AXIAL	CIRCUMF	NP	RADIAL	AXIAL	CIRCUMF
108	-0.147032E-01	0.102519E-05	0.147025E-01	109	-0.147018E-01	-0.104795E-01	0.147022E-01
110	-0.147008E-01	-0.209560E-01	0.147021E-01	111	-0.771616E-02	0.428691E-06	0.771634E-02
112	-0.771655E-02	-0.209571E-01	0.771648E-02	120	-0.730524E-03	-0.179417E-06	0.730539E-03
121	-0.730815E-03	-0.104790E-01	0.730799E-03	122	-0.730564E-03	-0.209582E-01	0.730728E-03
136	0.625512E-02	-0.276653E-06	-0.625512E-02	137	0.625537E-02	-0.209587E-01	-0.625495E-02
145	0.132408E-01	-0.267165E-06	-0.132411E-01	146	0.132415E-01	-0.104794E-01	-0.132413E-01
147	0.132416E-01	-0.209594E-01	-0.132408E-01	161	0.202275E-01	0.643972E-06	-0.202275E-01
162	0.202281E-01	-0.209591E-01	-0.202272E-01	170	0.272145E-01	0.174187E-05	-0.272144E-01
171	0.272136E-01	-0.104813E-01	-0.272138E-01	172	0.272142E-01	-0.209592E-01	-0.272138E-01
186	0.342020E-01	-0.128496E-05	-0.342014E-01	187	0.342001E-01	-0.209633E-01	-0.342006E-01
195	0.411853E-01	-0.402715E-05	-0.411874E-01	196	0.411894E-01	-0.104782E-01	-0.411884E-01
197	0.411924E-01	-0.209682E-01	-0.411882E-01				

STRESSES DUE TO APPLIED LOADS IN MEDIUM ELEMENTS

I	GPNU	SIGMX	SIGMY	SIGMZ	SIGMXY	SIGMXZ	SIGMYZ
1	1	-0.123030E-01	-0.125293E+00	-0.100250E+00	-0.699864E+00	0.000000E+00	0.000000E+00
1	2	0.231729E+00	-0.187607E-01	0.377101E+00	0.179748E+00	0.000000E+00	0.000000E+00
1	3	0.178949E+00	-0.195915E+00	0.725690E-01	-0.118107E+00	0.000000E+00	0.000000E+00
1	4	-0.322434E-01	-0.746583E+00	-0.257648E+00	-0.426715E+00	0.000000E+00	0.000000E+00
2	1	0.150035E+00	-0.442303E+00	-0.166158E-01	0.740888E-01	0.000000E+00	0.000000E+00

2	2	0.375099E+00	-0.575206E+00	0.888757E-01	-0.441292E+00	0.000000E+00	0.000000E+00
2	3	0.182691E+00	-0.661359E+00	-0.472290E-01	-0.558838E-01	0.000000E+00	0.000000E+00
2	4	0.486610E+00	-0.653083E+00	0.171573E+00	-0.190525E+00	0.000000E+00	0.000000E+00
3	1	0.282232E+00	-0.725772E+00	0.280404E-01	-0.623714E-01	0.000000E+00	0.000000E+00
3	2	0.222498E+00	-0.100827E+01	-0.866912E-01	-0.133787E-01	0.000000E+00	0.000000E+00
3	3	0.203744E+00	-0.847391E+00	-0.800004E-02	0.134833E-01	0.000000E+00	0.000000E+00
3	4	0.260126E+00	-0.936123E+00	0.170639E-01	0.108104E+00	0.000000E+00	0.000000E+00
4	1	0.128354E+00	-0.788146E+00	0.982477E-02	0.467556E-01	0.000000E+00	0.000000E+00
4	2	0.133144E+00	-0.858957E+00	0.137632E-01	0.164795E+00	0.000000E+00	0.000000E+00
4	3	0.591079E-02	-0.643213E+00	0.209817E-01	0.505380E-01	0.000000E+00	0.000000E+00
4	4	-0.704495E-01	-0.699459E+00	-0.164893E-01	0.189918E+00	0.000000E+00	0.000000E+00
5	1	-0.100790E+00	-0.533220E+00	0.735366E-02	0.412965E-01	0.000000E+00	0.000000E+00
5	2	-0.104785E+00	-0.491979E+00	0.426535E-01	0.161474E+00	0.000000E+00	0.000000E+00
5	3	-0.172313E+00	-0.353025E+00	0.262673E-01	0.341923E-01	0.000000E+00	0.000000E+00
5	4	-0.229686E+00	-0.362818E+00	0.316651E-02	0.123038E+00	0.000000E+00	0.000000E+00
6	1	-0.217381E+00	-0.258116E+00	0.189707E-01	0.208396E-01	0.000000E+00	0.000000E+00
6	2	-0.226124E+00	-0.229807E+00	0.331539E-01	0.721718E-01	0.000000E+00	0.000000E+00
6	3	-0.233527E+00	-0.140034E+00	0.253089E-01	0.135285E-01	0.000000E+00	0.000000E+00
6	4	-0.249030E+00	-0.134518E+00	0.220722E-01	0.474797E-01	0.000000E+00	0.000000E+00
7	1	-0.229009E+00	-0.839035E-01	0.223808E-01	0.465049E-02	0.000000E+00	0.000000E+00
7	2	-0.232401E+00	-0.757837E-01	0.251144E-01	0.157986E-01	0.000000E+00	0.000000E+00
7	3	-0.206108E+00	-0.359278E-01	0.188262E-01	0.200204E-02	0.000000E+00	0.000000E+00
7	4	-0.206399E+00	-0.324025E-01	0.201604E-01	0.861696E-02	0.000000E+00	0.000000E+00
8	1	-0.357685E+00	-0.294856E+00	-0.801177E+00	-0.174963E+01	0.000000E+00	0.000000E+00
8	2	0.174083E+01	0.409315E+00	0.157995E+01	-0.140917E+01	0.000000E+00	0.000000E+00
8	3	0.698180E+00	-0.232663E+00	0.334178E+00	-0.801768E+00	0.000000E+00	0.000000E+00
8	4	0.433666E-01	-0.209206E+01	-0.458669E+00	-0.129141E+01	0.000000E+00	0.000000E+00

45	1	-0.358124E+00	0.699531E-01	0.132462E+00	0.140652E+00	0.000000E+00	0.000000E+00
45	2	-0.298299E+00	0.124585E+00	0.181778E+00	-0.276150E-01	0.000000E+00	0.000000E+00
45	3	-0.336571E+00	-0.600336E-01	0.149310E-01	-0.596815E-01	0.000000E+00	0.000000E+00
45	4	-0.340372E+00	-0.712991E-01	0.534668E-02	0.824106E-01	0.000000E+00	0.000000E+00
46	1	-0.203947E+00	0.198561E-01	0.822782E-01	0.699650E-01	0.000000E+00	0.000000E+00
46	2	-0.189490E+00	0.244040E-01	0.905361E-01	-0.459196E-01	0.000000E+00	0.000000E+00
46	3	-0.176314E+00	-0.602277E-02	0.457611E-01	-0.588989E-01	0.000000E+00	0.000000E+00
46	4	-0.171943E+00	-0.622123E-02	0.480753E-01	0.517758E-01	0.000000E+00	0.000000E+00
47	1	-0.354875E+02	-0.152438E+02	-0.169998E+02	0.163846E+02	0.000000E+00	0.000000E+00
47	2	-0.673374E+02	-0.331242E+02	-0.390315E+02	0.237076E+02	0.000000E+00	0.000000E+00
47	3	-0.155327E+02	0.102610E+02	0.621850E+01	0.857918E+01	0.000000E+00	0.000000E+00
47	4	-0.342795E+02	0.374905E+00	-0.652684E+01	0.201801E+01	0.000000E+00	0.000000E+00
48	1	-0.176314E+02	-0.615548E+01	-0.691518E+01	0.499310E+01	0.000000E+00	0.000000E+00
48	2	-0.146290E+02	0.640926E+00	-0.254472E+01	0.187427E+01	0.000000E+00	0.000000E+00
48	3	-0.565262E+01	0.706970E+00	-0.368475E+00	0.156128E+01	0.000000E+00	0.000000E+00
48	4	-0.561799E+01	0.135812E+01	-0.339659E+00	-0.312238E+00	0.000000E+00	0.000000E+00
49	1	-0.319299E+01	-0.246362E+00	-0.506406E+00	0.412887E+00	0.000000E+00	0.000000E+00
49	2	-0.347717E+01	-0.915598E+00	-0.110035E+01	0.467275E+00	0.000000E+00	0.000000E+00
49	3	-0.953582E+00	0.655982E+00	0.482857E+00	0.380214E+00	0.000000E+00	0.000000E+00
49	4	-0.167821E+01	-0.130500E-01	-0.220481E+00	-0.241981E-01	0.000000E+00	0.000000E+00
50	1	-0.149349E+01	-0.665972E+00	-0.583005E+00	0.423040E-01	0.000000E+00	0.000000E+00
50	2	-0.715843E+00	0.133779E+00	0.141877E+00	0.148682E+00	0.000000E+00	0.000000E+00
50	3	-0.370739E+00	0.246308E+00	0.262986E+00	0.132687E+00	0.000000E+00	0.000000E+00
50	4	-0.536668E+00	0.628639E-01	0.796807E-01	-0.103836E+00	0.000000E+00	0.000000E+00
51	1	-0.488957E+00	-0.112332E+00	-0.284175E-01	-0.530048E-01	0.000000E+00	0.000000E+00
51	2	-0.378227E+00	-0.663584E-01	0.387919E-01	0.807529E-01	0.000000E+00	0.000000E+00
51	3	-0.177837E+00	0.103689E+00	0.165933E+00	0.895012E-01	0.000000E+00	0.000000E+00
51	4	-0.279529E+00	-0.360865E-02	0.641586E-01	-0.611137E-01	0.000000E+00	0.000000E+00
52	1	-0.258257E+00	-0.596061E-01	0.164794E-01	-0.526462E-01	0.000000E+00	0.000000E+00
52	2	-0.178222E+00	0.125101E-01	0.884936E-01	0.505948E-01	0.000000E+00	0.000000E+00
52	3	-0.149088E+00	0.140154E-01	0.690287E-01	0.535665E-01	0.000000E+00	0.000000E+00
52	4	-0.157646E+00	-0.234005E-02	0.575109E-01	-0.521146E-01	0.000000E+00	0.000000E+00

RESULTANT OF INITIAL AND APPLIED STRESSES IN MEDIUM ELEMENTS

I	GPNU	SIGMX	SIGMY	SIGMZ	SIGMXY	SIGMXZ	SIGMYZ
1	1	-0.159667E+03	-0.159780E+03	-0.100250E+00	-0.699864E+00	0.000000E+00	0.000000E+00

1	2	-0.159423E+03	-0.159674E+03	0.377101E+00	0.179748E+00	0.000000E+00	0.000000E+00
1	3	-0.135146E+03	-0.135521E+03	0.725690E-01	-0.118107E+00	0.000000E+00	0.000000E+00
1	4	-0.135357E+03	-0.136072E+03	-0.257648E+00	-0.426715E+00	0.000000E+00	0.000000E+00
2	1	-0.159505E+03	-0.160097E+03	-0.166158E-01	0.740888E-01	0.000000E+00	0.000000E+00
2	2	-0.159280E+03	-0.160230E+03	0.888757E-01	-0.441292E+00	0.000000E+00	0.000000E+00
2	3	-0.135143E+03	-0.135987E+03	-0.472290E-01	-0.558838E-01	0.000000E+00	0.000000E+00
2	4	-0.134839E+03	-0.135978E+03	0.171573E+00	-0.190525E+00	0.000000E+00	0.000000E+00
3	1	-0.159373E+03	-0.160381E+03	0.280404E-01	-0.623714E-01	0.000000E+00	0.000000E+00
3	2	-0.159432E+03	-0.160663E+03	-0.866912E-01	-0.133787E-01	0.000000E+00	0.000000E+00
3	3	-0.135121E+03	-0.136173E+03	-0.800004E-02	0.134833E-01	0.000000E+00	0.000000E+00
3	4	-0.135065E+03	-0.136261E+03	0.170639E-01	0.108104E+00	0.000000E+00	0.000000E+00
4	1	-0.159526E+03	-0.160443E+03	0.982477E-02	0.467556E-01	0.000000E+00	0.000000E+00
4	2	-0.159522E+03	-0.160514E+03	0.137632E-01	0.164795E+00	0.000000E+00	0.000000E+00
4	3	-0.135319E+03	-0.135968E+03	0.209817E-01	0.505380E-01	0.000000E+00	0.000000E+00
4	4	-0.135396E+03	-0.136025E+03	-0.164893E-01	0.189918E+00	0.000000E+00	0.000000E+00
5	1	-0.159756E+03	-0.160188E+03	0.735366E-02	0.412965E-01	0.000000E+00	0.000000E+00
5	2	-0.159760E+03	-0.160147E+03	0.426535E-01	0.161474E+00	0.000000E+00	0.000000E+00
5	3	-0.135498E+03	-0.135678E+03	0.262673E-01	0.341923E-01	0.000000E+00	0.000000E+00
5	4	-0.135555E+03	-0.135688E+03	0.316651E-02	0.123038E+00	0.000000E+00	0.000000E+00
6	1	-0.159872E+03	-0.159913E+03	0.189707E-01	0.208396E-01	0.000000E+00	0.000000E+00
6	2	-0.159881E+03	-0.159885E+03	0.331539E-01	0.721718E-01	0.000000E+00	0.000000E+00
6	3	-0.135559E+03	-0.135465E+03	0.253089E-01	0.135285E-01	0.000000E+00	0.000000E+00
6	4	-0.135574E+03	-0.135460E+03	0.220722E-01	0.474797E-01	0.000000E+00	0.000000E+00
7	1	-0.159884E+03	-0.159739E+03	0.223808E-01	0.465049E-02	0.000000E+00	0.000000E+00
7	2	-0.159887E+03	-0.159731E+03	0.251144E-01	0.157986E-01	0.000000E+00	0.000000E+00
7	3	-0.135531E+03	-0.135361E+03	0.188262E-01	0.200204E-02	0.000000E+00	0.000000E+00
7	4	-0.135532E+03	-0.135358E+03	0.201604E-01	0.861696E-02	0.000000E+00	0.000000E+00
8	1	-0.119654E+03	-0.119591E+03	-0.801177E+00	-0.174963E+01	0.000000E+00	0.000000E+00
8	2	-0.117555E+03	-0.118887E+03	0.157995E+01	-0.140917E+01	0.000000E+00	0.000000E+00
8	3	-0.991340E+02	-0.100065E+03	0.334178E+00	-0.801768E+00	0.000000E+00	0.000000E+00
8	4	-0.997888E+02	-0.101924E+03	-0.458669E+00	-0.129141E+01	0.000000E+00	0.000000E+00

45	1	-0.229706E+02	-0.225425E+02	0.132462E+00	0.140652E+00	0.000000E+00	0.000000E+00
45	2	-0.229107E+02	-0.224878E+02	0.181778E+00	-0.276150E-01	0.000000E+00	0.000000E+00
45	3	-0.156501E+02	-0.153736E+02	0.149310E-01	-0.596815E-01	0.000000E+00	0.000000E+00
45	4	-0.156539E+02	-0.153849E+02	0.534668E-02	0.824106E-01	0.000000E+00	0.000000E+00
46	1	-0.228164E+02	-0.225926E+02	0.822782E-01	0.699650E-01	0.000000E+00	0.000000E+00
46	2	-0.228019E+02	-0.225880E+02	0.905361E-01	-0.459196E-01	0.000000E+00	0.000000E+00
46	3	-0.154899E+02	-0.153196E+02	0.457611E-01	-0.588989E-01	0.000000E+00	0.000000E+00
46	4	-0.154855E+02	-0.153198E+02	0.480753E-01	0.517758E-01	0.000000E+00	0.000000E+00
47	1	-0.454580E+02	-0.252142E+02	-0.169998E+02	0.163846E+02	0.000000E+00	0.000000E+00
47	2	-0.773079E+02	-0.430946E+02	-0.390315E+02	0.237076E+02	0.000000E+00	0.000000E+00
47	3	-0.182043E+02	0.758944E+01	0.621850E+01	0.857918E+01	0.000000E+00	0.000000E+00
47	4	-0.369510E+02	-0.229666E+01	-0.652684E+01	0.201801E+01	0.000000E+00	0.000000E+00
48	1	-0.276018E+02	-0.161259E+02	-0.691518E+01	0.499310E+01	0.000000E+00	0.000000E+00
48	2	-0.245994E+02	-0.932951E+01	-0.254472E+01	0.187427E+01	0.000000E+00	0.000000E+00
48	3	-0.832419E+01	-0.196460E+01	-0.368475E+00	0.156128E+01	0.000000E+00	0.000000E+00
48	4	-0.828956E+01	-0.131345E+01	-0.339659E+00	-0.312238E+00	0.000000E+00	0.000000E+00
49	1	-0.131634E+02	-0.102168E+02	-0.506406E+00	0.412887E+00	0.000000E+00	0.000000E+00
49	2	-0.134476E+02	-0.108860E+02	-0.110035E+01	0.467275E+00	0.000000E+00	0.000000E+00
49	3	-0.362515E+01	-0.201559E+01	0.482857E+00	0.380214E+00	0.000000E+00	0.000000E+00
49	4	-0.434978E+01	-0.268462E+01	-0.220481E+00	-0.241981E-01	0.000000E+00	0.000000E+00
50	1	-0.114639E+02	-0.106364E+02	-0.583005E+00	0.423040E-01	0.000000E+00	0.000000E+00
50	2	-0.106863E+02	-0.983665E+01	0.141877E+00	0.148682E+00	0.000000E+00	0.000000E+00
50	3	-0.304231E+01	-0.242526E+01	0.262986E+00	0.132687E+00	0.000000E+00	0.000000E+00
50	4	-0.320824E+01	-0.260871E+01	0.796807E-01	-0.103836E+00	0.000000E+00	0.000000E+00
51	1	-0.104594E+02	-0.100828E+02	-0.284175E-01	-0.530048E-01	0.000000E+00	0.000000E+00
51	2	-0.103487E+02	-0.100368E+02	0.387919E-01	0.807529E-01	0.000000E+00	0.000000E+00
51	3	-0.284941E+01	-0.256788E+01	0.165933E+00	0.895012E-01	0.000000E+00	0.000000E+00
51	4	-0.295110E+01	-0.267518E+01	0.641586E-01	-0.611137E-01	0.000000E+00	0.000000E+00
52	1	-0.102287E+02	-0.100300E+02	0.164794E-01	-0.526462E-01	0.000000E+00	0.000000E+00
52	2	-0.101487E+02	-0.995792E+01	0.884936E-01	0.505948E-01	0.000000E+00	0.000000E+00
52	3	-0.282066E+01	-0.265755E+01	0.690287E-01	0.535665E-01	0.000000E+00	0.000000E+00
52	4	-0.282921E+01	-0.267391E+01	0.575109E-01	-0.521146E-01	0.000000E+00	0.000000E+00

STRESSES DUE TO APPLIED LOADS

IN HORIZONTAL FRICTION ELEMENTS

I	GPNU	SIGFNZ	SIGFSR	SIGFSC
1	1	0.817377E+07	-0.244023E+09	0.000000E+00
1	2	-0.205968E+08	0.835342E+06	0.000000E+00
1	3	0.817377E+07	-0.244023E+09	0.000000E+00
1	4	-0.205968E+08	0.835342E+06	0.000000E+00

IN VERTICAL FRICTION ELEMENTS

I	GPNU	SIGFNR	SIGFSZ	SIGFC
2	1	0.263099E+09	0.101507E+08	0.000000E+00
2	2	-0.489025E+08	-0.257534E+08	0.000000E+00
2	3	0.263099E+09	0.101507E+08	0.000000E+00
2	4	-0.489025E+08	-0.257534E+08	0.000000E+00
3	1	0.263107E+09	0.101633E+08	0.000000E+00
3	2	-0.489008E+08	-0.257521E+08	0.000000E+00
3	3	0.263107E+09	0.101633E+08	0.000000E+00
3	4	-0.489008E+08	-0.257521E+08	0.000000E+00
4	1	0.263100E+09	0.101905E+08	0.000000E+00
4	2	-0.488983E+08	-0.257554E+08	0.000000E+00
4	3	0.263100E+09	0.101905E+08	0.000000E+00
4	4	-0.488983E+08	-0.257554E+08	0.000000E+00
5	1	0.263325E+09	0.100188E+08	0.000000E+00
5	2	-0.489128E+08	-0.257458E+08	0.000000E+00
5	3	0.263325E+09	0.100188E+08	0.000000E+00
5	4	-0.489128E+08	-0.257458E+08	0.000000E+00

RESULTANT OF INITIAL AND APPLIED STRESSES

IN HORIZONTIAL FRICTION ELEMENTS

I	GPNU	SIGFNZ	SIGFSR	SIGFSC
1	1	0.817372E+07	-0.244023E+09	0.000000E+00
1	2	-0.205969E+08	0.835342E+06	0.000000E+00
1	3	0.817372E+07	-0.244023E+09	0.000000E+00
1	4	-0.205969E+08	0.835342E+06	0.000000E+00

IN VERTICAL FRICTION ELEMENTS

I	GPNU	SIGFNR	SIGFSZ	SIGFC
2	1	0.263099E+09	0.101507E+08	0.000000E+00
2	2	-0.489026E+08	-0.257534E+08	0.000000E+00
2	3	0.263099E+09	0.101507E+08	0.000000E+00
2	4	-0.489026E+08	-0.257534E+08	0.000000E+00
3	1	0.263107E+09	0.101633E+08	0.000000E+00
3	2	-0.489008E+08	-0.257521E+08	0.000000E+00
3	3	0.263107E+09	0.101633E+08	0.000000E+00
3	4	-0.489008E+08	-0.257521E+08	0.000000E+00
4	1	0.263100E+09	0.101905E+08	0.000000E+00
4	2	-0.488983E+08	-0.257554E+08	0.000000E+00
4	3	0.263100E+09	0.101905E+08	0.000000E+00
4	4	-0.488983E+08	-0.257554E+08	0.000000E+00
5	1	0.263325E+09	0.100188E+08	0.000000E+00
5	2	-0.489128E+08	-0.257458E+08	0.000000E+00
5	3	0.263325E+09	0.100188E+08	0.000000E+00
5	4	-0.489128E+08	-0.257458E+08	0.000000E+00

STRESSES DUE TO APPLIED LOADS IN PILE ELEMENTS

I	GPNU	SIGPX	SIGPY	SIGPZ	SIGPXY	SIGPXZ	SIGPYZ
1	1	0.259542E+03	0.101440E+03	0.337159E+02	-0.178226E+03	0.000000E+00	0.000000E+00
1	2	-0.237986E+03	-0.100992E+02	0.307366E+02	-0.180852E+03	0.000000E+00	0.000000E+00
1	3	0.164142E+03	-0.155263E+03	0.112901E+03	0.190963E+02	0.000000E+00	0.000000E+00

1	4	-0.112830E+03	-0.203724E+03	-0.113961E+03	0.292894E+02	0.000000E+00	0.000000E+00
2	1	-0.111494E+03	-0.125596E+03	-0.286923E+02	0.167408E+02	0.000000E+00	0.000000E+00
2	2	0.239484E+03	-0.258659E+01	0.867684E+01	-0.527097E+01	0.000000E+00	0.000000E+00
2	3	0.386448E+02	-0.221404E+03	-0.199289E+01	-0.606826E+02	0.000000E+00	0.000000E+00
2	4	-0.660237E+02	-0.393253E+03	0.131687E+02	-0.643597E+02	0.000000E+00	0.000000E+00
3	1	0.239610E+03	-0.937899E+02	0.291898E+02	-0.703802E+02	0.000000E+00	0.000000E+00
3	2	-0.299385E+03	-0.181476E+03	-0.104081E+03	-0.540401E+03	0.000000E+00	0.000000E+00
3	3	0.817881E+02	-0.385465E+03	0.119769E+03	0.610062E+01	0.000000E+00	0.000000E+00
3	4	0.198976E+03	-0.508730E+03	0.330015E+02	0.164069E+03	0.000000E+00	0.000000E+00
4	1	-0.797934E+03	-0.350373E+02	0.704279E+02	0.124765E+03	0.000000E+00	0.000000E+00
4	2	0.769151E+03	0.429509E+03	0.953601E+02	0.600255E+03	0.000000E+00	0.000000E+00
4	3	-0.560876E+03	-0.551490E+03	-0.450088E+03	-0.139063E+03	0.000000E+00	0.000000E+00
4	4	0.263125E+03	-0.578735E+03	0.250184E+03	-0.275020E+03	0.000000E+00	0.000000E+00

RESULTANT OF INITIAL AND APPLIED STRESSES IN PILE ELEMENTS

I	GPNU	SIGPX	SIGPY	SIGPZ	SIGPXY	SIGPXZ	SIGPYZ
1	1	0.211645E+03	0.535435E+02	0.337159E+02	-0.178226E+03	0.000000E+00	0.000000E+00
1	2	-0.285883E+03	-0.579956E+02	0.307366E+02	-0.180852E+03	0.000000E+00	0.000000E+00
1	3	0.123544E+03	-0.195860E+03	0.112901E+03	0.190963E+02	0.000000E+00	0.000000E+00
1	4	-0.153428E+03	-0.244321E+03	-0.113961E+03	0.292894E+02	0.000000E+00	0.000000E+00
2	1	-0.146748E+03	-0.160850E+03	-0.286923E+02	0.167408E+02	0.000000E+00	0.000000E+00
2	2	0.204230E+03	-0.378410E+02	0.867684E+01	-0.527097E+01	0.000000E+00	0.000000E+00
2	3	0.106892E+02	-0.249360E+03	-0.199289E+01	-0.606826E+02	0.000000E+00	0.000000E+00
2	4	-0.939792E+02	-0.421209E+03	0.131687E+02	-0.643597E+02	0.000000E+00	0.000000E+00
3	1	0.216998E+03	-0.116402E+03	0.291898E+02	-0.703802E+02	0.000000E+00	0.000000E+00
3	2	-0.321997E+03	-0.204089E+03	-0.104081E+03	-0.540401E+03	0.000000E+00	0.000000E+00
3	3	0.664745E+02	-0.400778E+03	0.119769E+03	0.610062E+01	0.000000E+00	0.000000E+00
3	4	0.183662E+03	-0.524044E+03	0.330015E+02	0.164069E+03	0.000000E+00	0.000000E+00
4	1	-0.807904E+03	-0.450077E+02	0.704279E+02	0.124765E+03	0.000000E+00	0.000000E+00
4	2	0.759180E+03	0.419539E+03	0.953601E+02	0.600255E+03	0.000000E+00	0.000000E+00
4	3	-0.563547E+03	-0.554162E+03	-0.450088E+03	-0.139063E+03	0.000000E+00	0.000000E+00
4	4	0.260453E+03	-0.581406E+03	0.250184E+03	-0.275020E+03	0.000000E+00	0.000000E+00

FORCES CALCULATED USING DISPLACEMENTS AT THE CENTRE OF THE PILE

NP	DEPTH	DISPLACEMENT	SLOPE	MOMENT	SHEAR	PRESSURE	SGRM	FRP
108	2.400	-0.147032E-01	-0.116450E-01	0.000000E+00	0.000000E+00	-0.852128E+06	0.579555E+08	0.113050E+09
111	2.100	-0.771616E-02	-0.232877E-01	-0.171893E+04	-0.220925E+02	-0.383458E+05	0.496954E+07	0.113050E+09
120	1.800	-0.730524E-03	-0.232855E-01	0.132555E+02	-0.284654E+04	0.195161E+05	-0.267152E+08	0.113050E+09
136	1.500	0.625512E-02	-0.232855E-01	-0.110059E+02	-0.234032E+04	-0.161412E+05	-0.258049E+07	0.113050E+09
145	1.200	0.132408E-01	-0.232873E-01	0.141744E+04	-0.409500E+03	0.290133E+05	0.219122E+07	0.113050E+09
161	0.900	0.202275E-01	-0.232895E-01	0.234694E+03	0.108092E+04	-0.190772E+05	-0.943132E+06	0.113050E+09
170	0.600	0.272145E-01	-0.232909E-01	0.768894E+03	0.946812E+04	0.749919E+05	0.275559E+07	0.113050E+09
186	0.300	0.342020E-01	-0.232847E-01	-0.544618E+04	0.128149E+04	-0.129569E+06	-0.378835E+07	0.113050E+09
195	0.000	0.411853E-01	-0.232780E-01	0.440000E+03	0.733330E+02	-0.131293E+06	-0.318786E+07	0.113050E+09

APPENDIX G3

INPUT AND OUTPUT DATA (USING PROGRAM PIER3DNL)

G3.1 INPUT DATA

```
BR16DP24
1      1          1
784    8 1080     6   15     8     9  456
385  386  387   388  441   442   443  444
487  496  559   568  631   640
  10   1   11   1   12   1   13   1   14   1   15   1   16   1   17   1
  19   1   20   1   21   1   22   1   23   1   24   1   25   1   26   1
  28   1   29   1   30   1   31   1   32   1   33   1   34   1   35   1
  37   1   38   1   39   1   40   1   41   1   42   1   43   1   44   1
  46   1   47   1   48   1   49   1   50   1   51   1   52   1   53   1
  55   1   56   1   57   1   58   1   59   1   60   1   61   1   62   1
1018   1 1019   1 1020   1 1021   1 1022   1 1023   1 1024   1 1025   1
1027   1 1028   1 1029   1 1030   1 1031   1 1032   1 1033   1 1034   1
1036   1 1037   1 1038   1 1039   1 1040   1 1041   1 1042   1 1043   1
1045   1 1046   1 1047   1 1048   1 1049   1 1050   1 1051   1 1052   1
1054   1 1055   1 1056   1 1057   1 1058   1 1059   1 1060   1 1061   1
1063   1 1064   1 1065   1 1066   1 1067   1 1068   1 1069   1 1070   1
  73   2   74   2   75   2   76   2   77   2   78   2   79   2   80   2
 145   2  146   2  147   2  148   2  149   2  150   2  151   2  152   2
 217   2  218   2  219   2  220   2  221   2  222   2  223   2  224   2
 289   2  290   2  291   2  292   2  293   2  294   2  295   2  296   2
 361   2  362   2  363   2  364   2  365   2  366   2  367   2  368   2
 433   2  434   2  435   2  436   2  437   2  438   2  439   2  440   2
 505   2  506   2  507   2  508   2  509   2  510   2  511   2  512   2
 577   2  578   2  579   2  580   2  581   2  582   2  583   2  584   2
 649   2  650   2  651   2  652   2  653   2  654   2  655   2  656   2
 721   2  722   2  723   2  724   2  725   2  726   2  727   2  728   2
 793   2  794   2  795   2  796   2  797   2  798   2  799   2  800   2
 865   2  866   2  867   2  868   2  869   2  870   2  871   2  872   2
 937   2  938   2  939   2  940   2  941   2  942   2  943   2  944   2
 136   2  137   2  138   2  139   2  140   2  141   2  142   2  143   2
 208   2  209   2  210   2  211   2  212   2  213   2  214   2  215   2
 280   2  281   2  282   2  283   2  284   2  285   2  286   2  287   2
 352   2  353   2  354   2  355   2  356   2  357   2  358   2  359   2
 424   2  425   2  426   2  427   2  428   2  429   2  430   2  431   2
 496   2  497   2  498   2  499   2  500   2  501   2  502   2  503   2
 568   2  569   2  570   2  571   2  572   2  573   2  574   2  575   2
 640   2  641   2  642   2  643   2  644   2  645   2  646   2  647   2
 712   2  713   2  714   2  715   2  716   2  717   2  718   2  719   2
 784   2  785   2  786   2  787   2  788   2  789   2  790   2  791   2
 856   2  857   2  858   2  859   2  860   2  861   2  862   2  863   2
 928   2  929   2  930   2  931   2  932   2  933   2  934   2  935   2
1000   2 1001   2 1002   2 1003   2 1004   2 1005   2 1006   2 1007   2
   1   4    2   4    3   4    4   4    5   4    6   4    7   4    8   4
  64   4   65   4   66   4   67   4   68   4   69   4   70   4   71   4
1009   4 1010   4 1011   4 1012   4 1013   4 1014   4 1015   4 1016   4
1072   4 1073   4 1074   4 1075   4 1076   4 1077   4 1078   4 1079   4
   9   7   18   6   27   6   36   6   45   6   54   6   63   6   72   7
  81   5   90   3   99   3  108   3  117   3  126   3  135   3  144   5
 153   5  162   3  171   3  180   3  189   3  198   3  207   3  216   5
 225   5  234   3  243   3  252   3  261   3  270   3  279   3  288   5
 297   5  306   3  315   3  324   3  333   3  342   3  351   3  360   5
 369   5  378   3  387   3  396   3  405   3  414   3  423   3  432   5
 441   5  450   3  459   3  468   3  477   3  486   3  495   3  504   5
 513   5  522   3  531   3  540   3  549   3  558   3  567   3  576   5
 585   5  594   3  603   3  612   3  621   3  630   3  639   3  648   5
 657   5  666   3  675   3  684   3  693   3  702   3  711   3  720   5
 729   5  738   3  747   3  756   3  765   3  774   3  783   3  792   5
 801   5  810   3  819   3  828   3  837   3  846   3  855   3  864   5
 873   5  882   3  891   3  900   3  909   3  918   3  927   3  936   5
 945   5  954   3  963   3  972   3  981   3  990   3  999   3 1008   5
1017   7 1026   6 1035   6 1044   6 1053   6 1062   6 1071   6 1080   7
0.0  2.3  4.5  6.6  8.6 10.0 11.2 12.0 12.8 14.0 15.4 17.4 19.5 21.7 24.0
```

```
0.0  2.3  4.5  6.6  8.6 10.0 11.2 12.0
0.0  0.6  1.2  1.8  2.4  3.2  4.4  6.0  8.0
  1.6     0.8
  0.0      1.0        21.07       0.0
  81.65   0.0   0.83   16.467    0.0   101.3   52.83
  0.48   207.0E6    0.25
    10
   0.0         500.00     0.0      0.0      -3000.00
```

G3.2 LIMITED OUTPUT DATA

NTNEL	NPE	NUMNP	NOLN	NPX	NPY	NPZ	NUMBC
784	8	1080	6	15	8	9	456

385 386 387 388 441 442 443 444

ELEMENT AND NODE NUMBERS FOR ELEMENTS

I	1	2	3	4	5	6	7	8
1	74	83	11	2	73	82	10	1
2	75	84	12	3	74	83	11	2
3	76	85	13	4	75	84	12	3
4	77	86	14	5	76	85	13	4
5	78	87	15	6	77	86	14	5
6	79	88	16	7	78	87	15	6
7	80	89	17	8	79	88	16	7
8	81	90	18	9	80	89	17	8
9	83	92	20	11	82	91	19	10
10	84	93	21	12	83	92	20	11

381	555	564	492	483	554	563	491	482
382	556	565	493	484	555	564	492	483
383	557	566	494	485	556	565	493	484
384	558	567	495	486	557	566	494	485
385	560	569	497	488	559	568	496	487
386	561	570	498	489	560	569	497	488
387	562	571	499	490	561	570	498	489
388	563	572	500	491	562	571	499	490
389	564	573	501	492	563	572	500	491
390	565	574	502	493	564	573	501	492

775	1061	1070	998	989	1060	1069	997	988
776	1062	1071	999	990	1061	1070	998	989
777	1064	1073	1001	992	1063	1072	1000	991
778	1065	1074	1002	993	1064	1073	1001	992
779	1066	1075	1003	994	1065	1074	1002	993
780	1067	1076	1004	995	1066	1075	1003	994
781	1068	1077	1005	996	1067	1076	1004	995
782	1069	1078	1006	997	1068	1077	1005	996
783	1070	1079	1007	998	1069	1078	1006	997
784	1071	1080	1008	999	1070	1079	1007	998

PIER ELEMENT NUMBERS

385 386 387 388 441 442 443 444

MESH DATA

COORDINATES ALONG X-AXIS

```
  0.0000     2.3000     4.5000     6.6000     8.6000    10.0000    11.2000    12.0000
 12.8000    14.0000    15.4000    17.4000    19.5000    21.7000    24.0000
```

COORDINATES ALONG Y-AXIS

```
  0.0000     2.3000     4.5000     6.6000     8.6000    10.0000    11.2000    12.0000
```

COORDINATES ALONG Z-AXIS

```
  0.0000     0.6000     1.2000     1.8000     2.4000     3.2000     4.4000     6.0000
  8.0000
```

NODAL POINT COORDINATES

NODE	X	Y	Z	NODE	X	Y	Z
1	0.00000	0.00000	0.00000	2	0.00000	0.00000	0.60000
3	0.00000	0.00000	1.20000	4	0.00000	0.00000	1.80000
5	0.00000	0.00000	2.40000	6	0.00000	0.00000	3.20000
7	0.00000	0.00000	4.40000	8	0.00000	0.00000	6.00000
9	0.00000	0.00000	8.00000	10	0.00000	2.30000	0.00000

11	0.00000	2.30000	0.60000	12	0.00000	2.30000	1.20000
13	0.00000	2.30000	1.80000	14	0.00000	2.30000	2.40000
15	0.00000	2.30000	3.20000	16	0.00000	2.30000	4.40000
17	0.00000	2.30000	6.00000	18	0.00000	2.30000	8.00000
19	0.00000	4.50000	0.00000	20	0.00000	4.50000	0.60000
21	0.00000	4.50000	1.20000	22	0.00000	4.50000	1.80000

1059	24.00000	10.00000	3.20000	1060	24.00000	10.00000	4.40000
1061	24.00000	10.00000	6.00000	1062	24.00000	10.00000	8.00000
1063	24.00000	11.20000	0.00000	1064	24.00000	11.20000	0.60000
1065	24.00000	11.20000	1.20000	1066	24.00000	11.20000	1.80000
1067	24.00000	11.20000	2.40000	1068	24.00000	11.20000	3.20000
1069	24.00000	11.20000	4.40000	1070	24.00000	11.20000	6.00000
1071	24.00000	11.20000	8.00000	1072	24.00000	12.00000	0.00000
1073	24.00000	12.00000	0.60000	1074	24.00000	12.00000	1.20000
1075	24.00000	12.00000	1.80000	1076	24.00000	12.00000	2.40000
1077	24.00000	12.00000	3.20000	1078	24.00000	12.00000	4.40000
1079	24.00000	12.00000	6.00000	1080	24.00000	12.00000	8.00000

NODAL POINT COORDINATES

NODE	X	Y	Z	NODE	X	Y	Z
1	0.00000	0.00000	0.00000	2	0.00000	0.00000	0.60000
3	0.00000	0.00000	1.20000	4	0.00000	0.00000	1.80000
5	0.00000	0.00000	2.40000	6	0.00000	0.00000	3.20000
7	0.00000	0.00000	4.40000	8	0.00000	0.00000	6.00000
9	0.00000	0.00000	8.00000	10	0.00000	2.30000	0.00000
11	0.00000	2.30000	0.60000	12	0.00000	2.30000	1.20000
13	0.00000	2.30000	1.80000	14	0.00000	2.30000	2.40000
15	0.00000	2.30000	3.20000	16	0.00000	2.30000	4.40000
17	0.00000	2.30000	6.00000	18	0.00000	2.30000	8.00000
19	0.00000	4.50000	0.00000	20	0.00000	4.50000	0.60000
21	0.00000	4.50000	1.20000	22	0.00000	4.50000	1.80000

1059	24.00000	10.00000	3.20000	1060	24.00000	10.00000	4.40000
1061	24.00000	10.00000	6.00000	1062	24.00000	10.00000	8.00000
1063	24.00000	11.20000	0.00000	1064	24.00000	11.20000	0.60000
1065	24.00000	11.20000	1.20000	1066	24.00000	11.20000	1.80000
1067	24.00000	11.20000	2.40000	1068	24.00000	11.20000	3.20000
1069	24.00000	11.20000	4.40000	1070	24.00000	11.20000	6.00000
1071	24.00000	11.20000	8.00000	1072	24.00000	12.00000	0.00000
1073	24.00000	12.00000	0.60000	1074	24.00000	12.00000	1.20000
1075	24.00000	12.00000	1.80000	1076	24.00000	12.00000	2.40000
1077	24.00000	12.00000	3.20000	1078	24.00000	12.00000	4.40000
1079	24.00000	12.00000	6.00000	1080	24.00000	12.00000	8.00000

HEIGHT OF WATER TABLE= 0.0000
KO VALUE= 1.0000
BULK DENSITY=21.0700
SUBMERGED DENSITY= 0.0000

NODES AT WHICH LOAD IS APPLIED

487 496 559 568 631 640

BOUNDARY CONDITIONS

NPB	CODE	NPB	CODE	NPB	CODE	NPB	CODE	NPB	CODE
10	1	11	1	12	1	13	1	14	1
15	1	16	1	17	1	19	1	20	1
21	1	22	1	23	1	24	1	25	1
26	1	28	1	29	1	30	1	31	1
32	1	33	1	34	1	35	1	37	1
38	1	39	1	40	1	41	1	42	1
43	1	44	1	46	1	47	1	48	1
49	1	50	1	51	1	52	1	53	1

585	5	594	3	603	3	612	3	621	3
630	3	639	3	648	5	657	5	666	3
675	3	684	3	693	3	702	3	711	3
720	5	729	5	738	3	747	3	756	3
765	3	774	3	783	3	792	5	801	5
810	3	819	3	828	3	837	3	846	3
855	3	864	5	873	5	882	3	891	3
900	3	909	3	918	3	927	3	936	5
945	5	954	3	963	3	972	3	981	3
990	3	999	3	1008	5	1017	7	1026	6
1035	6	1044	6	1053	6	1062	6	1071	6
1080	7								

SOIL PARAMETERS -HYPERBOLIC MODEL

COHESION	FRICT.ANGLE	FAIL.RATIO	STIFFN.NO	STIFFN.EXP	ATMOS.PRESS	U/R.STIFFN.NO
81.650	0.000	0.830	16.467	0.000	101.300	52.830

PIER AND SOIL ELEMENT PROPERTIES

SOIL POISSON RATIO	PIER MODULUS	POISSON RATIO
0.48000E+00	0.20700E+09	0.25000E+00

APPLIED LOADING.

VLOAD	XHLOAD	YHLOAD	CXLOAD	CYLOAD
0.000	500.000	0.000	0.000	-3000.000

BAND WIDTH = 249

INITIAL STRESSES

EL NO	SIGX	SIGY	SIGZ
1	-0.632100E+01	-0.632100E+01	-0.632100E+01
2	-0.189630E+02	-0.189630E+02	-0.189630E+02
3	-0.316050E+02	-0.316050E+02	-0.316050E+02
4	-0.442470E+02	-0.442470E+02	-0.442470E+02
5	-0.589960E+02	-0.589960E+02	-0.589960E+02
6	-0.800660E+02	-0.800660E+02	-0.800660E+02
7	-0.109564E+03	-0.109564E+03	-0.109564E+03
8	-0.147490E+03	-0.147490E+03	-0.147490E+03
9	-0.632100E+01	-0.632100E+01	-0.632100E+01
10	-0.189630E+02	-0.189630E+02	-0.189630E+02
11	-0.316050E+02	-0.316050E+02	-0.316050E+02
12	-0.442470E+02	-0.442470E+02	-0.442470E+02
13	-0.589960E+02	-0.589960E+02	-0.589960E+02
14	-0.800660E+02	-0.800660E+02	-0.800660E+02
15	-0.109564E+03	-0.109564E+03	-0.109564E+03

471	-0.109564E+03	-0.109564E+03	-0.109564E+03
472	-0.147490E+03	-0.147490E+03	-0.147490E+03
473	-0.632100E+01	-0.632100E+01	-0.632100E+01
474	-0.189630E+02	-0.189630E+02	-0.189630E+02
475	-0.316050E+02	-0.316050E+02	-0.316050E+02
476	-0.442470E+02	-0.442470E+02	-0.442470E+02
477	-0.589960E+02	-0.589960E+02	-0.589960E+02
478	-0.800660E+02	-0.800660E+02	-0.800660E+02
479	-0.109564E+03	-0.109564E+03	-0.109564E+03
480	-0.147490E+03	-0.147490E+03	-0.147490E+03
481	-0.632100E+01	-0.632100E+01	-0.632100E+01
482	-0.189630E+02	-0.189630E+02	-0.189630E+02
483	-0.316050E+02	-0.316050E+02	-0.316050E+02
484	-0.442470E+02	-0.442470E+02	-0.442470E+02
485	-0.589960E+02	-0.589960E+02	-0.589960E+02

773	-0.589960E+02	-0.589960E+02	-0.589960E+02
774	-0.800660E+02	-0.800660E+02	-0.800660E+02
775	-0.109564E+03	-0.109564E+03	-0.109564E+03
776	-0.147490E+03	-0.147490E+03	-0.147490E+03
777	-0.632100E+01	-0.632100E+01	-0.632100E+01
778	-0.189630E+02	-0.189630E+02	-0.189630E+02
779	-0.316050E+02	-0.316050E+02	-0.316050E+02
780	-0.442470E+02	-0.442470E+02	-0.442470E+02
781	-0.589960E+02	-0.589960E+02	-0.589960E+02
782	-0.800660E+02	-0.800660E+02	-0.800660E+02
783	-0.109564E+03	-0.109564E+03	-0.109564E+03
784	-0.147490E+03	-0.147490E+03	-0.147490E+03

INCN.NO. = 1

NODAL DISPLACEMENTS

	X-DISP		Y-DISP		Z-DISP
1	-0.9488E-17	2	0.1776E-15	3	0.1889E-03
4	0.1384E-16	5	0.2033E-15	6	0.1767E-03
7	0.2321E-16	8	0.2144E-15	9	0.1633E-03
10	0.3101E-16	11	0.2233E-15	12	0.1488E-03
13	0.4163E-16	14	0.2528E-15	15	0.1334E-03
16	0.6326E-16	17	0.3105E-15	18	0.1122E-03
19	0.7526E-16	20	0.3459E-15	21	0.8067E-04
22	0.6467E-16	23	0.3451E-15	24	0.4231E-04
25	0.4923E-16	26	0.3320E-15	27	-0.5046E-16

1699	-0.1221E-02	1700	0.2029E-04	1701	-0.1826E-15
1702	0.1953E-01	1703	-0.3438E-18	1704	-0.4443E-03
1705	0.1315E-01	1706	-0.1362E-18	1707	-0.4443E-03
1708	0.6780E-02	1709	0.2614E-19	1710	-0.4443E-03
1711	0.4076E-03	1712	0.3192E-19	1713	-0.4443E-03
1714	-0.5964E-02	1715	0.6755E-19	1716	-0.4443E-03
1717	-0.4460E-02	1718	-0.1032E-15	1719	-0.4056E-03
1720	-0.2378E-02	1721	-0.2307E-16	1722	-0.2760E-03
1723	-0.1497E-02	1724	-0.5787E-17	1725	-0.1327E-03
1726	-0.1236E-02	1727	-0.4009E-17	1728	-0.1563E-15

3214	0.7304E-16	3215	-0.1005E-15	3216	-0.2175E-03
3217	0.2428E-15	3218	-0.4310E-16	3219	-0.1949E-03
3220	0.3099E-15	3221	-0.1647E-16	3222	-0.1602E-03
3223	0.3956E-15	3224	0.5373E-17	3225	-0.1154E-03
3226	0.5753E-15	3227	0.3576E-16	3228	-0.6411E-04
3229	0.8223E-15	3230	0.6419E-16	3231	-0.2441E-06
3232	0.7902E-15	3233	0.3175E-16	3234	0.5800E-04
3235	0.6086E-15	3236	0.5071E-17	3237	0.6096E-04

3238	0.5109E-15	3239	-0.7810E-17	3240	0.4296E-15

NODAL POINT COORDINATES

NODE	X	Y	Z	NODE	X	Y	Z

ELEMENT STRESSES

EL NO	SIGX	SIGY	SIGZ	SIGXY	SIGYZ	SIGXZ	SIGMA1	SIGMA3	ETM
1	-.631E+01	-.623E+01	-.630E+01	0.246E-02	-.694E-04	0.738E-04	0.631E+01	0.626E+01	0.167E+04
2	-.189E+02	-.189E+02	-.189E+02	0.278E-02	-.592E-03	-.193E-03	0.189E+02	0.189E+02	0.167E+04
3	-.316E+02	-.315E+02	-.316E+02	0.290E-02	-.109E-02	-.565E-03	0.316E+02	0.315E+02	0.167E+04
4	-.442E+02	-.441E+02	-.442E+02	0.287E-02	-.149E-02	-.970E-03	0.442E+02	0.441E+02	0.167E+04
5	-.590E+02	-.589E+02	-.590E+02	0.270E-02	-.200E-02	-.146E-02	0.590E+02	0.589E+02	0.167E+04
6	-.800E+02	-.800E+02	-.800E+02	0.236E-02	-.273E-02	-.195E-02	0.800E+02	0.800E+02	0.167E+04
7	-.110E+03	-.109E+03	-.110E+03	0.192E-02	-.272E-02	-.174E-02	0.110E+03	0.109E+03	0.167E+04
8	-.147E+03	-.147E+03	-.147E+03	0.161E-02	-.123E-02	-.674E-03	0.147E+03	0.147E+03	0.167E+04
9	-.629E+01	-.624E+01	-.630E+01	0.786E-02	-.569E-03	-.644E-03	0.629E+01	0.626E+01	0.167E+04
10	-.189E+02	-.189E+02	-.189E+02	0.893E-02	-.159E-02	-.211E-02	0.189E+02	0.189E+02	0.167E+04
774	-.804E+02	-.801E+02	-.802E+02	0.168E-01	0.124E-01	-.558E-01	0.804E+02	0.801E+02	0.166E+04
775	-.110E+03	-.110E+03	-.110E+03	0.994E-02	0.124E-01	-.391E-01	0.110E+03	0.110E+03	0.167E+04
776	-.148E+03	-.148E+03	-.148E+03	0.617E-02	0.494E-02	-.132E-01	0.148E+03	0.148E+03	0.167E+04
777	-.643E+01	-.619E+01	-.623E+01	-.837E-03	0.192E-02	0.219E-02	0.643E+01	0.621E+01	0.166E+04
778	-.191E+02	-.188E+02	-.189E+02	0.104E-02	-.199E-03	0.246E-03	0.191E+02	0.188E+02	0.166E+04
779	-.318E+02	-.315E+02	-.315E+02	0.337E-02	-.125E-02	-.110E-01	0.318E+02	0.315E+02	0.166E+04
780	-.445E+02	-.442E+02	-.442E+02	0.557E-02	-.684E-03	-.288E-01	0.445E+02	0.442E+02	0.166E+04
781	-.593E+02	-.590E+02	-.590E+02	0.654E-02	0.112E-02	-.521E-01	0.593E+02	0.590E+02	0.166E+04
782	-.804E+02	-.801E+02	-.802E+02	0.527E-02	0.368E-02	-.620E-01	0.804E+02	0.801E+02	0.166E+04
783	-.110E+03	-.110E+03	-.110E+03	0.298E-02	0.352E-02	-.434E-01	0.110E+03	0.110E+03	0.166E+04
784	-.148E+03	-.148E+03	-.148E+03	0.176E-02	0.136E-02	-.144E-01	0.148E+03	0.148E+03	0.167E+04

INCN.NO.= 2

INCN.NO.= 10

NODAL DISPLACEMENTS

	X-DISP		Y-DISP		Z-DISP
1	-0.1051E-14	2	-0.2633E-15	3	0.3320E-03
4	-0.9174E-15	5	-0.2767E-15	6	0.4356E-03
7	-0.8128E-15	8	-0.1944E-15	9	0.5281E-03
10	-0.7113E-15	11	-0.5925E-16	12	0.6002E-03
13	-0.7500E-15	14	0.2120E-16	15	0.6480E-03
16	-0.7880E-15	17	0.1810E-15	18	0.6707E-03
19	-0.3564E-15	20	0.8773E-15	21	0.6072E-03
22	-0.5210E-16	23	0.1426E-14	24	0.3850E-03
25	-0.5765E-16	26	0.1546E-14	27	0.7764E-15
28	-0.1222E-14	29	0.1894E-04	30	0.3930E-03
31	-0.9451E-15	32	0.3457E-04	33	0.5045E-03
1699	-0.1376E-01	1700	0.6932E-03	1701	-0.8590E-14
1702	0.6361E+00	1703	0.5708E-17	1704	-0.1369E-01
1705	0.4377E+00	1706	-0.5932E-18	1707	-0.4229E-01
1708	0.2392E+00	1709	-0.2379E-17	1710	-0.7090E-01
1711	0.4073E-01	1712	-0.2787E-17	1713	-0.9950E-01
1714	-0.1577E+00	1715	0.4073E-17	1716	-0.1281E+00
1717	-0.5585E-01	1718	-0.7624E-13	1719	-0.1716E-01
1720	-0.2863E-01	1721	-0.1131E-13	1722	-0.8344E-02
1723	-0.1723E-01	1724	-0.2729E-14	1725	-0.4404E-02
1726	-0.1395E-01	1727	-0.1037E-14	1728	-0.8553E-14
1729	-0.4304E-02	1730	-0.1117E-14	1731	-0.4803E-03
1732	-0.4102E-02	1733	-0.1021E-14	1734	-0.2468E-03
3205	0.1300E-13	3206	-0.1062E-02	3207	0.1192E-02
3208	0.9213E-14	3209	-0.8497E-03	3210	0.1161E-02
3211	0.7283E-14	3212	-0.7604E-03	3213	0.7407E-14
3214	0.2604E-14	3215	-0.6490E-15	3216	-0.3821E-02
3217	0.4679E-14	3218	-0.2308E-15	3219	-0.3162E-02
3220	0.6213E-14	3221	-0.1450E-15	3222	-0.2435E-02
3223	0.6624E-14	3224	0.6003E-16	3225	-0.1623E-02
3226	0.8172E-14	3227	0.7481E-15	3228	-0.8069E-03
3229	0.1245E-13	3230	0.1294E-14	3231	0.2430E-03
3232	0.1185E-13	3233	0.6019E-15	3234	0.1207E-02
3235	0.8315E-14	3236	0.8791E-16	3237	0.1180E-02
3238	0.6483E-14	3239	-0.1068E-15	3240	0.6697E-14

NODAL POINT COORDINATES

NODE	X	Y	Z	NODE	X	Y	Z

ELEMENT STRESSES

EL NO	SIGX	SIGY	SIGZ	SIGXY	SIGYZ	SIGXZ	SIGMA1	SIGMA3	ETM
1	-.668E+01	-.644E+01	-.624E+01	0.918E-03	0.203E-01	-.306E-03	0.668E+01	0.629E+01	0.166E+04
2	-.193E+02	-.190E+02	-.189E+02	0.629E-02	0.380E-01	0.367E-02	0.193E+02	0.189E+02	0.166E+04
3	-.319E+02	-.316E+02	-.315E+02	0.112E-01	0.455E-01	0.810E-02	0.319E+02	0.315E+02	0.166E+04
4	-.445E+02	-.442E+02	-.442E+02	0.156E-01	0.467E-01	0.105E-01	0.445E+02	0.442E+02	0.166E+04
5	-.592E+02	-.589E+02	-.590E+02	0.196E-01	0.464E-01	0.121E-01	0.592E+02	0.589E+02	0.166E+04

6	-.802E+02	-.798E+02	-.801E+02	0.216E-01	0.457E-01	0.103E-01	0.802E+02	0.798E+02	0.166E+04
7	-.110E+03	-.109E+03	-.110E+03	0.244E-01	0.363E-01	0.753E-03	0.110E+03	0.109E+03	0.535E+04
8	-.147E+03	-.147E+03	-.148E+03	0.216E-01	0.860E-02	-.184E-02	0.148E+03	0.147E+03	0.535E+04
9	-.682E+01	-.665E+01	-.637E+01	-.115E-01	0.447E-01	0.766E-03	0.682E+01	0.643E+01	0.166E+04
10	-.194E+02	-.192E+02	-.190E+02	-.431E-03	0.103E+00	0.544E-02	0.194E+02	0.189E+02	0.166E+04

770	-.219E+02	-.173E+02	-.171E+02	0.167E+00	0.149E-01	-.219E+00	0.219E+02	0.171E+02	0.159E+04
771	-.351E+02	-.304E+02	-.302E+02	0.205E+00	-.655E-01	-.297E+00	0.351E+02	0.303E+02	0.159E+04
772	-.480E+02	-.434E+02	-.432E+02	0.300E+00	-.609E-01	-.424E+00	0.481E+02	0.432E+02	0.159E+04
773	-.634E+02	-.589E+02	-.590E+02	0.366E+00	0.428E-01	-.740E+00	0.634E+02	0.590E+02	0.159E+04
774	-.845E+02	-.809E+02	-.816E+02	0.304E+00	0.220E+00	-.892E+00	0.845E+02	0.810E+02	0.161E+04
775	-.113E+03	-.111E+03	-.112E+03	0.169E+00	0.230E+00	-.627E+00	0.113E+03	0.111E+03	0.163E+04
776	-.150E+03	-.149E+03	-.151E+03	0.889E-01	0.898E-01	-.204E+00	0.151E+03	0.149E+03	0.164E+04
777	-.855E+01	-.381E+01	-.399E+01	0.441E-01	0.633E-01	-.721E-01	0.855E+01	0.386E+01	0.159E+04
778	-.218E+02	-.169E+02	-.170E+02	0.385E-01	0.463E-01	-.229E+00	0.218E+02	0.169E+02	0.159E+04
779	-.351E+02	-.301E+02	-.302E+02	0.356E-01	0.308E-02	-.243E+00	0.351E+02	0.301E+02	0.159E+04
780	-.476E+02	-.425E+02	-.425E+02	0.686E-01	-.122E-01	-.273E+00	0.476E+02	0.425E+02	0.158E+04
781	-.632E+02	-.582E+02	-.584E+02	0.107E+00	0.116E-01	-.701E+00	0.632E+02	0.582E+02	0.159E+04
782	-.847E+02	-.805E+02	-.814E+02	0.950E-01	0.632E-01	-.986E+00	0.846E+02	0.807E+02	0.160E+04
783	-.113E+03	-.111E+03	-.112E+03	0.510E-01	0.629E-01	-.711E+00	0.113E+03	0.111E+03	0.163E+04
784	-.150E+03	-.149E+03	-.151E+03	0.249E-01	0.237E-01	-.229E+00	0.151E+03	0.149E+03	0.163E+04

APPENDIX H

PUBLICATIONS

H1 - CONVENTIONAL AND CENTRIFUGE MODEL STUDIES OF THE MOMENT CARRYING CAPACITY OF SHORT PIER FOUNDATIONS IN CLAY

H2 - NUMERICAL STUDIES OF THE MOMENT CARRYING CAPACITY OF SHORT PIER FOUNDATIONS IN CLAY